

THE EFFECT OF pH ON MICROBIAL
ACTIVITY AND COMMUNITY STRUCTURE
IN THE BIOLOGICAL REMOVAL OF RESIN ACIDS
FROM WASTEWATER

by

ALAN GIDEON WERKER

B.A.Sc., The University of Waterloo, 1985

M.Eng., The University of Toronto, 1988

A THESIS SUBMITTED IN PARTIAL FULFILMENT OF
THE REQUIREMENTS FOR THE DEGREE OF
DOCTOR OF PHILOSOPHY

in

THE FACULTY OF GRADUATE STUDIES

Department of Civil Engineering (Environmental Engineering)

We accept this thesis as conforming
to the required standard

THE UNIVERSITY OF BRITISH COLUMBIA

September 1998

© Alan Gideon Werker, 1998

In presenting this thesis in partial fulfilment of the requirements for an advanced degree at the University of British Columbia, I agree that the Library shall make it freely available for reference and study. I further agree that permission for extensive copying of this thesis for scholarly purposes may be granted by the head of my department or by his or her representatives. It is understood that copying or publication of this thesis for financial gain shall not be allowed without my written permission.

Department of CIVIL ENGINEERING

The University of British Columbia
Vancouver, Canada

Date DECEMBER 17/88

Abstract

Pulp mills in Canada rely on biological treatment systems for the removal of resin acids that are released from wood during pulping and bleaching. These are priority contaminants for the pulping industry, since they have been frequently associated with events of toxicity breakthrough. Although, tighter mill control has helped to minimize the losses of resin acids in wastewater, acute toxicity removal in downstream biological treatment systems may still be insufficient, particularly under dynamic loading conditions. The mechanisms responsible for these limitations are not fully understood. This dissertation documents a fundamental study into the fate of resin acids during biological treatment. The objective was to quantify the influence of pH on the resin acid bioavailability, metabolism, and retention time during biological treatment. A progression of two batch and two continuous flow bioreactor investigations were undertaken to consider the interrelated issues of pH-dependent microbial activity and resin acid hydrophobicity.

Changes in pH, within the typical range for biological treatment, significantly altered the bioavailability of resin acids and the community of microorganisms responsible for resin acid biodegradation. A sudden input of resin acids promoted an elevated level of community change during continuous treatment of bleached kraft mill effluent. The capacity of a treatment system to remove resin acids was found to be a function of the contaminant loading history. Time lag before biological removal in response to a shift-up in resin acid loading was significant and was also affected by the treatment system pH. Hence, the prevailing bioreactor pH operating condition, in conjunction with the period and amplitude of loading transients were shown to be key aspects controlling the microbial community structure and physiological state, which in turn determine the rate and extent of biological removal of resin acids.

Through the course of the four investigations, novel contributions have been made in the areas of surface tension and microbial fatty acid measurements that have engineering application in future modelling and monitoring of the behaviour of microbial wastewater treatment processes.

Table of Contents

Abstract	ii
Table of Contents	iii
List of Figures	iv
List of Tables	ix
Acknowledgement	xi
Dedication	xii
Chapter 1 - Resin Acids and Toxicity Breakthrough in Pulp Mill Effluent Treatment	1
Chapter 2 - Surfactancy and Solubility in the Biological Removal of Resin Acids	19
Chapter 3 - Microbial Community Structure in the Kinetics of Resin Acid Removal	80
Chapter 4 - A Resin Acid Shock Load During Continuous Biological Treatment	184
Chapter 5 - Transient Resin Acid Loading During Continuous Biological Treatment	263
Chapter 6 - Recommendations and Future Applications	336
Appendix A - Experimental Data	350

List of Figures

Figure 1-1. Common pine resin acids of the abietane skeletal class.	9
Figure 1-2. Common pine resin acids of the pimarane and isopimarane skeletal class.	10
Figure 1-3. Chlorinated resin acid derivatives formed during pulp bleaching.	10
Figure 2-1. A small (elemental) section of an arbitrarily curved gas/liquid interface.	27
Figure 2-2. Sample data from Hua and Rosen (1988) illustrating the effect of surfactant concentration (c) on dynamic surface tension for N-dodecyl-N-methylglycine at pH 9.0 and 25 °C.	32
Figure 2-3. The maximum bubble pressure method.	49
Figure 2-4. Experimental setup for the maximum bubble pressure method.	50
Figure 2-5. A typical maximum bubble pressure signal.	51
Figure 2-6. Detail of the critical points in the pressure signal.	51
Figure 2-7. Batch growth resin acid depletion curves for pH 6,7 and 8 from top to bottom.	57
Figure 2-8. Dynamic surface tension during biological removal of resin acids for pH 6,7 and 8 from top to bottom.	59
Figure 2-9. Derived surface pressure changes with time in the absence of resin acids that were believed to be due to the presence of kraft lignin in the media.	60
Figure 2-10. The quasi-static Langmuir concentration K_t (equation (2-20)) as a function of surface age and pH.	60
Figure 2-11. Normalized surface loading (γ) as a function of surface age (t) and resin acid concentration.	62
Figure 2-12. The derived initial flux of resin acid to a freshly generated gas/liquid interface at pH 8.	63
Figure 2-13. The derived initial flux of resin acid to a freshly generated gas/liquid interface at pH 6 and 7.	63
Figure 2-14. The experimentally derived dependency of the sticking factor Φ on the squared compliment of normalized surface loading based on the initial surface flux (equation (2-48) and (2-51)).	65
Figure 3-1. Chemical structure of abietic (left) versus pimaric acid (right).	84
Figure 3-2. Flow diagram for biochemical lipid analysis of natural microbial communities.	97
Figure 3-3. A schematic drawing depicting a segment of the classical lipid bilayer containing intrinsic (I) proteins.	99
Figure 3-4. Typical retention time data for a homologous series of saturated straight chain fatty acids (10:0 to 24:0) by GC/FID (HP Series II) with a DB5 (30 m, 0.32 mm ID and 0.25 μ m film thickness).	133
Figure 3-5. Equivalent chain length (ECL) template for monoenoic, branched and hydroxy fatty acids from a DB-5 column calibration (Figure 3-4) made with standard mixtures of fatty acid methyl esters (Supelco FAME and BAME component mixtures).	133
Figure 3-6. Relative peak positions as a function of double bond location for homologous cis and trans monoenoic fatty acids.	134

Figure 3-7. Mean logratio fatty acid compositional data ($y_i = \log(x_i / x_{16:0})$) by PLFA versus WCFA analysis from five replicate samples taken during log growth in Lauryl Tryptose Broth. .	137
Figure 3-8. Whole-cell fatty acid (TFA) increase with time representing biomass production during mixed culture batch growth in Lauryl Tryptose Broth.	138
Figure 3-9. Whole-cell fatty acid (TFA) extracts versus biomass measured as dry weight (■) or as Coomassie protein (▲) during mixed culture batch growth on Lauryl Tryptose Broth.	138
Figure 3-10. Relative WCFA composition similarity (I_s from equation (3-36)) with respect to the terminal time point during batch mixed culture growth on Lauryl Tryptose Broth.	139
Figure 3-11. Relative proportion (logratio) of the monoenoic fatty acid 16:1 ω 7c with respect to 16:0 for DhA-35 grown at pH 6.0, 7.0 and 7.5 on either dehydroabietic acid (▲) or pyruvate (▼) as sole carbon sources.	142
Figure 3-12. The derived soluble resin acid concentration as a function of pH for un-inoculated medium (Section 3.3.1) containing 39.8 ± 1.9 μ g/mL dehydroabietic acid (■-DHA) and 18.8 ± 1.0 μ g/mL abietic acid (●-ABA).	144
Figure 3-13. A typical total fatty acid (TFA) biomass growth curve on resin acid with an acclimated enrichment mixed culture, in this case, at pH 7.5 for experiment A.	145
Figure 3-14. Maximum specific growth rates for enrichment cultures of abietane resin acid degraders as a function of pH from three separate experiments (A, B, C from top to bottom).	147
Figure 3-15. Comparison of maximum specific growth rates (Q) for mixed cultures enriched for abietane resin acid degraders at 5 different pH levels inoculated into media containing either sodium acetate (▲) or abietane resin acids (■) as the sole carbon sources.	148
Figure 3-16. A typical linear yield approximation ($Y_{TFA} = -\Delta[TFA]/\Delta[TRA]$) for biomass production, as total fatty acid (TFA), versus total resin acid (TRA) consumption during exponential (balanced) growth ($t_1 < t < t_2$ in equation (3-57)) for an acclimated mixed culture.	149
Figure 3-17. Average molar total fatty acid (TFA) or biomass yield from three replicate experiments (A, B, C) monitoring microbial growth for total resin acid (TRA) depletion (left graph) as a function of pH.	149
Figure 3-18. Initial (▼) versus residuum (▲) resin acid concentrations obtained for replicated mixed culture batch experiments as a function of pH.	151
Figure 3-19. Experiment A model substrate depletion curves for pH conditions 6, 7 and 8 (Top to Bottom).	154
Figure 3-20. A more detailed consideration of total fatty acid TFA yield during mixed culture exponential growth ($t_1 < t < t_2$ in Figure 3-13).	155
Figure 3-21. A second example of a nearly linear biomass or total fatty acid TFA yield with respect to total resin acid removal (■) during mixed culture exponential growth ($t_1 < t < t_2$ in Figure 3-13).	155
Figure 3-22. Peak metabolite concentrations observed during mixed culture batch growth experiment A.	158
Figure 3-23. Two pathways for the initial biodegradation of dehydroabietic acid.	158
Figure 3-24. Relative proportions (logratios) of the monoenoic fatty acid 18:1 ω 7c with respect to 16:0 for resin acid enrichment cultures grown up on abietane resin acids (■) or sodium acetate (▲) as a function of pH.	160
Figure 3-25. Logratio fatty acid compositions for Experiment B as a function of pH.	161
Figure 3-26. The first logcontrast canonical component (LCC-1) for Experiment B summarising 80.4 percent of the enrichment culture between-group chemotype variability as a function of pH.	162
Figure 3-27. The normalized eigen vector for the first canonical component for experiment B. ..	163

Figure 3-28. Dendrogram from the similarity matrix for the mean WCFA compositions describing the enrichment cultures in Experiment B as a function of pH.	164
Figure 3-29. The first and second logcontrast canonical components in Experiment C for enrichment cultures grown on resin acids (right) and sodium acetate (left) as a function of pH (as labelled).	165
Figure 3-30. Normalized eigen vectors for the first and second logcontrast canonical components.	166
Figure 3-31. Dendrogram from the similarity matrix for the mean WCFA compositions describing the enrichment cultures in Experiment C as a function of pH.	166
Figure 3-32. Simulation of biphasic batch growth on two substrates using the system of equations given in Table 3-10.	175
Figure 4-1. Schematic of an ideally mixed chemostat with liquid volume, V.	193
Figure 4-2. Model transient substrate concentrations during ten hydraulic turn over periods in a well mixed chemostat.	195
Figure 4-3. Hypothetical Langmuir type sorption/desorption (Γ) progression during a changing surface concentration (C_0) with time (Top Left).	200
Figure 4-4. Idealized schematic of the experimental bench scale moving bed bioreactor (MBBR).	206
Figure 4-5. Photograph of the actual bench scale MBBR.	207
Figure 4-6. A sessile drop of ethylene glycol on an optically smooth surface of the ANOX carrier plastic.	217
Figure 4-7. The digitized ethylene glycol drop shown in Figure 4-6.	217
Figure 4-8. Experimental data (■) for the lithium washout curves following a spike load at time zero for reactor A (Top) and reactor B (Bottom).	219
Figure 4-9. Statistics for the surrogate (O-methylpodocarpic acid) extraction recoveries for biofilm and aqueous samples from the two reactors as well as for the aqueous feed samples.	221
Figure 4-10. Residence time distribution data and the functional fit ($f_a(t)$ in equation (4-28) and Table 4-6) for the aqueous concentration of total resin acids (TRA) in Reactors A and B.	223
Figure 4-11. Residence time distribution data and the functional fit ($f_a(t)$ in equation (4-28) and Table 4-6) for the aqueous concentration of chloro-dehydroabiatic acid (Cl-DHA) in Reactors A and B.	223
Figure 4-12. Residence time distribution data and the functional fit ($f_b(t)$ in equation (4-28) and Table 4-6) for the biofilm loading of total resin acids (TRA) in Reactors A and B.	224
Figure 4-13. Residence time distribution data and the functional fit ($f_b(t)$ in equation (4-28) and Table 4-6) for the biofilm loading of chloro-dehydroabiatic acid (Cl-DHA) in Reactors A and B.	224
Figure 4-14. Estimated total resin acid recovery from reactors A and B by the comparison of mass loss from the system (ΔM_{τ}^s) to mass loss in the effluent (ΔM_{τ}^e) for sample times (τ) less than and equal to 12 hours.	227
Figure 4-15. Estimated chloro-dehydroabiatic acid recovery from reactors A and B by the comparison of mass loss from the system (ΔM_{τ}^s) to mass loss in the effluent (ΔM_{τ}^e) for sample times (τ) less than and equal to 12 hours.	227
Figure 4-16. Resin acids in the surface scum that accumulated by 2.7 hours ($t/\theta_H \approx 1$) after the spike load.	228
Figure 4-17. Dendrogram from the similarity matrix for the mean whole cell fatty acid (WCFA) compositions for the suspended and biofilm from reactors A and B, as well as the WCFA composition of the BKME feed.	231

Figure 4-18. Average bioreactor biomass levels before ($-10 < \eta = t/\theta_H < 0$) and after ($0 < \eta < 10$) a resin acid shock load.	232
Figure 4-19. Logcontrast canonical components (LCC) of the fatty acid spectra for suspended and biofilm extracts.	234
Figure 4-20. The calculated and sorted probabilities for the logratio radius distributions (Chapter 3; equation (4-25)) for fatty acid compositions from Reactor B plotted against the uniform order statistic.	234
Figure 4-21. The trajectory describing the population dynamics of the suspended biomass in reactor A.	239
Figure 4-22. Data smoothing and differentiation of the first weighted canonical component from logcontrast canonical component analysis (LCCA) of the suspended biomass samples from reactor B.	242
Figure 4-23. A comparison of the average state speed (equation (4-42)) estimated from the indicated number of observations (n) over the 96 hour period of observation.	243
Figure 4-24. Population dynamics expressed as state speed (equation (4-42)) from fatty acid logcontrast canonical component analysis.	244
Figure 4-25. The derived correspondence between the state speed (equation (4-42)) and the total resin acid (TRA) levels after the shock load.	245
Figure 4-26. Pooled reactor TOC measurements taken before, during and after a spike load transient of resin acids.	247
Figure 4-27. Comparison of the estimated (equation (4-44)) versus the predicted (equation (4-17) and Table 4-16) flux of total resin acids to the carrier biofilms in reactors A and B.	249
Figure 4-28. Predicted equilibrium Langmuir isotherms for biofilm sorption of total resin acids (TRA) based on the experimental parameter estimates for equation (4-17) listed in Table 4-16. ..	249
Figure 4-29. Simulated TRA fate data for the set of ordinary differential equations (4-17) and (4-48).	252
Figure 5-1. The three classes of periodic bioreactor operation (adapted from Pickett (1982)).	270
Figure 5-2. Kinetics of sorption of resin acids to a biofilm based on the results of Chapter 4.	273
Figure 5-3. Idealized schematic of the experimental bench scale moving bed bioreactor (MBBR).	277
Figure 5-4. Photograph of the bench scale MBBR.	278
Figure 5-5. Tracer feed selection (Top) and sampling (Bottom) during the experiment.	279
Figure 5-6. Lithium input (top) and the measured lithium effluent levels in reactor A (middle) and B (bottom) during the course of the experiment.	284
Figure 5-7. Average TOC levels in the BKME feed and the two bioreactors from 84 samples taken over the 21 day experiment.	286
Figure 5-8. Measured TOC levels over time for the BKME feed (■), reactor A (●) and reactor B (▲).	286
Figure 5-9. Progress of TOC removal for reactors A and B over time.	288
Figure 5-10. The residual errors between the models plotted in Figure 5-9 and the measured TOC removal efficiencies.	289
Figure 5-11. Biomass levels as total fatty acid (TFA).	292
Figure 5-12. Amounts of suspended and dissolved total resin acids (TRA) and total fatty acids (TFA) expressed as a percent of the total concentration.	294

Figure 5-13. Dendrogram relating the similarities of fatty acid spectra from whole, filter and filtrate samples drawn from reactor A (A), reactor B (B) and the BKME feed (F).	294
Figure 5-14. Dendrogram relating the similarities of fatty acid spectra from biofilm and suspended samples from reactor A (A) and reactor B (B) for the experiment reported in Chapter 4 (1) and the current investigation (2).	296
Figure 5-15. Dendrogram relating the similarities of fatty acid spectra from biofilm, suspended and effluent samples from reactor A (A) and reactor B (B) for the current investigation.	296
Figure 5-16 Discrimination between the suspended and effluent microbial communities based on their fatty acid spectra.	297
Figure 5-17. Logcontrast canonical components (LCC) of the fatty acid spectra for suspended and biofilm extracts.	298
Figure 5-18. Reactor A suspended biomass community state and population dynamics.	301
Figure 5-19. Reactor B suspended biomass community state and population dynamics.	301
Figure 5-20. Reactor A biofilm biomass community state and population dynamics.	302
Figure 5-21. Reactor B biofilm biomass community state and population dynamics.	302
Figure 5-22. Retention (Reactor A) and selective withdrawal (Reactor B) of total resin acids (TRA).	304
Figure 5-23. The time course of the estimated total resin acid (TRA) specific uptake rate (■) in response to the step changes of the influent loading.	306
Figure 5-24. The transient response to a shift-up in total resin acids (TRA) was found to differ significantly with pH.	308
Figure 5-25. Logcontrast canonical component analysis of fatty acid compositions for the suspended biomass in reactor A (Top) and reactor B (Bottom) over selected time periods.	310
Figure 5-26. Logcontrast canonical component analysis of fatty acid compositions for the biofilm biomass in reactor A (Top) and reactor B (Bottom) over selected time periods.	311
Figure 5-27. The history of total resin acid (TRA) sorption to the carrier biofilm for the acidic conditions (pH 6) of reactor A.	313
Figure 5-28. The history of total resin acid (TRA) sorption to the carrier biofilm for the alkaline conditions (pH 8) of reactor B.	313
Figure 5-29. Shake flask B1 data illustrating the results of batch growth on BKME spiked with resin acids at pH 8. Biomass was measured as total fatty acid (TFA).	316
Figure 5-30. A comparison of effluent TOC levels from the moving bed bioreactors and after 30 hours of batch growth.	318
Figure 5-31. Mixed-culture batch growth rates estimated for replicate shake flasks at pH 6 (Top) and pH 8 (Bottom).	319
Figure 5-32. The estimated substrate specific growth rates for replicate shake flasks at pH 6. ...	321
Figure 5-33. The estimated substrate specific growth rates for replicate shake flasks at pH 8. ...	322
Figure 5-34. A comparison of lag times for growth (TFA) and for the specific removal of TOC and TRA.	323

List of Tables

Table 2-1. Weights of phosphate salts for a 100 mM pH buffered medium.	44
Table 2-2. Parameter values for the Monod model with a threshold substrate concentration (equation (2-32)) used to model the substrate depletion curves presented in Figure 2-7.	56
Table 3-1. Generalized chemical structures for the typical groups of bacterial fatty acids.	96
Table 3-2. Nomenclature for the common groups of fatty acids.	96
Table 3-3. The general structure and types of the important phospholipids found in microbial membranes (adapted from Harwood (1984)).	99
Table 3-4. Similarity measures for compositions x_A and x_B containing D fatty acids (Bousfield et al. 1983; Eerola and Lehtonen 1988).	111
Table 3-5. Marker phospholipid fatty acids in various cell types (adapted from (Basile et al. 1995; Kates 1964; Vestal and White 1989)).	114
Table 3-6. Weights of phosphate salts for a 100 mM pH buffered medium.	124
Table 3-7. Cellular fatty acid composition of the resin acid-degrading isolate DhA-35 (Mohn et al. 1997).	140
Table 3-8. Least squares estimates of biomass growth kinetic parameters (equation (3-57)) as illustrated in Figure 3-13.	146
Table 3-9. Comparison of average total fatty acid (TFA) or biomass yield coefficients for abietane resin acid enrichment culture growth on resin acids or sodium acetate as sole carbon sources.	150
Table 3-10. Reduced Synthetic Chemostat Model for batch growth on multiple carbon sources.	173
Table 4-1. Contact angle and solid-vapour surface energies for high density polyethylene, ANOX biofilm carriers and Teflon.	216
Table 4-2. MBBR volume estimated from measurements of effluent flow.	219
Table 4-3. Average nutrient levels (phosphorus and nitrogen) for the two MBBR reactors and the BKME feed.	220
Table 4-4. Estimated bioreactor volumetric inflow rates based on the conservation of mass balance for phosphorous and nitrogen and flow continuity.	220
Table 4-5. Values used to determine the total biofilm area.	220
Table 4-6. Least squares parameter values for equation (4-28) describing the experimental aqueous, $f_a(t)$, and biofilm, $f_b(t)$, residence time distributions.	225
Table 4-7. Average extracted fatty acid liquid concentrations and surface loadings for suspended and biofilm samples.	230
Table 4-8. Estimated total TFA biomass levels (μ moles) for Reactors A and B.	231
Table 4-9. Calculated values for the Anderson-Darling test statistic for the total fatty acid compositional data sampled over 96 hours.	235
Table 4-10. Critical values for the Anderson-Darling test statistic for assessing logistic normality from the d-dimensional radius distribution (adapted from Aitchison (1986)).	235
Table 4-11. Results of logcontrast canonical component analysis on the time series of suspended biomass samples taken from Reactor A.	239

Table 4-12. Results of logcontrast canonical component analysis on the time series of suspended biomass samples taken from Reactor B.	239
Table 4-13. Results of logcontrast canonical component analysis on the time series of biofilm biomass samples taken from Reactor A.	240
Table 4-14. Results of logcontrast canonical component analysis on the time series of biofilm biomass samples taken from Reactor B.	240
Table 4-15. Results of logcontrast canonical component analysis on the time series of fatty acid compositions taken from the BKME feed.	240
Table 4-16. Least-squares estimates for the model parameters of equation (4-17).	248
Table 5-1. Chemical amounts used to mix 1 L of concentrated tracer stock solutions.	276
Table 5-2. MBBR volume estimated from measurements of effluent flow.	283
Table 5-3. Average nutrient levels (phosphorus and nitrogen) for the two MBBR reactors and the BKME feed.	283
Table 5-4. Estimated bioreactor volumetric inflow rates based on the conservation of mass balance for lithium, phosphorus and nitrogen and flow continuity.	285
Table 5-5. Average extracted fatty acid liquid concentrations and surface loadings for suspended and biofilm samples.	291
Table 5-6. Estimated TFA biomass levels (μ moles) for Reactors A and B.	292
Table 5-7. Values used to determine the total biofilm area.	292
Table 5-8. Results of logcontrast canonical component analysis on the time series of suspended biomass samples taken from Reactor A.	299
Table 5-9. Results of logcontrast canonical component analysis on the time series of suspended biomass samples taken from Reactor B.	299
Table 5-10. Results of logcontrast canonical component analysis on the time series of biofilm biomass samples taken from Reactor A.	300
Table 5-11. Results of logcontrast canonical component analysis on the time series of biofilm biomass samples taken from Reactor B.	300
Table 5-12. Best fit parameters for a logistic function (equation (5-13)) empirically describing biomass production as total fatty acids (TFA) during replicate (1 and 2) batch growth as a function of pH on BKME effluent spiked with resin acids.	317
Table 5-13. Best fit parameters for a logistic function (equation (5-13)) empirically describing acid soluble total organic carbon (TOC) depletion during replicate (1 and 2) batch growth on BKME effluent as a function of pH.	317
Table 5-14. Best fit parameters for a Boltzman function (equation (5-14)) empirically describing total resin acid (TRA) depletion during replicate (1 and 2) batch growth on BKME effluent as a function of pH.	317

Acknowledgement

A friend once commented, that a doctoral degree is a measure of one's tenacity more than anything else. My own experience seems to support that hypothesis. As my father likes to remind me, life is what happens when we make plans. My four year plan expanded into six years, and led me in exciting directions that could not have been anticipated. However, the ability to hold on tightly through those valleys of despair, that I imagine engulf all Ph.D. candidates at some point (or points), is very much influenced by the support of friends, colleagues, and family. These individuals have a tremendous power to make or break one's resolve. In this regard I feel that I have been very fortunate. Foremost, Rebecca has been my rock through my deepest valleys and my highest peaks.

For my older friends, the "boys" (David, Michael, Karen and Joey), plus Jeff and Megan, my prolonged tenure as a student has been a constant source of amusement. It is a great comfort to have friends who know my history and help me to see the humour in myself. Learning is my secret for eternal youth. So there is no doubt that my activities will continue to be a source of amusement. What occupies my head most of the day, is so foreign to the "boys". If we all thought the same way there would be nothing to share, and nothing to laugh about. I toast to continued laughter, and learning.

Years from now I think that 1992-93 will be seen as one of the golden years for Environmental Engineering at UBC. At least from my perspective, I enrolled into the program along with a number of well motivated and seasoned students who added an unexpected richness to my time at UBC. Ron, Don and Jean are wonderful friends with whom I often regained perspective from "reality checks". They are also the kind of people who bring people together. If not for them, I would never have been treated to the friendships of Farahad, Loralee, Serena, Claire, Zarina, Emi and Erin, whose companionship, I similarly treasure and hope to enjoy for years to come.

Another pearl of wisdom from my father, is that one cannot teach experience. Since I entered the program from a disparate background in engineering, I was lucky to have had the technical support of Susan Harper, Paula Parkinson and Jufang Zhou. Additional technical and logistical help was always kindly provided by the staff at the UBC Pulp and Paper Centre, especially, Tim Paterson, Peter Taylor, Rita Penco and Lisa Brandly. Lina Madilao was very helpful on the initial mass spectrometry. Ron Dolling and Scott Jackson were always ready to share their ideas and talents in electronics. Sally Finora helped to kick start the surface tension work. For me, these people were the *sine qua non* for my research activities and progress. They are unsung heroes that see so many graduate students through to a degree.

The assistance of Ann Wilson was vital to the pure culture experiments. Similarly, Stephanie Ebelt worked as a temporary laboratory assistant, and was extremely meticulous and helpful. Dr. Paul Bicho was instrumental in getting me started with the microbiology and chemistry surrounding resin acids. Dr. Bill Mohn and Vincent Martin have been two other great resources in the microbiology.

I found that a little encouragement can go a long way. Andy Chan and Paulo Lin were high school students, who I had the pleasure to mentor with a science project in consecutive years, respectively. Rather than busy them with a make-work project, they were involved with and contributed directly to the goals of my own research. Andy helped to trouble shoot the method of analysis for the lithium tracer work, and Paulo worked on measuring biomass by a number of conventional techniques for the mixed culture control experiments. Both Andy and Paulo used an aspect of their projects for the annual Greater Vancouver Science Fair. It was nice to learn that in the fair they both won prizes. I hope that they continue in Science.

I feel indebted to Dr. Aat Voskamp, my friend and supervisor, during my employment in the Netherlands. Aat's compassion for research and truth, recharged my fire that was quenched after some former disillusionment with academia. I am also grateful to my current supervisor, Dr. Eric Hall whose commitment and support of my project continued unabated even when my direction may have seemed a little obtuse. It has been a privilege to have had his encouragement to explore new ideas. New ideas come from experience with things that do not work. A healthy research environment permits one to learn from, and look for opportunity in mistakes or unexpected results. I am also grateful to my supervisory committee, and especially Dr. Eric Hall for their guidance in research and in preparing this dissertation. Dr. Hall's attention to detail, and command of the English language are two of his many qualities that I aspire to someday attain.

Research costs time and money. For my time, I have been fortunate to have been supported from a number of sources. In kind, I have received much assistance from Jeanne Taylor and Western Pulp Limited Partnership in Squamish BC. I am extremely grateful to NSERC, PAPRICAN, the NSERC/COFI Industrial Research Chair in Forest Products Waste Management and the Sustainable Forest Management Network, for sustaining my existence as a graduate student and for funding my laboratory overhead.

Dedication

I would like to dedicate this dissertation to my parents, Fred and June Werker. The nature of my worries pale in comparison to those during times that they have lived through. For this luxury of an education that they have valued and helped to provide, I am eternally grateful.

Chapter 1
Resin Acids and Toxicity Breakthrough in Pulp Mill Effluent Treatment

Summary

Resin acids are hydrophobic carboxylic acids that are released from wood during pulping. These hydrophobic contaminants have been related to events of aquatic toxicity breakthrough from biological treatment systems treating pulp mill wastewaters. They are also one of a number of problematic contaminants that impede the reuse of process waters. Thus, although resin acids need to be consistently removed from mill effluents, biological treatment has been found to be periodically inadequate. Since hydrogen ion concentration strongly influences the nature of resin acids in solution, pH was thought to be the principal parameter controlling the fate of these compounds during biological treatment. A set of five research objectives was defined for assessing the mechanisms of pH influence on the biological removal of resin acids. Four experimental investigations were undertaken to address the stated objectives, and, thereby, answer fundamental questions of practical importance for the biological treatment of pulp mill effluent.

Table of Contents

1.1 Introduction	2
<i>1.1.1 Pulp Mill Effluent and Toxicity Breakthrough</i>	<i>3</i>
<i>1.1.2 Wood, Resin Acids and Toxicity Breakthrough</i>	<i>6</i>
<i>1.1.3 Resin acids</i>	<i>9</i>
1.2 Dissertation Question, Objectives and Overview	12
<i>1.2.1 Dissertation Question and Objectives</i>	<i>12</i>
<i>1.2.2 Dissertation Overview</i>	<i>14</i>
1.3 References	17

1.1 Introduction

This dissertation documents a fundamental study of physicochemical and biological interactions that influence the fate of resin acids during secondary biological treatment. The purpose of this first chapter is three fold. First, a general introduction will be given to pulp mill effluent, in order to identify resin acids as deleterious contaminants in discharged effluent and in retained process waters. This discussion provides the motivation for this research project, namely, a better understanding of the limitations in resin acid biodegradation that could lead to optimized or novel contaminant removal strategies. After providing this background information, the dissertation question is stated along with the hypothesis that defined the experimentation that needed to be undertaken. Finally, an outline of the dissertation is presented.

While the focus of the dissertation is resin acid removal from pulp mill effluent, many of the issues, concepts and experimental results are applicable to biological wastewater treatment in general. For instance, resin acids, like many other aquatic toxicants, are hydrophobic. Frequently, hydrophobic contaminants that cause wastewater to be acutely lethal, represent just a small fraction of the overall wastewater organic content. In addition, pulp mill effluents, like other seweraged wastewaters, are inherently variable in quantity and quality. Most wastewater treatment plants rely on a microbiological unit process to remove dissolved and suspended organic contaminants. Transient or non-steady state influent conditions are a challenge to biological treatment systems. Thus the topic of this dissertation applies also to the more general issue of trace, hydrophobic organic contaminant biological removal, from complex wastewater under non-steady state conditions.

It should be noted that over the six years of this research project, the intended application of the results has changed. In 1993, resin acids and events of toxicity breakthrough were topics of recurring concern in the pulping industry. It was this concern that motivated the project. As a result of improved in-mill practices, events of discharged toxic effluent are becoming rare. However, although upstream improvements have been made at pulp mills, a parallel increased understanding of the fate of these contaminants in the downstream biological treatment process is

still lacking. My effort has been to improve that understanding. Thus, the contribution of this study should not be viewed in the light of a problem that has been mitigated, but rather, in terms of the potential utility of the ideas, methods and quantitative results towards better monitoring, modelling and design of biological wastewater treatment processes.

The following background discussion is organized into three sections. First, a brief overview is given of pulp mill effluent and the occurrence of toxicity breakthrough from secondary biological treatment systems. Toxicity breakthrough at pulp mills is frequently caused by the inadvertent release of resin acids. The observed variability in the release and removal of resin acids during pulping is then briefly discussed. Finally, chemical properties of resin acids and their role as useful or problematic chemical by-products, and as aquatic toxicants, are summarized.

1.1.1 Pulp Mill Effluent and Toxicity Breakthrough

Production of pulp and paper requires extensive use of energy, chemicals and water. The large volumes of process effluents (in the order of two million cubic meters per day) that are discharged by the pulping industries have the potential for environmental impact (Hebron et al. 1997). In the United States, the pulp industry represents the third largest fresh water user (Beckett et al. 1992). Canada ranks second in the world for wood pulp production and first for export of this commodity (Gaston 1993). For the province of British Columbia in 1995, domestic and export revenue of pulp and paper products accounted for 5.5 billion Canadian dollars of the provincial economy (Hebron et al. 1997).

The current pulp and paper industry direction is towards progressive systems closure, whereby process waters would be reused and the fresh water intake would only replace losses due to evaporation (Ramamurthy and Wearing 1998). This industry objective is a considerable technical and economic challenge. The treated water quality requirements for water reuse are more stringent than those imposed by current environmental regulations for effluent discharge. More than likely the industry will move away from common sewers towards separate water circuits with specialized treatment kidneys refreshing selected process streams. Specialized contaminant

removal systems are best devised from a fundamental understanding of contaminant fate. Thus, while the prime motivation of this work was the issue of aquatic toxicity in externally discharged mill effluent, in view of the industry's current agenda, the results may have more direct engineering application in the design of process water treatment kidneys. It should not be surprising that material that is harmful to the environment can also be problematic in pulp and paper processing.

Waste from the pulp and paper industry was the major industrially-related environmental concern for British Columbia and New Brunswick in 1987 (Gaston 1993) and continues to raise environmental concerns that yet unidentified or unregulated compounds may exert subtle but quite deleterious chronic effects (Colborn et al. 1997; Servos et al. 1996). Mill wastewater discharged to the environment carries inorganic and organic compounds in both dissolved and particulate form, giving rise to environmental problems associated with colour, turbidity, biochemical oxygen demand (BOD) and aquatic toxicity (Colodey and Wells 1992). Canadian Federal Pulp and Paper Effluent Regulations (PPER) controlling the discharge of BOD, total suspended solids (TSS) and acutely lethal effluent (ALE) came into full effect in 1996 (Hebron et al. 1997). In 1996 there were ten days of recorded ALE discharge by mills in British Columbia as compared to 3,935 days in 1990, out of a total possible 8,395 discharge days per year.

This improvement of the ALE discharge record is likely due to tighter in-process control and the almost universal use of secondary biological treatment. The federal regulations require pulp and paper mills to report operating conditions and effluent quality. Federal or provincial inspectors work to verify the compliance of all pulp and paper mills by on-site inspections, audits, electronic reporting, and environmental impact assessment. Mills can apply to the government for authorization to temporarily exceed the normal limits for discharge. Noncompliance is met with warnings and can eventually lead to legal action. In 1996, one British Columbia pulp mill was convicted and fined 100 thousand Canadian dollars for discharge of toxic effluent (Hebron et al. 1997). Thus, while events of ALE are becoming rare, the legal ramifications for any one single event are becoming more significant.

Aquatic toxicity is commonly assessed with bioassays on juvenile fish (McLeay 1987). Fish are most frequently used because of their commercial significance, their role in the food chain and their sensitivity (Walden and Howard 1981). The standard acutely toxic threshold level is defined by the lethal concentration for 50 percent of the population after 96 hours, or the 96 hour LC₅₀. Sublethal concentrations of toxicants can induce changes in fish arterial tension, plasma glucose, blood cell counts, liver glycogen and muscle glucose levels. Studies (Walden and Howard 1981) indicate that a threshold response level for the sublethal effects is approximately 5 to 10 percent of the 96 hour LC₅₀ level.

Exposure of fish to sublethal concentrations of pulp and paper mill effluents elicits a response suggesting interference to respiration. Chronic effects of mill effluent, such as reduced fecundity and other physical or behavioural maladies due to endocrine disruption, are of current concern not just for fish, but for organisms further up the food chain. Thus, closure of mill aqueous discharges would certainly be helpful by translating many external environmental concerns into internal technological issues. In any pulp mill or bleach plant, increasing water recycling will promote the build up of extractives, either dispersed in the process water or deposited onto fibres or equipment (Jonasson et al. 1997). In spite of the technological hurdles to be overcome in contending with the problems of removing extractives and other elements or compounds from recycled water, the approach of closure as a means of environmental protection is a sound goal for pulp mills and for industry as a whole.

So long as wastewater is discharged to the environment, the short and long term impacts on aquatic life must be considered. There are many factors affecting the survival of fish that are subject to contact with pulp and paper mill effluent (Brouzes 1976; Ng 1977). Although BOD is the classical parameter used to measure wastewater strength, the removal of BOD cannot be equated with removal of toxicity (Mueller and Walden 1976). Toxic organic contaminants typically represent a small fraction of the overall influent BOD. Resin acids are a significant portion of the toxicity in mill effluent (McLeay 1987). In an Ontario Ministry of the Environment report (Water Resources Branch 1992) summarising acute lethality data for Ontario's pulp and

paper sector effluents over the winter and spring of 1990, resin acids were cited as one of the primary causes of acute lethality in the samples taken. Resin acids continue to be associated with issues of toxicity in the discharge of pulp mill effluent (Baley, B. (1998). Personal Communication, Environment Canada; Wasylenchuk, E.J. (1998). Personal Communication, Alberta Environment Protection; Funke 1996).

1.1.2 Wood, Resin Acids and Toxicity Breakthrough

The four major components of wood are polysaccharides, lignin, extractives and ash-forming minerals (Fengel and Wegener 1984). The polysaccharides, cellulose and hemicellulose, make up the wood structure. Lignin is the glue that interpenetrates, binds and strengthens this structure. The extractives, representing a small part of wood, contribute to the properties of colour, odour, taste and resistance to decay (U.S. Department of Agriculture 1955). Extractives can be removed from wood by solvents such as water, alcohol, acetone, benzene and ether. The volatile extractive fraction, such as the terpenes, can be isolated by steam distillation. Fatty acids, resin acids, tannins and colouring matter are the major substances that are extractable by non-polar solvents. The water-soluble components extracted from wood include carbohydrates, proteins and inorganic salts. Tree species differ widely in the type and amount of extractives, which can range from 0 to 10 percent of the wood composition. Extractive distribution throughout wood is also heterogeneous (Wangaard 1981).

Resin acids form part of the extractive content of wood. A natural wood component, these compounds are primarily located in the resin canals and parenchyma cells of trees, but are also to be found in sapwood, parenchyma tissue, heartwood, needles and bark (McCubbin 1983). The wood resin content is reported to be approximately the same for both coniferous and deciduous trees (Brouzes 1976), ranging from 1.0 to 2.3 percent of the dry wood weight. Softwoods, or conifers (gymnosperms) represent about 80 percent of available forests in Canada, with jack pine, spruce, fir and hemlock being the most important species for the forest industry (McCubbin 1983). During the pulping process, whether kraft, sulphite or mechanical, these wood extracts are washed away from the pulp fibres and form part of the wastewater stream.

Awareness of the acute toxicity of resin acids dates from as early as 1931 (Brouzes 1976). In 1936, Hagman (Hemingway and Greaves 1973) showed that resin acid concentrations in wastewater exceeding 1 ppm were toxic to fish. In 1950, Van Horn, Anderson and Katz (Hemingway and Greaves 1973) found that sodium salts of resin acids were toxic to minnows at 1 ppm and to *Daphnia* at 3 ppm. Motivated by periodic instances of inadequate detoxification of kraft mill effluent in the late 1960s, Rogers (1973) deduced the main toxic components to be two resin acids, namely, dehydroabietic and isopimaric acid. Rogers also noted the apparent relationship between resin acid content of the wastewater and its toxicity. Therefore, resin acids must be prevented from being discharged to receiving waters.

Differences are to be found in the relative proportions of resin acids present in different types of wood. The softwoods produce high resin acid yields. In spruce and pine, 27 and 29 percent of the wood resins are resin acids, respectively. In hardwoods, a significantly smaller proportion of the wood resins are present as resin acids. For example, in birch and aspen only 0.30 and 0.75 percent of the wood resins are present as resin acid, respectively. Therefore, changes to the wood furnish feeding the pulp mill will cause fluctuations in the resin acid concentrations of the raw mill effluent.

Reduction in resin acid content of wood can be accomplished by pre-treatment of wood prior to pulping. Seasoning of the wood attenuates toxicity levels in the effluent (Brouzes 1976). Chip aging decreases resin acid levels by natural oxidation augmented by the action of bacteria or fungi (Leach and Thakore 1976). Resin levels in the effluent are a function of wood chip age and also time of year, since resin acid content in trees is seasonal. Aging or "seasoning" of felled trees to reduce resin content takes 12 months in log form and 2 months in chip form. The capital costs and human resources required to manage wood storage are appreciable. Seasoning also reduces pulp brightness and yield (Rocheleau et al. 1998). Thus, the practical extent of pre-treatment of wood by aging for resin acid removal may be restricted due to the additional costs and the potential for the reduction in pulp quality. In the absence of extensive pre-treatment, the task of resin acid removal must be consistently accomplished during wastewater treatment.

Perhaps the most comprehensive studies of resin acid toxicity and wastewater removal were performed during the 1970s under the auspices of the Canadian Forestry Service, Department of the Environment, Canadian Pollution Abatement Research (CPAR) program. Dr. John Leach, one of the principal investigators under the CPAR program, studied the biodegradation of wood extractives important to bleached kraft mill effluent (Leach et al. 1977). Degradation rates, in order of most to least quickly degradable, were dehydroabietic, pimaric, monochloro-dehydroabietic, and dichloro-dehydroabietic acid. Thus, naturally-occurring wood extractives were more readily biodegradable than their chlorinated analogues. Pilot scale fermentation studies (Leach et al. 1978) demonstrated that when biotreatment was adequate to reduce the concentrations of resin and unsaturated fatty acids to less than 1 ppm, the resultant effluent demonstrated no acute toxicity. Degradation of dehydroabietic acid and pimaric acid went to completion in 1 to 3 days.

Much of the research in the 1970's regarding biological detoxification was driven by a concern for the wide temporal variations in the outfall toxicity. While the major toxicants were shown to be readily oxidized, results from 5-day aerated lagoons at mills in British Columbia indicated failure to eliminate toxicity up to 20 percent of the time (Leach et al. 1978). The current trend for biological detoxification in Coastal British Columbia has been to use the UNOX activated sludge system. Where topography does not restrict land usage, aerated lagoons remain the most often used secondary treatment system in Canada (Gaston 1993).

Incidents of periodic ALE discharge due to elevated outfall resin acid concentrations continue to occur today (Baley, B. (1998). Personal Communication, Environment Canada; Wasylenchuk, E.J. (1998). Personal Communication, Alberta Environment Protection). The fact that incidents of toxicity breakthrough are periodic, would suggest that biological wastewater systems cope poorly with transient contaminant loads. While mills work to tighten process control and to close process water circuits, they would benefit from an improved fundamental understanding of the limitations of biological wastewater treatment systems for removing transient loads of specific contaminants. Since the extent of plant wastewater monitoring is usually limited, it is often

impossible to trace the causes of toxicity breakthrough at pulp mills after the fact. Surprisingly, there have been no literature reports of studies in which laboratory scale bioreactors were subjected to resin acid load fluctuations that were carefully monitored. The existing literature indicates that previous laboratory bioreactor research experiments were typically steady state investigations, in which research success was linked to high removal efficiency. Laboratory research with bioreactors would be more informative if efforts were directed towards challenging biological systems with non-steady influent conditions in order to explore and understand the inherent limitations. The laboratory is the ideal setting for measuring bioreactor response to well controlled stimuli. Monitoring bioreactor response to dynamic conditions was one of the experimental approaches used for the present investigation.

1.1.3 Resin acids

Resin acids are weak tricyclic monocarboxylic acids of limited solubility (Soltes and Zinkel 1989; Taylor et al. 1988). Resin acids commonly found in pulp mill effluent are either abietic-type (Figure 1-1) or pimaric-type (Figure 1-2). Abietic-type acids have an isopropyl side chain at

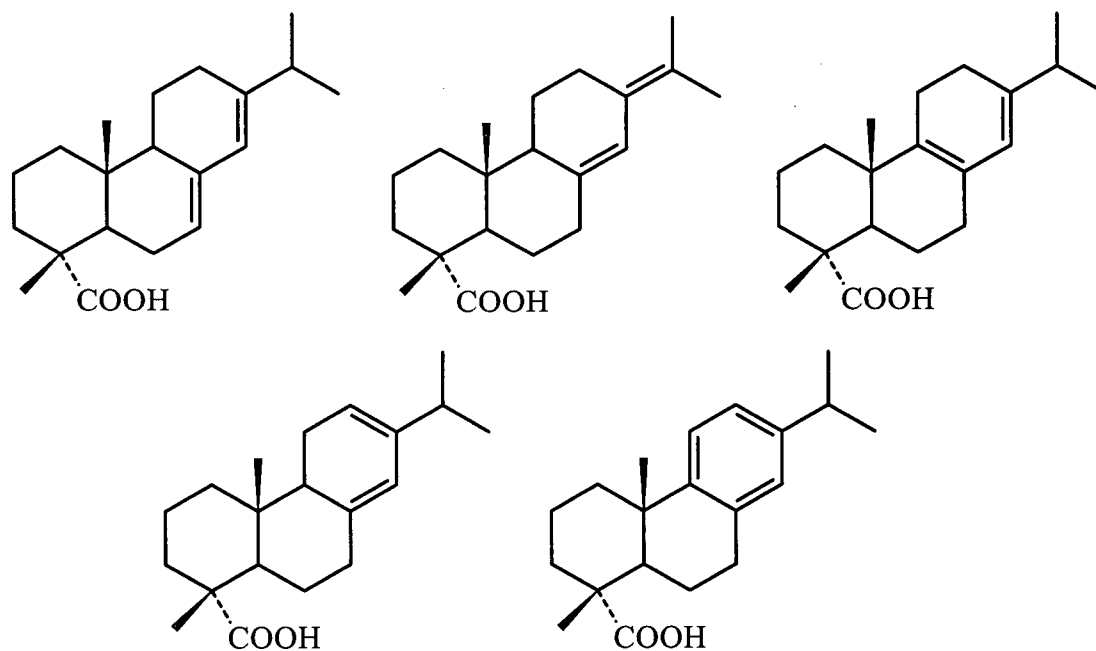


Figure 1-1. Common pine resin acids of the abietane skeletal class. Top row (left to right): Abietic, neoabietic and palustric acid. Bottom row (left to right): Levopimaric and dehydroabietic acid (Soltes and Zinkel 1989).

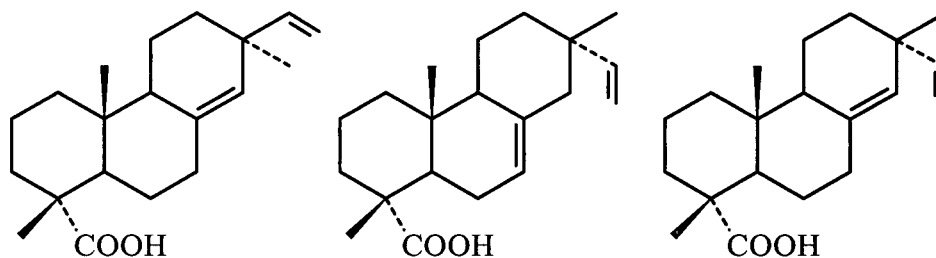


Figure 1-2. Common pine resin acids of the pimarane and isopimarane skeletal class. From left to right: Pimaric, isopimaric and sandaracopimaric acid (Soltes and Zinkel 1989).

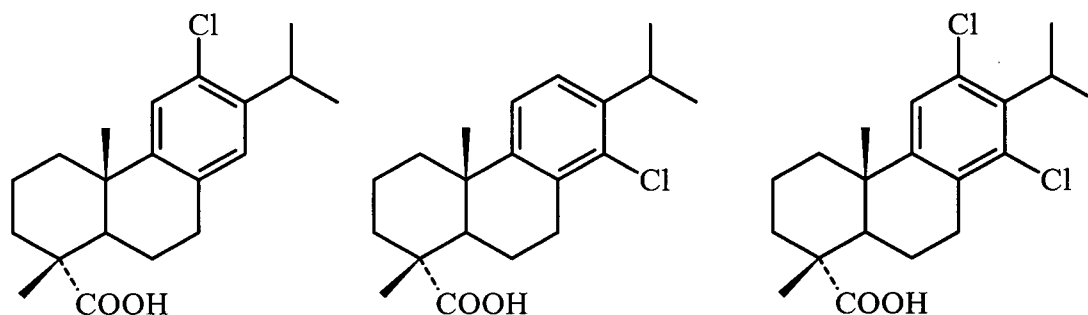


Figure 1-3. Chlorinated resin acid derivatives formed during pulp bleaching. From left to right: 12-Cl-dehydroabietic acid, 14-Cl-dehydroabietic acid, and 12,14-Cl₂-dehydroabietic acid.

position 13, while pimaric-type acids have methyl and vinyl substituents. Bleaching of pulp can result in chlorine substitution (Figure 1-3). Variations within each skeletal class arise due to the number and position of the double bonds. Dehydroabietic acid (DHA) exhibits an ionization constant (pKa) of 5.7 and a total solubility of 6.6 mg/L (Nyrén and Back 1958). The solubility of the unionized acid is 4.9 mg/L. DHA is the most soluble diterpene resin acid because it possesses the highest number of double bonds (Bruun 1952). Salts of the resin acids can readily be formed with sodium, calcium, zinc, magnesium and aluminium (Soltes and Zinkel 1989). Salts of resin acids, in contrast to the acids themselves, are orders of magnitude more soluble in water and exhibit amphiphilic properties that make them useful as soaps. The critical micelle concentration of potassium dehydroabietate is approximately $2.5\text{-}3.0 \times 10^{-2}$ molar (Corrin et al. 1946; Kolthoff and Stricks 1948).

One of the features of resin acids that make them interesting model compounds for research, is that they become less hydrophobic under alkaline conditions. Experiments examining the fate of

resin acids as a function of pH reveal general principles about the influence of contaminant hydrophobicity on biological removal.

Rosin soaps, which are refined saponified diterpene resin acids, find application in paper sizing (Strazdins 1989) and as emulsifiers for polymerization reactions (Davis 1989). Rosin is readily refined from tall oil, which comes initially from the soap skimmings off black liquor. The kraft pulping process acts to solubilize natural resinous material in trees by saponification. Therefore, resin acids in the effluent stream are initially in their resinate or soap form. The soaps can be converted back to their acids in the presence of free hydrogen ions. Carbon dioxide can precipitate resin acids from alkaline solutions (Soltes and Zinkel 1989). The pH changes following the combination of acidic or alkaline sewer lines will influence the dissolved resinate. If these soaps are converted back into acids, they may be precipitated, but they can also be held in solution by association with other soaps in solution (Nyrén and Back 1958; Soltes and Zinkel 1989) or with other dissolved organic matter such as lignin breakdown products (kraft lignin) (Kulovaara et al. 1987).

Resin acids may be a component of compounds referred to by the paper industry as “stickies” (Doshi and Dyer 1997) that form pitch deposits. During paper making, pitch deposits form on rolls, felts and fabrics. Their deposition can impede water removal, impact runnability and cause sheet defects. The reuse of pulping process water requires that “stickies” be effectively controlled. Thus resin acids are among the problematic compounds that must be contended with on the road of progressive systems closure.

As long as mills continue to discharge effluent into marine or riparian waters, environmental impact and toxicity will continue to be issues of investigation. More than seventy percent of the acute toxicity found in pulp mill effluent is attributable to the hydrophobic fraction (Ng et al. 1974). Within the hydrophobic fraction, resin acids are the primary toxicants, frequently related to incidents of toxicity breakthrough (Kovacs and O'Connor 1996; McLeay 1987; Taylor et al. 1988). Being natural wood extractives, resin acids are waste by-products endemic to the pulping process (Allen et al. 1993). They are of environmental concern primarily because they exhibit

acute toxicity (LC_{50}) towards aquatic life at concentrations in the order of 1 ppm (Taylor et al. 1988).

While aerobic secondary biological treatment can remove resin acids, periodic toxicity breakthrough continues to force mill shut downs (Kovacs and O'Connor 1996). Furthermore, even if sublethal concentrations at the outfall are achieved, these compounds can persist (Brownlee and Strachan 1977; Fox 1976) and bioaccumulate (Niimi and Lee 1992), posing a chronic threat to aquatic life (Oikari et al. 1988; Tana 1988). Local changes in environmental conditions can redistribute resin acids between aqueous, particulate and sedimentary phases (Volkman et al. 1993). A better understanding of the fate of resin acids in wastewater treatment systems should provide insight towards more reliable methods of removal, thereby reducing the risks of exposure for these, or similar contaminants in aquatic environments. Such advancement has been the underlying goal of this research project.

1.2 Dissertation Question, Objectives and Overview

1.2.1 Dissertation Question and Objectives

There is little doubt that hydrogen ion concentration is an important parameter in a biological treatment process. Most bacteria cannot proliferate at pH levels below 4.0 or above 9.5. Generally, the optimum pH for bacterial growth is between 6.5 and 7.5. The typical operating pH range for secondary treatment of pulp mill effluent is between 6.0 and 8.0. As will be discussed, a change in pH, over this same typical range for secondary biological treatment, significantly alters resin acid solubility and hydrophobicity. Therefore, the following dissertation question was posed.

What will be the dominant mechanism of pH influence on the biological removal of resin acids in kraft mill effluent?

The stated thesis question is based on the premise that:

change in pH, within the typical narrow operating range for secondary treatment of pulp mill effluent, will significantly influence the probability of resin acid biological removal.

The probability of contaminant removal in a bioreactor depends on the contaminant bioavailability, the microbial state, and the contaminant retention time. Thus, the hypothesized impact of pH on the likelihood of resin acid removal during secondary treatment, may be attributed to pH-dependent variations in resin acid bioavailability, fluctuations in metabolic activity or microbial community structure, and changes in the contaminant retention time. Therefore, an investigation was required to consider each of the following important factors. These will also be discussed later in more detail.

- i. Reduced contaminant aqueous solubility can serve to restrict the contaminant bioavailability. Resin acid solubility is a function of pH. While it is intuitively obvious that alkaline conditions, which increase resin acid solubility, are likely to enhance the extent of biological removal, the sensitivity of resin acid biodegradation to solubility has not been clearly quantified in the research literature.
- ii. Microbial communities in a bioreactor are shaped by reactor environmental conditions, such as pH. The influence of pH on community selection and on growth kinetics for microorganisms that can degrade resin acids, has not been established in the scientific literature. Hydrophobic compounds can also inhibit microbial activity. The possibility of pH-dependent changes in microbial inhibition, due to pH-dependent changes in resin acid hydrophobicity, has also not been previously studied. Further, studies of the time lags in microbial response to fluctuating resin acid loadings during continuous treatment, are lacking.
- iii. Contaminant retention time during secondary treatment can be influenced by the kinetics and the extent of contaminant sorption on biomass, which are a function of hydrophobicity. Resin acid hydrophobicity is a function of pH. The influence of pH on resin acid hydrophobicity and any associated change in resin acid sorption kinetics have not been

adequately quantified in the research literature.

Consequently, the following five research objectives were defined.

- A. To determine the influence of resin acid solubility on contaminant bioavailability.
- B. To determine the influence of pH on the microbial community structure and the uptake rate of resin acids.
- C. To determine the influence of resin acid hydrophobicity on microbial activity.
- D. To determine the influence of resin acid hydrophobicity on contaminant sorption to biomass and, consequently, retention time.
- E. To determine the influence of pH on the time lag in increased metabolic activity for resin acid biodegradation.

1.2.2 Dissertation Overview

In order to consider the stated objectives, it was recognized that pH must be the principal independent parameter for experiments designed to elucidate the importance of bioavailability, metabolic activity, microbial community structure, and adsorption kinetics in the biological removal of resin acids from pulp mill effluent. Little attention has been given to pH-sensitivity in the removal of resin acids. It will be seen that in this regard the scientific literature is also in apparent contradiction. A progression of two batch and two continuous flow microbiological investigations were undertaken in order to clearly assess the role of pH in resin acid biodegradation. Due to the specific aspects of each investigation, they have been organized chronologically into separate chapters as follows:

Chapter 2. Surfactancy and Solubility in the Biological Removal of Resin Acids

Batch growth experiments were performed to determine the extent to which resin acid solubility influences bioavailability during biological treatment (**Objective A**). In these

experiments, changes in adsorption kinetics were monitored using dynamic surface tension measurements. Deriving the adsorption kinetics from surface tension data required the development of a novel quasi-static approach to isotherm modelling. From the isotherm modelling, it was possible to quantify pH-induced changes in resin acid diffusivity. This measure of diffusivity provided a means to explain observed changes in resin acid bioavailability.

Chapter 3. Microbial Community Structure in the Kinetics of Resin Acid Removal

In a second series of batch growth experiments, it was necessary to consider the influence of microbial community structure on the hypothesized pH-dependent rate of resin acid removal (**Objective B**). Microbial communities were distinguished by comparing compositions of fatty acids extracted from culture samples. The ability to assess changes in community structure was a key contributor to the success of this investigation. Measurements of mixed culture growth kinetics are notoriously variable. Valuable insight was gained by using community structure as the basis of comparison to interpret the observed variability within and between experiments. Control experiments were performed to assist in the interpretation of the observed changes in the microbial fatty acid spectra.

Chapter 4. A Resin Acid Shock Load During Continuous Biological Treatment

Based on the results from the batch experimentation, the first continuous flow experiment was then undertaken. Two parallel, bench scale, single stage, completely mixed moving bed bioreactors, treating whole bleached kraft mill effluent, were operated and compared. One of the bioreactors was operated under constant acidic conditions (pH 6) while the other was run under constant alkaline conditions (pH 8). Resin acid adsorption onto the biomass and the possibility for resin acid-induced growth inhibition were investigated (**Objectives C and D**). Analytical techniques developed for comparing microbial communities and quantifying population dynamics from microbial fatty acid compositions were advanced and became principal tools that were applied for data interpretation.

Chapter 5. Transient Resin Acid Loading During Continuous Biological Treatment

Biological response to transient loads of resin acids was monitored in a second similar continuous flow experiment. It was of interest to know the extent to which the acclimation of a microbial community to a change in contaminant loading, was pH-dependent (**Objective E**). An acclimation period or lag time is a well known phenomenon for bacteria responding to changing environmental conditions. Since pulp mill effluents are known to have variable organic contents, the dynamic response of communities is of practical importance.

In this dissertation, background, concepts, theories, and methods are presented in the chapters in which they were first used. This format was chosen, in part, to help in the readability of a dissertation that has delved into a number of rather specialized areas of mathematics and science that were unique to each aspect of the investigation. Much of the mathematical detail is included because these developments were integral to the data analysis and interpretation. Such detail is important to those wishing to further test and pursue the ideas presented. The second objective of the thesis format was to preserve the development of ideas, since the earlier research strongly influenced the approach taken in later experiments. The scope of the research unfortunately resulted in an unexpectedly long treatise. To assist in the readability, each experimental chapter was written as a relatively self-contained extended publication. Experimental methods, results and ideas that become established in the earlier chapters form points of reference later in the thesis.

1.3 References

- Allen, S. L., Allen, L. H., and Flaherty, T. H. (1993). Defoaming in the pulp and paper industry. Defoaming, P. R. Garret, ed., Marcel Dekker, Inc., Surfactant Science Series, 151-175.
- Beckett, R., Wood, J. W., and Dixon, D. R. (1992). Size and chemical characterization of pulp and paper mill effluents by flow field fractionation and resin adsorption. *Environmental Technology*, 13, 1129-1140.
- Brouzes, R. J. P. (1976). Fish toxicity with specific reference to the pulp and paper industry. *EPS 3-WP-76-4*, Environment Canada.
- Brownlee, B., and Strachan, W. M. J. (1977). Distribution of some organic compounds in the receiving waters of a kraft pulp and paper mill. *Journal of the Fisheries Research Board of Canada*, 34, 830-837.
- Bruun, H. (1952). Properties of monolayers of rosin acids. *Acta Chemica Scandinavica*, 6, 494-501.
- Colborn, T., Dumanoski, D., and Myers, J. P. (1997). *Our Stolen Future*, Plume/Penguin.
- Colodey, A. G., and Wells, P. G. (1992). Effects of pulp and paper mill effluents on estuarine and marine ecosystems in Canada: a review. *Journal of Aquatic Ecosystem Health*, 1, 201-226.
- Corrin, M. L., Klevens, H. B., and Harkins, W. D. (1946). The determination of critical concentrations for the formation of soap micelles by the spectral behavior of pinacyanol chloride. *Journal of Chemical Physics*, 14(8), 480-486.
- Davis, C. B. (1989). Rosin soaps as polymerization emulsifiers. Navel Stores, D. F. Zinkel and J. Russell, eds., Pulp Chemicals Association, New York, 625-642.
- Doshi, M. R., and Dyer, J. M. (1997). Paper Recycling Challenge, Volume I, Stickies. , Doshi & Associates.
- Fengel, D. and Wegener, G. (1984). *Wood: Chemistry, Ultrastructure, Reactions*, Walter de Gruyter.
- Fox, M. E. (1976). Fate of selected organic compounds in the discharge of kraft paper mills into lake superior. Identification and analysis of organic pollutants in water, L. H. Keith, ed., Ann Arbor Science, 641-659.
- Funke, L. (1996). Order issued to pulp mill for exceeding effluent limits. *96-034*, Government of Alberta.
- Gaston, C. (1993). Pulp and paper industry compliance costs. *11-528E*, Statistics Canada.
- Hebron, K., Krahn, P., and Bannister, G. (1997). 1996 Annual compliance report for pulp and paper effluent regulations in British Columbia. *Regional Program Report 97-27*, Environment Canada.
- Hemingway, R. W., and Greaves, H. (1973). Biodegradation of resin acid sodium salts. *Tappi Journal*, 56(12), 189-192.
- Jonasson, R. G., Tosto, F., Holloway, L., Rawluk, M., Goulet, C., Fuhr, B., and Leary, G. Comparison of extractives in pulps from mechanical and chemical pulp mills: Composition and impact. *Spring Conference*, Whistler, British Columbia.
- Kolthoff, I. M., and Stricks, W. (1948). Solubilization of dimethylaminoazobenzene in solutions of detergents - I. The effect of temperature on the solubilization and upon the critical concentration. *Journal of Physical and Colloidal Chemistry*, 52, 915-941.
- Kovacs, T., and O'Connor, B. (1996). Insights for toxicity-free pulp and paper mill effluents. *MR 331*, Paprican.
- Kulovaara, M., Kronberg, L., and Pensar, G. (1987). Recoveries of some chlorophenolics and resin acids from humic water. *The Science of the Total Environment*, 62, 291-296.
- Leach, J. M., Mueller, J. C., and Walden, C. C. (1977). Biodegradability of toxic compounds in pulp mill effluents. *Transactions of the technical section CPPA*, 3(4), TR126-TR130.
- Leach, J. M., Mueller, J. C., and Walden, C. C. (1978). Biological detoxification of pulp mill effluents. *Process Biochemistry*, 13(1), 18-21.
- Leach, J. M., and Thakore, A. N. (1976). Toxic constituents in mechanical pulping effluents. *Tappi Journal*, 59(2), 129-132.

- McCubbin, N. (1983). The basic technology of the pulp and paper industry and its environmental protection practices. *EPS 6-EP-83-1*, Environment Canada.
- McLeay, D. (1987). Aquatic Toxicity of Pulp and Paper Mill Effluents: A Review. *EPS Report 4/PF/1*, Environment Canada.
- Mueller, J. C., and Walden, C. C. (1976). Detoxification of bleached kraft mill effluents. *Journal of the Water Pollution Control Federation*, 48(3), 502-510.
- Ng, K. S. (1977). Detoxification of bleached kraft mill effluents by foam separation, PhD, University of British Columbia, Vancouver.
- Ng, K. S., Mueller, J. C., and Walden, C. C. (1974). Study of foam separation as a means of detoxifying bleached kraft mill effluents, removing suspended solids and enhancing biotreatability. *CPAR Project Report 233-1*, Ottawa.
- Niimi, A. J., and Lee, H. B. (1992). Free and conjugated concentrations of nine resin acids in rainbow trout (*Oncorhynchus mykiss*) following waterborne exposure. *Environmental Toxicology and Chemistry*, 11, 1403-1407.
- Nyrén, V., and Back, E. (1958). The ionization constant, solubility product and solubility of abietic and dehydroabietic acid. *Acta Chemica Scandinavica*, 12(7), 1516-1520.
- Oikari, A., Lindström-Seppä, P., and Kukkonen, J. (1988). Subchronic metabolic effects and toxicity of a simulated pulp mill effluent on juvenile lake trout, *Salmo trutta m. lacustris*. *Ecotoxicology and Environmental Safety*, 16, 202-218.
- Ramamurthy, P., and Wearing, J. T. System closure: A Canadian perspective. *84th Annual Meeting, Technical Section of the CPPA*, Montreal, A215-A222.
- Rocheleau, M. J., Sithole, B. B., Allen, L. H., Iverson, S., Farrell, R., and Noel, Y. (1998). Fungal treatment of Aspen chips for wood resin reduction: A laboratory evaluation. *Journal of Pulp and Paper Science*, 24(2), 37-42.
- Rogers, I. H. (1973). Isolation and chemical identification of toxic components of kraft mill wastes. *Pulp & Paper Magazine of Canada*, 74(9), 303-308.
- Servos, M. R., Munkittrick, K. R., Carey, J. H., and van der Kraak, G. J. (1996). Environmental fate and effects of pulp and paper mill effluents. , St. Lucie Press.
- Soltes, E. J., and Zinkel, D. F. (1989). Chemistry of rosin. Navel Stores, D. F. Zinkel and J. Russel, eds., Pulp Chemicals Association, 261-345.
- Strazdins, E. (1989). Paper sizes and sizing. Navel Stores, D. F. Zinkel and J. Russell, eds., Pulp Chemicals Association, New York, 575-624.
- Tana, J. J. (1988). Sublethal effects of chlorinated phenols and resin acids on rainbow trout (*Salmo Gairdneri*). *Water Science and Technology*, 20(2), 77-85.
- Taylor, B. R., Yeager, K. L., Abernethy, S. G., and Westlake, G. F. (1988). *Resin Acids*, Queen's Printer for Ontario.
- U.S. Department of Agriculture. (1955). *Wood Handbook*, U.S. Government Printing Office.
- Volkman, J. K., Holdsworth, D. G., and Richardson, D. E. (1993). Determination of resin acids by gas chromatography and high-performance liquid chromatography in paper mill effluent, river waters and sediments from the upper Derwent Estuary, Tasmania. *Journal of Chromatography*, 643, 209-219.
- Walden, C. C., and Howard, T. E. (1981). Toxicity of pulp and paper mill effluents - a review. *Pulp & Paper Canada*, 82(4), T143-T148.
- Wangaard, F. F. (1981). *Wood: Its Structure and Properties*. Clark C. Heritage Memorial Series on Wood, Pennsylvania State University.
- Water Resources Branch. (1992). Acute lethality data for Ontario's pulp and paper sector effluents covering the period from January 1990 to June 1990. ISBN 0-7729-8926-5, Ontario Ministry of the Environment.

Chapter 2

Surfactancy and Solubility in the Biological Removal of Resin Acids

Summary

The objective of this investigation was to determine the influence of resin acid solubility on the contaminant bioavailability (Objective A - Chapter 1). The solubility and surfactancy of resin acids are strongly influenced by pH within the range typically used for biological treatment. Changes in solubility and surfactancy for hydrophobic contaminants can be sensed by dynamic surface tension measurements. Relative changes in the contaminant diffusivity can also be derived from dynamic surface tension measurements. Such changes impact on the bioavailability of resin acids during batch treatment. Under acidic conditions, resin acids form associations with other dissolved organic matter contained in pulp mill effluent, while under alkaline conditions, they behave as relatively soluble surfactants. A residuum of a contaminant at the end of a batch treatment represents an important limitation for biological removal. The resin acid residuum, or threshold concentration, was found to increase under acidic growth conditions. This residuum increase corresponded to an inferred reduction in resin acid bioavailability.

Table of Contents

2.1 Introduction	20
<i>2.1.1 The Fate of Resin Acids</i>	<i>21</i>
<i>2.1.2 Dynamic Surface Tension Measurement</i>	<i>25</i>
<i>2.1.3 Modelling Adsorption by Dynamic Surface Tension Measurements</i>	<i>28</i>
<i>2.1.4 Quasi-static Langmuir Adsorption</i>	<i>33</i>
<i>2.1.5 Modelling Kinetics of Batch Growth with Threshold Concentrations</i>	<i>39</i>
2.2 Experimental Methods and Materials	43
<i>2.2.1 Mixed Culture Batch Growth</i>	<i>43</i>
<i>2.2.2 Dynamic Surface Tension Measurement</i>	<i>48</i>
<i>2.2.3 Nonlinear Regression Analysis</i>	<i>52</i>
2.3 Results	55
<i>2.3.1 Mixed Culture Batch Growth</i>	<i>55</i>
<i>2.3.2 Dynamic Surface Tension Measurements</i>	<i>58</i>
2.4 Discussion	66
2.5 Conclusions	73
2.6 References	75

2.1 Introduction

The purpose of this study was to determine if pH could alter the bioavailability of resin acids (Objective A - Chapter 1). It was felt that a fundamental study into the fate of resin acids was justifiable if this effect could be shown to be valid from a very limited preliminary investigation. Hence, batch growth experiments were performed as a function of pH, using a representative medium of kraft mill effluent. The experimental objective was to monitor the influence of pH on biological removal in relation to the resin acid chemical properties of surfactancy and solubility. Of particular interest was the issue of bioavailability. Surfactancy was considered by isotherm modelling of resin acid adsorption kinetics determined from dynamic surface tension measurements. Solubility was estimated according to the Standard Methods (Clesceri et al. 1989) definition for suspended solids.

Necessary background literature and theory used for the interpretation of the experimental results are presented in the introduction. First, a review of the relevant literature is presented, indicating that adsorptive properties of resin acids are linked to pH and that adsorption is an important aspect of the contaminant fate. This review also describes how previous literature data on the influence of pH on resin acid degradation are incomplete and in apparent contradiction. The ability of surface tension measurements to follow resin acid adsorption is then explained with references to a relevant body of literature. Since surface tension is an indirect measurement of adsorption, the relationships that couple the kinetics of surface tension change to the kinetics of adsorption are described. Thermodynamic justification is then given for the Quasi-static Langmuir Adsorption model that was developed to interpret the experimental data. Along with the physico-chemical properties of resin acids, quantifying microbiological activity was an important part of this study. Therefore, some important issues surrounding the modelling of batch growth kinetics are also covered in the introduction. Due to their toxicity, some organic pollutants may be of concern even at trace levels. Thus, the contaminant concentration at which microbial growth can no longer be sustained is an important parameter to be derived from batch growth experiments. This concentration level is often referred to as a threshold for microbial

growth. The required modification to the Monod model to include such a threshold resin acid concentration is also presented in the introduction.

2.1.1 The Fate of Resin Acids

The hydrophobicity of resin acids makes them surface active compounds that will tend to gravitate towards interfaces in aqueous environments. This property is manifested in conventional secondary biological treatment systems by resin acid accumulation in surface foams. Resin acid concentrations in surface foams above biobasins can attain levels that are orders of magnitude higher than those in the underlying liquid (Chandrasekaran et al. 1978; Fein et al. 1992; Servizi et al. 1975; Zitko and Carson 1971). Collapse of the foam layer is a probable cause for some of the treatment detoxification failures that have been reported in the past (Leach et al. 1977; Servizi et al. 1975).

In a more recent example of contaminant concentration in surface foam (Kruzynski 1995), foam sampled from the discharge pond at a British Columbia pulp mill exhibited an LC₅₀ of 0.75 percent for rainbow trout (van Agglin 1995). The resin acid concentration in the collapsed foam was in the order of 5 ppm, which was a thousand fold greater than that in the underlying wastewater (Bicho 1995). Foam sampled downstream of this pulp mill on the Fraser river also contained elevated levels of resin acids (Duncan 1993). While only resin acids were assayed for these samples, they would not have been the only contaminant in the foam causing toxicity. In spite of its toxic contents, foam from pulp mill lagoons has been reduced to that of an aesthetic problem that is a (public) nuisance, especially if it is blown to the surrounding community (Palermo and Holzer 1992). Although foam is problematic, the tendency for resin acids to adsorb onto the gas bubbles that generate foams has been of some benefit for their selective oxidation by ozone treatment (Roy-Arcand and Archibald 1996).

Hence, resin acids are readily collected at gas/liquid interfaces of bubbles and foams. Adsorption at gas/liquid interfaces can be sensed by measuring surface tension reduction (Burcik 1950; Burcik 1953). The rate and extent of surface tension lowering should be related to the

contaminant bulk liquid concentration. Therefore, if resin acid adsorption is an important controlling aspect of the contaminant fate during secondary treatment, then it should be possible to characterize this transport mechanism from surface tension measurements.

The fate of these chemicals in wastewater treatment systems mirrors their behaviour in the open environment. One can consider the partitioning of a pollutant from an effluent stream into biological (lipid), solid (suspended or settled particulate matter), aqueous, or gaseous environmental compartments. Partitioning is dependent on the physico-chemical properties of a pollutant. The fate of pulp mill effluent contaminants in treatment systems (Mackay and Southwood 1992; Mackay et al. 1996) and in the environment (Kolset and Heiberg 1988) has been modelled using fugacity concepts. Fugacity measures the thermodynamic driving force for partitioning into air, soil, water, biota, suspended solids and sediment. From such considerations, predictions are made about where most of the solute will partition and where the highest concentrations should occur (Mackay and Paterson 1981). Each compartment can have associated rate constants for physical or biological degradation. A chemical will persist in the environment, or in a treatment system, if it is partitioned away from the more rapid degradative processes.

In biotreatment systems, resin acids could exhibit limited bioavailability because they are likely to be transported into surface foams (Leach et al. 1977) as surfactants. The bioavailability of resin acids can also be limited as a result of close association with particulate organic matter due to their hydrophobicity (Alexander 1994). For instance, Brownlee (1977) estimated that the half-life of dehydroabietic acid discharged into Lake Superior was 21 years in the sediment, as compared to 0.12 years in the water column. It is unclear if the prolonged half-life in the sediment was due to reduced bioavailability or due to persistence under anaerobic conditions.

It has been stated that the major dispersal mechanism for resin acids at the final effluent outfall is by adsorption onto, or sedimentation with, suspended particulates (Carlberg and Stuthridge 1996). Therefore, an important part of understanding the fate of trace hydrophobic compounds in treatment systems or the environment, is in the determination of the governing thermodynamic

potentials driving contaminant partitioning behaviour. Interfaces, either gas/liquid or solid/liquid, between environmental compartments, are regions where significant amounts of hydrophobic chemicals collect and concentrate (Hoff et al. 1993; Valsaraj 1994). In this respect, surface tension measurements should also be able to indicate the extent to which the surface phase should be considered as a distinct compartment for fugacity type fate models.

The literature suggests that pH is the dominant parameter determining whether resin acids partition as a soluble surfactant or as an insoluble particulate-bound contaminant. Ng (1974a) found that an alkaline pH resulted in more consistent effluent detoxification by foam fractionation for the same duration of treatment. Hence under alkaline conditions, resin acids appear to be better surfactants. The dispersive power of resin acids has also been shown to be much greater under alkaline conditions (Drobosyuk et al. 1982). Conversely, the extraction recovery of resin acids from slightly acidic humic water was found to decrease over time (Kulovaara et al. 1987). This reduction in extraction recovery indicates that under acidic conditions resin acids become bound to other organic matter in solution. Reduced extraction recovery over time was probably due to "aging" interactions with dissolved organic matter (Hassett and Anderson 1979; Kukkonen 1992). Aging refers to the observed reduction of the bioavailability of a sequestered compound over time (Alexander 1994). Hence, the fate of resin acids changes in the transition from acidic to alkaline environments.

This observed change with pH can readily be understood if one considers that the pKa value for resin acids predicts a significant change in the dissociated fraction in the pH range from 6 to 8 (Nyrén and Back 1958). The direct effect of an increased dissociated fraction of resin acid in solution with increased pH is a parallel increase in total solubility. For instance, in the pH range from 6 to 8, the total solubility of abietic acid increases from a few micrograms per millilitre to over 100 µg/mL (Nyrén and Back 1958).

The pH range from 6 to 8 needs to be further emphasized because it also defines the normal operating range of a mill secondary biological treatment process. Therefore, within the normal operating pH conditions of pulp mill secondary biological treatment systems, resin acids, which

need to be metabolized to well below 1 $\mu\text{g}/\text{mL}$, undergo a dramatic change in nature.

There have been only two studies that explicitly considered the effect of pH on biodegradation of resin acids. One investigation utilized batch growth conditions (Hemingway and Greaves 1973) and the other, twenty years later, yielded conflicting results with a bench scale continuous system (Liu et al. 1993). Hemingway and Greaves (1973) monitored pH during batch growth on resin acids (40 $\mu\text{g}/\text{mL}$) in a Dubos buffered medium containing 10% bisulfite liquor. With slightly acidic starting conditions, it was found that no significant resin acid removal occurred until the pH exceeded 7.3. Unfortunately, little can be derived from this aspect of their investigation. Without pH control, it is unclear if the significance of pH 7.3 had more to do with diauxic growth on other organic acids in the bisulfite liquor, than a supposed limiting pH for biological removal.

Liu et al. (1993) operated bench scale, continuous flow stirred-tank reactors with a 3 day hydraulic retention time (HRT) on chemi-thermomechanical pulping (CTMP) effluent containing 45 $\mu\text{g}/\text{mL}$ resin acid. In contradiction to Hemingway and Greaves' conclusion regarding the effect of pH, this study demonstrated that under steady state conditions, a consistent 98% removal of influent resin acid could be achieved in the pH range from 5 to 8. Unfortunately, the possibility of changes in biodegradation kinetics with pH was not considered, perhaps due to the relatively long HRT used for this part of the study. Had a shorter HRT been used it might have been possible to observe different steady state effluent concentrations which could have been related to pH-dependent removal kinetics. Additionally, while the observed 98% removal efficiency is significant, it should be noted that, depending on pH (McLeay et al. 1979a; McLeay et al. 1979b; Zanella 1983), the residual 2% resin acid in the effluent could still be considered acutely toxic to aquatic life. If this observed 2% residual persisted due to a limitation in bioavailability, it would likely not be reduced by increasing the HRT further. In other words, it remains unclear if the observed contaminant residual concentration was an inherent limit for removal or a function of the removal kinetics during continuous treatment. Therefore, a shortcoming exists when contaminant removal efficiencies are used to indicate efficacy in the reduction of toxicants in wastewater, when the goal is detoxification.

There are five major conclusions to be drawn from this discussion of the literature. Surfactancy and solubility are important determinants of the fate of resin acids in kraft pulp mill effluents. Dissociation of resin acids as a function of pH strongly influences their surfactancy and solubility. The significance of surfactancy and solubility with respect to biological removal of these contaminants has not been well established in the literature. The two published investigations that explicitly examined the effect of pH on biodegradation are in apparent contradiction. Finally, the properties of resin acids significantly change within the typical pH range used for secondary treatment of pulp mill effluents.

In order to clarify the results and the apparent contradictions between the published findings about the influence of pH on resin acid biodegradation kinetics, batch growth experiments were conducted with abietic and dehydroabietic acid in a well buffered matrix of treated and filtered bleached kraft mill effluent. Growth curves were generated at constant pH in the range from 6 to 8 in order to determine whether changes in total resin acid solubility could either alter the uptake kinetics or affect bioavailability. Resin acids that are mobile enough to become adsorbed at a gas/liquid interface, may be mobile enough to diffuse into a microbe to be metabolized. Hence, availability for adsorption was considered to be a potential indicator for relative differences in bioavailability. Kinetics of adsorption were calculated from dynamic surface tension measurements.

2.1.2 Dynamic Surface Tension Measurement

Since adsorption of solute at the gas/liquid interface will act to lower the liquid surface tension, measurements of surface tension as a function of solute concentration and pH would provide information about differences in the mobility of resin acids in solution. Dynamic surface tension measurements can indicate both the extent and the rate of surfactant adsorption at a gas/liquid interface (Burcik 1950; Burcik 1953).

There are a few reports in the literature of the use of surface tension measurement in conjunction with pulp mill effluent or its constituents. Brasch (1974) measured the equilibrium surface tension

of black liquor, producing a surface tension versus concentration relationship similar to those of common surfactants. Berk et al. (1979) reported a strong correlation between *Daphnia magna* median survival time and surface tension, for foam fractionated spent sulphite liquor. In that study, foam fractionation reduced toxicity by 40%, by concentrating the toxicants in 20% of the original volume. Keirstead (1978) reported the influence of fungal treatment on the surface tension of a 1% (w/v) sodium lignosulfonate solution. Werker et al. (1996) followed surface tension changes during the hydroxylation of dehydroabietic acid by the fungus *Mortierella isabellina*. These studies indicate that surface tension measurements of wastewater can be used as a method to quickly screen for the presence of hydrophobic contaminants. In pulp mill effluent, where toxicity is, to a large extent, associated with such hydrophobic compounds as resin acids, surface tension measurement offers promise as a rapid monitoring tool in effluent treatment quality control.

The kinetics of surfactant adsorption at the gas/liquid interface can be monitored by dynamic surface tension measurements. This approach depends on the surface aging phenomenon (Adamson 1982) whereby a fresh gas/liquid interface is experimentally generated and the progress of surface tension lowering due to solute adsorption is monitored with time. By the application of a suitable thermodynamic model, the reduction in surface tension can be related to solute loading at the interface (Kohler 1993). Measurement of dynamic surface tension is especially relevant for dynamic engineering processes in which equilibrium conditions may not be attained. For example, dynamic surface tension measurements have been used to explain the lack of correlation between equilibrium surface tensions (by contact angle measurements) and the flotation recovery of mining ores (Finch and Smith 1972). This fundamental information has engineering application in modelling of the kinetics of adsorption for the purpose of industrial process design (Bing et al. 1988; Clarke and Wilson 1983). Dynamic surface tension measurement has also been used to study the effects of surfactant adsorption on oxygen transfer in aerobic biological treatment systems (Masutani and Stenstrom 1991).

A number of experimental techniques that cover a range of adsorption time scales have been

devised to assess the kinetics of surface aging by indirectly monitoring gas/liquid surface tension changes in time. Whether one considers surface aging over tens of milliseconds by the oscillating jet method (Thomas and Potter 1975), over tens of seconds by the maximum bubble pressure method (Mysels 1990), or over minutes by the pendant drop or drop volume method (Adamson 1982), the theory of capillarity (Adamson 1982) is the important theoretical starting point.

The theory of capillarity centres on Laplace's equation relating the radii of curvature (R_1 and R_2) across an interface (Figure 2-1) to the differential pressure (Δp) and surface tension (σ_t) of a gas/liquid interface aged for the time period t (Adamson 1982):

$$\Delta p = \sigma_t \left(\frac{1}{R_1} + \frac{1}{R_2} \right) \quad (2-1)$$

Measuring surface tension lowering provides an indirect indication of the progress of surfactant adsorption at a gas/liquid interface with time. However, it is usually of interest to estimate the actual progression of the contaminant surface loading. Since the contaminant surface loading cannot be measured directly, it is necessary to apply a theoretical model in order to translate the surface tension σ_t for an interface aged over the time, t , to a corresponding surface loading, Γ_t . Contaminant surface loading is expressed in units of moles per unit area.

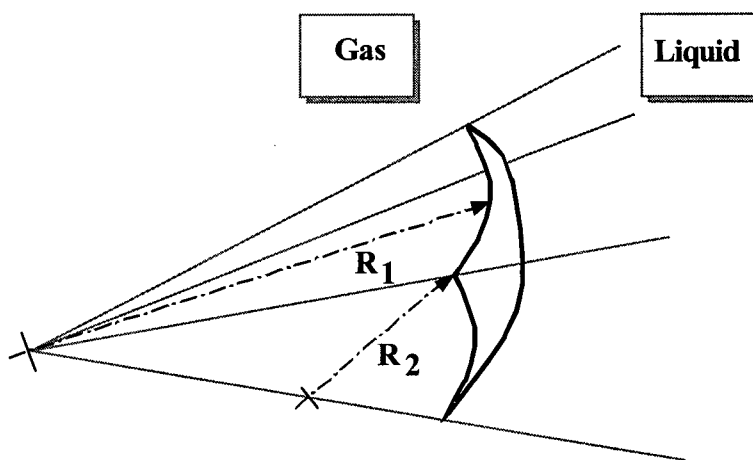


Figure 2-1. A small (elemental) section of an arbitrarily curved gas/liquid interface. In general it is necessary to use two radii of curvature to describe the curved surface. The two radii would be equal if the section was an element of a sphere. There will be a pressure difference Δp across the surface which will be balanced by the interfacial surface tension, σ , according to the equation of Young and Laplace (Adamson 1982).

2.1.3 Modelling Adsorption by Dynamic Surface Tension Measurements

Much of the theory surrounding dynamic surface tension measurement seems to be directed towards deriving the solute diffusivity. Estimating changes in resin acid diffusivity was felt to be important for the present investigation. A change in diffusivity with pH would indicate a relative change in mobility which could be related to differences in bioavailability. In contrast to the current investigation, the motivation for previous theoretical research on modelling dynamic surface tension measurements arose due to the relationship between solute diffusivity and foaming (Burcik 1950). The transport of surfactant from the bulk liquid solution to a perturbed or non-equilibrium gas/liquid interface represents an important destabilising effect for the thin films that make up foams (Bendure 1975). In the case of foam stability, the rate of surfactant adsorption to the film surface needs to be relatively low (Davies and Rideal 1963b).

The problem of relating solute diffusivity to adsorption at a gas/liquid interface was solved originally by Ward and Tordai (1946). Their derivation required the definition of a *near surface*, being the bulk liquid layer directly adjacent to the interface. By assuming that the kinetics of attainment of adsorption equilibrium between the near surface and the interface were instantaneous, they asserted that the process of adsorption was diffusion-limited by solute transport from bulk solution to the near surface. Mathematically, the problem then became analogous to the temperature as a function of the distance from a surface of a semi-infinite solid with surface temperature varying in time. Under this construct, surface loading, Γ_t , as a function of time, t , was modelled to be:

$$\Gamma_t = 2c_b \sqrt{\frac{Dt}{\pi}} - 2\sqrt{\frac{D}{\pi}} \int_0^t c_s(t-\tau) d[\sqrt{\tau}] \quad (2-2)$$

where c_b is the liquid solute concentration, D the diffusion coefficient and c_s the *near surface* concentration as a function of time. Note that while the liquid concentrations (c_b and c_s) are expressed in moles per unit volume, the surface loading (Γ_t) is given in moles per unit area. If the Ward and Tordai model (equation (2-2)) is restricted to just the initial short time interval of adsorption, it can be simplified to:

$$\Gamma_t = 2c_b \sqrt{\frac{Dt}{\pi}} \quad (2-3)$$

Thus Ward and Tordai predicted a linear dependence of the initial adsorption rate on the square root of time. Since the surface loading (Γ_t) could not be measured directly, a model relating surface loading to surface tension was required in order to test the experimental validity of equation (2-3) and to estimate a surfactant diffusivity (D).

The theory of diffusion-controlled adsorption kinetics for systems obeying Langmuir's adsorption isotherm was developed by Hansen (1960). By adopting a specific adsorption isotherm relationship, the measured quantity of surface tension (σ) could be used to determine the model parameter of diffusivity (D). Hansen made short and long term time approximations of the Ward and Tordai model and arrived at the following equation based on Gibbs adsorption theorem:

$$\sigma_t - \sigma_e = -\Gamma_L RT \ln \left(1 - \frac{\Gamma_L}{c_b \sqrt{\pi Dt}} \right) \quad (2-4)$$

for small times and:

$$\sigma_t - \sigma_e = \frac{\Gamma_L^2 RT}{c_b \sqrt{\pi Dt}} \quad (2-5)$$

for long times. In these equations, σ_t is the surface tension as a function of time, σ_e is the equilibrium surface tension, Γ_L is the limiting surface loading, R is the universal gas constant and T is the temperature. Hansen concluded that a diffusion-controlled adsorption mechanism was not a good representation of the initial dependence of surface tension aging with time. Bendure (1971) also noted that diffusion-limited adsorption modelling did not fit the measured data over all time scales. Joos and Rillaerts (1981) incorporated convection into the Ward and Tordai model to improve the estimation of solute diffusivity from dynamic surface tension measurements. However, if convection is indeed significant, one would expect that the near surface would maintain essentially the bulk liquid concentration thereby contradicting the underlying premise of the original Ward and Tordai theory. Without a near surface deficit of solute, no diffusion barrier

would exist for the adsorption process. In any event, the necessity to define short and long time scales (equations (2-4) and (2-5)), whose delineation would be a function of bulk solute concentration, severely limits the practical application of the Ward and Tordai representation.

With reference to traditional continuum mechanics mass transport modelling (Incropera and de Witt 1981), there is more practical gain in relating dynamic surface tension measurements to a relationship describing the flux of solute to the gas/liquid interface while ascribing some probability for the adsorption of any impinging solute molecule:

$$\frac{d\Gamma}{dt} = \Phi J = \Phi B f(c_b) \quad (2-6)$$

where Γ is the solute loading at the interface, J is the flux of solute to the interface and Φ is a sticking coefficient (Ertl 1983) specifying the probability that a particle striking the surface becomes adsorbed. The flux is a function of solute mobility, B , times some function of the bulk solute concentration, c_b . The solute mobility will be a constant characteristic of the solute for the particular conditions of the solvent. The sticking probability is conceivably related to both the degree of coverage (Ertl 1983) and also to the spreading pressure. Spreading pressure (Π) is the surface analogue to pressure in a closed container. It represents a depression in the solvent surface tension (σ_o) due to solute surface loading (Γ). The adsorbed solute monolayer behaves similarly to a two dimensional gas. In its simplest form, the equation of state for the adsorbed phase is an analogue to the ideal gas law:

$$\Pi = \sigma_o - \sigma = \Gamma RT \quad (2-7)$$

Thus, for the sticking probability, the degree of coverage (Γ) relates to the chances of finding an empty site and the spreading pressure (Π) to the surface forces that must be overcome in squeezing yet another molecule into the surface monolayer.

There are two possible models that could describe the flux of solute to the interface. Flux of solute to the interface could be thought of as being a passive process that is dependent on random occurrences from Brownian motion. Flux in this case would be directly related to bulk solute

concentration. The higher the solute concentration, the greater the chances of solute collisions with the interface would be. Conversely, based on a thermodynamic model, adsorption could be seen to be driven by solute chemical potential differences between the bulk solution and the surface (Ruthven 1984). In this case, the flux would be dependent on the natural logarithm of bulk solute concentration. The question is, which, if either, of these two models provides the best representation.

Modelling single-stage removal of a surfactant from a water column by bubble fractionation (solvent sublation), Clarke and Wilson (1983) assumed, on the basis of intuitive justification, that the kinetics of adsorption are governed by an equation of form:

$$\frac{d\Gamma}{dt} = \left(1 - \frac{\Gamma}{\Gamma_e}\right) B\Gamma_e \quad (2-8)$$

where Γ_e is the equilibrium surface loading of a Langmuir isotherm. The rate of mass transfer to the interface is proportional to the difference between the actual surface loading and the equilibrium surface loading. Equating equation (2-8) to equation (2-6), the sticking coefficient is given by the expression in parenthesis and the function of bulk concentration is contained within Γ_e , the equilibrium surface loading. No experimental results have been found in the literature that confirm the validity of equation (2-8).

Hua and Rosen (1988) have shown (Figure 2-2) that the process of surface aging for a constant surfactant concentration can be generalized empirically by a sigmoid on a logarithmic time scale:

$$\sigma_t = \sigma_m + \frac{\sigma_o - \sigma_m}{1 + (t/t^*)^n} \quad (2-9)$$

where the surface tension σ_t , falls with time from the level of the freshly generated interface (σ_o) to a so-called meso-equilibrium surface tension, σ_m , for the aged surface. Meso-equilibrium is differentiated from the equilibrium surface tension because over much longer time scales, surfactant conformational changes at the interface can act to lower the surface tension even further. For the present investigation, *meso-equilibrium* was considered as the operational

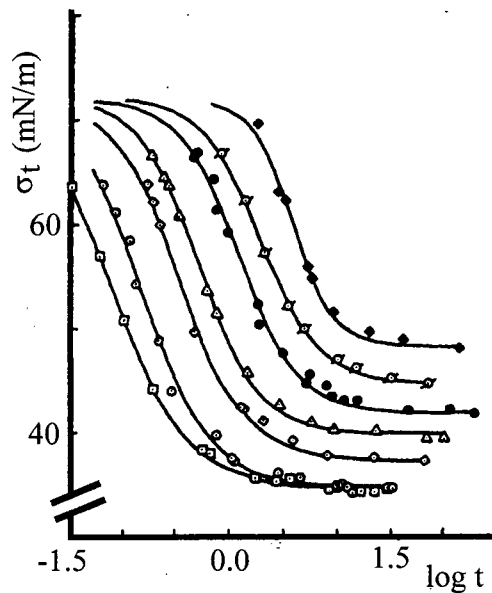


Figure 2-2. Sample data from Hua and Rosen (1988) illustrating the effect of surfactant concentration (c) on dynamic surface tension for N-dodecyl-N-methylglycine at pH 9.0 and 25 °C. The data show surface tension lowering (σ_t) in terms of surface age or $\log(t)$ for a family of surfactant concentrations. The log-surfactant concentrations, $\log(c)$, in water were equal to: -2.992 (\square), -3.224 (\circ), -3.410 (\diamond), -3.525 (Δ), -3.701 (\bullet), -3.826 (\emptyset), and -4.108 (\blacklozenge). Solid lines were calculated by Hua and Rosen using best fit parameters for equation (2-9). Note the change in the time lag before the onset of the log-linear decrease in the surface tension.

definition for equilibrium.

The Hua and Rosen (1988) empirical curve parameters $\{\sigma_m, n, t^*\}$ are functions of ionic strength, temperature and solute bulk liquid concentration (Figure 2-2). Systematic changes in surfactant concentration, with all other things held constant, produces a family of similar curves, each of which is described by equation (2-9). The duration of the initial plateau, or the time before significant surface tension lowering, is referred to as an induction period. In a subsequent publication (Gao and Rosen 1995), the induction period, which is defined by the parameters $\{n, t^*\}$, was shown to be related to solute diffusivity as defined by the Ward and Tordai model (Ward and Tordai 1946) for diffusion-controlled adsorption.

Upon reviewing the literature, it became apparent that modelling of adsorption kinetics (Clarke and Wilson 1983) requires a “time implicit” mathematical description (equation (2-8)). Time implicit refers to the fact that surface age is not explicitly considered in determining the flux of surfactant to the interface. Each increment in surface loading depends on the current state of the interface. In contrast, experimental theorists appear, since the work of Ward and Tordai, to be

locked onto a time explicit description of adsorption at a gas/liquid interface. A time explicit description of adsorption, such as equation (2-4) or equation (2-9), means that the surface age must be known explicitly before the increment in surface loading can be calculated. It is probably for this reason that, other than providing qualitative insight, theoretical developments in dynamic surface tension measurements seem to have had limited engineering application. That the parameters, $\{\sigma_m, n, t^*\}$, were found to be systematic functions of solute concentration (Hua and Rosen 1988) means that, in principle, it should be possible to similarly obtain an expression describing the family of iso-time dynamic surface tension curves relating the dependence of surfactant concentration on a particular surface age. Cast in this form, it will be shown that such an expression would help to justify or improve upon the model relationships assumed by Clarke and Wilson (1983). It was found that, for the purpose of the present investigation, such a time implicit approach became the only means with which to obtain useful information from dynamic surface tension measurements. The method applied was to idealize the adsorption process as a locus of quasi-static equilibrium states (Callen 1985).

2.1.4 Quasi-static Langmuir Adsorption

Real adsorption processes involve considerations of rate, making them a temporal succession of non-equilibrium states leading to some terminal equilibrium. In contrast, a quasi-static process is defined in terms of a dense, ordered succession of equilibrium states. A quasi-static adsorption process would not involve consideration of rate or time *per se* although it may be possible to contrive a temporal relationship to the quasi-static process.

The quasi-static process can be understood from a conceptual example. Consider a closed system containing a freshly formed gas/liquid interface in an aqueous solution with a surfactant solute. Conceptually the surface aging process is seen to move from its initial state, A, through a locus of points $\{B, C, D, \dots\}$ in thermodynamic configuration space by the successive relaxation of some constraint. With the relaxation of the constraint, more solute adsorbs at the interface. Each state given by the locus of points defines equilibrium conditions of adsorbed solute. In the initial relaxation of the constraint, the system is permitted to proceed from A to B but no further. The

system *disappears* from A and subsequently *appears* at B after passing through non-representable non-equilibrium states. Relaxing the constraint further, the system proceeds to C, and so forth. At each point a greater level of solute is adsorbed at the interface. The quasi-static locus of states can be approximated by a real process in a closed system only if the entropy is monotonically increasing along the quasi-static locus of points (Callen 1985). The correspondence between each state on the locus of points to experimentally-measured steps of increasing surface age provides the temporal relationship of the real process to the quasi-static one.

Theoretical justification for modelling adsorption as a quasi-static process can be found in the thermodynamic relations for non-equilibrium surfaces presented by Kohler (1993). This justification starts with the definition of Gibbs free energy of adsorption (ΔG^a):

$$\Delta G^a = G^e - G^r \quad (2-10)$$

where G^e is the actual free energy at equilibrium and G^r is a hypothetical reference free energy if adsorption did not take place. For simplicity, but with no loss of generality, the system being considered for this discussion is restricted to two chemical components. Component 1 is the solvent and component 2 the solute surfactant. The location of the (*dividing*) surface is defined by the plane where the “surface excess” of the solvent (component 1) is zero.

The term surface excess comes as a result of the need to mathematically define a surface plane between two phases that in reality do not change sharply from one to the other (Adamson 1982). If one considers the interface between two bulk phases (gas and liquid), the mass balance for any chemical component across the interface will include a term for the mass located in the phase transition region. The surface excess per unit area refers to the amount of any component in this transition region. Since it is convenient to suppose that the two bulk phases are uniform up to some arbitrary dividing plane, the location of this plane must be clearly defined. With the definition for the dividing surface given above, surface loading (Γ) refers unambiguously to the solute surface excess (component 2). In addition, any references to chemical potential (μ) are also made with respect to the solute.

For an ideal dilute solution, where the bulk liquid phase is large with respect to the surface phase, the surface tension of the reference state can be approximated by the solvent surface tension and the chemical potential within the bulk solution will be negligibly affected by adsorption. Hence, the above mentioned Gibbs reference state (G^r) is approximated by the free energy of the system when no solute is adsorbed at the interface. Under these conditions the Gibbs free energy of adsorption simplifies to:

$$\Delta G^a = (\sigma - \sigma_0)A = -\Pi A \quad (2-11)$$

where σ is the surface tension, σ_0 is the surface tension for zero solute surface excess, A is the surface area and Π is the surface pressure (equation (2-7)).

From equation (2-11), the *specific* Gibbs free energy of adsorption is ΔG^a normalized by the surface area (A):

$$\Delta g_A^a = \sigma - \sigma_0 = -\Pi \quad (2-12)$$

Since surface pressure (Π) relates to surface loading or *surface excess* (Equation (2-7)), Gibbs free energy is minimized by the exchange of solute from solution to the surface phase. Equation (2-12) can be combined with Gibbs adsorption equation at constant temperature:

$$d\sigma = -\Gamma d\mu \quad (2-13)$$

and this combination yields:

$$\Delta g_A^a = (\sigma - \sigma_0) = \int_{\sigma_0}^{\sigma} d\tilde{\sigma} = - \int_0^{\mu^b} \tilde{\Gamma} d\tilde{\mu} \quad (2-14)$$

where the tilde is used to specify integration variables and μ^b is the chemical potential for the solute in the bulk solution which is approximately constant. Integrating equation (2-14) by parts expresses the Gibbs free energy change occurring when the solute amount Γ is exchanged between the bulk liquid phase (with constant chemical potential μ^b) and the surface phase:

$$\Delta g_A^a = \int_{\sigma_0}^{\sigma_e} d\sigma = \int_0^{\Gamma_e} (\tilde{\mu} - \mu^b) \cdot d\tilde{\Gamma} \quad (2-15)$$

Again the tilde is used to specify integration variables. At the beginning of the exchange process of solute from solution to the surface, surface loading (Γ) is zero. Ultimately the surface phase reaches equilibrium with the bulk liquid phase which, at constant pressure, is defined by:

$$\tilde{\mu}(T, \Gamma_e) = \mu^b(T, c_b) \quad (2-16)$$

Although the adsorption process passes through non-equilibrium states, from equation (2-15) the chemical potentials of the surface can still be identified with equilibrium potentials of the form:

$$\tilde{\mu} = \tilde{\mu}(T, \Gamma) \quad (2-17)$$

A surface phase cannot exist without the existence of two neighbouring extended bulk phases, namely, gas and liquid. Hence, the intensive surface state thermodynamic variables depend not only on T and Γ but also in general on the bulk solute concentration. If equation (2-17) represents an equilibrium potential then a quasi-static equilibrium condition can be defined by:

$$\tilde{\mu}'(T, \Gamma_t) = \mu^b(T, c_b) \quad (2-18)$$

where Γ_t is the surface loading at a surface age of t . With reference to the locus of points describing the quasi-static adsorption process, at constant temperature and pressure, the corresponding states in thermodynamic configuration space are defined by the sequence of surface loadings $\{\Gamma_A, \Gamma_B, \Gamma_C, \Gamma_D, \dots\}$. To be valid, the states must be along a path of decreasing Gibbs free energy of adsorption, thereby moving the system along the route towards a minimum Gibbs free energy. According to the quasi-static equilibrium condition of equation (2-18), there exists an isotherm type relationship of the form:

$$\Gamma_t = \Gamma_t(T, c_b) \quad (2-19)$$

describing the surface loading for a surface age at a given temperature and bulk solute concentration. The experimental validity of a *quasi-static* equilibrium condition is demonstrated,

for instance, by the ability of *dynamic* surface tension measurements to determine critical micelle concentrations (Brown et al. 1952).

Resin acids have been shown to adsorb to biosolids according to the Langmuir isotherm (Liu et al. 1996a). The Langmuir isotherm describes adsorption to identical independent sites and, in keeping with the notation of equation (2-19), is given by:

$$\theta_t = \frac{\Gamma_t}{\Gamma_L} = \frac{c_b}{c_b + K_t} \quad (2-20)$$

The limiting surface loading (Γ_L) is a constant, dependent on steric and charge interactions that influence the packing of the solute at the interface. For instance, a monolayer of protonated resin acids will collapse (buckle) at a surface coverage of 42.0 and 40.4 Å per molecule for abietic and dehydroabietic acid respectively (Bruun 1952b). The difference between the two abietanes is due to the higher polarity of dehydroabietic acid because of its extra double bond. Therefore, Γ_L is a physical constant for the family of isotherms described by equation (2-20). The limiting surface loading will, however, be a function of the condition of the aqueous matrix. In the case of resin acids, ionization, with increased pH, influences the molecular configuration at the interface which in turn affects the degree of molecular surface coverage and interaction (Bruun 1952a). The presence of inorganic salts or the formation of molecular complexes also influences solute interactions in the monolayer (Davies and Rideal 1963a).

The parameter K_t measures the standard state parameters of the surfactant (Lucassen-Reynders and van den Tempel 1964):

$$K_t = K_t^r \exp\left(\frac{\Delta h^{ad}}{RT}\right) \quad (2-21)$$

where Δh^{ad} is the enthalpy of adsorption (Kohler 1993) and K_t^r is an isotherm constant. With the quasi-static equilibrium condition of equation (2-18) written in terms of the partial molar adsorption enthalpy and entropy:

$$\Delta\mu^{ad} = \Delta h^{ad} - T\Delta s^{ad} = 0 \quad (2-22)$$

the adsorption entropy can be written in terms of the Langmuir parameters:

$$\Delta s^{ad} = R \ln \left(\frac{c_b}{K_t} \frac{1-\theta_t}{\theta_t} \right) \quad (2-23)$$

Therefore, K_t has entropic meaning and the standard adsorption entropy increases if K_t decreases. For the family of isotherms describing the quasi-static adsorption along a locus of points in thermodynamic configuration space, K_t is the relaxation constraint, where by definition:

$$K_A \geq K_B \geq K_C \geq \dots \quad (2-24)$$

must be true.

Combining Gibbs' adsorption equation (2-13) for an ideally dilute solution with the quasi-static Langmuir isotherm of equation (2-20) provides the link between surface loading and the measured quantity of surface tension:

$$\sigma_t = \sigma_0 - RT\Gamma_L \ln \left(1 + \frac{c_b}{K_t} \right) \quad (2-25)$$

Therefore, from isothermal dynamic surface tension data that can be modelled by a Langmuir isotherm, it should be possible to relate the surface tension at particular surface age (t) to a corresponding bulk surfactant concentration. In defining this relationship, one should be able to estimate the limiting surface loading which is independent of surface age. The kinetics of adsorption are related to this quasi-static adsorption model, by the manner in which the parameter K_t decreases with surface age. For the data to be considered thermodynamically admissible, K_t must be continuously decreasing with surface age.

2.1.5 Modelling Kinetics of Batch Growth with Threshold Concentrations

In batch growth experiments, beyond answering the basic question of biodegradability of a target contaminant, one is often interested in describing the data in terms of the parameters specified by the equation originally used for enzymology by Michaelis-Menton and for microbial growth by Monod (Bailey and Ollis 1986; Panikov 1995):

$$q = \frac{QS}{k_s + S} \quad (2-26)$$

where, q is the specific growth rate, S is the limiting substrate concentration, Q is the maximum specific growth rate when $S \gg k_s$, and k_s is the limiting nutrient concentration at which the specific growth rate is half its maximum value. These two constants can be derived from the period of exponential or balanced growth during batch cultivation. The constants are typically used for model predictions in the design of biological treatment systems (Liu et al. 1996b).

Balanced microbial growth can be expressed by,

$$\frac{dX}{dt} = qX = \frac{QSX}{k_s + S} \quad (2-27)$$

and growth proceeds with a parallel substrate depletion,

$$\frac{dS}{dt} = -\frac{QSX}{Y(k_s + S)} \quad (2-28)$$

where, X is the concentration of biomass and Y is the biomass yield coefficient. If the biomass yield coefficient is assumed to be constant, equation (2-28) can be integrated to give the non-linear Monod equation (Simkins and Alexander 1984) describing substrate concentration as a function of time:

$$k_s \ln\left(\frac{S}{S_0}\right) = (S_0 + X_0/Y + k_s) \ln\left(\frac{X_0/Y + S_0 - S}{X_0/Y}\right) - (S_0 + X_0/Y)Q \cdot t \quad (2-29)$$

where X_0 and S_0 are the initial biomass and substrate concentrations respectively.

The attraction of equation (2-29) is that, given experimental data for X_0 and $S(t)$, estimates of Y , Q , and k_s can be obtained from non-linear least squares curve fitting of just the substrate depletion curve or, with S_0 and $X(t)$, just the biomass production curve (Dang et al. 1989; Robinson and Tiedje 1983; Simkins and Alexander 1985; Templeton and Grady (1988)). However, because the parameters Q and k_s have similar sensitivity functions, their identifiability is susceptible to measurement noise. The sensitivity functions express the influence, of a small perturbation in the model parameters being estimated, on the state variables of the system. The state variables in this case are biomass and substrate concentrations.

Both measurement noise and sampling frequency influence the accuracy of the estimates. Simulation studies have shown that the correct parameters cannot generally be obtained from stochastic data (Holmberg 1982). The objective function to be minimized in modelling a data set will vary only slightly over wide ranges of parameter values, all giving a good fit. Therefore, rate constants obtained from just the substrate depletion curve must be viewed with some degree of scepticism. Linearisation techniques are possible (Levenspiel 1984), but these introduce statistical bias that may influence the experimentally-determined parameters (Berthouex and Brown 1994; Robinson 1985). However, the linearized equations are useful for obtaining initial guesses required for non-linear parameter estimation methods (Panikov 1995; Robinson 1985).

The Monod model suffers from systematic errors at modestly small values of S (Panikov 1995). Monod kinetics predict the complete removal of a contaminant with the depletion rate becoming first order (Simkins and Alexander 1984) when S becomes much less than k_s . However, complete removal may not be achievable and this is important if the residuum remains acutely toxic or if the contaminant tends to bioconcentrate or worse, is biomagnified (Muir and Servos 1996).

Therefore, in a study of toxicity removal kinetics from wastewater, threshold levels for removal need to be addressed. The threshold contaminant concentration is defined by the level at which microbial growth on that contaminant can no longer be supported. Typical threshold concentrations for contaminants in aerobic systems have been reported in the 0.1 to 1.0 mg/L concentration range (Kobayashi and Rittmann 1982).

One probable cause for the limitation in the biological removal of hydrophobic contaminants is substrate availability (Providenti et al. 1993; Sikkema et al. 1995). Mass transfer from the particulate phase to the aqueous phase can be rate limiting. For example, the delivery rate of polycyclic aromatic hydrocarbons to competent bacteria, rather than the kinetics of oxidation, has been shown to be a limiting step (Stuck and Alexander 1987; Volkering et al. 1992; Volkering et al. 1995). Optimising environmental parameters, such as temperature or pH, which alter the physico-chemical properties of targeted wastewater contaminants so as to increase their bioavailability, should be a primary engineering design strategy. With reference to resin acid solubility, the tolerance range for biotreatment pH control may need to be tighter than the limits currently defined by the discharge regulations. The general opinion is that microbial uptake of cyclic hydrocarbons is a passive process (Sikkema et al. 1995). With reference to dynamic surface tension measurements, dissolution and passive transport of a contaminant to a microbe is akin to dissolution and adsorption at a gas/liquid interface. Thus, surface activity could, in principle, provide an indirect indication of bioavailability.

The other aspect of limitation for biological removal is related to microbial energetics. A respiration threshold exists when the carbon requirements for cell maintenance fall below the diffusion rate of the chemical to the cell surface (Alexander 1994). This threshold can be lowered by the presence of alternate carbon sources. A threshold substrate concentration, S^* , below which growth is impossible, is therefore, a biologically justified modification of Monod's equation (Panikov 1995):

$$q = Q \frac{S - S^*}{K_s + S} \quad (2-30)$$

For the purpose of this investigation, the operational definition made for the threshold S^* is a residuum at the cessation of observable growth. For an assumed constant yield, the rate of change in substrate concentration can again be derived based on the modified Monod equation (2-30). However, for a numerical solution method, it is best to first normalize the equations. The non-dimensional variables and parameters that were chosen are as follows:

$$x = \frac{X}{X_0}, \quad s = \frac{S}{S_0}, \quad s^* = \frac{S^*}{S_0}, \quad \kappa = \frac{k_S}{S_0}, \quad \eta = Qt, \quad \Psi = \frac{S_0}{X_0} Y \quad (2-31)$$

Similar to equation (2-28), the non-dimensional Monod rate of substrate depletion with a threshold concentration and a constant yield is equal to:

$$g(\eta) = \frac{ds}{d\eta} = \frac{s - s^*}{\kappa + s} \left(s - \left(1 + \frac{1}{\Psi} \right) \right) \quad (2-32)$$

There are two approaches to solving equation (2-32). The first approach entails analytical integration giving an implicit function similar to equation (2-29) which can be solved by numerical iteration. The second approach is to solve equation (2-32) directly by numerical integration. Since both methods are numerical and integration algorithms are easy to program and have more general usage, the latter approach was chosen.

2.2 Experimental Methods and Materials

2.2.1 Mixed Culture Batch Growth

Medium and Batch Culture Preparation

For these experiments, both microbiological inoculum and treated effluent were kindly supplied by Western Pulp Limited Partnership in Squamish, British Columbia. In Squamish, Western Pulp Limited Partnership has a coastal bleached kraft mill. At the time samples were obtained, the mill was pulping a fir:cedar:hemlock furnish and bleaching with 75% chlorine dioxide substitution at a 700 ADt/day production rate. Whole mill effluent undergoes secondary biological treatment by a high rate UNOX process that, at the time, was operating with an 8 hour HRT. Further references made to Squamish effluent refer to biologically (secondary) treated and filtered (Whatman 40) whole bleached kraft mill effluent (BKME).

Abietane resin acid was recrystallized from commercial rosin (Hercules Pamite 79) following the method of Halbrook (1966). A 30:70 mixture of abietic (ABA) and dehydroabietic (DHA) acid was obtained. A concentrated solution of resin acid was prepared by reflux boiling 2.5 grams abietane resin acid stock, in 25 mL of HPLC grade methanol (MeOH).

Parallel shake flask cultures were maintained at three buffered pH conditions. All glassware was thoroughly washed and fired at 475°C to remove any trace organic residue prior to use. Medium was prepared by adding a 1½ mL aliquot of concentrated resin acid to 1.5 L of heated (60°C) Squamish effluent adjusted to pH 10 with 2 N NaOH. From this bulk solution, aliquots of 500 mL were decanted into 2 litre Erlenmeyer flasks containing weighed mixtures of Na_2HPO_4 and $\text{NaH}_2\text{PO}_4 \cdot \text{H}_2\text{O}$ salts to yield a 100 mM phosphate buffer at pH 6, 7 or 8 (Table 2-1).

This method of adding resin acid to a hot effluent at an alkaline pH, before pH adjustment, was chosen to produce an aqueous matrix that would resemble kraft mill effluent. Methanol helped to disperse the resin acid in the matrix and also supplied a carbon source typical of pulp mill effluent (McCubbin 1983; Springer 1986). Just prior to inoculation, 5 mL of 10% sterilized NH_4Cl was added to each flask and the pH was trimmed, if necessary, dropwise, with 50% H_2SO_4 or 2 N

Table 2-1. Weights of phosphate salts for a 100 mM pH buffered medium.

pH	NaH ₂ PO ₄ (GMW = 137.99) g/500 mL	Na ₂ HPO ₄ (GMW = 141.96) g/500 mL
6	6.05	0.87
7	2.69	4.33
8	0.37	6.72

NaOH. In preliminary batch tests, a 5 mL aliquot of a sterilized 7.5% stock solution of sodium acetate was also added to the medium at this time to provide a representative readily biodegradable primary carbon source (McCubbin 1983). The carbon source combination of resin acid, methanol and sodium acetate in the kraft mill secondary treated effluent matrix formed a synthetic kraft mill effluent having a well defined BOD content for controlled batch experimentation on resin acids.

A 1% inoculum was taken from mature cultures acclimated at the respective pHs. All cultures were initiated with a common inoculum of mixed liquor from the Western Pulp UNOX biobasin. Flasks were agitated on a reciprocal shaker table (40 rpm) in the dark within a 37°C thermostated room. Cultures were acclimated by two batch growth cycles prior to an experimental run.

Resin Acid Sampling and Analysis

During the time course of an experimental run, whole samples and filtered samples were taken for resin acid analysis. Filtered samples were used to compare the time course for depletion of the suspended versus the dissolved resin acid fraction. For filter samples, broth aliquots of 1 mL were drawn through 2.5 cm diameter, 0.45 µm cellulose acetate membrane filters. The filters were rinsed with 2 mL physiological saline (8.5 g/L NaCl) and transferred to 10 mL glass tubes with Teflon caps. For whole broth samples, 1 mL aliquots drawn from the shake flasks were transferred to similar 10 mL glass tubes. To these extraction samples, 1 mL of 1 N NaOH spiked with O-methylpodocarpic acid (O-MPCA) was added immediately. The 1 N NaOH acted to arrest microbial activity while also solubilizing resin acid and microbial constituents alike. Alkaline storage was chosen to prevent time-dependent loss in extraction recovery (Kulovaara et al. 1987). The O-MPCA served as a sample extraction surrogate. Samples were stored frozen at minus 10°C pending extraction.

Prior to extraction, sealed sample tubes were brought to 90°C for 30 minutes to fully solubilize resin acids. Samples were extracted twice with 2 mL methyl-tert-butyl ether (MTBE) with intense vortex mixing followed by centrifugation (20 minutes at 2060 × g) for complete phase separation. With the addition of the first 2 mL of MTBE, 1 mL of 2 N H₂SO₄ was used to acidify the sample in order to reduce the aqueous solubility of the resin acids for improved extraction. For each extraction, the solvent was transferred directly to 2 mL GC vials and dried under vacuum. Resin acid recovery from BKME by solvent extraction under acidic conditions has been shown to be relatively poor (Voss and Rapsomatiotis 1985). Voss and Rapsomatiotis report optimum extraction efficiency around pH 9. However, spiked sample recoveries have been shown to be optimal at low pH (Li et al. 1997). The method of alkaline saponification followed by acidic extraction was chosen to create the conditions of spiked sample extraction. Solvent emulsions could always be collapsed by centrifugation. Recoveries with respect to O-MPCA were typically greater than 90 percent.

Gas chromatographic analysis of underivatized resin acids (Gref 1988) was found to be possible. However, consistent results could only be obtained by the formation of the resin acid methyl esters prior to chromatographic analysis. Methylation was accomplished by dispensing and vortexing, in the dried GC vials, 500 µL of chilled (0 to 4°C) MTBE and HPLC grade methanol (80:20) containing excess dissolved diazomethane, and spiked with heneicosanoic acid methyl ester (HCA-ME) and tricosanoic acid (TCA). Diazomethane gas was dissolved in the MTBE/methanol mixture within a closed vessel (Pierce 28131). The diazomethane gas was generated by reacting N-methyl-N-nitroso-N'-nitroguanidine with 5 N NaOH.

Extracted resin acids and cellular fatty acids were identified and measured by GC/FID (HP5890 Series II with a DB5 column of 30 m having a 0.32 mm ID and 0.25 µm film thickness). Samples of 1 µL were injected at 280°C with an initial column temperature of 100°C. After a 5 minute holding time, the temperature was taken up to 200°C at 20°C/min and followed by a ramp of 1°C/min to 230°C. A post-run ramp to 290°C at 20°C/min was used to clean out the column. A helium carrier gas was used with a column head pressure of 10 psi. Resin acids were quantified

using the response factor of 99% pure dehydroabiatic acid (Helix) standards prepared from a 1000 µg/mL stock solution in MTBE. Internal standards and extraction surrogates were quantified with their respective 99% pure standards as 1000 µg/mL stock solutions in MTBE. With a 1 µL injection, the GC/FID detection limit for DHA was found to be approximately 0.10 µg/mL.

Protein Sampling and Analysis

For this investigation, biomass was measured in terms of protein using the Coomassie Brilliant Blue G dye binding assay (Bradford 1976; Gogstad and Krutnes 1982; Read and Northcote 1981; Stoscheck 1990). The method was chosen for its simplicity and sensitivity. Time-varying inert suspended solids in the medium precluded using the more traditional optical density or gravimetric techniques for biomass.

Filter samples were taken for protein biomass measurements as bovine serum albumin (BSA). Broth aliquots of 1 mL were drawn through 2.5 cm diameter, 0.45 µm cellulose acetate membrane filters. The filters were rinsed with 2 mL physiological saline (8.5 g/L NaCl) and transferred to 10 mL glass tubes with Teflon caps and stored at minus 10°C. Protein was extracted from the filter-harvested cells by adding 2 mL 0.1 N filter-sterilized NaOH and incubating the filters in the sealed tubes at 100°C for 5 minutes. A Coomassie dye reagent was made by dissolving 100 mg of Sigma (B-0770) Brilliant Blue G in a mixture of 100 mL 85% phosphoric acid and 50 mL 95% ethanol. Once the dye was dissolved the final volume was brought up to 1 litre with deionized water. Colour change at a wave length of 595 nm was calibrated against Bovine Serum Albumin (Sigma) standards. To accommodate the expected range of protein in the samples, a number of sample and standard volumes (75, 100 and 150 µL) were combined with a fixed reagent volume (150 µL) producing a range of sensitivities in terms of colour change versus protein concentration. Adsorption was measured with Corning disposable sterile ELISA 96 well (300 µL) flat bottom polystyrene plates in a Molecular Devices Thermo Max Microplate reader. The ELISA plate wells were first referenced with just the 150 µL reagent aliquot. Replicate standards and sample volumes were added and the plate promptly

measured again for colour development. All calibration and sample readings for any one growth curve were made within one ELISA plate. The method detection limit was found to be approximately 0.5 mg/L protein as Bovine Serum Albumin.

Methanol Sampling and Analysis

For methanol, 1 mL samples were taken and stored frozen in 10 mL glass tubes with Teflon caps pending analysis. Methanol in the samples was quantified by GC/FID. Sealed sample tubes were vortexed and then incubated at 90°C for 10 minutes in order to reduce the potential for bioactivity during analysis. After centrifuging ($2060 \times g$) for 30 minutes, a 200 μ L sub-sample was diluted with a 200 μ L aliquot of deionized water spiked with iso-propyl alcohol as an internal standard. Methanol in the samples was quantified against a dilution series from a 1000 ppm stock solution of HPLC grade methanol in distilled and deionized water prepared in the same manner. The gas chromatogram was generated on an HP 5890 Series II with a DB624 column (30 m with a 0.32 mm ID and 3.0 μ m film thickness) and a column head pressure of 5.5 psi. One microlitre aqueous injections were made with injection and detection temperatures of 110 and 200°C respectively. The column temperature was held at 40°C for 3 minutes after injection and then ramped to 120°C at 20°C/min.

Sodium Acetate Sampling and Analysis

For the analysis of sodium acetate, 1 mL samples were drawn and immediately acidified with 200 μ L of 10 % phosphoric acid and then frozen at minus 10°C in 2 mL crimped-top GC autosampler vials pending analysis. Sodium acetate was measured by GC/FID (HP 5880A Series) as acetic acid following the method outlined in the Supelco GC Bulletin 751G (Supelco 1982).

pH Sampling and Analysis

To confirm that the medium buffering capacity was not exceeded, 1 mL samples were dispensed into standard glass disposable test tubes and measured directly with a calibrated Accumet pH electrode (No. 69488) with a Cole Palmer CP Chemcadet (5986-40) pH meter.

2.2.2 Dynamic Surface Tension Measurement

Aliquots of 1 mL broth samples were drawn from the shake flasks and transferred to 10 mL glass tubes. To inhibit biological activity, 10 μ L of 10% sodium azide were added. All glassware had been thoroughly washed and rinsed with deionized water and then fired at 475°C in a muffle furnace for over an hour to remove any organic material. Dynamic surface tension was measured directly after sample temperature equilibration to 20 \pm 1°C. After the surface tension measurement, the sample pH was taken.

Dynamic surface tension measurements were made using the maximum bubble pressure (MBP) method. Since this technique was developed by Sugden (1922; 1924), it has become a readily applied tool for experimental research in surface thermodynamics (Bendure 1971; Bing et al. 1988; Brown et al. 1952; Finch and Smith 1972; Hirt 1990; Hua and Rosen 1988; Iliev and Dushkin 1992; Kuffner 1961; Masutani and Stenstrom 1991; Posner et al. 1952). Mysels (1990) has written a relatively recent review of the history and experimental considerations for the method.

With this method, gas is forced out of a capillary tube of radius, r , immersed at a depth, h (Figure 2-3). From Laplace's equation (2-1), the pressure, p , required to produce an assumed spherical bubble reaches a maximum (p_M) when the emerging bubble becomes a hemisphere with the capillary's radius:

$$p_M = p - p_a = 2\frac{\sigma_t}{r} + \rho gh \quad (2-33)$$

where p_a is the atmospheric pressure, ρ is the liquid density (0.99821 g/cm³ at 20°C), g is the acceleration due to gravity (980.98 cm/s²) and σ_t is the dynamic surface tension as a function of the bubble formation time, t . For a pure solvent, p_M is theoretically independent of the rate of bubble production. However, if surfactants are present in solution, a longer time for bubble formation permits a greater extent of surfactant adsorption at the gas/liquid interface. Increased surfactant concentration at the gas/liquid interface lowers the surface tension, as observed by a

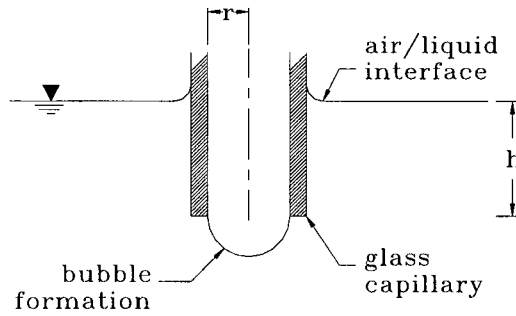


Figure 2-3. The maximum bubble pressure method. Gas bubbles are blown through a glass capillary tube of radius, r , that is immersed to a depth, h , into a liquid sample. The pressure needed to generate the bubbles is monitored and interpreted.

corresponding change in the measured p_M .

Equation (2-33) is not exact. The existence of a pressure gradient with liquid depth results in a formed half bubble that is not exactly hemispherical. The MBP surface tension is calculated precisely from the formula:

$$\sigma_t = \frac{r(p_M - \rho gh)f_c}{2} \quad (2-34)$$

where f_c is a correction factor for non-sphericity. Sugden (1922) tabulated the correction factor as a function of the dimensionless ratio (r/α) , where α is the capillary constant defined as:

$$\alpha = \sqrt{\frac{2\sigma_t}{\rho g}} \quad (2-35)$$

Bendure (1971) approximated the tabulated values by an empirical power series:

$$f = a_0 + a_1(r/\alpha) + a_2(r/\alpha)^2 + a_3(r/\alpha)^3 + \dots \quad (2-36)$$

$$\begin{aligned} a_0 &= 0.99951 & a_2 &= -0.69498 & a_3 &= -0.11133 \\ a_1 &= 0.01359 & a_4 &= 0.56447 & a_5 &= -0.20156 \end{aligned}$$

The shape correction calculation was refined by Johnson and Lane (1974). However, the correction factor differs from unity only in the third decimal place when the capillary radius is around 0.02 cm.

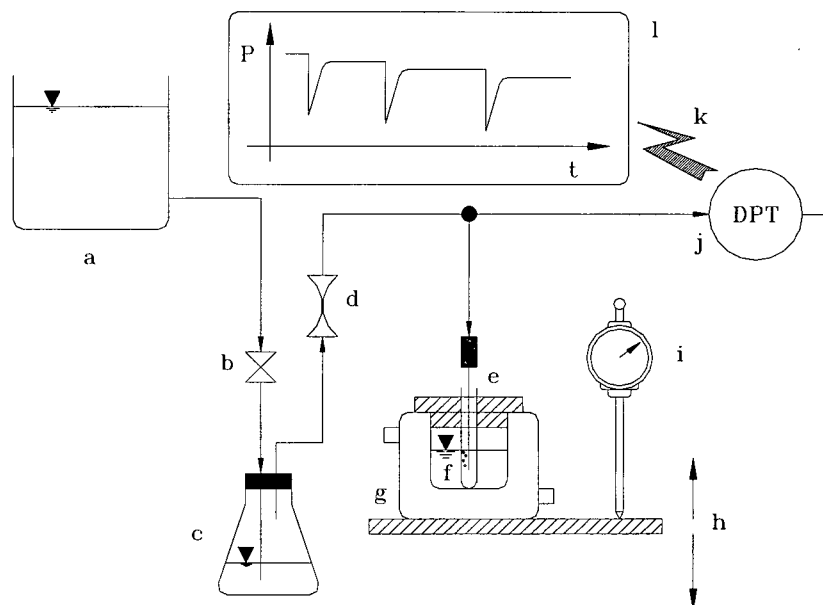


Figure 2-4. Experimental set-up for the maximum bubble pressure method. Regulated flow (b) of distilled water from a constant head tank (a) pressurizes a closed reservoir (c). Transmission of the reservoir pressure to the rest of the system is damped by a fixed orifice (d). Pressure at the capillary tube (e) produces gas bubbles in the sample contained within a test tube (f). The test tube temperature is regulated through a thermostated jacketed beaker (g). Gage pressure at the capillary is measured by an electronic differential pressure transducer (j) whose signal is recorded (l). Capillary immersion depth is set by the stage height (h) whose level is referenced by a needle gauge micrometer (i).

Bubbles were produced with the sample tube immersed in a thermostated bath at $20 \pm 1^\circ\text{C}$ (Figure 2-4). Bubble formation proceeded at constant pressure supplied by an air-charged reservoir. The air reservoir was pressurized by displacement with deionized water. Bubbling frequency decreased as the reservoir pressure decreased with gas lost from the system in each bubble. Bubbling frequencies from about 10 Hz down to 0.04 Hz were monitored. Micropipet capillaries ($10 \mu\text{L}$) having a radius in the order of 0.02 cm were used. The effective capillary radius was assessed by measurement and calibration against the surface tension of deionized water ($\sigma = 72.75 \text{ dyne/cm}$ at 20°C). Although the capillary lumen radius could be measured with a microscope, in practice the anchoring radius for the bubble can be slightly outside the lumen. Since surface tension determination is sensitive to capillary radius, the radius was determined indirectly by calibration against the reference liquid. The radius calculated in this manner implicitly included the correction factor, f_c , which was approximated to be constant for all other measurements.

Capillary immersion depth, h , was measured to the closest 0.025 mm by a needle gauge micrometer. The change in liquid level due to liquid displacement by the capillary or by bubble

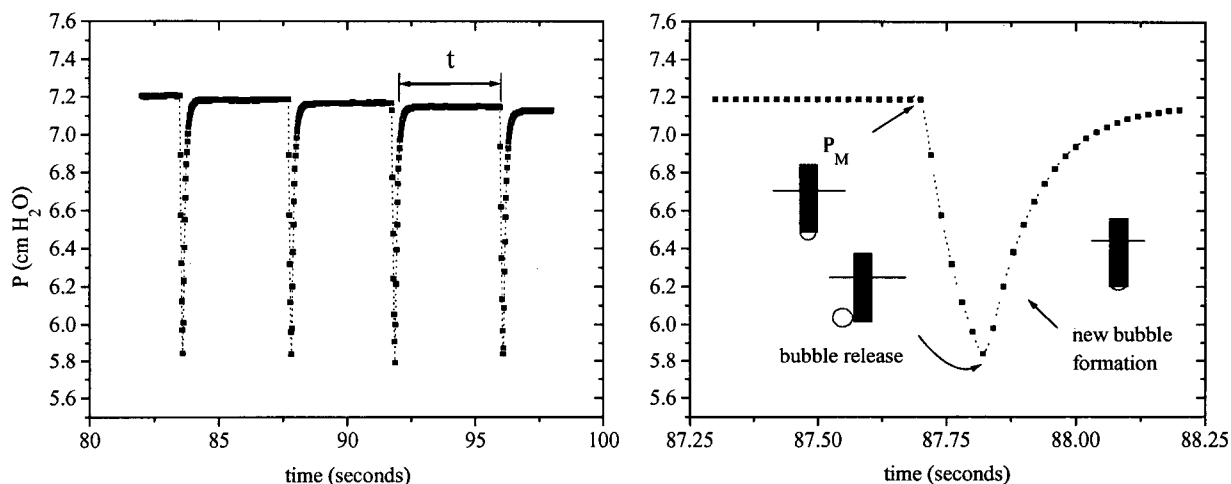


Figure 2-5. A typical maximum bubble pressure signal (Left). This signal contains four bubble events corresponding to the four transient pressure dips. The plateau pressure decreases slightly with gas lost from the reservoir in each bubble. Bubble life or surface age (t) is defined from a point of minimum pressure to the next point of maximum pressure.

Figure 2-6. Detail of the critical points in the pressure signal (Right). Surfactant adsorption at constant pressure (p_M) terminates at the critical point of a hemispherical geometry. A bubble is *explosively* produced leading to a fresh gas-liquid interface that forms the next bubble. The dead time is the period between maximum pressure and bubble release.

formation affects the MBP. The influence of this type of error was minimized by the use of a micro-capillary tube and was standardized by maintaining the same immersion depth of 0.508 cm for all sample and reference measurements.

Pressure values during bubble formation were logged at 50 Hz directly onto a computer (PC-LabCard Series PCL-812G 12 bit A/D driven by Labtech Notebook LE software on an IBM-PC clone with a 486 DLC 40 MHz CPU with math co-processor) through a calibrated differential pressure transducer (0-20 cm H₂O Celesco VR Series Differential Pressure Transducer with a LCCD-110 Carrier Demodulator) producing a 1 volt/cm H₂O signal.

In real time, the digitized pressure signal was analyzed by applying Savitzky and Golay (1964) least squares smoothing and differentiation. Figure 2-5 illustrates a typical segment from a pressure-time trace showing the release of four bubbles. A slight decrease in the (plateau) reservoir pressure level can be seen with the release of each bubble. Figure 2-6 is a close-up of the pressure data during one bubble release. First and second time derivatives of the raw pressure trace helped to define the distinct *calm* and *explosive* phases of bubble production permitting the

discretization of the pressure-time signal into single bubble events. Identification of bubble events by pressure gradients enabled automatic triggering of data acquisition, minimizing the amount of information that needed to be stored to disk. Since a measurement sequence could take as long as 30 minutes, data files would have become unmanageably large had a triggering scheme not been used. Two data files were created. One stored the start and stop times of each bubble event and the other logged the time series of pressure values at 50 Hz during each event typified by Figure 2-6. For each bubble produced, the formation time (or bubble life) and the corresponding maximum pressure were ascertained by numerical data smoothing, cubic spline interpolation and extremum search algorithms (Hornbeck 1975; Press et al. 1989). Bubble life or *surface age* (t) is defined by the period from the point of bubble release of one event to the point of maximum pressure (p_M) in the next (Figure 2-5). The bubble production dead time defined by the period of explosive bubble release (Figure 2-6) was therefore accounted for. A sample measurement was defined by a recorded log of around 100 bubble events distributed over a range of surface ages.

Bubble life represents the time available for surfactant adsorption at the bubble's gas/liquid interface. A longer bubble life allows more surfactant to be adsorbed at the bubble surface with a correlated lower p_M and surface tension. The incremental extent of adsorption for a longer bubble life depends on the surfactant's bulk concentration, interfacial concentration, molecular diffusivity and chemical structure. In order to analyse the compiled adsorption data as a function of concentration for a constant surface age, the derived experimental σ_t data, obtained over a range of random t values for each sample measurement, were interpolated by a cubic spline on a log time scale. In this manner, all sample measurements were aligned to a set of common times or surface ages.

2.2.3 Nonlinear Regression Analysis

Nonlinear regression was required to estimate the parameters of the equation (2-32) that best fit the experimental substrate depletion curve. Parameter values $\{S_0, S^*, Q, k_s, \Psi\}$ were estimated by non-linear least squares regression by Taylor series linearization (Draper and Smith 1966) modified by a logarithmic data transformation for variance stabilisation. Since the substrate

depletion curve involved experimental concentrations over four orders of magnitude, a lack of variance constancy would unduly influence the numerical results (Berthouex and Brown 1994). There are two kinds of random errors that combine to affect experimental data. Background noise is omnipresent and is assumed to have a constant variance. Measurement error is assumed to be proportional to the level of signal. Least squares regression on the untransformed concentration data would be biased by larger absolute experimental errors for the data at higher concentration. This bias resulted in a poor estimate of the threshold concentration. In order to give all data in the depletion curve equal weight, log-transformed concentrations were used.

The objective function was the sum of square errors, $SS(\Theta)$, between the natural logarithm of the measured and estimated concentration:

$$SS(\Theta) = \sum_{k=1}^N (u_k - U_k)^2 \quad (2-37)$$

where Θ is the vector of p parameters (the five, $\{S_0, S^*, Q, k_s, \Psi\}$, in this case), N is the number of observations of the transformed experimental concentrations (u_k) and U_k is the natural logarithm of the integral of equation (2-32):

$$U_k = U(\eta_k, \Theta) = \ln(g(\eta_k, \Theta)) = \ln \left(\int_0^{\eta_k} \frac{s - s^*}{\kappa + s} \left(s - \left(1 + \frac{1}{\Psi} \right) \right) d\eta \right) \quad (2-38)$$

$$u_k = \ln(s_k)$$

Given the j^{th} estimate of the parameter set, Θ^j , the Taylor series method predicts the next best estimate, Θ^{j+1} in minimising the objective function as follows:

$$\Theta^{j+1} = \Theta^j + (G^T G)^{-1} (G^T Z) \quad (2-39)$$

where Z is the discrepancy vector and G is the matrix of partial derivatives with respect to the parameters:

$$Z = \begin{bmatrix} u_1 - U(\eta_1, \Theta^j) \\ \vdots \\ u_N - U(\eta_N, \Theta^j) \end{bmatrix} \quad G = \begin{bmatrix} \frac{\partial U(\eta_1, \Theta^j)}{\partial \Theta_1} & \dots & \frac{\partial U(\eta_1, \Theta^j)}{\partial \Theta_p} \\ \vdots & \ddots & \vdots \\ \frac{\partial U(\eta_N, \Theta^j)}{\partial \Theta_1} & \dots & \frac{\partial U(\eta_N, \Theta^j)}{\partial \Theta_p} \end{bmatrix} \quad \Theta^j = \begin{bmatrix} S_0 \\ S^* \\ Q \\ k_s \\ \Psi \end{bmatrix} \quad (2-40)$$

Since the partial derivatives in the matrix G could not be determined analytically, they were numerically calculated by a second order finite difference approximation (Hornbeck 1975):

$$\frac{\partial U(\eta_k, \Theta^j)}{\partial \Theta_i} = \frac{1}{g(\eta_k, \Theta^j)} \frac{-3g(\eta_k, \Theta^j) + 4g(\eta_k, \Theta^j + \Delta\Theta_i) - g(\eta_k, \Theta^j + 2\Delta\Theta_i)}{2\Delta\Theta_i} \quad (2-41)$$

The numerical solution is doubly iterative. It is iterative in the first instance due to the successive integration of equation (2-32) for calculated values of U_k as a function of the parameter set. The second level of iteration is in the search for numerical convergence to a minimum objective function. Numerical integration was accomplished with a fourth order Runge-Kutta (Hornbeck 1975) algorithm with self-limiting step-size halving optimisation.

An approximate 100(1- α) percent confidence contour for the best parameter estimate $\langle \Theta \rangle$ is defined by (Draper and Smith 1966):

$$SS(\theta) = SS(\langle \Theta \rangle) \left(1 + \frac{p}{N-p} F(p, N-p, 1-\alpha) \right) \quad (2-42)$$

where $F(p, N-p, 1-\alpha)$ is the 1 - α point of the $F(p, N-p)$ distribution. The precision of the estimated parameters was considered by generating the approximate 1- α joint confidence regions for logical pairs of the parameters. This was done by calculating $SS(\Theta)$ in the neighbourhood of the minimum by varying the parameters in pairs, such as $\{Q, k_s\}$ or $\{S_0, S^*\}$, while holding all other parameters constant. From the objective function mapping as a function of the parameter pair, a contour plot was then generated with the help of commercial software (Surfer Version 6.01, Golden Software Incorporated).

2.3 Results

The experimental results have been organized in two sections. In the first section, the experimental results and considerations for assessing the mixed culture batch growth data are presented. Diauxic growth was observed for the medium containing the combined carbon sources of resin acids and sodium acetate. Due to the experienced inconsistency of resin acid biodegradation in the presence of sodium acetate, the additions of sodium acetate were abandoned. Unfortunately, biomass measurements using the protein assay were also unsuccessful due to matrix interferences. However, the substrate depletion data could still be modelled by Monod kinetics with the incorporation of a threshold concentration. The threshold concentration appeared to be greatest under acidic growth conditions.

The results of the dynamic surface tension measurements are subsequently reported. The surface tension data were found to be well represented by the model of quasi-static Langmuir adsorption. Differences in pH greatly influenced the flux and adsorption of resin acids at a gas/liquid interface. It was interesting to observe a lower bound or threshold concentration for resin acid flux in solution. The increase in this flux threshold corresponded qualitatively with the observed threshold concentration for biodegradation.

2.3.1 Mixed Culture Batch Growth

Initial batch experiments with the three carbon sources (sodium acetate, methanol, and resin acids) in BKME effluent gave unpredictable results. While acetate was always consumed over a twenty-four hour period, the resin acids were often left essentially untouched. Under these mixed substrate conditions, resin acids were depleted most consistently at pH 6. After the first few experiments, sodium acetate was no longer added to the medium, due to the uncertainty that it introduced. The remainder of the results describe batch growth studies with the Squamish effluent media containing only resin acids and associated methanol as carbon sources. It should be noted, however, that methanol was also not consistently metabolized.

Figure 2-7 shows total and suspended resin acid depletion data for pH 6, 7 and 8. Regression

Table 2-2. Parameter values for the Monod model with a threshold substrate concentration (equation (2-32)) used to model the substrate depletion curves presented in Figure 2-7.

Total Resin Acid Depletion					
pH	S_0 μM	S^* μM	k_s μM	Q Hr^{-1}	$1/\Psi$
6	171	2.7	292	3.0	0.00003
7	179	0.8	66	1.0	0.00007
8	180	0.7	13	0.2	0.03226
Suspended Resin Acid Depletion					
pH	S_0 μM	S^* μM	k_s μM	Q Hr^{-1}	$1/\Psi$
6	94	2.3	155	3.0	0.00005
7	32	0.7	8	1.0	0.00004
8	5	0.5	0	0.2	0.10489

curves were generated according to the best fit parameters obtained for the model of Monod growth with a substrate threshold (equation (2-32)). The optimal parameter values used to fit the data are reported in Table 2-2. Unfortunately, biomass measurements as protein (BSA), that were quite precise during method trials, were found to suffer from an interference that increased with decreasing pH. Without a reliable measurement for biomass, neither the batch growth lag time, or the biomass concentrations, could be reliably estimated. Therefore, the constants Ψ , Q and k_s served solely as empirical curve fit parameters. However, from a visual inspection of the substrate data, the rate of substrate removal was influenced by pH and this difference was reflected by differences in Q and k_s .

A threshold resin acid concentration (S^*) was also observed (Table 2-2). Error in the estimation of the threshold concentration based on the approximate 95% joint confidence interval for $\{S_0, S^*\}$ was found to be no more than 15 percent of the absolute value. The residuum can be seen to be essentially suspended and was highest (2.7 μM) for the pH 6 condition (Figure 2-7). A resin acid concentration of 2.7 μM translates to approximately 0.8 mg/L which is still a level that could be acutely lethal towards fish. Therefore, in this case, biological treatment alone did not appear to be sufficient for detoxification.

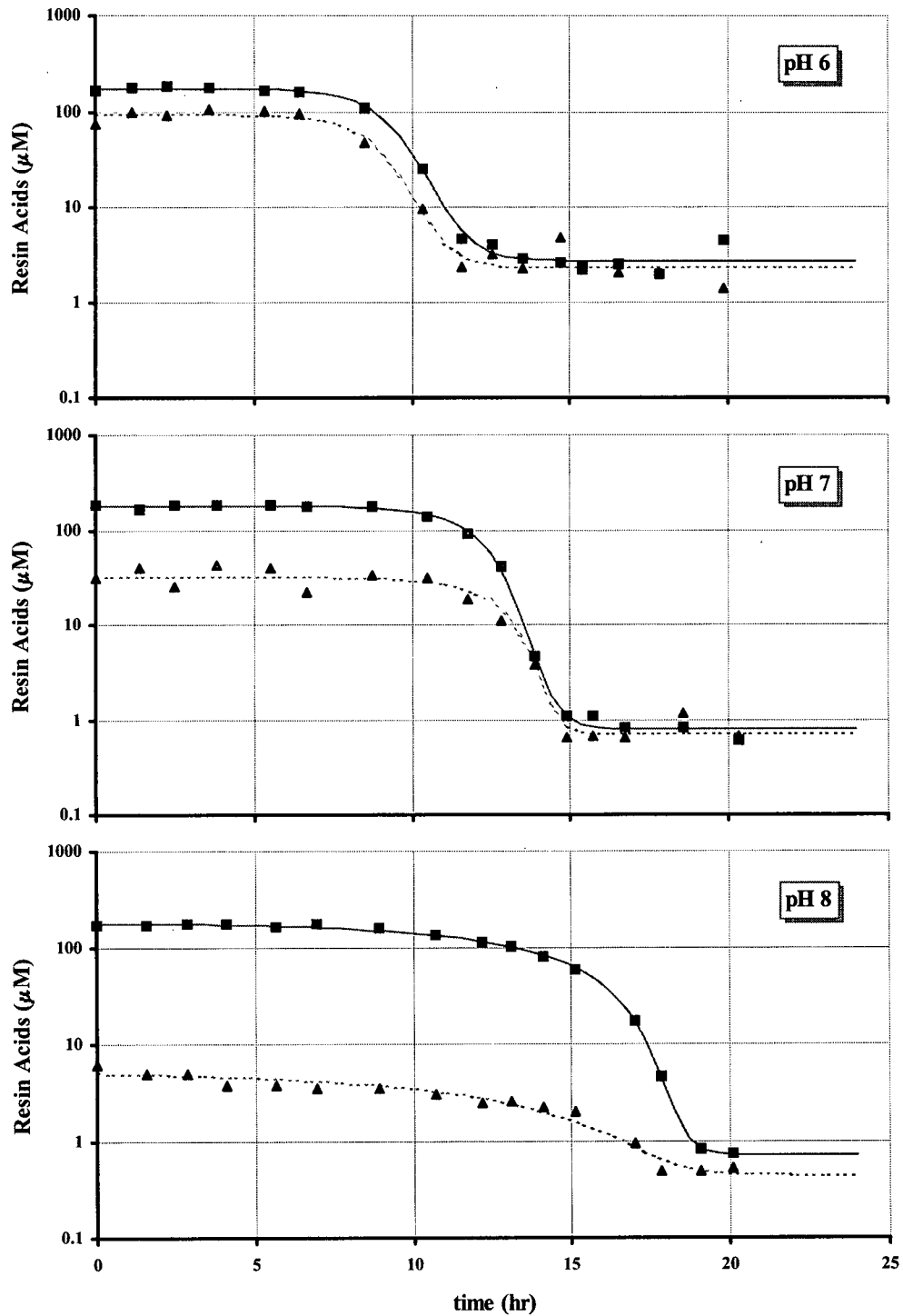


Figure 2-7. Batch growth resin acid depletion curves for pH 6,7 and 8 from top to bottom. The data show the time courses of removal for both total (■) and particulate (▲) resin acid modelled by best fit curves from equation (2-32). See Table 2-2 for model parameter values.

2.3.2 Dynamic Surface Tension Measurements

Results of the corresponding dynamic surface tension measurements made during batch growth are shown in Figure 2-8. The data are presented for a number of surface ages, forming a family of quasi-static Langmuir isotherms. The group of isotherms was fitted simultaneously to equation (2-25) by generalized reduced gradient non-linear optimisation (Microsoft Excel 97 SR-1 Solver) with the constraint of a common Γ_L . The resultant limiting surface loading, Γ_L , is noted on the graph for each pH. Kraft mill effluent contains a significant amount of amorphous high molecular weight poly-electrolytes which are the recalcitrant breakdown products of lignin. These compounds impart the characteristic colour to the effluent. Because of their high molecular weight, kraft lignins can also be surface active. Therefore it was not surprising to find a changing reference surface tension, σ_0 (equation (2-25)) corresponding to a background matrix surfactancy, varying both with pH and surface age. Inherent surface aging that was believed to be due to kraft lignin adsorption is shown in Figure 2-9 in terms of the derived matrix surface pressure change with age.

The trend in the isotherm data, shown in Figure 2-8 for the condition of pH 7, suggested the presence of a critical micelle resin acid concentration in the neighbourhood of 100 μM . In this case, isotherm modelling was restricted to concentrations below 100 μM . The parameter K_e was estimated by fitting respective K_t values to an exponential decay curve on a logarithmic time scale (Figure 2-10). The extrapolated value, K_e is a minimum representing the point of maximum entropy or minimum Gibbs free energy.

From the values of K_t and Γ_L the surface loading Γ_t was calculated as a function of solute concentration (equation (2-20)). Based on the extrapolated equilibrium value, K_e , the normalized surface loading (γ_t) with time as a function of solute concentration was calculated from:

$$\gamma_t = \frac{\Gamma_t}{\Gamma_e} = \frac{c_b + K_e}{c_b + K_t} \quad (2-43)$$

The γ_t data at constant pH were empirically found to be well represented by an equation of form:

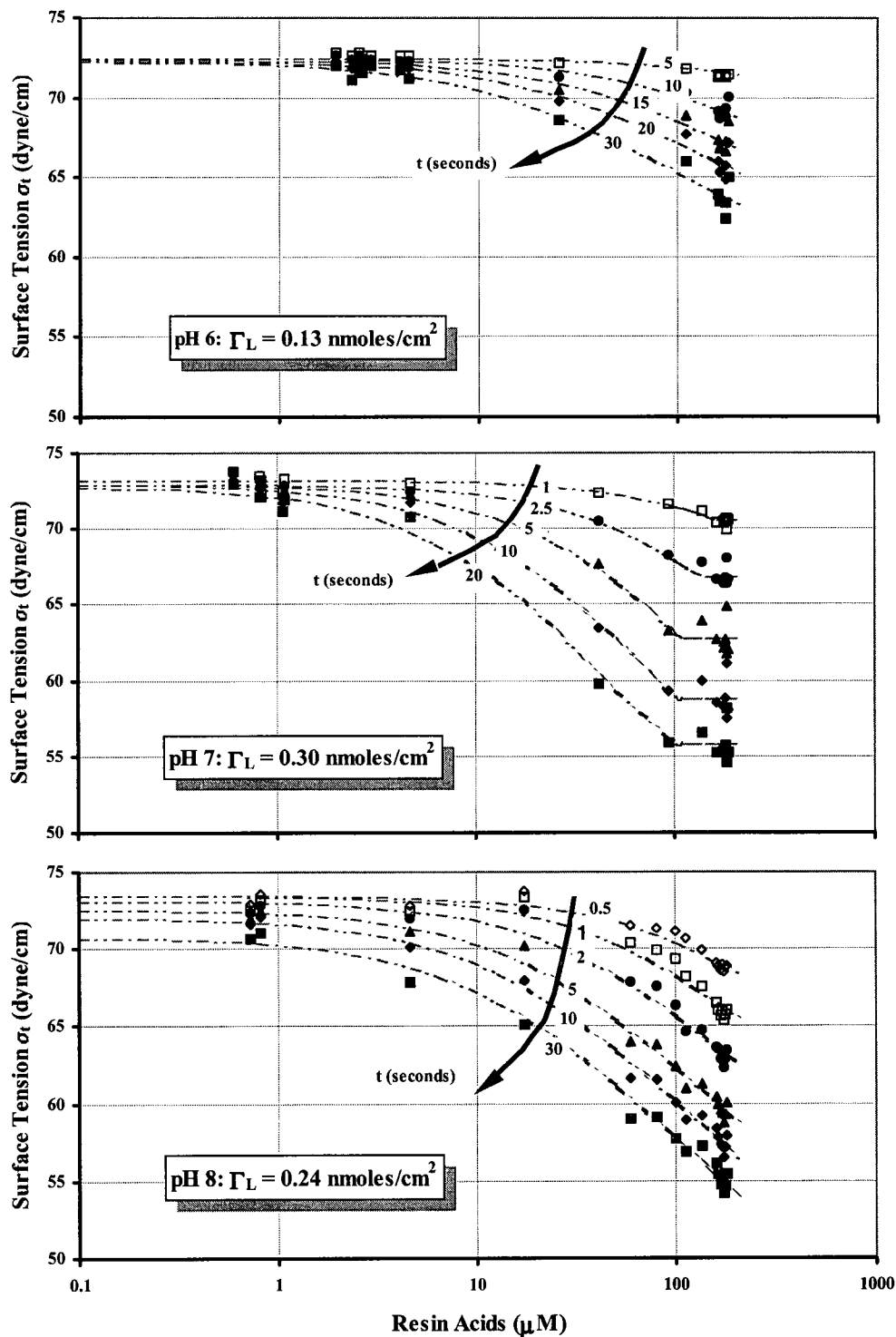


Figure 2-8. Dynamic surface tension during biological removal of resin acids for pH 6,7 and 8 from top to bottom. Experimental data at the indicated surface ages is shown along with the family of quasi-static Langmuir isotherms (equation (2-25)) that were fitted to the data. The isotherms generated for the data at pH 7 suggest the presence of a critical micelle concentration in the neighbourhood of 100 μM .

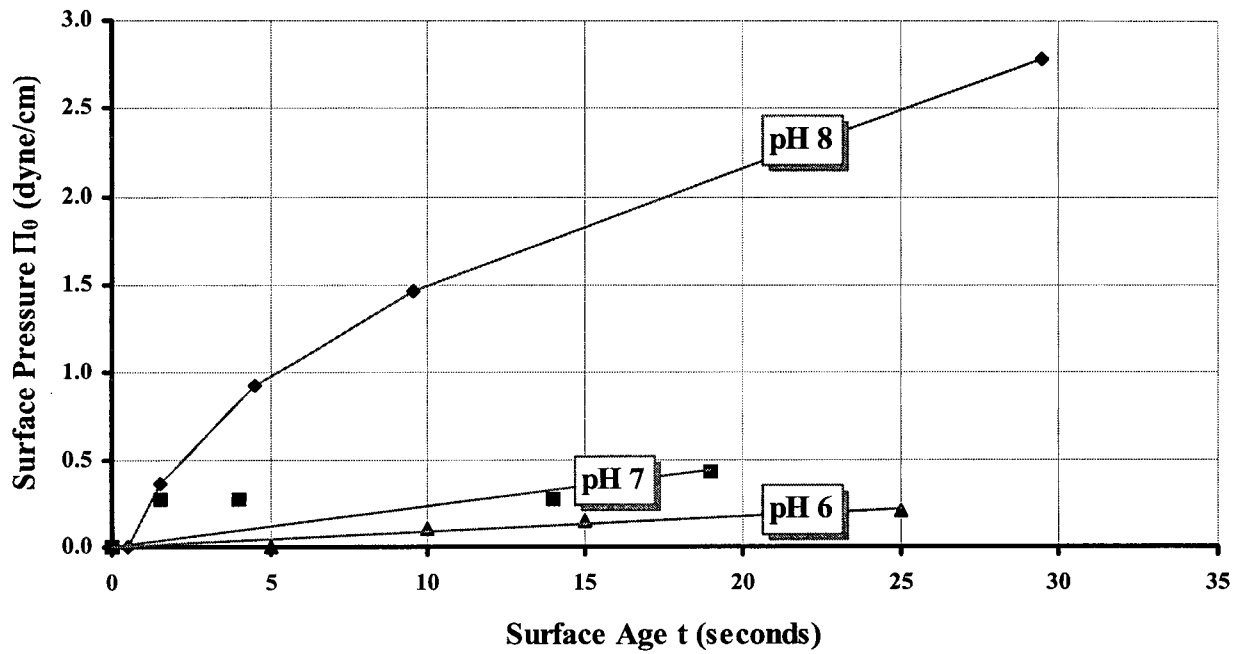


Figure 2-9. Derived surface pressure changes with surface age in the absence of resin acids that were believed to be due to the presence of kraft lignin in the media.

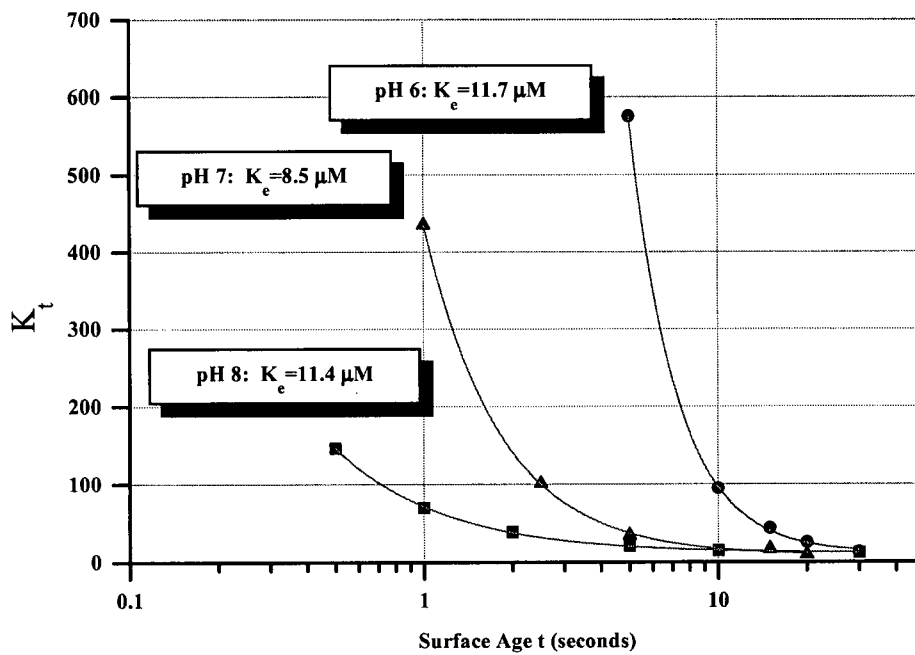


Figure 2-10. The quasi-static Langmuir concentration K (equation (2-20)) as a function of surface age and pH. Equilibrium values (K_e) for an infinite surface age were estimated from regression analysis to an exponential decay function.

$$\gamma_t = \frac{\beta_a t}{1 + \beta_a t}, \quad \beta_a = \frac{q_a}{\tau_a} \quad (2-44)$$

Equation (2-44) describes a sigmoid on a logarithmic time scale, where q_a is the rate constant for adsorption and τ_a is the lag time to reach a normalized surface loading of 50 percent.

The rate constant (q_a) was found to be independent of resin acid concentration. The lag time (τ_a) taken to reach 50 percent surface loading increased with decreasing solute concentration (Figure 2-11). Equation (2-44) is analogous to equation (2-9) used by Hua and Rosen (1988), except in this case adsorption is expressed directly in terms of surface loading. Figure 2-11 shows that both the rate of surface loading (q_a) and the lag time (τ_a) increases with decreasing pH.

From equation (2-44), the rate change in surface loading can be calculated explicitly in time and this expression can also be equated to the general surface loading rate equation (2-6):

$$\frac{\partial \Gamma}{\partial t} = \Gamma_e \frac{\partial \gamma}{\partial t} = \frac{\Gamma_e \beta_a}{(1 + \beta_a t)^2} = \Phi J \quad (2-45)$$

If the sticking coefficient (Φ) is assumed to be initially equal to one, then the initial solute flux should be related to the solute mobility B times some function of solute concentration (equation (2-6)):

$$J_0 = \Gamma_e \beta_a = Bf(c_b) \quad (2-46)$$

The initial solute flux from the adsorption data at pH 8 was linearly dependent on resin acid concentration (Figure 2-12). However, the data at pH 6 and 7 were both better represented by a linear dependence on the logarithm of resin acid concentration (Figure 2-13). In Figure 2-13 it can be seen that the adsorption data for pH 6 and 7 both displayed a knee or threshold concentration below which solute flux became independent of resin acid concentration. The initial solute flux at pH 8 is an order of magnitude higher than the fluxes at pH 6 and 7. The flux at pH 7 is greater than at pH 6.

If the surface flux J is assumed to be constant and equal to the initial flux of solute to the interface

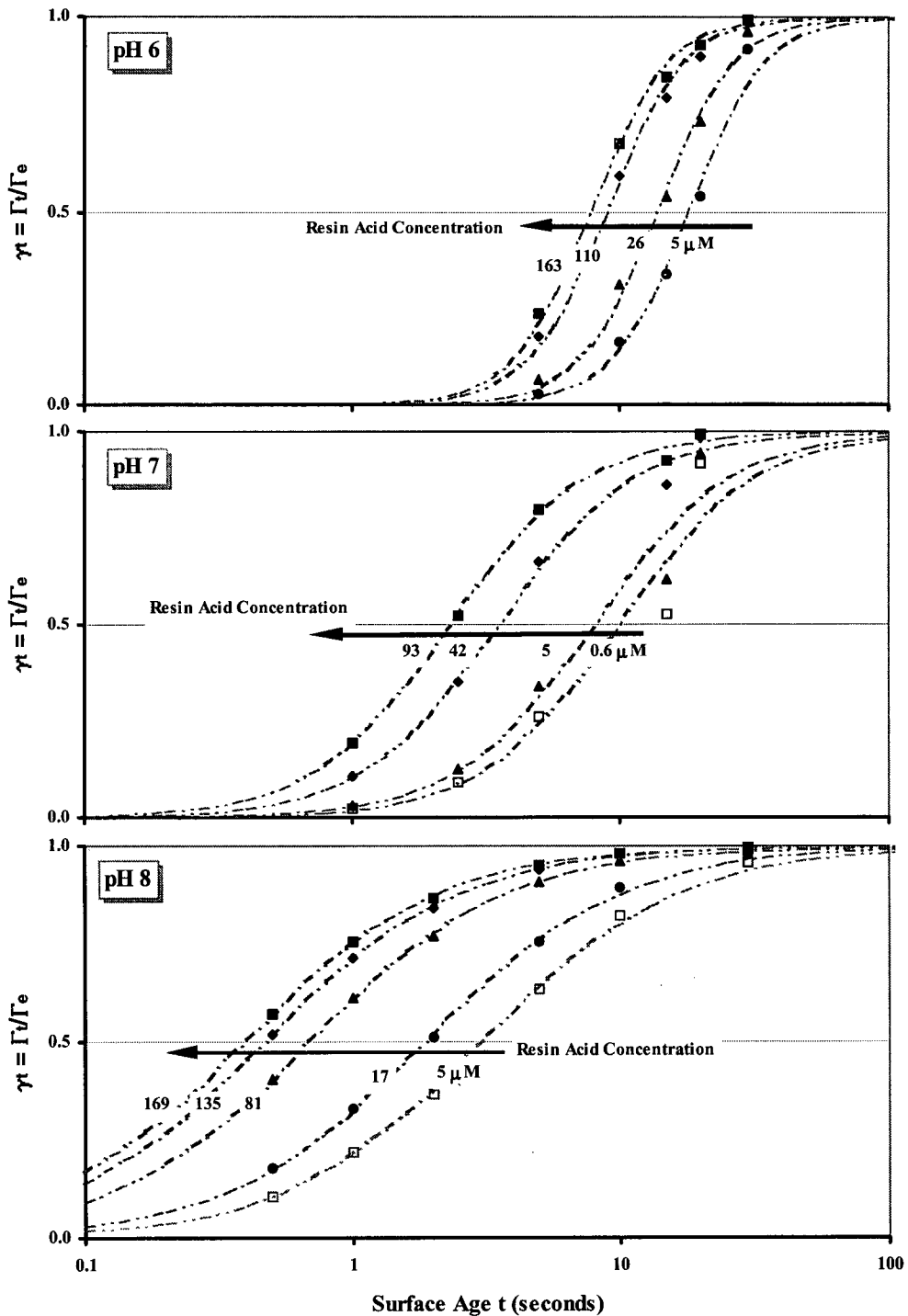


Figure 2-11. Normalized surface loading (γ) as a function of surface age (t) and resin acid concentration. Experimental data are shown for pH 6, 7 and 8 (top to bottom) along with best fit model curves (equation (2-44)) obtained by generalized reduced gradient nonlinear optimisation (Microsoft Excel SR-1 Solver) for the whole data set at each pH condition respectively. With reference to equation (2-44) the q_a values are 3.07, 1.72 and 1.18 for pH 6, 7 and 8. The τ_a values can be read from the curves at a surface loading $\gamma_t = 1/2$. Not all data have been shown to allow for better visual clarity.

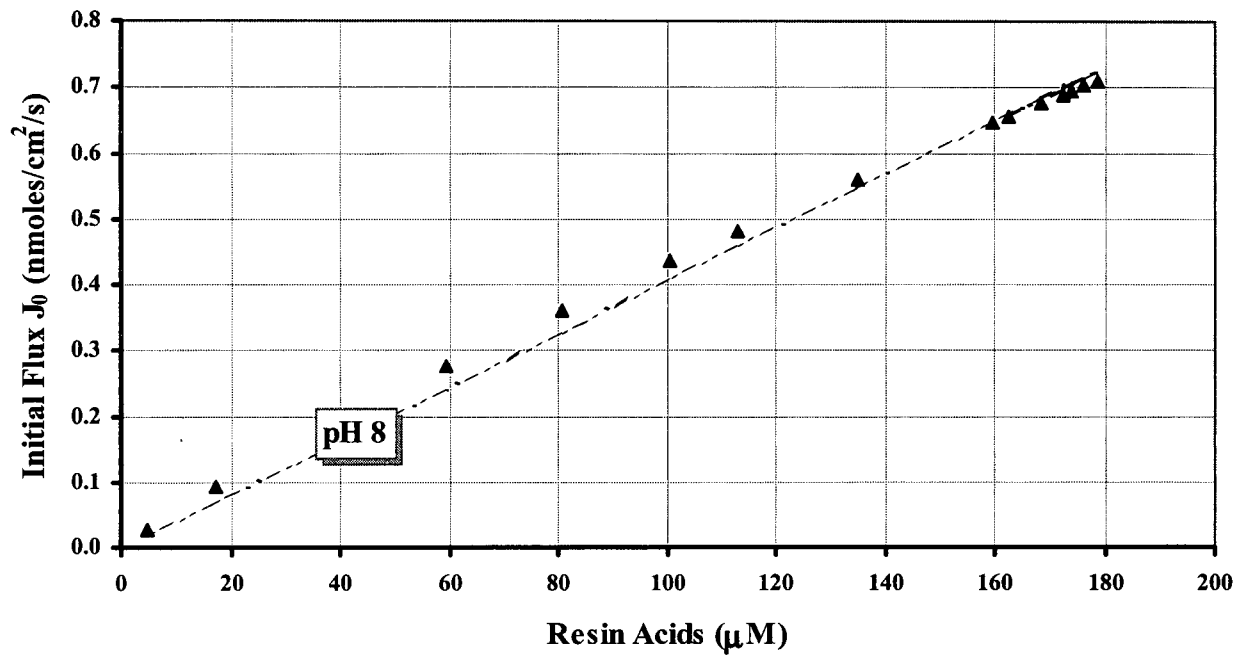


Figure 2-12. The derived initial flux of resin acid to a freshly generated gas/liquid interface at pH 8. The initial flux is directly proportional to resin acid concentration.

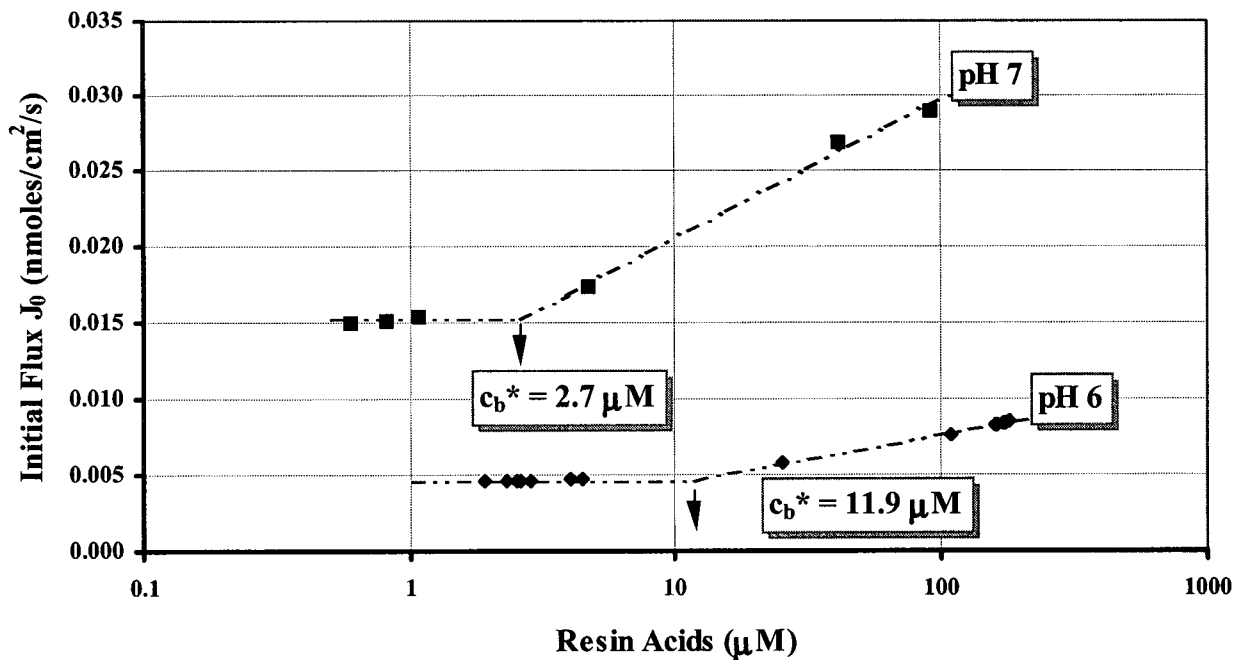


Figure 2-13. The derived initial flux of resin acid to a freshly generated gas/liquid interface at pH 6 and 7. The initial flux is directly proportional to the logarithm of resin acid concentration, c_b^* .

then from equation (2-45) and (2-46):

$$\Phi = \frac{1}{(1 + \beta_a t)^2} \quad (2-47)$$

By manipulating equation (2-45), it can be shown that the assumption of a constant surface flux leads to a time-implicit expression of the sticking factor in terms of the squared compliment of the normalized surface loading:

$$\Phi = (1 - \gamma_t)^2 = \frac{1}{(1 + \beta_a t)^2} \quad (2-48)$$

Accordingly, a time implicit expression for the sticking factor, Φ , was sought in the form of:

$$\Phi = \Phi \left((1 - \gamma_t)^2 \right) \quad (2-49)$$

The results plotted in Figure 2-14 however, show that equation (2-48) is not strictly valid, meaning that the surface flux is not constant but is also dependent on surface loading. However, it is still possible to write a time-implicit relationship for the rate change of surface loading in terms of the initial surface flux as follows:

$$\frac{\partial \Gamma}{\partial t} = \Phi J_0, \quad \Phi = \sum_{i=1}^{\infty} \phi_i (1 - \gamma_t)^{2i}, \quad \sum_{i=1}^{\infty} \phi_i \leq 1 \quad (2-50)$$

The crudest approximation of equation (2-50), which works reasonably well at pH 8 but progressively poorer at pH 7 and 6, is a linear representation as shown in Figure 2-14:

$$\frac{\partial \Gamma}{\partial t} \approx \phi (1 - \gamma_t)^2 J_0, \quad \phi \leq 1 \quad (2-51)$$

The sticking probability is highest for pH 8 and decreases with increasing surface coverage. The experimental data (Figure 2-12 and Figure 2-13) suggest that, depending on the pH condition, the initial flux J_0 is related to concentration by an equation of form:

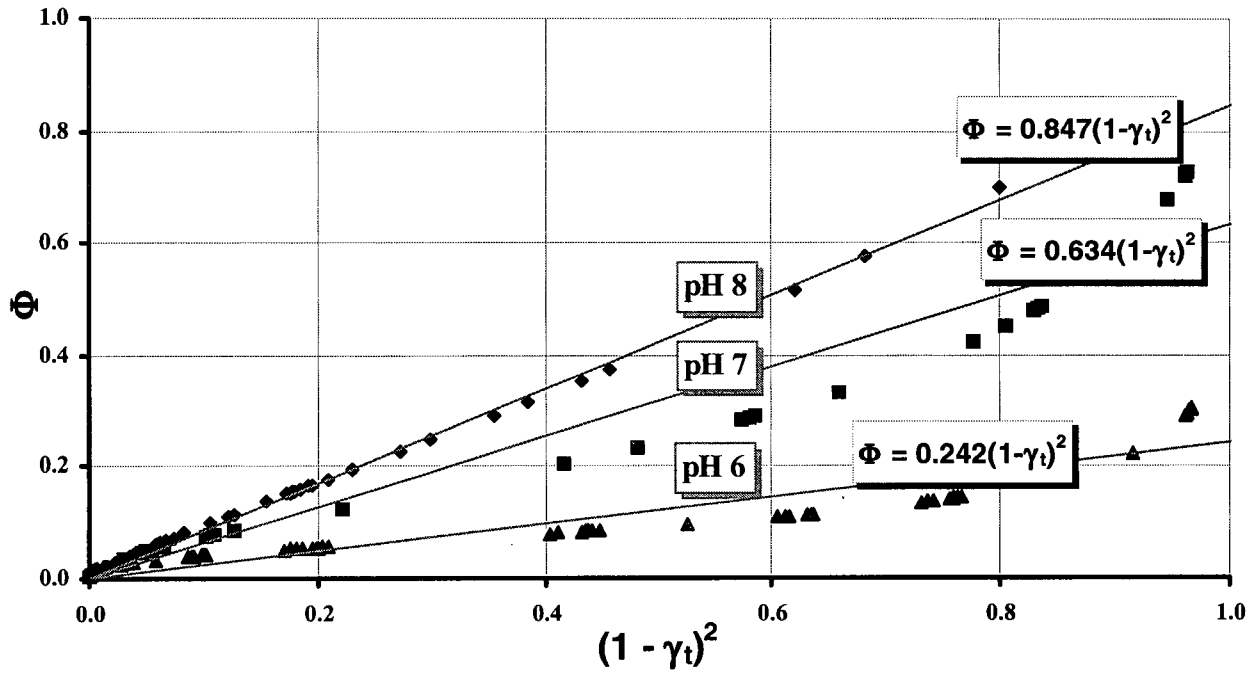


Figure 2-14. The experimentally derived dependency of the sticking factor Φ on the squared compliment of normalized surface loading based on the initial surface flux (equation (2-48) and (2-51))

$$J_0 = \begin{cases} j_0 + H(c_b - c_b^*) \cdot (\ln c_b - \ln c_b^*) & pH \leq 7 \\ Bc_b & pH \approx 8 \end{cases} \quad (52)$$

where $H(c_b - c_b^*)$ is Heaviside's unit step function defining the threshold concentration for the adsorption dependency on resin acid concentration and j_0 is a background adsorption flux.

2.4 Discussion

For the present investigation, batch removal of resin acids was found to be greater than 98%, however the residuum or threshold concentration was still well within the resin acid concentration range reported for sublethal effects to aquatic organisms (McLeay 1987). In the research literature on the biological removal of resin acids, to the author's knowledge, no mention has previously been made of such threshold concentrations. Thus, microbial oxidation can achieve significant depletion of a contaminant, but final absolute concentrations cannot be neglected in the consideration of toxicity removal. The residuum was greatest at pH 6 indicating the potential of reduced bioavailability of resin acids under acidic conditions. This result corresponds to the fact that resin acid extractability has been observed to diminish with time after storage under slightly acidic conditions (Kulovaara et al. 1987).

A good fit to the experimental substrate depletion data was obtained with a Monod model that was modified to include a threshold concentration (equation (2-32)). Thus, conventional Monod kinetics (equation (2-28)), that are commonly used to design wastewater treatment systems, may not give the best representation for toxicity removal. While a compound may be readily biodegradable, a residuum concentration, that is not predicted by traditional Monod kinetics, can persist. Even if this residuum is below the level of acute toxicity, its discharge can still pose an environmental threat if the contaminant is known to bioaccumulate. Resin acids have been reported to concentrate in tissues of fish (Niimi and Lee 1992). Therefore, although biological treatment may provide an economic means to remove the bulk of a toxic contaminant from a wastewater stream, the presence of a threshold concentration after biological treatment may necessitate subsequent effluent polishing. Literature reports of high removal efficiencies for a particular contaminant can be misleading. Typically, literature data are obtained for the removal of a given contaminant, under steady state conditions, for a particular hydraulic retention time. Such work is incomplete since it cannot be known if the observed effluent concentration is either an inherent threshold due to a restriction in bioavailability, or whether it is a function of the removal kinetics. The wastewater treatment design strategy to contend with limitations in

contaminant bioavailability would need to be quite different. For instance it might be necessary to introduce surfactants to help solubilize the hydrophobic contaminants. For ionogenic contaminants like resin acids, pH control appears to be an important factor for controlling solubility and associated bioavailability.

While these results support the findings of Liu (1993) for resin acid biodegradation under either acidic or alkaline media conditions, the findings of Hemingway and Greaves' (1973) were also reproduced in the sense of a reduced extent of removal below pH 7. The observed preferential microbial growth on sodium acetate when this carbon source was included in the medium further suggests that diauxic growth was indeed a factor in the results presented by Hemingway and Greaves.

The collected dynamic surface tension data were modelled well by a family of quasi-static adsorption isotherms. Similar to a previous investigation of resin acid adsorption (Liu et al. 1996a), a Langmuir isotherm provided a good representation of the data. The method of data reduction that was developed for the present study has a far greater scope of application, since the theory is independent of the isotherm chosen. For example, solute interaction at the surface can be accounted for by Temkin adsorption (Kohler 1993). Solute interaction and molar surface area would be incorporated by a Van der Waals adsorption model. However, a practical complexity may arise with the use of more comprehensive isotherm models due to the increased number of parameters that would need to be determined.

The observed qualitative differences in the isotherms at different pH conditions reflect significant changes to the properties of resin acids in the BKME. These changes do not occur in isolation, but are probably influenced by the presence of other dissolved organic compounds in the effluent. Lignin is the second most abundant component of wood, representing 25-30 percent of its weight. The ubiquitous high molecular weight kraft lignin released during wood fibre pulping is a poly-electrolyte with surfactancy that was also found to diminish with pH. Marton (1964) has shown that, like resin acids, the solubility of kraft lignin decreases with decreasing pH. The increased colloidal nature of resin acids at lower pH is evident from the higher suspended fraction observed.

Therefore, as pH decreases, both resin acids and kraft lignin exhibit reduced solubility. As a result, it is likely that, under acidic conditions, resin acids will form associations with other resin acids in solution, and also with the kraft lignin. Decreased diffusivity with increased effective molecular weight (size) was reflected by the lag time for adsorption that increased with decreasing pH. Surface tension lowering, under acidic conditions, indicated that resin acids, complexed with other organic matter in solution (kraft lignin), were still surface active. However, the larger effective size for the hydrophobic complex, should mean a less efficient packing arrangement at the interface. This notion was confirmed by the fact that the limiting resin acid loading (Γ_L) at pH 6 was roughly half that at pH 8. The limiting surface loading (Γ_L) was observed to be 0.13 nmoles/cm² at pH 6, versus 0.24 nmoles/cm² at pH 8.

The solubility of kraft lignin is influenced by ionic strength, however, up to a 0.10 molar salt concentration, the change in solubility is most pronounced below pH 7 (Marton 1964). Therefore, association between kraft lignin and resin acids in solution is likely to become more significant only below pH 7. The adsorption data at pH 7 suggest that resin acid self-association dominated the resin acid interactions at this pH. Tendency towards self-association at pH 7 was observed in the first instance by the presence of a critical micelle concentration. The critical micelle concentration (CMC) of potassium dehydroabietate is approximately $2.5-3.0 \times 10^{-2}$ molar (Corrin et al. 1946; Kolthoff and Stricks 1948). A mixture of dehydroabietic acid with dehydroabietate should have a lower CMC.

Further, the lag time for adsorption (τ_a in Figure 2-11) was longer than at pH 8, indicating a higher effective molecular weight of the adsorbing solute. In contrast to the limiting surface loading at pH 6, Γ_L at pH 7 was higher than at pH 8. The derived value for Γ_L at pH 7 was 0.30 nmoles/cm², versus 0.24 nmoles/cm² at pH 8. Therefore, the adsorbed complex at pH 7 likely consisted of an arrangement of the more hydrophobic protonated resin acids sequestered by the more soluble dissociated resin acids. Changes in the limiting surface loading with pH therefore indicate the presence of a maximum in the absorbable amount of resin acid, depending on the extent of molecular association induced by changing solubility with pH. Hence, a wastewater

treatment unit process, that makes use of contaminant adsorption, must consider both the potential extent for adsorption (Γ_L) in addition to the kinetics of adsorption (β_a in equation (2-44)). The potential for micelle formation is another practical consideration. Thus, although the potential surface loading at pH 7 was greater than at pH 8, these gains may be offset by the observed increased lag time and also micelle formation above a 100 micromolar concentration.

As part of the CPAR program, Ng (1977; 1974b) investigated the feasibility of foam separation as a stand-alone physical unit process to detoxify bleached kraft mill effluent. Foam separation removed up to 65 percent of the resin acid content of the effluent and a pH greater than 7 was necessary for consistent detoxification. Branion (1992) more recently made preliminary tests into foam fractionation for thermomechanical pulping wastewater. Similarly to Ng et al.'s results on BKME, no significant removal was noted at pH 5, while a 60 percent reduction occurred at pH 9. The surface tension data and accompanying adsorption theory of the present investigation have provided the model framework to predict and explain the empirical observations of these previous investigations. Ng et al. experimentally tested a number of parameters in order to optimize their unit process. Such experimental investigations of trial and error may not be the most efficient for determining optimal design parameters. From the results of this experiment it should be apparent that a number of systematic *dynamic* surface tension measurements can yield more fundamental information about the adsorption process. Armed with kinetic parameters for adsorption, a sensitivity analysis for the factors that most influence the adsorption unit process can be readily made numerically by computer simulation (Clarke and Wilson 1983). Once the important process parameters have been identified, an engineer would have better guidelines with which to base the process prototype design.

That limiting bioavailability is a factor behind the observed increased Monod threshold concentration (S^*) at pH 6 is supported by the corresponding adsorption flux threshold concentration (c_b^*) that increased from pH 7 to pH 6 (Figure 2-13). The observed flux threshold, c_b^* , indicated a limiting concentration at which the resin acids could no longer be considered as free solutes in solution. Below c_b^* , what adsorbed was likely an amorphous complex of high

molecular weight material into which some resin acid was dissolved. Adsorption of the kraft lignin was expected since high molecular weight organochlorines in pulp mill effluent have been shown to adsorb to biomass (Yan and Allen 1994). The overall drop in solute flux with pH, measured by the adsorption lag time (τ_a in Figure 2-11) can be related to an increased effective size of the complexed solute molecule in solution. In other words, the observed decrease in resin acid diffusivity with pH is explained by an effective increase in molecular size of the adsorbing solute. The change in the functionality (equation (2-52)) relating solute flux to the concentration also reflects the change in the nature of resin acids in solution over the pH range tested.

Therefore, much insight has been gained by studying the surfactancy of resin acids during their biological oxidation. Since compounds like resin acids are believed to be degraded intracellularly (Sikkema et al. 1995), the transport and adsorption to biomass are important steps in their removal. A fundamental understanding of the conditions that can strongly influence the delivery of a contaminant to a microorganism can only assist in identifying causes of limitations and routes for optimisation in treatment processes. Limitations in contaminant transport become increasingly relevant when trace residual concentrations are sufficient to cause acute or chronic toxicity.

The approach taken in the interpretation of the dynamic surface tension measurements provided model time-implicit relationships and parameter values that have engineering application in computer simulation for the design of new or optimized treatment processes. The derived rate expression for surface loading (equation (2-51)) was not the same as the equation (2-8) assumed by Clarke and Wilson (1983). Therefore, modelling the fate of a surfactant solute requires parameters and relationships that should first be determined experimentally.

While the attention of this study has been directed towards resin acids in pulp mill effluent, it should be noted that toxic organic contaminants are, in general, weakly soluble and hydrophobic. Thus the technique used for this investigation should be equally informative for a similar study on pentachlorophenol for example. In addition to the application of dynamic surface tension measurements to expose the nature of hydrophobic contaminants in wastewater, the measurement technique also has application as rapid method for effluent monitoring. Resin acids are one of a

plethora of hydrophobic contaminants in pulp mill effluent (Sunito et al. 1988). XAD resin adsorption experiments (Dixon et al. 1992) have demonstrated that 70-75 percent of the total organic carbon content from whole mill effluent is composed of hydrophobic molecules. A reduction in effluent foaming tendency, which is related to the concentration of these hydrophobic compounds, has also been shown to parallel BOD removal (Carpenter and Gellman 1966). Therefore, BOD and toxicity removal from pulp mill effluent by biological treatment can, in principle, be calibrated to dynamic surface tension measurements. However, the factors affecting the survival of fish exposed to pulp and paper mill effluent also include ammonia, carbon dioxide, chlorine, dissolved oxygen, dissolved solids, heavy metals, pH, sulphur compounds, suspended solids and temperature (Brouzes 1976). Thus dynamic surface tension monitoring would only test for the onset of one probable cause for toxicity breakthrough.

The acute toxicity of BKME varies widely between mills and between effluents from the same mill discharged at different times (Walden and Howard 1981). Toxicity variation can occur over periods as short as 15 minutes. At the other extreme, fluctuations in bleachery effluent toxicity occur on the time scale of one or two hours. Further, some pulp and paper mills are equipped to run more than one kind of pulping process simultaneously. Dixon (1992), characterising the molecular weight distribution of contaminants in mill effluents, found from successive samples that, while colour and total organic carbon remained similar, the molecular weight distributions shifted. These shifts represent changes in the organic components, which may in turn influence biological treatability. It may be possible to relate shifts in the organic content of pulp mill wastewater prior to biological treatment to trends in dynamic surface tension.

While inherent variability seems to be a natural aspect of pulp mill effluent, limitations in the frequency and extent of treatment plant monitoring mean that it is often difficult to retrace the causes of toxic breakthrough after the fact. Occurrences of toxic discharges are not highly publicized and data are not readily available. Toxicity monitoring is typically performed by weekly LC₅₀ bioassays on *Daphnia magna* and monthly LC₅₀ bioassays on fish. Knowledge of a toxicity breakthrough event may therefore lag days or weeks behind its occurrence. Periodic

events would go unnoticed. Therefore, a reliable technique that can flag the onset of an upset has significant practical application for environmental protection. Dynamic surface tension measurements made as a regular process control measurement could be used to signal the alarm of a potential toxicity event due to compounds like resin acids if a trend of increasing surfactancy is monitored. The technique is amenable to automation.

2.5 Conclusions

The pH-dependent resin acid flux to a gas/liquid interface suggests that acidic conditions promote the association of resin acids with other dissolved organic matter. Under alkaline conditions, resin acids are relatively mobile surfactants in solution. Under acidic conditions, a significant threshold concentration exists, at which the flux of resin acids to a gas/liquid interface becomes independent of the resin acid concentration.

In parallel to the surface tension measurements, after batch growth treatment an elevated threshold concentration for resin acid removal was observed under acidic growth conditions. This threshold or residuum was modelled as the level at which microbial growth could no longer be supported. The residuum was observed to be present primarily in the suspended resin acid fraction of the medium. Thus, although resin acids were shown to be readily removed under acidic or alkaline conditions, the observed residuum in conjunction with the solubility and surface tension data indicate a pH-dependence for the contaminant bioavailability. Resin acids become less mobile under acidic conditions, resulting in a reduced potential extent of biological removal.

It is important to note that the removal of resin acids during the reported batch treatments was assumed to be due to biological activity. Although biomass changes were monitored, the resultant microbial protein data were unreliable. Therefore, for the subsequent investigations, a better monitor for biomass was required.

Therefore, with respect to objective A in Chapter 1, the data from this preliminary investigation indicate that pH-dependent resin acid solubility significantly influences the contaminant bioavailability under acidic pH conditions. Differences in the growth rates were observed. However, without reliable biomass data, the kinetic coefficient values could not be interpreted with confidence. Therefore, a second batch treatment investigation was required to reaffirm the present conclusions (Objective A - Chapter 1) and to better consider any pH-dependence for the microbial growth kinetics (Objective B - Chapter 1). The second batch treatment investigation is reported in Chapter 3, Microbial Community Structure in the Kinetics of Resin Acid Removal.

Dynamic surface tension measurements made by the maximum bubble pressure method during batch microbial growth were instrumental in interpreting the interactions of resin acids in solution. The quasi-static adsorption theory that was developed for the purpose of this investigation, facilitated the formulation of mathematical models that were useful for explaining both the current results and the related literature. The development of such adsorption models has application in computer simulation for process design. Further, the results suggest that dynamic surface tension measurements could be utilized as an informative treatment process monitor. Such a process monitor would serve as an early warning indicator of a mill or bioreactor upset that would have a high potential of leading to an event of toxicity breakthrough.

2.6 References

- Adamson, A. W. (1982). *Physical Chemistry of Surfaces*, John Wiley & Sons.
- Alexander, M. (1994). *Biodegradation and bioremediation*, Academic Press.
- Bailey, J. E., and Ollis, D. F. (1986). *Biochemical Engineering Fundamentals*, McGraw-Hill.
- Bendure, R. L. (1971). Dynamic surface tension determination with the maximum bubble pressure method. *Journal of Colloid and Interface Science*, 35(2), 238-248.
- Bendure, R. L. (1975). Introduction to foams and their physical-chemical properties. *Tappi Journal*, 58(2), 83-87.
- Berk, D., Zajic, J. E., and Behie, L. A. (1979). Foam Fractionation of Spent Sulphite Liquor Part II: Separation of Toxic Components. *The Canadian Journal of Chemical Engineering*, 57, 327-332.
- Berthouex, P. M., and Brown, L. C. (1994). *Statistics for Environmental Engineers*, Lewis Publishers.
- Bicho, P. (1995). Personal communication. , Forest Products Biotechnology, University of British Columbia, Vancouver, BC.
- Bing, Y., Xiu, D., and Yajun, S. (1988). Foam fractionation technique II. Design method about foam fractionation column. *Journal of East China Institute of Chemical Technology*, 14(5), 579-587.
- Branion, R. (1992). Treatment of thermomechanical pulping wastewaters. #13(RC 18), #13(RC 20), *STDF-AGAR 13(SA-2)*, Science Council of British Columbia Research Grants, Vancouver.
- Brasch, D. J. (1974). The foam fractionation of spent kraft pulping liquor. *Appita*, 28(1), 29-32.
- Brouzes, R. J. P. (1976). Fish toxicity with specific reference to the pulp and paper industry. *EPS 3-WP-76-4*, Environment Canada.
- Brown, A. S., Robinson, R. U., Sirois, E. H., Thibault, H. G., McNeill, W., and Tofias, A. (1952). Critical micelle concentrations by a bubble pressure method. *Journal of Chemical Physics*, 56, 701-705.
- Brownlee, B., Fox, M. E., Strachan, M. J., and Joshi, S. R. (1977). Distribution of dehydroabiatic acid in sediments adjacent to a kraft pulp and paper mill. *Journal of the Fisheries Research Board of Canada*, 34, 838-843.
- Bruun, H. (1952a). An interpretation of the effect of ionization upon monolayer properties of rosin acids. *Acta Chemica Scandinavica*, 6, 955-957.
- Bruun, H. (1952b). Properties of monolayers of rosin acids. *Acta Chemica Scandinavica*, 6, 494-501.
- Burcik, E. J. (1950). The rate of surface tension lowering and its role in foaming. *Journal of Colloid Science*, 5, 421-436.
- Burcik, E. J. (1953). Effect of electrolytes on the rate of surface tension lowering; the rate of surface equilibrium attainment as a factor in detergency. *Journal of Colloid Science*, 8, 520-528.
- Callen, H. B. (1985). *Thermodynamics and an introduction to thermostatics*, John Wiley & Sons.
- Carlberg, G. E., and Stuthridge, T. R. (1996). Environmental fate and distribution of substances. *Environmental Fate and Effects of Pulp and Paper Mill Effluents*, M. R. Servos, K. R. Munkittrick, J. H. Carey, and G. J. van der Kraak, eds., St. Lucie Press, 169-178.
- Carpenter, W. L., and Gellman, I. Measurement, control and changes in foaming characteristics of pulping wastes during biological treatment. *Industrial Waste Conference*, Purdue, 203-213.
- Chandrasekaran, K., Reis, R., Tanner, G., and Rogers, H. (1978). Removing toxicity in an aerated stabilization basin. *Pulp & Paper Canada*, 79(10), T304-309.
- Clarke, A. N., and Wilson, D. J. (1983). *Foam flotation: theory and applications*, Marcel Dekker.
- Clesceri, L. S., Geenberg, A. E., and Trussell, R. R. (1989). Standard Methods for the Examination of Water and Wastewater. , M. A. H. Franson, ed., APHA, AWWA, WPCF.
- Corrin, M. L., Klevens, H. B., and Harkins, W. D. (1946). The determination of critical concentrations for the formation of soap micelles by the spectral behavior of pinacyanol chloride. *Journal of Chemical Physics*, 14(8), 480-486.
- Dang, J. S., Harvey, D. M., Jobbagy, A., and Leslie Grady Jr., C. P. (1989). Evaluation of biodegradation

- kinetics with respirometric data. *Journal of the Water Pollution Control Federation*, 61(11/12), 1711-1721.
- Davies, J. T., and Rideal, E. K. (1963a). Chapter 5 - Properties of monolayers. *Interfacial Phenomena*, Academic Press, 217-281.
- Davies, J. T., and Rideal, E. K. (1963b). Chapter 8 - Disperse Systems and Adhesion. *Interfacial Phenomena*, Academic Press, New York and London, 343-451.
- Dixon, D. R., Wood, F. J., and Beckett, R. (1992). Characterization of organics in pulp and paper mill effluents before and after physicochemical treatment. *Environmental Technology*, 13, 1117-1127.
- Draper, N. R., and Smith, H. (1966). *Applied Regression Analysis*, John Wiley & Sons.
- Drobosyuk, V. M., Borodulina, M. R., Krylatov, Y. A., and Talmud, S. L. (1982). The dispersive power of resin acids and fatty acids. *Journal of Applied Chemistry of the USSR*, 55(9), 2105-2107.
- Duncan, B. (1993). Foam samples collected from the Fraser River. , BC Environment.
- Ertl, G. (1983). Kinetics of chemical processes on well-defined surfaces. *Catalysis Science and Technology*, J. R. Anderson and M. Boudart, eds., Springer-Verlag, 209-282.
- Fein, J., Beavan, M., Effio, A., Gray, N., Moubayed, N., and Cline, P. (1992). Comprehensive study of a bleached kraft mill aerobic secondary treatment system. *Water Pollution Research Journal of Canada*, 27(3), 575-599.
- Finch, J. A., and Smith, G. W. (1972). Dynamic surface tension of alkaline dodecylamine acetate solutions in oxide flotation. *Mining and Metallurgy*(12), C213-218.
- Gao, T., and Rosen, M. J. (1995). Dynamic surface tension of aqueous surfactant solutions 7. Physical significance of dynamic parameters and the induction period. *Journal of Colloid and Interface Science*, 172, 242-248.
- Gref, R. (1988). Gas chromatographic analysis of underivatized resin acids. *Journal of Chromatography*, 448, 428-432.
- Halbrook, N. J., and Lawrence, R. V. (1966). The isolation of dehydroabietic acid from disproportionated rosin. *J. Org. Chem.*, 31, 4246-4247.
- Hansen, R. S. (1960). The theory of diffusion controlled absorption kinetics with accompanying evaporation. *Journal of Chemical Physics*, 64, 637-641.
- Hassett, J. P., and Anderson, M. A. (1979). Association of hydrophobic organic compounds with dissolved organic matter in aquatic systems. *Environmental Science and Technology*, 13(12), 1526-1529.
- Hemingway, R. W., and Greaves, H. (1973). Biodegradation of resin acid sodium salts. *Tappi Journal*, 56(12), 189-192.
- Hirt, D. E. (1990). Dynamic surface tension of hydrocarbon and fluorocarbon surfactant solutions using the maximum bubble pressure method. *Colloids and Surfaces*, 44, 101-117.
- Hoff, J. T., Mackay, D., Gillham, R., and Shiu, W. Y. (1993). Partitioning of organic chemicals at the air-water interface in environmental systems. *Environmental Science and Technology*, 27, 2174-2180.
- Holmberg, A. (1982). On the practical identifiability of microbial growth models incorporating Michaelis-Menten type nonlinearities. *Mathematical Biosciences*, 62, 23-43.
- Hornbeck, R. W. (1975). *Numerical Methods*, Quantum Publishers.
- Hua, X., Y., and Rosen, M. J. (1988). Dynamic surface tension of aqueous surfactant solutions 1. Basic parameters. *Journal of Colloid and Interface Science*, 124(2), 652-659.
- Iliev, T. H., and Dushkin, C. D. (1992). Dynamic surface tension of micellar solutions studied by the maximum bubble pressure method. *Colloid & Polymer Science*, 270, 370-376.
- Incropera, F. P., and de Witt, D. P. (1981). *Fundamentals of Heat Transfer*, John Wiley & Sons.
- Johnson, C. H. J., and Lane, J. E. (1974). Surface shape and the calculation of surface tension from maximum bubble pressure. *Journal of Colloid and Interface Science*, 47(1), 117-121.
- Joos, P., and Rillaerts, E. (1981). Theory on the determination of the dynamic surface tension with the drop volume and maximum bubble pressure methods. *Journal of Colloid and Interface Science*, 79(1), 96-100.

- Keirstead, K. F. (1978). Foam fractionation and surface tension method of characterizing soluble lignins. *Pulp & Paper Magazine of Canada*, 4, T6-9.
- Kobayashi, H., and Rittmann, B. E. (1982). Microbial removal of hazardous organic compounds. *Environmental Science and Technology*, 15(3), 170-183.
- Kohler, H.-H. (1993). Thermodynamics of adsorption from solution. Coagulation and Flocculation: theory and applications, B. Dobiás, ed., Marcel Dekker, 1-36.
- Kolset, K., and Heiberg, A. (1988). Evaluation of the "FUGACITY" (FEQUM) and the "EXAMS" chemical fate and transport models: A case study on the pollution of the Norrsundet Bay (Sweden). *Water Science and Technology*, 20(2), 1-12.
- Kolthoff, I. M., and Stricks, W. (1948). Solubilization of dimethylaminoazobenzene in solutions of detergents - I. The effect of temperature on the solubilization and upon the critical concentration. *Journal of Physical and Colloidal Chemistry*, 52, 915-941.
- Kruzynski, G. (1995). Personal communication. , Department of fisheries and Oceans, Vancouver, BC.
- Kuffner, R. J. (1961). The measurement of dynamic surface tensions of solutions of slowly diffusing molecules by the maximum bubble pressure method. *Journal of Colloid Science*, 16, 497-500.
- Kukkonen, J. (1992). Effects of lignin and chlorolignin in pulp mill effluents on the binding and bioavailability of hydrophobic organic pollutants. *Water Research*, 26(11), 1523-1532.
- Kulovaara, M., Kronberg, L., and Pensar, G. (1987). Recoveries of some chlorophenolics and resin acids from humic water. *The Science of the Total Environment*, 62, 291-296.
- Leach, J. M., Mueller, J. C., and Walden, C. C. (1977). Biodegradability of toxic compounds in pulp mill effluents. *Transactions of the technical section CPPA*, 3(4), TR126-TR130.
- Levenspiel, O. (1984). *The Chemical Reactor Omnibook*, OSU Book Stores, Inc.
- Li, K., Chen, T., Bicho, P., Breuil, C., and Saddler, J. N. (1997). Factors affecting gas chromatographic analysis of resin acids present in pulp mill effluents. .
- Liu, H. W., Lo, S. N., and Lavallée, H. C. (1993). Study of the performance and kinetics of aerobic biological treatment of a CTMP effluent. *Tappi Journal*, 94(12), 172-176.
- Liu, H. W., Lo, S. N., and Lavallée, H. C. (1996a). Mechanisms of removing resin and fatty acids in CTMP effluent during aerobic biological treatment. *Pulp & Paper Canada*, 79(5), 145-154.
- Liu, H. W., Lo, S. N., and Lavallée, H. C. (1996b). Theoretical study on two-stage anaerobic-aerobic biological treatment of a CTMP effluent. *Water Quality Research Journal of Canada*, 31(1), 1-35.
- Lucassen-Reynders, E. H., and van den Tempel, M. Surface equation of state for adsorbed surfactants. *Chemistry, Physics and Application of Surface Active Substances*, Brussels, 779-791.
- Mackay, D., and Paterson, S. (1981). Calculating fugacity. *Environmental Science and Technology*, 15(9), 1006-1014.
- Mackay, D., and Southwood, J. M. (1992). Modelling the fate of Organochlorine chemicals in pulp mill effluents. *Water Pollution Research Journal of Canada*, 27(3), 509-537.
- Mackay, D., Southwood, J. M., Kukkonen, J., Shiu, W. Y., Tam, D. D., Varhanickova, D., and Lun, R. (1996). Modelling the fate of 2,4,6-trichlorophenol in pulp and paper mill effluent in Lake Saimaa, Finland. *Environmental Fate and Effects of Pulp and Paper Mill Effluents*, M. R. Servos, K. R. Munkittrick, J. H. Carey, and G. J. van der Kraak, eds., St. Lucie Press, 219-228.
- Marton, J. (1964). On the structure of Kraft lignin. *Tappi Journal*, 47(11), 713-719.
- Masutani, G. K., and Stenstrom, M. K. (1991). Dynamic surface tension effects on oxygen transfer. *Journal of Environmental Engineering*, 117(1), 126-142.
- McCubbin, N. (1983). The basic technology of the pulp and paper industry and its environmental protection practices. *EPS 6-EP-83-1*, Environment Canada.
- McLeay, D. (1987). Aquatic Toxicity of Pulp and Paper Mill Effluents: A Review. *EPS Report 4/PF/1*, Environment Canada.
- McLeay, D. J., Walden, C. C., and Munro, J. R. (1979a). Effect of pH on toxicity of kraft pulp and paper mill effluent to salmonid fish in fresh and seawater. *Water Research*, 13, 249-254.

- McLeay, D. J., Walden, C. C., and Munro, J. R. (1979b). Influence of dilution water on the toxicity of kraft pulp and paper mill effluent, including mechanisms of effect. *Water Research*, 13, 151-158.
- Muir, D. C. G., and Servos, M. R. (1996). Bioaccumulation of bleached kraft pulp mill related organic chemicals by fish. Environmental Fate and Effects of Pulp and Paper Mill Effluents, M. R. Servos, K. R. Munkittrick, J. H. Carey, and G. J. van der Kraak, eds., St. Lucie Press, 283-296.
- Mysels, K. J. (1990). The maximum bubble pressure method of measuring surface tension, revisited. *Colloids and Surfaces*, 43, 241-262.
- Ng, K. S. (1977). Detoxification of bleached kraft mill effluents by foam separation, PhD, University of British Columbia, Vancouver.
- Ng, K. S., Mueller, J. C., and Walden, C. C. (1974a). Process parameters of foam detoxification of kraft effluent. *Pulp & Paper Magazine of Canada*, 75(7), T263-268.
- Ng, K. S., Mueller, J. C., and Walden, C. C. (1974b). Study of foam separation as a means of detoxifying bleached kraft mill effluents, removing suspended solids and enhancing biotreatability. 233-1, Canadian Forestry Service, Ottawa.
- Niimi, A. J., and Lee, H. B. (1992). Free and conjugated concentrations of nine resin acids in rainbow trout (*Oncorhynchus mykiss*) following waterborne exposure. *Environmental Toxicology and Chemistry*, 11, 1403-1407.
- Nyrén, V., and Back, E. (1958). The ionization constant, solubility product and solubility of abietic and dehydroabietic acid. *Acta Chemica Scandinavica*, 12(7), 1516-1520.
- Palermo, D. R., and Holzer, K. A. (1992). Degradation of BOD and foam in a paper mill aerated lagoon by biological methods. *Tappi Environmental Conference Proceedings*, 811-819.
- Panikov, N. S. (1995). *Microbial Growth Kinetics*, Chapman & Hall.
- Posner, A. M., Anderson, J. R., and Alexander, A. E. (1952). The surface tension and surface potential of aqueous solutions of normal aliphatic alcohols. *Journal of Colloid Science*, 7, 623-644.
- Press, W. H., Flannery, B. P., Teukolsky, S. A., and Vetterling, W. T. (1989). *Numerical Recipes in Pascal*, Cambridge University Press.
- Providenti, M. A., Lee, H., and Trevors, J. T. (1993). Selected factors limiting the microbial degradation of recalcitrant compounds. *Journal of Industrial Microbiology*, 12, 379-395.
- Robinson, J. A. (1985). Determining microbial kinetic parameters using nonlinear regression analysis. *Advances in Microbial Ecology*, K. C. Marshall, ed., Plenum Press, 61-114.
- Robinson, J. A., and Tiedje, J. M. (1983). Nonlinear estimation of Monod growth kinetic parameters from a single substrate depletion curve. *Applied and Environmental Microbiology*, 45(5), 1453-1458.
- Roy-Arcand, L., and Archibald, F. (1996). Selective removal of resin and fatty acids from mechanical pulp effluents by ozone. *Water Research*, 30(5), 1269-1279.
- Ruthven, D. M. (1984). *Principles of adsorption and absorption processes*, John Wiley & Sons.
- Savitzky, A., and Golay, M. J. E. (1964). Smoothing and Differentiation of Data by Simplified Least Squares Procedures. *Anal. Chem.*, 36(8), 1627-1639.
- Servizi, J. A., Gordon, R. W., Rogers, I. H., AND, and Mahood, H. W. (1975). Chemical Characteristics, acute toxicity and detoxification of foam on two aerated lagoons. *Environment Improvement Conference*, 45-52.
- Sikkema, J., De Bont, J. A. M., and Poolman, B. (1995). Mechanisms of membrane toxicity of hydrocarbons. *Microbiological Reviews*, 59(2), 201-222.
- Simkins, S., and Alexander, M. (1984). Models for mineralization kinetics with the variables substrate concentration and population density. *Applied and Environmental Microbiology*, 47(6), 1299-1306.
- Simkins, S., and Alexander, M. (1985). Nonlinear estimation of the parameters of Monod kinetics that best describe mineralization of several substrate concentrations by dissimilar bacterial densities. *Applied and Environmental Microbiology*, 50(10), 81-824.
- Springer, A. M. (1986). *Industrial environmental control - Pulp and Paper Industry*, John Wiley & Sons.
- Stuck, G., and Alexander, M. (1987). Role of dissolution rate and solubility in biodegradation of aromatic compounds. *Applied and Environmental Microbiology*, 53(2), 292-297.

- Sugden, S. (1922). The determination of surface tension from the maximum pressure in bubbles. *Journal of the Chemical Society - Transactions Part 1*, 121, 858-866.
- Sugden, S. (1924). The determination of surface tension from the maximum pressure in bubbles - Part II. *Journal of the Chemical Society - Transactions Part 1*, 125, 27-31.
- Sunito, L. R., Shiu, W. Y., and Mackay, D. (1988). A review of the nature and properties of chemicals present in pulp mill effluents. *Chemosphere*, 17(7), 1249-1290.
- Supelco. (1982). Separating aqueous free carboxylic acids (C2-C5) at ppm concentrations. *GC Bulletin 751G*, Supelco Inc.
- Templeton, L. L., and Leslie Grady Jr., C. P. (1988). Effect of culture history on the determination of biodegradation kinetics by batch and fed-batch techniques. *Journal of the Water Pollution Control Federation*, 60(5), 651-658.
- Thomas, W. D. E., and Potter, L. (1975). Solution/Air Interfaces 1. An oscillating jet relative method for determining dynamic surface tensions. *Journal of Colloid and Interface Science*, 50(3), 397-412.
- Valsaraj, K. T. (1994). Hydrophobic compounds in the environment: adsorption equilibrium at the air-water interface. *Water Research*, 28(4).
- van Agglin, G. (1995). Personal communication. , Ministry of the Environment, Vancouver, BC.
- Volkering, F., Breure, A. M., Sterkenburg, A., and van Andel, J. G. (1992). Microbial degradation of polycyclic aromatic hydrocarbons: effect of substrate availability on bacterial growth kinetics. *Microbiology and Biotechnology*, 36, 548-552.
- Volkering, F., Breure, A. M., van Andel, J. G., and Rulkens, W. H. (1995). Influence of nonionic surfactants on bioavailability and biodegradation of polycyclic aromatic hydrocarbons. *Applied and Environmental Microbiology*, 61(5), 1699-1705.
- Voss, R. H., and Rapsomatiotis, A. (1985). An improved solvent-extraction based procedure for the gas chromatographic analysis of resin and fatty acids in pulp mill effluents. *Journal of Chromatography*, 346, 205-214.
- Walden, C. C., and Howard, T. E. (1981). Toxicity of pulp and paper mill effluents - a review. *Pulp & Paper Canada*, 82(4), T143-T148.
- Ward, A. F. H., and Tordai, L. (1946). Time-dependence of boundary tensions of solutions - 1. The role of diffusion in time-effects. *Journal of Chemical Physics*, 14(7), 453-461.
- Werker, A. G., Bicho, P. A., Saddler, J. N., and Hall, E. R. (1996). Surface tension changes related to the biotransformation of dehydroabiatic acid by *Mortierella Isabellina*. Environmental Fate and Effects of Pulp and Paper Mill Effluents, M. R. Servos, K. R. Munkittrick, J. H. Carey, and G. J. van der Kraak, eds., St. Lucie Press, 139-150.
- Yan, G., and Allen, D. G. (1994). Biosorption of high molecular weight organochlorines in pulp mill effluent. *Water Research*, 28(9), 1933-1941.
- Zanella, E. (1983). Effect of pH on acute toxicity of dehydroabiatic acid and chlorinated dehydroabiatic acid to fish and Daphnia. *Bulletin for Environmental Contamination and Toxicology*, 30, 133-140.
- Zitko, V., and Carson, W. V. (1971). Resin acids and other organic compounds in groundwood and sulfate mill effluents and foams. *Manuscript Report Series No. 1134*, Fisheries Research Board of Canada.

Chapter 3
Microbial Community Structure in the Kinetics of Resin Acid Removal

Summary

The objective of this investigation was to determine the influence of pH on the microbial community structure and the uptake rate of resin acids (Objective B - Chapter 1). The microbial community structures of enrichment cultures degrading resin acids were compared by the statistical analysis of microbial fatty acid compositions. The data indicate that there exists a diversity of communities that can degrade resin acids in nature. Different communities of resin acid-degrading microorganisms exhibited different growth kinetics. For any one experiment, alkaline pH conditions were observed to exhibit optimal removal kinetics. Acidic conditions again resulted in an elevated residuum or threshold concentration for biological removal (Objective A - Chapter 1). While the community of resin acid-degrading organisms varied with the time of sampling from a full scale treatment system, the enrichment culture selected from a biosolids sample was sensitive to pH. A comparison of pure versus mixed culture experimental results, indicated that changes in fatty acid compositions of mixed cultures reflect a change in community structure, more than an adaptative membrane response of individual species.

Table of Contents

3.1 Introduction	81
3.1.1 <i>Understanding Biological Removal of Resin Acids</i>	83
3.1.2 <i>Moving Beyond Black Box Wastewater Treatment</i>	88
3.1.3 <i>Biomass and Community Structure from Microbial Fatty Acid Analysis</i>	92
3.1.4 <i>Microbial Lipids, Fatty Acids and Their Analysis</i>	95
3.1.5 <i>A Review of Fatty Acid Compositional Analysis</i>	101
3.1.6 <i>The Principal Objective and Method Specific Issues</i>	121
3.2 Experimental Methods and Materials	123
3.2.1 <i>Mixed Culture Batch Growth Experiments</i>	123
3.2.2 <i>Pure Culture Batch Growth Experiments</i>	127
3.2.3 <i>Mixed Culture Method Control Experiments</i>	128
3.3 Results	132
3.3.1 <i>Equivalent Chain Length (ECL) Methodology</i>	132
3.3.2 <i>Mixed Culture Method Control Experiments</i>	136
3.3.3 <i>Pure Culture Batch Growth Experiments</i>	139
3.3.4 <i>Mixed Culture Batch Growth Experiments</i>	142
3.4 Discussion	167
3.5 Conclusions	177
3.6 References	179

3.1 Introduction

The objective of this phase of the overall study was to consider how changes in pH may affect the microbial growth kinetics in resin acid removal (Objective B- Chapter 1). Secondary wastewater treatment plants are designed to reduce effluent biochemical oxygen demand (BOD) and total suspended solids (TSS) (Metcalf & Eddy 1991), but are relied upon for consistent effluent detoxification. The removal of specific organic contaminants is one aspect of detoxification. Toxic organic contaminants can represent just a small fraction of the overall influent BOD while being a significant proportion of the effluent toxicity towards aquatic life in the receiving water. The removal of BOD cannot necessarily be equated with the removal of toxicity (Mueller and Walden 1976). A challenge in biological detoxification is in the consistent removal of these specific pollutants down to non-toxic levels. Organic pollutants that are toxic to aquatic life at low concentrations, in the order of one part per million, tend to be relatively stable and hydrophobic. Resin acids are such a group of aquatic toxicants specific to pulp mill effluent (Chapter 1).

The previous study (Chapter 2) served to characterize important pH-dependent physico-chemical properties of resin acids that affect the contaminant bioavailability. The nature of resin acid associations in solution can impact the contaminant transport by passive diffusion, which is a required step for microbial uptake. In Chapter 2, a threshold level for biological resin acid removal was observed to increase with decreasing pH. Based on solubility and dynamic surface tension data, the increase in residuum was related to a decrease in the solute mobility. Resin acid uptake kinetics were also observed to change with pH but could not be completely characterized due to the absence of a reliable biomass measure. The previous difficulties encountered with attempts at quantifying biomass by more conventional non-specific assays, were overcome in the present stage of the investigation by extracting, identifying and measuring specific microbial constituents during batch growth. Microbial fatty acids hydrolyzed and extracted from cellular lipid were used to quantify and interpret the growth kinetics of mixed cultures on resin acids as a function of pH. The added benefit of analysing microbial fatty acids

was that relative differences in the structure of microbial communities cultured at different pH levels could be compared. This added information became essential to the data interpretation.

Since solution pH, in the 6 to 8 range, that defines typical treatment operating limits, strongly affected the mobility of resin acids in solution (Chapter 2), it was of interest to know if an optimum growth-linked resin acid removal rate existed in this pH range. Bacteria in a biological treatment system are sensitive to selective pressures like pH. Consequently, the question of the extent to which the community of resin acid degraders is altered by pH has implications for process control. Since pH and the form of resin acids in solution are separate but interdependent effects, it was necessary to try to distinguish between the direct effects of pH on microbial activity and the indirect pH-related effect of a change in resin acid hydrophobicity.

Experiments were therefore undertaken to consider the mechanism of pH-dependence that most influenced the kinetics of resin acid removal. The batch growth kinetics and ecology of mixed cultures enriched for resin acid degraders and acclimated to a number of different pH levels were compared. Pure culture experiments were performed to help in the interpretation of the observations made on the mixed cultures. In addition, control experiments were conducted to help in the interpretation of the results of microbial lipid analysis from mixed cultures.

Research to assess the community structure, as well as the quantity of biomass in a biological treatment system, moves beyond the more traditional black box engineering approach of wastewater treatment. A better understanding of microbial ecology in secondary treatment systems has been pivotal for success in understanding and controlling sludge bulking phenomena (Blackall et al. 1991; Fahmy and Hao 1990; Khan and Forster 1991; Lemmer 1986; Lemmer and Baumann 1988; Richards et al. 1990). An analogous contribution was seen as necessary for understanding and optimising organic toxicant removal in biological systems. The development of this understanding required a readily measurable fingerprint for complex microbial communities that could be used to monitor the kinetics of change and adaptation in response to a variety of environmental stresses. By establishing cause and effect relationships, a fingerprint for the system microbial community could serve ultimately in treatment process control. A

microbial fingerprinting assay that can be adapted to on-line measurement has significant engineering application. Fatty acids extracted from microbial lipids were found to have the potential to be used as such a fingerprint. It is a measurement that is also amenable to some degree of automation. Therefore, microbial fatty acid analysis and its interpretation became a major part of this investigation.

3.1.1 Understanding Biological Removal of Resin Acids

The applied experimental methodology of mixed culture batch growth, following steps of enrichment (Brock and Madigan 1991) with selected resin acids as the sole carbon source, is a simplification of a full scale secondary treatment system. The scientific approach of reduction of complicated processes can provide data that have little bearing on the system of interest. Therefore, it is important to consider the engineering relevance of this experimental approach to full scale biological wastewater treatment.

The conundrum in laboratory wastewater experiments is in the sufficient simplification of a complex system to yield general and meaningful results that have engineering application for the real process. By oversimplification, the important features of the real system may be lost. The disadvantage of attempting to include too much of the system complexity is that the relationships underlying the results may be difficult to clearly interpret.

Fundamental understanding of microbial activity toward specific organic compounds comes from basic research on pure culture isolates. It is on this footing that some experimental simplification has been made. As noted in Chapter 1, resin acids can be classed into two chemical groups, abietanes and pimaranes (Figure 3-1). Bacterial isolates have been cultured that are quite specific in their ability to degrade either abietanes or pimaranes (Mohn 1995; Wilson et al. 1996). Furthermore, the ability to metabolize the naturally-occurring resin acids does not necessarily confer an ability to metabolize the chlorinated forms (Mohn et al. 1997) which are degraded more slowly (Leach et al. 1977). Pure culture research into the metabolic pathways for the catabolism of dehydroabietic acid indicates that different organisms have

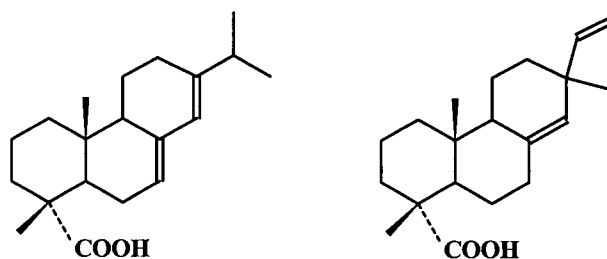


Figure 3-1. Chemical structure of abietic (left) versus pimaric acid (right). Both abietanes and pimaranes are based on the same diterpene hydrocarbon skeleton. Abietic-type acids have an isopropyl side chain, while pimaric-type acids have the methyl and vinyl substituents at this site. Abietanes have greater isomerization reactivity than the pimaranes due to their two conjugated double bonds. Some microorganisms are specific in their abilities to degrade either of these two forms of resin acid.

developed similar, but distinct strategies of enzymatic attack (Biellmann et al. 1973a; Biellmann et al. 1973b). Therefore, results from mixed culture laboratory experiments using a cocktail of resin acids would be clouded by the uncertainty of community variability due to the complex feed composition. In other words, if each individual resin acid can support the growth of a number of individual microbial species, then the number of possible distinct communities of resin acid degrading microorganisms increases with the number of resin acids composing the substrate mix.

To constrain the number of possible community permutations, only abietane resin acids were considered. A study using only these selected resin acids is without any loss in generality because, based on the literature, enrichment cultures for pimaranes, chlorinated resin acids or mixtures thereof, could have also been generated. The decision to use only one resin acid type, was to more clearly isolate the influence that pH and pH-dependent resin acid solubility have on biodegradation. Although pimaranes and abietanes are a part of the same chemical family and will have similar pH-dependent solubility characteristics, they are, from a microbial perspective, distinct compounds.

Generally, the effect of pH on the removal of a particular compound should decrease with increased diversity of the group of competent microorganisms (Alexander 1994). By including only abietane resin acids in the medium, it was expected that the role of microbial diversity on the contaminant uptake as a function of pH could be assessed. Alexander also comments that the effect of pH on biodegradation of polluting chemicals has received little attention. A lack of

literature experience on pH effects was felt to be further impetus for avoiding any unnecessary experimental complication.

Pure culture microbial research is an extreme, but necessary level of experimental reductionism for obtaining fundamental scientific knowledge about the nature of microorganisms. However, natural or engineered microbial systems contain many interacting species. Neutralism, or the null response of one organism due to the presence of another is apparently rare (Bailey and Ollis 1986). Pure culture studies are inadequate for predicting the fate of substances in the environment if, in practice, removal enlists many interactions between different organisms (Kobayashi and Rittmann 1982). Therefore, pure culture kinetics have limited engineering application. Applied research in wastewater treatment must allow for the potential, if only in a restricted sense, for interactions between microorganisms.

Mutualism, the ability of species to grow faster together, than in isolation, is more common than neutralism (Bailey and Ollis 1986). Mutualism can involve a symbiotic exchange of growth factors, such as dissolved gas exchange between aerobic bacteria and photosynthetic algae. Commensalism is also a form of symbiosis where one species enjoys benefits, such as moderated environmental conditions, provided by the activity of the first. Competition between microorganisms can produce amensalism, or the suffering of a second species as a result of its interaction with the first. Amensalism could be due to the production of toxic compounds (antibiotics) or the removal of essential nutrients. Panikov (1995) discusses a survival or life strategy triad characteristic of microbes, that shape the resultant communities in natural ecosystems. Survival of individual populations within a community will depend on their ability to (a) compete with other populations, (b) recover from environmental perturbations and (c) survive periods of stress.

Real microbial systems involve many interacting populations, operating on a number of trophic levels, that make up a complicated food web of predator and prey (Bailey and Ollis 1986). Meaningful simplification would, therefore, appear to be an oxymoron. However, the experimental method of mixed culture, batch enrichment for resin acid degraders does represent

an important facet of the complete system that can be clearly defined. There are three conceivable mechanisms for the biological removal of a selected organic compound, namely, growth-linked metabolism, uncoupled metabolism and cometabolism (Alexander 1994; Brock and Madigan 1991; Kobayashi and Rittmann 1982).

In growth-linked metabolism, culture biomass increases at a rate that parallels the disappearance of the limiting substrate (Alexander 1994). As a rule, organisms convert organic substrate to CO_2 and water for energy to proliferate. In the process, leaked products of catabolism may similarly support the growth of other organisms. Oxygen serves not only as the terminal electron acceptor in aerobic respiration, but also as a substrate, in oxygenase-catalyzed reactions necessary for ring cleavage and hydroxylation (Providenti et al. 1993). The cellular efficiency in the conversion or yield of biomass from organic carbon varies with metabolic pathway, organism, substrate, concentration and environmental conditions. For growth to occur, the compound must first be transformed enzymatically to chemical intermediates that are components of the major metabolic pathways such as the tricarboxylic acid cycle (Brock and Madigan 1991), that are common to heterotrophic microorganisms. The initial catabolic steps could be accomplished as a consorted effort of a number of species in the community.

In some situations, organic mineralization is uncoupled from growth and acts only to maintain rather than proliferate populations (Alexander 1994). Catabolism for maintenance energy sustains motility, intracellular and extracellular concentration gradients, and the replenishment of hydrolysed macromolecules (Sherrard and Schroeder 1973). Another form of non-growth related respiration is in the cellular response to abrupt environmental transitions such as swings of 'famine to feast' (Panikov 1995). Thresholds of removal exist when slow substrate utilisation kinetics that occur with very low concentrations, provide insufficient energy flux for maintenance (Kobayashi and Rittmann 1982). Contaminants may also persist if their concentrations are too low to induce the production of the necessary catabolic enzymes.

Co-metabolism occurs when other organic material is present as the primary energy source for growth and a secondary breakdown of the target contaminant occurs (Brock and Madigan 1991;

Kobayashi and Rittmann 1982). For example, pentachlorophenol degradation is enhanced with the addition of glutamate to the growth medium (Providenti et al. 1993). However, diauxic growth, or the preferential metabolism of alternate carbon sources may limit biodegradation of the target contaminant. Diauxic growth was observed in the present study for batch growth on a mixture of sodium acetate and resin acids (Chapter 2). It is also possible that the target contaminant can be gratuitously metabolized by the production of enzymes induced by the presence of another substrate. If the microbial community removing the target substrate is small and is governed solely by co-metabolism, then an increase in the contaminant loading will not increase the community size and the conversion rate will be maintained (Alexander 1994).

In a secondary biological treatment process, the contribution of growth-linked, uncoupled and cometabolic mechanisms will sum to yield the net observed removal rate. Respirometric methods have been developed for determining the extant or *in situ* biodegradation kinetics of specific organic compounds (Ellis et al. 1998). However, such a measurement cannot distinguish the relative contributions of the three separate mechanisms. Measurement of extant kinetics provides information of an immediate nature that is specific to the history of the biomass sample. Determining extant kinetics relies on an assumption about the biomass fraction metabolising the test compound. The respective biomass fraction is usually assumed to be proportional to the fraction of the influent biodegradable chemical oxygen demand (COD) contributed by the target compound. However, this estimate of the biomass fraction implicitly assumes only growth-linked metabolism. Instead of assuming growth-linked metabolism, the approach of the current investigation was to explicitly measure growth-linked mixed culture metabolism. This was seen as a starting point from which, in future work, the other possible mechanisms of biological resin acid removal could eventually be considered. Selection for growth-linked metabolism can be ensured by culture enrichment using the target contaminant as the sole carbon source.

Culture enrichment is the first step in the protocol used by microbiologists to obtain isolates that grow on one selected carbon source (Alexander 1994; Brock and Madigan 1991). Small

inoculum transfers from sequential batch growth cycles will dilute out of the system those organisms that do not grow. Contributions of cometabolism and uncoupled growth are thereby washed out. By the competitive exclusion principle (Bailey and Ollis 1986), when two species compete in a common environment, one species eventually disappears. Competitive exclusion through culture enrichment selects for the fastest growing community of bacteria. Some members of the community may grow quickly on the substrate, others may be able to maintain their numbers by mutualism or commensalism. Therefore, while enrichment on a sole carbon source may procure isolates, the procedure selects for the fittest growth-linked community that will entail both isolates and partnerships. Prey dynamics are also not ruled out, but these will only become important once growth on the primary carbon source slows down during the decline phase (Alexander 1994).

The existence of only growth-linked substrate removal by the enrichment culture can be verified from experimental data of substrate depletion and biomass production. The specific rate of substrate removal should correspond directly to the specific rate of biomass production. Microbial diversity can be assessed by the variability between the ecology of one enrichment culture and another. Assessment of the microbial community structure, moves beyond the more traditional approach of black box wastewater treatment.

3.1.2 Moving Beyond Black Box Wastewater Treatment

Biological treatment processes are complex, controlled microbial ecosystems containing a mixed community of microorganisms interacting with each other, and their local environment to affect the concentrations of individual pollutants. There are many examples in the literature that demonstrate how activated sludge can acclimate to degrade many organic contaminants under steady state conditions, with a variety of bioreactor configurations. Demonstration of biodegradability is necessary for determining the feasibility of using a *biological* system to remove toxic organic contaminants, versus other physical, or chemical treatment methods. However, the requirement for microbial acclimation does limit the ability of biological systems to accommodate process transients. This limitation has often been implicitly neglected in the

research reported in the literature, since steady state removal is typically investigated.

Experimental studies into biological treatment generally utilize steady state bioreactor operation, in which the success of the process is equated to a high removal efficiency. In contrast, real systems continually experience both hydraulic and contaminant loading transients. The rate at which microorganisms acclimate to these transients is, therefore, an important facet of treatment reliability.

If a microbiological wastewater treatment approach has been shown to be feasible, then representative rates of biodegradation are needed to assess its practical application. For instance, tank volume and aeration cost are important design constraints. Conservative mathematical modelling used to design and predict the expected performance of full scale biological treatment systems requires intrinsic rate constants (Grady 1990). Rate constants must be obtained experimentally with bench or pilot scale biological treatment processes. Generally, the mixed microbial culture in a continuous flow treatment system is considered to be a single, so-called "pseudo-species" (Bailey and Ollis 1986). Effective kinetics for any given pseudo-species can be determined from batch growth experiments inoculated with biomass from continuous flow systems (Ellis et al. 1998; Klecka and Maier 1985; Shamat and Maier 1980).

Computer simulations of a full scale process can then be made assuming that those kinetic parameters are valid and that the fraction of the total biomass acting on the xenobiotic compound is proportional to its contribution to the total biodegradable chemical oxygen demand (COD). However, unqualified use of these experimentally-determined microbiological rate constants is tenuous, because the history of the mixed culture in a batch growth experiment influences the resulting kinetic parameters (Templeton and Grady 1988). Mixed microbial populations are dynamic entities that are strongly dependent on the culture history and the selective pressures created by the growth conditions (Chiu et al. 1972). Changes in selective pressures on mixed populations by altering such factors as cell recycle rate, inlet flow rate, feed composition, temperature and pH will produce markedly changed microbiological communities or so called pseudo-species.

Degradation experiments using a pure microbiological culture will provide kinetic parameters which are intrinsic to that particular organism under the particular set of growth conditions chosen. Unfortunately, due to the inherent variability of mixed-microbial populations, similar kinetic characterization of mixed culture systems cannot be intrinsic without a means to distinguish one mixed population from another. Hence, if the black box or pseudo-species approach is applied to experimentation with mixed microbial populations, experimentally-derived kinetic parameters should be taken as extrinsic and, strictly speaking, locally and temporally limited in their scope of application. A black box approach to mixed populations makes it impossible to be sure of the source of the variability in the growth parameters estimated with repeated experimentation. Comparison of kinetic constants by researchers has little value unless it can be confirmed that the substance in the black box is of a similar or dissimilar nature. If similar rate constants are consistently found with a variety of pseudo-species, then more confidence is generated regarding the robustness of the biological process with respect to the target contaminant. Conversely, if a variety of pseudo-species produce a range of rate constants, then a large factor of safety must be employed in designing the treatment process. If pseudo-species changes are sensitive to particular bioreactor conditions then tighter process control may be required. Therefore, significant advancement could be made in the interpretation and application of mixed population kinetic parameters, if some form of fingerprint could be obtained to characterize a degree of similarity between microbial communities.

One attractive method to compare mixed communities of microorganisms originates from the study of lipid extracts from biomass samples (Vestal and White 1989). The attraction of this approach for the present study is related to the ability of the method to quantify low concentrations of biomass during batch growth in a pulp mill effluent matrix. Since bacterial lipid analysis also enables the measurement of the community structure (quality) as well as the quantity of the biomass, a significant step can be made beyond the limitations of more conventional environmental engineering black box microbiology. In the present study, a measure for biomass was needed for determining growth yields and specific growth rates. A measure for biomass community structure was useful for the interpretation of variability in

growth yields and rates for different experimental conditions.

The need for a non-conventional measure of microbial biomass arose due to problems with the more conventional methods. Resin acids were a component of the medium suspended solids, whose interference in gravimetric or optical density methods changed with pH and time. Interference from the background high molecular weight dissolved organic matter (HMW DOM) or kraft lignin in the medium was also pH-dependent because these constituents become increasingly colloidal with decreasing pH (Marton 1964). While protein assays were found to be relatively sensitive, the Coomassie Brilliant Blue G dye protein-binding dye assay on membrane filter-harvested cells (Chapter 2) suffered from interference, which increased with decreasing pH. Protein assay interference was attributed to colloidal kraft lignin and resin acid. The dye binding protein assay depends on Van der Waals forces and hydrophobic interactions (Compton and Jones 1985). Aromatic structures show a strong affinity for the dye. Native lignin contains many aromatic functional groups which makes its concentration quantifiable by a related colourimetric technique (see Standard Methods section 5550 (Clesceri et al. 1989)) that is also used for protein assays (Deutscher 1990; Peterson 1977). Time restrictions and other practical limitations during sampling ruled out the use of direct measures of biological activity such as oxygen uptake respirometry or microbial adenosine triphosphate (ATP) extraction. As part of the method development for the present study, attempts at ATP measurement by cold acid extraction (Karl and Craven 1980) and photometric quantification by firefly bioluminescence (Karl 1980) were found to be laborious and imprecise. The extreme labile nature of ATP was a factor in the difficulty of using ATP as a biomass measure. The indicator of viable biomass required for the present experiments needed to be an easily preservable analyte and a conserved microbial constituent with a relatively rapid *in situ* turnover rate.

Microbial fatty acids were selected both as a biomass measurement and a means to differentiate the communities cultured. The assay for microbial fatty acids (see Section 3.2) also offered significant practical advantage since the substrate resin acids could be quantified from the same measurement. Reduction of the sampling and analytical burden permitted the testing of many

more experimental conditions.

3.1.3 Biomass and Community Structure from Microbial Fatty Acid Analysis

Lipid analysis has been developed by microbial ecologists to measure microbial community biomass, structure and activity under *in situ* conditions (Vestal and White 1989). Microorganisms rarely exist in nature as monocultures. The culturing of microorganisms is a process of elimination that allows only certain microbes with specific metabolic properties to grow under the selected conditions of incubation. Growth of microbes on artificial media may reveal only a small fraction of the total microorganisms present in the original system. In principle, isolation techniques may filter out those organisms that are the key members of the communities from the environment under study. Advancement in biological wastewater treatment research requires understanding of the behaviour of complete communities of microorganisms in treatment systems.

Phospholipid fatty acids are a relatively conserved constituent of every cellular membrane. They are not found in storage lipids and furthermore, they undergo a relatively rapid turnover rate in both living cells and non-viable cells added to the environment (White 1983). Cell lipid extracts contain ester-linked fatty acids, typically with carbon chain lengths of 12 to 20 atoms (Harwood and Russell 1984). Gas chromatographic identification of phospholipid fatty acid (PLFA) compositions of pure microbial cultures has application in taxonomic classification of different bacterial and fungal species (Bousfield et al. 1983; Eerola and Lehtonen 1988; Lechevalier and Lechevalier 1988; Moss and Dees 1976; Stahl and Klug 1996). The fatty acid spectra for bacterial members of the same family are qualitatively similar and, for different families, distinguishably different (Kates 1964). While quantitative variations in the relative abundance of fatty acids in a given profile have been observed with changes in the composition of the growth medium and with the age of the culture, the characteristic family pattern remains distinctive (Haack et al. 1994; Kates 1964). Thus, pure bacterial cultures grown under controlled growth conditions have unique whole cell fatty acid profiles which can be used to differentiate even closely related organisms (Miller and Berger 1985). Microorganism genera

and species can be distinguished by the presence or absence of a particular fatty acid and, for well controlled conditions, their relative abundance.

Since changes in the relative abundance of phospholipid fatty acids coincide with physical, chemical or temporal changes in the growth conditions, fatty acid analysis can be used to follow the kinetics of microbial adaptations to transient conditions in biological treatment systems. Cells alter the fatty acids in their lipids as they adapt to environmental conditions to maintain membrane fluidity. Cell viability depends on membrane fluidity necessary for sustaining membrane protein function (Harwood and Russell 1984; Rose 1989). For example, a decrease in growth temperature has been found to result in an increase in the proportion of unsaturated fatty acids (Marr and Ingraham 1962).

Hydrophobic organic contaminants can also influence microbial membrane lipid composition. The general opinion is that: (a) uptake of cyclic hydrocarbons by microorganisms is a passive process, (b) partitioning of these lipophilic compounds into the cytoplasmic membrane is integral to their uptake, and (c) these substrates must enter the cell prior to their metabolism (Sikkema et al. 1994; Sikkema et al. 1995). Since hydrophobic, organic contaminants partitioning to the cell membrane can disrupt membrane lipid-protein interactions (fluidity), they can exert a toxic effect, requiring microbial adaptation before resumption of normal metabolic activity. Analogous to the observed temperature response noted above, fatty acid composition alterations have been induced by alcohols or organic solvents in the growth medium (Ingram 1976; Ingram 1977; Pinkart et al. 1996).

Phospholipid fatty acids have been found useful to track the biomass and community structure in terrestrial (Bruggemann et al. 1995; Cavigelli et al. 1995; Franzmann et al. 1996; Frostegard et al. 1997; Reichardt et al. 1997; Sundh et al. 1997; Tunlid and White 1992; Zelles et al. 1992; Zelles et al. 1994) and marine (Bobbie and White 1980; Gillan and Hogg 1984; Khandekar and Johns 1990; Reemtsma and Ittekkot 1992; White et al. 1979) environments. Recently, lipid analysis has been utilized for monitoring bench scale biofilters treating hydrogen sulfide and volatile organic compounds at a wastewater treatment plant (de Castro et al. 1997; Webster et al.

1997).

Lipid-based biomass measures correlate well with ATP, direct cell enumeration, DNA synthesis and respirometric assays (Balkwill et al. 1988; White et al. 1979; Zelles et al. 1994). Some discrepancy in the correspondence of plate counts to fatty acid concentrations in a biofilter study by Webster et al. (1997), was reported to be due to a decrease in culturable organisms. Due to the presence of non-culturable organisms, plate counts are anticipated to yield lower values than the true numbers present in mixed culture systems (Lechevalier and Lechevalier 1988).

Although phospholipid fatty acid (PLFA) concentration is, in itself, a biomass measure, just as dry weight, protein, ATP, or volatile suspended solids (VSS), conversion of PLFA to more traditional measures is often preferred. *Escherichia coli* has been used as a reference microorganism for conversion of PLFA to numbers of microorganisms. One pica mole of palmitic acid, a fatty acid that is ubiquitous in microbial lipids, is equivalent to about 5×10^5 cells the size of *E. coli* (Baird and White 1985; White 1983). Balkwill et al. (1988) estimated that 100 μmol PLFA is equivalent to one gram dry weight of cells. The conversion by Balkwill et al. assumes a specific cell weight of 5×10^{-13} grams per cell. However, this value for *E. coli* has been reported to be 2.8×10^{-13} g/cell (Brock and Madigan 1991). Thus, there exists some discrepancy in the attempts to estimate cell numbers from PLFA data.

The phospholipid contents of various bacteria have further been shown to vary between 4 and 91 milligrams per gram dry weight (Kates 1964). Specific taxa of bacteria can yield significantly different fatty acid contents, ranging from 11 to 197 μmol of PLFA per gram of dry weight (Haack et al. 1994). The lipid content of microorganisms is also known to vary with environmental conditions (Tunlid and White 1992). Therefore, due to this well-documented variability, a reliance on literature "constants" for conversion of PLFA data is not advisable practice. The PLFA to dry weight ratio could itself be a monitor of community change. PLFA conversion should not be considered necessary since it is, by itself, a reference parameter to be compared and monitored in the same manner as VSS.

Conversion of PLFA data may have some utility when constructing a carbon balance of a treatment system for assessing microbial energetics. The carbon content of bacteria is typically 50% of the dry weight (Metcalf & Eddy 1991). From experimentally-derived PLFA to dry weight ratios, biomass carbon produced, can be estimated and compared to the corresponding organic carbon consumed.

The monitoring of phospholipid fatty acids in bioreactors, as opposed to natural environments, has the advantage that engineered biological systems tend to be relatively well controlled and easily monitored systems. Repeated experiments with bioreactors can be used to establish links between process variables and community adaptations based on phospholipid fatty acid profiles.

3.1.4 Microbial Lipids, Fatty Acids and Their Analysis

The analysis of lipids in microbial samples can entail a suite of assays (Figure 3-2), of which microbial fatty acid identification and quantification is one component (White 1983). The assays inform on biomass, community structure or nutritional status. This information has engineering application in the control of biological wastewater treatment systems (Riebel et al. 1997). Of the measurable constituents shown in Figure 3-2, only fatty acid analysis measures both biomass and community structure. There are a number of fatty acids of varying chain length commonly associated with microorganisms. The major fatty acid groupings are the saturated, unsaturated, branched, cyclic and hydroxy types (Table 3-1). Unsaturated fatty acids in bacteria are typically monoenoic (mono-unsaturated), indicating that the presence of polyenoic fatty acids in a sample can be attributed to contributions from plant, algae, fungi or cyanobacteria (Harwood and Russell 1984).

The nomenclature of fatty acids (Ratledge and Wilkinson 1988a) needs some clarification since different formats appear in the literature, leading to possible confusion. Fatty acids always have a systematic name and, often, a trivial name. For instance, palmitic acid is the trivial name for the saturated sixteen carbon fatty acid, hexadecanoic acid. For clarity, only systematic names will be used in this text. Due to their compactness, shorthand designations will also be

Table 3-1. Generalized chemical structures for the typical groups of bacterial fatty acids.

Bacterial Fatty Acid	Generalized Chemical Structure
Straight Chain Saturated	$\text{CH}_3-(\text{CH}_2)_n-\overset{\text{O}}{\parallel}{\text{C}}-\text{OH}$
Straight Chain Unsaturated	$\text{CH}_3-(\text{CH}_2)_n-\text{CH}=\text{CH}-(\text{CH}_2)_m-\overset{\text{O}}{\parallel}{\text{C}}-\text{OH}$
Branched Saturated	$\begin{array}{c} \text{CH}_3-(\text{CH}_2)_n \\ \quad \quad \quad \diagdown \\ \quad \quad \quad \text{CH}_2-(\text{CH}_2)_m-\overset{\text{O}}{\parallel}{\text{C}}-\text{OH} \\ \quad \quad \quad \diagup \\ \quad \quad \quad \text{CH}_3 \end{array}$
Iso-Branched Saturated	$\begin{array}{c} \text{CH}_3 \\ \diagdown \\ \text{CH}_2-(\text{CH}_2)_n-\overset{\text{O}}{\parallel}{\text{C}}-\text{OH} \\ \diagup \\ \text{CH}_3 \end{array}$
Anteiso-Branched Saturated	$\begin{array}{c} \text{CH}_3-\text{CH}_2 \\ \quad \quad \quad \diagdown \\ \quad \quad \quad \text{CH}_2-(\text{CH}_2)_n-\overset{\text{O}}{\parallel}{\text{C}}-\text{OH} \\ \quad \quad \quad \diagup \\ \quad \quad \quad \text{CH}_3 \end{array}$
Cyclopropane Saturated	$\text{CH}_3-(\text{CH}_2)_n-\overset{\text{O}}{\parallel}{\text{C}}-\text{OH}$ $\begin{array}{c} \text{CH} \\ \diagdown \quad \diagup \\ \text{CH} \quad \text{CH} \\ \quad \quad \quad \diagdown \quad \diagup \\ \quad \quad \quad \text{CH}_2 \end{array}$
α -Hydroxy Saturated	$\text{CH}_3-(\text{CH}_2)_n-\overset{\text{O}}{\parallel}{\text{C}}-\text{OH}$ $\begin{array}{c} \text{CH} \\ \\ \text{OH} \end{array}$
β -Hydroxy Saturated	$\text{CH}_3-(\text{CH}_2)_n-\overset{\text{O}}{\parallel}{\text{C}}-\text{OH}$ $\begin{array}{c} \text{CH}-\text{CH}_2 \\ \quad \quad \\ \text{OH} \quad \quad \text{O} \end{array}$

Table 3-2. Nomenclature for the common groups of fatty acids. Generally the shorthand notation is of the form N:x where N is the number of carbon atoms and x is the number of double bonds. The “ ω n” indicates the nth carbon counting from the methyl end of the chain. Otherwise position of elements should be counted from the carboxyl end of the chain. Shorthand abbreviations are as follows: c-cis, t-trans, br-branched, i-iso, a-anteiso, Me-methyl, cy-cyclo, and OH-hydroxy.

Type	Systematic Name	Shorthand designation		
		Nonspecific	Specific	Alternate
saturated	octadecanoic acid	-	18:0	-
cis-monoenoic	cis-octadec-11-enoic acid	18:1	18:1(11c)	18:1 ω 7c
trans-monoenoic	trans-octadec-11-enoic acid	18:1	18:1(11t)	18:1 ω 7t
dienoic	cis,cis-octadeca-9,12-dienoic acid	18:2	18:2(9c12c)	18:2 ω 6
polyenoic	cis,cis,cis-octadeca-9,12,15-trienoic acid	18:3	18:3(9c12c15c)	18:3 ω 3
branched	10-methyloctadecanoic acid	br19:0	10Me18:0	-
iso-branched	16-methylheptadecanoic acid	br18:0	i18:0	16Me17:0
anteiso-branched	15-methylheptadecanoic acid	br18:0	a18:0	15Me17:0
cyclopropane	cis-11,12-methyleneoctadecanoic acid	cy19:0	cy19:0 ω 7	-
α -hydroxy	2-hydroxyoctadecanoic acid	OH-18:0	2OH-18:0	α OH-18:0
β -hydroxy	3-hydroxyoctadecanoic acid	OH-18:0	3OH-18:0	β OH-18:0

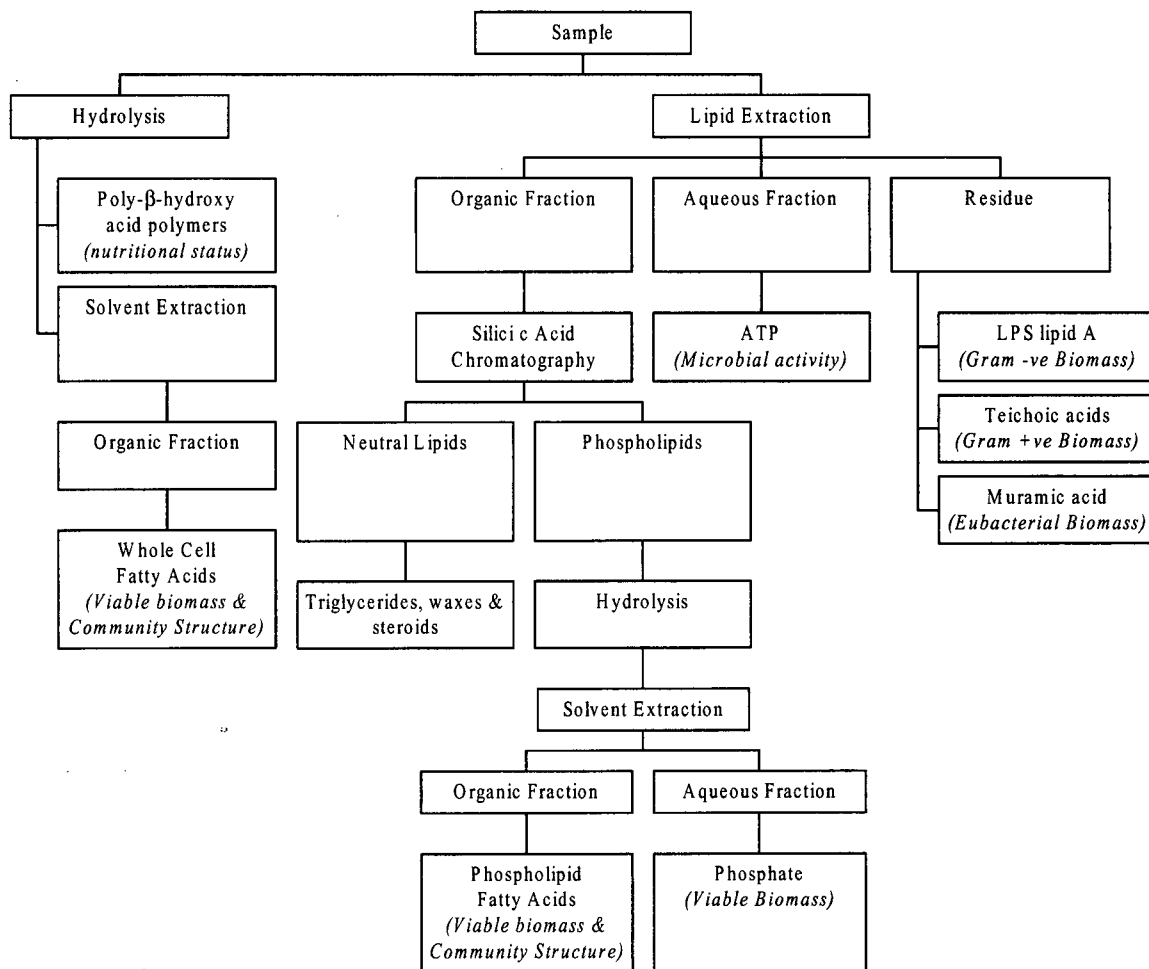


Figure 3-2. Flow diagram for biochemical lipid analysis of natural microbial communities (adapted from Vestal and White (1989)).

frequently used. However, shorthand designations are complicated by non-specific and multiple specific forms of notation. The shorthand notation conventions adopted here are summarized by example in Table 3-2. Generally, carbon locations in a fatty acid are referenced either to the ω -end (methyl end) of the chain or to the carboxyl end. Thus " $\omega 1$ " is the carbon atom furthest from the carboxyl end. With respect to the carboxyl end, the alpha position is the second carbon atom and the beta position is the third carbon atom in the chain.

The specificity of some lipids to particular kinds of microorganisms makes it possible to identify certain biomass fractions. As shown in Figure 3-2, the residue fraction can be assayed for constituents specific to gram negative or gram positive bacteria. For bacterial fatty acid enumeration there are two methodologies in use, namely phospholipid fatty acid (PLFA) and

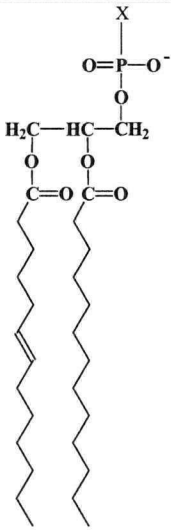
whole cell fatty acid (WCFA) analysis.

Phospholipid fatty acid analysis by definition considers only those fatty acids linked to phospholipids. This form of lipid analysis requires careful separation of microbial fractions before fatty acids are released from their lipids by hydrolysis. The established method of lipid extraction (Tunlid and White 1992; White et al. 1979) is the procedure developed by Bligh and Dyer (1959). Exposing a sample to a single-phase mixture of chloroform, methanol, and water (1.0:2.0:0.8) dissolves lipids while arresting metabolic activity (Vestal and White 1989). Changing the proportions of water and chloroform generates a biphasic mixture and the lipids partition to the lower solvent phase. The extracted lipids can be purified by silicic acid chromatography and the ester-linked fatty acids converted to their methyl esters by mild alkaline methanolysis. The fatty acid methyl esters (FAMES) are readily analysed by gas chromatography (GC) using a flame ionisation detector (FID). This extraction procedure has recently been used to simultaneously follow microbial community structure and the uptake of polyaromatic hydrocarbons (Fang and Findlay 1996).

The advantage of a more detailed lipid analysis is that sometimes the source of the fatty acid can provide more information than the type of fatty acid obtained. Since fatty acids do not occur in the cells as free acids but are generally linked to other compounds, the taxonomic value of fatty acid analysis can be markedly improved if the lipids are fractionated into at least polar and neutral lipids before they are released by saponification (Lechevalier and Lechevalier 1988). The most common phospholipids consist of two long chain fatty acids esterified to phosphoglycerol (Table 3-3). The typical phosphoglycerides are phosphatidylinositol (PI), phosphatidylglycerol (PG), phosphatidylcholine (PC), phosphatidylethanolamine (PE), phosphatidylserine (PS) and diphosphatidylglycerol (DPG). These lipids are associated with cytoplasmic membranes, with some being more common in some microbial groups than in others (Harwood and Russell 1984). The lipid content of a microorganism reflects its genetic make-up.

The cytoplasmic membrane is a selectively permeable barrier that isolates the cell contents from

Table 3-3. The general structure and types of the important phospholipids found in microbial membranes (adapted from Harwood (1984)).

General Formula	Regions	X-substituent	phospholipid
	Polar Head Group Phosphoglycerol backbone	H	phosphatidic acid
		serine	phosphatidylserine
	Non-polar Tails Two long chain ester linked fatty acids	ethanolamine	phosphatidylethanolamine
		choline	phosphatidylcholine
		glycerol	phosphatidylglycerol
		inositol	phosphatidylinositol
		phosphatidylglycerol	diphosphatidylglycerol

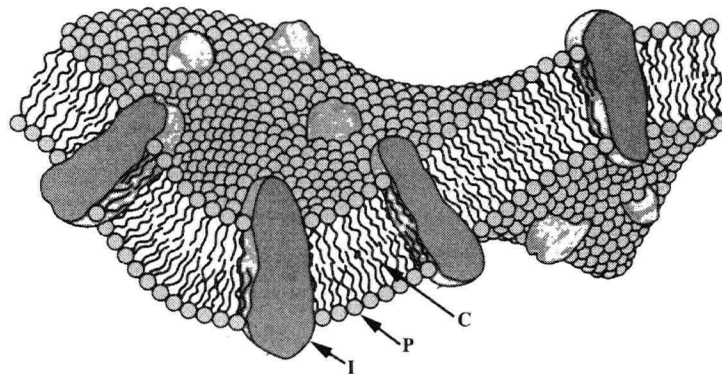


Figure 3-3. A schematic drawing depicting a segment of the classical lipid bilayer containing intrinsic (I) proteins. The bilayer is an arrangement of phospholipids with their polar head groups (P) facing out and their long chain hydrocarbon (fatty acid) tails (C) facing in. The membrane is said to be fluid in the plane of the layer. Protein function depends on membrane fluidity (adapted from Brock and Madigan (1991)).

the surrounding environment (Figure 3-3). Membranes also provide a special hydrophobic environment where enzymes and special cellular processes can operate (Brock and Madigan 1991; Harwood and Russell 1984). The alkyl (fatty acid) chains of the lipids in the membrane core are in a liquid-crystalline phase and the membrane is said to be *fluid*. Fluidity allows both intrinsic proteins and lipids to move in the plane of the membrane. The presence of *iso* or *anteiso* branched-chain acids in membrane lipids increases fluidity as does the presence of *cis* and *trans* double bonds. Shifts in relative proportions of fatty acids in the cytoplasmic

membrane are a direct microbial response to environmental factors.

The disadvantages of the Bligh and Dyer lipid extraction method are the number of analytical steps required and the fact that the organic (extract) phase ends up below the aqueous phase.

Whole cell fatty acid analysis is a more rapid alternative to PLFA, that was developed for clinical microbiology use (Miller and Berger 1985). Fatty acids from whole cell hydrolysates are obtained without regard to their source from within the cell. Fatty acids are released from whole cell samples by hot methanolic alkaline saponification. The cellular solution is acidified and the liberated fatty acids are methylated by heating the solution in the presence of methyl alcohol. Fatty acid methyl esters can be extracted from the acidified aqueous solution, but the organic extract must be washed with a dilute base to remove acid carryover. Once again the fatty acids are measured and identified by GC/FID.

Whole cell fatty acid (WCFA) analysis will contain fatty acids from all cellular sources. For example, the outer membrane of gram-negative bacteria consists of lipopolysaccharide or LPS which is known to yield α -hydroxy, β -hydroxy and non-hydroxy fatty acids (Wilkinson 1989). However, data acquired by WCFA and PLFA protocols have been found to be of a similar nature (Haack et al. 1994). Hence, for the comparison of fatty acid spectra obtained from mixed cultures, both methods appear to be equally valid.

Quantification of fatty acid mixtures by GC/FID requires the use of standards for peak identification. Due to the number of possible fatty acids that could be present, a commercial standard mixture (Supelco Inc.) of common bacterial fatty acid methyl esters (FAMES) may not contain all the FAMES found in an environmental sample. Unknown peaks can be tentatively identified by equivalent chain length (ECL) calibration of the GC column for a specific temperature program. The ECL expresses the relative elution position of any peak with respect to the closest saturated fatty acid. Gas chromatograms of a standard mixture containing a homologous series of saturated fatty acid methyl esters are used to equate retention time to an equivalent chain length or ECL (Gillan 1983; Miller and Berger 1985). The ECL for a peak, x , is calculated by interpolation of the retention times (t) of the two neighbouring saturated fatty

acids (n:0 and (n+1):0):

$$ECL_x = \frac{t_x - t_n}{t_{n+1} - t_n} + n \quad (3-1)$$

A family plot of carbon length (n) versus relative peak position ($ECL_x - n$) for the FAMES in the standard mixture serves as an identification template. Since members of a homologous series of fatty acids tend to be linear on the family plot, probable identification of FAME peaks is made from their ECL and interpolation on the family plot. Increased confidence in the identity of a fatty acid peak can be made by a confirmatory result using the same analysis with a different column or by GC with mass spectrometry (MS) on selected samples. Commercial hardware and software is available for FAME analysis (Microbial Identification System, MIDI, Inc. Newark, Delaware).

Some other protocols for FAME analysis that have been recently published are pyrolysis mass spectrometry (Basile et al. 1995), *in situ* supercritical fluid extraction and derivatization followed by GC/MS (Gharaibeh and Voorhees 1996), and sodium methoxide methylation (Rozes et al. 1993).

For the purpose of the present investigation, whole cell fatty acids were monitored during mixed culture batch growth experiments on resin acids in kraft pulp mill effluent as a function of pH. A modified WCFA type protocol was used for quantitative extraction, derivatization and analysis of both resin and fatty acids. The WCFA method applied was verified by experimental comparison to the more traditional PLFA analysis. FAME peak confirmation was accomplished by ECL calibration followed by GC/MS analysis on selected samples.

3.1.5 A Review of Fatty Acid Compositional Analysis

Analysis of fatty acid compositions is a multivariate statistical problem that requires special consideration (Aitchison 1986). However, it became evident that, in the research literature, these important considerations have not always been given due regard. Valid

interpretation of experimental data requires some understanding of the appropriate statistical methods. Thus, the purpose of this section is to provide the reader with a concise technical review of the statistical methods required for fatty acid compositional data used to compare microbial communities.

From this review the reader should understand a number of important concepts that will be essential in following the experimental results. This review begins with a mathematical definition of fatty acid compositional data. Each sample or observation is often referred to as a fatty acid profile, or spectrum. Due to the interdependence between elements of a composition, a valid statistical comparison of fatty acid spectra requires that a logratio data transformation be made. Logratio transformation of zero values necessitates some special data handling.

Spectra can also be compared by an analysis of similarity. A similarity index was derived based on the research literature. Although this index of similarity can be used to discern compositional differences, specific patterns of change within the fatty acid spectra can not be identified by this approach. One method to interpret the fatty acid spectra is in the consideration of certain marker fatty acids. Principal component analysis (PCA) is a multivariate statistical tool that can also facilitate a greater level of data interpretation. Logcontrast principal component analysis, the method of PCA for compositional data, can be used to summarize the compositional variability for a number of observations from one sample population. A sample population is defined by a community of microorganisms constrained by a set of environmental and growth conditions. However, in the literature and for the present investigation, it is of interest to assess the variability between sample populations. Discrimination between two or more groups of sample populations of compositional data, can be accomplished by logcontrast canonical component analysis.

In this section of the introduction, the above mentioned concepts are reviewed. This literature survey of fatty acid compositional analysis, has been divided into five sub-sections, namely, (1) Compositional Data and Logratio Transformations, (2) Analysis of Compositional Similarity, (3) An Introduction to Marker Fatty Acids and Chemotypes, (4) Logcontrast Principal and

Canonical Component Analysis, and (5) Summary of Fatty Acid Compositional Analysis.

Compositional Data and Logratio Transformations

For this discussion, an experiment is considered to consist of N samples (observations) taken from any one of M culture conditions. Therefore, the fatty acid data are a collection of N fatty acid profile observations for M conditions where N is not necessarily the same for each condition. Statistical analysis is required to assess the *intra* and *inter*-condition variability. Each observation X is a vector of D molar fatty acid concentrations which sum to give the sample total fatty acid (TFA) concentration:

$$TFA = X_1 + X_2 + X_3 + \dots + X_D = \sum_{j=1}^D X_j \quad (3-2)$$

where TFA quantifies biomass. To remove the influence of biomass in comparing one sample composition to another, the vector X is first normalized by TFA to produce a compositional data vector, x, called a fatty acid profile or spectrum:

$$x = \{x_1, x_2, x_3, \dots, x_D\} = \frac{X}{TFA} \quad (3-3)$$

Thus x is a vector of proportions with non-negative elements x_1, \dots, x_D subject to the constraint:

$$\sum_{j=1}^D x_j = 1 \quad (3-4)$$

The crude compositional covariance (σ_{kl}) between elements k and l estimated from N observations of the vector x is defined as:

$$\sigma_{kl} = \text{cov}\{x_k, x_l\} = \frac{1}{N-1} \sum_{n=1}^N (x_{kn} - \bar{x}_k)(x_{ln} - \bar{x}_l), \quad \bar{x}_j = \frac{1}{N} \sum_{n=1}^N x_{jn} \quad (3-5)$$

However, elements of the composition are not mutually independent. By the compositional constraint of equation (3-4), the D-part composition is completely specified by a d-part subvector (x_1, \dots, x_d) where

$$d = D - 1 \quad (3-6)$$

Mathematically expressed, the subvector forms a d-dimensional simplex, S^d , embedded in D-dimensional real space. The simplex is defined by:

$$S^d = \{(x_1, \dots, x_D) : x_1 > 0, \dots, x_D > 0; x_1 + \dots + x_D = 1\} \quad (3-7)$$

A simplex is a restricted part of real space. The constraint imposed on the data by the simplex requires special statistical consideration due in part to the absence of an interpretable covariance structure based on the crude compositional data (equation (3-5)). Spurious correlation arises since if one element of the composition increases, others by definition must decrease. Therefore, the correlation coefficient is not free to range from -1 to 1 . Biologists have been warned of the prospect of spurious correlation between (normalized) indices since the turn of the century (Aitchison 1986). Aitchison addresses statistical analysis of compositional data with considerable mathematical rigour. Due to the particular requirements of compositional data, specialized computer programs were written (Microsoft Visual Basic in Excel 97 SR-1) to perform the statistical analysis in the present study. A summary of some of the important aspects of the mathematics underlying these algorithms is presented in the ensuing text.

Since the study of compositions concerns the relative magnitudes of the elements rather than their absolute values, it is suggested that correlations be made on the covariance of element ratios (quotients). Mathematical awkwardness in manipulating ratios can be overcome by considering logarithms of the quotients. For a D-part composition x , the *compositional variation array* is defined by the expected value and variance for logratios of the composition:

$$\xi_{ij} = E\{\log(x_i / x_j)\}, \quad \tau_{ij} = \text{var}\{\log(x_i / x_j)\}, \quad i = 1, \dots, d; j = i + 1, \dots, D \quad (3-8)$$

Estimates from the experimental data follow standard formulae for means and variances:

$$\xi_{ij} \approx \frac{1}{N} \sum_{n=1}^N \log(x_i / x_j)_n \quad (3-9)$$

$$\tau_{ij} \approx \frac{1}{N-1} \sum_{n=1}^N \left(\log(x_i / x_j)_n - \xi_{ij} \right)^2 \quad (3-10)$$

The estimated values can be presented in an ordered matrix from which obvious features of the compositional data are readily seen. The matrix lower triangle is used for the logratio means and the upper triangle reports the logratio variances as follows:

$$\begin{bmatrix} \cdot & \tau_{12} & \cdots & \tau_{1d} & \tau_{1D} \\ \xi_{12} & \cdot & \ddots & \vdots & \tau_{2D} \\ \vdots & \ddots & \cdot & \ddots & \vdots \\ \xi_{1d} & \vdots & \ddots & \cdot & \tau_{dD} \\ \xi_{1D} & \xi_{2D} & \cdots & \xi_{dD} & \cdot \end{bmatrix} \quad (3-11)$$

Information such as relative compositional magnitudes ($\xi > 0$ or $\xi < 0$) or the relative variations ($\tau > \xi^2$ or $\tau < \xi^2$) is gathered directly from the ordered array. The covariance structure of a D-part composition is completely determined by the $\frac{1}{2}dD$ independent logratio (τ) variances. The covariance structure is the set of all

$$\sigma_{ij,kl} = \text{cov}\{\log(x_i / x_k), \log(x_j / x_l)\} \quad (3-12)$$

as i, j, k and l run through the values $1, \dots, D$. The variation matrix $T = [\tau_{ij}]$ determines the covariance structure by the relationships:

$$\sigma_{ij,kl} = \frac{1}{2} (\tau_{il} + \tau_{jk} - \tau_{ij} - \tau_{kl}) \quad (3-13)$$

In addition to the variation matrix T , there are two other ways in which the logratio compositional covariance structure can be specified. The *logratio covariance matrix* is formed by choosing a common divisor, x_D , for all the logratios and by restricting the consideration of compositional covariance to the set of covariances defined by the $d \times d$ logratio covariance matrix:

$$\Sigma = [\sigma_{ij,DD}] = [\sigma_{ij}] = \text{cov}\{\log(x_i / x_D), \log(x_j / x_D)\}, \quad i, j = 1, \dots, d \quad (3-14)$$

This covariance structure is contained by the set of relationships:

$$\sigma_{ij,kl} = \sigma_{ij} + \sigma_{kl} - \sigma_{il} - \sigma_{jk} \quad (3-15)$$

The logratio covariance matrix, Σ , is the covariance matrix of a d-dimensional random vector of the logratio transformed compositional data:

$$y_i = \log(x_i / x_D), \quad i = 1, \dots, d \quad (3-16)$$

The order of parts and the choice of component divisor should make no difference to the outcome of the statistical analyses performed.

The third covariance matrix is the *centred logratio covariance matrix*, Γ . The common component divisor is the geometric mean, g , of the D components:

$$g(x) = (x_1 \cdots x_D)^{1/D} \quad (3-17)$$

The centred logratio covariance matrix is defined by:

$$\Gamma = [\gamma_{ij}] = \text{cov}\{\log(x_i / g(x)), \log(x_j / g(x))\}, \quad i, j = 1, \dots, D \quad (3-18)$$

and is similarly related to the covariance structure by the relationships:

$$\sigma_{ij,kl} = \gamma_{ij} + \gamma_{kl} - \gamma_{il} - \gamma_{jk} \quad (3-19)$$

The matrix Γ is the covariance matrix of the random vector, z , of the transformed compositional data:

$$z_i = \log(x_i / g(x)), \quad i = 1, \dots, D \quad (3-20)$$

The three matrix specifications $\{T, \Sigma, \Gamma\}$ are equivalent. The necessity for three separate specifications is one of mathematical flexibility, depending on the analysis performed. Each specification has disadvantages relative to the other. T is not a covariance matrix, Σ is not symmetric in the compositional parts and Γ is a singular matrix.

Zero values are an obstacle to logratio transformation (Aitchison 1986). One practical solution is to treat a zero as an analytical trace value, δ , below the method detection limit. For an observation x with D elements each zero value can be replaced by:

$$x_i = 0 \Rightarrow x'_i = \delta \frac{(O+1)(D-O)}{D^2} \quad (3-21)$$

where O is the number of zero elements. The non-zero values must also be adjusted accordingly:

$$x_i \neq 0 \Rightarrow x'_i = x_i - \delta \frac{O(O+1)}{D^2} \quad (3-22)$$

Sensitivity analysis can be performed to test for any influence of the choice of δ on the statistical outcome. Another strategy of zero replacement is to assign zero values a random number in the range $(0, \delta]$, where δ is the compositional detection limit. The latter approach was used.

Estimation of mean and covariance logratio transformed compositional data statistics follow standard definitions:

$$\psi = \{\psi_1, \dots, \psi_d\}, \quad \psi_i \approx \frac{1}{N} \sum_{n=1}^N y_{in} \quad (3-23)$$

$$\Sigma = [\sigma_{ij}], \quad \sigma_{ij} \approx \frac{1}{N-1} \sum_{n=1}^N (y_{in} - \psi_i)(y_{jn} - \psi_j) \quad (3-24)$$

A test for logistic normality can be made by considering the d -dimensional radius (Mahalanobis distance) distribution computed from the matrix equation:

$$\rho_n = (y_n - \psi)^T \Sigma^{-1} (y_n - \psi), \quad n = 1, \dots, N \quad (3-25)$$

where the superscript "T" is the transpose operator. For the assumption of multivariate normality of the y_n observations, the radii ρ_n should be approximately distributed as $\chi^2(d)$. If the computed value of the radius ρ is r , then the sorted calculated probabilities $\Pr(\rho \geq r)$ plotted against the order statistic $(2n-1)/2N$ should approximately follow the diagonal of the unit square

for logistic normality.

Consider ψ and Σ estimated from two sets of observations of fatty acid profiles identified as conditions A and B. Assuming that both are described by logistic normal distributions $L_A^d(\psi, \Sigma)$ and $L_B^d(\psi, \Sigma)$, statistical tests are made of the likelihood (Λ) of the parameter θ being valid for the random logratio variable y . The likelihood that θ is true for y is written “ $\Lambda(\theta | y)$ ”. The logarithm of the generalized likelihood ratio test statistic (Q) contrasts the likelihood for the hypothesis (θ_h) versus the model (θ_m) parameter estimates:

$$Q = 2 \log(R(y)) = 2 \log \left(\frac{\Lambda(\theta_h | y)}{\Lambda(\theta_m | y)} \right) \quad (3-26)$$

The test statistic Q is approximately distributed as $\chi^2(c)$ where c is the constraint in calculating the statistical parameter θ . If the computed value of the test statistic Q is q , then the probability $\Pr(Q \geq q)$ is calculated from the incomplete gamma function as follows:

$$\Pr(Q \geq q) = 1 - \frac{1}{\Gamma(\beta)} \int_0^t w^{\beta-1} e^{-w} dw, \quad \Gamma(\beta) = \int_0^\infty w^{\beta-1} e^{-w} dw, \quad \beta = \frac{c}{2}, \quad t = \frac{q}{2} \quad (3-27)$$

The approximate generalized likelihood ratio test statistic (equation (3-26)), for examining hypotheses in the comparison of compositions, is of the form:

$$Q = N_A \log \left(\frac{|\Sigma_{hA}|}{|\Sigma_A|} \right) + N_B \log \left(\frac{|\Sigma_{hB}|}{|\Sigma_B|} \right) \quad (3-28)$$

where “ $|\Sigma|$ ” is the determinant of the respective estimated hypothesis and model covariance matrices.

Testing for equivalence of sample population variance ($\Sigma_A = \Sigma_B$) requires the calculation of a pooled (Σ_p) sample population estimate:

$$\Sigma_p \approx \frac{1}{N_A + N_B} (N_A \Sigma_A + N_B \Sigma_B) \quad (3-29)$$

The test statistic for the hypothesis Σ_A equal to Σ_B is calculated from equation (3-28) assigning

both Σ_{hA} and Σ_{hB} to Σ_p and the probability $\Pr(Q \geq q)$ is based on $\chi^2(\frac{1}{2}d(d+1))$. A combined sample estimate, Σ_C , is required for the hypothesis of equal means and variances ($\psi_A = \psi_B$ and $\Sigma_A = \Sigma_B$):

$$\Sigma_C \approx \Sigma_p + \frac{N_A N_B}{(N_A + N_B)^2} (\psi_A - \psi_B)(\psi_A - \psi_B)^T \quad (3-30)$$

In this case q is calculated by assigning both Σ_{hA} and Σ_{hB} to Σ_C and the probability $\Pr(Q \geq q)$ is based on $\chi^2(\frac{1}{2}d(d+3))$. Should the hypothesis ($\psi_A = \psi_B$ and $\Sigma_A = \Sigma_B$) be valid, the combined mean fatty acid profile is estimated by the equation:

$$\psi_C \approx \frac{1}{N_A + N_B} (N_A \psi_A + N_B \psi_B) \quad (3-31)$$

The hypothesis of equal means ($\psi_A = \psi_B$) allowing for the possibility of Σ_A different from Σ_B does not have explicit forms of the likelihood estimates similar to the expressions of the pooled and combined estimate of Σ given by equations (3-29) and (3-30). The likelihood estimates in this case are calculated following an iterative process:

initialize :

$$\Sigma_{hA} = \Sigma_A$$

$$\Sigma_{hB} = \Sigma_B$$

iterate :

$$\psi_h = (N_A \Sigma_{hA}^{-1} + N_B \Sigma_{hB}^{-1})^{-1} (N_A \Sigma_{hA}^{-1} \psi_A + N_B \Sigma_{hB}^{-1} \psi_B)$$

$$\Sigma_{hA} = \Sigma_A + (\psi_A - \psi_h)(\psi_A - \psi_h)^T$$

$$\Sigma_{hB} = \Sigma_B + (\psi_B - \psi_h)(\psi_B - \psi_h)^T$$

(3-32)

Successive approximations of Σ_{hA} and Σ_{hB} are made until they change negligibly with further iteration. The test statistic q is then obtained from equation (3-28) and the probability $\Pr(Q \geq q)$ is based on $\chi^2(d)$.

Therefore, with logratios of compositional data the standard battery of tests for the analysis of variance are readily made in order to compare groups of samples. In terms of comparisons of

microbial community structure from fatty acid analysis, one can ask whether two sample populations are the same. With a representative number of observations from a given sample population, it is also possible to test the likelihood of another sample being a *member* of the same community of microorganisms from the hypothesis of the population mean being equal to the unknown sample composition. Since fatty acid extracts from mixed cultures are an ensemble average of the condition and species of microorganisms within a sample, then a test of sample population similarity considers likeness in terms of both condition and content.

Analysis of Compositional Similarity

Microbial taxonomists use a different approach for identifying and categorising microbial isolates. In clinical microbiology, microorganisms are clustered according to an index of similarity (I_s) ranging from 0 to 1 for increasing likeness between profiles from two isolates (Bousfield et al. 1983; Eerola and Lehtonen 1988). The similarity index is like a distance scale which can be used for cluster analysis (Aldenderfer and Blashfield 1984; Manly 1986; Spath 1980). Cluster analysis is a multivariate classification tool for applying a hierarchy to measurements by agglomerating the compositions into groups of nearest neighbours. Results of this analysis are illustrated with dendrograms.

Although the index of similarity seems to have been exclusively used in clinical microbiology for discriminating between bacterial isolates, there is no reason why such an index could not also be a meaningful tool for assessing the relative likeness of mixed cultures. The idea is quite simple but it is complicated by the number of methods used to calculate I_s . A number of the equations that have been used in clinical microbiology are reported in Table 3-4.

Different equations of profile similarity show differences in the sensitivity of classification. Increased sensitivity to discriminate between two profiles is compromised by an increased probability of false differentiation due to experimental variability. Eerola and Lehtonen (1988) demonstrated the best results with an exponential function weighted by peak size (Table 3-4, row 6). From their data they concluded that for a mean peak area around 1%, the coefficient of variation (CV) was about 30%. As the mean peak area increased, the CV decreased to around

Table 3-4. Similarity measures for compositions x_A and x_B containing D fatty acids (Bousfield et al. 1983; Eerola and Lehtonen 1988). Similarity ranges from 0 (no likeness) to 1 (identical). Note that for the weighted exponential function, the parameters $\{k_1, k_2, k_3\}$ are empirical constants.

Method	Formula
Correlation Coefficient	$\frac{1}{2} \left(1 + \frac{\sum_{i=1}^D (x_{iA} - \bar{x}_A)(x_{iB} - \bar{x}_B)}{\left(\sqrt{\sum_{i=1}^D (x_{iA} - \bar{x}_A)^2} \sqrt{\sum_{i=1}^D (x_{iB} - \bar{x}_B)^2} \right)} \right)$
Angle of Separation of Vectors	$\sum_{i=1}^D \sqrt{x_{iA}} \sqrt{x_{iB}}$
Degree of Overlap	$1 - \frac{1}{2} \sum_{i=1}^D x_{iA} - x_{iB} $
Stack Method	$\frac{1}{D} \sum_{i=1}^D \min \left\{ \left(\frac{x_{iA}}{x_{iB}} \right), \left(\frac{x_{iB}}{x_{iA}} \right) \right\}$
Weighted Stack Method	$\sum_{i=1}^D \frac{x_{iA} + x_{iB}}{2} \min \left\{ \left(\frac{x_{iA}}{x_{iB}} \right), \left(\frac{x_{iB}}{x_{iA}} \right) \right\}$
Weighted Exponential Function	$\sum_{i=1}^D \frac{x_{iA} + x_{iB}}{2} f(\omega), \omega = \max \left\{ \left(\frac{x_{iA}}{x_{iB}} \right), \left(\frac{x_{iB}}{x_{iA}} \right) \right\}, f(\omega) = \frac{k_1}{(\omega - k_2)^{k_3} - 1 + k_1}$

10%. Thus, the minor peaks of a spectrum tend to be more variable, adding merit to the weighted approach for calculating an index of similarity. Further, with an expected CV range from 0 to 30%, the cost in lost similarity for peak ratios between 1 and 1.3 should be small relative to the peak ratios greater than 1.3. Based on the observed within-species variability of fatty acid peaks, Eerola and Lehtonen adjusted the empirical constants $\{k_1, k_2, k_3\}$ of their similarity index (Table 3-4, row 6) to optimize their success in discrimination. However, the use of three empirical constants to adjust the width of a probability distribution function is excessive. The features of Eerola and Lehtonen's observations can be more simply expressed by defining a peak ratio random variable:

$$v_i = \ln \left(\frac{x_{iA}}{x_{iB}} \right), \quad i = 1, \dots, D \quad (3-33)$$

The variable v_i sampled from the same microbial species is assumed to be normally distributed as $N(0, \sigma_i)$ over the range $[-\infty, +\infty]$. The standard deviation, σ_i , represents the above mentioned coefficient of variability that increases with decreasing peak area. However, Eerola and Lehtonen were successful in using a globally representative CV of 30% which is the same as saying:

$$\sigma_i \approx \sigma \approx \ln(1.3), \quad i = 1, \dots, D \quad (3-34)$$

Errors in this approximation are compensated for by making a weighted sum for the index of similarity. The hypothesis that two peaks, x_{iA} and x_{iB} , are equal can be tested for each v_i by calculating the probability of finding another value even more removed from zero mean. If the observed value of v_i is ζ_i then the probability $\Pr(v_i \geq |\zeta_i|)$ is equal to:

$$F(\zeta_i, \sigma) = \Pr(v_i \geq |\zeta_i|) = \frac{2}{\sigma\sqrt{2\pi}} \int_{|\zeta_i|}^{\infty} e^{-\frac{1}{2}\left(\frac{\eta}{\sigma}\right)^2} d\eta = 1 - \operatorname{erf}\left(\frac{|\zeta_i|}{\sqrt{2}\sigma}\right) \quad (3-35)$$

Based on equation (3-35) the weighted similarity index will be defined for the present investigation as follows:

$$I_s = \sum_{i=1}^D \frac{x_{iA} + x_{iB}}{2} F(\zeta_i, \sigma), \quad \zeta_i = \ln\left(\frac{x_{iA}}{x_{iB}}\right) \quad (3-36)$$

Equation (3-36) preserves the basic features of the findings of Eerola and Lehtonen while presenting a more fundamentally-rooted calculation for a similarity index. The function is derived from purely statistical considerations and involves only one scaling term (σ) versus the three empirical factors of the Eerola and Lehtonen equation. The standard deviation, σ , could conceivably be used as a tuning parameter that adjusts the sensitivity of trend alarms in the application of microbial ecology assessment as a process control tool in wastewater treatment.

While the statistics for compositions and similarity indexes discussed so far, are helpful in comparing microbial fatty acid compositions, they are not as informative when it comes to understanding any underlying patterns for differences in fatty acid profiles. It is therefore, of interest to identify trends in elements of the composition that relate to external causes.

Hypothetically, fatty acid patterns that indicate early signs of sludge bulking or the onset of microbial stress would necessitate different operator interventions. Correct process control action depends on valid pattern recognition. The ability to identify deterministic factors influencing coherent patterns in the fatty acid composition could ultimately lead to meaningful

input signals for process control, using this approach of fingerprinting microbial communities.

An Introduction to Marker Fatty Acids and Chemotypes

Identification of a direct microbial response to changing bioreactor conditions can be interpreted from the identification of certain marker fatty acids. For example, direct isomerization of *cis* unsaturated fatty acids to their complementary *trans* configurations by aerobic bacteria is a reported, rapid response mechanism to growth inhibition due to a toxic shock (Keweloh and Heipieper 1996). Conversion from *cis* to *trans* configuration changes membrane fluidity and could be an important survival mechanism if lipid synthesis is also inhibited by the adverse stimulus. The relative proportion of *trans* monoenoic (16:1 ω 7t and 18:1 ω 7t) to *cis* monoenoic fatty acids (16:1 ω 7c and 18:1 ω 7c) has been used as a so-called microbial *stress ratio* (Frostegard et al. 1997; Reichardt et al. 1997; Webster et al. 1997). Membrane fluidity is tuned to temperature, or to the adsorption of hydrophobic contaminants, by a change in the proportion of saturated to unsaturated fatty acids (Harwood and Russell 1984; Ingram 1976; Ingram 1977; Marr and Ingraham 1962; Pinkart et al. 1996; Rose 1989; Sikkema et al. 1994; Sikkema et al. 1995). Microbial *stress* levels can be monitored by following the ratio of poly- β -hydroxybutyrate (PHB) to phospholipid fatty acid concentrations (Nichols and White 1989; Zelles et al. 1994). PHB is a prokaryotic endogenous storage polymer that accumulates in cells when the absence of one or more essential nutrients prevents the complete oxidation of an otherwise available carbon source. Increased relative PHB levels indicate unbalanced growth.

With the accumulation of research data on microbial lipids (Ratledge and Wilkinson 1988b), some patterns have emerged, although often with notable exceptions, identifying certain fatty acids with particular groups of microorganisms (Table 3-5). Most bacteria can be classified as either straight or branched-chain producers and chain-length specificity or geometry and position of unsaturation is a further distinction (Gillan and Hogg 1984). Therefore, instead of attempting to identify specific individual organisms from fatty acid compositions, groupings of marker fatty acids can be made to follow bacterial *chemotypes* or distinct chemical "families" of bacteria. This approach has been taken by a number of researchers, allowing distinctions to be made

Table 3-5. Marker phospholipid fatty acids in various cell types (adapted from (Basile et al. 1995; Kates 1964; Vestal and White 1989)).

Eubacteria:	
Common markers	15:0, i15:0, 16:1 ω 9, 16:1 ω 5, i17:0, a17:0, 18:1 ω 7t, 18:1 ω 5, i19:0, a19:0
Aerobes	16:1 ω 7, 16:1 ω 7t, 18:1 ω 7
Anaerobes	cy17:0, cy19:0
Stationary phase	cy17:0, cy19:0
Gram-positive	i15:0, a15:0
Gram-negative	β OH 14:0
Sulphate-reducers	i17:1 ω 7, 10Me-16:0, 17:1 ω 6
Clostridia	cy15:1
Barophilic, psychrophilic	20:5, 22:6
Cyanobacteria:	same as eubacteria plus 18:2 ω 6
Actinomycetes:	same as eubacteria plus 10Me-18:0
Fungi:	16:0, 18:1 ω 8, 18:2 ω 6, 18:3 ω 6, 18:3 ω 3
Protozoa:	20:3 ω 6, 20:4 ω 6
Plants and Green Algae:	
Diatoms	16:1 ω 3t, 20:5 ω 5, 20:5 ω 3
Green algae	16:1 ω 13t, 18:3 ω 3, 18:1 ω 9
Microalgae	16:3 ω 6
Higher plants	18:1 ω 9, 18:1 ω 11, 18:3 ω 3, 20:5 ω 3, 26:0

between communities in time and space (Baird and White 1985; Bobbie and White 1980; Cavigelli et al. 1995; Gillan and Hogg 1984; Sundh et al. 1997; Webster et al. 1997; Zelles et al. 1992; Zelles et al. 1994).

While it is interesting that fatty acid composition can be used to discern community differences, the results beg answers to questions of “why” and of “what impact”, that do not seem to have been addressed in the literature. Cause and effect relationships are difficult to establish in open environmental systems because of the multitude of factors involved. The engineering utility of a measurable difference comes from the understanding that these observations can be linked to reproducible and associated behaviour or performance of a system or process. As an analogy, the ethnic differences of people around the world are readily observable but do not translate to any differences in performance, ability or intellect. However recognition and knowledge of cultural backgrounds is essential to diplomacy and to the general ability of disparate groups of people to get along. A sensitivity to cultural differences does have utility in a social context. Advancement and engineering application for chemotype monitoring will likely come from well-

controlled perturbation experiments of engineered environmental systems.

Logcontrast Principal and Canonical Component Analysis

Subcompositional analysis of fatty acid profiles can allow meaningful interpretations to be made of the variability within experimental data. However, there is the risk that subjective grouping will bias information contained in the data. It is also possible that chemotype grouping does not provide any insight to the data. Furthermore, due to the high dimensionality of the compositions (large D in equation (3-2)), interpretation may not be obvious.

For high dimensional systems, principal component and canonical component analyses (Dunteman 1989; Jackson 1991; Manly 1986) are useful multivariate statistical tools for analysing the variability within and between sample populations respectively. Both techniques attempt to reduce the dimensionality of multivariate systems by expressing most of the measured variability in terms of a few mutually orthogonal (independent) parameters that are weighted sums of the original system parameters. The weighting factors (loadings) of the original parameters and relationships of the weighted sums or principal components to experimental covariants can lead to meaningful data interpretation. Therefore, principal component analysis is a data reduction technique to condense the information contained in D variables of the fatty acid composition into p new variables where $p \ll D$. Canonical component analysis achieves the same ends, but discriminates between sample populations by accounting for both *intra* and *inter*-population variability.

In general, principal component analysis (PCA) involves the formation of linear composites. For an experimental system consisting of N observations of D variables, $\{\Omega_1, \dots, \Omega_D\}$, a linear composite of those variables is simply defined by:

$$\omega_k = \sum_{j=1}^D a_{kj} (\Omega_j - \bar{\Omega}_j), \quad \bar{\Omega}_j = \frac{1}{N} \sum_{n=1}^N (\Omega_j)_n, \quad k = 1, \dots, D \quad (3-37)$$

where $\{a_{k1}, \dots, a_{kD}\}$ is a vector of weighting coefficients. This linear transformation therefore defines a new coordinate variable scaled by the coefficient vector (a_k) and centred around the

multivariate mean vector $\bar{\Omega}$. The variance of the variable ω_k defined by the linear composite is:

$$\lambda_k = \sum_{i=1}^D \sum_{j=1}^D a_{ki} a_{kj} \sigma_{ij} = a'_k C a_k \quad k = 1, \dots, D \quad (3-38)$$

where σ_{ij} is the element of the matrix C describing the covariance between the variables Ω_i and Ω_j . The variable ω_k is called a principal component when the weight vector a_k is chosen such that it maximizes λ_k subject to the constraint:

$$\sum_{i=1}^D a_{ki}^2 = a_k \cdot a_k = 1 \quad (3-39)$$

This definition for the principal components leads to the standard eigen value problem defined by the matrix equation:

$$(C - \lambda_k I) a_k = 0 \quad (3-40)$$

where I is the identity matrix. The solution to equation (3-40) results in D characteristic (latent) roots, $\{\lambda_1, \dots, \lambda_D\}$ and D corresponding eigen vectors $\{a_1, \dots, a_D\}$ defining D principal components $\{\omega_1, \dots, \omega_D\}$. The eigen vectors are orthonormal:

$$\sum_{i=1}^D a_{ki} a_{li} = a_k \cdot a_l = 0, \quad k \neq l \quad (3-41)$$

Orthonormality means that the principal components are uncorrelated with each other. The characteristic a-vectors can be scaled to their roots:

$$a'_k = \sqrt{\lambda_k} a_k \quad (3-42)$$

Principal components scaled by their roots will have the same units as the original variables.

The characteristic a-vectors can also be normalized by their roots:

$$a''_k = a_k / \sqrt{\lambda_k} \quad (3-43)$$

resulting in principal components with unit variances.

With the latent roots ordered in decreasing value ($\lambda_1 > \lambda_2 > \dots > \lambda_D$) from equation (3-38) it can be seen that the corresponding principal components represent decreasing amounts of the variance contained in the N observations of Ω . The overall variability of the multivariate data is quantified by the determinant of the covariance matrix, $|C|$ (generalized variance), or by the sum of the variances given by the trace of C, $Tr(C)$. Variance in the data is preserved by the transformation to principal components where:

$$|C| = \lambda_1 \lambda_2 \lambda_3 \dots \lambda_D, \quad Tr(C) = \lambda_1 + \lambda_2 + \lambda_3 + \dots + \lambda_D \quad (3-44)$$

The benefit of principal component analysis is that most of the variance of the original data is contained by just the first few principal components:

$$Tr(C) \approx \lambda_1 + \lambda_2 + \lambda_3 \quad (3-45)$$

Therefore the D parameters, $\{\Omega_1, \dots, \Omega_D\}$, used to describe an experimental system can often be adequately represented by a few ($p \ll D$) parameters, $\{\omega_1, \dots, \omega_p\}$, enabling significant dimensional reduction. Data interpretation is sought in the groupings of the original D parameters implied by the weighting factors (loadings) and also in the appearance of relationships between the principal components and any covariants for the experiment. For instance, in a study of bird mortality, the chance of survival might be related to a principal component that weights a variety of measures of bird dimension (Manly 1986). Success in PCA analysis occurs when the principal components can help to provide meaningful interpretation of, or interrelationships between, the experimental variables and conditions. PCA therefore acts to condense the experimental and natural variability contained within observations of many potentially interrelated parameters, into a few independent, and hopefully, relevant new parameters.

Principal component analysis considers the variability contained in the observations of a single sample population. Often, one needs to compare groups of observations from a number of

sample populations. The statistical variability between groups of observations can be assessed by canonical component analysis. Canonical component analysis addresses the question of how well it is possible to separate (distinguish) two or more groups, given measurements from these groups on several variables. Consider M different groups from which N_1, \dots, N_M random samples of D parameters, $\{\Omega_1, \dots, \Omega_D\}$, are obtained. The canonical discriminant function is the linear combination of the parameters, like equation (3-37) but with a global mean, that gives the maximum possible F ratio on a one-way analysis of variance. In this case the eigen value problem takes the form:

$$\begin{aligned}
 (B - \lambda_k W)b_k &= 0 \\
 W_{ij} &= \frac{1}{N-M} \sum_{m=1}^M \sum_{n=1}^{N_m} (\Omega_{in} - \bar{\Omega}_{in})(\Omega_{jn} - \bar{\Omega}_{jn}), \quad N = \sum_{m=1}^M N_m, \quad \bar{\Omega}_{jm} = \frac{1}{N_m} \sum_{n=1}^{N_m} \Omega_{jn} \\
 B_{ij} &= \frac{1}{N} \sum_{m=1}^M N_m (\bar{\Omega}_{im} - \bar{\Omega}_i)(\bar{\Omega}_{jm} - \bar{\Omega}_j), \quad \bar{\Omega}_j = \frac{1}{N} \sum_{m=1}^M \sum_{n=1}^{N_m} \Omega_{jn}
 \end{aligned} \tag{3-46}$$

where B is the between group covariance matrix and W is the within group covariance matrix. The resultant eigen vectors, $\{b_1, \dots, b_D\}$, are standardized by the constraint:

$$b^T W b = 1 \tag{3-47}$$

The solution of equation (3-46) subject to equation (3-47) is somewhat more complicated to solve. However, since B and W are both positive definite, the eigen value problem can be reduced to standard form by Choleski decomposition (Hornbeck 1975; Kreyszig 1983):

$$\begin{aligned}
 (H - I\lambda)b' &= 0 \\
 W &= LL^T, \quad L \equiv \text{lower triangular} \\
 H &= L^{-1} B L^{-T} \\
 b &= L^{-T} b'
 \end{aligned} \tag{3-48}$$

Principal component analysis is a common approach for data reduction and analysis of fatty acid profiles (Basile et al. 1995; Cavigelli et al. 1995; de Castro et al. 1997; Frostegard et al. 1997; Gharaibeh and Voorhees 1996; Haack et al. 1994; Sundh et al. 1997; Zelles et al. 1994).

However, these authors have used principal component analysis simply to discriminate between microbial communities. Microbial communities from samples taken from different sediments or soils were compared. In cases where inter-community differences are being assessed, canonical component analysis is the more appropriate method for data reduction and statistical analysis. Furthermore, out of these eight literature examples only Fostegard (1997) explicitly addressed the considerations that are required for treating compositional data. It is unclear from the remaining seven publications whether such consideration was given. There is a danger of missed or invalid interpretation from principal component analysis of compositional data, due to spurious correlation, if standard multivariate statistical methods are applied (Aitchison 1986; Jackson 1991; Reyment 1989). In order to avoid the chances of false or spurious correlation of compositional data, a data transformation to either logratio (equation (3-16)) or centred logratio (equation (3-20)) random variables is necessary. Here lies the pitfall in the availability of commercial statistical software. The convenience afforded by the software does guarantee complete awareness of the propriety of various statistical techniques. Principal component analysis of logratio transformed data is referred to as logcontrast principal component analysis.

Logcontrast principal component analysis (LPCA) is a valid method for PCA of compositional data (Aitchison 1986). Maintaining the notation for compositional data analysis (equations (3-2) to (3-32)), a logcontrast of a D-part composition, x , is any loglinear combination:

$$a_k^T \log x = a_{k1} \log x_1 + \dots + a_{kD} \log x_D, \quad \sum_{i=1}^D a_{ki} = 0 \quad (3-49)$$

The condition that the logcontrast coefficients sum to zero, means that a logcontrast can always be expressed as a linear combination of logratios with a common divisor making them scale free:

$$a_k^T \log x = a_k^T \log \frac{x}{\beta} \quad (3-50)$$

where β is an arbitrary constant. A logcontrast is said to be standard if the coefficients

$\{a_{k1}, \dots, a_{kD}\}$ form a unity vector ($a_k^T a_k = 1$). Two logcontrast vectors are orthogonal if their dot

product is zero. From N samples of a composition, x , the variance of a logcontrast of the composition is:

$$\text{var}(a_k^T \log x) = a_k^T \Gamma a_k \quad (3-51)$$

Therefore, the problem of LPCA is finding the standardized logcontrast of maximum variance which amounts to the solution of the eigen value problem, as for PCA, but using the centred logratio covariance matrix:

$$(\Gamma - \lambda_k I) a_k = 0, \quad k = 1, \dots, d \quad (3-52)$$

Note that although Γ is a $D \times D$ matrix, it is singular, meaning that equation (3-52) produces one trivial eigen value ($\lambda = 0$) with the corresponding unit length vector $a = \{D^{-1/2}, \dots, D^{-1/2}\}_k$.

Logcontrast canonical component analysis (LCCA) similarly follows equation (3-46) subject to equation (3-47), with the substitution of the logratio transformed random variable, y_j (equation (3-16)) for the generalized parameter Ω_j .

$$\begin{aligned} (B - \lambda_k W) b_k &= 0 \\ W_{ij} &= \frac{1}{N - M} \sum_{m=1}^M \sum_{n=1}^{N_m} (y_{in} - \bar{y}_{in})(y_{jn} - \bar{y}_{jn}), \quad N = \sum_{m=1}^M N_m, \quad \bar{y}_{jm} = \frac{1}{N_m} \sum_{n=1}^{N_m} y_{jn} \\ B_{ij} &= \frac{1}{N} \sum_{m=1}^M N_m (\bar{y}_{im} - \bar{y}_i)(\bar{y}_{jm} - \bar{y}_j), \quad \bar{y}_j = \frac{1}{N} \sum_{m=1}^M \sum_{n=1}^{N_m} y_{jn} \end{aligned} \quad (3-53)$$

The logcontrast canonical components are usually translated so that their origin corresponds to the overall mean logratio vector. The k^{th} logcontrast canonical component value (LCC- k) is calculated from the vector scalar product of the k^{th} eigen vector and the translated logratio compositional vector as follows:

$$LCC_k = b_k \cdot (y - \bar{y}) \quad (3-54)$$

Summary of Fatty Acid Compositional Analysis

To summarize, logratio transformations of compositional data achieve statistical independence of the elements within a spectra. The likeness between logratio transformed fatty acid spectra can be calculated following the standard techniques of multivariate analysis of variance. Logcontrast principal component analysis of fatty acid compositions is a method to interpret the compositional variability contained within a number of samples from a single microbial population. Such an analysis could be used, for instance, to consider a trend in the microbial community structure of a sample population over time. Logcontrast canonical component analysis of fatty acid compositions can be used to discriminate between samples from a number of microbial communities. Logcontrast canonical component analysis could be used, for example, to consider the effect of pH on culture enrichment for resin acid degraders. It is also possible to quantify relative differences in fatty acid compositions by calculating an index of similarity. However, the index of similarity can not be used to consider any underlying fatty acid patterns that might be responsible for the observed differences. Finally, there are a number of marker fatty acids that can be used to infer either microbial stress or adaptation to changing environmental conditions.

3.1.6 The Principal Objective and Method Specific Issues

The principal objective at this stage of the investigation was to determine the mechanism and extent of pH influence on the removal kinetics of resin acids (Objective B - Chapter 1). It was also necessary to replicate the observations of the residuum reported in Chapter 2 (Objective A - Chapter 1). Microbial fatty acid analysis was the chosen method for monitoring growth-linked removal kinetics and for assessing relative differences between the microbial communities in the enrichment cultures. The literature reviewed in this introduction supports the validity of microbial fatty acid analysis as a tool in microbial ecology. However, the employment of this tool for the purpose of the present investigation necessitated that three important issues be addressed.

- i. The use of microbial fatty acids to monitor biomass is not conventional in wastewater engineering. Consequently, a control experiment was designed to confirm that total microbial fatty acid extracted from a mixed culture was a conserved biomass quantity during batch growth. In this control mixed culture experiment, microbial growth was monitored in a model medium that permitted the assessment and comparison of a number of biomass quantities.
- ii. The chosen method of whole cell fatty acid analysis (WCFA) is less specific than phospholipid fatty acid analysis (PLFA). It follows that fatty acid compositions obtained by PLFA should be a subset of those derived by WCFA. To test this hypothesis, the fatty acid spectra generated by WCFA and PLFA were compared for replicate samples obtained during the above-mentioned control mixed culture experiment.
- iii. Any observed difference in the fatty acid spectra between two microbial communities enriched as a function of pH may be due, in part or in combination, to (a) a membrane adaptation to pH, (b) a membrane adaptation to the pH-dependent resin acid hydrophobicity, and (c) an overall change in the community structure. The issue of membrane versus community level adaptation was felt to be a question of fundamental importance for considering the mechanism of pH influence. Therefore, interpretation of the mixed culture fatty acid spectra required model data for a typical microbial membrane response. These model data were acquired by monitoring, the membrane response of a resin acid degrading pure culture isolate, to pH and substrate hydrophobicity. In parallel, a similar experiment was also performed using enrichment cultures.

The stated research objective was considered by monitoring mixed culture growth kinetics in a medium of pulp mill effluent with resin acids as the sole carbon source. The data interpretation was based on the results of the above-mentioned, control mixed culture and control pure culture experiments.

3.2 Experimental Methods and Materials

3.2.1 Mixed Culture Batch Growth Experiments

Batch growth on resin acid or sodium acetate as the sole carbon sources was monitored for mixed cultures enriched for abietane resin acid degraders as a function of pH. Sodium acetate was a control used to consider the influence of pH, versus the combination of pH and resin acid hydrophobicity. Methyl esters of resin and bacterial fatty acids were analysed over the time course of batch growth by solvent extraction, methylation and GC/FID quantification as described below.

Medium and Batch Culture Preparation

For all these experiments, both the starting microbiological inoculum and treated effluent were kindly supplied by Western Pulp Partnership in Squamish, British Columbia, as previously described (Chapter 2). Treated effluent was used as the aqueous matrix for the growth medium. This treated effluent was further aerated for two days to exhaust the biologically degradable carbon. Further references made to Squamish effluent refer to biologically treated, aerated and filtered (Whatman 40) whole bleached kraft mill effluent. All glassware was thoroughly washed and fired at 475°C to remove any trace organic residue prior to use.

As before (Chapter 2), recrystallized resin acid from commercial rosin (Hercules Pamite 79) yielding a 30:70 mixture of abietic (ABA) and dehydroabietic (DHA) acid was used. However, instead of dissolving the resin acid in methanol (Chapter 2), a concentrated resinate solution was prepared by reflux boiling 1 g of abietane resin acid, in 50 mL of 0.1 N NaOH filtered (0.45 µm nitrocellulose) Squamish effluent. In this manner, resin acids were truly made the sole carbon source. In the former experiments (Chapter 2) in which methanol was used as a co-solvent to help disperse resin acids into the medium, microbial uptake of the methanol was inconsistent. Solubilized wood compounds act to stabilize suspensions of wood resin in solution (Sundberg et al. 1996b) so long as the wood resin can be initially dissolved or dispersed into the matrix. For the case of resin acids, initial uniform dispersion can be accomplished by using a co-solvent or by

Table 3-6. Weights of phosphate salts for a 100 mM pH buffered medium.

pH	NaH ₂ PO ₄ (GMW = 137.99) g/500 mL	Na ₂ HPO ₄ (GMW = 141.96) g/500 mL
5.5	6.60	0.31
6.0	6.05	0.87
6.5	4.71	2.25
7.0	2.69	4.34
7.5	1.09	5.98
8.0	0.37	6.72
8.5	0.13	6.97

starting from an elevated pH (Sundberg et al. 1996a).

Parallel shake flask cultures were maintained for up to seven, buffered pH conditions. Resin acid medium was prepared by adding an aliquot of concentrated resinate to 2.6 L of heated (55°C) Squamish effluent adjusted to pH 10 with 2 N NaOH. From this bulk solution, aliquots of 500 mL were decanted into respective 2 L Erlenmeyer flasks, containing weighed mixtures of Na₂HPO₄ and NaH₂PO₄ salts to yield a 100 mM phosphate buffer ranging from pH 5.5 to 8.5, as required (Table 3-6). This method of adding saponified resin acid to a hot effluent at an alkaline pH before pH adjustment, was chosen to produce an aqueous matrix that would closely resemble native resin acid in kraft mill effluent. Kraft pulping saponifies up to 90% of the wood extractives (Allen et al. 1993). Sodium acetate medium was prepared in the same way, omitting the addition of the resinate aliquot. Instead, for these flasks a 2.5 mL aliquot from a sterile solution of 0.5 M sodium acetate in 0.1 N NaOH was added just prior to inoculation.

Flasks were autoclaved for 20 minutes and left overnight at 37°C. Just prior to inoculation, 5 mL of 10% sterilized NH₄Cl was added to each flask and the pH was trimmed, if necessary, dropwise, with 50% H₂SO₄ or 2 N NaOH. A 1% inoculum was taken from mature cultures acclimated to resin acid at the same pHs. Acclimation was initiated with a common inoculum of mixed liquor from a 1 L grab sample from the Western Pulp UNOX biobasin. Flasks were agitated on a reciprocal shaker table (40 rpm) in the dark, within a 37°C thermostated room. Cultures were acclimated (enriched for growth-linked abietane resin acid degraders) by two batch growth cycles prior to each experimental run. Parallel shake flasks with sodium acetate medium were similarly inoculated with the resin acid-acclimated cultures at their respective pHs.

Resin and Bacterial Fatty Acid Sampling and Analysis

Trace organic analysis by solvent extraction and GC/FID quantification is a straightforward though somewhat laborious exercise when large numbers of samples need to be processed. Therefore, the novel method to monitor both substrate and biomass from a single sample assay was a tremendous benefit for these experiments. The extraction procedure described in Chapter 2 was modified for WCFA analysis based on the Moss FAME method described by Miller and Berger (1985). Since WCFA analysis yields similar results to the more involved PLFA analysis (Haack et al. 1994), whole-cell fatty acid extracts are dominated by cellular phospholipid fatty acids. The Moss FAME preparation of whole cell extracts consists of a saponification step, followed by acidification with methyl alcohol methylation, and then solvent extraction with a base wash. The purpose of the base wash is to recover acid carry-over into the solvent in order to protect the GC column and injection liner from reactive site build up. The extraction method employed for the present investigation was similarly, saponification, then acidification followed by solvent extraction. However, methyl esters were formed instead in the solvent phase with diazomethane. The main reason for the method change was to enable the simultaneous quantitative extraction and methylation of resin acids with a reduced risk of isomerization. Strong acids in combination with heat can isomerize resin acids (Soltes and Zinkel 1989). A base wash was not required because reagents of reduced molarity were used. Extraction efficiencies were monitored by surrogate recovery.

During the time course of an experimental run, 2 or 3 mL whole broth samples were drawn from the shake flasks and transferred to 15 mL glass tubes with Teflon screw caps. These 15 mL glass tubes contained 1 mL of 1 N NaOH in 50 percent HPLC grade methanol, spiked with O-methylpodocarpic acid (O-MPCA). The alcoholic NaOH solution acted to arrest microbial activity while also solubilizing resin acid and microbial constituents alike. The O-MPCA served as the sample extraction surrogate. Samples were stored frozen at minus 10°C pending extraction.

The effect of pH on the resin acid media solutions was assessed by harvesting, in triplicate,

suspended resin acid from a 1 mL sample onto a 0.45 μm cellulose acetate membrane filter. The suspended resin acid was compared to the contents of triplicate 1 mL whole samples. Filter and whole samples were similarly amended with 1 mL alcoholic 1 N NaOH and then stored frozen.

Prior to extraction, the sealed sample tubes were incubated at 90°C for 30 minutes to saponify the resin and cellular phospholipid fatty acids. Samples were extracted twice with 1 mL methyl-ter-butyl ether (MTBE). While no problems with emulsions were encountered, cellular debris suspended in the solvent phase was forced to the aqueous-solvent interface by centrifugation (2060 \times g for 20 minutes). With the addition of the first 1 mL of MTBE, 1 mL of 2 N H₂SO₄ was used to acidify the sample and to reduce the aqueous solubility of both resin and fatty acids prior to extraction. For each extraction, the solvent was transferred directly to 2 mL GC vials and dried under vacuum. After the second drying, a 100 μL aliquot of MTBE spiked with heneicosanoic acid methyl ester (HCA-ME) and tricosanoic acid (TCA) was added to each vial. HCA-ME was the internal standard and TCA the control for methylation. Methylation was accomplished by dispensing and vortexing, in the dried GC vials, 400 μL of chilled (0 to 4°C) MTBE and HPLC grade methanol (80:20) containing excess dissolved diazomethane.

Diazomethane was dissolved into the chilled MTBE methanol mixture by using nitrogen gas flow to purge the diazomethane from a reaction vessel into the solvent. The reaction vessel held 10 mL of MTBE, 5 mL of HPLC grade methanol into which approximately 0.5 g of Diazald (N-methyl-N-nitroso-p-toluenesulfonamide) was dissolved and then 5 mL of 10 N KOH was added to start the diazomethane generation. Diazomethane dissolved in MTBE in this manner would remain potent for weeks when stored in the freezer in 25 mL vials sealed with teflon lined caps. This open sparging diazomethane preparation method was superior to the closed reaction vessel described in Chapter 2. Larger volumes of more consistently dissolved diazomethane solvent solutions were produced with more consistent methylation results and less overall effort.

Extracted resin acids and microbial fatty acids were identified and measured by GC/FID (HP5890 Series II with a DB5 column of 30 m having a 0.32 mm ID and 0.25 mm film thickness) with 1 μL splitless injection. The inlet and detector temperatures were 250°C and 300°C, respectively.

The temperature program was 4 minutes at 130°C followed by a ramp of 4°C/min to 250°C and a post-run temperature of 290°C for 5 minutes. A hydrogen carrier gas was used with a column head pressure of 10 psi providing a total flow of 30 mL/min. Extraction efficiencies were typically greater than 90 percent. All chromatographic peaks were positively identified with pure standards, equivalent chain length calibration using fatty acid standard mixtures (Supelco 37 component FAME mix and 26 component BAME mix) and subsequent GC/MS confirmation (HP 6890 Series GC System with the 5973 Mass Selective Detector) on selected samples using the same column and temperature program except for a slower ramp of 2°C/min to 250°C. Resin acids and metabolites were quantified using the response factor of 99% pure dehydroabietic acid (Helix) standards prepared from a 1000 µg/mL stock solution in MTBE. Fatty acids were quantified using the response factor of 99% pure hexadecanoic acid standards (Sigma) prepared from a 1000 µg/mL stock solution in MTBE. Internal standards and extraction surrogates were quantified with their respective 99% pure standards as 1000 µg/mL stock solutions in MTBE. The detection limit for GC/FID with a 1 µL injection was found to be approximately 0.1 µg/mL for both resin and fatty acids.

Sodium Acetate Sampling and Analysis

For the shake flasks in which sodium acetate was the sole carbon source, additional 1 mL samples were withdrawn, stored and analysed as described in Chapter 2. The method detection limit was found to be approximately 4 mg/L.

pH Sampling and Analysis

Medium pH was monitored as described in Chapter 2.

3.2.2 Pure Culture Batch Growth Experiments

In order to better interpret the results from the mixed culture batch growth experiments described above, pure culture batch growth experiments were also conducted using the bacterial isolate DhA-35 (Mohn 1995) that is capable of growing on dehydroabietic and abietic acid. DhA-35 was grown on resin acid or pyruvate at pH 6.0, 7.0 and 7.5. Analogous to the use of sodium

acetate in the mixed culture experiments, pyruvate was a soluble control substrate with which to consider the influence of pH apart from the effect of a hydrophobic substrate.

Pure Culture Medium Preparation

The growth medium used was as described by Mohn (1995) with the exception of a 50 mM sodium phosphate buffer to better maintain a constant pH. The growth time course was determined by periodically sacrificing identically prepared and inoculated individual 2 or 4 mL cultures following the method described by Wilson et al. (1996). Entire cultures were used for each analysis because of the expected difficulty in obtaining representative samples due to the clumping nature of DhA-35. Cultures were contained in 15 mL glass tubes with Teflon lined caps. Each culture received a 1 % inoculum from a late-log phase culture acclimated to the respective pH on a tube roller at 37°C.

Resin and Bacterial Fatty Acid Sampling and Analysis

All cultures were frozen at minus 10°C pending analysis. To culture tubes sacrificed for resin and fatty acid analysis, 1 mL of 1 N NaOH in 50 percent HPLC grade methanol, spiked with O-MPCA, was added. The remainder of the extraction procedure was identical to the one used for the mixed culture batch growth experiments.

Pyruvate Sampling and Analysis

Pyruvate was measured as pyruvic acid by first acidifying samples with H_2SO_4 . Pyruvic acid was quantified by HPLC (Aminex HPX-87H 300x7.8 mm column at 65°C with UV detection at 220 nm) using 50 μ L injections with a 0.012 M H_2SO_4 eluant at a 0.7 mL/min flow rate.

3.2.3 Mixed Culture Method Control Experiments

Mixed culture batch growth experiments using a common general purpose medium were conducted to assess the whole cell fatty acid extraction method and the bacterial fatty acid measure of biomass. After the calibration of dry weight in terms of optical density, batch growth cycles were monitored with the objective of comparing independent methods of biomass

measurement. Thus, during the growth cycle, samples were taken for optical density, protein and total fatty acid (TFA) assays as described below. To compare the extraction method that was developed for the simultaneous recovery of resin acids and whole cell fatty acids, with the classic lipid PLFA extraction method, replicate samples were also taken from an early stationary culture.

Medium and Batch Culture Preparation

Lauryl Tryptose Broth (DIFCO Catalogue # 0241-17-0) was used as a standard medium with which to test the validity of using bacterial fatty acids as a biomass equivalent and of the extraction method used to simultaneously separate resin acids and the bacterial fatty acids from media samples. The Lauryl Tryptose Broth (LTB) was prepared according to the label instructions, mixing 500 mL deionized water with 17.8 grams powdered media in 2 L Erlenmeyer shake flasks. All glassware was thoroughly washed and fired at 475°C to remove any trace organic residue prior to use. Once the LTB was dissolved, the medium was autoclaved at 124°C for 15 minutes and then was left to stand in the dark overnight at 37°C.

A 1% inoculum taken from mature cultures acclimated to the LTB was used to maintain the culture. Acclimation was initiated with an inoculum of mixed liquor from a 1 L grab sample from the Western Pulp UNOX biobasin. Flasks were agitated on a reciprocal shaker table (40 rpm) in the dark within a 37°C thermostated room.

WCFA Sampling and Analysis

Analysis for WCFA was the same as described for the mixed culture batch growth experiments.

PLFA Sampling and Analysis

The chloroform-methanol-water lipid extraction procedure (Bligh and Dyer 1959) is an accepted method of microbial lipid analysis (Vestal and White 1989). Broth samples of 5 mL were drawn, transferred to 10 mL glass tubes with Teflon screw caps and centrifuged (15 minutes at $2060 \times g$). The supernatant was poured off and the cell pellet retained. A 1.6 mL aliquot of a

50 mM pH 7.4 phosphate buffer, plus 4.0 mL of methanol spiked with heneicosanoic acid methyl ester (HCA-ME) and tricosanoic acid (TCA), and 2.0 mL of chloroform were added to the pellet. The HCA-ME was used as the extraction surrogate and the TCA as a control for methylation. This monophasic mixture was vortexed for two minutes to solubilize any lipids present in the sample. A further 2.0 mL of chloroform were added and the mixture was intensely mixed by vortexing for 30 seconds. Then 2.0 mL distilled water were added, followed by another 30 seconds vortex mixing. The resultant biphasic mixture was centrifuged (15 minutes at $2060 \times g$) to achieve complete phase separation. A layer of insoluble (cell) debris was found between the upper aqueous and lower solvent layers. The upper aqueous and the solid phase was removed with a glass pipette. In this process, a small fraction of the chloroform phase was sacrificed to ensure complete aqueous removal. The remaining chloroform was transferred to a clean tube and was blown down with a stream of nitrogen gas to dryness.

The dried lipids were dissolved in 1 mL of a 1:1 mixture of methanol and toluene. The lipid extract was subjected to mild alkaline methanolysis by mixing into the sample 1.0 mL of 0.2 N methanolic KOH followed by incubation at 37°C for 15 minutes. After methanolysis, the sample pH was lowered to 6 by adding 50 μL of 25% acetic acid. Similarly to the lipid extraction step, a biphasic solution was obtained by adding 2.0 mL chloroform, vortexing, adding 2.0 mL distilled water and vortexing again. The sample was centrifuged (15 minutes at $2060 \times g$) to clearly separate the two phases. The upper aqueous phase was again removed and discarded. The remaining chloroform was transferred directly to 2 mL HP autosampler GC vials and then dried with a gentle stream of nitrogen gas. To the extracted residue in the GC vials, 100 μL O-MPCA spiked MTBE was added. In this case, the O-MPCA was the internal standard. Finally, 400 μL of chilled MTBE with dissolved diazomethane was mixed into the extraction sample. Although fatty acid methylation should have been accomplish during the alkaline methanolysis stage, initial tests revealed that without diazomethane, the surrogate (TCA) methylation was not complete.

Protein Sampling and Analysis

Biomass was measured as protein using the Coomassie Brilliant Blue G dye binding assay. Sample collection was as previously described (Chapter 2). Colour change at a wave length of 595 nm was again calibrated against Bovine Serum Albumin standards. The relative colour development of a 1 mL aliquot Coomassie reagent in standard glass test tube with three successive sample additions of 100 μ L was measured in a Turner Model 690 Spectrophotometer.

Optical Density Sampling and Analysis

Broth optical density was measured by light absorption at a wave length of 510 nm on a Turner Model 690 Spectrophotometer. Samples of 5 mL were transferred to a standard glass test tube and the optical density of the medium in the tube was referenced to the optical density taken of the same tube with 5 mL deionized water.

Dry Weight

Bacterial dry weight was calibrated to optical density for this system by measuring the dry weight of the culture at the start of the stationary phase. To the 500 mL culture, 1 mL of 10 percent sodium azide was added to inhibit further biological activity. Cells were harvested from the broth by filtration onto 47 mm diameter 0.45 μ m nitro-cellulose membrane filters. The filters were dried for 1 hour at 105°C. The resultant dry weights were referenced to the previously obtained tare weights and corrected according to blank sample weight loss. At the same time optical density measurements were taken on a dilution series from a parallel sample of the same culture. From these data, the correspondence between broth optical density and culture dry weight was estimated.

3.3 Results

The main objective of this study was to determine the sensitivity of mixed culture growth kinetics to cultivation pH for enrichment cultures removing abietane resin acids as the sole carbon source (Objective B - Chapter 1). General experimental results of equivalent chain length (ECL) fatty acid identification will be presented first. Next, the suitability of the whole-cell fatty acid (WCFA) extraction method as a representative biomass measure are discussed with the results of the mixed culture method control experiments (Section 3.2.3). Pure culture batch experimental results (Section 3.2.2) are then reported to provide a reference from which to consider the mixed culture batch growth experimental data (Section 3.2.1) that were the main focus of this investigation.

3.3.1 Equivalent Chain Length (ECL) Methodology

Fatty acid compositional analysis depends on the accurate identification of microbial fatty acids from sample extracts. Reducing large volumes of raw experimental data necessitates some degree of analytical standardisation and, where possible, numerical processing. The purpose of this section is to highlight the important features of the ECL methodology that was applied to the raw chromatographic data.

With a DB5 column and a 4°C/min constant temperature ramp, the retention times for a homologous series of saturated straight chain fatty acids (10:0 to 24:0) very nearly followed a linear dependence on carbon chain length (Figure 3-4). However, the retention time trend was not strictly linear. Retention times for the homologous series deviated from a linear trend line in a predictable manner. As a result, the ECL could be approximately calculated over the entire retention time range by least squares fitting of the retention time data for the homologous saturated fatty acid series, {11:0, ..., 24:0}, to the empirical equation:

$$ECL = A_0 + A_1t + A_2t^2 + A_3t^3 + A_4t^4 + A_5t^5 + A_6t^6 + A_7t^7 \quad (3-55)$$

where A_i ($i=0, \dots, 7$) is a constant coefficient. The coefficients for equation (3-55) were

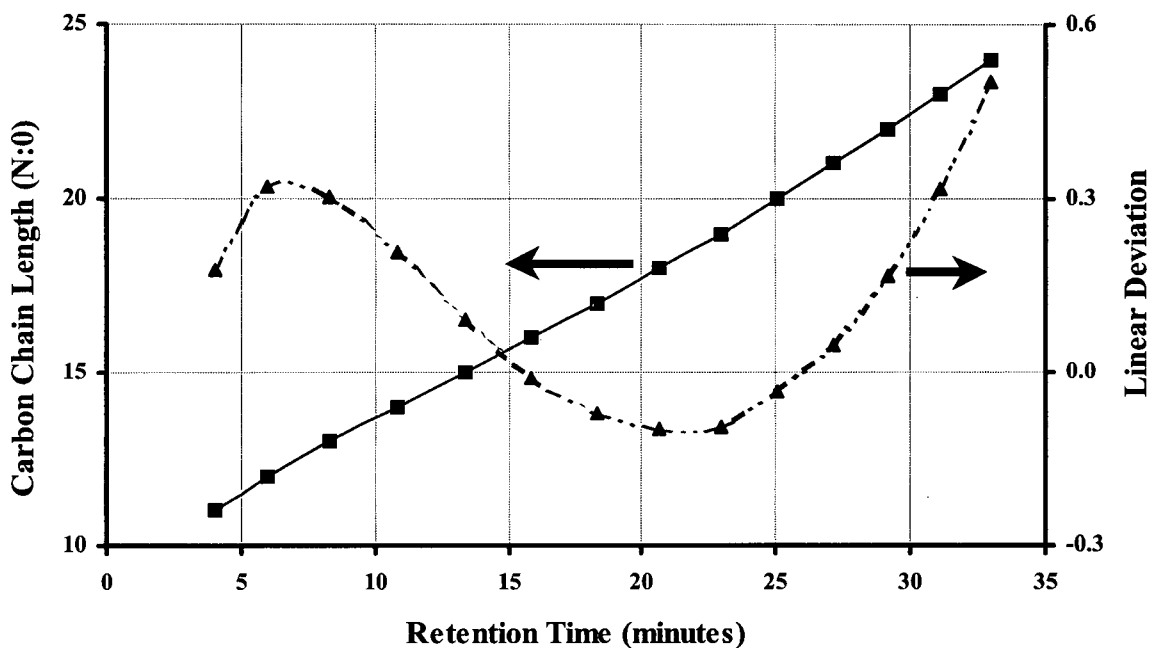


Figure 3-4. Typical retention time data for a homologous series of saturated straight chain fatty acids (10:0 to 24:0) by GC/FID (HP Series II) with a DB5 (30 m, 0.32 mm ID and 0.25 μm film thickness). Injection Port, detector and oven temperatures were as follows: $T_{\text{inj}} = 250^\circ\text{C}$; $T_{\text{det}} = 300^\circ\text{C}$; $T_{\text{oven}} = 130^\circ\text{C}$ for 4 minutes followed by a constant ramp of $4^\circ\text{C}/\text{min}$ to 250°C . The two graphs illustrate how the relationship between retention time and carbon chain lengths deviates from an apparent linear relationship.

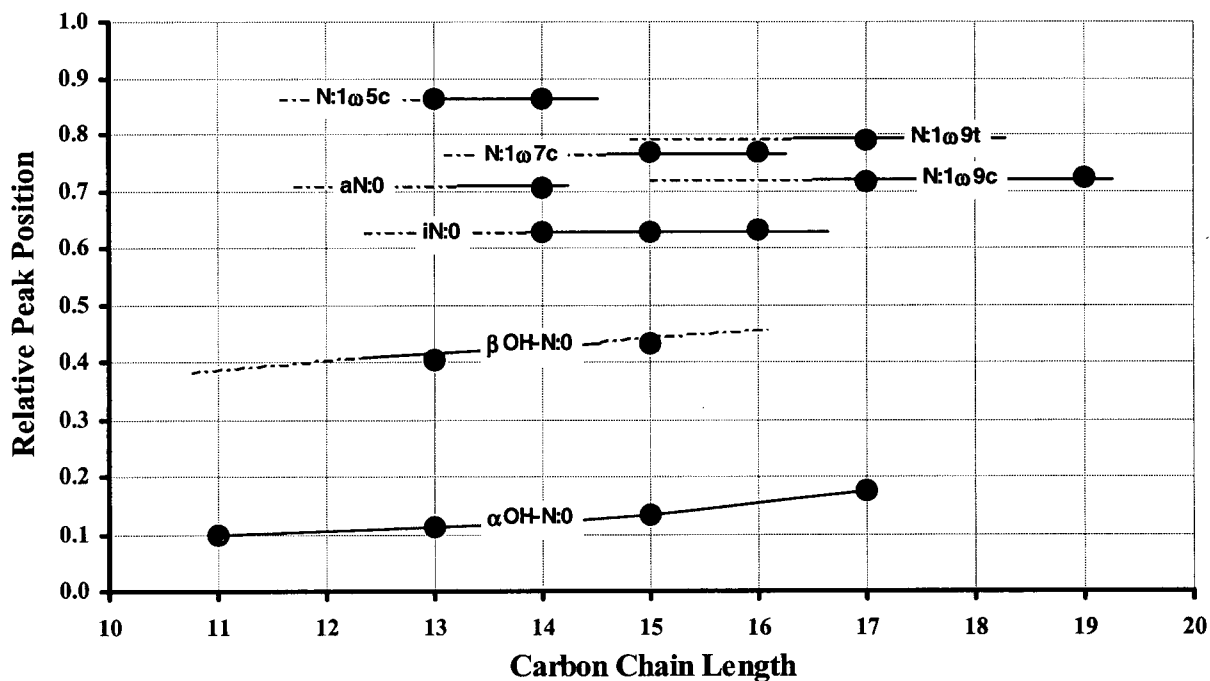


Figure 3-5. Equivalent chain length (ECL) template for monoenoic, branched and hydroxy fatty acids from a DB-5 column calibration (Figure 3-4) made with standard mixtures of fatty acid methyl esters (Supelco FAME and BAME component mixtures).

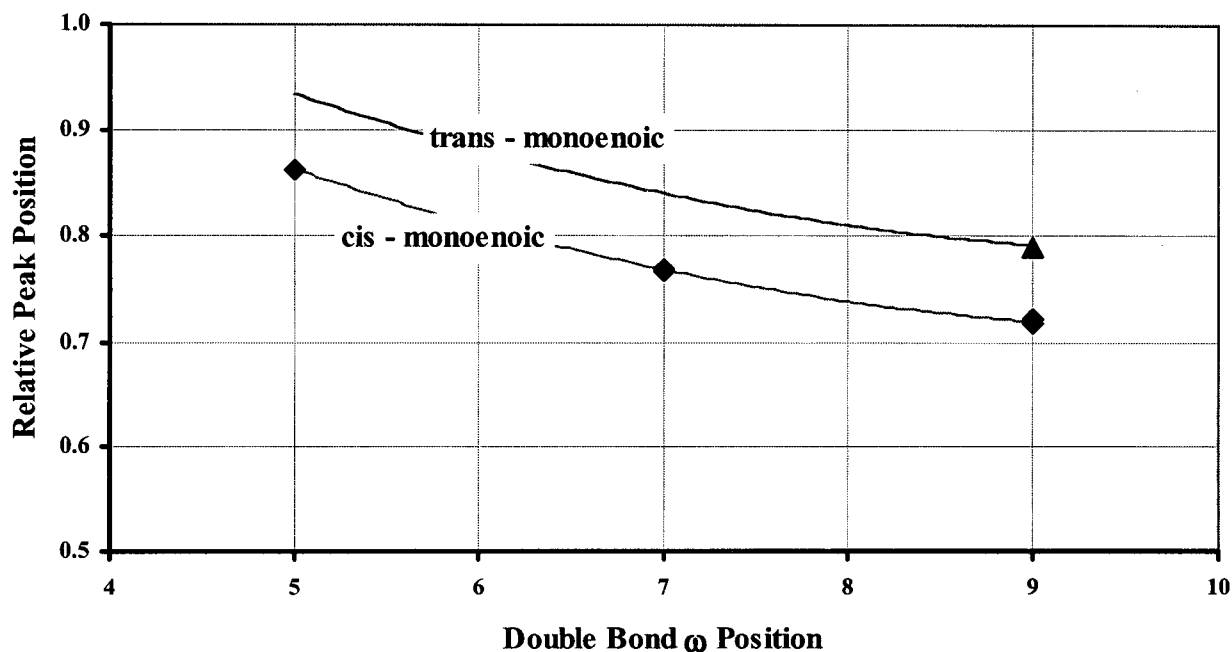


Figure 3-6. Relative peak positions as a function of double bond location for homologous cis and trans monoenoic fatty acids.

determined for each sequence of samples that were analysed in batch loads by the autosampler on the gas chromatograph. While the coefficients varied slightly due to retention time shifts that were dependent on the column condition, the relative peak positions in terms of ECL remained consistent. Therefore, ECL retention time calibration was a good method to standardize the chromatographic results. From the relative peak positions of the other types of fatty acids in the standard mixtures (Supelco) a template was generated to facilitate probable identification of fatty acid peaks in sample chromatograms (Figure 3-5). For example, suppose that, based on the carbon chain length calibration (equation (3-55) and Figure 3-4), a chromatographic peak was identified with an ECL of approximately 12.100 (ie. Carbon Chain Length = 12, Relative Peak Position = 0.100). Then from the template in Figure 3-5, constructed from fatty acid standard component mixtures, the ECL 12.100 peak would be tentatively identified as α OH-12:0. The *tentative identification* would be advanced to *probable identification* following peak confirmation by GC/MS.

Due to the reproducibility of relative peak positions of homologous monoenoic fatty acids, it was possible to construct a template for probable identification of the monoenoic isomers based on the

contents of the standard mixtures (Figure 3-6). From the shape of the curves in Figure 3-6, it can be seen that ω -double bond positions become harder to unambiguously determine with increasing ω -value. To illustrate the method of isomer identification, consider a peak that eluted with an ECL of 18.750 (ie. Carbon Chain Length = 18, Relative Peak Position = 0.750). Such an ECL does not coincide with any of the groups of homologous fatty acids in the template of Figure 3-5. However, from Figure 3-6, the peak could be tentatively identified as 18:1 ω 8c. Once again probable identification would require peak confirmation by GC/MS.

ECL-identified peaks for a sequence of GC chromatograms from samples taken during batch cultivation were confirmed on selected samples by GC/MS. It should be noted however that although mass spectrometry was helpful in identifying peaks as fatty acid methyl esters (FAMES), the similarity of long chain fatty acid ion mass fragmentation patterns between isomers decreased the confidence in the most probable mass spectral matches from standard library (Wiley) searches. A more detailed study of the mass spectrometry could have been used as an alternate approach for identifying isomers of FAME extracts (Basile et al. 1995; Gharaibeh and Voorhees 1996). However, more subtle analysis of mass spectra beyond FAME peak confirmation on selected samples was not undertaken, given the adequate sensitivity of retention time data for fatty acid isomer identification based on ECL.

The GC/FID-ECL approach was better suited to the purposes of this investigation than a GC/MS methodology, for logistical reasons of data storage, acquisition time and measurement sensitivity. In all, hundreds of samples were analysed. Data files for GC/MS were considerably larger than the ones produced for GC/FID and electronic data storage and manipulation was essential. Due to the number of samples analysed, software routines were written to scan the data files and summarize measurement sequences in order to tabulate the raw retention time and area of integration data for subsequent spreadsheet analysis. GC/FID analysis took half the machine time per sample as GC/MS analysis. The slope of the GC/FID temperature ramp was double that used for GC/MS analysis. In part, this was possible because a hydrogen carrier gas could be used for GC/FID. GC/FID peak detection was also more sensitive than GC/MS. Optimal sensitivity was

necessary in the lag phase of growth to detect low biomass concentrations and in the cell decline phase to detect any substrate residuum.

In summary, the ECL methodology was found to be a sensitive method of fatty acid peak identification. The analysis was amenable to numerical data handling, which facilitated the processing of hundreds of sample chromatograms in a reasonable amount of time. Confidence in the validity of the reduced chromatographic data was generated by subsequent GC/MS confirmation of tentatively identified peaks on a number of selected samples.

3.3.2 Mixed Culture Method Control Experiments

Mixed culture control experiments were undertaken in order to test the validity of the whole-cell fatty acid (WCFA) extraction method used for the present investigation to measure microbial ecology and biomass. Traditional analysis of microbial phospholipid fatty acids (PLFA) to assess mixed culture community structure is more specific in terms of the fraction of the cell from which the fatty acids are being extracted. For this reason it was of interest to compare the fatty acid spectra obtained by either a WCFA or a PLFA protocol. Secondly, the use of microbial fatty acid enumeration to measure biomass is not a conventional method in wastewater engineering. Hence, some justification was warranted to substantiate the hypothesis that microbial fatty acids are a conserved cellular constituent during mixed culture batch growth.

Replicate samples from log phase mixed cultures grown on Lauryl Tryptose Broth (LTB) were extracted for whole-cell fatty acids (WCFAs) and phospholipid fatty acids (PLFAs). The resultant compositional data are presented in Figure 3-7 as logratios using hexadecanoic acid (16:0) as the common divisor. Hexadecanoic acid is the logical choice of divisor for microbial fatty acid logratios because it is ubiquitous in fatty acid extracts (Baird and White 1985). Since PLFA analysis is more selective than WCFA analysis, the PLFA profile should be a subcomposition of the WCFA profile. Indeed, the total PLFA concentration was 48 μM and 75 percent of the WCFA concentration of 64 μM . The seven fatty acids, {14:0, 16:1 ω 7c, 16:0, cy17:0 ω 7, 18:1 ω 7c, 18:0, cy19:0 ω 9}, were present in common and in similar proportion for both extraction

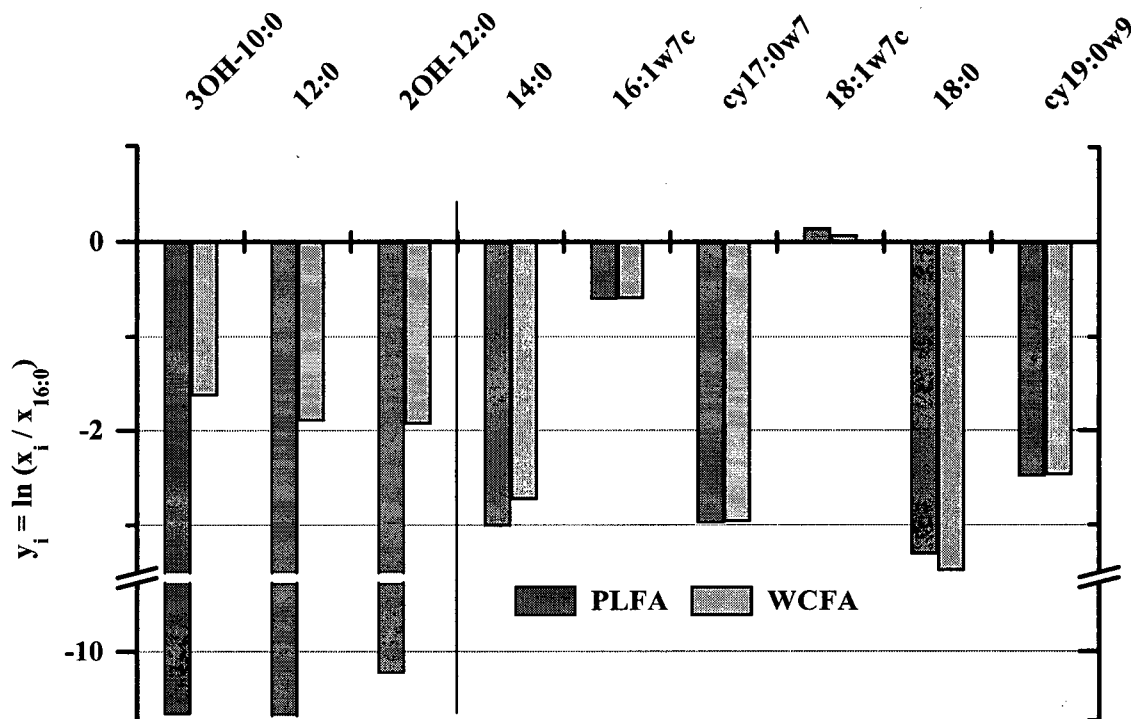


Figure 3-7. Mean logratio fatty acid compositional data ($y_i = \log(x_i / x_{16:0})$) by PLFA versus WCFA analysis from five replicate samples taken during log growth in Lauryl Tryptose Broth. The logratios can be interpreted as follows: $y_i > 0 \rightarrow x_i > x_{16:0}$; $y_i \approx 0 \rightarrow x_i \approx x_{16:0}$; $y_i < 0 \rightarrow x_i < x_{16:0}$; $y_i \ll 0 \rightarrow x_i \approx 0$. The PLFA profile forms a sub-composition of the WCFA profile. Total extracted fatty concentrations were 48 μM and 64 μM for PLFA and WCFA analysis respectively.

methods. WCFA extracts contained three additional fatty acids, {3OH-10:0, 12:0, 2OH-12:0}, that were absent from the PLFA analysis. These three WCFA are typical of those present in the lipopolysaccharide of gram-negative bacterial cell walls (Wilkinson 1989). The WCFA and the PLFA profiles were different, but the differences can be explained in terms of the specificity of the PLFA protocol. Therefore, it is important to note the extraction procedure for the comparison of fatty acid spectral data used to monitor changes in microbial community structure.

Figure 3-8 shows the time course of WCFA production during batch growth on LTB. Parallel measurements of biomass as dry weight (based on optical density calibration) and protein as bovine serum albumin (BSA), revealed a direct correspondence between the three quantities (Figure 3-9). WCFA production of 265 μmoles was equivalent to approximately one gram dry weight of biomass. Note that although the total amount of microbial fatty acid remained proportional to dry weight and protein during batch growth, the WCFA profile changed with culture age (Figure 3-10). The fatty acid composition changed most significantly during early and

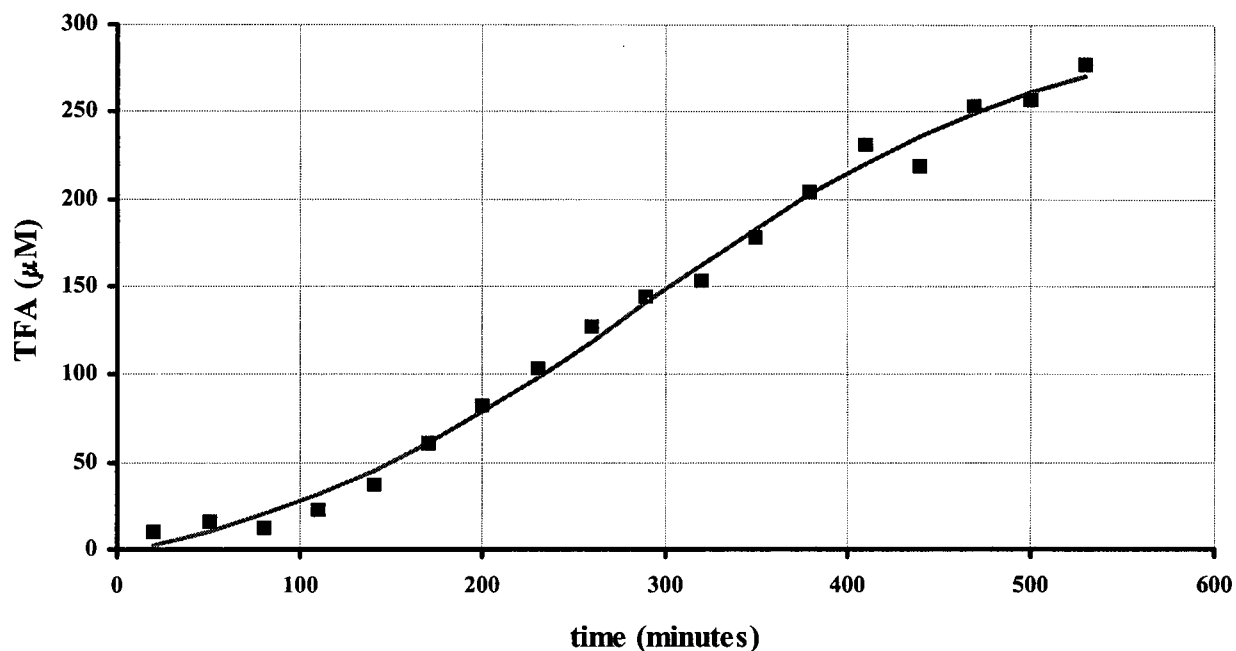


Figure 3-8. Whole-cell fatty acid (TFA) increase with time representing biomass production during mixed culture batch growth in Lauryl Tryptose Broth.

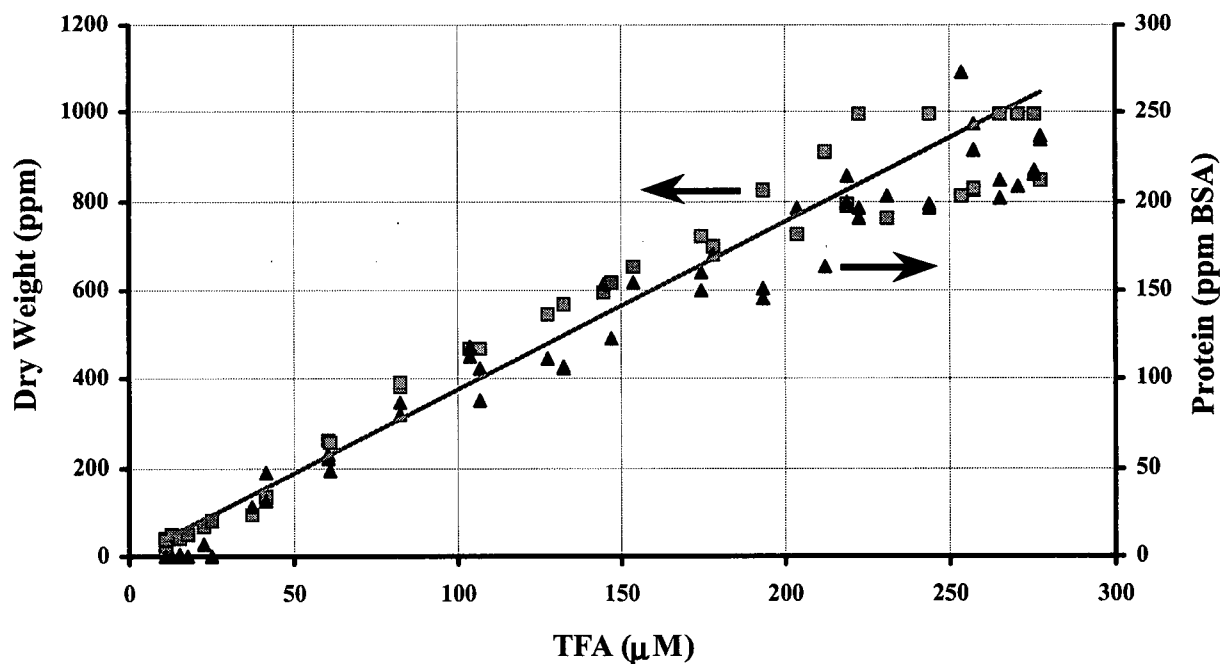


Figure 3-9. Whole-cell fatty acid (TFA) extracts versus biomass measured as dry weight (■) or as Coomassie protein (▲) during mixed culture batch growth on Lauryl Tryptose Broth. Fatty acid production for the mixed culture is approximately 265 μmoles WCFA per gram dry weight and 1.15 μmoles WCFA per milligram BSA.

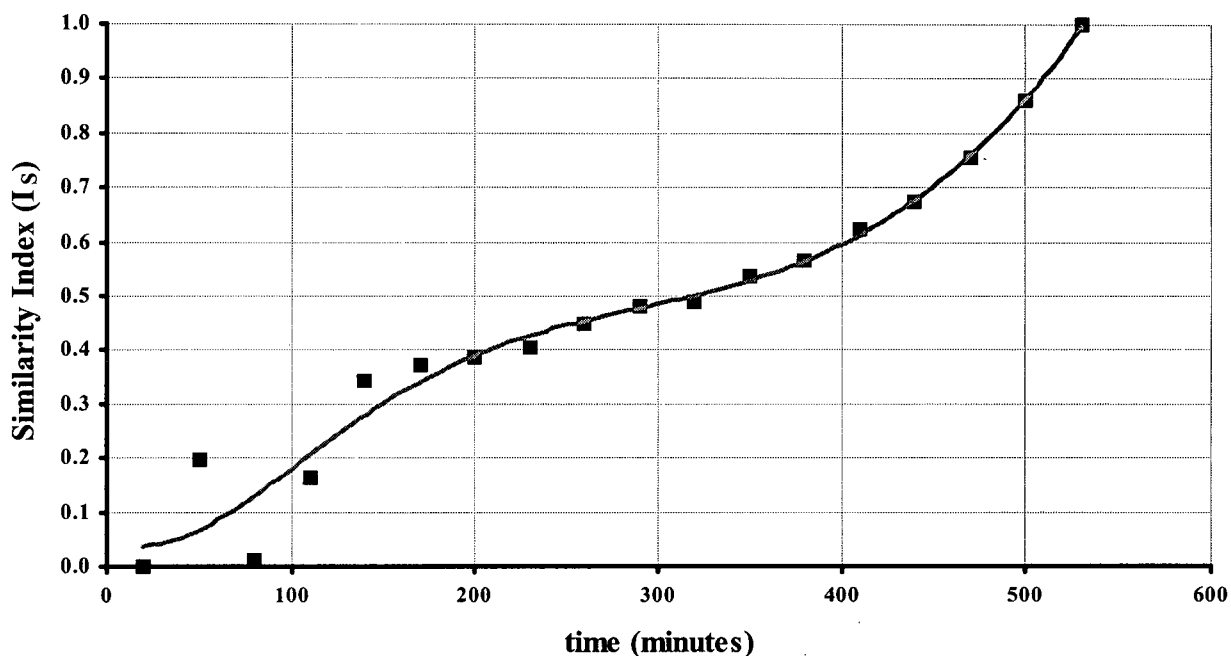


Figure 3-10. Relative WCFA composition similarity (I_s from equation (3-36)) with respect to the terminal time point during batch mixed culture growth on Lauryl Tryptose Broth. Fatty acid composition changes with culture age. I_s calculations were made with $\sigma = 1.3$.

late exponential growth. For example, the cyclopropane fatty acids {cy17:0, cy19:0} appeared later in the log growth phase. These control experiments supported the validity of WCFA extracts as a conserved microbial constituent that can be used to measure biomass during batch growth of mixed cultures. While the total fatty acid remained at a fixed proportion to biomass, the fatty acid composition changed during batch growth, reflecting changing conditions of the community with time.

3.3.3 Pure Culture Batch Growth Experiments

One of the important questions for the current investigation was whether any observed change in fatty acid spectra, for the enrichment cultures as a function of pH, was due to membrane adaptation by common individual species or due to a more general change in the microbial community. The adaptation of individuals to pH could only be unambiguously observed from pure culture experimentation. Since resin acid hydrophobicity increases with decreasing pH, pure culture experiments were undertaken in order to see if resin acids elicit a microbial membrane response commensurate with literature findings. For example, a known microbial

response to the presence of non-polar solvents in the growth medium, is a membrane adaptation that results in a decrease in the proportion of the major monoenoic PLFA (Ingram 1977).

The initial experimental design was to use the mixed culture resin acid medium (Section 3.2.1) for uniformity in comparing mixed to pure culture data. The microorganism DhA-35 had been isolated by Mohn (1995) from enrichment cultures of bacteria originally sampled from a laboratory scale (10-litre) sequencing batch reactor treating a synthetic, high strength, mechanical pulping whitewater (Johnson 1995). This whitewater was a mixture of plug screw pressate from a thermomechanical pulp mill and evaporator bottoms from a closed-cycle chemi-thermomechanical pulp mill. After a number of failed attempts at culturing DhA-35 in the mixed culture medium of Section 3.2.1 at pH 6, 7 and 8, the original enrichment medium used by Mohn (1995) was adopted in order to try to improve the chances of experimental success. The isolate seemed to be sensitive to both the medium and the pH condition. Even with the original enrichment medium of Mohn, growth at pH 6 was inconsistent and growth at pH 8 was never achieved. Replicate growth curves at pH 6, 7 and 7.5 were finally obtained using either dehydroabiatic acid (DHA) or pyruvate as the sole carbon source.

DhA-35 has been well characterized (Mohn 1995) with its whole-cell fatty acid profile being one of the methods used for its phylogenic fingerprinting (Mohn et al. 1997). Table 3-7 reports the cellular fatty acid composition of DhA-35, determined by the standard methods and equipment of the Microbial Identification System, MIDI, Inc., Newark, Delaware. The two fatty acids {16:1 ω 7c, 16:0} dominate, amounting to 80 percent of the total fatty acid content.

A change in the relative proportion of the major monoenoic fatty acid is a demonstrated response of bacterial membrane lipids to hydrophobic compounds such as long chain alcohols and solvents

Table 3-7. Cellular fatty acid composition of the resin acid-degrading isolate DhA-35 (Mohn et al. 1997).

Fatty Acid	10:0	3OH-10:0	12:0	3OH-12:0	16:1 ω 7c	16:0	18:1 ω 7c
Content (% of total)	0.8	5.0	3.6	2.4	52.4	28.1	7.5
$\ln x_i / x_{16:0}$	-3.56	-1.73	-2.05	-2.46	0.62	0	-1.32

(Ingram 1976; Ingram 1977; Pinkart et al. 1996). Dehydroabietic acid was similarly expected to influence the amount of 16:1 ω 7c with respect to 16:0. The proportion of 16:1 ω 7c with respect to 16:0 is readily expressed by their logratio (Table 3-7). Due to changes in the lipid composition with cell age, comparison of fatty acid profiles extracted from different batch cultures need to be compared at similar points of the growth cycle (Kates 1964). Therefore, the lipid contents of DhA-35 under the different growth conditions of substrate and pH were compared for the isolate by averaging WCFA profiles from samples taken in the neighbourhood of the height of the exponential growth phase (Figure 3-11). The logratio of 16:1 to 16:0 around pH 7 was an optimum that approached the value of 0.62 (Table 3-7) obtained by Mohn (1997) for this isolate. It is likely that the saturated to monoenoic logratio represents an optimum membrane condition around pH 7, since DhA-35 was isolated by enrichment at neutral pH and was found in this work to be temperamental when cultured at pH values away from neutral.

With both substrates (DHA or pyruvate) the general response to pH values away from neutral was a decrease in the proportion of 16:1. While the influence of pH on lipid composition is reported to not be clearly defined (Harwood and Russell 1984; Rattray 1988), the experimental observation of a decrease with pH of the major monoenoic fatty acid component has been previously reported for some yeast (Rattray 1988). It is plausible that the observed decrease in hexadecenoic acid represents a common microbial adaptation, or stress response, to sub-optimal pH values.

The membrane composition for growth on DHA versus pyruvate was significantly different at pH 6, where the resin acid is protonated and in its most hydrophobic form. The hydrophobicity of the substrate appeared to promote a pronounced decrease in the proportion of the major monoenoic acid 16:1 ω 7c (Figure 3-11). This response is consistent with the observed adaptation of *E. coli* cells to non-polar solvents, such as benzene and chloroform (Ingram 1977).

Therefore, the pure culture experiments suggested a microbial membrane response to both pH and substrate hydrophobicity. Further, DhA-35 exhibited an optimum pH-dependent membrane fatty acid composition that corresponded qualitatively with the ease with which the isolate could

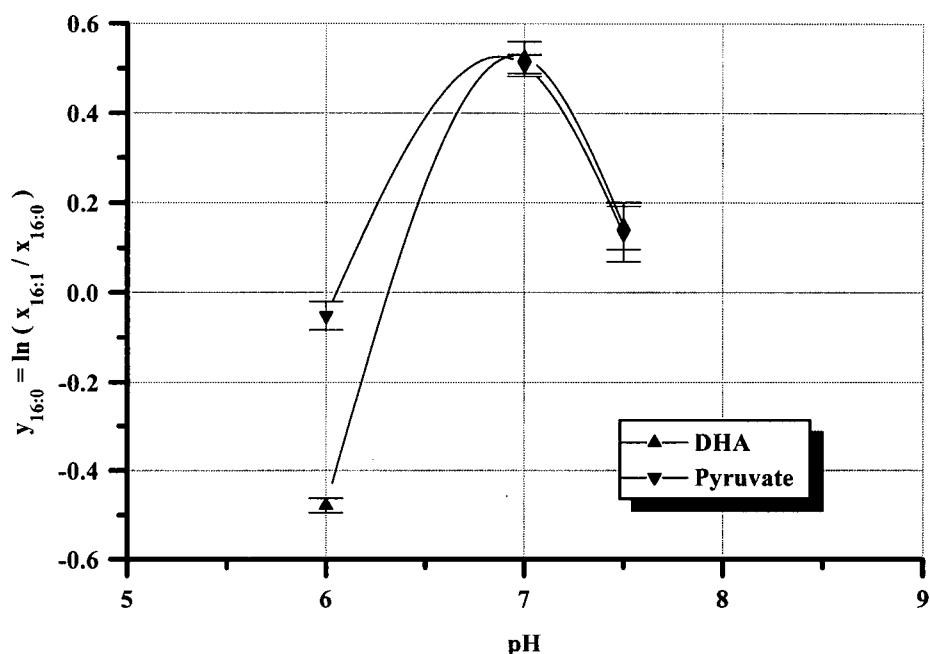


Figure 3-11. Relative proportion (logratio) of the monoenoic fatty acid 16:1 ω 7c with respect to 16:0 for DhA-35 grown at pH 6.0, 7.0 and 7.5 on either dehydroabiatic acid (▲) or pyruvate (▼) as sole carbon sources. WCFA extracts were compared for the same relative culture age of late exponential growth.

be cultured. Based on the pure culture experimental data, typical microbial membrane adaptations to pH and to a hydrophobic substrate were demonstrated. Sub-optimal pH conditions appeared to cause a decrease in the relative proportion of the major membrane monoenoic acid. The presence of a hydrophobic substrate in the medium seemed to extend this response. Therefore, if similar changes in the fatty acid spectra were observed in the mixed culture experimentation, then the pure culture data would suggest that the spectral changes were dominated by membrane adaptations of individual species. Conversely, fatty acid spectral changes, differing from the pure culture results, for the mixed culture experiments, as a function of pH and the presence of a hydrophobic substrate, would suggest that a transition in microbial content was likely to be dominating the results.

3.3.4 Mixed Culture Batch Growth Experiments

The demonstrated validity of WCFA extraction for quantifying mixed culture biomass and the observed response of an isolate to pH and resin acid hydrophobicity give some perspective with which to consider the results of the mixed culture batch growth experiments. The purpose

of the mixed culture experiments was to consider the extent to which pH influences the growth-linked kinetics and the microbial community structure of resin acid removal.

Three replicate experiments were performed and will be referred to as mixed culture experiments A (March 1996), B (June 1996) and C (November 1996). For each experiment, a fresh 1 L mixed liquor sample from the Western Pulp Partnership UNOX biobasin was obtained as a starting inoculum. Experiment A was the first in which microbial fatty acids were used as a measure for biomass. At this time, only the major saturated and monoenoic fatty acids, {16:0 and 18:1}, were considered. An increased understanding of the potential for the method promoted the more thorough WCFA analysis that was performed during experiments B and C. Experiment C was undertaken in conjunction with the pure culture experiments with DhA-35 and included the parallel inoculations of the enrichment mixed cultures into medium with sodium acetate.

Due to the greater number of pH conditions tested, the depletion of the particulate resin acid fraction, that was previously monitored (Chapter 2), was not followed as part of these mixed culture experiments. However, the particulate resin acid fraction in the medium prepared for experiment B was analysed. The medium contained approximately 40 µg/mL DHA and 19 µg/mL ABA. The soluble resin acid fraction in the medium was determined for the un-inoculated medium by subtracting suspended (filter) resin acid from the total concentration. These extractions were made in triplicate (Figure 3-12) and were fitted by least squares with a sigmoidal function (Origin v4.0, Microcal Software, Inc.) which predicted that DHA and ABA were 50 percent dissolved at pH 6.6 ± 0.03 and 7.1 ± 0.1 , respectively. Further, the limiting solubilities in the Squamish effluent for DHA and ABA were estimated to be 3.6 ± 0.8 µg/mL and 1.9 ± 1.2 µg/L respectively. Above pH 7.5, essentially all of the resin acid was dissolved. The effective solubility of the resin acids in these experiments was lower than their solubilities found during the batch experiments described in Chapter 2. However, in the earlier experiments methanol was used to help disperse the wood extractives in the medium.

The WCFA concentration used to monitor biomass followed the characteristic three phase log-linear batch growth pattern (Figure 3-13) with distinct lag, exponential growth, and cell decline

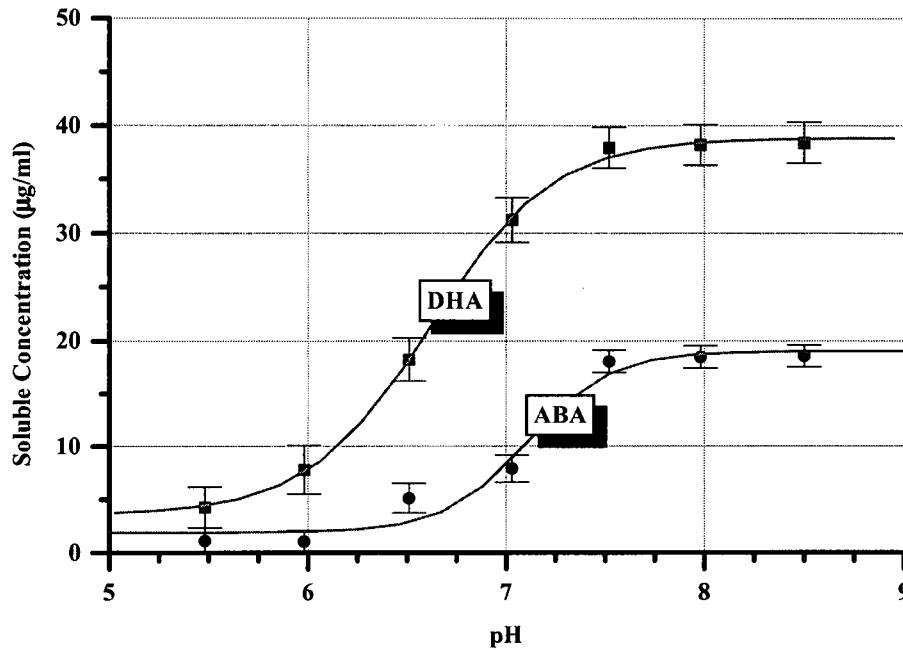


Figure 3-12. The derived soluble resin acid concentration as a function of pH for un-inoculated medium (Section 3.3.1) containing $39.8 \pm 1.9 \mu\text{g/mL}$ dehydroabiatic acid (■-DHA) and $18.8 \pm 1.0 \mu\text{g/mL}$ abiatic acid (●-ABA). Error bars represent the standard deviation for samples made in triplicate. The estimated limiting solubilities were 3.6 ± 0.8 and $1.9 \pm 1.2 \mu\text{g/mL}$ for DHA and ABA respectively. DHA and ABA were estimated to be 50 percent dissolved at pH 6.6 ± 0.03 and 7.1 ± 0.10 respectively.

(endogenous growth) phases (Bailey and Ollis 1986; Metcalf & Eddy 1991). Logarithmic growth indicated (Simkins and Alexander 1984) that the initial total resin acid (TRA) concentration ($\approx 60 \mu\text{g/mL}$) was much larger than k_s , the limiting concentration at which the specific growth rate is half its maximum value (Chapter 2). Therefore, the modified Monod's equation presented in Chapter 2 could be simplified as follows:

$$q \approx Q \left(1 - \frac{S^*}{S} \right), \quad k_s \ll S \quad (3-56)$$

By directly monitoring the change in biomass with time, growth rates were obtained unambiguously, as compared to other methods which attempt to define growth rate indirectly from the substrate depletion curve (Holmberg 1982). The growth kinetic parameters were defined by least squares regression of the total fatty acid (TFA) concentration data in time to a function of the form:

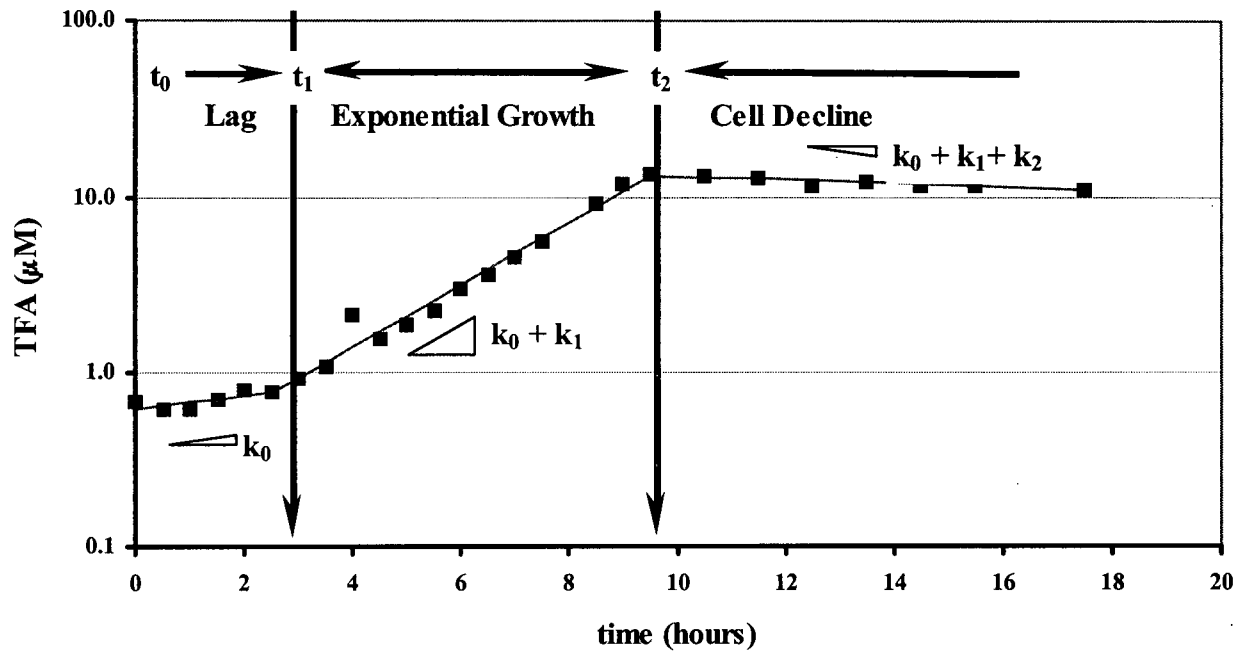


Figure 3-13. A typical total fatty acid (TFA) biomass growth curve on resin acid with an acclimated enrichment mixed culture, in this case, at pH 7.5 for experiment A. The three log-linear phases are delineated by times t_1 and t_2 . The model curve was the least squares best fit of equation (3-57).

$$\ln(X) = \ln(X_0) + \sum_{i=0}^2 H(t-t_i) k_i (t-t_i) \quad (3-57)$$

where X is the biomass concentration (TFA), X_0 is the initial TFA concentration, k_i are the cumulative rate constants, t_i are characteristic growth curve time points and $H(t)$ is Heaviside's unit step function (Figure 3-13). The least-squares estimates for the growth curves in experiments A, B and C are listed in Table 3-8.

The maximum growth rates (Q), shown in Figure 3-14, were calculated from the rate constants of equation (3-57) as follows:

$$Q = k_0 + k_1 \quad (3-58)$$

Upon repeated experimentation, the maximum growth rates for the pH-acclimated enrichment cultures, initiated with mixed liquor samples from the Western Pulp Partnership UNOX biobasin in Squamish BC, were different. Although all the important aspects of the experiment were held constant, some variability between experiments was anticipated due to natural population

differences in the mixed liquor samples obtained for each case. The potential growth-linked removal rate of resin acids for the mill biobasin varied by as much as 50 percent between experiments and almost that much again, as a function of pH. In experiment B, a replicate shake flask was included at pH 7. The maximum specific growth rate for the duplicate flask very closely matched the first. Therefore, differences in the growth rates between pH levels for each experiment were most likely indicative of the growth conditions and not of uncontrolled experimental variability.

Table 3-8. Least squares estimates of biomass growth kinetic parameters (equation (3-57)) as illustrated in Figure 3-13. For the growth curves, points 0, 1, and 2 refer to time zero, the end of the lag phase and the end of exponential growth. The TFA yield coefficient is the linear approximation of molar microbial fatty acid production per mole of substrate removed during exponential growth ($t_1 < t < t_2$).

Experimental Condition		Rate Constants 1/Hr			Characteristic Times (Hr)		Biomass Concentrations $\mu\text{M TFA}$			Yield $\mu\text{mole TFA}/\mu\text{mole}$
Exp. ID Substrate	pH	k_0	k_1	k_2	t_1	t_2	X_0	X_1	X_2	Y_{TFA}
A Resin Acid	6.04	0.098	0.330	-0.452	3.184	9.112	0.786	1.073	13.580	0.057
	7.03	0.110	0.318	-0.459	3.430	9.678	0.733	1.069	15.483	0.057
	7.55	0.087	0.320	-0.432	2.532	9.540	0.620	0.772	13.343	0.049
	8.06	0.000	0.430	-0.450	2.928	9.455	0.734	0.735	12.172	0.048
	8.44	0.032	0.235	-0.279	3.287	12.429	0.703	0.779	8.944	0.030
B Resin Acid	5.50	0.000	0.239	-0.257	2.750	10.286	0.630	0.630	3.813	0.047
	6.01	0.000	0.295	-0.286	2.522	8.755	0.575	0.575	3.607	0.067
	6.51	0.000	0.197	-0.202	4.285	16.719	0.794	0.794	9.199	0.062
	7.03	0.000	0.329	-0.346	4.910	11.750	1.176	1.176	11.167	0.050
	7.02	0.000	0.327	-0.340	6.385	11.766	2.113	2.113	12.264	0.051
	7.55	0.000	0.367	-0.377	3.987	11.721	0.750	0.750	12.786	0.067
	8.08	0.000	0.314	-0.331	4.437	12.733	1.044	1.044	14.153	0.052
8.53	0.000	0.228	-0.267	5.034	17.367	0.807	0.807	13.379	0.053	
C Resin Acid	5.95	0.000	0.389	-0.391	4.141	11.522	0.584	0.584	10.331	0.058
	6.45	0.000	0.427	-0.435	3.642	11.142	0.472	0.472	11.585	0.066
	6.96	0.000	0.394	-0.403	3.334	11.169	0.534	0.534	11.704	0.070
	7.47	0.000	0.459	-0.472	3.096	10.125	0.444	0.444	11.210	0.062
	8.04	0.045	0.332	-0.408	3.626	12.112	0.413	0.486	11.913	0.073
C Sodium Acetate	5.99	0.000	0.568	-0.582	5.253	9.917	0.694	0.694	9.830	0.003
	6.46	0.127	0.564	-0.702	4.524	8.802	0.308	0.548	10.557	0.004
	6.98	0.137	0.487	-0.632	4.249	8.776	0.369	0.661	11.184	0.004
	7.51	0.173	0.543	-0.730	3.540	7.756	0.309	0.571	11.669	0.004
	8.09	0.050	0.485	-0.551	2.634	9.362	0.272	0.310	11.311	0.004

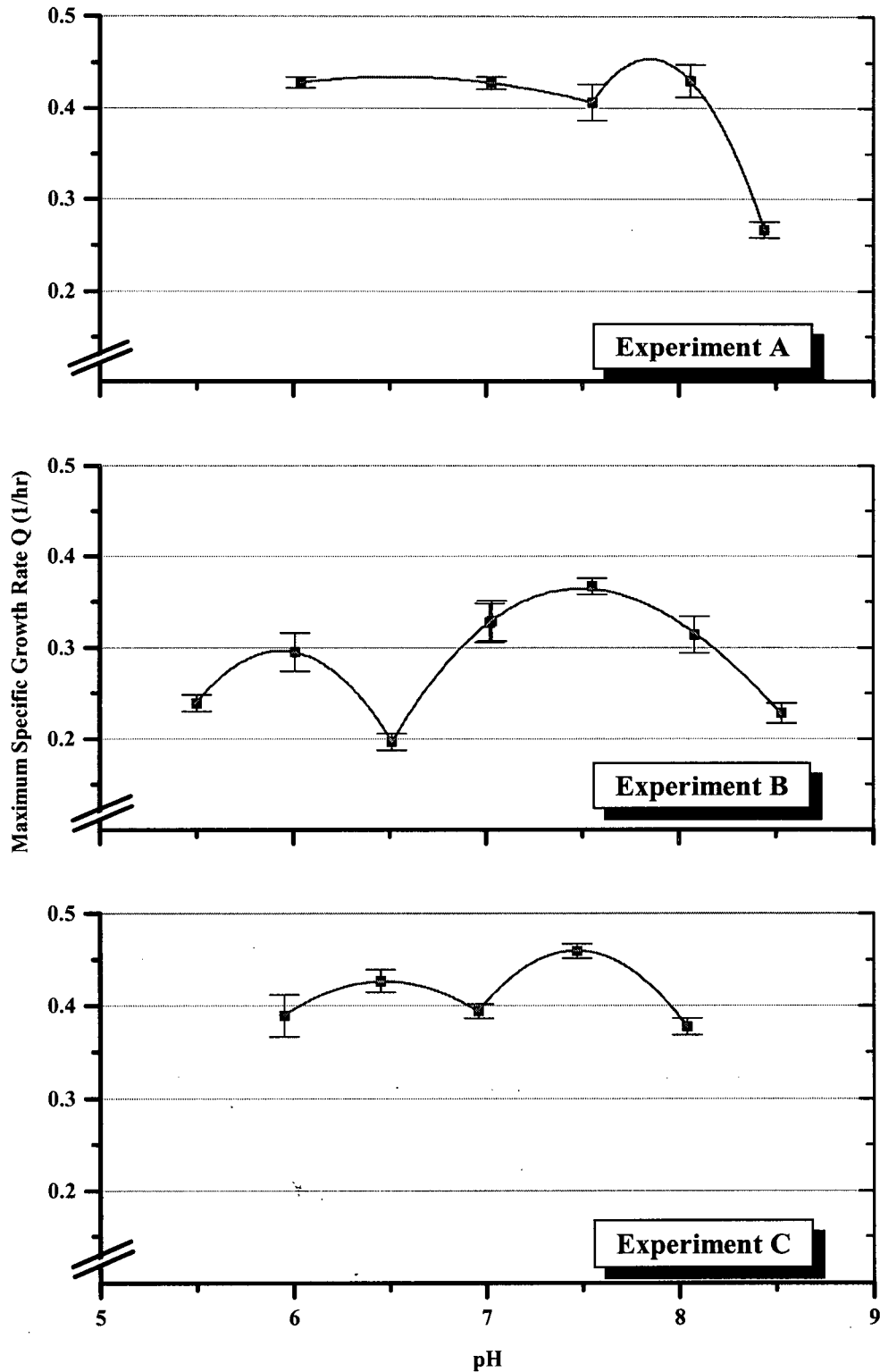


Figure 3-14. Maximum specific growth rates for enrichment cultures of abietane resin acid degraders as a function of pH from three separate experiments (A, B, C from top to bottom). For each experiment the enrichments were all initiated from a common inoculum of mixed liquor from the Western Pulp Partnership UNOX biobasin in Squamish BC. Since all other parameters were held constant, the differences between experiments reflect differences in the initial inoculum. Parabolic curves were fitted based on the data interpretation of separate growth optima under acid and alkaline conditions. Error bars represent the standard deviation in estimating Q (" $k_0 + k_1$ " in equation (3-57)) from the TFA data. Overlapping data points from replicate growth curves made at pH 7 for the experiment B (middle) give an indication of experimental reproducibility.

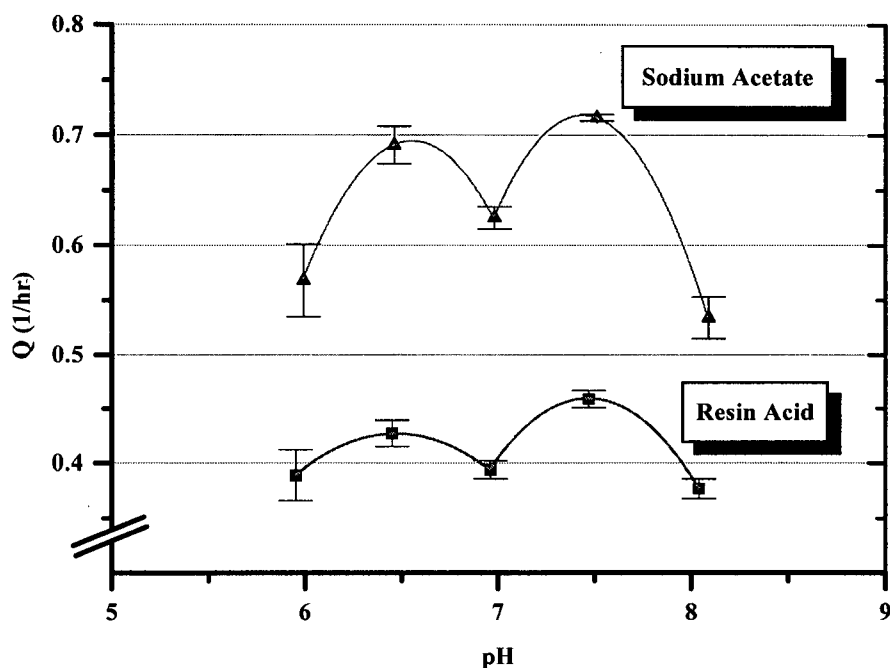


Figure 3-15. Comparison of maximum specific growth rates (Q) for mixed cultures enriched for abietane resin acid degraders at 5 different pH levels inoculated into media containing either sodium acetate (▲) or abietane resin acids (■) as the sole carbon sources. Parabolic curves were fitted based on the data interpretation of separate growth optima under acid and alkaline conditions. Error bars represent the standard deviation in estimating Q (" $k_0 + k_1$ " in equation (3-57)) from the TFA data.

A consistent pattern in maximum growth rate as a function of pH was observed. The data showed evidence of separate optima in the removal rate under acidic and alkaline conditions (Figure 3-14). In experiment C for the parallel shake flasks containing sodium acetate, the maximum growth rates were influenced by the change in carbon source but the two optima persisted (Figure 3-15).

In the period of balanced growth, delimited by times t_1 and t_2 in equation (3-57), plots of total resin acid (TRA) depletion versus total fatty acid (TFA) production indicated the consistency of the TFA growth yield or Y_{TFA} . The approximately linear, balanced growth yields were estimated by linear regression (Table 3-8 and Figure 3-16). For each of the three experiments, no dependency of yield on pH was observed. Therefore, these data were reduced further by calculating a pooled average TFA yield for each experiment (Figure 3-17). The molar resin acid TFA yields between replicate experiments were of similar magnitude but did differ, reflecting again some variability in the mixed liquor grab samples taken for each experiment. In experiment A, only the two major fatty acids, {16:0, 18:1}, were enumerated. For this reason the calculated

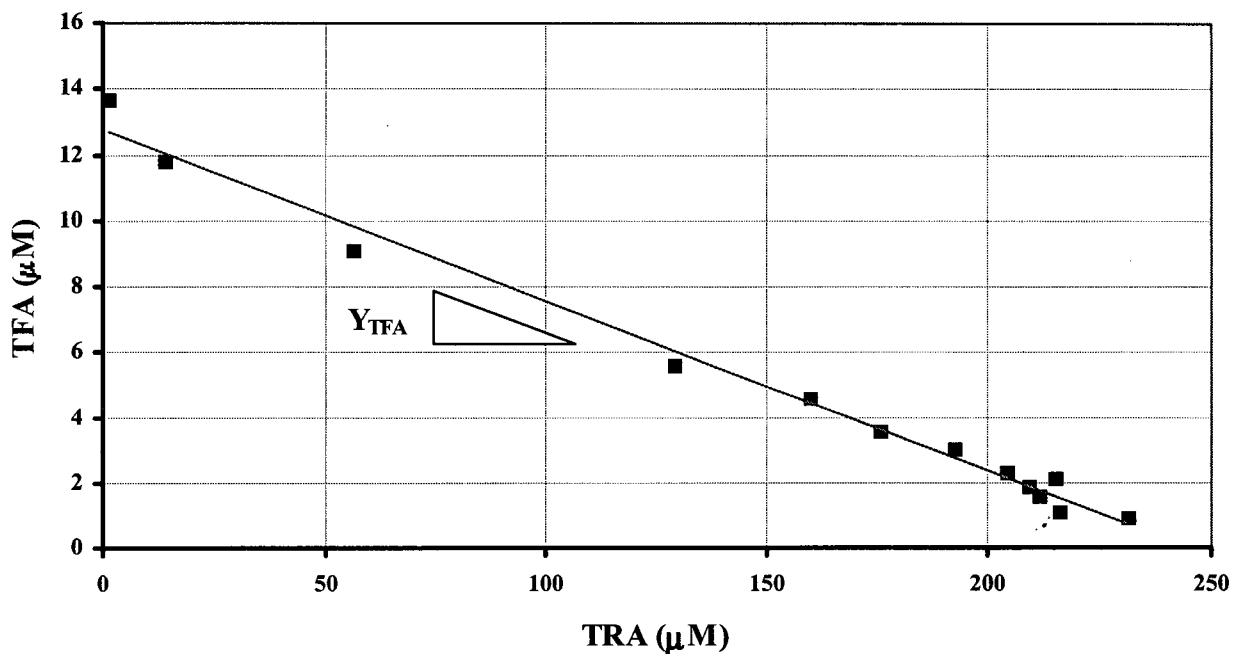


Figure 3-16. A typical linear yield approximation ($Y_{TFA} = -\Delta[TFA]/\Delta[TRA]$) for biomass production, as total fatty acid (TFA), versus total resin acid (TRA) consumption during exponential (balanced) growth ($t_1 < t < t_2$ in equation (3-57)) for an acclimated mixed culture. These data correspond to the growth data presented in Figure 3-13. Yield values were estimated by linear regression.

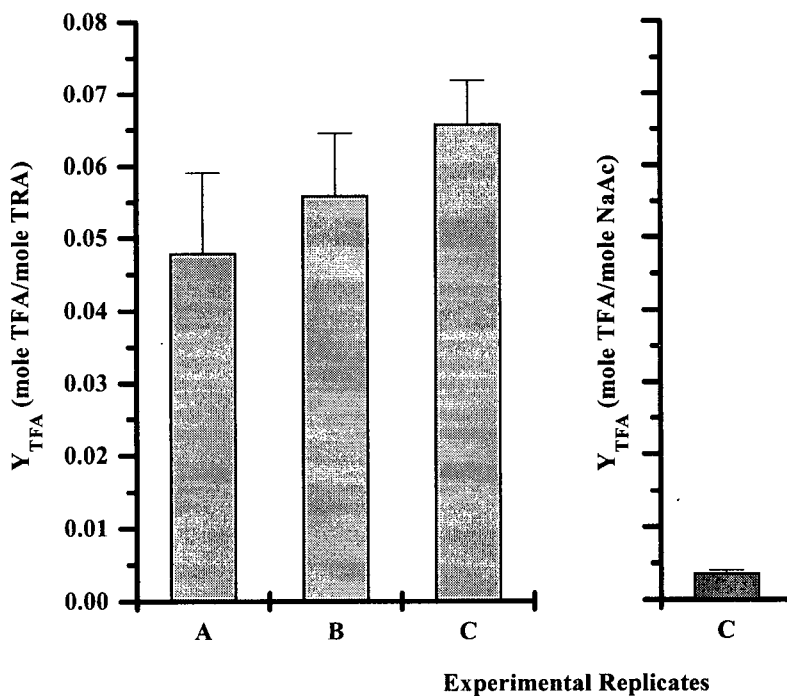


Figure 3-17. Average molar total fatty acid (TFA) or biomass yield from three replicate experiments (A, B, C) monitoring microbial growth for total resin acid (TRA) depletion (left graph) as a function of pH. For replicate C, molar TFA yield on sodium acetate (NaAc) was determined for parallel shake flasks (right graph).

Table 3-9. Comparison of average total fatty acid (TFA) or biomass yield coefficients for abietane resin acid enrichment culture growth on resin acids or sodium acetate as sole carbon sources.

Carbon Source	Resin Acid	Sodium Acetate
Molar Yield	65.89 mmole TFA/mole	3.63 mmole TFA/mole
Balanced Reaction	$C_{20}H_{30}O_2 + \frac{53}{2}O_2 \rightarrow 20CO_2 + 15H_2O$	$C_2H_3O_2^- + \frac{7}{4}O_2 \rightarrow 2CO_2 + \frac{3}{2}H_2O$
$-\Delta G_f$	50.9 kJ/mole	369.9 kJ/mole
$-\Delta G_r$	11,410.65 kJ/mole	776.26 kJ/mole
ThOD	0.848 mg O ₂ /mole	0.056 mg O ₂ /mole
Oxygen Yield	77.70 mmole TFA/mg O ₂	64.82 mmole TFA/mg O ₂
Energy Yield	5.77 mmole TFA/J	4.68 mmole TFA/J

Standard Gibbs formation energies: $\Delta G_f(CO_2) = -394.90$ kJ/mole and $\Delta G_f(H_2O) = -237.57$ kJ/mole

Reaction free energy yield: $\Delta G_r = \Sigma \Delta G_f(\text{products}) - \Sigma \Delta G_f(\text{reactants})$

ThOD = Theoretical Oxygen Demand

References: (Brock and Madigan 1991; Daubert et al. 1995; Metcalf & Eddy 1991)

TFA yields for experiment A were lower than those of experiments B and C (Figure 3-17).

In experiment C, the estimated molar TFA yield on sodium acetate was much lower than the TFA yield on resin acids (Figure 3-17 and Table 3-9). The theoretical oxygen demand is 56 g O₂/mole for acetate and is 848 g O₂/mole for resin acid (C₂₀H₃₀O₂). Converting the two TFA yields to a common basis of theoretical oxygen demand, the mixed culture yield on acetate would be 83 percent of the resin acid yield. Another way to compare the two yields is on a chemical energy basis. On this basis, the acetate yield is calculated to be about 81 percent of the resin acid yield. By applying a common basis, the growth yields on the two substrates can be seen to be similar but not equal. Biomass yield on resin acids was significantly greater than the yield on sodium acetate.

In Chapter 2 a resin acid residuum was exhibited by the substrate depletion curves. This residuum was estimated, in the absence of adequate biomass data, with a Monod model modified to include a threshold concentration. According to the model, the threshold represents a substrate level below which growth is no longer supported. At the threshold, the flux of organic carbon to the microorganism becomes low with respect to cellular requirements for maintenance energy. In the present investigation, the lag and cell decline periods of the batch growth cycles were defined by the characteristic times t_1 and t_2 identified from the biomass TFA data (see equation (3-57), Figure 3-13 and Table 3-8). Using this information, an initial substrate concentration (S_0) and a substrate

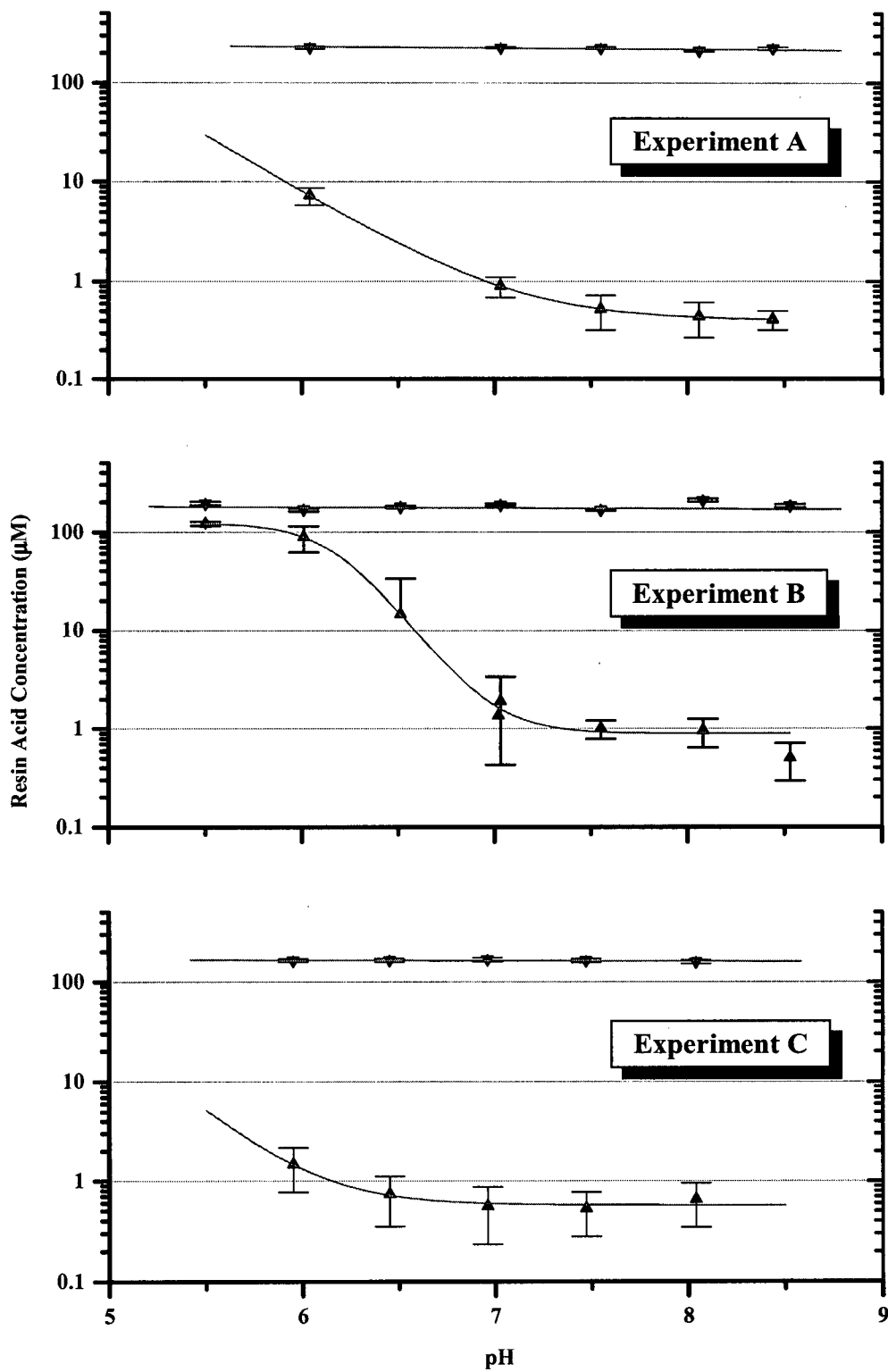


Figure 3-18. Initial (▼) versus residuum (▲) resin acid concentrations obtained for replicated mixed culture batch experiments as a function of pH. The initial (S_0) resin acid concentrations were estimated from the experimental substrate depletion curves by averaging extracted values for growth times less than t_1 (see Figure 3-13 and Table 3-8). Similarly threshold (S^*) values were obtained by averaging the experimentally determined resin acid concentrations for growth times greater than t_2 . Averages were typically made from five or more sample points. The error bars represent the standard deviation of the average. Large error bars reflect a decrease over the period averaged.

threshold (S^*) were estimated from the depletion curves by averaging the substrate concentrations for times less than t_1 and for times greater than t_2 respectively (Figure 3-18). In agreement with the results of Chapter 2, upon repeated experimentation, for pH values less than 7, an elevated threshold was observed. The threshold level for alkaline pH levels remained relatively constant between experiments, but the residuum level under acidic conditions was found to be variable. From the dynamic surface tension measurements described in Chapter 2, the residuum was hypothesized to be related to a decreased bioavailability of resin acids under acidic conditions. Differences in the residuum levels, between experiments A, B and C, could be due to variability in the extent of resin acid dispersion in the media for each experiment. The initial concentration of sodium acetate in Experiment C was $3067 \pm 88 \mu\text{M}$ and, in this case, no residuum was detected.

In this investigation, all of the kinetic parameters of the Monod model described in Chapter 2 were estimated from the data without the uncertainties introduced in non-linear regression curve fitting of the substrate depletion curve only. Further, it was determined that the Monod constant, k_s , was negligible, based on the observation of exponential growth independent of substrate concentration. Although k_s values were estimated in Chapter 2, this study demonstrates that it would have been unwise to have given those parameters any significance beyond their ability to empirically represent the data. The importance of the kinetic parameters derived in Chapter 2 was for satisfactory modelling of the data for the estimation of threshold resin acid levels. The list of the characteristic times, t_1 , in Table 3-8, shows further that each batch cycle exhibited a distinct lag phase. Traditional Monod kinetics do not account for the lag phase (Bailey and Ollis 1986; Panikov 1995). Serious errors are possible in estimated parameters with batch growth data, when a lag phase is neglected (Chiu et al. 1972).

The lag phase can be minimized experimentally by using acclimated cultures enriched on the target substrate and by using a late log phase culture as the inoculum. However, changes in environment, such as a sudden change in substrate concentration, may result in an induction period, during which mixed cultures make physiological adjustments. Even with these

precautions, biological systems are temperamental, meaning that the absence of the lag phase cannot be assured, and therefore, it is better to explicitly determine lag phase duration. Errors in neglecting a lag phase can affect the magnitude of the rate constants which depend on the estimation of the initial biomass concentration (X_0). Careful culture dilution techniques can be used to accurately measure low initial culture concentrations (Dang et al. 1989; Simkins and Alexander 1985). However, in this investigation it was found that the initial concentration may not be the same by the end of the lag phase (X_1). More confidence in derived kinetic parameters was facilitated by explicitly determining the duration of the lag phase and the biomass concentration entering the balanced growth phase.

By offsetting the time scale so that t_1 corresponds to time zero, the model substrate depletion curves were calculated by numerically integrating the equation (Chapter 2):

$$g(\eta) = \frac{ds}{d\eta} = \frac{s - s^*}{\kappa + s} \left(s - \left(1 + \frac{1}{\Psi} \right) \right) \quad (3-59)$$

$$x = \frac{X}{X_1}, \quad s = \frac{S}{S_0}, \quad s^* = \frac{S^*}{S_0}, \quad \kappa = \frac{k_s}{S_0}, \quad \eta = Qt, \quad \Psi = \frac{S_0}{X_1} Y \quad (3-60)$$

with input parameters from the estimated initial conditions S_0 (Figure 3-18) and X_1 (Table 3-8), the growth rate constants Q ($k_0 + k_1$ in Table 3-8) assuming k_s approximately zero, the TFA yield coefficients (Y_{TFA} in Table 3-8) and the threshold concentrations S^* (Figure 3-18). Figure 3-19 illustrates the general ability of the model to describe the substrate depletion curves, confirming growth-linked metabolism. Attempting to determine the parameter values by non-linear regression of the substrate depletion curve could also yield a reasonable empirical fit, but the parameter estimates would be different and fundamentally ungrounded.

Although the approximation of a constant Y_{TFA} during balanced growth was found to be reasonable, the yield coefficient was observed to depart from linearity in what may be considered transition zones near t_1 and t_2 (Figure 3-20 and Figure 3-21). Further, the removal of the individual abietane resin acids was not concurrent, but rather biphasic (sequential). Consumption

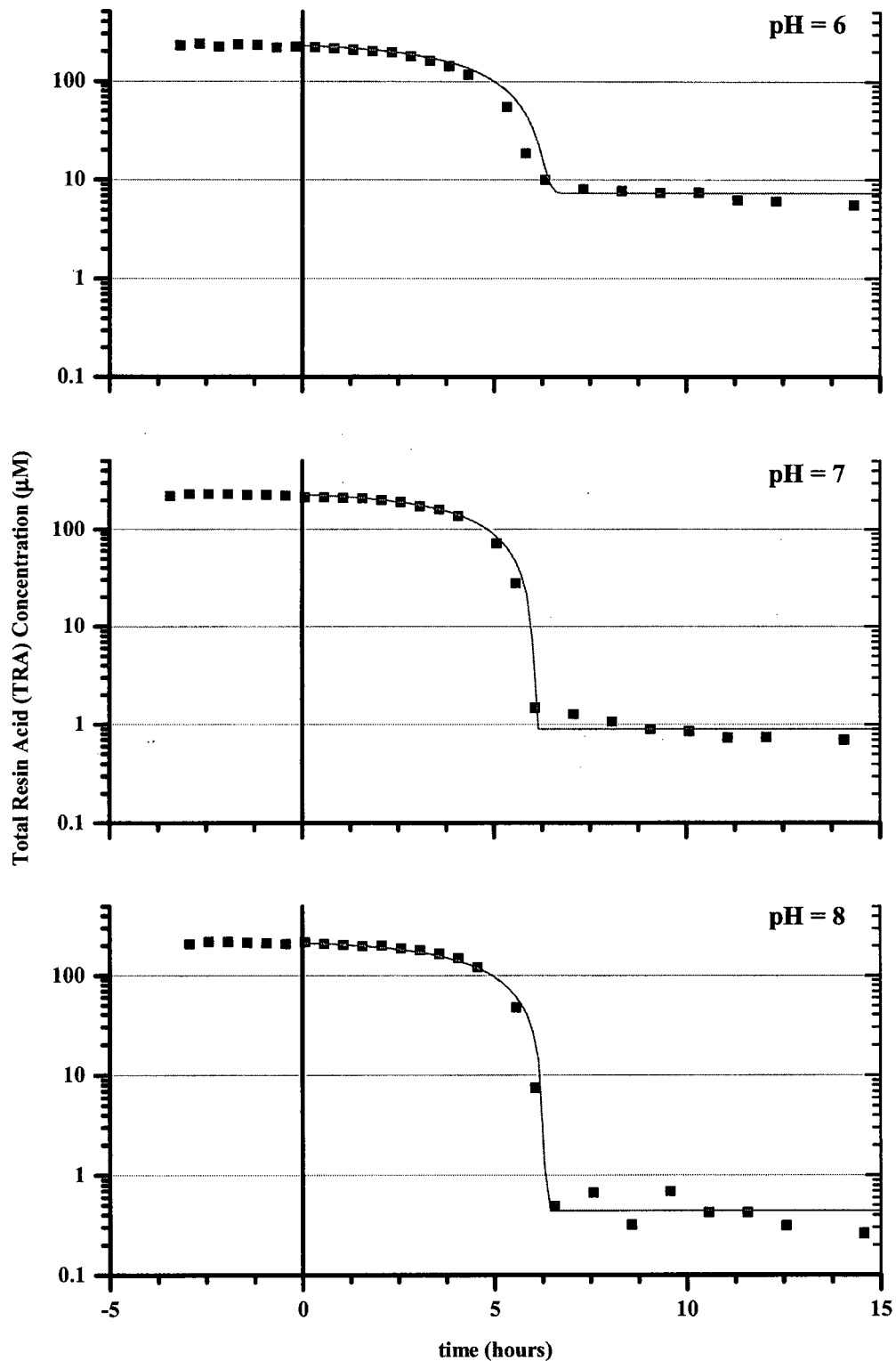


Figure 3-19. Experiment A model substrate depletion curves for pH conditions 6, 7 and 8 (Top to Bottom). The growth time was offset by t (equation (3-57)) so that time zero corresponded with the start of exponential growth. Model curves were generated by integrating equation (3-59) with the parameters $\{S_0, X_1, Q, k_s, Y_{TFA}, S^*\}$ derived from the analysis of the TFA biomass production curve in conjunction with the substrate depletion data. The parameter values applied for the model curves were $\{227.7, 1.073, 0.428, 0.0, 0.057, 7.3\}$, $\{227.3, 1.069, 0.428, 0.0, 0.057, 0.9\}$, and $\{212.2, 0.735, 0.430, 0.0, 0.048, 0.4\}$ in units of $\{\mu\text{M TRA}, \mu\text{M TFA}, \text{Hr}^{-1}, \mu\text{M TRA}, \mu\text{M TFA}/\mu\text{M TRA}, \mu\text{M TRA}\}$ from top to bottom respectively. Growth-linked kinetics are qualitatively confirmed.

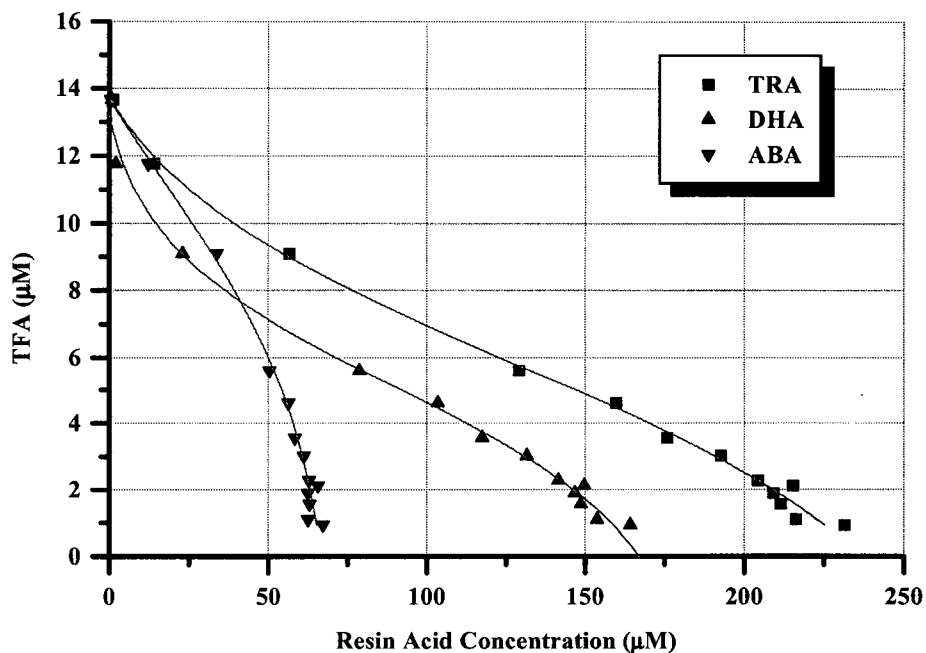


Figure 3-20. A more detailed consideration of total fatty acid TFA yield during mixed culture exponential growth ($t_1 < t < t_2$ in Figure 3-13). The resin acids dehydroabietic (\blacktriangle) and abietic (\blacktriangledown) acid in the mixture sum to the total resin acid (TRA) concentration (\blacksquare). Y_{TFA} deviates from linearity near the beginning and end of exponential growth. Consumption of ABA initially lags behind DHA. These data correspond to the growth curve in Figure 3-13.

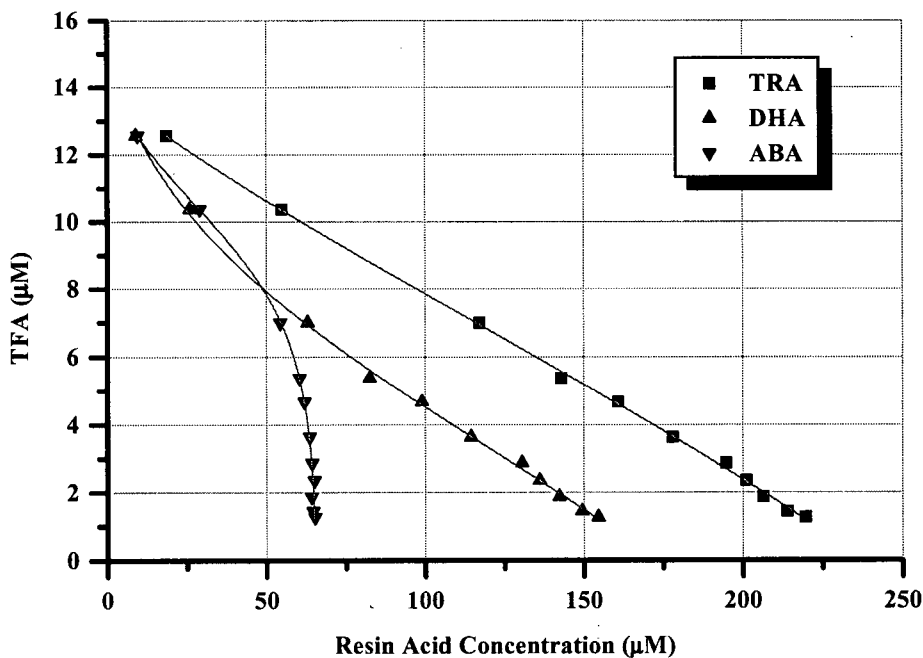


Figure 3-21. A second example of a nearly linear biomass or total fatty acid TFA yield with respect to total resin acid removal (\blacksquare) during mixed culture exponential growth ($t_1 < t < t_2$ in Figure 3-13). Removal of dehydroabietic (\blacktriangle) precedes abietic (\blacktriangledown) acid. The data are for pH 6.0 in experiment A.

of dehydroabietic acid (DHA) preceded abietic acid (ABA) until they were of similar concentration. The initial concentration of dehydroabietic acid was always about twice that of abietic acid. In some experiments (not shown) when the initial concentration of abietic acid was greater than DHA, the reverse sequence of removal was observed. The order of removal was dependent on relative concentration.

Balanced growth is succeeded by a decline phase in which essential nutrient(s) become limiting or waste products become inhibiting. Classical Monod kinetics do not account for cellular decay and thus have been modified by incorporating an additional first order term (Bailey and Ollis 1986):

$$\frac{dX}{dt} = qX - q_D X \quad (3-61)$$

where q is the specific growth rate (Chapter 2) and q_D is the decay coefficient that is meant to represent endogenous metabolism. A sensitivity analysis of the Monod model with decay shows that the influence of q_D can only be distinguished in the portion of the data from a biomass production curve after the decay phase begins (Holmberg 1982). The maintenance requirements of aged and dying cells at the end of batch growth are different from cells rapidly multiplying during exponential growth. The relative change in the cellular fatty acid composition during batch growth shown in Figure 3-10 would indicate a general change in the make-up or condition of mixed populations during batch growth. Thus, applying a single decay coefficient across the entire growth time domain may not be appropriate, even if it does produce a model which adequately describes the data.

Including q_D in the model will also alter the other kinetic parameter values from those obtained from the balanced growth phase in isolation. Furthermore, while the assumption that the yield coefficient is constant may be reasonable during balanced growth, this approximation was observed to fail near the tail of the exponential growth phase. The net loss in TFA biomass after t_2 (Figure 3-13) would indicate an onset of endogenous growth. However, at the same time, the

residuum was observed to also decrease during this period at a reduced rate, presumably due to diffusion rate limitation (Chapter 2).

The combination of catabolic and endogenous metabolic activities after t_2 make for a more complicated model. For example, the high residuum levels that occurred in Experiment B were sufficient to support a net, though slight, biomass increase during the decline phase. Therefore, batch growth kinetics are best approached by separately considering the three distinct phases in order to arrive at kinetic parameters that reflect the three distinct physiological conditions of the mixed culture. Due to its complexity, the decline phase was not modelled for this investigation. Only the exponential growth phase was considered since only in this phase of the batch growth cycle could growth parameters be explicitly determined.

During the growth cycle time period when the activity on abietic acid began to increase, two metabolites were observed to briefly accumulate in the system. These two metabolites were tentatively identified as the methyl esters of 6-dehydro-dehydroabietic acid and 7-keto-dehydroabietic acid on the basis of their mass spectrograms. The 7-keto DHA metabolite was later confirmed by comparison with a pure standard. Acidic conditions favoured the production of 6-dehydro-dehydroabietic acid while 7-keto-dehydroabietic acid dominated under alkaline conditions (Figure 3-22). The metabolite 7-keto DHA has been recovered from kraft mill effluent and receiving water samples (Taylor et al. 1988). In previous studies (reviewed by Rogers (1989) and Taylor (1988)) on breakdown pathways of DHA by *F. resinovorum*, metabolic intermediates were obtained by retarding the rate of metabolic activity either by the omission of nutrients such as NH_4^+ , Fe^{2+} , or Mg^{2+} or by the addition of an inhibitor. In this investigation, retardation of DHA metabolism occurred as the rate of ABA uptake began to increase (Figure 3-20 and Figure 3-21). This period of transition in the biphasic process could explain the observed accumulation of DHA metabolic intermediates in the batch system.

In studies with *F. resinovorum*, Biellmann et al. (1973a) found that this isolate could utilize two routes for the metabolism of DHA. However, both pathways started with oxidative attack at C-3 and C-7, forming either 3 or 7-keto DHA (Figure 3-23). Both the 3 and the 7 sites needed to be

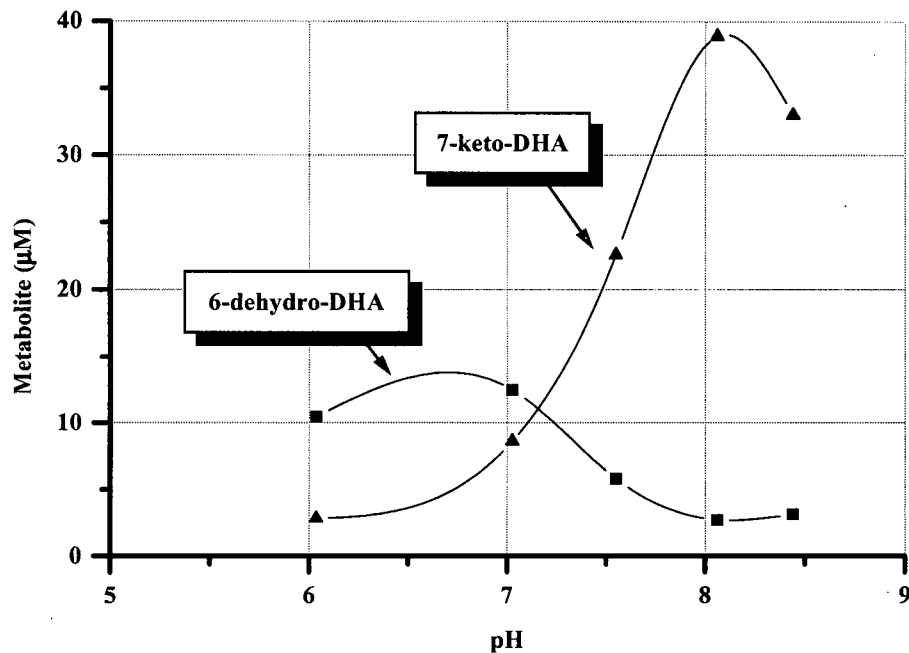


Figure 3-22. Peak metabolite concentrations observed during mixed culture batch growth experiment A. The timing of metabolite peaks coincided with the period in the growth cycle when the removal of DHA became secondary to ABA.

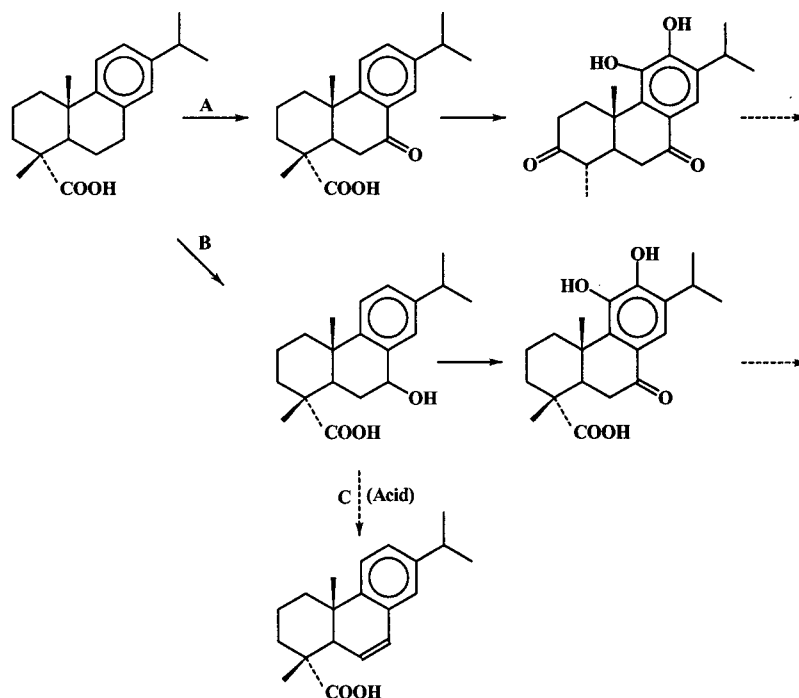


Figure 3-23. Two pathways for the initial biodegradation of dehydroabietic acid. *F. resinovorum* (A) begins with oxidative attack at C-3 and C-7 forming 3-keto and 7-keto DHA (Biellmann et al. 1973a). Both the C-3 and C-7 positions must be oxidized before dihydroxylation of the aromatic ring. *Pseudomonas sp.* and *A. eutrophus* (B) similarly attack the C-7 position to form 7-hydroxy DHA but do not oxidatively attack position C-3 before aromatic ring hydroxylation (Biellmann et al. 1973b). Different bacteria seem to have adopted different approaches to DHA utilisation. Extraction under acidic conditions is believed to have promoted the dehydration of 7-hydroxy DHA to form 6-dehydro DHA (C).

oxidized before dihydroxylation of the aromatic ring at C-11 and C-12 could proceed. Biellmann et al. (1973b) subsequently isolated two other Gram-negative organisms, *Pseudomonas sp.* and *A. eutrophus*, that also grew on DHA as a sole carbon source. These two organisms were found to use a similar pathway to *F. resinovorum*. The first step in DHA oxidation by these other bacteria was again an attack on C-7 but in this case, 7-hydroxy DHA was collected as the first intermediate (Figure 3-23). Dehydrogenation of the alcohol and dihydroxylation of the aromatic ring followed the first oxidation step. Hence, different bacteria seem to have acquired similar, but different, approaches to the utilization of resin acids. It is reported (Soltes and Zinkel 1989) that 7-hydroxy DHA readily dehydrates to form 6-dehydro dehydroabietic acid. Since dehydration reactions are catalysed by acidic conditions (Morrison and Boyd 1992), it is possible that the H_2SO_4 acidification step during sample extraction would convert 7-hydroxy DHA in the media to 6-dehydro DHA. Therefore, the literature suggests that the relative proportions of 7-keto and 6-dehydro DHA found in the media as a function of pH for these experiments reflect different levels of separate metabolic activities. Differences in the observed metabolites could indicate pH-induced changes in a particular organism, or a pH-induced shift in the community.

As was observed for the fatty acid composition of DhA-35, the dominant saturated fatty acid in the spectra for the mixed cultures was hexadecanoic acid. However, the principal monoenoic fatty acid was cis-octadecenoic acid. With reference to the pure culture results and the literature, it was initially felt that the response to pH and resin acid hydrophobicity would be seen by a change in the relative proportion of these two major fatty acids. Indeed, repeated experiments revealed a reproducible trend in the logratio of 18:1ω7c with respect to 16:0 (Figure 3-24). For the mixed culture, the proportion of the dominant monoenoic fatty acid increased with pH. Such a response would be consistent with an expected pseudo-species response to changing substrate hydrophobicity. However, data for the enrichment cultures grown on sodium acetate produced a similar pattern. In addition, the relative level of octadecenoic acid was lower with sodium acetate, which is in contradiction to an expectation founded on observations made with DhA-35 (Figure 3-11). A change in substrate is known to have the ability to influence the lipid content of a single microorganism. The observed change in the proportion of the monoenoic fatty acid 18:1

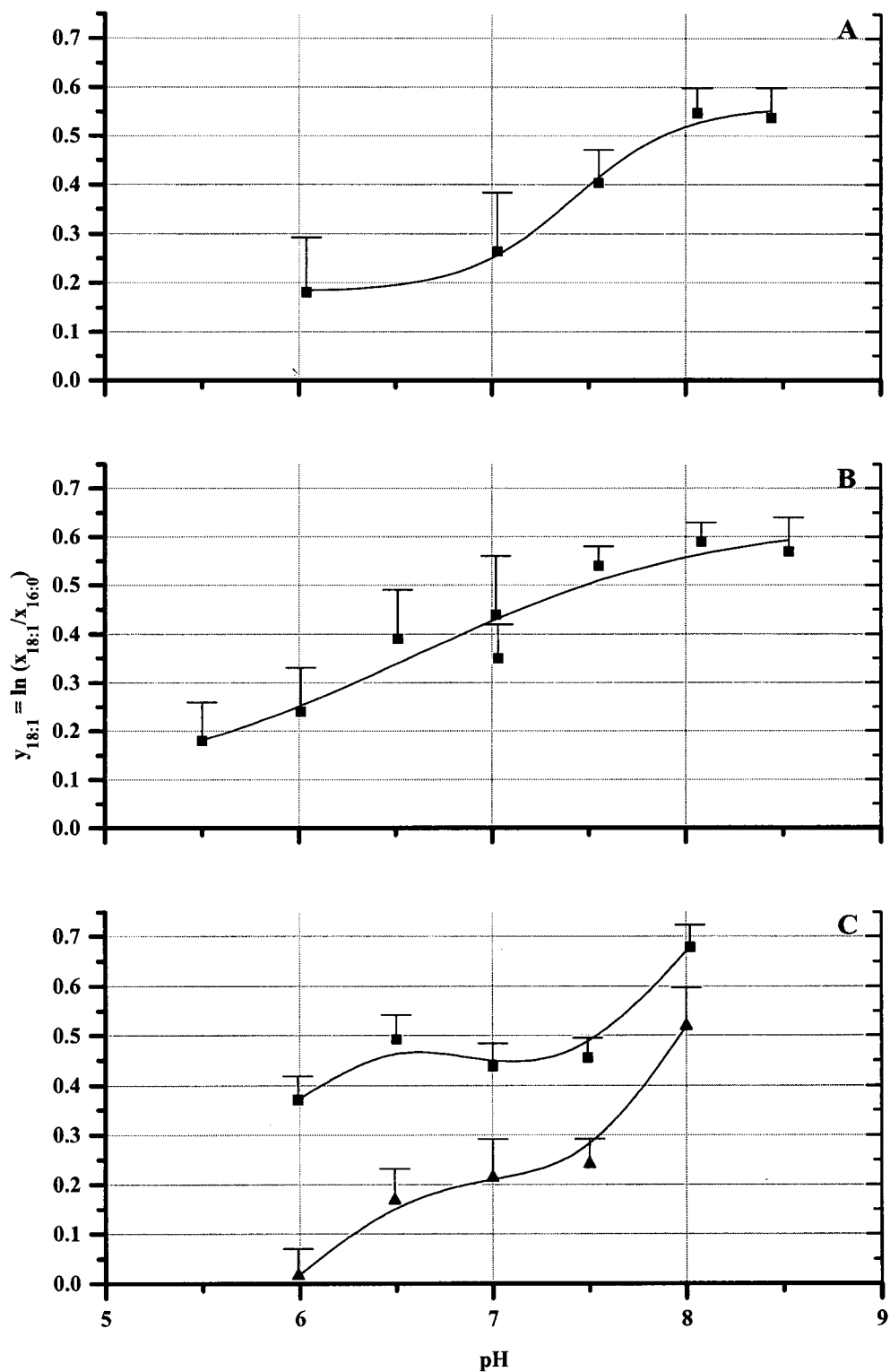


Figure 3-24. Relative proportions (logratios) of the monoenoic fatty acid 18:1 ω 7c with respect to 16:0 for resin acid enrichment cultures grown up on abietane resin acids (■) or sodium acetate (▲) as a function of pH. Results are given for three separate experiments (A, B, C from top to bottom). In each case the enrichment cultures were initiated from a common inoculum of mixed liquor from the Western Pulp Partnership UNOX biobasin in Squamish BC. The proportion of 18:1 ω 7c increased with pH and decreased for growth on sodium acetate. Error bars represent the standard deviation for samples taken in the vicinity of the height of balanced growth.

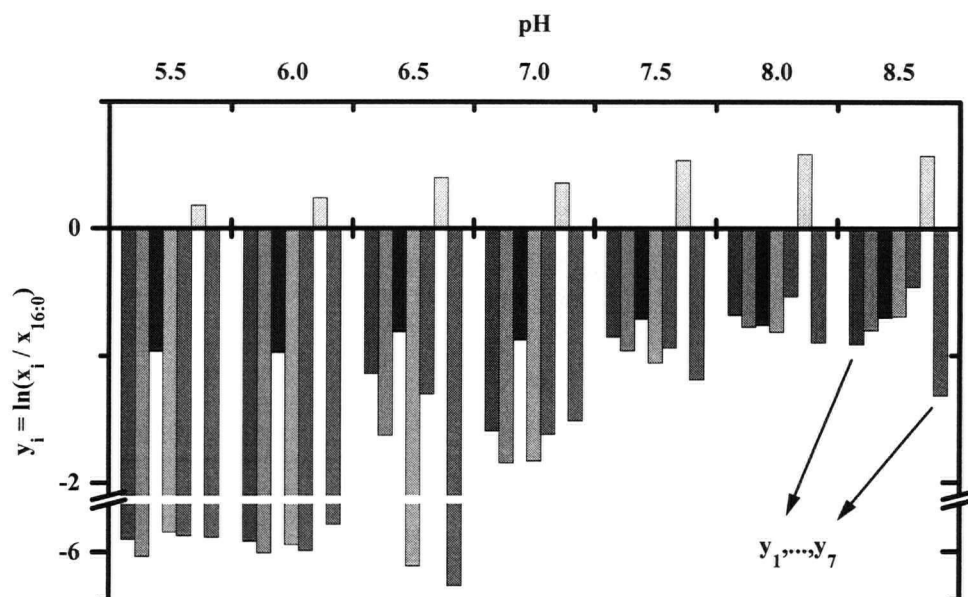


Figure 3-25. Logratio fatty acid compositions for Experiment B as a function of pH. Logratios are with respect to 16:0 and $\{y_1, \dots, y_7\}$ correspond to logratios of $\{12:0, 15:0, 16:1\omega7c, 17:1\omega7c, 17:0, 18:1\omega7c, 18:0\}$ respectively. Note that for $y_i = 0 \rightarrow x_i = x_{16:0}$.

was not consistent with the observed response of DhA-35.

These results suggested that the mixed culture fatty acid compositional changes with pH were not a general response or adaptation of a single representative pseudo-species, but rather a change in the content of the community of microorganisms. In other words, the fatty acid spectra indicate that different pseudo-species were obtained as a function of pH. The results presented thus far support this conclusion. The fact that different metabolite concentrations were observed, depending on pH, could be a consequence of different pathways used by different selected communities. The appearance of the two growth rate maxima could correspond to respective optimal pH conditions for the selected communities under acidic or alkaline conditions. The local minimum between the maxima would represent the transition zone from one community to the next. Variability in the growth rate patterns between repeated experiments could be a product of the diversity of enrichment cultures that arose from mixed liquor samples taken at different times. Therefore, the fatty acid spectra were considered in more detail in order to consider the microbial content as the underlying cause of the growth rate variability.

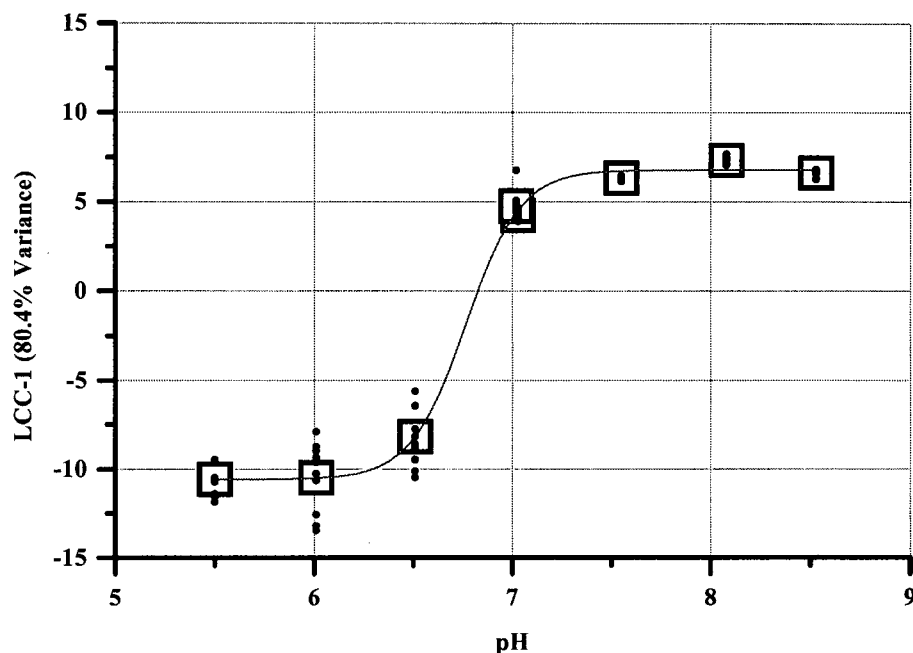


Figure 3-26. The first logcontrast canonical component (LCC-1) for Experiment B summarising 80.4 percent of the enrichment culture between-group chemotype variability as a function of pH. Mean values (\square) are shown for 10 samples (\bullet) taken around the height of the growth curve ($t \approx t_c$). The canonical components were calculated using logratios with $x_{16.0}$ as the common divisor.

Figure 3-25 shows qualitatively how the WCFA spectra changed as a function of pH for Experiment B. The relative proportions of the minor fatty acids increased to produce a greater chemotype diversity in the community under alkaline conditions. In total, the following 8 fatty acids characterized the cultures: 12:0, 15:0, 16:1 ω 7c, 16:0, 17:1 ω 7c, 17:0, 18:1 ω 7c and 18:0. From an analysis of variance, the hypothesis of equal spectra was not rejected for only the WCFA growth data at pH 5.5 and 6.0. Communities were compared on the basis of ten samples of WCFA compositions around the height of their TFA growth curves. Differences between enrichment cultures were quantitatively expressed by logcontrast canonical component analysis. The first and second logcontrast canonical components (LCC) accounted for 80.4 and 17.5 percent of the between group variance, respectively. The first component (LCC-1) is strongly correlated to pH. Figure 3-26 illustrates the well defined transition in the enrichment culture over the experimental pH range. The LCC-1 data were empirically fit to a sigmoidal function of pH. From this function, the most sensitivity (variability) to pH was predicted to be around pH 6.7. This pH value corresponds to the observed local minimum obtained for the maximum growth rate (Figure 3-14). Thus, logcontrast canonical component analysis of WCFA spectra identifies a pH

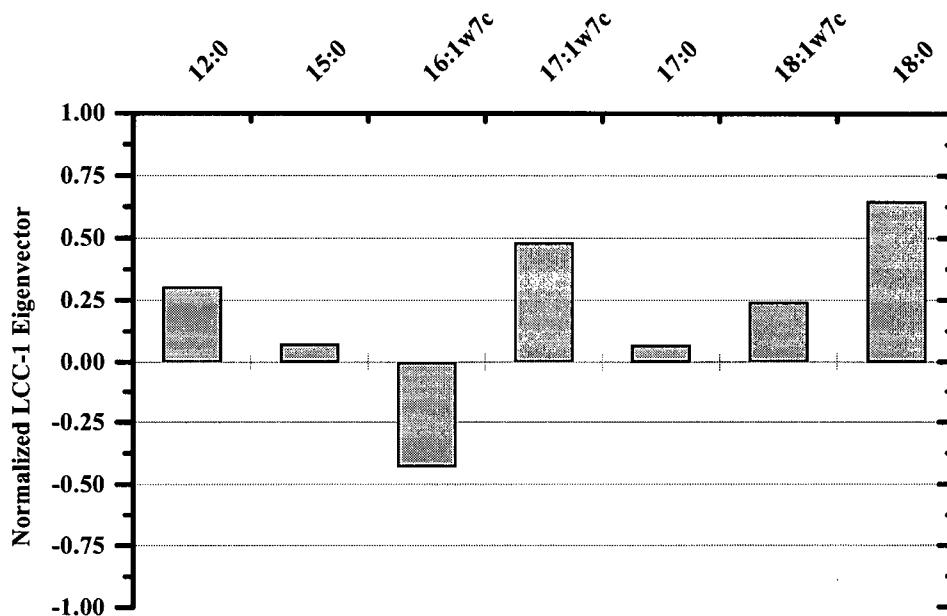


Figure 3-27. The normalized eigen vector for the first canonical component for experiment B. The relative loadings on the fatty acids show that logratios of 12:0, 15:0, 17:1w7c, 17:0 16:1w7c and 18:0 with respect to 16:0 increase with pH and the logratio of 16:1w7c decreases.

range of maximum sensitivity of mixed culture community structure to pH. It is of interest that where the microbial content was found to be the most sensitive to the environmental condition of pH, lower batch growth kinetics were also observed. These results would suggest that, for full scale treatment systems targeting specific contaminants, the sub-optimal conditions may occur at settings where the microbial content is most sensitive to small operational control errors.

The logcontrast canonical component is a weighted sum of the centred logratio fatty acid composition (equation (3-54)). The relative magnitudes of the weighting coefficients (ie. the logcontrast eigen vector) for LCC-1 are shown in Figure 3-27. Loading factors much different from zero indicate fatty acids most responsible for the between-group variability. Positive and negative loading factors correlate positively and negatively with pH, respectively. Logratios with respect to 16:0 show that increasing pH promoted the fatty acids {12:0, 15:0, 17:1w7c, 17:0, 18:1w7c, 18:0} while the logratio for 16:1w7c decreased. It was initially expected that the identification of certain marker fatty acids would be possible from the consideration of the component loading factors. However, once it was apparent that the changes in fatty acid profiles were more a consequence of a change in pseudo-species rather than a specific membrane

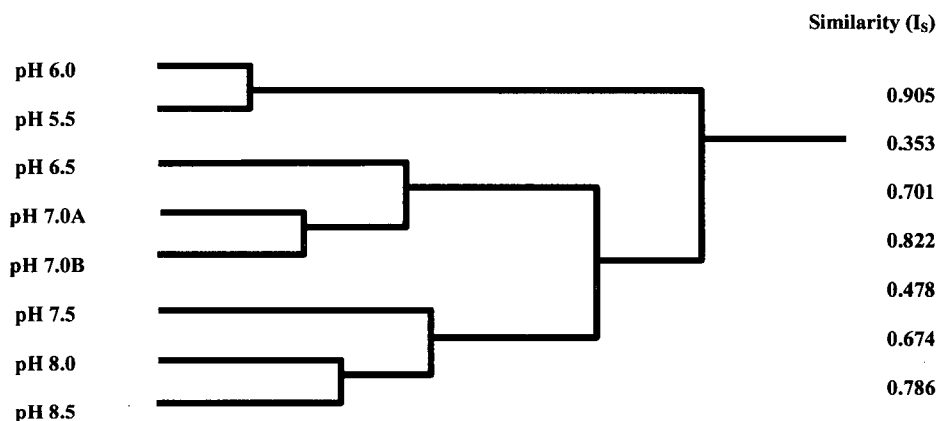


Figure 3-28. Dendrogram from the similarity matrix for the mean WCFA compositions describing the enrichment cultures in Experiment B as a function of pH. Composition similarity was calculated with equation (3-36) based on σ of 1.3. The dendrogram was created by single linkage agglomeration. The WCFA compositions can be clustered into three groups defined by pH around 6.0, 7.0 and 8.0 respectively.

adaptation, the significance of the individual loading factors became less important. The trend in any one fatty acid logratio as a function of pH most likely reflects an overall change in the balance of species for the respective enrichment cultures. Therefore, the utility of the fatty acid profile analysis was most useful in its ability to provide statistical comparisons of the enrichment cultures. Had fatty acid shifts due to membrane adaptation been a more dominant factor, then the consideration of the loading factors would have facilitated some general conclusions about microbial membrane response. In a limited sense, such general conclusions were assumed from the results of the pure culture experiments.

Experiment B TFA data were also considered by cluster analysis of compositional similarity (equation (3-36)) between each group's averaged fatty acid profiles calculated for the same respective sets of samples. Figure 3-28 shows the resultant dendrogram indicating the hierarchy of nearest neighbours. The enrichment cultures can be grouped into three clusters according to pH levels around 6.0, 7.0 and 8.0 respectively. This alternate approach of multivariate analysis also indicated a pH-related transition in the WCFA profile which most likely represents a pH-dependent change in community make-up.

A much richer chemotype diversity was obtained for Experiment C. In this case the following 21 fatty acids characterized the communities: 11:0, 3OH-10:0, 12:0, 13:0, 2OH-12:0, 14:0, i15:0,

15:0, 16:1 ω 7c, 16:1 ω 7t, 16:0, i17:0, 17:1 ω 8c, 17:1 ω 8t, cy17:0, 17:0, 18:1 ω 7c, 18:1 ω 7t, 18:1 ω 5c, 18:0, and cy19:0. Logcontrast canonical component analysis of the late log growth samples summarized 98 percent of the fatty acid compositional variance between pH conditions into the first two canonical components (Figure 3-29). Both LCC-1 and LCC-2 correlated with pH. LCC-1 explained 75% of the variance and correlated positively with pH. LCC-2 explained 18% of the variance and correlated negatively with pH. The influence of substrate (resin acid versus sodium acetate) for the same enrichment culture inoculum was clearly separated by LCC-1. From the logcontrast loadings for logratios with 16:0 (Figure 3-30), increasing pH in experiment C promoted an increase in the proportion of 18:1 ω 7c. In this respect, the influence of a change to sodium acetate was similar to that of a decrease in pH. In Figure 3-31, the dendrogram from cluster analysis based on WCFA composition similarity, links sodium acetate cultures with the resin acid cultures at pH 6.0. Nearest neighbours were otherwise in order of pH as found in experiment B. Thus, it would appear that pH exhibited a less selective impact on the community of resin acid degraders when the sole carbon source was sodium acetate.

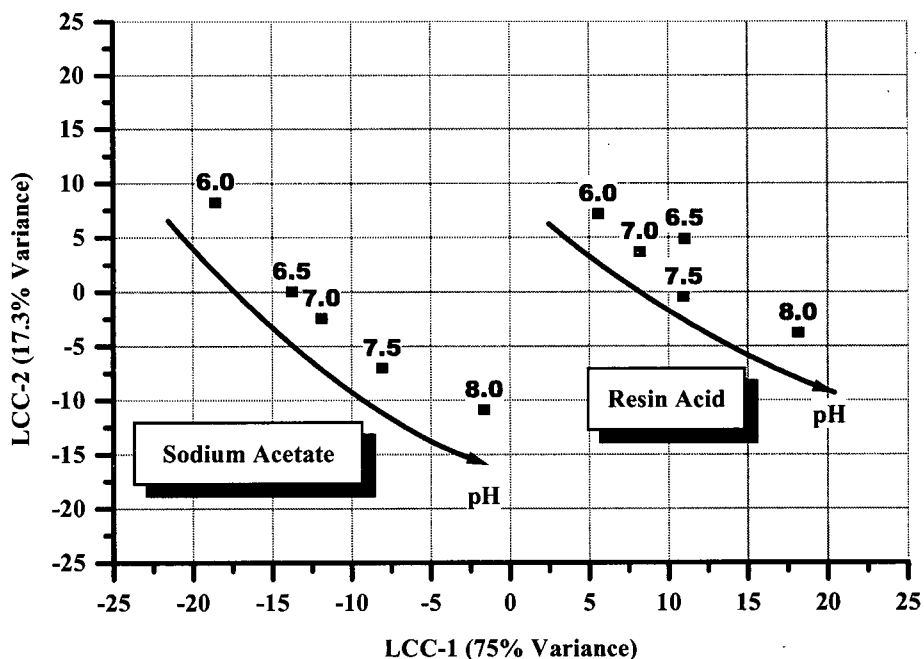


Figure 3-29. The first and second logcontrast canonical components in Experiment C for enrichment cultures grown on resin acids (right) and sodium acetate (left) as a function of pH (as labelled). The effect of substrate is separated along the first canonical component. The influence of pH correlates positively with the first canonical component and negatively with the second canonical component.

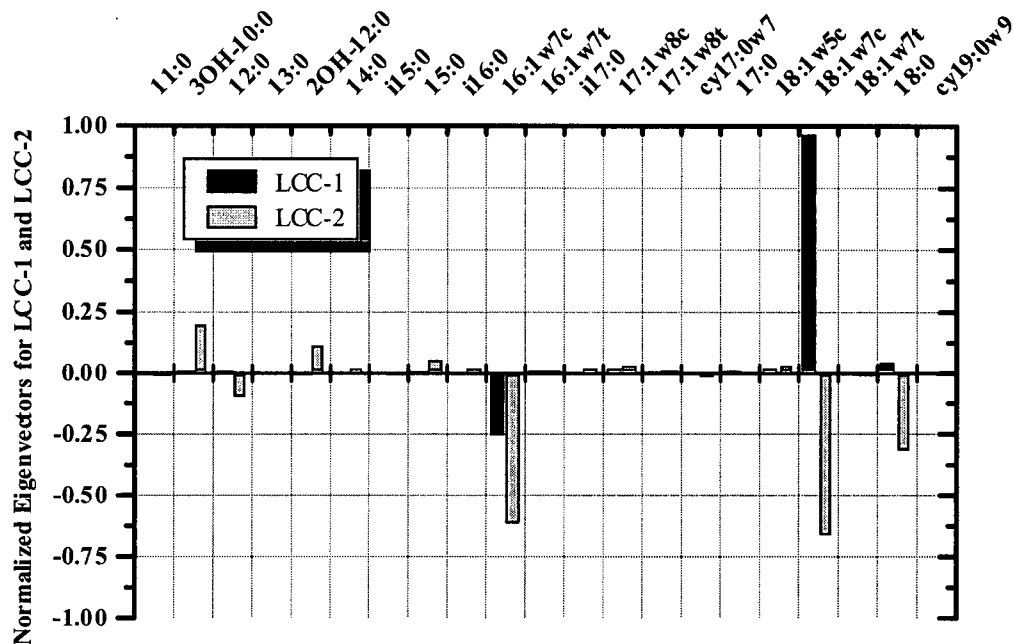


Figure 3-30. Normalized eigen vectors for the first and second logcontrast canonical components. The eigen vectors are for logratios with $x_{16:0}$ as the common divisor. The influence of resin acid on the chemotypes appears to be a significant increase in the logratio of 18:1w7c. The pH also increases the logratio of 18:1w7c.

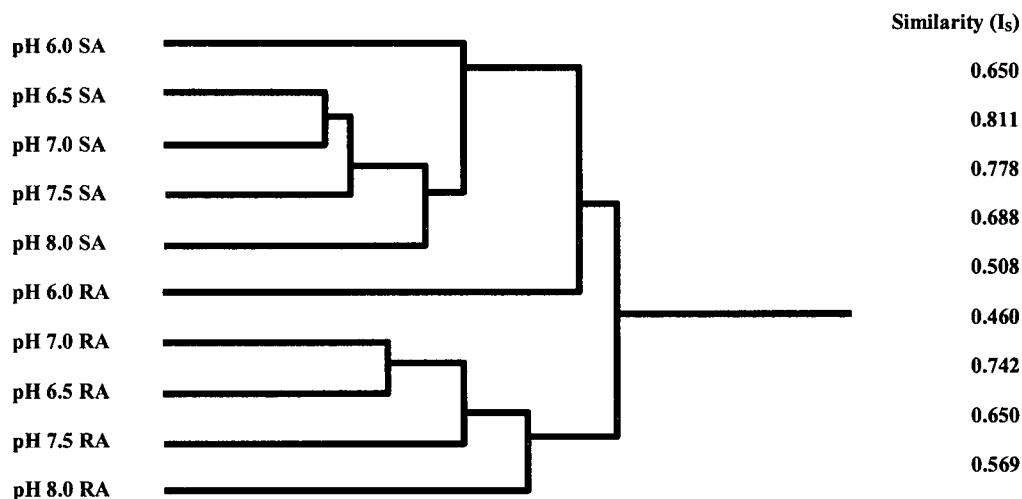


Figure 3-31. Dendrogram from the similarity matrix for the mean WCFA compositions describing the enrichment cultures in Experiment C as a function of pH. Cultures were supplied either sodium acetate (SA) or resin acid (RA) as a sole carbon source. Composition similarity was calculated with equation (3-36) based on σ of 1.3. The dendrogram was created by single linkage agglomeration. The WCFA compositions can be clustered into groups according to substrate and neighbours defined in order of pH similar to Experiment B.

3.4 Discussion

The results of this investigation augment the literature findings (Balkwill et al. 1988; White 1983; White et al. 1979; Zelles et al. 1994) by demonstrating that microbial fatty acids are a conserved representation of biomass during batch growth experiments. Although the fatty acid composition was observed to change during the growth cycle, the total fatty acid (TFA) concentration was shown to remain proportional to dry weight or protein biomass. Total fatty acid biomass offered particular benefits for the purpose of this work. The approach of assaying for specific microbial constituents side-stepped the problems encountered with other, more conventional, biomass measures. Specifically, interference from humic substances and from inert suspended organic matter was avoided. The sensitivity of GC/FID for trace analysis meant that small changes of low biomass concentrations could be accurately followed.

Based on initial TFA concentrations of about 0.5 μM (Table 3-8) and an estimated conversion factor of 265 $\mu\text{moles/g}$ dry weight (Figure 3-9), biomass levels in the order of 5 mg/L could be readily detected. For a two millilitre sample, this would be equivalent to gravimetric sensitivity of about 10 μg . The 2 mL samples were extracted to a 400 μL final solvent volume, making a 5-fold concentration factor. Without altering the extraction method or sample volume, it would have been possible to reduce the solvent down to 50 μL , equivalent to a 40-fold concentration factor. This means that, in principle, an equivalent gravimetric dry weight detection on the order of 1 μg was measurable from a 2 mL sample. Based on the specific weight of *E. coli* being 2.8×10^{-13} g/cell (Brock and Madigan 1991), a 1 μg detection is equivalent to about 3.6×10^6 cells. Detection of such low biomass levels is especially important for studies on the removal of trace organic contaminants, in which a representative microbiological response is best acquired from known initial concentrations.

The added advantage of FAME analysis for research on hydrophobic contaminant biodegradation, is that both substrate and biomass can be measured from the same extraction, making for considerable savings in time and expense. Simultaneous recovery of microbial lipids and organic pollutants, as recently advocated by Fang and Findlay (1996), have helped to produce meaningful

results for the present investigation.

While Monod batch growth kinetics can be assessed from the substrate depletion curve alone, model coefficients so determined may be useful only to the extent of providing a good empirical fit to the data. The theory of batch growth kinetics is founded on pure culture experiments (Panikov 1995). Mixed cultures are complicated systems that are more difficult to predict and control. Uncontrollable sources of variability in experiments are best eliminated for obtaining the most meaningful results. There are three distinct phases of batch growth with quite different respective physiological conditions and population dynamics. The lag phase is difficult to control and the decline phase is complicated by the interplay of nutrient limitation, endogenous growth and heightened prey dynamics. The experience of this investigation has been that better insight into the growth cycle of mixed cultures is obtained from simultaneous monitoring of substrate depletion and biomass production. The growth curves could be delineated and each phase considered as a separate process. Model assumptions and simplifications were tested explicitly. The k_s parameter value was observed to be negligible and the growth yield coefficient approximately constant during the balanced growth phase. The assumption of growth-linked substrate removal by the enrichment cultures was confirmed.

As reported by Alexander (1994), the impact of pH on the removal of resin acids appeared to be less severe in mixed, than in pure culture. Presumably, the lesser influence of pH in the enriched cultures relative to DhA-35, was due to an increased diversity of competent microorganisms in a mixed culture. However, the rate of growth-linked resin acid uptake with the enriched cultures varied significantly with pH and between experiments.

Based on WCFA compositional analysis, mixed liquor samples taken on different dates from the pulp mill biobasin produced different chemotypic enrichment cultures of resin acid degraders. By both canonical component analysis and cluster similarity analysis, the selective pressures of pH resulted in a relatively smooth transition of community chemotype for the enrichment cultures. While pure culture experiments on DhA-35 showed a fatty acid response to substrate hydrophobicity that was consistent with literature findings, the opposite mixed culture response

suggests a change in community structure with pH as a reasonable interpretation. Changes in fatty acid profiles of mixed cultures were most likely dominated by community level or “pseudo-species” changes rather than adaptations of individuals.

The growth of each individual in a community will be governed by that organism's optima to environmental factors like substrate, temperature and pH (Brock and Madigan 1991). How well each organism survives in the community is also a function of how well it fits into the web of the community. Perturbations of environmental factors will force a change in the balance by favouring the success of some individuals or partnerships while antagonising others. It is therefore, not unreasonable to speculate that community level, rather than individual level adaptations dominate the variability in fatty acid compositions from mixed cultures. Secondary experimental evidence also supports the notion that WCFA variability of mixed cultures occurs predominantly at the community level. Different peak metabolite concentrations representing different potential degradation pathways were recovered at different pH levels. Growth rates following the same enrichment procedure from the same source were variable, indicating intrinsic kinetics of different pseudo-species. Growth rates as a function of pH appeared to be bimodal, indicating distinct optima for different communities.

The fact that different pseudo-species of resin acid degraders produce a range of specific uptake rates would indicate that a large factor of safety should be employed in a bioreactor design with respect to resin acid removal. Identifying the most probable source of variability in these mixed culture kinetic experiments by WCFA fingerprinting, adds significantly to the usefulness and engineering application of these results.

Batch growth on resin acids below pH 7 tended to leave a relatively higher residuum level, than above pH 7. The variability in the residuum upon repeated experimentation may have originated from differences in the enrichment cultures and in the extent of resin acid dispersion between experiments. However, the extent of resin acid removal in the alkaline pH range was consistent. Therefore, the threshold resin acid levels observed in the present investigation lead to the recommendation that resin acid removal under alkaline conditions ($\text{pH} \approx 7.5$) is likely to be more

reliable.

It is not unusual to observe significant experimental variability in microbial growth kinetics. This inherent variability may be considered with the specific example of the work of Ellis et al. (1996; 1998) in the research literature. Ellis et al. (1996) developed a sensitive respirometric method for determining the extant kinetics of activated sludge on specific organic contaminants.

Measurement of extant kinetics provides an important assessment of the actual capabilities of biomass in a continuous system at a given time. In a recent study, Ellis et al. (1998) considered extant kinetics for well-controlled activated sludge samples for the removal of phenol. Mixed liquor samples were taken from a well controlled continuously operated laboratory-scale completely mixed activated sludge system fed a synthetic wastewater, containing both biogenic and xenobiotic organic nutrients. The extant specific uptake rate of phenol on two different dates differed by 75 percent. Although this difference was not commented on by the authors, its implication for treatment reliability is quite important. Without a characteristic fingerprint of the biosolids it is not possible to judge the role of community variability in these results. The enigma of variable removal kinetics may be very much a product of natural cycles in microbial communities. WCFA analysis is a promising method to detect such cycles of microbial content if they exist.

The benefit of measuring the extant removal kinetics is that all contributing mechanisms of mineralization are involved. Growth-linked, uncoupled, and co-metabolic catabolism can all be important routes of contaminant removal. However, extant rate calculations rely on the assumption that the competent biomass fraction is proportional to the relative contaminant loading, which in turn, assumes growth-linked metabolism. The number of competent microorganisms can increase without growth on that contaminant as a sole carbon source. Conjugation of plasmid genotypes is an important mechanism of gene transfer. Plasmids can contain genes for the catabolism of substrates (Brock and Madigan 1991). Quantitative gene probe analysis of a plasmid-bound naphthalene-degrading genotype was shown to correspond to activity on naphthalene (Blackburn et al. 1987). Therefore, the biomass degrading a contaminant

may not have originally grown up on that carbon source. This factor makes it hard to be sure of the substrate specificity for fractions of a microbial community at any given time. Therefore, without a direct measure of the contributing biomass, derived extant specific uptake rates may be significantly in error. The potential advantage of measuring extant uptake rates, is in determining the *in situ* (relative) activity on a particular substrate for biosolids from a full scale treatment system.

In the present investigation, growth-linked metabolism was explicitly measured by culture enrichment. However, the question of whether the experimental results are relevant to full scale secondary treatment systems needs some consideration. Since growth-linked metabolism will contribute only a portion of the overall biodegradation capacity of a mixed culture system, the estimated kinetic parameters for biodegradation should be conservative. However, the physiology of cells is quite different during rapid cell division in balanced growth versus the limiting low-growth-rate environments found in most wastewater treatment bioreactors. Therefore, in order to apply the kinetic parameters observed during the current investigation, to full scale treatment, the influence of physiological state needs to be accounted for.

Full consideration of physiological state was beyond the scope of the objectives for this dissertation. However, the determination of maximal removal kinetics has significant engineering application, given a representation of physiological state in full scale modelling. One accounting for the variation of cell physiology has been embraced by Panikov's (1995) synthetic chemostat model (SCM). This model was given preliminary consideration for the present investigation.

According to the SCM, macromolecular cell constituents can be divided into either primary or survival components. Primary components (P-components) are essential for growth, while survival components (U-components) help to maintain the organism in any kind of growth-restricted environment. The P-components are the constituents such as RNA, proteins and key enzymes controlling the principal metabolic pathways. The average RNA concentration within a cell increases directly with population growth rate (Bailey and Ollis 1986). The U-components are the enzymes of secondary metabolism and the reserved substances that improve an organism's

chances of survival during limiting or adverse situations. The U-component contribution to the cell biomass decreases with an increase of growth rate. Thus, a physiological state (Φ) of a culture can be defined by its macromolecular “P” and “U” cell compositions. Defining basal P and U component levels (P_0 and U_0 respectively) and a well defined cellular range for P and U (ΔP and ΔU respectively) leads to the following linear approximation of physiological state:

$$\Phi = P_0 + U_0 + r\Delta P + (1-r)\Delta U \quad (3-62)$$

The parameter r is a “variable of physiological state” that depends on conditions of nutrient limitation and can range from zero to one. As the r -variable moves from zero to one, the cell moves from a state of starvation to one of maximal growth. For the case of organic carbon limitation, cell regulation of physiological state may be empirically expressed in terms of a generalized sigmoidal function of substrate concentration (Panikov 1995):

$$r = \frac{S^n}{k_r + S^n} \quad (3-63)$$

where k_r and n are constants and S is the limiting substrate concentration. The *driving force* for a change in r may be expressed as the difference between the equilibrium and instantaneous r -values as follows:

$$\frac{dr}{dt} = \beta (q_g + q_d) \left(\frac{S^n}{k_r + S^n} - r \right) - q_d r \quad (3-64)$$

where q_g is the specific growth rate, q_d is the endogenous macromolecule decay rate, and β is a constant that models either induction ($\beta > 1$) or retardation ($0 < \beta < 1$) for the onset of new growth conditions.

Unfortunately, the experimental design was not developed to prove the suitability of the SCM model to incorporate the concept of physiological state for mixed cultures. However, the ability of such a model to qualitatively reproduce the basic features of the experimental data, could be taken as a preliminary indication for the promise of such a modelling approach.

Table 3-10. Reduced Synthetic Chemostat Model for batch growth on multiple carbon sources.

Variable	Equation
Limiting Substrate	$\frac{dS_i}{dt} = -q_{Si}X + q_{di}X, \quad i = 1, 2, \dots$ $q_{Si} = \rho_i Q_S \frac{S_i - S_i^*}{k_S + \sum S_i}$ $q_{di} = \rho_i Q_d$
Biomass	$\frac{dX}{dt} = Y(\sum q_{Si})X - \sum q_{di}$
r-Variable	$\rho_i = \beta q_{Si} + q_{di} \left(\frac{\left(1 - \sum_{k \neq i} \rho_k\right) (S_i - S_i^*)^n}{k_r + (\sum S_i)^n} - \rho_i \right) - q_{di}$
<p>X = biomass Y = biomass yield (Y = -ΔX/ΔS) Q_S = maximum specific growth rate Q_t = maximum specific turnover rate S_i = ith substrate S_i[*] = ith substrate threshold ρ_i = r-variable with respect to the ith substrate (r = Σρ_i ≤ 1)</p>	

To qualitatively test the applicability of the parameter of physiological state for the prediction of the behaviour of mixed cultures, a reduced SCM model was constructed. The purpose of this exercise was to observe the extent to which this model could reproduce the exhibited biphasic growth pattern on dehydroabietic and abietic acid.

The model equations, based on the work of Panikov (1995), are given in Table 3-10. The model is essentially a carbon balance between substrate and biomass. Biomass and substrate are both expressed in units of organic carbon concentration. For the purpose of numerical simulation, the model parameters and variables were normalized as follows:

$$x = \frac{X}{\sum S_{0i}}, \quad s_i = \frac{S_i}{\sum S_{0i}}, \quad s_i^* = \frac{S_i^*}{\sum S_{0i}}, \quad \eta = Q_S t \quad (3-65)$$

$$\kappa_S = \frac{k_S}{\sum S_{0i}}, \quad \kappa_r = \frac{k_r}{\sum S_{0i}}, \quad \vartheta_{Si} = \frac{q_{Si}}{Q_S}, \quad \vartheta_{di} = \frac{q_{di}}{Q_S}$$

where S_{0i} is the initial concentration of the ith substrate. Simulation (Simnon Version 1.03, SSPA

Systems, Sweden) of the non-dimensionalized system of equations in Table 3-10 reproduces the basic trends of biphasic growth observed during this investigation (Figure 3-32). In Figure 3-32, biomass production can be seen to follow a three phase log-linear pattern, as was found for the enrichment cultures grown on resin acids. Further, the most abundant substrate (S_1) is predicted to be the first to be metabolized in the model biphasic growth pattern, and, when model biomass production ceases, a residuum of S_1 and S_2 remains in the model system. Finally, the graph, in Figure 3-32, relating the model substrate depletion to biomass production, bears good qualitative similarity to the experimental data shown in Figures 3-20 and 3-21. This ability of the model to reproduce the basic features of the biphasic growth pattern, suggests that applying a parameter of physiological state in conjunction with representative maximal growth kinetic parameters has potential for modelling the behaviour of mixed culture systems. The true potential of this approach will become more apparent with rigorous testing and well designed experimentation in the future.

Assume that SCM models can be used to describe the overall behaviour of mixed cultures in organic substrate removal. The application of the physiological state parameter for a pseudo-species representing a mixed culture could be applied to the modelling of full scale treatment systems. Physiological states in terms of the r -variable are defined and driven with respect to relative and absolute contaminant concentration levels (Table 3-10). In this manner, the whole biomass is considered, without the need to make assumptions about the relative contributing biomass fractions, that are currently required for assessing experimentally-determined extant kinetic parameters. Thus, by introducing the parameter of physiological state to bioreactor models used for process treatment design, the most appropriate kinetic data would be the maximum uptake rates obtained by enrichment culture experiments similar to the ones performed for this investigation. However, the results of this experiment suggest that the pseudo-species contributing to resin acid degradation in full scale treatment systems change over time. With a change in pseudo-species, a significant change in the uptake rate was observed. In terms of the model presented in Table 3-10, a change in pseudo-species would result in a corresponding change in the uptake kinetics of Q_s and Q_d . However, if conservative values of Q_s and Q_d are

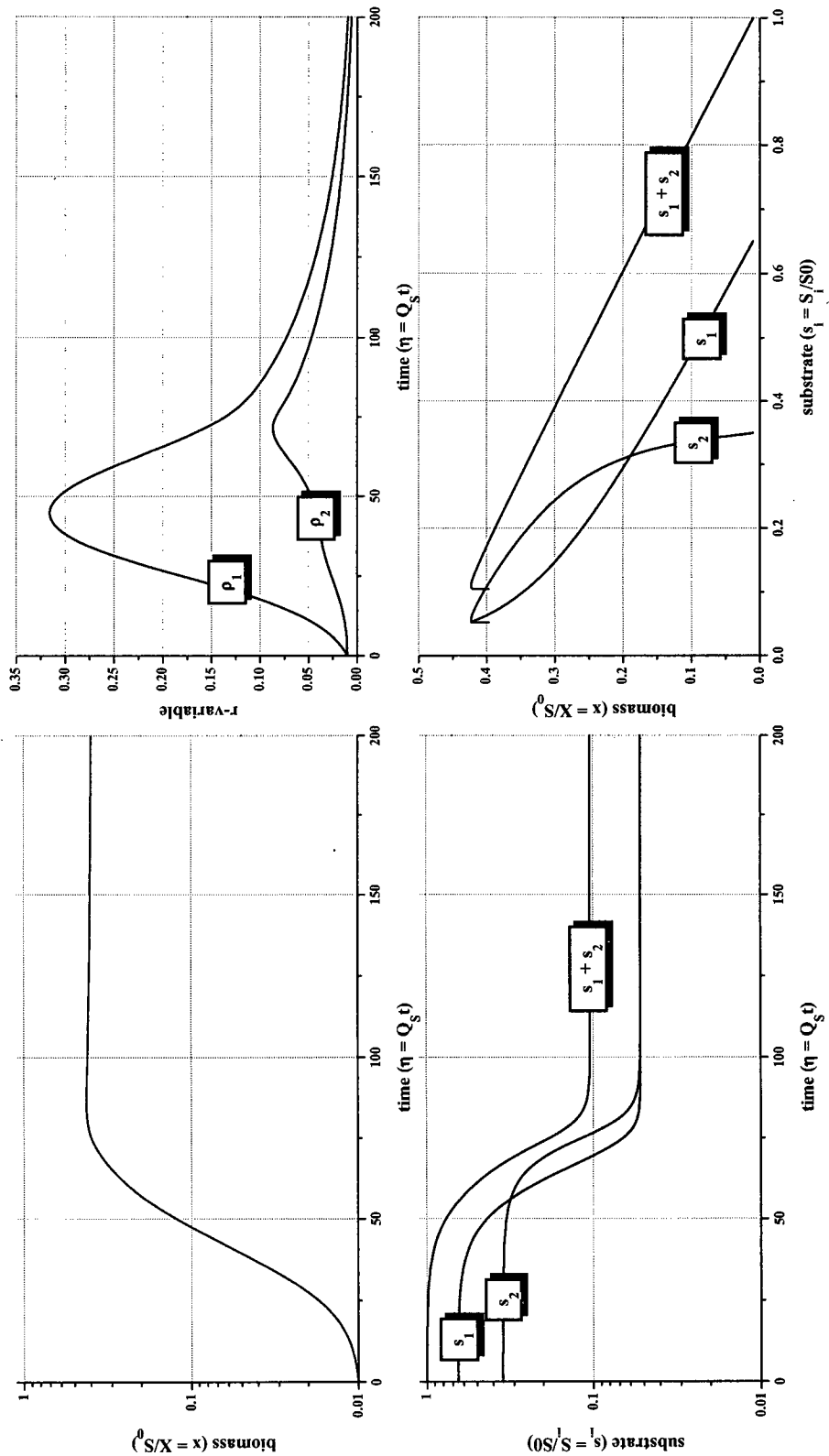


Figure 3-32. Simulation of biphasic batch growth on two substrates using the system of equations given in Table 3-10. Parameters and variables are normalized according to equation (3-65). Non-dimensional parameter values used to create the model data were as follows: $Y=0.5$, $\beta=1.0$, $n=1.5$, $\kappa_s=0.0001$, $\kappa=0.001$, $Q_d/Q_s = 0.02$, $s_{01} = 0.65$, $s_{02}=0.35$, $s_1^*=s_2^*=0.05$, $x_0=0.01$, $\rho_{01}=\rho_{02}=0.01$. The SCM qualitatively reproduces the observed trends of batch growth on a mixture of dehydroabiatic and abiatic acids. Model trends reproduce the experimental observations.

selected based on replicate experimental data of growth-linked biodegradation, realistic predictions of bioreactor responses to transient loadings should be possible by the application of this parameter of physiological state. In this way, model bioreactor performance could be assessed with respect to the expected wastewater loading variability. Should this model approach be proven, it would provide a method to predict dynamic metabolic behaviour that is important for the design of biological unit processes subject to fluctuating organic loading conditions.

3.5 Conclusions

Whole cell fatty acid analysis of enrichment cultures degrading abietane resin acids in a kraft mill effluent matrix, indicated that the community of resin acid-degrading microorganisms in a full scale treatment system change significantly over time. Therefore, a diversity of resin acid degraders exists in nature. Changes in microbial content were concluded to be the major cause in the variability of growth-linked removal kinetics between three otherwise identical experiments.

System pH also influenced the selection of resin acid degraders. Starting with a common inoculum, enrichment cultures that developed over the pH range 6 to 8 displayed a pH-dependent chemotype transition. Optimal mixed cultures with respect to removal kinetics were obtained for both acidic and alkaline conditions. The bimodal specific growth rate as a function of pH indicated selection of enrichment cultures suited to either acidic or alkaline conditions. For each experiment, the greatest specific removal rate was observed near pH 7.5. The extent of resin acid removal was found to be higher under alkaline conditions. For each experiment, with pH levels of less than 7, an increased residuum level was measured. Based on the results of Chapter 2, the presence of a resin acid residuum was attributed to reduced resin acid bioavailability with decreased solubility under acidic conditions.

The order of metabolism for multiple resin acids in batch growth medium was dependent on their relative concentrations. This behaviour could be modelled by Monod kinetics modified to include a parameter of physiological state (SCM model). A physiological state parameter is believed to be the link needed for relating the growth-linked kinetic data from the present investigation, to model predictions of full scale treatment systems.

Therefore, with respect to objective A in Chapter 1, the data from this second investigation have replicated the observed pH-dependent residuum first reported in Chapter 2. With respect to objective B in Chapter 1, it is concluded that the kinetics of resin acid removal are more sensitive to the composition of the microbial community than to pH. However, community selection is pH-dependent and in this regard alkaline conditions appear to promote more rapid removal. Having

established growth characteristics of well-acclimated enrichment cultures of resin acid degrading microorganisms, the next stage of the investigation was designed to assess the impact of resin acids on heterotrophic microbial activity in general. Hydrophobic substrates can inhibit microbial activity. An investigation was required to determine the influence of resin acid hydrophobicity on microbial activity (Objective C - Chapter 1). In conjunction, the influence of resin acid hydrophobicity on the contaminant retention time was also considered (Objective D - Chapter 1). The results of this subsequent stage to the larger investigation are reported in Chapter 4, A Resin Acid Shock Load During Continuous Biological Treatment.

3.6 References

- Aitchison, J. (1986). *The Statistical Analysis of Compositional Data*, Chapman and Hall.
- Aldenderfer, M. S., and Blashfield, R. K. (1984). *Cluster Analysis*, Sage Publications.
- Alexander, M. (1994). *Biodegradation and bioremediation*, Academic Press.
- Allen, S. L., Allen, L. H., and Flaherty, T. H. (1993). Defoaming in the pulp and paper industry. Defoaming, P. R. Garret, ed., Marcel Dekker, Inc., Surfactant Science Series, 151-175.
- Bailey, J. E., and Ollis, D. F. (1986). *Biochemical Engineering Fundamentals*, McGraw-Hill.
- Baird, B. H., and White, D. C. (1985). Biomass and community structure of the abyssal microbiota determined from the ester-linked phospholipids recovered from Venezuela basin and Puerto Rico trench sediments. *Marine Geology*, 68, 217-231.
- Balkwill, D. L., Leach, F. R., Wilson, J. T., McNabb, J. F., and White, D. C. (1988). Equivalence of microbial biomass measures based on membrane lipid and cell wall components, adenosine triphosphate and direct counts in subsurface aquifer sediments. *Microbial Ecology*, 16, 73-84.
- Basile, F., Voorhees, K. J., and Hadfield, T. L. (1995). Microorganism gram-type differentiation based on pyrolysis-mass spectrometry of bacterial fatty acid methyl ester extracts. *Applied and Environmental Microbiology*, 61(4), 1534-1539.
- Biellmann, J. F., Branlant, G., Gero-Robert, M., and Poiret, M. (1973a). Degradation bacterienne de l'acide dehydroabietique par *Flavobacterium reinovorum*. *Tetrahedron*, 29, 1227-1236.
- Biellmann, J. F., Branlant, G., Gero-Robert, M., and Poiret, M. (1973b). Degradation bacterienne de l'acide dehydroabietique par un *Pseudomonas* et une *Alcaligenes*. *Tetrahedron*, 29, 1237-1241.
- Blackall, L. L., Harbers, A. E., Greenfield, P. F., and Hayward, A. C. (1991). Activated sludge foams: Effects of environmental variables on organism growth and foam formation. *Environmental Technology*, 12, 241-248.
- Blackburn, J. W., Jain, R. K., and Sayler, G. S. (1987). Molecular microbial ecology of a naphthalene-degrading genotype in activated sludge. *Environmental Science and Technology*, 21, 884-890.
- Bligh, E. G., and Dyer, W. J. (1959). A rapid method of total lipid extraction and purification. *Canadian Journal of Biochemistry and Physiology*, 37(8), 911-917.
- Bobbie, R. J., and White, D. C. (1980). Characterization of benthic microbial community structure by high-resolution gas chromatography of fatty acid methyl esters. *Applied and Environmental Microbiology*, 39(6), 1212-1222.
- Bousfield, I. J., Smith, G. L., Dando, T. R., and Hobbs, G. (1983). Numerical analysis of total fatty acid profiles in the identification of Coryneform, Nocardioform and some other bacteria. *Journal of General Microbiology*, 129, 375-394.
- Brock, T. D., and Madigan, M. T. (1991). *Biology of Microorganisms*, Prentice Hall.
- Bruggemann, R., Zelles, L., Bai, Q. Y., and Hartmann, A. (1995). Use of Hasse diagram technique for evaluation of phospholipid fatty acids distribution as biomarkers in selected soils. *Chemosphere*, 30(7), 1209-1228.
- Cavigelli, M. A., Robertson, G. P., and Klug, M. J. (1995). Fatty acid methyl ester (FAME) profiles as measures of soil microbial community structure. *Plant and Soil*, 170, 99-113.
- Chiu, S. Y., Fan, L. T., Kao, I. C., and Erickson, L. E. (1972). Kinetic behaviour of mixed populations of activated sludge. *Biotechnology and Bioengineering*, 14, 179-199.
- Clesceri, L. S., Geenberg, A. E., and Trussell, R. R. (1989). Standard Methods for the Examination of Water and Wastewater. , M. A. H. Franson, ed., APHA, AWWA, WPCF.
- Compton, S. J., and Jones, G. C. (1985). Mechanism of dye response and interference in the Bradford protein assay. *Analytical Biochemistry*, 151, 369-374.
- Dang, J. S., Harvey, D. M., Jobbagy, A., and Leslie Grady Jr., C. P. (1989). Evaluation of biodegradation kinetics with respirometric data. *Journal of the Water Pollution Control Federation*, 61(11/12), 1711-1721.

- Daubert, T. E., Danner, R. P., Sibul, H. M., and Stebbins, C. C. (1995). *Physical and Thermodynamic Properties of Pure Chemicals: Data Compilation.*, Taylor & Francis.
- de Castro, A., Allen, D. G., and Fulthorpe, R. F. (1997). Characterization of the microbial population during biofiltration and the influence of the inoculum source. .
- Deutscher, M. P. (1990). *Guide to Protein Purification.* Methods in Enzymology, J. N. Abelson and M. I. Simon, eds., Academic Press.
- Dunteman, G. H. (1989). *Principal Component Analysis*, Sage Publications.
- Eerola, E., and Lehtonen, O. (1988). Optimal data processing procedure for automatic bacterial identification by gas-liquid chromatography of cellular fatty acids. *Journal of Clinical Microbiology*, 26(9), 1745-1753.
- Ellis, T. G., Barbeau, D. S., Smets, B. F., and Grady, C. P. L., Jr. (1996). Respirometric technique for determination of extant kinetic parameters describing biodegradation. *Water Environment Research*, 68, 917.
- Ellis, T. G., Smets, B. F., and Leslie Grady Jr., C. P. (1998). Effect of simultaneous biodegradation of multiple substrates on the extant biodegradation kinetics of individual substrates. *Water Environment Research*, 70(1), 27-38.
- Fahmy, G. T., and Hao, O. J. (1990). Characterization of Activated sludge foams from two plants. *Journal of Environmental Engineering*, 116(5), 991-997.
- Fang, J., and Findlay, R. H. (1996). The use of classic lipid extraction method for simultaneous recovery of organic pollutants and microbial lipids from sediments. *Journal of Microbiological Methods*, 27, 63-71.
- Franzmann, P. D., Patterson, B. M., Power, T. R., Nichols, P. D., and Davis, G. B. (1996). Microbial biomass in a shallow, urban aquifer contaminated with aromatic hydrocarbons: analysis by phospholipid fatty acid content and composition. *Journal of Applied Bacteriology*, 80, 617-625.
- Frostegard, A., Petersen, S. O., Baath, E., and Nielsen. (1997). Dynamics of a microbial community associated with manure hot spots as revealed by phospholipid fatty acid analysis. *Applied and Environmental Microbiology*, 63(6), 2224-2231.
- Gharaibeh, A. A., and Voorhees, K. J. (1996). Characterization of lipid fatty acids in whole-cell microorganisms using in situ supercritical fluid derivatization/extraction and gas chromatography/mass spectrometry. *Analytical Chemistry*, 68(17), 2805-2810.
- Gillan, F. T. (1983). Analysis of complex fatty acid methyl ester mixtures on non-polar capillary GC columns. *Journal of Chromatographic Science*, 21(7), 293-297.
- Gillan, F. T., and Hogg, R. W. (1984). A method for the estimation of bacterial biomass and community structure in mangrove-associated sediments. *Journal of Microbiological Methods*, 2, 275-293.
- Grady, C. P. L. J. (1990). Biodegradation of toxic organics: status and potential. *Journal of Environmental Engineering*, 116(5), 805-828.
- Haack, S. K., Garchow, H., Odelson, D. A., Forney, L. Y., and Klug, M. J. (1994). Accuracy, reproducibility, and interpretation of fatty acid methyl ester profiles of model bacterial communities. *Applied and Environmental Microbiology*, 60(7), 2843-2493.
- Harwood, J. L., and Russell, N. J. (1984). *Lipids in Plants and Microbes*, George Allen & Unwin, London.
- Holmberg, A. (1982). On the practical identifiability of microbial growth models incorporating Michaelis-Menten type nonlinearities. *Mathematical Biosciences*, 62, 23-43.
- Hornbeck, R. W. (1975). *Numerical Methods*, Quantum Publishers.
- Ingram, L. O. (1976). Adaptation of membrane lipids to alcohols. *Journal of Bacteriology*, 125(2), 670-678.
- Ingram, L. O. (1977). Changes in lipid composition of *Escherichia coli* resulting from growth with organic solvents and with food additives. *Applied and Environmental Microbiology*, 33(5), 1233-1236.
- Jackson, J. E. (1991). *A User's Guide to Principal Components*, John Wiley & Sons, Inc.
- Johnson, R. M. (1995). Biological Treatment of Recirculated Mechanical Newsprint Whitewater at High

- Temperatures, M.A.Sc., University of British Columbia, Vancouver.
- Karl, D. M. (1980). Cellular nucleotide measurements and applications in microbial ecology. *Microbiological Reviews*, 44(4), 739-796.
- Karl, D. M., and Craven, D. B. (1980). Effects of alkaline phosphatase activity on nucleotide measurements in aquatic microbial communities. *Applied and Environmental Microbiology*, 40(3), 549-561.
- Kates, M. (1964). Bacterial lipids. *Advances in Lipid Research*, 2, 17-90.
- Keweloh, H., and Heipieper, H. J. (1996). Trans unsaturated fatty acids in bacteria. *Lipids*, 31(2), 129-137.
- Khan, A. R., and Forster, C. F. (1991). Aspects of the nutrition and the growth of *Rhodococcus Rubra* in relation to the formation of stable foams. *Environmental Technology*, 12, 271-277.
- Khandekar, N., and Johns, R. B. (1990). Marine corrosion studies -II. A biomarker study tracing the early formation of biofilms on steel plates in a marine environment. *Organic Geochemistry*, 15(5), 531-538.
- Klecka, G. M., and Maier, W. J. (1985). Kinetics of microbial growth on pentachlorophenol. *Applied and Environmental Microbiology*, 49(1), 46-53.
- Kobayashi, H., and Rittmann, B. E. (1982). Microbial removal of hazardous organic compounds. *Environmental Science and Technology*, 15(3), 170-183.
- Kreyszig, E. (1983). *Advanced Engineering Mathematics*, John Wiley & Sons.
- Leach, J. M., Mueller, J. C., and Walden, C. C. (1977). Biodegradability of toxic compounds in pulp mill effluents. *Transactions of the technical section CPPA*, 3(4), TR126-TR130.
- Lechevalier, H., and Lechevalier, M. P. (1988). Chemotaxonomic use of lipids - an overview. *Microbial Lipids*, C. Ratledge and S. G. Wilkinson, eds., Academic Press, 869-902.
- Lemmer, H. (1986). The ecology of scum causing actinomycetes in sewage treatment plants. *Water Research*, 20(4), 531-535.
- Lemmer, H., and Baumann, M. (1988). Scum actinomycetes in sewage treatment plants - part 3: synergisms with other sludge bacteria. *Water Research*, 22(6), 765-767.
- Manly, B. F. J. (1986). *Multivariate Statistical Methods - A Primer*, Chapman and Hall.
- Marr, A. G., and Ingraham, J. L. (1962). Effect of temperature on the composition of fatty acids in *Escherichia Coli*. *Journal of Bacteriology*, 84, 1260-1267.
- Marton, J. (1964). On the structure of Kraft lignin. *Tappi Journal*, 47(11), 713-719.
- Metcalf & Eddy, I. (1991). *Wastewater Engineering: Treatment, Disposal, and Reuse*, McGraw-Hill, Inc.
- Miller, L., and Berger, T. (1985). Bacterial identification by gas chromatography of whole cell fatty acids. 228-41, Hewlett-Packard Company.
- Mohn, W. W. (1995). Bacteria obtained from a sequencing batch reactor that are capable of growth on dehydroabiatic acid. *Applied and Environmental Microbiology*, 61(6), 2145-2150.
- Mohn, W. W., Wilson, A. E., Bicho, P., and Moore, E. R. B. (1997). Diversity of Bacteria Growing on Resin Acids (Draft).
- Morrison, R. T., and Boyd, R. N. (1992). *Organic Chemistry*, Prentice-Hall.
- Moss, C. W., and Dees, S. B. (1976). Cellular fatty acids and metabolic products of *Pseudomonas* species obtained from clinical specimens. *Journal of Clinical Microbiology*, 4(6), 492-502.
- Mueller, J. C., and Walden, C. C. (1976). Detoxification of bleached kraft mill effluents. *Journal of the Water Pollution Control Federation*, 48(3), 502-510.
- Nichols, P. D., and White, D. C. (1989). Accumulation of poly-beta-hydroxybutyrate in a methane-enriched, halogenated hydrocarbon-degrading soil column: implications for microbial community structure and nutritional status. *Hydrobiologia*, 176/177, 369-377.
- Panikov, N. S. (1995). *Microbial Growth Kinetics*, Chapman & Hall.
- Peterson, G. L. (1977). A simplification of the protein assay method of Lowry et al. which is more generally applicable. *Analytical Biochemistry*, 83, 346-356.

- Pinkart, H. C., Wolfram, J. W., Rogers, R., and White, D. C. (1996). Cell envelope changes in solvent-tolerant and solvent-sensitive *pseudomonas putida* strains following exposure to o-Xylene. *Applied and Environmental Microbiology*, 62(3), 1129-1132.
- Providenti, M. A., Lee, H., and Trevors, J. T. (1993). Selected factors limiting the microbial degradation of recalcitrant compounds. *Journal of Industrial Microbiology*, 12, 379-395.
- Ratledge, C., and Wilkinson, S. G. (1988a). Fatty acids, related and derived lipids. , C. Ratledge and S. G. Wilkinson, eds., Academic Press, 23-79.
- Ratledge, C., and Wilkinson, S. G. (1988b). Microbial Lipids. , Academic Press.
- Ratray, J. B. M. (1988). Yeasts. Microbial Lipids, C. Ratledge and S. G. Wilkinson, eds., Academic Press, 555-697.
- Reemtsma, T., and Ittekkot, V. (1992). Determination of factors controlling the fatty acid composition of settling particles in the water column by principal-component analysis and their quantitative assessment by multiple regression. *Organic Geochemistry*, 18(1), 121-129.
- Reichardt, W., Mascarina, G., Padre, B., and Doll, J. (1997). Microbial communities of continuously cropped, irrigated rice fields. *Applied and Environmental Microbiology*, 63(1), 233-238.
- Reyment, R. A. (1989). Compositional data analysis. *Terra Nova*, 1, 29-34.
- Richards, T., Nungesser, P., and Jones, C. (1990). Solution of Nocardia foaming problems. *Research Journal WPCF*, 62(7), 915-919.
- Riebel, P., Owen, M., and Yazer, M. (1997). Toxicity prevention and response. *Pulp & Paper Canada*, 98(5), 23-26.
- Rogers, I. H. (1989). Biological Interactions. Naval Stores, D. F. Zinkel and J. Russell, eds., Pulp Chemicals Association, Inc., 942-976.
- Rose, A. H. (1989). *Influence of the environment on microbial lipid composition*, Academic Press.
- Rozes, N., Garbay, S., Denayrolles, M., and Lonvaud-Funel, A. (1993). A rapid method for the determination of bacterial fatty acid composition. *Letters in Applied Microbiology*, 17, 126-131.
- Shamat, N. A., and Maier, W. J. (1980). Kinetics of biodegradation of chlorinated organics. *Journal of the Water Pollution Control Federation*, 52(8), 2158-2166.
- Sherrard, J. H., and Schroeder, E. D. (1973). Cell yield and growth rate in activated sludge. *Journal of the Water Pollution Control Federation*, 45(9), 1889-1897.
- Sikkema, J., de Bont, J. A. M., and Poolman, B. (1994). Interactions of cyclic hydrocarbons with biological membranes. *Journal of Biological Chemistry*, 269(11), 8022-8028.
- Sikkema, J., De Bont, J. A. M., and Poolman, B. (1995). Mechanisms of membrane toxicity of hydrocarbons. *Microbiological Reviews*, 59(2), 201-222.
- Simkins, S., and Alexander, M. (1984). Models for mineralization kinetics with the variables substrate concentration and population density. *Applied and Environmental Microbiology*, 47(6), 1299-1306.
- Simkins, S., and Alexander, M. (1985). Nonlinear estimation of the parameters of Monod kinetics that best describe mineralization of several substrate concentrations by dissimilar bacterial densities. *Applied and Environmental Microbiology*, 50(10), 81-824.
- Soltes, E. J., and Zinkel, D. F. (1989). Chemistry of rosin. Naval Stores, D. F. Zinkel and J. Russell, eds., Pulp Chemicals Association, 261-345.
- Spath, H. (1980). *Cluster Analysis Algorithms*, Ursula Bull, translator, Ellis Horwood Limited.
- Stahl, P. D., and Klug, M. J. (1996). Characterization and differentiation of filamentous fungi based on fatty acid composition. *Applied and Environmental Microbiology*, 62(11), 4136-4146.
- Sundberg, K., Pettersson, C., Eckerman, C., and Holmbom, B. (1996a). Preparation and properties of a model dispersion of colloidal wood resin from Norway spruce. *Journal of Pulp and Paper Science*, 22(7), 248-252.
- Sundberg, K., Thornton, J., Holmbom, B., and Ekman, R. (1996b). Effects of wood polysaccharides on the stability of colloidal wood resin. *Journal of Pulp and Paper Science*, 22(7), 226-230.
- Sundh, I., Nilsson, M., and Borga, P. (1997). Variation in microbial community structure in two boreal

- peatlands as determined by analysis of phospholipid fatty acid profiles. *Applied and Environmental Microbiology*, 63(4), 1476-1482.
- Taylor, B. R., Yeager, K. L., Abernethy, S. G., and Westlake, G. F. (1988). *Resin Acids*, Queen's Printer for Ontario.
- Templeton, L. L., and Grady, C. P. L. J. (1988). Effect of culture history on the determination of biodegradation kinetics by batch and fed-batch techniques. *Journal of the Water Pollution Control Federation*, 60(5), 651-658.
- Tunlid, A., and White, D. C. (1992). Biochemical analysis of biomass, community structure, nutritional status, and metabolic activity of microbial communities in soil. *Soil Biochemistry*, G. Stotzky and J. M. Bollag, eds., Marcel Dekker Inc., 229-262.
- Vestal, J. R., and White, D. C. (1989). Lipid analysis in microbial ecology. *BioScience*, 39, 535-541.
- Webster, T. S., Deviny, J. S., Torres, E. M., and Basrai, S. S. (1997). Microbial ecosystems in compost and granular activated carbon biofilters. *Biotechnology and Bioengineering*, 53(3), 296-303.
- White, D. C. (1983). Analysis of microorganisms in terms of quantity and activity in natural environments. *Microbes in their natural environments*, R. Whittenberg and J. W. T. Wimpenny, eds., Society for General Microbiology, 37-66.
- White, D. C., Davis, W. M., Nickels, J. S., King, J. D., and Bobbie, R. J. (1979). Determination of the sedimentary microbial biomass by extractible lipid phosphate. *Oecologia*, 40, 51-62.
- Wilkinson, S. G. (1989). Gram-negative bacteria. *Microbial Lipids*, C. Ratledge and S. G. Wilkinson, eds., Academic Press, 299-488.
- Wilson, A. E. J., Moore, E. R. B., and Mohn, W. W. (1996). Isolation and characterization of isopimaric acid-degrading bacteria from a sequencing batch reactor. *Applied and Environmental Microbiology*, 62(9), 3146-3151.
- Zelles, L., Bai, Q. Y., Beck, T., and Beese, F. (1992). Signature fatty acids in phospholipids and lipopolysaccharides as indicators of microbial biomass and community structure in agricultural soils. *Soil Biology and Biochemistry*, 24(4), 317-323.
- Zelles, L., Bai, Q. Y., Rackwitz, R., Winter, K., and Beese, F. (1994). Microbial biomass, metabolic activity and nutritional status determined from fatty acid patterns and poly-hydroxybutyrate in agriculturally-managed soils. *Soil Biology and Biochemistry*, 26(4), 439-446.

Chapter 4
A Resin Acid Shock Load During Continuous Biological Treatment

Summary

The objective of this investigation was to determine the influence of resin acid hydrophobicity on heterotrophic metabolic activity (Objective C - Chapter 1) and the contaminant retention time (Objective D - Chapter 1) during continuous biological treatment. A shock load of resin acids was applied to bench scale bioreactors treating primary bleached kraft mill effluent. The two parallel bench scale moving bed bioreactors were operated at pH 6 and pH 8, respectively. From pH 6 to pH 8, resin acid hydrophobicity decreases by approximately two orders of magnitude. Although these bioreactors were well acclimated to remove background levels of resin acids, no biological removal of the spike input could be detected. The added input of resin acids appeared to strongly influence the community structure of the reactor biomass, but without any detected loss in reactor performance. Thus, although there was no evidence of a hydrophobicity-dependent decrease in the overall metabolic activity, the spike load did appear to induce a shift in the community structure. Sorption of resin acids to the reactor biomass did extend the contaminant retention time beyond the bioreactor hydraulic retention time.

Table of Contents

4.1 Introduction	185
<i>4.1.1 Insight and Engineering Perspective</i>	<i>186</i>
<i>4.1.2 Resin Acid Hydrophobicity and Sorption to Biomass</i>	<i>187</i>
<i>4.1.3 Kinetics of Sorption to a Biofilm</i>	<i>195</i>
<i>4.1.4 Method Specific Issues</i>	<i>202</i>
4.2 Methods and Materials	205
<i>4.2.1 Bioreactor design and operation</i>	<i>205</i>
<i>4.2.2 Sampling and Chemical Analysis</i>	<i>208</i>
<i>4.2.3 Bio-carrier Material Characterization</i>	<i>211</i>
4.3 Results	215
<i>4.3.1 Bio-carrier Material Characterization</i>	<i>216</i>
<i>4.3.2 Bioreactor Operating Conditions</i>	<i>218</i>
<i>4.3.3 Resin Acid Analysis</i>	<i>221</i>
<i>4.3.4 Biomass Characterization</i>	<i>229</i>
<i>4.3.5 Assessment of Microbial Community Structure and Population Dynamics</i>	<i>232</i>
<i>4.3.6 Resin Acid Sorption Kinetics</i>	<i>248</i>
4.4 Discussion	253
4.5 Conclusions	258
4.6 References	260

4.1 Introduction

The probability of metabolism for any organic contaminant during secondary biological treatment will depend on its residence time, bioavailability, and the status of the microbial community (Chapter 1). This investigation was designed to consider the extent to which resin acid hydrophobicity could influence the activity of the reactor biomass (Objective C - Chapter 1) and the contaminant residence time (Objective D - Chapter 1). To assess the significance of resin acid sorption on retention time and for the potential of resin acid-induced inhibition on microbial activity, a resin acid shock load was imposed on well acclimated, bench scale, completely mixed moving bed bioreactors. During the wash-out of this spike load, samples were taken to follow the resin acid residence time distribution function, as well as to monitor for any changes in microbial activity. For comparison, two identical bench scale bioreactors treating bleached kraft mill effluent were operated in parallel. One reactor was maintained at pH 6 and the other at pH 8. Resin acids have been shown to be dissociated and dissolved at pH 8, and protonated and particulate at pH 6 (Chapters 2 and 3).

In this introduction, the motivation for this study is reviewed, based on the perspective from the batch growth investigation results from the previous two chapters, which have provided insight and some engineering perspective on factors controlling the removal of resin acids during continuous biological treatment. The adsorptive characteristics of resin acids and their potential for bacterial inhibition are then related to the hydrophobicities of the components, which are pH-dependent. Aspects of resin acid hydrophobicity are discussed in the introduction, with references to the literature. A brief description of the four steps of contaminant sorption to biosolids is then provided and is followed by a description of the model used to consider the experimental data. Consideration of time scales and of the method of sampling was important to the experimental design for this investigation. Therefore, the rationale for the experimental set-up is also explained in the introduction.

4.1.1 Insight and Engineering Perspective

The batch growth experiments described in the previous two chapters have shown that while acidic pH conditions reduce the bioavailability of resin acids, enrichment cultures of resin acid degraders can be acclimated to either acidic or alkaline conditions. The resultant enrichment cultures of resin acid degraders were sensitive to pH conditions and the communities were also found to vary between experiments. This variation was likely due to the fact that enrichment cultures obtained from inocula taken from the same full scale biobasin on different dates were distinct. Differences in the communities were distinguishable by their fatty acid proportions and their overall chemotype diversity. These results indicated that there exists a diversity of competent organisms capable of degrading resin acids and that pH is one important selective pressure. The enrichment cultures, varying with pH and time, were also observed to metabolize resin acids at different rates. These data suggested, therefore, that the rate of biological removal of these contaminants due to growth-linked metabolism in full scale systems will likely also vary due to natural or process-induced changes of the biobasin community structure. If the biological removal rate of a targeted contaminant is variable, then the bioreactor must be designed using the most conservative removal rate, such that the contaminant will be adequately metabolized during the time over which it is retained within the system. The slower the steady state uptake rate, the longer the contaminant retention time must be. The retention time of a soluble contaminant is dependent on hydraulic retention time (HRT) (Metcalf & Eddy 1991) which is equal to:

$$HRT = \theta_H = \frac{V}{Q_e} \quad (4-1)$$

where Q_e is the effluent flow rate and V is the reactor volume. For a specified flow rate, conservative design for an inherently variable uptake rate, requires that a large factor of safety be applied to the design HRT. To accommodate a greater HRT, the tank volume must be oversized. Construction and operation costs increase with tank volume, making it an important design constraint in the process economics. Therefore, aspects of a treatment process that prolong the retention of a targeted contaminant beyond the hydraulic retention time will relax the influence of

that contaminant on HRT and, ultimately, on tank volume (cost).

Due to their hydrophobicity, resin acids are driven out of polar aqueous environments and, consequently, sorb or partition to biomass. The kinetics of resin acid adsorption at a gas/liquid interface were followed by dynamic surface tension measurements that were described in Chapter 2. Sorption is an important aspect of contaminant fate and treatment process design, since by contaminant sorption to biosolids, residence time in the biobasin can be extended beyond the hydraulic retention time. For example, significant resin acid levels have been measured at the sludge dewatering press during an audit at one British Columbia pulp mill (Bicho and Saddler 1994). Therefore, sludge wasting is one important route of contaminant removal. For anaerobic treatment systems, in which resin acids do not appear to be metabolized (Liver and Hall 1996), sludge wasting would be the only mechanism of removal. Conversely, discharge of biosolids from secondary clarifiers due to bulking sludge, may have a deleterious environmental impact because of the sorbed contaminants (Taylor and Ross 1993). Therefore resin acid hydrophobicity and sorption to biomass are important contributors to the contaminant fate.

4.1.2 Resin Acid Hydrophobicity and Sorption to Biomass

Being weak hydrophobic organic acids, resin acids dissociate as a function of pH. For dehydroabietic acid and abietic acid, pKa values of 5.7 and 6.4 respectively, have been estimated (Nyrén and Back 1958). The pKa values from Nyrén (1958) are in qualitative agreement with the work of Bruun (1952a; 1952b) who followed pH-induced changes in surface pressure for monolayers of resin acids.

The polar forces that produce the high cohesive energy density within a water phase act to squeeze out any component with less attractiveness (Hansch and Leo 1995). Thus, the direct effect of dissociation for weak hydrophobic organic acids, is an increased polarity resulting in an increased aqueous solubility with pH. The influence of changing solubility on bioavailability was demonstrated in the previous two investigations (Chapters 2 and 3). Decreased solubility was shown to result in an increased residuum in batch aerobic assays.

Solubility is thermodynamically related to hydrophobicity (Mackay et al. 1980), which can in turn, influence a contaminant's toxicity. The influence of resin acid dissociation on aquatic toxicity has been investigated with a variety of bioassays by varying pH (McLeay et al. 1979a; McLeay et al. 1979b; Zanella 1983). Dissociated resin acid elicits less acute toxicity. Since hydrophobic compounds can collect in the cytoplasmic membrane of bacteria and disrupt membrane function (Sikkema et al. 1994; Sikkema et al. 1995), the potential for resin acid-induced microbial inhibition is important to consider for microbiological treatment systems. Resin acids have been shown to have an inhibitory effect on methanogens in anaerobic batch assays but were not found to measurably alter the growth characteristics of biosolids in aerobic batch reactors (Liver and Hall 1996). The effect of pH on the impact of a resin acid shock load under continuous aerobic treatment conditions has not previously been considered. While previous studies have related pH to changes in resin acid aquatic toxicity, it is important to keep in mind that pH provides the means to change resin acid hydrophobicity. Therefore the topic of resin acid hydrophobicity should be considered.

The octanol-water partition coefficient (P_{ow}) is a standard measure of hydrophobicity (Hansch and Leo 1995). The partition coefficient is the ratio of the distribution of a chemical between two immiscible liquid phases. Water is the most obvious choice for the polar phase and octanol has become the conventional choice for the nonpolar phase in the pair. Most frequently, the octanol-water partition coefficient is expressed on a logarithmic scale or $\log P_{ow}$. A reliable experimental measure of resin acid P_{ow} was not found in the literature. However, an approximation can be made, based on the correlations that have been developed between the experimentally determined P_{ow} for other solutes and the parameters of solubility and melting point (Mackay et al. 1980) as follows:

$$\ln P_{OW} = 9.804 - \ln C_S + 6.79(1 - T_M/T) \quad (4-2)$$

where C_S is the aqueous solubility (mol/m³) and T_M is the melting point (degrees Kelvin). Based on the reported limiting solubilities and melting points for undissociated dehydroabietic and abietic acid (16 μ M and 12 μ M (Nyrén and Back 1958); 173°C and 172°C (Soltes and Zinkel

1989) respectively), equation (4-2) predicts $\log P_{ow}$ values of 4.6 and 4.7, respectively at 25°C. However, equation (4-2) may not be accurate for resin acids, since octanol and water activity coefficients have been reported to be influenced by molecular size, when molecular weights are greater than 290 (Mackay et al. 1980). The molecular weight of resin acids is approximately 302.

Octanol-water partition coefficients can also be estimated by the method of fragments (Hansch and Leo 1995). This method was established by correlations developed from a comprehensive database of the measured values for many organic contaminants, with the goal of advancing the understanding in quantitative structure-activity relationships (QSAR). From the database, contributions to the P_{ow} by simple chemical fragments such as C, CH, CH₂, CH₃, OH and NH₂, were estimated. By the appropriate fragmentation of any chemical structure, the partition coefficient can be estimated. Using commercial CLOGP software (Daylight Chemical Information Systems, Inc.) the predicted octanol-water partition coefficients ($\log P_{ow}$) for undissociated dehydroabietic and abietic acid are 5.1 and 5.2.

Based on the similarity of the predicted $\log P_{ow}$ values obtained by these two very different theoretical approaches, resin acids in their protonated form can be expected to have log octanol-water partition coefficients of around 5. Organic chemicals with hydrophobicities ($\log P_{ow}$) in the neighbourhood of 5, tend to bioconcentrate in fish but do not biomagnify (Muir and Servos 1996). The extent of bioconcentration is dependent on the ability of fish to biotransform the contaminant to more polar compounds (via hydroxylation and conjugation), that can then be excreted. Resin acids are relatively rapidly biotransformed (Muir and Servos 1996) but they have been observed to accumulate in fish tissue (Niimi and Lee 1992).

Westall (1985) and Jafvert (1990) demonstrated how the P_{ow} of ionogenic hydrophobic organic compounds decreases with ionisation. In simple systems, the partition coefficient is a function of pH and pK_a as follows:

$$K_{OW} = \frac{P_{OW}}{1 + K_a/[H^+]} \quad (4-3)$$

where K_{ow} is the partition coefficient, assuming that only the neutral species are present in the nonaqueous phase and that activity corrections are negligible. In general, the distribution of organic acids between octanol and water is also strongly influenced by ionic strength in the aqueous phase (Jafvert et al. 1990). In the absence of other cations in solution, measured resin acid K_{ow} may be expected to decrease by two orders of magnitude over the pH range from 6 to 8. Thus, the log octanol-water partition coefficient also decreases, under alkaline conditions, to approximately 3, which is a level below which organic chemicals do not bioconcentrate (Muir and Servos 1996). In this respect, resin acids are of general research interest since the effect of hydrophobicity on contaminant fate can be experimentally tested by a change in pH.

Due to their hydrophobicity, resin acids will sorb and thereby partition to biomass. Sorption is an important aspect of contaminant fate, since, through such interactions, contaminant residence time in a treatment process can extend beyond the hydraulic retention time. While it was stated that solubility and hydrophobicity are thermodynamically coupled (Mackay et al. 1980), hydrophobicity in terms of K_{ow} , is said to be a better indicator for the relative extent of sorption (Selvakumar and Hsieh 1988). Partition coefficients, describing the sorption equilibria between aqueous and sorbed phases, have been shown to correlate to the octanol-water partition coefficient (Karickhoff et al. 1979). Therefore, changes in pH will alter the resin acid octanol-water partition coefficient, which will, in turn, influence resin acid interactions with biomass.

Sorption of hydrophobic organic contaminants to biomass has been found to be reversible, following standard isotherms (Bell and Tsezos 1987), and proportional to P_{ow} (Dobbs et al. 1989). Schellenberg (1984) and, later, Jacobsen (1996) followed sorption of chlorinated phenols, another group of ionogenic hydrophobic compounds, to sediments and biomass (respectively) as a function of pH and ionic strength. Sorption dependency on pH and ionic strength corresponded to K_{ow} dependency on pH (equation (4-3)) and ionic strength. A primary parameter for modelling pentachlorophenol sorption to natural soils, was shown to be pH (Christodoulatos and Mohiuddin 1996). Hence, literature findings do show that pH-induced changes of K_{ow} are important to contaminant fate. Surprisingly, little attention has been given in the literature to the

sensitivity of resin acid fate to pH, during full scale biological treatment.

Resin acids have been shown to sorb to biomass according to standard Langmuir or Freundlich isotherms, although the reversibility of sorption and the role of pH has not been demonstrated (Hall and Liver 1996; Liu et al. 1996). From the investigation of Chapter 2, kinetics of resin acid adsorption at a gas-liquid interface was modelled by quasi-static Langmuir isotherms, for which the parameters were definitely a function of pH. Hall and Liver (1996) have determined partitioning coefficient values for resin acid association at pH 7 with inactivated aerobic biomass to be 0.31 and 1.14 l/g TSS for dehydroabietic and abietic acid respectively. These partition coefficients are at least in qualitative agreement with their relative hydrophobicities predicted by their K_{ow} values given above. Therefore, it seems reasonable to expect that resin acids will sorb to biomass reversibly, according to their pH-dependent hydrophobicities.

However, in practice, resin acids also interact with high molecular weight dissolved organic matter (HMW DOM) that is common in pulp mill effluent (Chapter 2). The HMW DOM are amorphous polyelectrolytes derived from lignin, that will also gain and lose protons as pH changes (Sarkanen and Ludwig 1971). Molecular association with the HMW DOM increases with decreasing pH and increasing ionic strength (Marton 1964). The sorption of HMW DOM to biomass has been investigated because of concern regarding the release of organic halides. Organic halides are measured in terms of Adsorbable Organic Halide or AOX. AOX compounds were brought into focus following fisheries closures related to dioxin and furan contamination associated with bleached kraft mill effluent (Colodey and Wells 1992).

In pulp mill effluent, HMW DOM has been observed to sorb to biomass, in accordance with standard isotherms, either conditionally reversibly (Amy et al. 1988) or irreversibly (Yan and Allen 1994). The fate of contaminants, sequestered by the HMW DOM in solution, will be governed indirectly by the nature of these HMW DOM sorption interactions. Hydrophobic organic compounds, like resin acids, have been shown to associate with dissolved organic matter (Carter and Suffet 1982; Hassett and Anderson 1979; Kulovaara et al. 1987; Robinson and Novak 1994). Further, the data from Chapter 2 suggested that resin acid association with HMW DOM

becomes most significant under slightly acidic conditions. Therefore, resin acids in association with HMW DOM under acidic conditions are likely to sorb more tenaciously.

The retention of resin acids in association with biomass-sorbed HMW DOM will increase the resin acid residence time in a secondary biological treatment process. However, the literature reports that hydrophobic contaminants bound to dissolved organic matter also exhibit decreased bioavailability (Kukkonen 1992; Kukkonen and Oikari 1992; Robinson and Novak 1994; Shimp and Pfaender 1985). The uptake of hydrophobic compounds by microorganisms is believed to be passive and restricted to molecular masses less than 1,000 Da (Sikkema et al. 1995). Since the metabolism of hydrophobic compounds is believed to take place intracellularly, components in association with HMW DOM are likely to be prevented from entering the cytoplasm due to their effective size. For this reason, HMW DOM-bound contaminants are probably not readily biodegraded.

While HMW DOM-associated resin acids may not be readily bioavailable, there still remains the potential for membrane toxicity exerted by resin acids that eventually diffuse passively to microorganisms. Hydrophobic compounds can collect in the cytoplasmic membrane of bacteria and disrupt membrane function (Sikkema et al. 1995). Microbial membrane-buffer partition coefficients of lipophilic compounds correlate directly with their octanol-water partition coefficients. Accumulation of cyclic terpene hydrocarbons in the cytoplasmic membrane can cause a loss of membrane integrity and a dissipation of the proton motive force (Sikkema et al. 1994). Loss of the barrier function of the membrane to protons impairs pH homeostasis, which may lead to impairment of cellular viability (Sikkema et al. 1995). Growth inhibition due to the presence of a toxic compound can be modelled by Monod-type kinetics, with a modification of the form (Bailey and Ollis 1986):

$$q = Q \frac{S_g}{k_g + S_g} \frac{k_t}{k_t + S_t} \quad (4-4)$$

where Q is the maximum specific growth rate, S_g is the total concentration of the substrates sustaining growth, S_t is the total concentration of any toxic substrates, and k_g and k_t are respective

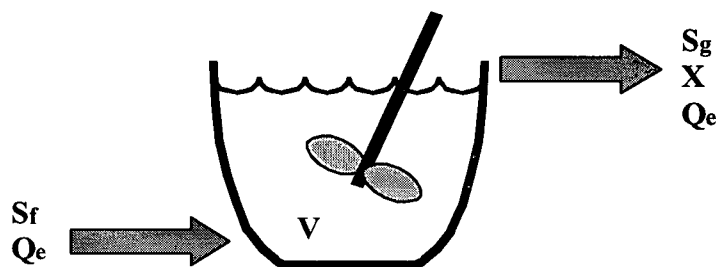


Figure 4-1. Schematic of an ideally mixed chemostat with liquid volume, V . The chemostat supports a biomass community X that consumes the organic feed substrate S_f to the bioreactor level S_g . The volumetric liquid flow rate through the reactor is Q_e .

Monod constants. Equation (4-4) predicts that, for a chemostat operating at steady state, the sudden introduction of a toxic substrate should cause a transient decrease in the biomass level and an increase in the growth substrate concentration commensurate with the sensitivity (k_t) and concentration (S_t) of the inhibiting compound. Based on the previous discussion, k_t should be a function of resin acid hydrophobicity which, in turn, is inversely related to pH. If membrane toxicity is caused by a hydrophobic compound, then greater hydrophobicity would result in a lower corresponding k_t value.

It should be possible to detect toxic inhibition caused by a contaminant, by injecting a spike input of the contaminant into a well acclimated chemostat. If equation (4-4) is a valid model for the concentration-dependence of the contaminant toxicity, then resumption of metabolic activity, measured by a recovered biomass level or substrate consumption rate, should progress in step with the wash-out of the spiked contaminant from the chemostat. The expected effect can be shown, for example, with the simplified model of the system illustrated schematically in Figure 4-1. A mass balance for the growth substrate (S_g) leads to the differential equation:

$$\frac{\partial S_g}{\partial t} = \frac{1}{\theta_H} S_f - \frac{1}{\theta_H} S_g - \frac{m_b'}{V} \quad (4-5)$$

where θ_H is the hydraulic retention time, S_f is the influent ("feed") concentration level of S_g , V is the reactor volume and m_b' is the biological mass uptake rate of S_g in the chemostat. The mass

uptake rate divided by the reactor volume is equal to:

$$\frac{m_b'}{V} = \left(\frac{X}{Y} \right) q \quad (4-6)$$

where q is defined in equation (4-4), X is the biomass concentration and Y is the biomass yield coefficient. Assuming that the biomass level remains essentially constant and that $k_b \ll S_g$, equation (4-6) can be simplified to:

$$\frac{m_b'}{V} = k_b \frac{k_t}{k_t + S_t} \quad (4-7)$$

where k_b is the steady-state uptake rate of S_g . The parameters and variables can be non-dimensionalized for numerical simulation as follows:

$$\eta = \frac{t}{\theta_H}, \quad s_g = \frac{S_g}{S_f}, \quad \kappa_b = \frac{k_b \theta_H}{S_f}, \quad s_t = \frac{S_t}{k_t} \quad (4-8)$$

The differential equation (4-5) can then be written in its non-dimensional form:

$$\frac{\partial s_g}{\partial \eta} = 1 - s_g - \kappa_b \left(\frac{1}{1 + s_t} \right) \quad (4-9)$$

If this model chemostat is assumed to be operating at steady state ($\partial s_g / \partial \eta = 0$), with s_t initially equal to zero, then s_g would initially be given by:

$$s_g = 1 - \kappa_b \quad (4-10)$$

To illustrate, equation (4-9) was integrated (Simnon, Version 1.03) twice in order to model two shock loads at a constant κ_b equal to 0.5. Two model toxic contaminant spike inputs, applied at η equal to zero, with s_t equal to 1 and 10, respectively, were simulated (Figure 4-2). From Figure 4-2, it can be seen that for an actual experiment, substrate data for $\eta < 0$ should be randomly distributed and for $0 < \eta < 5$ a definite trend in substrate concentration would be expected. The

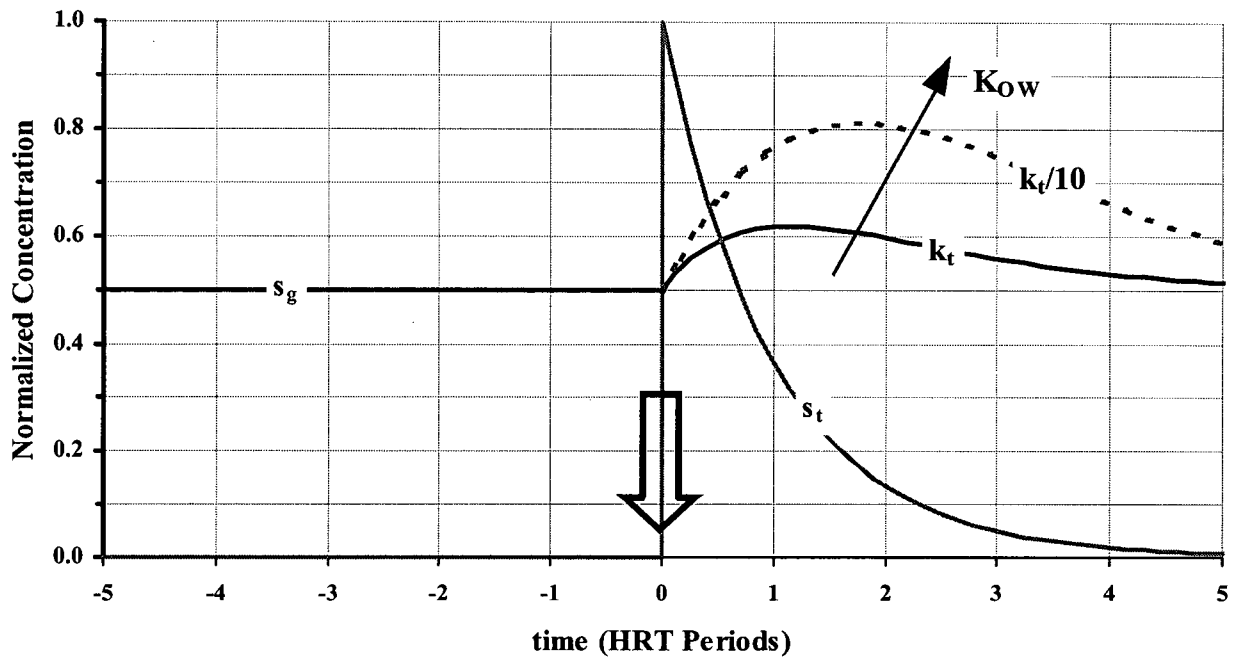


Figure 4-2. Model transient substrate concentrations during ten hydraulic turn over periods in a well mixed chemostat. At steady state the chemostat removes 50 percent of the growth substrate (s_g). At time zero a spike load of an inhibiting substrate (s_i) is introduced and washes out following an exponential decay. Due to microbial inhibition, the growth substrate concentration increases as a function of the s_i level (Equation (4-9)). Simulation results show how microbial sensitivity (k_t) to the inhibiting substrate changes the level of response. Presumably an increase in contaminant hydrophobicity, measured by K_{ow} , decreases k_t . Resin acid K_{ow} is inversely related to pH.

magnitude of this trend would depend on k_t , which should be related to substrate hydrophobicity.

In other words, since partitioning of lipophilic compounds correlates directly with their octanol-water partition coefficients, a more hydrophobic contaminant should collect to a greater extent in the cytoplasmic membrane, and result in a greater level of disruption of membrane function.

Therefore, if resin acids have a toxic impact, then a shock load at pH 6 should be more inhibiting and should produce a stronger response, than at pH 8. While hydrophobicity may influence the extent and impact of sorption, it must not be forgotten that sorption to biomass is a kinetic process.

4.1.3 Kinetics of Sorption to a Biofilm

Sorption of a contaminant to a biofilm is a complex mass transfer process with four major steps (Nauman 1987; Weber 1972). The first step is bulk transport of the contaminant to the vicinity of the biofilm. Bulk transport is followed by inter-phase mass transfer through the hydrodynamic boundary layer formed by fluid motion relative to the biofilm. The boundary layer

accounts for the fluid velocity distribution close to the surface. Since the fluid dynamics in the boundary layer are typically not well defined, the resistance to mass transfer at the surface is normally referred to as a *film diffusion* process. If the biofilm is porous, then pore diffusion of the sorbent to interior surfaces follows the mass transfer by film diffusion. Once at the surface, the contaminant may sorb to the biofilm.

Under well mixed conditions, bulk transport of a contaminant should be rapid. Further, from the dynamic surface tension measurements described in Chapter 2, the adsorption of resin acids at a gas-liquid interface proceeds quite rapidly, with equilibrium conditions being approached on a time scale of a few minutes. In modelling of a continuous flow bioreactor on the time scale of tens of minutes to hours, the sorption process would most likely be rate limited by the film and pore diffusion steps. Therefore, it should be possible to neglect resistance to mass transfer due to the initial bulk transport step and to the final sorption step (Weber 1972).

Given that both the boundary layer and the porous nature of a biofilm are difficult to characterize, resistance due to film and pore diffusion may be lumped together and represented in terms of an effective film diffusion process to an idealized biofilm surface. If the concentration of a contaminant (C_0) at this idealized biofilm surface differs from the concentration in bulk solution (C_∞), a concentration boundary layer will develop whose thickness (δ) is defined by the distance (z) away from the surface as follows (Incropera and de Witt 1981):

$$(C_0 - C_z)/(C_0 - C_\infty) = 0.99 \quad (4-11)$$

Contaminant molar flux due to diffusion (J_D) is approximated by Fick's law:

$$J_D = -D \frac{\partial C}{\partial z} \quad (4-12)$$

where D is the binary diffusion coefficient. In general, species flux in the boundary layer is due to both bulk fluid motion (convection) and diffusion. However, at the surface ($z=0$) there can be no

fluid motion and contaminant transport reduces to that of diffusion alone. Since the contaminant flux across the boundary layer must be constant for mass continuity, it follows that the total flux (J) can be determined by the surface condition:

$$J = -D \left. \frac{\partial C}{\partial z} \right|_{z=0} \quad (4-13)$$

Unfortunately, the concentration gradient at the surface cannot be readily measured. Instead a convection mass transfer coefficient (h) can be defined as follows:

$$h = \frac{-D \left. \frac{\partial C}{\partial z} \right|_{z=0}}{C_0 - C_\infty} \quad (4-14)$$

Therefore the contaminant flux to the biofilm is represented by:

$$J = h(C_0 - C_\infty) \quad (4-15)$$

Hence the mass transfer coefficient (h) is a function of contaminant diffusivity and the surface concentration gradient at the idealized biofilm surface. Hydrodynamic and biofilm morphology both factor into the effective surface concentration gradient and, consequently, any experimentally determined value for h . For two systems with similar and constant mixing intensities and biofilm morphologies, differences found in h for the same contaminant should reflect a change in the contaminant diffusivity. Therefore, monitoring resin acid sorption at pH 6 and pH 8 for otherwise identical bioreactors should reveal the same pH-dependent diffusivity changes observed in Chapter 2.

If the sorption step can be assumed to be relatively rapid, then the surface concentration (C_0) immediately adjacent to the biofilm will be in equilibrium with the biofilm loading. Based on the

results of Chapter 2 and on literature findings (Liu et al. 1996), a Langmuir isotherm is likely to be a good model for resin acid sorption to the biofilm:

$$\Gamma = \Gamma_L \frac{C_0}{K_e + C_0} \quad (4-16)$$

where Γ is the solute concentration per unit weight of sorbent (biofilm), Γ_L is the limiting sorbed concentration, K_e is the equilibrium Langmuir constant (Chapter 2), and C_0 is the surface aqueous concentration. Combining equations (15) and (16), the flux equation can be written in terms of readily measured quantities:

$$J = -\frac{\partial \Gamma}{\partial t} = h \left(\frac{K_e (\Gamma/\Gamma_L)}{1 - (\Gamma/\Gamma_L)} - C_\infty \right) \quad (4-17)$$

Therefore, assuming that film and pore diffusion can be effectively lumped together and that a Langmuir isotherm applies, the parameters $\{h, K_e, \Gamma_L\}$ can be estimated by experimentally monitoring the time course of biofilm loading (Γ) during conditions of changing bulk contaminant concentration (C_∞).

To experimentally test for the applicability of the sorption model presented by equation (4-17), the time varying bulk contaminant concentration should be such that conditions for both sorption and desorption are created. The failure of equation (4-17) to adequately describe the experimental data could indicate that either (1) film diffusion is not rate limiting, (2) Langmuir sorption is not followed, (3) the sorption process is not reversible, or (4) metabolism of the contaminant by microorganisms in the biofilm is significant.

If suitable parameter values, $\{h, K_e, \Gamma_L\}$, cannot be found, then an alternate sorption model can be combined with equation (4-15). For instance if $K_e \gg C$ then the data may be over-specified by equation (4-16) and the sorption equilibrium would be better expressed in terms of a partition

coefficient (K_p) as follows:

$$\Gamma = K_p C_0 \quad (4-18)$$

Partition coefficients of this form were determined by Hall and Liver (1996) for resin acid association with inactivated biomass. Alternatively, Freundlich or BET isotherm models (Weber 1972) could be tested for their respective abilities to fit the observed data.

A degree of irreversibility in the sorption process would be measured if the rate of desorption was slower than the rate of sorption. On a plot of C_0 versus Γ , such irreversibility would appear as a counter clockwise hysteresis (Figure 4-3). Thus while film diffusion would be rate limiting for sorption, sorption kinetics would be rate limiting for desorption. In this case, equation (4-17) may provide a good fit during sorption but would systematically overestimate the magnitude of the biofilm loading rate during times of desorption.

Since resin acids are readily metabolized by microorganisms (Chapter 2 and 3), the potential for biological removal must also be considered. The most direct way to control for contaminant loss due to metabolism without altering the morphology of the biofilm would be to inhibit biological activity with sodium azide (Hall and Liver 1996). However, inactivation of the biosolids would prevent the observation of microbial inhibition due to resin acid toxicity. As an alternative, the duration of an experiment could be kept short with respect to the time scale of microbial acclimation. A sudden elevation of resin acids in a biofilm is not unlike the conditions created for batch removal experiments by activated sludge. Removal of resin acids in batch experiments with activated sludge has been reported to take from 1 (Liver and Hall 1996) to 3 (Leach et al. 1977) days for dehydroabietic acid. A lag time of 8 to 12 hours has been reported before significant biological removal begins (Liu et al. 1996). The lag time for chloro-dehydroabietic acid is longer (Leach et al. 1977). Therefore, based on the literature, in order to minimize biological removal by the biofilm during an experiment, contact times should not extend much beyond 12 hours. Since

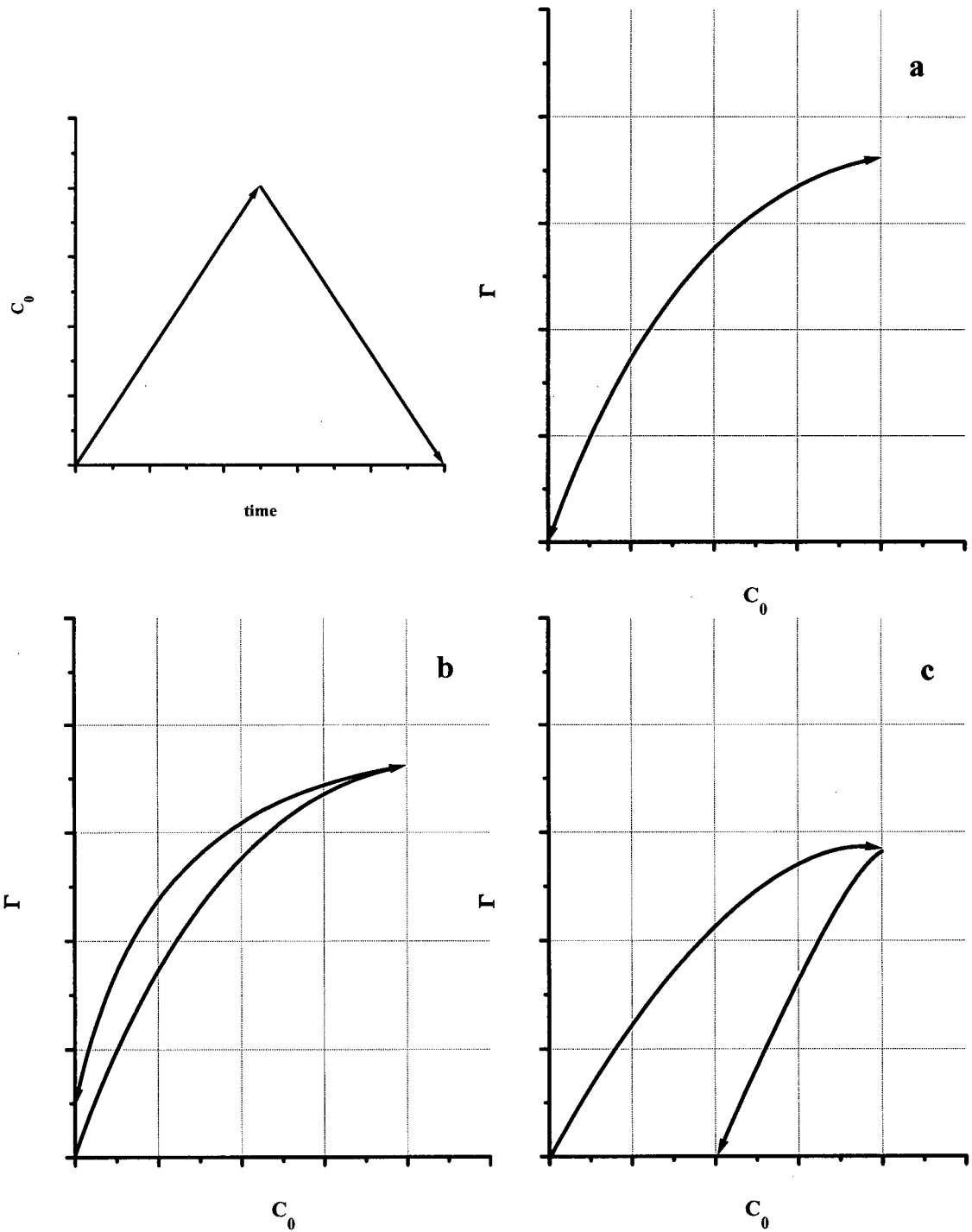


Figure 4-3. Hypothetical Langmuir type sorption/desorption (Γ) progression during a changing surface concentration (C_0) with time (Top Left). For reversible sorption conditions, assuming that sorption kinetics are relatively rapid with respect to the time frame of concentration change, a typical Langmuir isotherm should be followed (Top Right). If sorption is not completely reversible then a counter clockwise hysteresis should result (Bottom Left). If metabolic activity in the biofilm becomes significant then a clockwise hysteresis should be apparent (Bottom Right).

chloro-dehydroabiatic acid is more resistant to biological oxidation than its native form, it would make a good “conserved” control during such an experiment.

Evidence of biological removal of resin acids by the biofilm should be apparent in the observed data. On a plot of C_0 versus Γ , biological removal would appear as a clockwise hysteresis. In this case, the rate of sorption would be apparently slower than the rate of desorption (Figure 4-3). A good fit of equation (4-17) to the data during times of sorption would systematically underestimate the magnitude of the biofilm loading rate during apparent times of desorption. In this event, the model of equation (4-17) could be modified to include contaminant loss due to metabolism.

Therefore, based on the expected time scale for resin acid sorption and the anticipated lag before significant biological removal of a spike resin acid input, this experiment was designed with the objective of determining,

- i. the extent to which pH-dependent resin acid hydrophobicity could interfere with microbial activity (Objective C - Chapter 1), and
- ii. how resin acid sorption kinetics could influence the contaminant retention time in a bioreactor (Objective D - Chapter 1).

The pH levels 6 and 8 were chosen to contrast the effect of high versus low resin acid hydrophobicity on the contaminant fate.

4.1.4 Method Specific Issues

Given that the expectations and model responses to a resin acid shock load have been addressed in the preceding discussion, the actual method of measuring sorption requires some further consideration. The common procedure reported in the literature for measuring the extent of sorption of organic pollutants to biomass entails contacting aqueous solutions of predetermined contaminant concentrations to different quantities of biosolids over a set time period (Amy et al. 1988; Bell and Tsezos 1987; Hall and Liver 1996; Jacobsen et al. 1996; Liu et al. 1996; Selvakumar and Hsieh 1988). The extent of sorption on the biosolids is measured by extracting the contaminant(s) from the biosolids with an organic solvent. Thus, after the set contact period, the biosolids must be separated from the aqueous solution. Separation is typically performed by filtration or by centrifugation. The results of Chapter 2 and 3 indicated that a portion of resin acids in pulp mill effluent is particulate and will, therefore, be separated alongside the biosolids by either filtration or centrifugation.

Liu et. al (1996) reported that resin acid sorption to biosolids was initially very rapid and this initial sorption was shown to remove 50 percent of the initial concentration. These experiments were conducted at pH 7 where the particulate fraction of resin acid could have been around 50 percent (Chapter 3). The use of sample controls to verify the methods in the absence of biosolids was not mentioned in this work. It would not be surprising to find that the observed rapid sorption was in fact, an artefact of the separation method used to isolate the biosolids from solution.

Similarly, Hall and Liver (1996) reported that the partitioning of resin acids onto biosolids was apparently a two-phase process in which the major portion of the adsorbate was rapidly removed by the biomass. Once again, these experiments were carried out nominally at neutral pH and centrifugation was used to isolate the biosolids from solution. Further, over a range of resin acid to biomass ratios, the final concentration of resin acids in the liquid phase was similar in all the partitioning experiments. These partitioning experiments were conducted by varying the biomass concentration by orders of magnitude with respect to a relatively constant resin acid

concentration in solution. A nominal total resin acid concentration of 200 mg/L dispersed with methanol in a nutrient buffered medium was used. At pH 7, the total solubility of resin acids can be expected to be around 30 mg/L (Nyrén and Back 1958). Therefore, centrifugation could have stripped the medium of the colloidal fraction, leaving only the truly dissolved resin acids in the supernatant. As the medium and the pH for these partitioning experiments was kept approximately constant, it is understandable that the remaining concentration in the supernatant was independent of the biosolids concentration.

In contrast to these reported methods, the experimental procedure for this investigation made use of a fixed film biological process. Well mixed, single tank, bench scale, moving bed bioreactors were used (Strehler and Welander 1994). The moving bed consisted of small, free-floating, plastic elements, with a specific gravity close to unity. The plastic elements or carriers were held in suspension by a combination of mechanical mixing and aeration. Over time, a steady-state biofilm formed on the carriers. Such moving bed biofilm reactors (MBBR) are being used successfully in full scale applications (Broch-Due et al. 1994; Rusten et al. 1995). They are an attractive option for treatment plant upgrades, since they enable existing systems to support a higher loading rate without the need for expansion.

The MBBR was selected for this investigation for a number of reasons. First, sorption of contaminants to the biofilm could be monitored by simply sacrificing suspended carriers from the bioreactor. Secondly, centrifugation or filtration to isolate the biosolids would not be required. Thus, the potential for measurement artefacts created by the particulate resin acid fraction could be avoided. Furthermore, the use of a simple, well mixed, one tank system, without a clarifier and biosolids recycle, considerably simplified the bioreactor operation and, ultimately, the interpretation of the experimental results. The bench scale bioreactor could be operated with a very short hydraulic retention time without the risk of biosolids washout. In this manner, contact times for transient resin acid loads to the carrier biofilms could be kept as short as necessary.

The fact that the laboratory MBBR would support two distinct communities of microorganisms was also seen as a research advantage. The microbial community that composed the carrier

biofilm would effectively have an infinite solids retention time (SRT). The bioreactor would also support a community of more rapidly growing suspended biosolids, whose SRT would be approximately equal to the reactor HRT. Since both these communities could be sampled separately, the sensitivity of short or long SRT communities, to the changing bioreactor operating conditions during an experiment, could be concurrently monitored.

4.2 Methods and Materials

4.2.1 Bioreactor design and operation

For these experiments, both microbiological inoculum and primary mill effluent were kindly supplied by Western Pulp Partnership in Squamish, British Columbia. At the time sludge samples and effluent were obtained, the mill was kraft pulping a fir:cedar:hemlock furnish with 75% chlorine dioxide substitution in bleaching for a 700 ADt/day production rate yielding a mill primary effluent of approximately 1200 mg/L COD (Chemical Oxygen Demand) and 325 mg/L BOD (Biochemical Oxygen Demand).

Primary effluent, delivered weekly in 25 L Nalgene carboys, was adjusted to pH 10 with 50 mL of 2 N NaOH and stored at 4°C. On a daily basis, approximately one carboy was screened to remove fibre fines and then decanted into a 50 litre holding tank, also refrigerated at 4°C.

Primary effluent was pumped (Cole Parmer MasterFlex) at a constant rate from the holding tank to two parallel bench scale moving bed bioreactors. In addition to the main effluent feed, a constant drip feed of concentrated ammonium chloride (6 g/L) supplied the microorganisms with excess nitrogen. Dosing the reactors with phosphoric acid (Cole Parmer Series 7142 pH/pump system) to maintain a constant pH of 6 and 8 in reactor A (“Acidic”) and B (“Basic”), respectively, provided excess phosphorus with pH control.

The two parallel bioreactors were identical 3 litre (total volume) Plexiglas jacketed cylindrical vessels with a 5-inch inside diameter (Figure 4-4 and Figure 4-5). The water jacket was thermostated to maintain biological treatment at 37°C. Magnetic stirrers were used for mixing. Air, feed and phosphoric acid (pH control) were pumped into the reactors in close proximity to the magnetic stir bars through a ¼ inch stainless steel tube inserted down the axis of symmetry. In this manner, gas sparging and rapid mixing of the feed and phosphoric acid was achieved. Rapid mixing was especially important to minimize any time lag and overshoot in the pH control. Sparging the air and feed together also provided an air lock, preventing back diffusion, inoculation and growth in the feed lines. The air was pre-humidified by passage through two 4

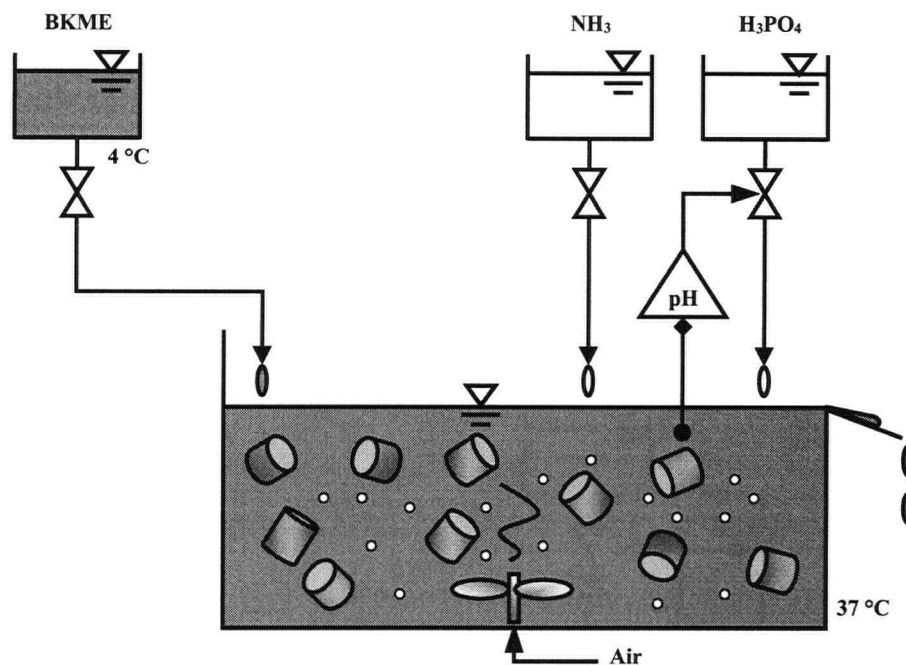


Figure 4-4. Idealized schematic of the experimental bench scale moving bed bioreactor (MBBR). Two parallel bioreactors (one at pH 6.0 and the other at pH 8.0) were continuously fed whole bleached kraft mill effluent. The effluent was kept at 4 °C and pH adjusted to 10. Additional nutrients were supplied to maintain excess levels of nitrogen and phosphorus. The phosphorus supply was added at a rate to maintain constant pH in the bioreactors. The bioreactors were thermostated at 37 °C.

litre bottles filled with distilled water and thermostated at 37°C. Air flow was sufficient to maintain a dissolved oxygen level around 2 mg/L. The nitrogen drip was separately supplied to the liquid surface. Treated effluent was discharged through a constant level overflow. The carriers were prevented from leaving the reactors at the overflow due to their size.

The biofilm suspended carriers were cut from an extruded cylinder made from a proprietary plastic (ANOX AB, S223 70 Lund Sweden). This plastic was a high density polyethylene that was combined with fillers to arrive at a specific gravity of about 0.98-0.99. Ideally, moving bed carriers would have a specific gravity just under that of water, so that once a biofilm is established, the carrier becomes neutrally buoyant and is, thereby, easily fluidized. The carriers were cylindrical units, nominally, 8 mm \varnothing by 1.25 mm wall thickness by 10 ± 2 mm long. Due to the extrusion molding process, the carrier diameter and wall thickness were approximately constant. The 900 carriers used in each reactor occupied about 25 percent of the empty bed

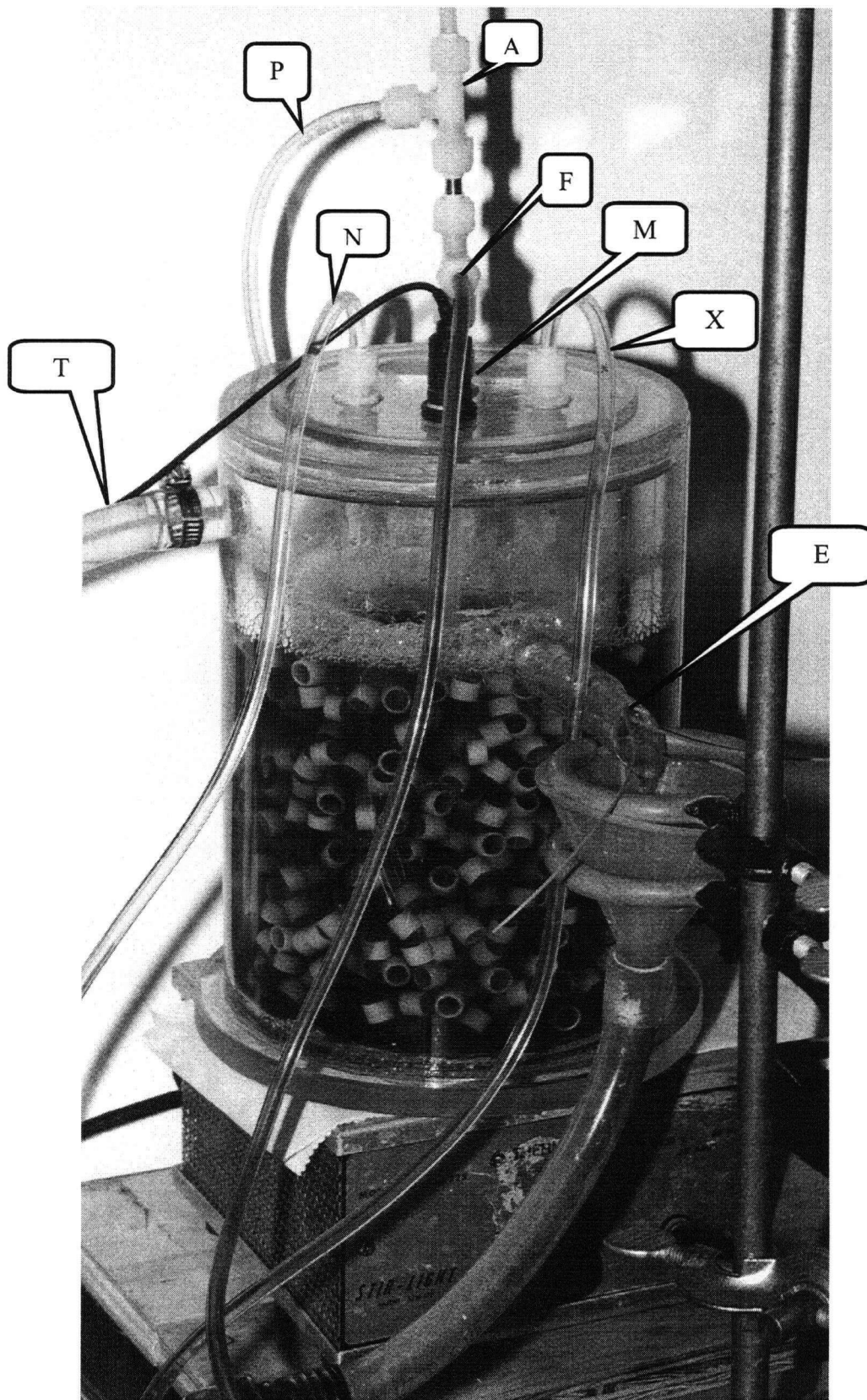


Figure 4-5. Photograph of the actual bench scale MBBR. Air (A), BKME feed (F), and phosphorus (P) were supplied through a common $\frac{1}{4}$ inch stainless steel tube down the axis of the Plexiglas tank in close proximity to the magnetic stir bar. The pH probe (M) can be seen supported by the top plate. The extra drip feed port (X) was not used in this experiment. Treated effluent exited the reactor by a constant level overflow (E). Thermostated water (T) was constantly supplied to the water jacket to maintain the bioreactor temperature.

reactor volume. Mechanical mixing and aeration kept the carriers fluidized.

The bioreactors were acclimated over a month of continuous operation (November 1996).

Surface scum and attached growth were cleaned regularly from the two reactors. Wall growth generally occurred at the liquid surface and around the outlet, but this tended to diminish as the carrier biofilm became established. Constant contact of the carriers with the tank walls below the surface prevented attached growth elsewhere in the tanks.

Twenty-four hours prior to introducing the resin acid shock load, the reactors were closely monitored to characterize the operational conditions. The resin acid shock load was a 10 mL aliquot of a saponified concentrate of pimaric (16%), abietic (62%), dehydroabietic (16%), and chloro-dehydrabiatic (6%) acid in a solution of 0.1 N LiOH and 0.6 N LiCl. Lithium served as a conserved non-interacting tracer and was used to assess the actual reactor mixing conditions, the liquid volume, and the hydraulic retention time (HRT). Chloro-dehydroabietic acid was assumed to be a conserved interacting tracer that would behave similarly to the other resin acids introduced to the system. Periodically for 72 hours after the shock load, aqueous samples were drawn and suspended carriers were sacrificed for chemical analysis. The residence time distribution (RTD) was determined for lithium, the resin acids in the liquid phase and, concurrently, the resin acids sorbed to the carrier biofilm.

4.2.2 Sampling and Chemical Analysis

Resin and Microbial Fatty Acid Sampling and Analysis

Resin and microbial fatty acid concentrations were measured by solvent extraction, methylation and GC/FID quantification. Microbial fatty acids provided a quantitative and qualitative assessment for suspended and biofilm biomass in the two chemostats.

At regular intervals, 5 mL aqueous samples from the two reactors and the feed were transferred to 15 mL glass tubes with Teflon screw caps. To these samples, a 1 mL aliquot of 2 N NaOH in 50 percent HPLC grade methanol spiked with O-methylpodocarpic acid (O-MPCA) was added.

Similarly, carriers were randomly plucked from the reactor with forceps and placed into capped tubes containing 1 mL of 1 N NaOH in 50 percent HPLC grade methanol also spiked with O-methylpodocarpic acid (O-MPCA). Samples were stored frozen at minus 10°C pending extraction.

The extraction procedure described in Chapter 3 was followed with a couple of minor modifications due to the larger aqueous reactor samples taken and due to special considerations required for the carrier/biofilm samples. After the biofilm carrier samples were incubated at 90°C for 30 minutes to saponify the resin and whole cell fatty acids (WCFA), these samples were vigorously vortexed to fully detach the biofilm from the carrier. The liquid contents were carefully transferred to a clean tube. The carrier was rinsed with distilled water and then dried and weighed. From this weight (W_c), the carrier surface area was estimated based on the manufacturer's reported plastic density ($\rho_c = 0.985 \text{ g/cm}^3$) and the tubular geometry as follows:

$$A_c = 2 \frac{W_c (D_c - t_c)}{\rho_c (D_c t_c - t_c^2)} \quad (4-19)$$

where D_c is the diameter (8 mm) and t_c is the wall thickness (1.25 mm).

As before (Chapter 3) the liquid samples were extracted twice with 1 mL methyl-ter-butyl ether (MTBE). With the addition of the first millilitre of MTBE, the 5 mL reactor samples were acidified with 1 mL $2 \text{ N H}_2\text{SO}_4$ and the solubilized biofilm samples were acidified with $\frac{1}{2}$ mL $2 \text{ N H}_2\text{SO}_4$. The remaining steps of the extraction method, sample analysis by GC/FID, peak identification by equivalent chain length calibration, and peak confirmation by GC/MS were as described in Chapter 3.

Lithium Tracer Sampling and Analysis

Lithium was analysed by flame emission spectrophotometry. Reactor samples of 10 mL were acidified with 1 mL of 10% nitric acid in 15 mL glass tubes with Teflon caps. Lithium was quantified from the supernatant of vortexed and centrifuged samples (20 minutes at $2060 \times g$)

with a Thermo Jarrell Ash Video 22 aa/ae spectrophotometer. An acetylene/air oxidising flame was used with detection at a 670.8 nm wavelength with a 0.3 nm band width. Samples were calibrated against similarly prepared standards diluted from the same Li stock solution used to dissolve and saponify the resin acids.

Total Organic Carbon (TOC) Sampling and Analysis

Reactor performance was measured in terms of total organic carbon (TOC) removal. Reactor samples of 1 mL were diluted to 5 mL in 10 mL glass tubes with Teflon caps, acidified with 100 μ L of 10 % phosphoric acid and stored frozen prior to analysis. TOC was quantified for the supernatant of vortexed and centrifuged samples (20 minutes at 2060 \times g) with a Shimadzu TOC 500 Analyzer against similarly acidified calibration standards prepared with dried $\text{KHC}_8\text{H}_4\text{O}_4$ (KHP). A stock solution of 2.125 mg of KHP in 1 litre created a 1000 mg C/L calibration standard. Acidification and centrifugation of TOC samples was found to remove acid insoluble compounds from the water column. Resin acids contributed negligibly to the measured TOC.

Nitrogen and Phosphorus Sampling and Analysis

Reactor nitrogen and phosphorus levels were measured on a Lachat QuikChem AE system. Reactor samples of 5 mL were stored frozen in 10 mL glass tubes with Teflon caps. On a diluted aliquot of the 5 mL sample, total Kjeldahl nitrogen and total phosphorous were determined following the QuikChem method No. 10-107-06-2-E and No. 10-115-01-1-I, respectively.

Effluent Flow Rate Sampling and Analysis

The effluent volumetric flow rate was regularly monitored. The chemostat effluent overflow was collected in dry tarred Nalgene beakers for a timed period of about 15 minutes. From the net weight (W_l) of the collected liquid, a flow rate was estimated based on the approximate liquid density (ρ_l) of 1.0 g/cm³ as follows:

$$Q_e = \frac{(W_l / \rho_l)}{t} \quad (4-20)$$

where Q_e is the average volumetric flow rate over the time (t) during which the effluent was collected.

pH Control

Primary BKME effluent feed, adjusted to a pH around 10, maintained a “driving force” for pH control. Automatic dosing of phosphoric acid solutions with a Cole Parmer Series 7142 pH/pump system kept the pH constant. The dosing stock was 0.85 percent H_3PO_4 for reactor A and 2 percent $NaH_2PO_4 \cdot H_2O$ for reactor B. Confirmation of a steady pH was made by continuously logging the pH to a strip chart. Reactor A was maintained at pH 6.0 and reactor B at pH 8.0 to within ± 0.1 pH units.

4.2.3 Bio-carrier Material Characterization

The plastic carrier was considered to be integral to the development of the biofilm. Modifications to the carrier materials that generate a more hydrophilic surface have been shown to effect microbial colonisation (Strehler and Welander 1994). As a consequence, some effort was made to characterize the plastic surface, especially since the exact chemical composition of the carriers was proprietary. Colonisation of the carrier relies on adhesion of the biofilm to the plastic surface. The reversible work of adhesion between a particle (p) and a solid (s) in a liquid (l) is given by (Israelachvili 1985):

$$W_{pls} = \gamma_{pl} + \gamma_{sl} - \gamma_{ps} \quad (4-21)$$

where γ is the interfacial energy for the particle-liquid (pl), solid-liquid (sl) and particle-solid (ps) surfaces. The “interfacial” energy represents the free energy change in expanding an interface by one unit of area.

The interfacial energies of a solid surface are indicated by forming a liquid drop on the solid surface. In most instances, the drop will not wet the surface but remains instead as a sessile drop having a definite angle of contact to the solid surface. When the liquid drop, the solid and the surrounding vapour are in equilibrium, the Gibbs free energy of the system is at a minimum, and

this condition is expressed by Young's equation (Adamson 1982):

$$\gamma_{lv} \cos \theta_e = \gamma_{sv} - \gamma_{sl} \quad (4-22)$$

where θ_e is the equilibrium contact angle and γ is the interfacial energy for the liquid-vapour (lv), solid-vapour (sv) and solid-liquid (sl) interfaces. The solid-vapour interfacial energy (γ_{sv}) was chosen as a meaningful quantity with which to characterize the biofilm carrier for this investigation.

The geometry of a sessile drop is predicted by Laplace's equation of capillarity (Neumann 1974a):

$$\gamma_{lv} \left(\frac{1}{R_1} + \frac{1}{R_2} \right) = \Delta \rho g z + P_0 \quad (4-23)$$

where R_1 and R_2 are the principal radii of curvature at any point on the liquid-vapour drop surface, $\Delta \rho$ is the density discontinuity across the liquid-vapour interface, g is the acceleration due to gravity, z is the ordinate in the liquid along the drop's axis of symmetry and P_0 the capillary pressure at z equal to zero. From a digitized image of the sessile drop profile, the liquid-vapour interfacial energy (γ_{lv}) and the contact angle (θ) can be estimated by least-squares regression to equation (4-23) by means of a numerical iterative curve fitting procedure (Maze and Burnet 1969).

Given experimental values for γ_{lv} and θ_e , estimation of γ_{sl} and γ_{sv} with equation (4-22) requires an additional relationship between these quantities. The solid-liquid, solid-vapour and liquid-vapour interfacial energies of a two-component, three-phase system are related by an equation of state which has been empirically determined to be (Neumann 1974a; Neumann 1974b):

$$\gamma_{sl} = \frac{(\sqrt{\gamma_{sv}} - \sqrt{\gamma_{lv}})^2}{1 - 0.015 \sqrt{\gamma_{sv} \gamma_{lv}}} \quad (4-24)$$

The surface energies for the ANOX carrier plastic along with pure high density polyethylene and Teflon were estimated from digitized images of sessile drops created with water (Millipore Alpha

Q Ultra-pure Water System) and 99% pure chromatographic quality ethylene glycol (Matheson, Coleman and Bell).

Optically smooth surfaces of the samples were generated by warm forming the plastic between glass microslides (Fisher Scientific Co.). Small (2 cm × 2 cm × 0.2 cm) plastic samples were first cleaned with water and were then rinsed with HPLC grade acetone (Fisher Scientific Co.). The glass slides were thoroughly rinsed with acetone and then heated to 475°C for two hours to remove any organic impurities. The samples were formed by clamping the plastic between two slides and then by gradually applying heat until the clamping pressure was sufficient to mold the plastic to the slide surface.

The drops were formed by the careful deposition of small liquid volumes (5-10 µL) on the plastic surfaces. In a manner similar to Zisman's technique (Neumann and Good 1979), the liquid volume was hung from the tip of a thoroughly cleaned and rinsed microlitre syringe with a fine stainless steel needle. The test surface, placed on an x-y-z micrometer stage, was brought slowly to the drop until it made contact and the liquid flowed off the tip to form a sessile drop. Measurements were made at room temperature (20°C) on an open stage, which is allowable for high boiling point liquids such as water and ethylene glycol, so long as measurements are made quickly after drop formation (Neumann and Good 1979).

A video image of the drop was recorded with a Panasonic Model WV-D5000 video camera through a Titan Tool 1-6.5 Zoom Objective long focal length lens with a 2× extension tube and an additional 2× magnification lens. Gentle back lighting through a diffuser screen was used to produce a sharp silhouette. The surface was tilted slightly with respect to the tele-microscope so that the front edge of the surface was out of the line of sight (Neumann and Good 1979). The image was quickly framed and focused on a Panasonic video monitor by careful stage manipulation. The image was then digitally captured (Snappy Video Image Version 1.0, Play Incorporated) and stored as a pixel image file (IBM-PC clone with a 486 DLC 40 MHz CPU with math co-processor). The pixel image was scaled by capturing an additional image of a stage micrometer slide (Fisher Scientific Co.) held parallel to the plane of focus with the same lens

settings. The pixel conversion was nominally 2 $\mu\text{m}/\text{pixel}$.

The pixel image of the drop silhouette was digitized (Surfer Version 6.01, Golden Software Inc.). Co-ordinates for the sessile drop were then numerically fit to equation (4-23) with a modified form of the mathematical procedure employed by Maze and Burnet (1969) and the contact angles formed on the surfaces by the liquid drops were thereby measured. Estimates for the solid-liquid and solid-vapour interfacial energies were obtained by solving for γ_{sl} and γ_{sv} with Young's equilibrium equation (4-22) and Neumann's state equation (4-24).

4.3 Results

The experimental results have been organized into the six major aspects of the measurements made for this investigation. First, the results of the bio-carrier material characterization are presented. The bio-carrier plastic was found to have properties similar to native high-density polyethylene, on the basis of surface energy. This information is deemed to be an important reference for research work with biofilms. In the next section, the operating characteristics of the two parallel bioreactors are described. From the lithium tracer analysis, the moving bed bioreactors closely followed the model of complete mixing. Next, the results of the resin acid analysis are given. A mass balance indicated that little, if any, biological removal of the spike input of resin acids occurred. A significant amount of resin acids was partitioned into a surface scum layer for the bioreactor operating under the alkaline pH conditions. Assessment of the impact of the resin acid shock load is then considered from the analysis of the biomass as total fatty acids (TFAs) and from the data for bioactivity in terms of total organic carbon (TOC) removal. There was no evidence to suggest microbial inhibition due to a resin acid shock load. However, from the analysis of the fatty acid compositions, there was a strong indication that the ecology of the suspended biomass community rapidly changed in correlation with the bioreactor resin acid concentration.

In order to assess the microbial community response, a novel parameter, called "state speed", was derived by mathematically reducing the fatty acid compositional data into a form that could be interpreted as a trajectory for the community structure. The community state speed was defined as the rate of passage on the path of this trajectory and measured relative shifts in the bioreactor community structure. The greater community response for the suspended biomass than that of the biofilm biomass, supported the notion that faster growing, short SRT, microbial populations should adapt more rapidly to environmental change.

Finally, the results of resin acid sorption kinetics to the biofilm are considered. These data could be modelled by Langmuir sorption, rate limited by film diffusion. From these results, it was confirmed that sorption was reversible and that biological removal of the resin acid input could

not have been significant. Based on the derived model parameters, the influence of sorption on the fate of resin acids during biological treatment was estimated from a numerical simulation. It was determined that the higher rate of sorption under alkaline conditions was more important than the greater extent of sorption under acidic conditions, when it came to prolonging the resin acid retention time in the bioreactors.

4.3.1 Bio-carrier Material Characterization

Table 4-1 lists the solid-vapour surface energies determined from contact angles with high purity water and with chromatographic grade ethylene glycol for the ANOX biofilm carrier, the high density polyethylene (HDPE) and the Teflon (PTFE) test surfaces. Average contact angles were determined from at least three separate measurements. Typical data are illustrated by Figure 4-6 and Figure 4-7.

It was expected that γ_{sv} estimated with contact angles from the two liquids would have similar values. However, in all cases, the surface energies determined from water contact angles were higher. The boiling point of water (100°C) is considerably less than that for ethylene glycol (198°C) and the water drops were observed to have been more susceptible to evaporation during the measurements. Evaporation would tend to produce a receding contact angle which can underestimate the equilibrium value due to any surface heterogeneity (Adamson 1982).

Literature values for advancing contact angles of water on Teflon have been reported to be in the order of 110 degrees (Adamson 1982). A contact angle of 110 degrees for water on Teflon would have resulted in a γ_{sv} approximately equal to the value obtained with ethylene glycol. Therefore, the ethylene glycol data are likely to be more accurate.

Table 4-1. Contact angle and solid-vapour surface energies for high density polyethylene, ANOX biofilm carriers and Teflon. Contact angles were formed with high purity water ($\gamma_{lv}=72.8$ erg/cm²) and ethylene glycol ($\gamma_{lv}=47.7$ erg/cm²). Standard deviations are for an average for three separate sessile drops.

Material	Contact Angle Degrees		Surface Energy (γ_{sv}) erg/cm ²	
	H ₂ O	Ethylene Glycol	H ₂ O	Ethylene Glycol
HDPE	98 ± 1	76 ± 1	25	21
ANOX Carrier	101 ± 1	76 ± 1	23	21
Teflon	102 ± 1	87 ± 1	22	16

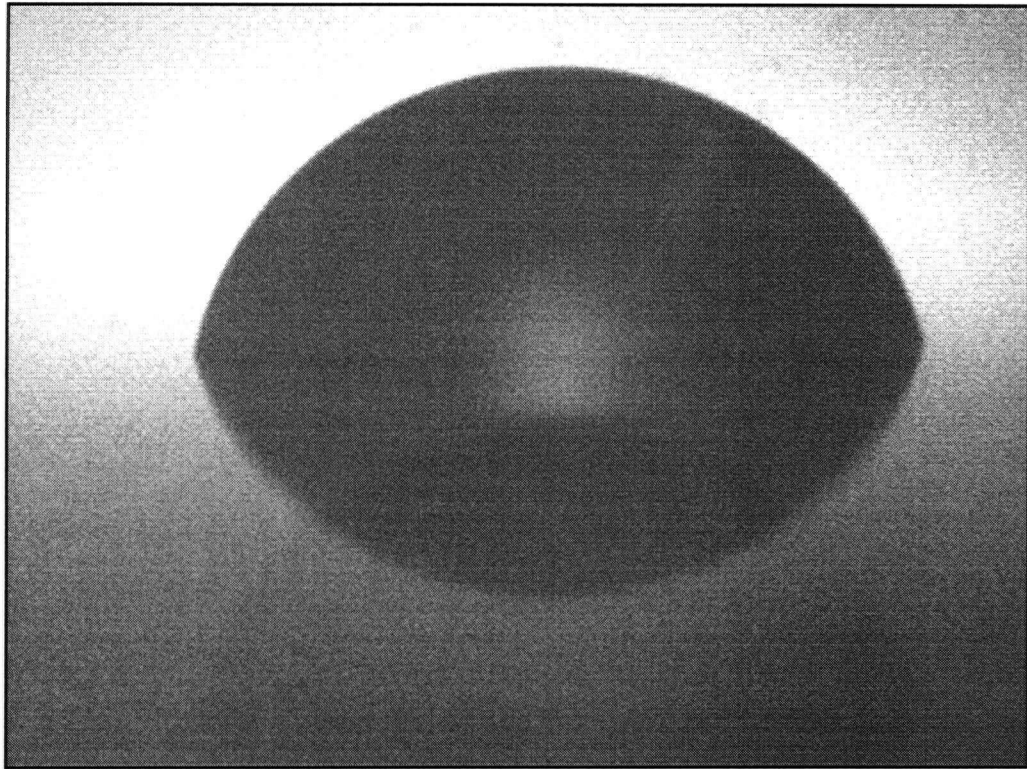


Figure 4-6. A sessile drop of ethylene glycol on an optically smooth surface of the ANOX carrier plastic. The plastic is a high density polyethylene with added fillers to make the specific gravity just below one. A mirror image of the drop is seen in the surface. The drop is approximately 1 mm in diameter.

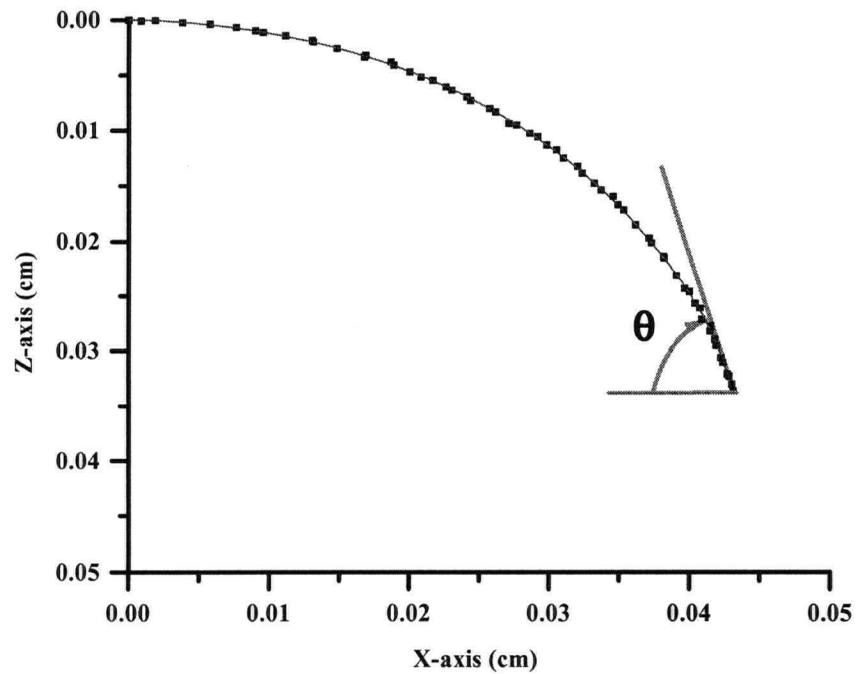


Figure 4-7. The digitized ethylene glycol drop shown in Figure 4-6. A line of best fit (—) for the data points (■) was found by solving Laplace's equation (4-23) and the value for the contact angle θ was determined from the slope of the least squares curve.

Based on the ethylene glycol data, the surface energy of the ANOX lab carrier was the same as the value for the pure high density polyethylene. Therefore, the fillers combined with HDPE to create the ANOX carrier material, of a higher specific gravity, did not seem to have altered the surface energy of the plastic. In so far as biofilm surface interactions were concerned, the ANOX carrier plastic should have behaved similarly to native HDPE. For the present investigation, this information about the bio-carrier plastic surface energy documents the nature of the carrier material surface used to establish a biofilm reactor biomass.

4.3.2 Bioreactor Operating Conditions

Figure 4-8 shows the lithium wash-out curves for the pulse injection of the tracer that contained resin acids saponified by lithium salts. Lithium concentrations in the bioreactors were observed to decrease with a trend closely following an exponential decay function. This type of stimulus-response indicated conditions of ideally mixed flow (Levenspiel 1984). The data were fitted by least squares regression to the function:

$$L = L_0 \exp\left(-\frac{t}{\theta_H}\right) \quad (4-25)$$

where L is the lithium concentration and L_0 is the concentration at time zero. The best fit parameter values used to generate the curves in Figure 4-8 are listed in Table 4-2. Lithium recovery was approximately 100 percent. From the measured effluent flow rate (Q_e) and the derived HRT (θ_H), the liquid volume (V) of the two reactors was estimated (Table 4-2) with equation (4-1). Completely mixed reactor conditions were assumed, based on the good agreement between the ideally mixed reactor model and the experimental lithium wash-out data.

The average measured nutrient levels in the two reactors, as well as in the feed, are given in Table 4-3. From these data it was possible to solve for the experimental feed and supplemental influent flows based on considerations of continuity and conservation of mass. By continuity:

$$Q_e = Q_f + Q_N + Q_P \quad (4-26)$$

Table 4-2. MBBR volume estimated from measurements of effluent flow. From the wash-out function for a pulse injection of lithium salt, the reactors were determined to be ideally mixed and an HRT was calculated.

Parameter	Reactor A pH = 6.0 ± 0.1	Reactor B pH = 8.0 ± 0.1	Units	Description
Q _e	566 ± 10	567 ± 11	mL/hr	effluent flow rate
L ₀	31.61 ± 0.40	33.22 ± 0.33	mg/L	initial lithium concentration
HRT	2.80 ± 0.13	2.87 ± 0.10	hr	hydraulic retention time
V	1583 ± 28	1630 ± 32	mL	liquid volume

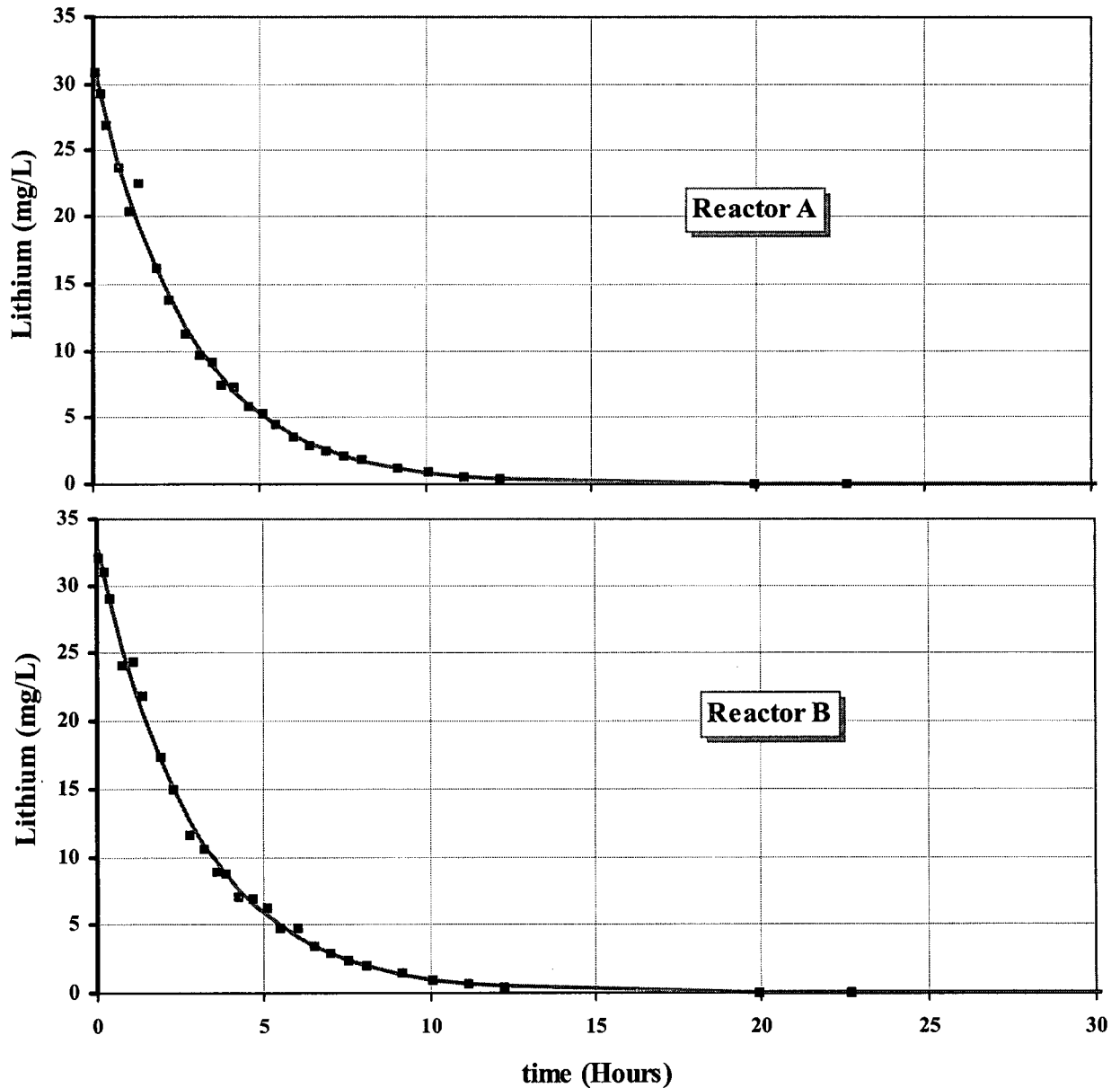


Figure 4-8. Experimental data (■) for the lithium wash-out curves following a spike load at time zero for reactor A (Top) and reactor B (Bottom). For both reactors the wash-out curves were modelled by an exponential decay function (—) which indicated ideal mixing conditions (Levenspiel 1972).

Table 4-3. Average nutrient levels (phosphorus and nitrogen) for the two MBBR reactors and the BKME feed.

	Reactor A pH = 6.0 ± 0.1	Reactor B pH = 8.0 ± 0.1	Feed
Total-P (mg P/L)	288 ± 20	184 ± 19	0.2 ± 0.2
Kjeldahl-N (mg N/L)	41 ± 3	38 ± 3	9.4 ± 1.0

Table 4-4. Estimated bioreactor volumetric inflow rates based on the conservation of mass balance for phosphorous and nitrogen and flow continuity. Volumetric flow rates are in mL/Hr.

Flow Variable	Reactor A	Reactor B	Description
Q_e	566	567	MBBR effluent (total) flow
Q_f	493	535	BKME feed rate
Q_N	12	10	N-feed rate
Q_P	61	22	P-feed rate

Table 4-5. Values used to determine the total biofilm area.

Variable	Value	Units	Description
W_c	0.222 ± 0.020	g	Average weight
ρ_c	0.985	g/cm ³	Plastic density
A_c	3.471 ± 0.445	cm ²	Average surface area
N	900 ± 25		Number of units
A	3124	cm ²	Total biofilm Area

where the subscripts f, P, and N refer to BKME feed, phosphorus and nitrogen inflow rates respectively. Mass balance of nitrogen (N) and phosphorus (P) are described by:

$$N_f Q_f + N_N Q_N = N_e Q_e \quad (4-27)$$

$$P_f Q_f + P_P Q_P = P_e Q_e$$

where N and P are nitrogen and phosphorus concentrations with the same subscript notation defined by equation (4-26). The estimated bioreactor volumetric inflow rates based on equations (4-26) and (4-27) for the measured nutrient levels in Table 4-3 are listed in Table 4-4. A good estimate of the actual feed volumetric inflow rate was necessary for comparing the TOC removal kinetics as a function of bioreactor pH (Section 4.3.4). The average bio-carrier parameters are listed in Table 4-5.

4.3.3 Resin Acid Analysis

There was some initial uncertainty about the efficiency of the extraction method from Chapter 3, for the analysis of the sorbed resin acids and biofilm on the support carriers. The statistics for surrogate recoveries obtained with the sample solvent extractions are presented in Figure 4-9. Generally, the recovery of O-methylpodocarpic acid was greater than 80 percent. Surrogate recoveries for the biofilm A samples, from the reactor operating at pH 6, were on average lower. These samples were also observed to be more highly coloured than the biofilm samples from reactor B. Hence, a greater extent of kraft lignin was observed to be adsorbed along with the biofilm onto the plastic carriers. Molecular interactions with this HMW DOM may have reduced the extraction efficiency for the biofilm samples from reactor A.

Due to the native resin acid content of the BKME feed, the reactor biomass was considered to be well-acclimated towards resin acids. The background total resin acid (TRA) concentration in the BKME feed, was $3.86 \pm 0.54 \mu\text{M}$. Prior to the shock load, both reactors were removing about 75 percent of the influent resin acids. No chlorinated resin acids were detected in the BKME

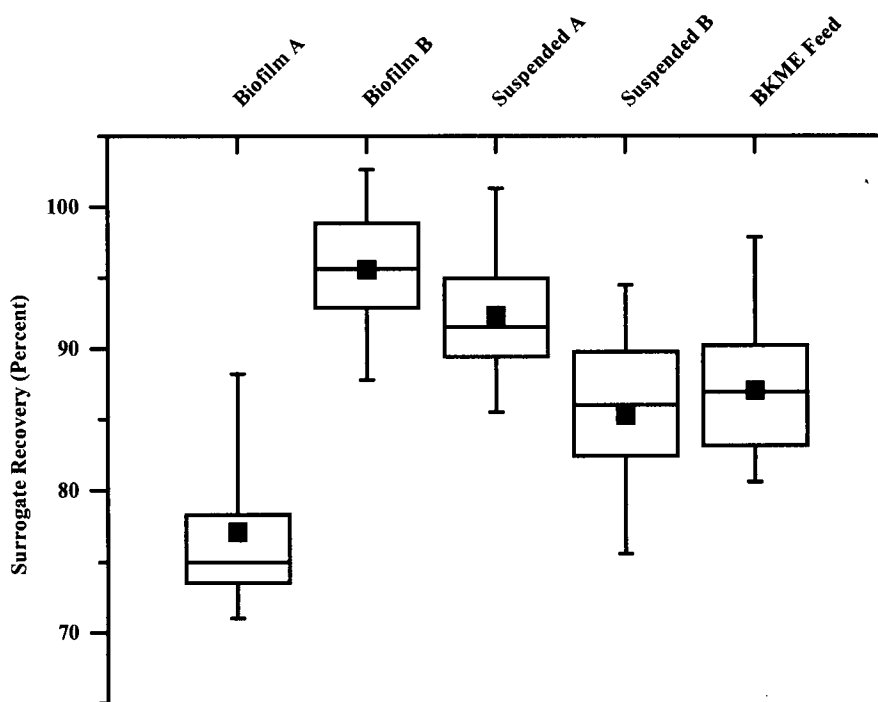


Figure 4-9. Statistics for the surrogate (O-methylpodocarpic acid) extraction recoveries for biofilm and aqueous samples from the two reactors as well as for the aqueous feed samples.

feed. Thus the biosolids in the reactors were acclimated to remove only non-chlorinated forms of resin acids.

Assessment of the fate of the resin acid spike input required that a functional representation be made of the experimental data. The resin acid data were observed to follow the residence time distribution (RTD) model for a tracer in a well stirred tank reactor with mass transfer to a separate stagnant region (Levenspiel 1972). However, in this case, the “stagnant region” was not a secondary volume, but rather, the biofilm surface phase. In keeping with the general form of the equations derived for this type of non-ideal reactor (Levenspiel 1972), the instantaneous concentrations for the liquid and surface phases were empirically described by an equation of form:

$$f_a(t) \text{ or } f_b(t) = \xi_0 + \xi_1 \exp(-v_1 t) + \xi_2 \exp(-v_2 t) + \xi_3 \exp(-v_3 t) \quad (4-28)$$

where $f(t)$ is the instantaneous concentration for the aqueous or biofilm resin acid levels as a function of time (t) and the subscripts “a” and “b” refer to the aqueous and biofilm data respectively. The set of parameters $\{\xi_0, \xi_1, \xi_2, \xi_3, v_1, v_2, v_3\}$ are best fit constants that were determined by nonlinear least squares analysis (Microsoft Excel 97 SR-1, Solver). Note that $f_a(t)$ and $f_b(t)$ are expressed in terms of moles per unit volume and moles per unit biomass, respectively. Biomass was measured as moles total fatty acid (TFA).

No physical significance was assigned to these best fit parameters in equation (4-28) other than their ability to provide a smooth functional representation of the experimental data. Functional representation was necessary for the analytical data interpretation that follows below. By the appropriate choice of an empirical fit to the data, a continuous and differentiable representation of the raw results was obtained. Figures 4-10 through to Figure 4-13 show the resin acid aqueous concentration and biofilm loading data along with the best fit empirical curves modelled by equation (4-28). Total resin acid (TRA) and chloro-dehydroabietic acid (Cl-DHA) concentrations are reported in these graphs. Cl-DHA was used as a control to ascertain whether non-biological removal was significant during the experiment. Since the biomass was not acclimated to Cl-DHA

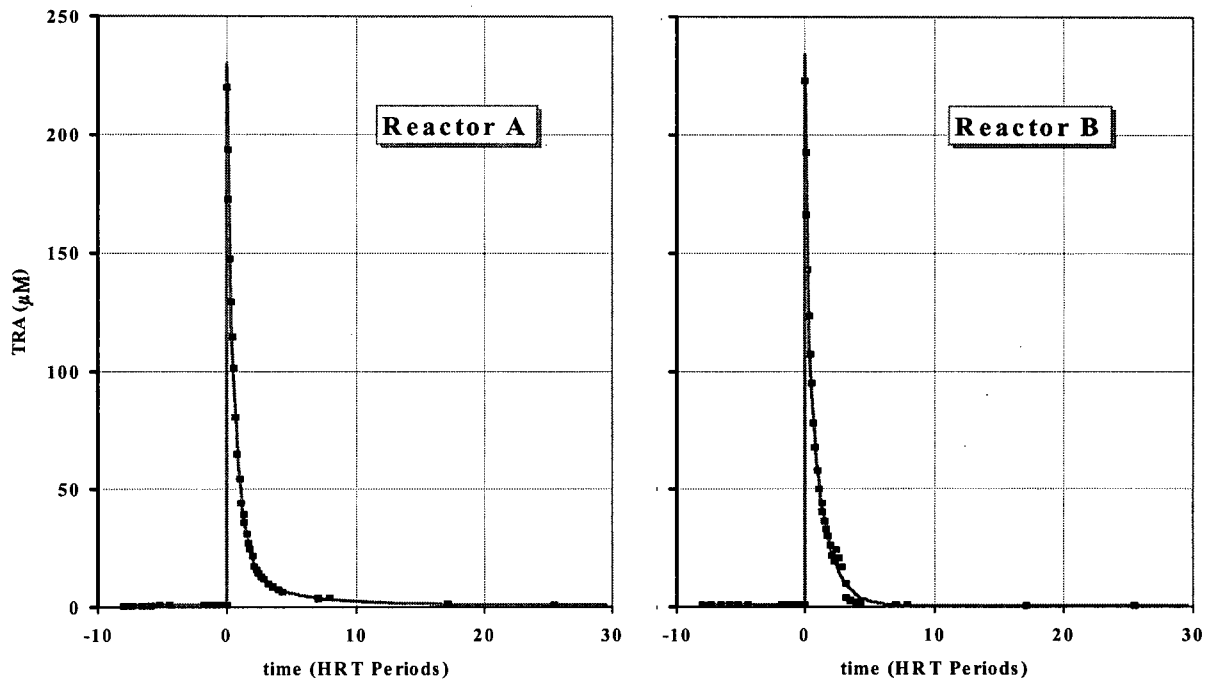


Figure 4-10. Residence time distribution data and the functional fit ($f_a(t)$ in equation (4-28) and Table 4-6) for the aqueous concentration of total resin acids (TRA) in Reactors A and B.

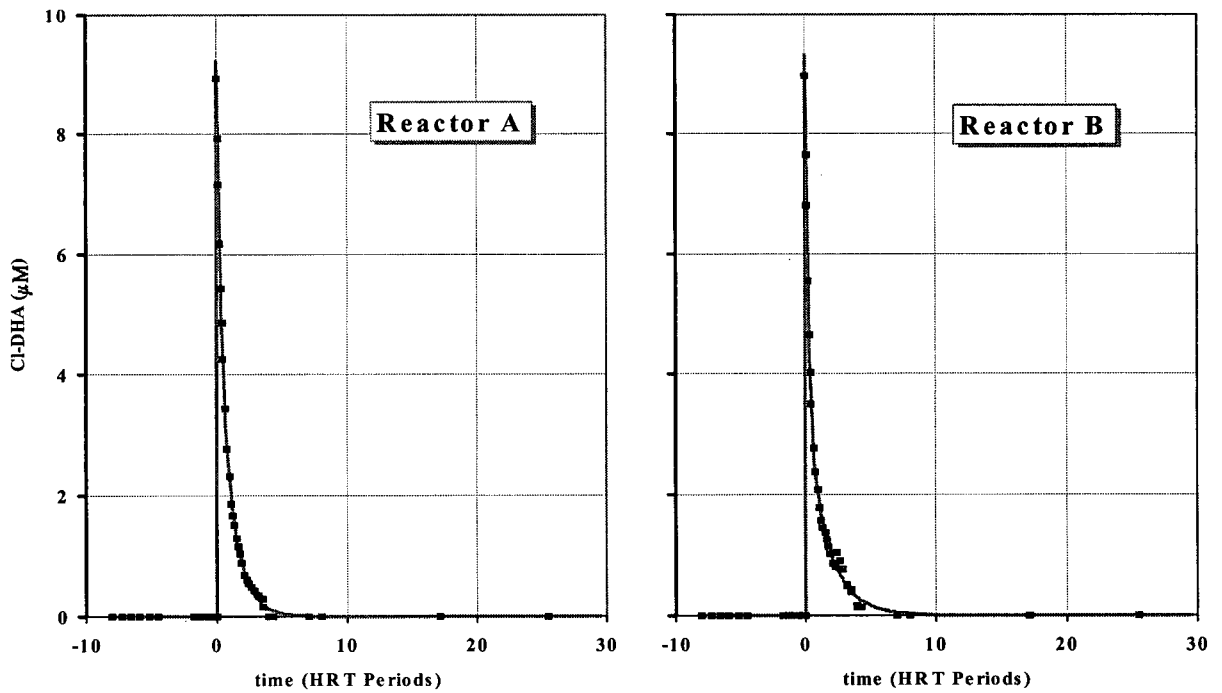


Figure 4-11. Residence time distribution data and the functional fit ($f_a(t)$ in equation (4-28) and Table 4-6) for the aqueous concentration of chloro-dehydroabiatic acid (Cl-DHA) in Reactors A and B.

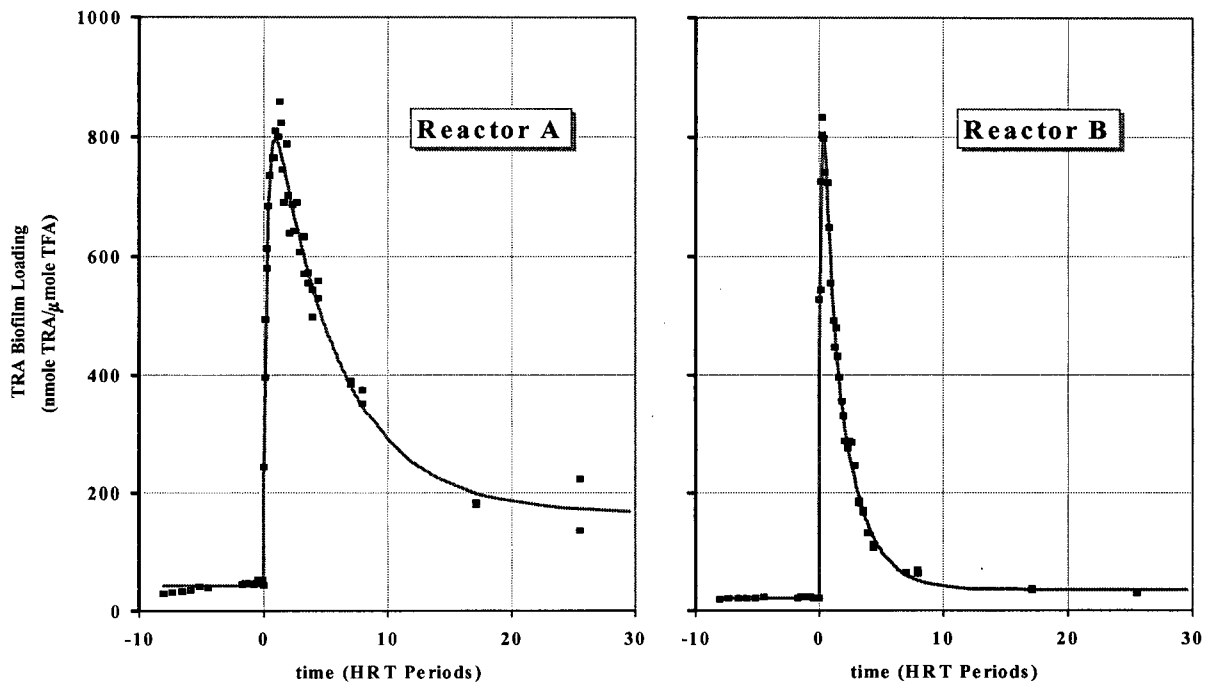


Figure 4-12. Residence time distribution data and the functional fit ($f_b(t)$ in equation (4-28) and Table 4-6) for the biofilm loading of total resin acids (TRA) in Reactors A and B.

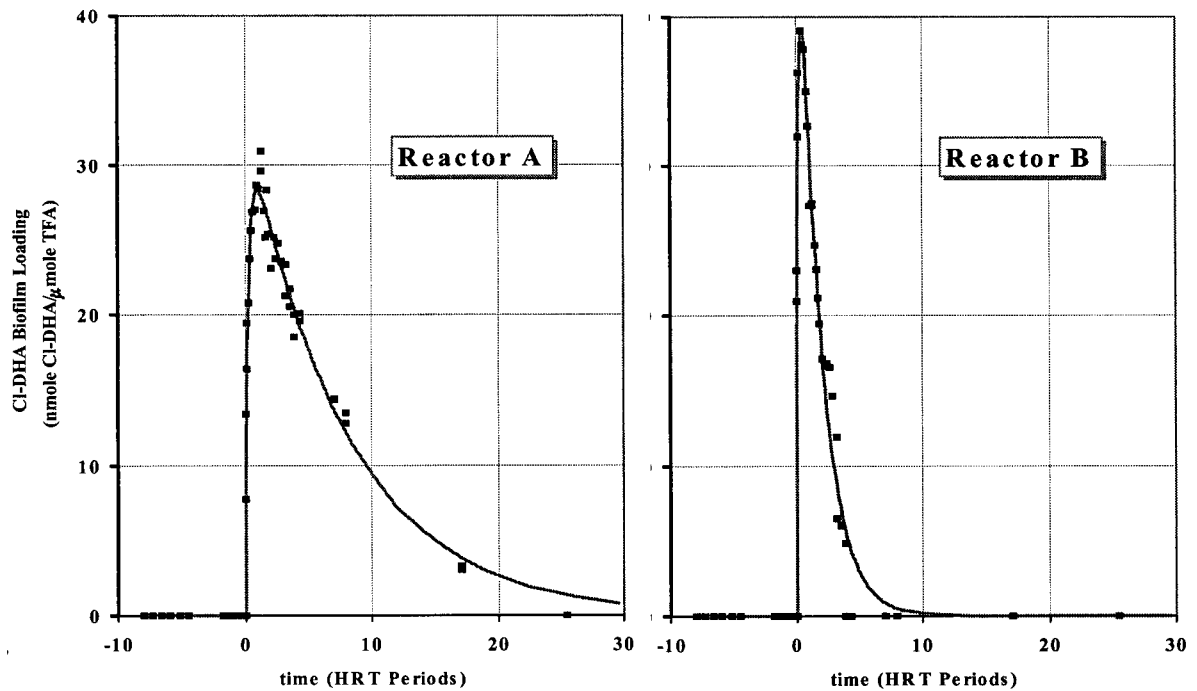


Figure 4-13. Residence time distribution data and the functional fit ($f_b(t)$ in equation (4-28) and Table 4-6) for the biofilm loading of chloro-dehydroabiatic acid (Cl-DHA) in Reactors A and B.

and since chlorinated resin acids are only slowly degraded, any loss of Cl-DHA from the system would have most likely been via mechanisms other than biological oxidation. The best fit parameter values for equation (4-28) are reported in Table 4-6.

The resin acid mass balance was assessed by comparing the estimated cumulative effluent mass to the estimated change in mass in the reactors over fixed time intervals. The mass of resin acids leaving the bioreactor in the effluent ("e") over the time period ($0 \leq t \leq \tau$) was calculated from:

$$\Delta M_{\tau}^e = Q_e \int_0^{\tau} f_a(t) dt \quad (4-29)$$

At any time (τ) greater than or equal to zero, the total mass of resin acids in the system ("s") was estimated from:

$$M_{\tau}^s = V f_a(\tau) + A_T X_b f_b(\tau) \quad (4-30)$$

where V is the reactor liquid volume [L], A_T is the total biofilm surface area [cm^2] and X_b is the average carrier biomass loading [$\mu\text{mole TFA}/\text{cm}^2$]. The actual loss or disappearance of resin acids from the system over the time period ($0 \leq t \leq \tau$) was then estimated from:

$$\Delta M_{\tau}^s = M_0^s - M_{\tau}^s \quad (4-31)$$

Table 4-6. Least squares parameter values for equation (4-28) describing the experimental aqueous, $f_a(t)$, and biofilm, $f_b(t)$, residence time distributions. The functional representations for total resin acid (TRA) and chloro-dehydroabiatic acid (Cl-DHA) concentrations and loadings are listed. Aqueous concentrations are in units of μM and biofilm loadings are in $\text{nmoles RA}/\mu\text{mole TFA}$. TFA represents biomass as total fatty acid. Time (t) is in hours.

	Reactor A				Reactor B			
	TRA		Cl-DHA		TRA		Cl-DHA	
	$f_a(t)$	$f_b(t)$	$f_a(t)$	$f_b(t)$	$f_a(t)$	$f_b(t)$	$f_a(t)$	$f_b(t)$
ξ_0	0.8470			0.0003	0.4399	36.0605		0.0003
ξ_1	14.6343	171.4859	0.8051	39.2186	7.4634	756.7282	5.9825	60.3668
ξ_2	167.5022	789.0445	4.6392	33.4622	120.1323	3407.6230	3.4292	
ξ_3	47.3438	-732.1160	3.8524	-65.3440	106.4708	-3768.2763		-43.2020
v_1	0.07841	0.00039	3.31388	1.20582	0.29457	0.17308	1.39426	0.21213
v_2	0.50685	0.06632	0.31444	0.04468	0.29452	1.11395	0.21482	
v_3	2.45815	1.14558	0.86349	1.15815	1.82542	1.34069		1.47726

If resin acids in the system were not being biodegraded and therefore, only exited the system in the effluent, then a plot of ΔM_t^s versus ΔM_t^e should have been a straight line with a slope equal to one. A slope of less than one would indicate mass recoveries of less than 100 percent, suggesting that biodegradation may have occurred. The mass recoveries for TRA and Cl-DHA were considered using for the data for times (τ) up to 12 hours ($\tau/\theta_H = 4.2$). A 12 hour cut-off was imposed because the most significant portion of the RTD was completed by 12 hours and the tails of the distribution were not as well defined by the remaining low level concentration data. Values for biomass used to evaluate equation (4-30) are reported with the more detailed account of the TFA analysis that follows below. The derived mass recovery data for TRA and Cl-DHA are shown in Figure 4-14 and Figure 4-15, respectively. Overall recovery of TRA was almost identical to the mass recovery of Cl-DHA, indicating that over the duration of the experiment the observed disappearance of TRA was most likely not due to bio-oxidation. The mass recovery at pH 8 (Reactor B) was only about 70 percent while at pH 6 (Reactor A) almost 90 percent of the resin acid mass could be accounted for.

The cause for the incomplete mass balance was believed to be the formation of surface scum. Shortly after the shock load, a distinct residue formed on the surface of the bioreactors. This surface scum on the two reactors was sampled at about 2.7 hours ($\eta = t/\theta_H \approx 1$). The samples were weighed, stored and later extracted for resin acids. These results are shown in Figure 4-16. Corresponding to the differences in mass recovery between the two reactors noted above, the scum on the surface of reactor B contained much higher levels of resin acids. Furthermore, the proportional difference in total resin acids found in the scum was approximately the same as that for chloro-dehydroabietic acid. Scum formation was caused by aeration and bubble fractionation to the surface. An elevated level of resin acids at the surface would tend to exceed the resin acid aqueous solubility limit leading to the formation of an insoluble scum. This would be not unlike the scum and foam commonly experienced on full scale treatment systems. Although resin acid mass closure was not attained in this experiment, the data do suggest that the apparent mass loss was most likely due to the formation of surface scum. Based on the results of Chapter 2, some level of bubble fractionation had been anticipated. Even though coarse bubble aeration was used

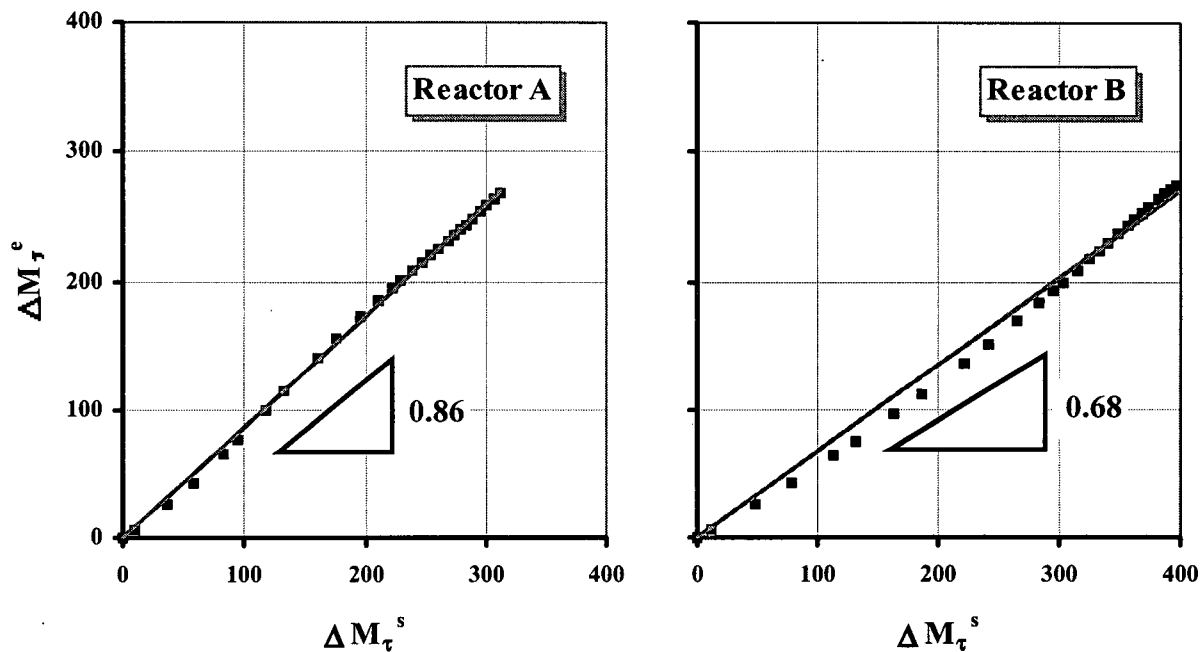


Figure 4-14. Estimated total resin acid recovery from reactors A and B by the comparison of mass loss from the system (ΔM_{τ}^s) to mass loss in the effluent (ΔM_{τ}^e) for sample times (τ) less than and equal to 12 hours. Refer to equation (4-29) through to (4-31). Mass loss (ΔM) is given in units of μmoles . TRA recovery for reactor A and B was 86 and 68 percent, respectively. Overall TRA recovery was similar to chloro-dehydroabiatic acid (Figure 4-15).

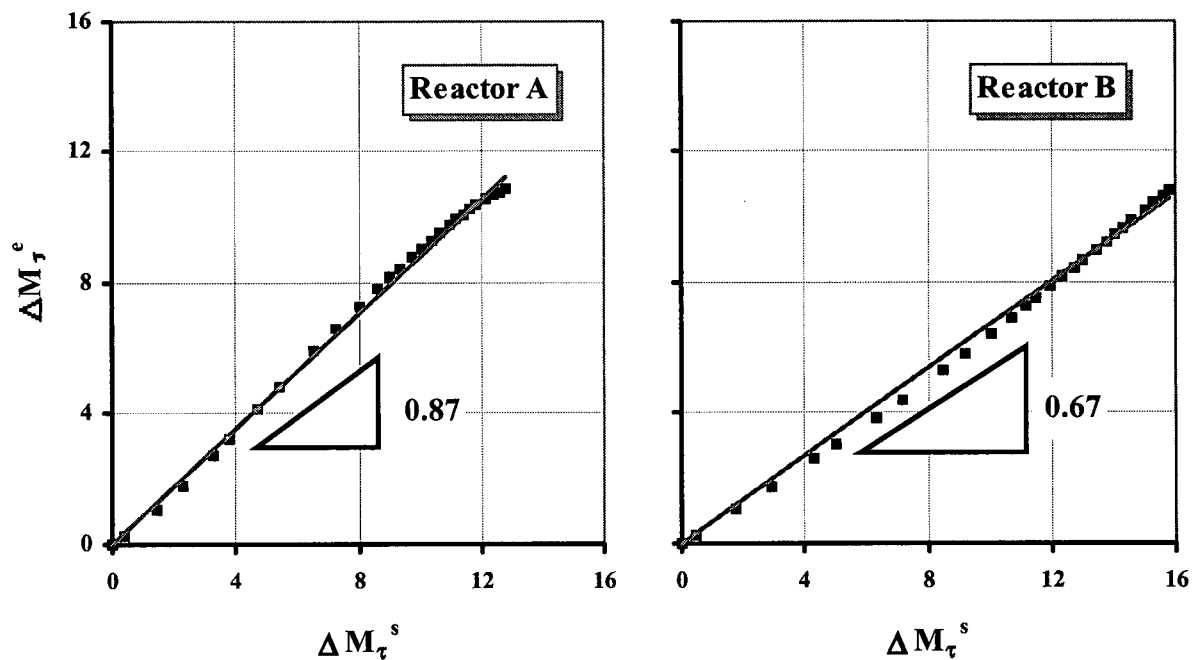


Figure 4-15. Estimated chloro-dehydroabiatic acid recovery from reactors A and B by the comparison of mass loss from the system (ΔM_{τ}^s) to mass loss in the effluent (ΔM_{τ}^e) for sample times (τ) less than and equal to 12 hours. Refer to equation (4-29) through to (4-31). Mass loss (ΔM) is given in units of μmoles . Chloro-dehydroabiatic acid recovery for reactor A and B was 87 and 67 percent, respectively. For the purpose of this experiment chloro-dehydroabiatic acid was considered to be an inert control tracer.

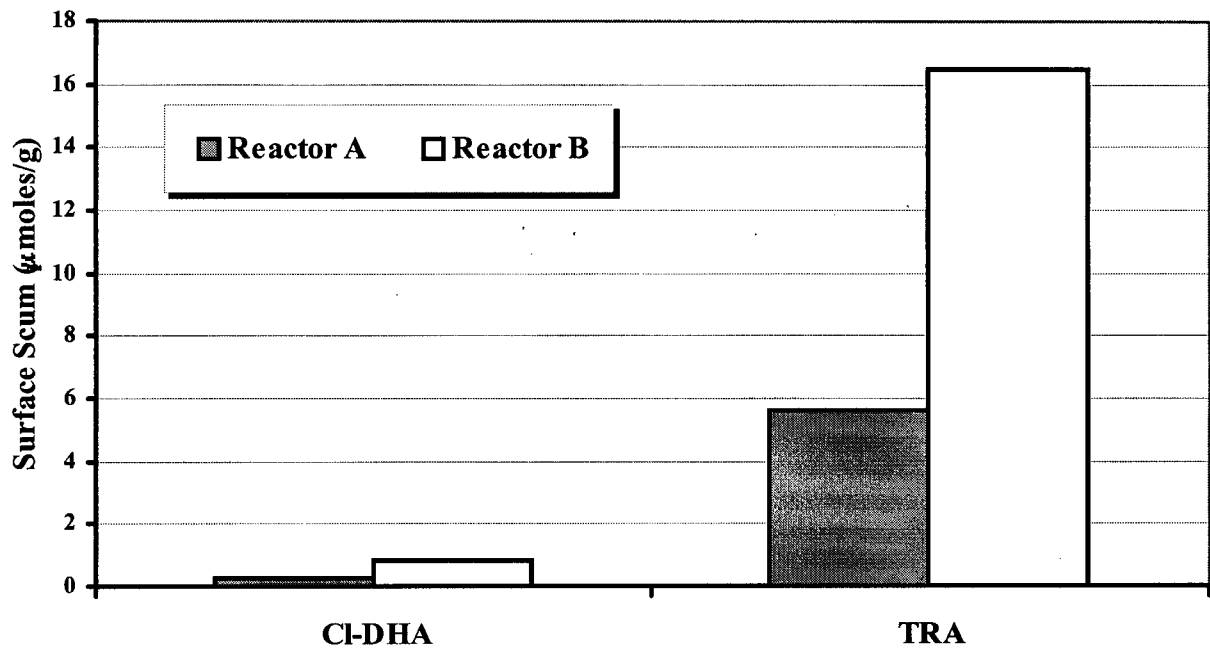


Figure 4-16. Resin acids in the surface scum that accumulated by 2.7 hours ($t/\theta_H \approx 1$) after the spike load. The scum in Reactor B at pH 8.0 had much higher concentrations of total resin acids (TRA) and chloro-dehydroabietic acid (Cl-DHA).

purposefully to minimize the significance of this fate mechanism, apparently bubble fractionation still played an important role in the experiment.

Since the probability of contaminant metabolism during biological treatment depends on its residence time in the bioreactor, it was of interest to calculate the effect of pH on resin acid retention time. The mean aqueous resin acid retention time (θ_{RA}) for the shock load was estimated from equation (4-28) as follows (Levenspiel 1972):

$$\theta_{RA} = \frac{\int_0^{\infty} t(f_a(t) - \xi_0) dt}{\int_0^{\infty} (f_a(t) - \xi_0) dt} \quad (4-32)$$

where $f_a(t)$ refers specifically to the RTD of the aqueous resin acid concentrations. In equation (4-32), the estimated background level (ξ_0) was subtracted to remove the contribution of the resin acid input from the BKME feed. The mean resin acid residence time for the shock load was 5.67 and 3.06 hours for reactors A and B respectively. Mass loss due to bubble fractionation and partitioning of resin acids to the surface scum would act to reduce the mean contaminant aqueous residence time for the bioreactors. However, the effective resin acid retention time was still

longer than the bioreactor HRT, in spite of this mass sink due to scum formation. Even with a 13 and 32 percent resin acid loss in reactors A and B, the mean residence time of the resin acids was extended substantially beyond the 2.84 hour hydraulic retention time, presumably due to sorption interactions with the carrier biofilm. Thus the influence of sorption appears to have been significant, but the exact estimation of this effect was compromised by bubble fractionation and partitioning to the surface scum.

4.3.4 Biomass Characterization

Significant microbial inhibition due to the resin acid shock load was anticipated to be measurable as a change in biomass levels. Biomass was quantified in terms of extractable microbial fatty acids. The average quantities for the twenty-five, positively identified fatty acids that were present to varying degrees in the samples are listed in Table 4-7. The averages summarize the spectra derived from GC chromatograms obtained for up to 53 sample extracts taken for each group (suspended and biofilm samples from reactors A and B) over the 96 hour period of experimental operation. The biofilm surface loadings are based on the total surface area estimated from the dry weight of the sacrificed carriers (Table 4-5).

The use of fatty acids to quantify biomass was complicated by the potential for interference due to the presence of wood-derived fatty acids in the BKME primary effluent. Since dienoic fatty acids are not typically of microbial origin (Harwood and Russell 1984), the extent of interference from wood-derived fatty acids could be estimated with the marker acid, octadecadienoic acid (18:2c9c12). The kraft mill primary effluent contained on average, 1.28 $\mu\text{mole/L}$ of octadecadienoic acid that was not detected in either reactor A or B. The free (background) fatty acids were therefore assumed to be readily degraded or incorporated into active microorganisms (White 1983). A cluster analysis of the matrix of similarities (Chapter 3) between the mean fatty acid compositions further indicated how the BKME feed (influent) fatty acid composition was quite distinct from the reactor compositions (Figure 4-17). Hence, fatty acid extracts from the bioreactors were assumed to be of essentially viable microbial origin.

Table 4-7. Average extracted fatty acid liquid concentrations and surface loadings for suspended and biofilm samples. Samples were obtained over 96 hours of operation. Fatty acids are identified by their shorthand designation (Chapter 3). Equivalent chain length (ECL) values are also reported.

Fatty Acid	ECL	BKME Influent ($\mu\text{mole/L}$) (n=22)	Reactor A		Reactor B	
			Suspended ($\mu\text{mole/L}$) (n=50)	Biofilm (nmole/sq.cm) (n=53)	Suspended ($\mu\text{mole/L}$) (n=53)	Biofilm (nmole/sq.cm) (n=53)
3OH-10:0	11.350		0.831 \pm 0.063	0.877 \pm 0.059	1.097 \pm 0.091	0.842 \pm 0.083
12:0	12.000		0.373 \pm 0.146	0.613 \pm 0.070	0.810 \pm 0.232	0.984 \pm 0.089
i14:0	13.628			0.388 \pm 0.029		0.297 \pm 0.062
14:0	14.000		0.398 \pm 0.024	0.891 \pm 0.067	0.265 \pm 0.032	0.475 \pm 0.034
i15:0	14.632			1.484 \pm 0.114		0.956 \pm 0.073
a15:0	14.709		0.285 \pm 0.056	1.977 \pm 0.214	0.492 \pm 0.107	1.350 \pm 0.147
15:0	15.000			0.497 \pm 0.101	0.225 \pm 0.219	0.455 \pm 0.035
3OH-14:0	15.431			0.683 \pm 0.061		0.584 \pm 0.031
i16:0	15.631			0.590 \pm 0.047		0.527 \pm 0.045
16:1w7c	15.772		7.544 \pm 0.359	2.636 \pm 0.271	8.557 \pm 0.399	3.252 \pm 0.296
16:1w7t	15.827				0.144 \pm 0.135	
16:0	16.000	1.924 \pm 0.274	8.455 \pm 0.316	10.208 \pm 0.962	9.836 \pm 0.422	6.927 \pm 0.571
i17:0	16.632			0.213 \pm 0.065		
a17:0	16.714	1.115 \pm 0.065		0.394 \pm 0.049		0.439 \pm 0.037
cy17:0w7	16.836		0.330 \pm 0.036	3.702 \pm 0.401	0.227 \pm 0.091	1.892 \pm 0.212
17:0	17.000			0.478 \pm 0.075		0.386 \pm 0.030
2OH-16:0	17.182		4.349 \pm 1.110	1.467 \pm 0.335	5.804 \pm 0.881	1.539 \pm 0.398
3OH-16:0	17.406	3.837 \pm 0.943	2.310 \pm 0.304	0.226 \pm 0.152	2.247 \pm 0.260	
18:2(9c,12c)	17.648	1.280 \pm 0.105				
18:1w9c	17.720	1.661 \pm 0.286	0.147 \pm 0.083		0.438 \pm 0.075	
18:1w7c	17.772	0.537 \pm 0.143	3.472 \pm 0.339	7.635 \pm 0.999	4.046 \pm 0.207	7.282 \pm 0.573
18:1w7t	17.827			0.545 \pm 0.110		0.600 \pm 0.064
18:0	18.000	0.307 \pm 0.051	0.252 \pm 0.025	1.906 \pm 0.224	0.293 \pm 0.027	1.007 \pm 0.090
cy19:0w7	18.836			8.897 \pm 0.840		
cy19:0w9	18.846		0.376 \pm 0.070			2.997 \pm 0.277
Total		10.662 \pm 1.042	29.124 \pm 1.308	46.308 \pm 1.778	34.481 \pm 1.175	32.792 \pm 1.042

Total biomass was then estimated (Table 4-8), given the approximate liquid volume (Table 4-2) and the total carrier surface area (Table 4-5). The ratio of biofilm to suspended biomass, on a molar basis, was 3.1:1 and 1.8:1 for reactors A and B respectively. While the effluent TOC levels for reactor B were higher, by accounting for differences in the reactor flow rates (Table 4-4), both reactors were found to be removing about 57 percent of the influent TOC. The effective mean influent TOCs to reactor A and B were 392 and 423 mg C/L. The TOC in the BKME feed degraded slightly over the course of the experiment. The BKME feed had an initial TOC level of about 491 mg C/L and decayed approximately following first order kinetics with a rate constant of about 0.0017 Hr⁻¹. Even with this influent TOC decay, the effluent TOC remained constant. This constancy would indicate that, in spite of operating at a very short hydraulic retention time, both bioreactors were removing 100 percent of the biologically available organic content in the

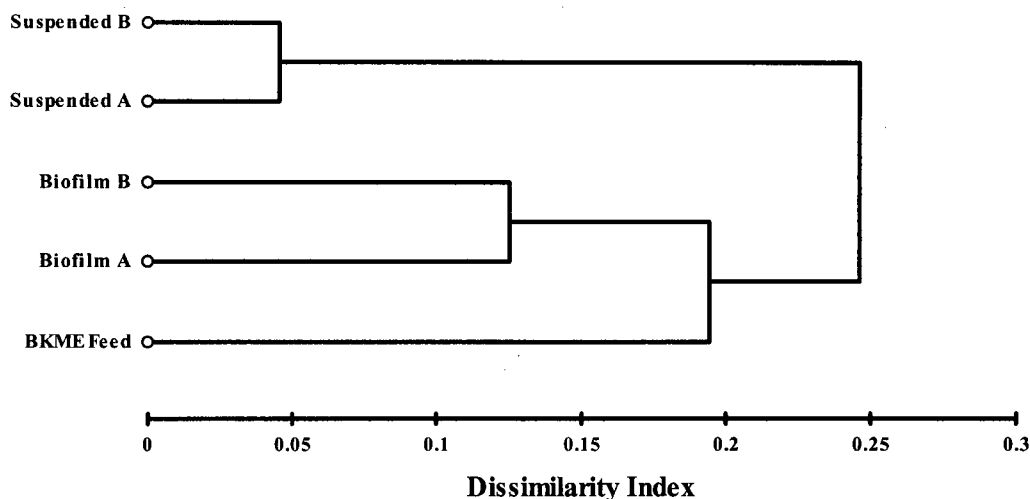


Figure 4-17. Dendrogram from the similarity matrix for the mean whole cell fatty acid (WCFA) compositions for the suspended and biofilm from reactors A and B, as well as the WCFA composition of the BKME feed. The dendrogram was generated (XLSTAT Version 3.4) by Ward's method (Aldenderfer and Blashfield 1984). The WCFA compositions for the suspended samples are relatively similar. Suspended, biofilm and feed compositions appear to cluster distinctly from one and other.

Table 4-8. Estimated total TFA biomass levels (μmoles) for Reactors A and B.

	Reactor A	Reactor B
Total Suspended	46	56
Total Biofilm	145	102
Total Biomass	191	158

feed. However, reactor A maintained 20 % more biomass while its removal efficiency was approximately the same.

Biomass levels before and after the shock load were compared (Figure 4-18). If resin acid inhibition had been significant, suspended biomass levels would have been expected to decrease over the course of the transient. Reactor B suspended biomass levels were not significantly different ($\alpha=0.05$) after the shock load. Reactor A suspended biomass was observed to be increasing prior to the shock load. As a result, reactor A suspended biomass levels were, on average, slightly higher for η greater than zero. However, there was no evidence to support the hypothesis of microbial inhibition due to a resin acid shock load in terms of a change in biomass level. Microbial activity was also monitored by following the removal of acid soluble total organic carbon (TOC). Considering the before and after shock load data as two separate sample

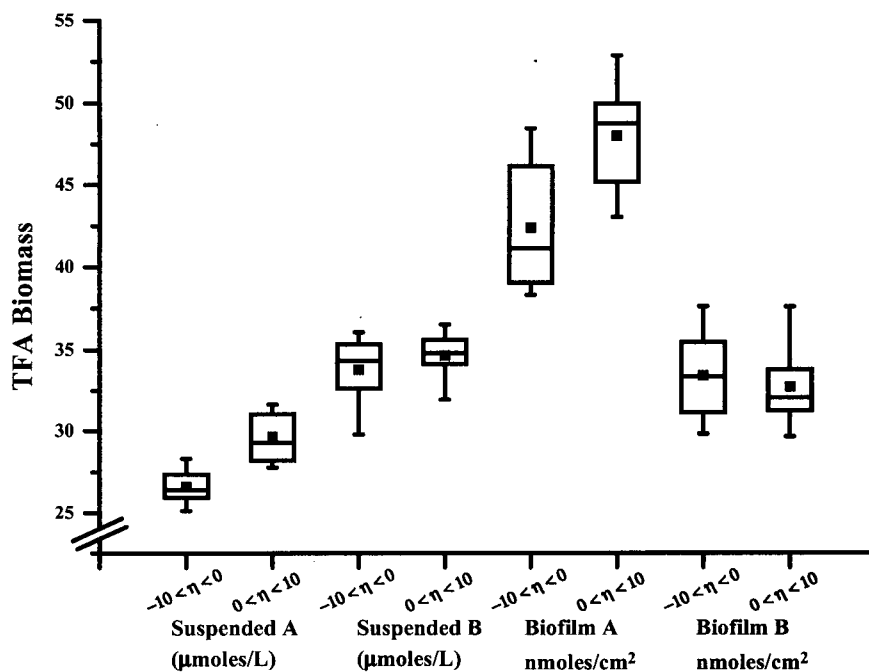


Figure 4-18. Average bioreactor biomass levels before ($-10 < \eta = t/\theta_H < 0$) and after ($0 < \eta < 10$) a resin acid shock load. Biomass is expressed as total fatty acid (TFA) concentration (Suspended) and TFA surface loading (Biofilm) for reactors A and B. No significant difference ($\alpha=0.05$) was found between the before and after biomass levels in reactor B. The “after” biomass levels in reactor A were slightly higher but the change appeared to be due to background fluctuations not associated with the shock load. For reactor A, a trend of increasing biomass preceded the shock load. Inhibition due to resin acids would be expected to cause a decrease in the “after” biomass average level.

populations, no significant differences ($\alpha = 0.05$) between the respective means for reactor A and B were found. Therefore, there was no evidence of toxic inhibition from a consideration of either biomass quantity or overall microbial activity.

4.3.5 Assessment of Microbial Community Structure and Population Dynamics

The ecology of the biofilm and suspended growth microbial communities sampled from the two reactors were compared, based on their average fatty acid compositions, by logcontrast canonical component analysis (Chapter 3). Figure 4-19 summarizes the variability between the groups in terms of the first three logcontrast canonical components, which accounted for all of the data variance. The first component (LCC-1) clearly distinguishes between the biofilm and suspended communities. The second and third components appear to reflect the influence of pH on the biofilm and on the suspended growth respectively. Logcontrast canonical component analysis indicated that pH exerted a slightly more pronounced effect on the biofilm than the

suspended growth communities.

Evidence of a microbial response to the resin acid shock load was expected to be apparent from the fatty acid compositions for each individual group of samples. The first approach used to test for evidence of a deterministic trend in each sample population was the test for logistic normality (Chapter 3). Considering the radius distribution of the logratio transformed compositional data, an absence of trends in the TFA compositions for each sample group should have resulted in a distribution of the radial distances that approximately followed a χ^2 -distribution (Aitchison 1986). For example, Figure 4-20 shows the sorted probabilities for the calculated radii against the order statistic of the Reactor B suspended and biofilm data. Logistic normal data should closely follow the unit square diagonal. The Anderson-Darling statistic (Q_A), used to quantitatively test the hypothesis of logistic normality, was calculated for each of the sample populations (Table 4-9) as follows (Aitchison 1986):

$$Q_A = -\frac{1}{n} \sum_{k=1}^n (2k-1) \{ \log p_k + \log(1-p_{n+1-k}) \} - n \quad (4-33)$$

where n is the number of observations and p_k is the k^{th} ordered probability (Chapter 3). Critical values for the Anderson-Darling test statistic are given in Table 4-10. Higher values of the test statistic indicate a greater departure from logistic normality. Rejection of the hypothesis of logistic normality for compositional data, implies the presence of a coherent trend for the sequence of samples.

Since the fatty acids present as background in the BKME feed would have been of wood origin, these compositions should have remained relatively constant during the experiment. Indeed, the fatty acid compositions from the feed fitted best to the hypothesis of logistic normality, since they exhibited the lowest Q_A value. The hypothesis of logistic normality for the microbial communities was marginally retained for the reactor sample groups. The hypothesis could not be rejected at the 2.5 percent significance level for any of the sample populations and at the 5 percent level for all except the suspended growth in Reactor A. Had there been a pronounced microbial response

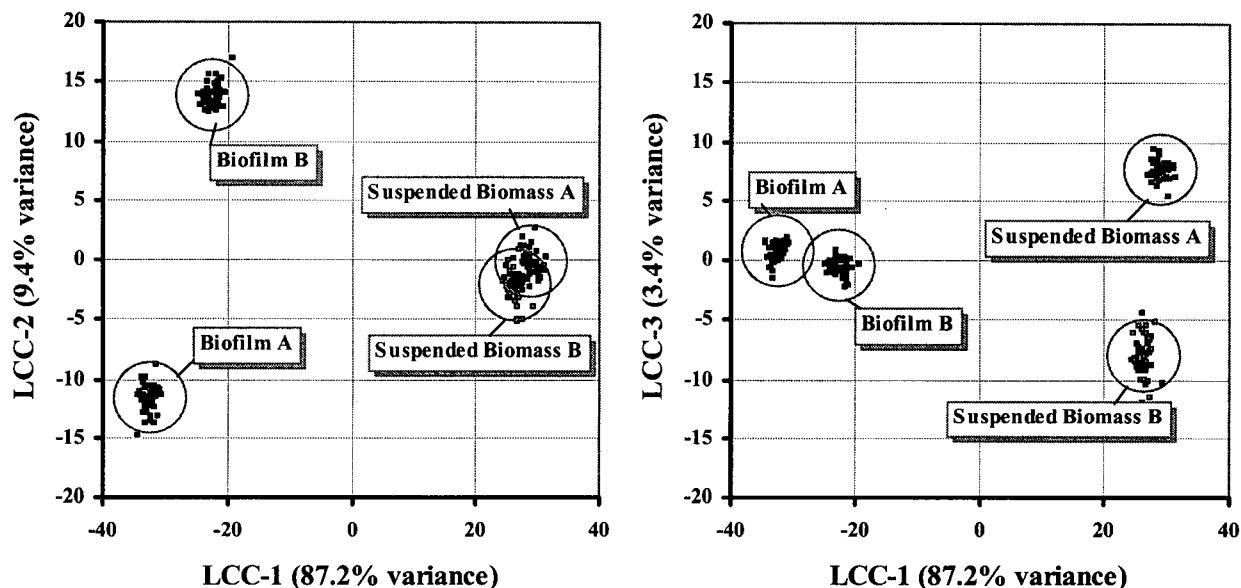


Figure 4-19. Logcontrast canonical components (LCC) of the fatty acid spectra for suspended and biofilm extracts. Individual observations are shown (■) along with the mean values given by the centre of the circle around the respective data clusters. The canonical components were calculated using logratios with hexadecanoic acid (16:0) as the common divisor. The first component (LCC-1) distinguishes biofilm from suspended communities while the second and third components separate the influence of pH on the biofilm and suspended microbial ecology respectively.

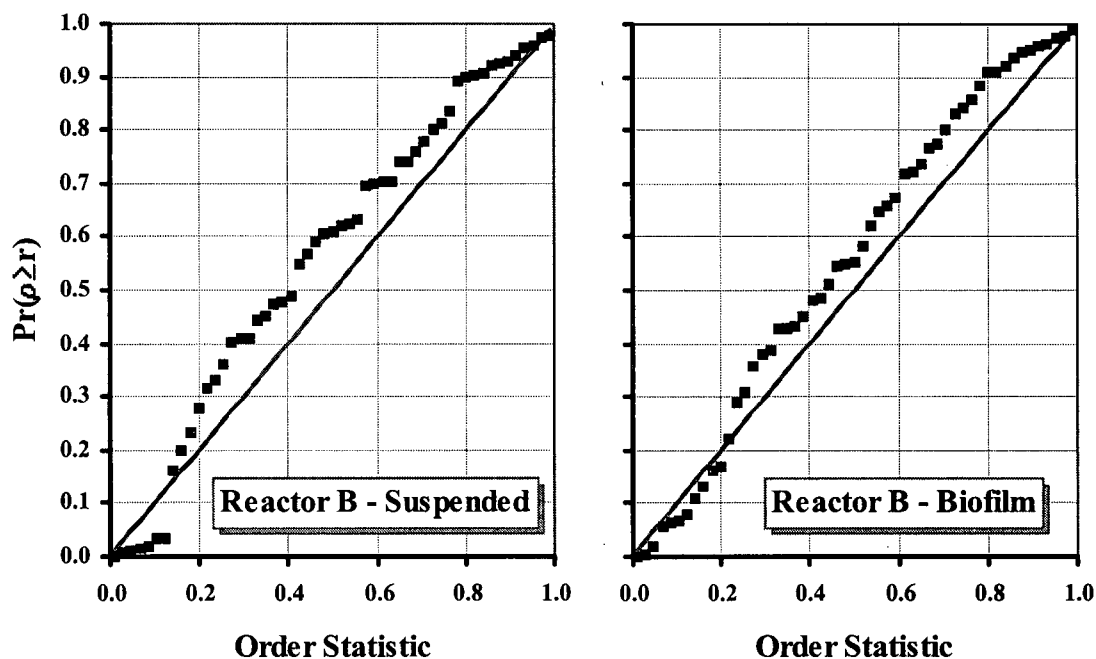


Figure 4-20. The calculated and sorted probabilities for the logratio radius distributions (Chapter 3; equation (4-25)) for fatty acid compositions from Reactor B plotted against the uniform order statistic. Qualitatively, conformity with logistic normality corresponds to the degree to which the data pattern follows the diagonal of the square (Aitchison 1986).

Table 4-9. Calculated values for the Anderson-Darling test statistic for the total fatty acid compositional data sampled over 96 hours.

Sample Population	Anderson-Darling Test Statistic
BKME Feed	1.30
Reactor A – Suspended	2.67
Reactor A – Biofilm	2.05
Reactor B – Suspended	2.36
Reactor B – Biofilm	1.84

Table 4-10. Critical values for the Anderson-Darling test statistic for assessing logistic normality from the d-dimensional radius distribution (adapted from Aitchison (1986)).

Significance Level (α)	Critical Value
0.10	1.933
0.05	2.492
0.025	3.070
0.01	3.857

to the shock load, a more significant departure from logistic normality might have been expected. For instance, membrane toxicity due to resin acid hydrophobicity might have been expected to induce a significant change in the balance of monoenoic fatty acids in the community (Chapter 3). However, by the test of logistic normality there was no strong evidence in the data of a community response to the shock load of resin acids. The “marginality” for the normality of the data describing the reactor microbial communities could be thought of as a reflection of the inherent natural cycles of population dynamics within the communities. However, there was some doubt as to the sensitivity of this test and, as a consequence, the possibility of trends in the data was considered more explicitly.

The five groups of data (Table 4-9) were assessed for the possibility of underlying trends by logcontrast principal component analysis (LPCA). Since principal component analysis is unable to distinguish between different sources of variability, the method was found to be quite sensitive to spurious data values. This sensitivity was most apparent for a set of observations of compositions that contained concentration values that crossed in and out of the limits of detection.

To remedy this problem found with LPCA, logcontrast canonical component analysis (LCCA)

was performed by breaking each sample group into sequential sub-groups of observations. The advantage of this approach appeared to be that much of the experimental variability was filtered out due to the fact that this method discriminates between groups by comparing both the within- and the between-group variability. Hence, the sources of spurious, within-group variability should not have figured largely in the overall between-group discrimination. This approach is analogous to a moving average calculation applied to a data series. The moving average tends to reduce signal noise, although with some loss in signal. For the LCC analysis, observations within a sample population were combined into sub-groups of five. This sub-population size of five was chosen as a compromise between the need to have a large enough sub-group to provide an assessment of measurement variability and of having enough sub-groups to still follow any compositional trends over time.

For any given observation, the fatty acid composition was considered to be a representation of the microbial community. Changes in the composition were assumed to reflect changes in the community structure. Therefore, this assessment of between-group variability by logcontrast canonical component analysis provided an indication of fatty acid compositional trends which were felt, based on previous results (Chapter 3), to correlate with population dynamics. The analytical problem was reduced to how best quantify and compare these population dynamics.

To evaluate the population dynamics, a function of sample population state (Ξ) was considered to be defined by the d-dimensional random vector of the logratio transformed D-dimensional compositional data as follows:

$$\Xi = \Xi(y_1, \dots, y_d), \quad y_i = \ln(x_i/x_D), \quad d = D - 1 \quad (4-34)$$

where x_i is the i^{th} fatty acid in the composition and x_D is the fatty acid composition chosen as the common denominator. For all the calculations reported, hexadecanoic acid (16:0) was kept as the common x_D divisor. The state vector Ξ is implicitly a function of time (t) since all the logratio components are time dependent:

$$y_i = y_i(t) \quad (4-35)$$

The primary objective of logcontrast canonical component analysis (LCCA) is to assess the between-group variability with dimensional reduction. By LCCA, the logratios (y_i) were transformed to their weighted logcontrast canonical components (Ψ) by the scalar vector product as follows:

$$\Psi_k = \sqrt{\lambda_k} b_k \cdot (y - \bar{y}), \quad y = (y_1, \dots, y_d) \quad (4-36)$$

where λ_k is the k^{th} latent root, b_k is the corresponding k^{th} eigenvector $\{b_1, \dots, b_d\}_k$, and \bar{y} is the overall mean logratio vector defined in Chapter 3. The variance in the data is preserved by this transformation. Note that since the latent roots decrease in value (Chapter 3):

$$\lim_{k \rightarrow d} \lambda_k = 0 \quad (4-37)$$

the sample population state variable (Ξ) could be described by just a few of the weighted canonical components (Ψ_k) while still embracing the same dependence with time:

$$\begin{aligned} \Xi &= \Xi(\Psi_1, \dots, \Psi_p), \quad p \ll d \\ \Psi_k &= \Psi_k(t) \end{aligned} \quad (4-38)$$

The state vector can be written as follows:

$$\Xi = \Psi_1 \hat{e}_1 + \Psi_2 \hat{e}_2 + \dots + \Psi_p \hat{e}_p \quad (4-39)$$

where \hat{e}_i are the unit vectors of the orthogonal canonical components. Thus the change in the sample population state with time is simply given by:

$$\Theta = \frac{\partial \Xi}{\partial t} = \frac{\partial \Psi_1}{\partial t} \hat{e}_1 + \frac{\partial \Psi_2}{\partial t} \hat{e}_2 + \dots + \frac{\partial \Psi_p}{\partial t} \hat{e}_p \quad (4-40)$$

where Θ was considered as the sample population velocity vector. The measure taken to quantify the population dynamics in the reactor was the scalar rate of sample population change or a so-called "state speed":

$$|\Theta| = \sqrt{\frac{\partial \Xi}{\partial t} \cdot \frac{\partial \Xi}{\partial t}} \quad (4-41)$$

The natural time unit for a completely mixed chemostat is the hydraulic retention time (HRT or θ_H). Hence, the state speed multiplied by HRT yields a non-dimensional measure that was used to assess the population dynamics:

$$v_c = |\Theta| \cdot \theta_H = \sqrt{\frac{\partial \Xi}{\partial \eta} \cdot \frac{\partial \Xi}{\partial \eta}}, \quad \eta = \frac{t}{\theta_H} \quad (4-42)$$

A stable community would have a state speed (v_c) of zero. Any environmental perturbation to the community that affected the average species composition of the community should have been seen to induce a corresponding response in terms of a measurable population dynamic or elevated state speed above the natural background level.

To illustrate this idea of state speed, Figure 4-21 shows the trajectory of the suspended community in terms of the first three weighted canonical components for Reactor A during the course of the experiment. These first three components represented 90 percent of the variability contained in the original 11-dimensional logratio dataset. Hence the high-dimensional multivariate problem could be approximated by this more amenable, three-dimensional representation. The plotted points are the calculated sub-group mean positions and serve to illustrate how the community shifted during the course of the experiment. Although the biomass level did not change significantly, the biomass was measurably dynamic in the sense of community fluctuation. The expression of state speed in equation (4-42) would describe the rate at which the sample population moved along the path of the trajectory in Figure 4-21.

The question being considered was the extent of apparent correlation between state speed and the event of the spike load of resin acids. In the consideration of this question, the fatty acid composition of the BKME feed served as an experimental control since the fatty acids in the feed were deemed to be predominantly of wood origin and the feed itself was also not subject to any sudden changes.

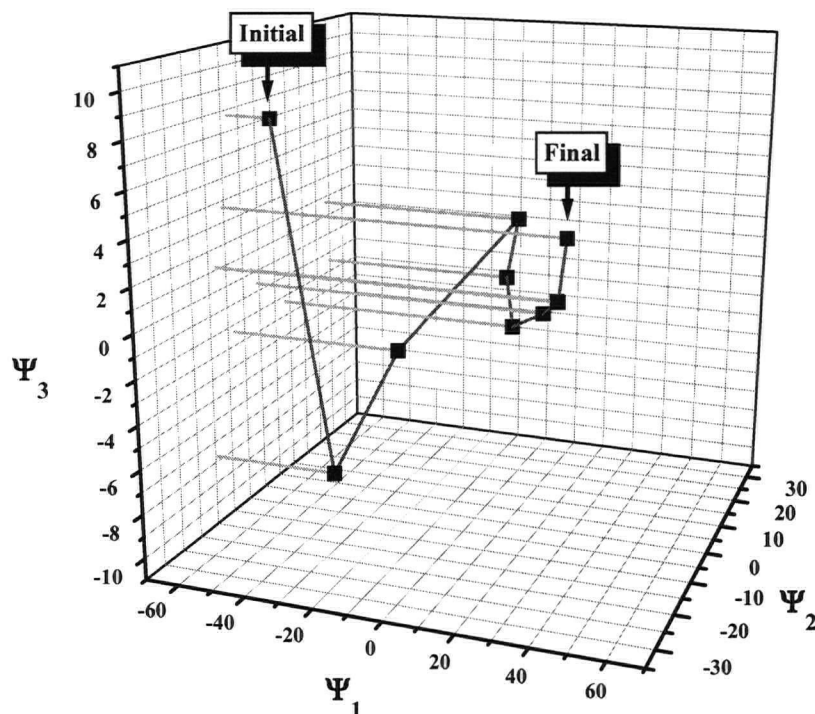


Figure 4-21. The trajectory describing the population dynamics of the suspended biomass in reactor A. The time series of data for this sample population was broken up into sequential sub-groups of five observations. The first three weighted logcontrast canonical components $\{\Psi_1, \Psi_2, \Psi_3\}$, defined in equation (4-36), accounted for 90 percent of the between group variability. Note how the scale decreases in order of the components. The plotted points represent mean values for each of the sub-groups in the sequence. Initial and final conditions are noted. The trajectory was made over the course of the 96 hour period of the experiment.

Table 4-11. Results of logcontrast canonical component analysis on the time series of suspended biomass samples taken from Reactor A. Sequential sub-groups of at least 5 observations were used.

Eigen Values				
Latent Root	λ_1	λ_2	λ_3	$\Sigma\lambda_i$
Eigen Value	28.07	13.73	3.89	45.69
Percent	55.04	26.92	7.62	89.58
Eigen Vectors				
Fatty Acid	ECL	b_1	b_2	b_3
3OH-10:0	11.350	13.76	-9.38	-9.30
12:0	12.000	-0.19	1.02	-0.55
14:0	14.000	-3.10	-17.32	-7.80
a15:0	14.709	-3.96	0.59	1.17
16:1w7c	15.772	-11.31	43.36	91.51
cy17:0w7	16.836	-9.23	1.47	2.79
2OH-16:0	17.182	-4.35	12.81	-5.54
3OH-16:0	17.406	-4.04	6.18	-4.45
18:1w7c	17.772	46.23	-34.04	-4.53
18:0	18.000	-4.78	2.27	-2.41
cy19:0w9	18.846	7.67	9.80	6.92

Table 4-12. Results of logcontrast canonical component analysis on the time series of suspended biomass samples taken from Reactor B. Sequential sub-groups of at least 5 observations were used.

Eigen Values				
Latent Root	λ_1	λ_2	λ_3	$\Sigma\lambda_i$
Eigen Value	37.42	11.31	4.23	52.95
Percent	67.14	20.28	7.58	95.00
Eigen Vectors				
Fatty Acid	ECL	b_1	b_2	b_3
3OH-10:0	11.350	-10.80	-22.04	-1.66
12:0	12.000	-0.86	0.42	1.08
14:0	14.000	1.49	-5.55	-2.71
a15:0	14.709	16.28	-6.18	-6.18
15:0	15.000	0.33	-0.09	0.05
16:1w7c	15.772	9.79	-7.76	5.33
16:1w7t	15.827	0.19	0.36	0.04
cy17:0w7	16.836	-0.26	0.03	-0.01
2OH-16:0	17.182	-9.69	6.59	-19.04
3OH-16:0	17.406	2.65	-6.77	-4.24
18:1w9c	17.720	-0.79	10.96	-3.51
18:1w7c	17.772	-9.34	32.34	36.84
18:0	18.000	0.95	-10.74	4.14

Table 4-13. Results of logcontrast canonical component analysis on the time series of biofilm biomass samples taken from Reactor A. Sequential sub-groups of at least 5 observations were used.

Eigen Values				
Latent Root	λ_1	λ_2	λ_3	$\Sigma\lambda_i$
Eigen Value	19.08	7.59	3.43	30.10
Percent	56.25	22.38	10.12	88.75
Eigen Vectors				
Fatty Acid	ECL	b_1	b_2	b_3
3OH-10:0	11.350	-16.01	-2.89	-3.36
12:0	12.000	3.80	1.23	-0.35
i14:0	13.628	4.68	11.21	36.81
14:0	14.000	27.03	-39.61	8.90
i15:0	14.632	1.21	15.60	53.39
a15:0	14.709	-11.43	-31.65	1.04
15:0	15.000	-41.90	20.41	-51.94
3OH-14:0	15.431	26.92	-10.49	-7.10
i16:0	15.631	12.88	-7.16	-5.47
16:1w7c	15.772	-18.55	26.33	0.42
i17:0	16.632	-0.05	-0.14	0.02
a17:0	16.714	-3.01	12.43	-4.75
cy17:0w7	16.836	-27.47	-3.89	-15.32
17:0	17.000	3.22	-9.69	8.10
2OH-16:0	17.182	-1.69	-0.01	-4.95
3OH-16:0	17.406	0.22	0.18	-0.23
18:1w7c	17.772	40.29	19.37	30.90
18:1w7t	17.827	-3.83	0.99	-3.67
18:0	18.000	-12.33	-4.08	13.49
cy19:0w7	18.836	9.78	-20.66	-23.29

Table 4-14. Results of logcontrast canonical component analysis on the time series of biofilm biomass samples taken from Reactor B. Sequential sub-groups of at least 5 observations were used.

Eigen Values				
Latent Root	λ_1	λ_2	λ_3	$\Sigma\lambda_i$
Eigen Value	37.91	8.40	3.32	49.63
Percent	71.44	15.83	6.25	93.52
Eigen Vectors				
Fatty Acid	ECL	b_1	b_2	b_3
3OH-10:0	11.350	20.15	10.12	1.42
12:0	12.000	-17.80	-4.68	-9.04
i14:0	13.628	-0.19	0.16	0.54
14:0	14.000	-20.97	53.88	15.61
i15:0	14.632	-15.83	-105.01	25.59
a15:0	14.709	-0.45	33.95	-5.30
15:0	15.000	-10.68	-32.93	-31.92
3OH-14:0	15.431	-20.68	-4.73	-4.18
i16:0	15.631	5.04	8.04	23.68
16:1w7c	15.772	45.16	-28.52	39.39
a17:0	16.714	3.96	4.05	-8.37
cy17:0w7	16.836	48.44	48.74	-24.08
17:0	17.000	35.94	13.70	-17.25
2OH-16:0	17.182	0.14	0.10	-2.63
18:1w7c	17.772	-1.91	6.25	-18.37
18:1w7t	17.827	4.15	-0.32	-5.82
18:0	18.000	-9.58	-2.75	31.65
cy19:0w9	18.846	-16.50	-9.65	17.58

Table 4-15. Results of logcontrast canonical component analysis on the time series of fatty acid compositions taken from the BKME feed. Sequential sub-groups of at least 5 observations were used.

Eigen Values				
Latent Root	λ_1	λ_2	λ_3	$\Sigma\lambda_i$
Eigen Value	6.41	1.57	0.47	8.45
Percent	75.87	18.62	5.51	100.00
Eigen Vectors				
Fatty Acid	ECL	b_1	b_2	b_3
a17:0	16.714	3.18	20.54	-15.37
3OH-16:0	17.406	2.89	-4.80	-1.81
18:2(9c,12c)	17.648	-27.70	1.94	14.82
18:1w9c	17.720	28.41	-1.57	3.03
18:1w7c	17.772	-3.21	-2.02	-0.49
18:0	18.000	-2.69	-2.85	-1.64

The results of the logcontrast canonical component analysis are reported in Table 4-11 through to Table 4-15. Only the first three components were used, as these retained about 90 percent of the community variance. As seen in Figure 4-21, by noting the relative axis scales, each successive weighted canonical component accounted, in ever decreasing extent, for the variability associated with the sample population changes.

The relative degrees for trends of community change could be appraised by the differences in the

magnitude of the sum of the first three latent roots ($\Sigma\lambda_i \approx \lambda_1 + \lambda_2 + \lambda_3$). A greater degree of “sub-group discrimination” or “between sub-group variability” is indicated by a corresponding larger value for $\Sigma\lambda_i$. It can be seen from Table 4-11 through to Table 4-15, that the suspended biomass communities exhibited the most variance, and BKME feed fatty acid composition exhibited the least variance. This observation agrees qualitatively with the results from the tests for logistic normality. A greater departure from logistic normality, as shown by a larger Anderson-Darling test statistic, indicated a greater extent of deterministic trend over time. Similarly, a larger variance ($\Sigma\lambda_i$) measured by LCCA revealed a greater level of between sub-group discrimination that suggested a more pronounced level of community change over time.

Evaluation of equation (4-42) required the estimation of the first derivative with respect to time for the weighted logcontrast components. Derivatives of the experimental data were determined by Savitzky-Golay smoothing and differentiation least squares procedures (Savitzky and Golay 1964). This approach was modified to accommodate irregularly sampled data over time. By this method of analysis, the raw data are represented by a sliding polynomial window to reduce the influence of experimental noise. Derivatives of the sliding polynomial estimate the rates of change. For example, Figure 4-22 shows the raw data, the result of Savitzky-Golay smoothing, and the estimated first derivative for the Ψ_1 -component for the reactor B suspended biomass dataset.

An initial impression of the relative differences in population dynamics was considered by calculating the average state speed over time (Figure 4-23). The average state speeds for the microbial communities within the bioreactors were significantly greater than the value calculated for the BKME feed. Since the fatty acid composition of the BKME feed was considered to be of non-microbial origin, the dynamic response of the biomass in the bioreactors were well above this background reference level. From Figure 4-23 it can be seen that the suspended community in reactor B exhibited the greatest level of community change during the experiment.

A rapid change in the fatty acid spectra, that corresponded to the timing of the spike load of resin acids, was assumed to infer a community response to the stimulus. Some loss in the temporal

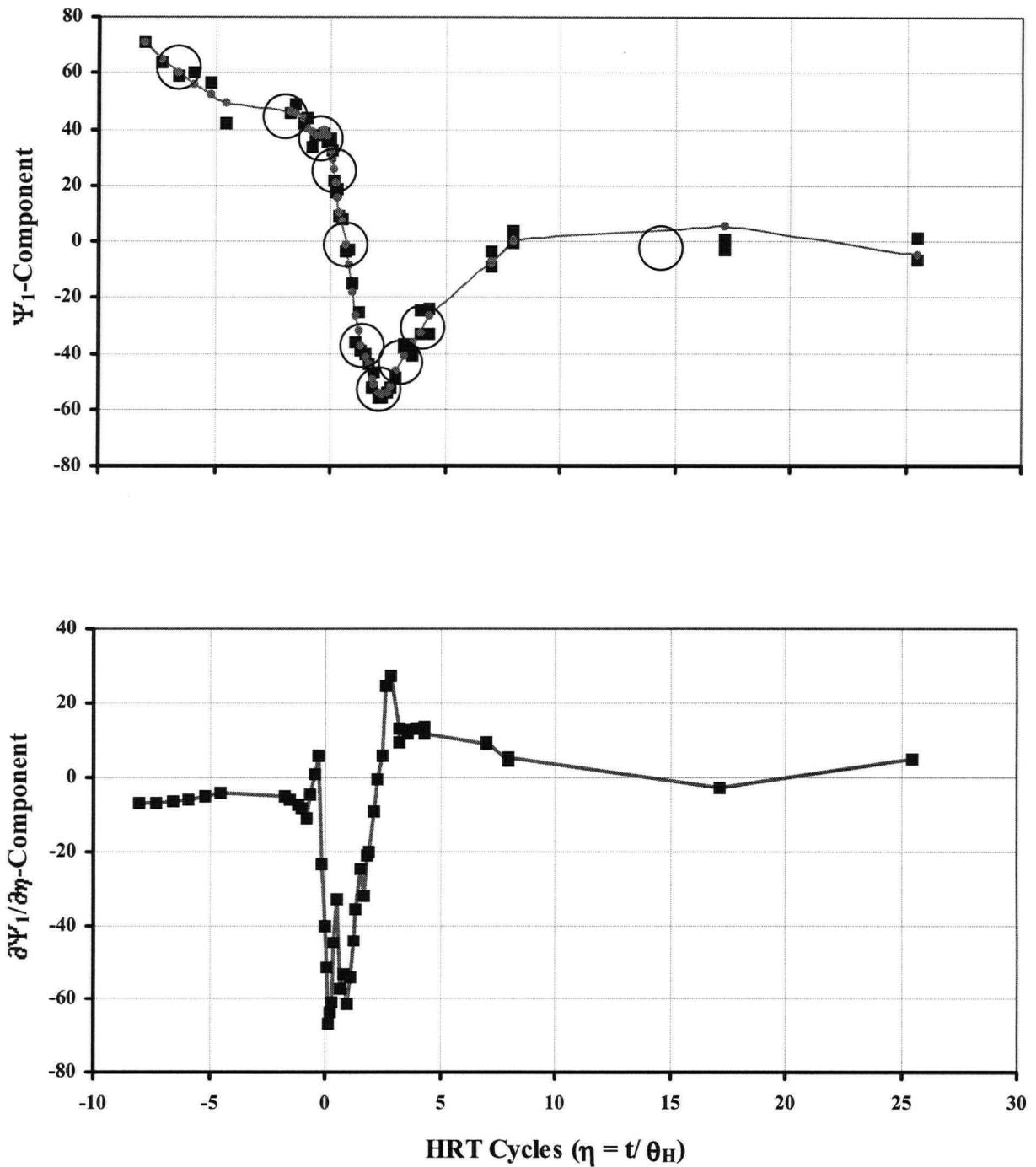


Figure 4-22. Data smoothing and differentiation of the first weighted canonical component from logcontrast canonical component analysis (LCCA) of the suspended biomass samples from reactor B. The Ψ_1 -component (Top) was determined according to equation (4-36). Sub-group mean values are also indicated (o). The line graph plotted on top the experimental data (Top) was generated by Savitzky-Golay type data smoothing (Savitzky and Golay 1964). In this case a 9-point 3rd-order sliding polynomial was used. The first derivative of this sliding least-squares best fit polynomial provided an estimate of the rate change of the Ψ_1 -component (Bottom). Numerical calculations were performed with software written in Microsoft Excel 97-SR1 Visual Basic.

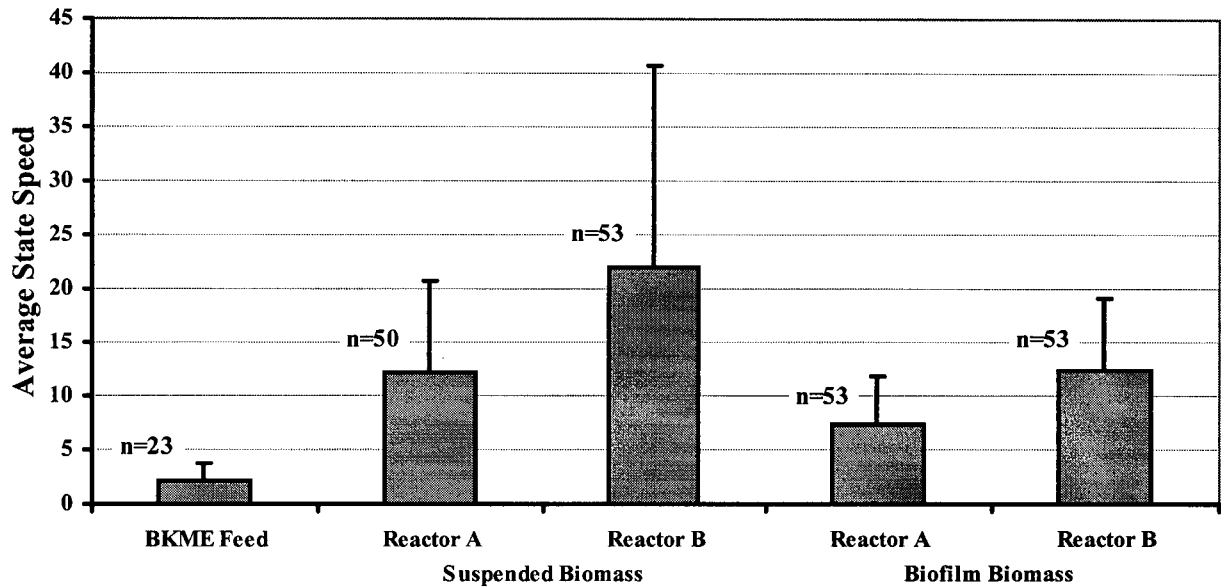


Figure 4-23. A comparison of the average state speed (equation (4-42)) estimated from the indicated number of observations (n) over the 96 hour period of observation. State speed was adopted as a measure of microbial population dynamics based on fatty acid compositional analysis. The BKME feed, whose fatty acid composition was of wood origin and, therefore, of non-microbial origin, was considered to be a control and background reference for the calculation. Judging from the relative means and standard deviations, the suspended biomass in Reactor B exhibited the greatest response.

definition of the data was expected due to the “moving average” effect of sub-grouping the observations within a sample population. The estimated state speed values as a function of time are shown in Figure 4-24. These results indicate a low or inherent background level of community change that apparently increased suddenly in conjunction with the resin acid shock load. The levels of this response in decreasing order were as follows: Suspended B > Suspended A > Biofilm B > Biofilm A.

The scatter in the state speed was reduced by modelling the data to a function of form:

$$v_c(\eta) = \xi_0 + \xi_1 \exp(-v_1\eta) + \xi_2 \exp(-v_2\eta), \quad \eta \geq 0 \quad (4-43)$$

The parameters were estimated by least-squares nonlinear regression. The resultant curves are also shown in Figure 4-24.

If the elevated state speed could be attributed to the resin acid input, then it follows that the level of response should have corresponded directly to the instantaneous resin acid concentration or

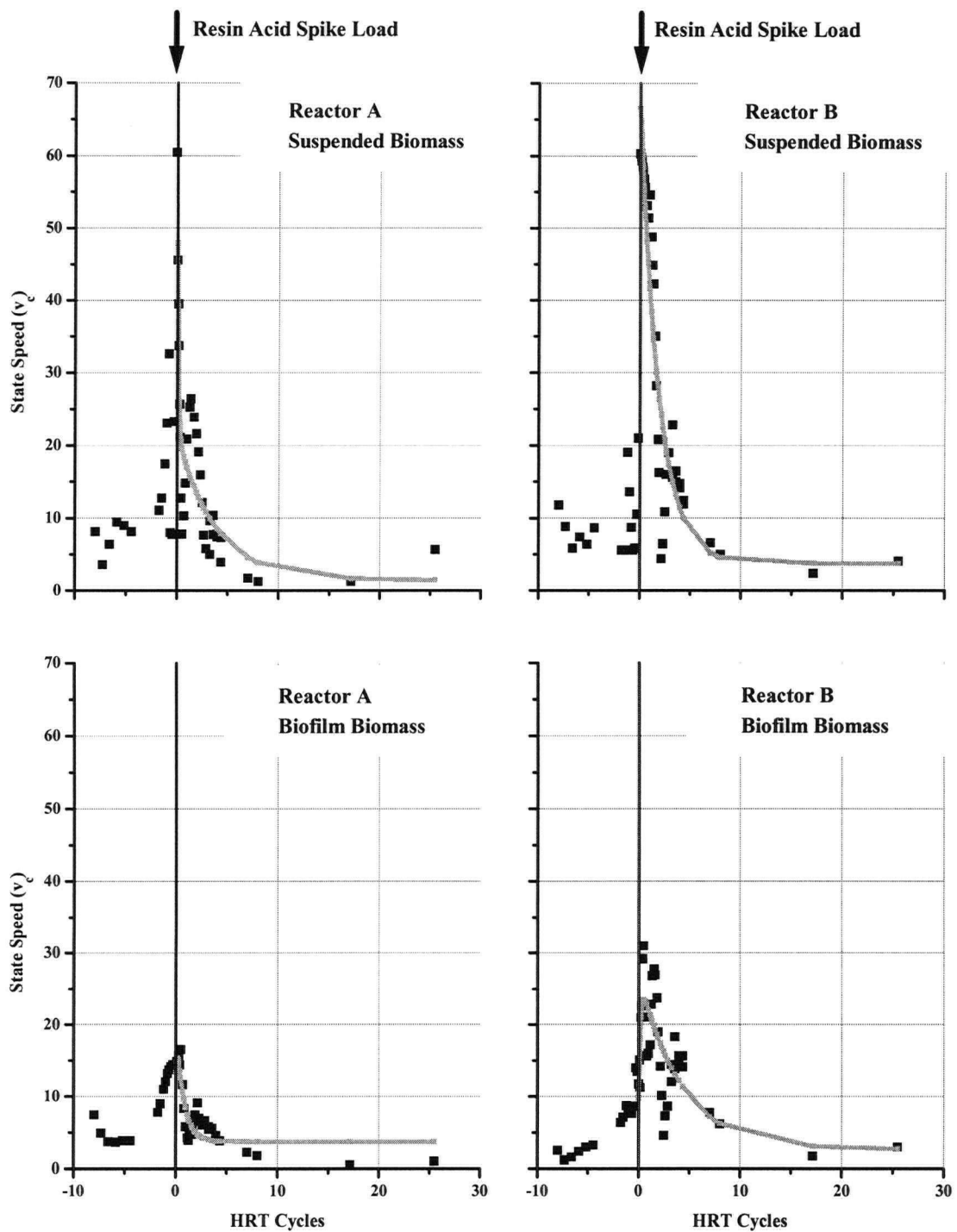


Figure 4-24. Population dynamics expressed as state speed (equation (4-42)) from fatty acid logcontrast canonical component analysis. A community response to the spike load of resin acids was most apparent for the suspended biomass in reactors A (pH 6) and B (pH 8). Best fit lines were determined for the model of equation (4-43) by least squares nonlinear regression analysis (Excel 97 SR-1 Solver).

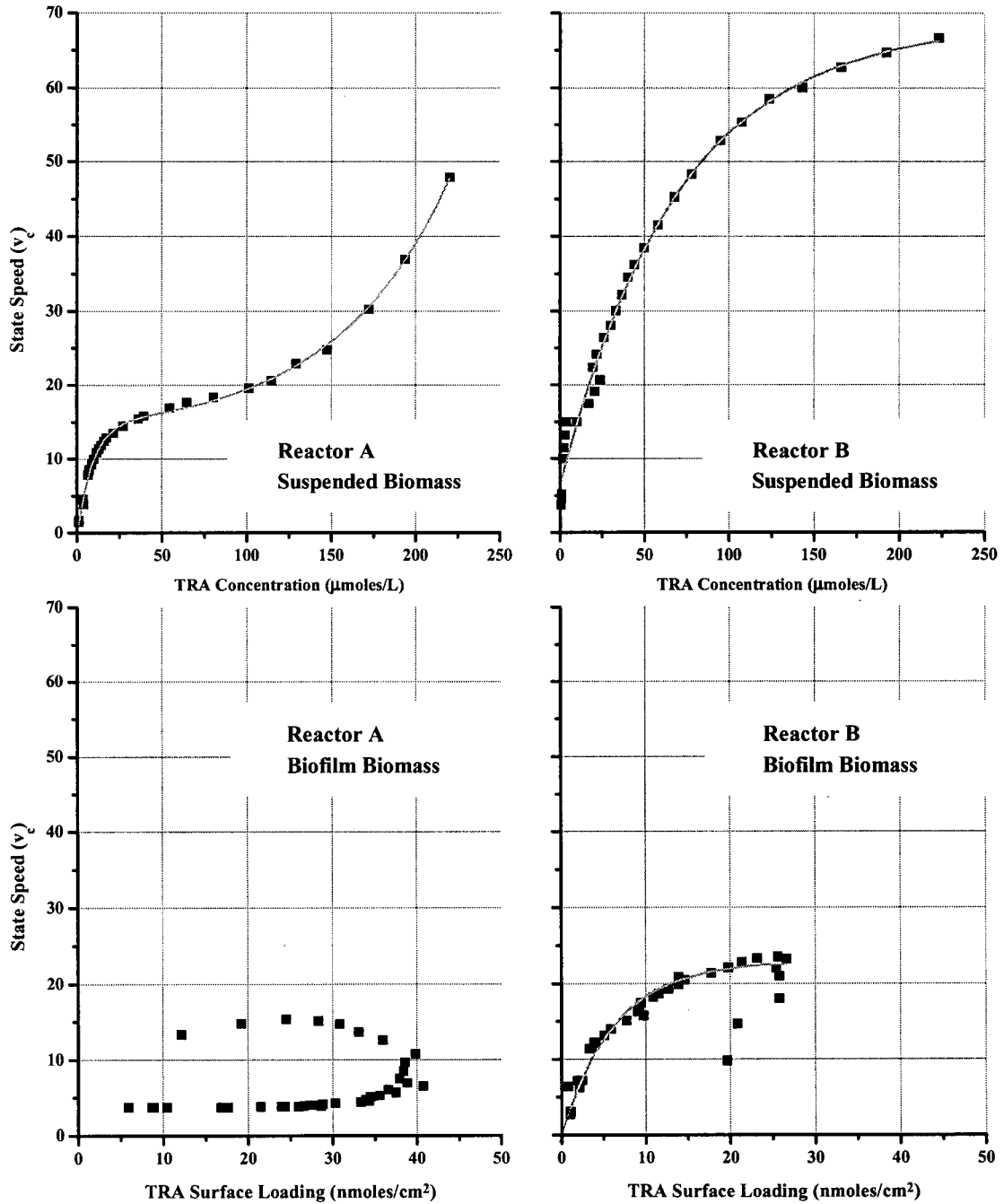


Figure 4-25. The derived correspondence between the state speed (equation (4-42)) and the total resin acid (TRA) levels after the shock load. The values of state speed used for this assessment were those determined from the trend lines (equation (4-43)) shown in Figure 4-24. The suspended biomass from the two reactors exhibited the strongest correspondence between population dynamics and resin acid level.

surface loading for the suspended or biofilm biomass respectively. To test the validity of this hypothesis, the best fit data (Figure 4-24) were plotted against total resin acid (TRA) levels (Figure 4-25). The suspended biomass state speeds from reactors A and B did exhibit strong relationships with TRA concentration. The biofilm biomass state speed for reactor B appeared to be more weakly related to TRA surface loading. No such correspondence for the biofilm biomass in reactor A was evident.

The observation of these sample population responses to the shock load prompted the question of whether these fatty acid compositional changes were a product of individual, or community level, acclimations. If the compositional changes were due to adaptation in response to membrane toxicity from a hydrophobic substrate then one might have expected that some corresponding microbial inhibition would have been observed.

Microbial inhibition should have caused a reduction in microbial activity. The pooled and sorted TOC data plotted against their order statistic (Figure 4-26) fitted well to a linear trend indicating that any variability in the TOC was random and well represented by a normal distribution. If a shock load of a hydrophobic substrate caused a toxic shock that decreased overall metabolic activity, then the observed population dynamic response could infer an adaptation response of individuals. However, no change in TOC removal was observed. Furthermore, a general species-level response to membrane toxicity should, in principle, have appeared for both the biofilm and suspended biosolids. In addition, the hydrophobicity of resin acids is greater under acidic conditions, yet it was the suspended biomass under alkaline conditions that appeared to have exhibited the greater response. These results suggest that the population dynamics observed through microbial fatty acid compositional analysis are best interpreted as a shift in the balance of populations in the community. This conclusion is also consistent with the results of Chapter 3.

A decline in some species within a community due to toxic inhibition would permit the emergence of other organisms with no net change in the removal rate of TOC. Thus, the introduction of the resin acid shock load appears to have caused a shift in the community favouring those organisms that would not have been impeded by the hydrophobic substrate. Resin acids are known to inhibit

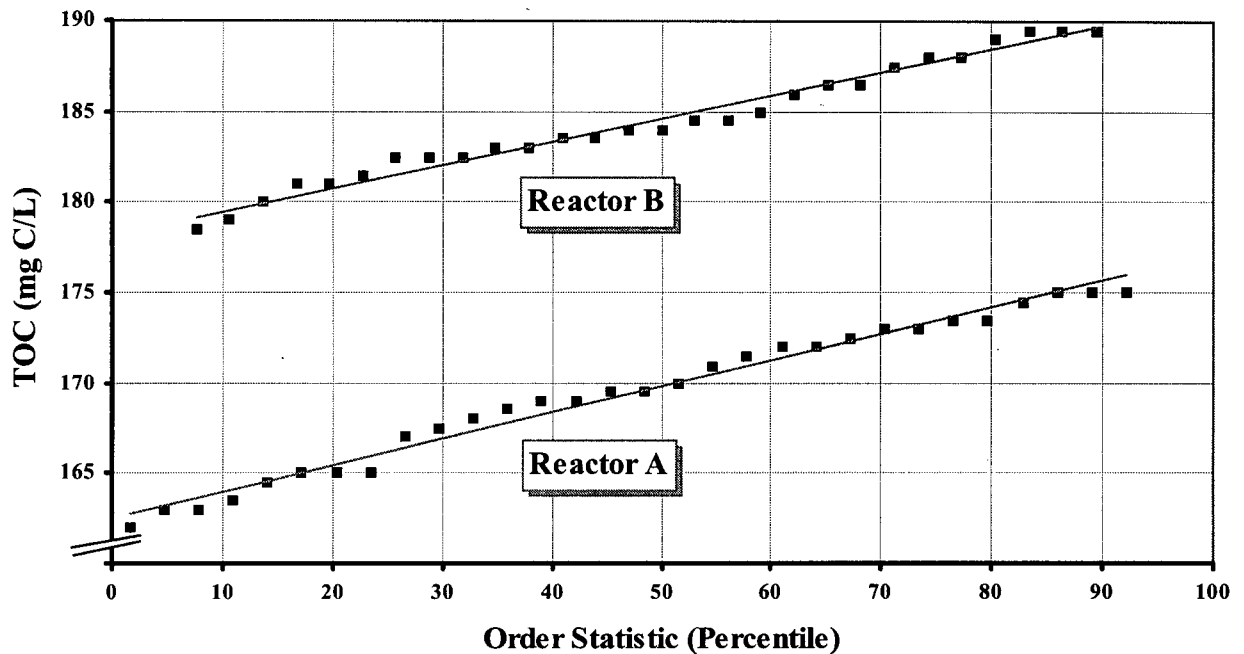


Figure 4-26. Pooled reactor TOC measurements taken before, during and after a spike load transient of resin acids. During the transient, there was no significant increase in the reactor TOC levels to suggest microbial inhibition. The effluent TOC data plotted against the order statistic (Gilbert 1987) indicate that these measurements were normally distributed. Both distributions have similar slope which implies that the variability was due solely to measurement errors. Differences in the mean values (Order Statistic = 50 percent) are a combined effect of difference in uptake rates and flow rates. In fact, the removal rate of TOC for reactor B was significantly greater than the one for A.

anaerobic bacteria (Liver and Hall 1996). If the mechanism of inhibition is non-specific, then it is not unreasonable to suspect that some organisms within a complex microbial ecosystem could be similarly affected.

A community level adaptation implies a degree of plasticity. Although biological removal of the resin acid shock load appears to have been negligible, the community, as a whole, maintained sufficient diversity and an adequate growth rate to accommodate the imposed stress. The observation that the community response was greater for the suspended biomass is consistent with the expectation that faster growing, short SRT, microbial populations adapt more rapidly to environmental change.

4.3.6 Resin Acid Sorption Kinetics

Sorption to the biofilm was modelled by equation (4-17). With the functional representation of the data given by equation (4-28), estimates for the resin acid aqueous concentration, biofilm loading and rate of change of biofilm loading were obtained for each observation as follows:

$$C_{\infty} = f_a(t), \quad \Gamma = f_b(t), \quad \frac{\partial \Gamma}{\partial t} = \frac{\partial f_b(t)}{\partial t} \quad (4-44)$$

Estimates for the parameters $\{h, K_e, \Gamma_L\}$ were obtained by least-squares non-linear regression (Microsoft Excel 97 SR-1, Solver) and are listed in Table 4-16. A plot, of the predicted versus estimated (measured) values of the rate change in surface loading (Figure 4-27), illustrates that the model of equation (4-17) provided a good representation of the data during periods of both sorption and desorption. The absence of major departures from the diagonal of Figure 4-27 confirms that biological removal of resin acid during the shock load period was not a factor for this experiment. Therefore, resin acid sorption to the carrier biofilm appeared to be reversible and followed a Langmuir isotherm. The isotherms predicted for pH 6 and pH 8 by the estimated parameters in Table 4-16 are shown in Figure 4-28. Note that although a much greater biofilm

Table 4-16. Least-squares estimates for the model parameters of equation (4-17). The extent of resin acid sorption to the biofilm at pH 8.0 (Reactor B) is about twice the level for pH 6.0. Mobility (B) of resin acids at pH 8.0 was also found to be significantly greater.

Parameter	Reactor A	Reactor B	units	Description
h	3.08	6.09	mL/ μ mole TFA/Hr	Specific biofilm mass transfer coefficient
K_e	13.20	175.50	μ mole TRA/L	Langmuir equilibrium constant
Γ_L	977.11	1964.14	nmole TRA/ μ mole TFA	Limiting sorbed TRA biofilm loading
r^2	0.99	0.99		Correlation coefficient in fitting the data to the model
X_b	46.31	32.79	nmole TFA/cm ²	Average carrier biomass concentration
$B = h \cdot X_b$	0.14	0.20	cm/Hr	Mass transfer coefficient (TRA mobility)

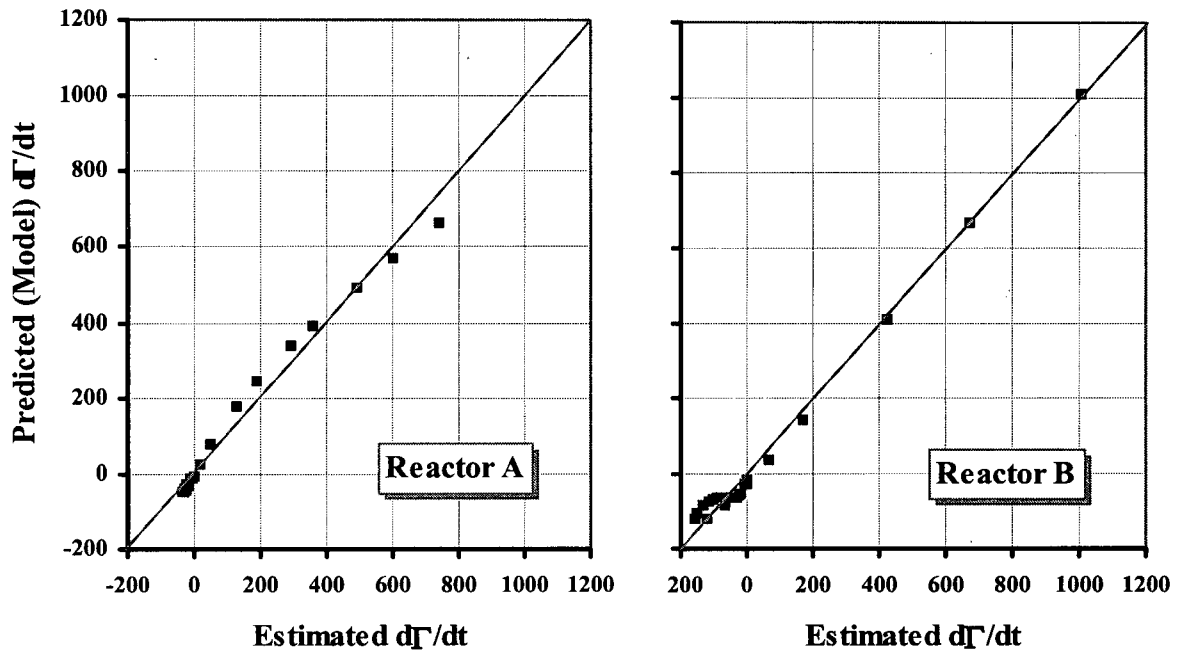


Figure 4-27. Comparison of the estimated (equation (4-44)) versus the predicted (equation (4-17) and Table 4-16) flux of total resin acids to the carrier biofilms in reactors A and B. By the data correspondence to the graph diagonal, the model of equation (4-17) appears to approximately represent the sorption and desorption of resin acids during the transient shock load. The data for this experiment suggest that sorption was reversible.

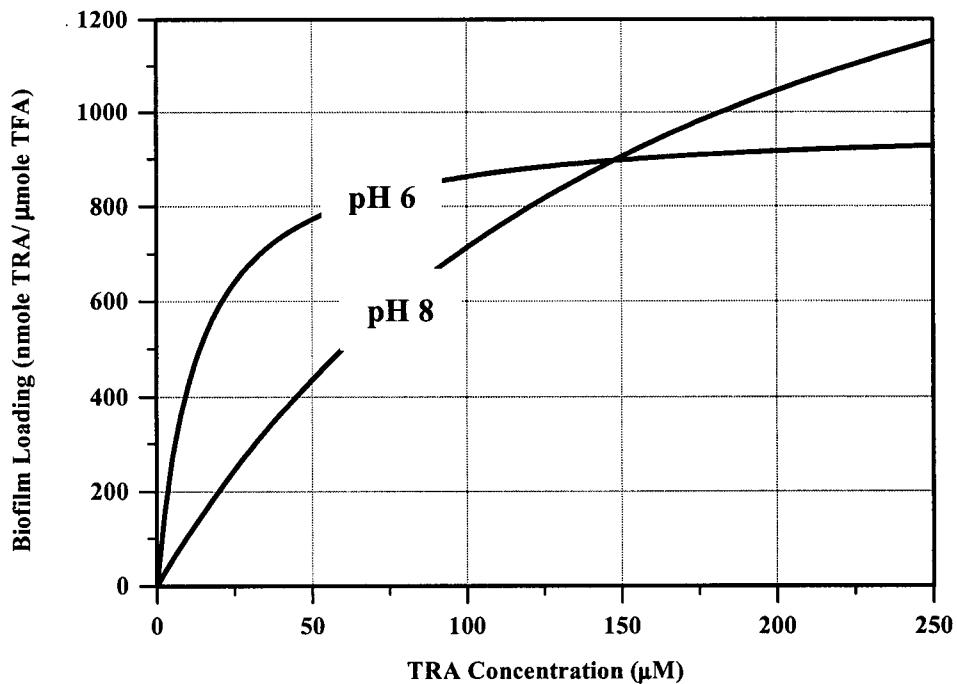


Figure 4-28. Predicted equilibrium Langmuir isotherms for biofilm sorption of total resin acids (TRA) based on the experimental parameter estimates for equation (4-17) listed in Table 4-16. The extent of sorption possible is predicted to be greater at pH 8 but the level of sorption is greater at pH 6 up to a TRA concentration of about 150 μ M.

loading is predicted to be possible at pH 8, the equilibrium surface loading up to a TRA concentration of about 150 μM will be greater at pH 6. However, the rate of sorption is limited by film diffusion and the mobility of resin acids at pH 8 (Reactor B) was found to be significantly greater than at pH 6. Retention of resin acids due to sorption on the biomass was found to extend beyond the bioreactor HRT. However, due to the difference in mass loss in the surface scum between the two reactors, it was not possible to directly compare the values of θ_{RA} (equation (4-32)) and the role of biomass sorption on resin acid retention as a function of pH.

The effect of pH on the retention of resin acids due to biomass sorption could be considered instead by a numerical simulation using the experimentally-derived parameters as input. If bubble fractionation and scum formation are neglected, the mass balance for resin acids in the MBBR is as follows:

$$\frac{\partial m_r}{\partial t} = m'_f - m'_e - m'_b \quad (4-45)$$

where m_r is the TRA mass in the MBBR, m'_f is the mass flow rate into the MBBR from the feed, m'_e is the mass flow rate out of the MBBR in the effluent, and m'_b is the mass sorption rate to the biofilm. Assuming that the MBBR is subject to a spike load of resin acids at time zero and that the feed TRA level is negligible then:

$$\frac{\partial m_r}{\partial t} = -m'_e - m'_b \quad (4-46)$$

Substituting parameters defined in Table 4-2 and Table 4-16, equation (4-46) can be written as:

$$\frac{\partial c}{\partial t} = -\frac{Q_e}{V}c - X_b \frac{A}{V} \frac{\partial \Gamma}{\partial t} \quad (4-47)$$

where c is the TRA concentration in the MBBR and A is the total biofilm area (Table 4-5).

Substituting equation (4-17) into equation (4-47) yields:

$$\frac{\partial c}{\partial t} = -\frac{1}{\theta_H}c + B \frac{A}{V} \left(K_e \frac{\left(\frac{\Gamma}{\Gamma_L} \right)}{1 - \left(\frac{\Gamma}{\Gamma_L} \right)} - c \right) \quad (4-48)$$

where B is the TRA mobility as defined in Table 4-16. Equations (4-17) and (4-48) form a coupled set of ordinary differential equations that can be solved by numerical integration.

Starting with the initial conditions of $c(t=0)$ equal to 240 μM and $\Gamma(t=0)$ equal to zero, model simulations were generated (Simnon, Version 1.03) for reactors A and B with their respective estimated parameters (Table 4-2 and Table 4-16). These predicted fate data were similarly fitted to equation (4-28) and the ideal resin acid retention time (θ_{RA} of equation (4-32)), due to sorption, was estimated. The numerical simulations are shown in Figure 4-29. These calculations predicted that, in the absence of scum formation, the TRA retention time at pH 6 would be 2.37 times θ_H , which agrees closely with the experimental result. This predicted θ_{RA} of 2.37 times the HRT was expected to be close to the experimental value of 2.00 times the HRT for reactor A since about 90 percent of the TRA mass was recovered in reactor A. In other words, scum formation was not a large resin acid mass sink during the experiment for reactor A. However, the TRA retention time at pH 8 was estimated to be 3.39 times the HRT. This θ_{RA} value of 3.39 times the HRT is much larger than the experimentally observed value of 1.08 times the HRT for reactor B. Therefore, from this investigation it was determined that the velocity of sorption was more important than the extent of sorption when it comes the retention of a contaminant in a treatment system due to sorption. The influence of resin acid sorption to biomass on the contaminant retention time was greater at pH 8.

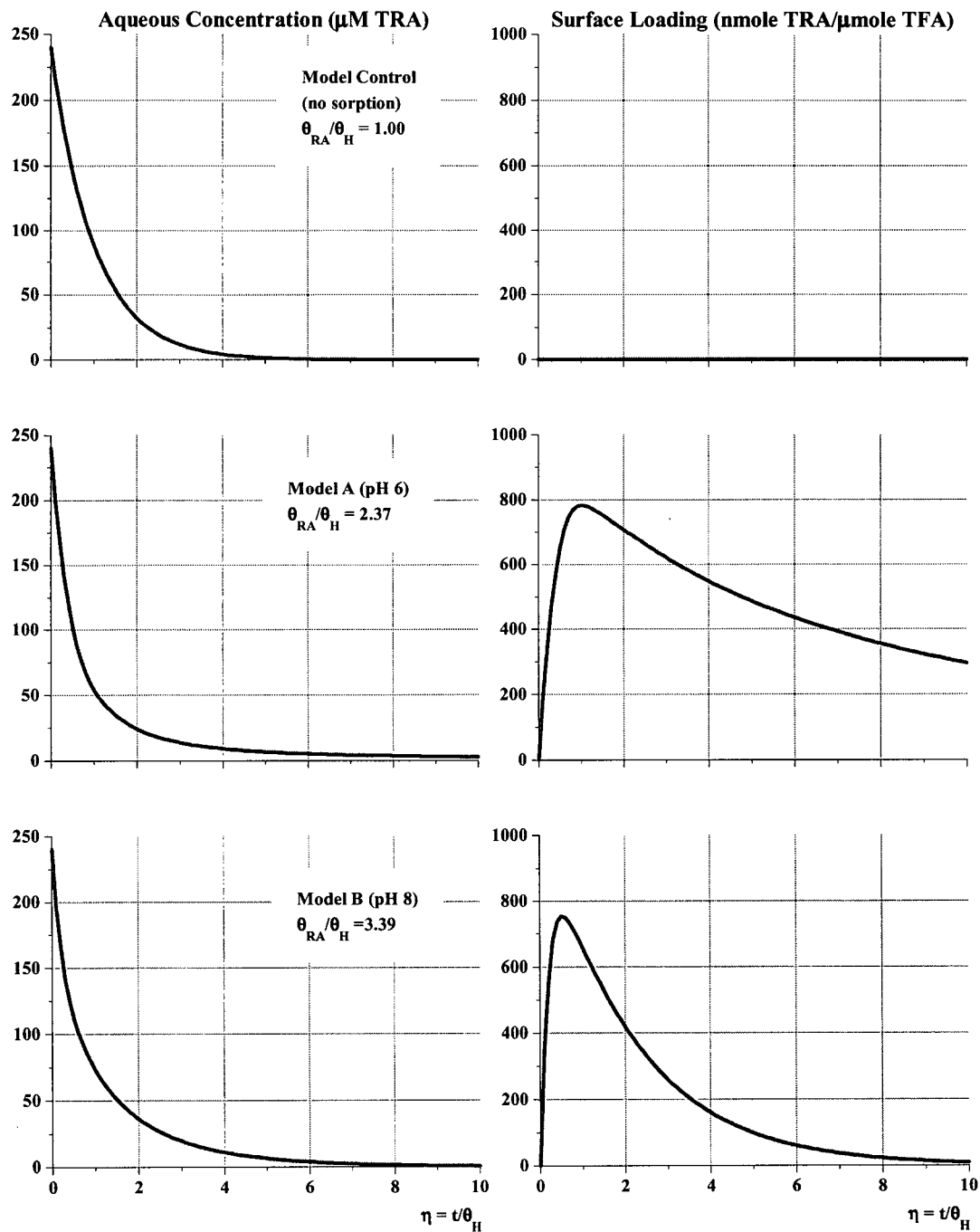


Figure 4-29. Simulated TRA fate data for the set of ordinary differential equations (4-17) and (4-48). Numerical integration was performed (Simnon, Version 1.03) for the case of no sorption (Top), and for the conditions of reactor A (Middle) and reactor B (Bottom). The reactor parameters used are defined in Table 4-2 and Table 4-16. The case of no sorption was created by setting h (equations (4-17)) equal to zero. The initial simulation conditions were a total resin acid concentration of 240 μM and zero biofilm loading. From the simulation data, θ_{RA} values were calculated (equation (4-32)). Retention of resin acids due to biofilm sorption is predicted to be most significant at pH 8.

4.4 Discussion

Contact angle measurements were found to be useful to characterize and document the nature of the biofilm carrier material. The proprietary ANOX plastic surface energy was the same as native high density polyethylene. While this issue was ancillary to the principal objectives of the investigation, surface energy would be a meaningful parameter to use for future work should the role of the support material in biofilm development become a focal issue.

Previous studies that reported a two-step sorption process of resin acids onto biosolids (Hall and Liver 1996; Liu et al. 1996) were discussed in the introduction (Section 4.14). In these past investigations, resin acid partitioning was studied by separation of the biosolids from the water column by centrifugation. In the present study, acidification followed by centrifugation was similarly found to separate resin acids from the supernatant. The acidification and centrifugation of the TOC samples effectively eliminated the contribution of resin acids to the TOC measurements made during the shock load. The spike input raising the TRA concentration from about 1 to 240 μM was equivalent to a step of 57 mg C/L. No sudden step change in TOC was measured, in spite of this significant input of additional carbon. The results from the previous partitioning studies were most likely confounded by the presence of suspended resin acids in solution. The formation of insoluble particulates must be accounted for when determining the partitioning characteristics of hydrophobic contaminants. The use of a biofilm system avoided interference from the suspended solids and eliminated the requirement for centrifugation to achieve biomass separation from the bulk liquid. By the elimination of the centrifugation step in the analytical protocol, the experimental results of resin acid sorption kinetics could be considered without ambiguity.

Resin acids were observed to adsorb reversibly to the biofilm, according to a kinetic model with a Langmuir sorption rate limited by film diffusion. In Chapter 2, adsorption equilibrium at a gas-liquid interface was seen to be reached within a couple of minutes, given relatively quiescent aqueous conditions. Since sorption to the biofilm was measured under ideally mixed reactor conditions, biofilm morphology, as opposed to reactor hydrodynamics, likely contributed more

significantly to “film diffusion” mass transport resistance. Resin acid mobility and the predicted Langmuir limiting surface loading were dependent on pH. Decreases in the estimated extent (Γ_L) and kinetics (h) of sorption at lower pH would be attributable to the higher effective mass of resin acid agglomerates that have been shown to form under acidic conditions (Chapter 2 and 3). The formation of resin acid colloids occurs due to the decrease in resin acid solubility with pH.

These relative pH-dependent differences in the sorption parameters were consistent with the analogous values determined by the dynamic surface tension measurements reported in Chapter 2. Therefore, the results of this continuous flow experiment serve to support the general applicability of the adsorption parameters previously determined by the maximum bubble pressure method. The correspondence of the results in Chapter 2 to the current investigation is of significant engineering application because many experimental conditions could have been more readily investigated by dynamic surface tension measurements and quasi-static isotherm modelling.

Extraction for microbial fatty acid methyl esters, introduced in Chapter 3, proved to be an effective method to account for both the suspended and biofilm reactor biomass. That the total fatty acid (TFA) concentrations in the reactors could be deemed to represent the active biomass was supported by the fact that an influent fatty acid, octadecadienoic (linoleic) acid of known wood origin (McLeay 1987), was not detected in the bioreactors. Further, the influent fatty acid composition was distinct from the suspended and biofilm TFA spectra. Fatty acids in BKME effluent are known to be degraded at such a rapid rate that a reliable fatty acid LC₅₀ from bioassay experiments has been difficult to determine (McLeay 1987). It is true that any viable biomass in the feed would not have been well represented by TFA. However monitoring the feed TFA composition was an important control in the use of the reactor TFA as a valid biomass measure.

Once justified, fatty acid compositions provided a convenient basis upon which to quantify, compare and combine the biofilm and suspended biomass content of the two reactors. Reactor A (pH 6), maintained a larger biofilm community with a similar suspended biomass concentration in comparison to reactor B, even though the reactors exhibited similar treatment efficiencies.

Overall, reactor A produced 20 percent more biomass than reactor B. It is interesting that the

greater biofilm content in reactor A was not generated at the expense of suspended biomass. This observation suggests that growth yields could have also been influenced by pH.

The results of the TFA compositional analysis demonstrated that pH within the typical operating range for pulp mill effluent secondary treatment influenced the resultant pseudo-species (Chapter 3) or microbial communities. Community fatty acid spectra were compared by similarity and logcontrast canonical component analyses. The first canonical component distinguished between suspended and biofilm biomass sources. The community variability due to inter-reactor pH differences appeared to be represented by the second and third components. The influence of pH seemed to have resulted in a greater variability on the between-population variance of the biofilm community.

It is interesting to speculate on the importance of chemotype differences in relation to solids retention time. The suspended biomass SRT was equal to the bioreactor HRT (2.84 hours) while the biofilm SRT was essentially infinite. Most likely, the biofilm established itself on the more recalcitrant fraction of the influent. From this hypothesis it follows that the more slowly biodegradable portion of the influent was consumed by the slower growing, longer SRT fraction of the biomass. Since this sample population was affected more by pH, then operational pH shifts in full scale treatment systems could have bearing on treatment performance. Slower growing, high SRT biomass would require more time to acclimate to changing environmental conditions. Although the suspended, short SRT biomass community was also measurably influenced by pH, the impact of a pH shift on this group would be adsorbed more readily due to its faster growth rate.

Therefore, the data suggest that pH control will be important for maintaining the reliability of biological treatment for pulp mill effluent. Process upsets at kraft pulp mills usually result in simultaneous organic and pH shocks to the biological treatment process. Equalization or rapid mixing tanks to stabilize pH swings might, therefore, improve the ability of such biological systems to cope with transient loads.

Selective resin acid withdrawal by bubble fractionation is believed to have been the main reason for the observed mass loss of resin acids. Higher levels of resin acids measured in the surface scum layer at pH 8, and the decreased mass recovery at pH 8, are consistent with expectations based on results from foam fractionation research (Branion 1992; Ng 1977) and from the results of Chapter 2. There was no evidence of biological oxidation of the transient load, since the mass recovery of chloro-dehydroabietic acid was almost identical to the overall resin acid recovery during the experiment. Liu et al. (1996) made measurements to suggest that air-oxidation was an important mechanism of resin acid removal. In their investigation, untreated effluent was sparged with air, resulting in an initial rapid 10 percent removal. No control conditions were mentioned and no account of scum formation was made. The results of the present investigation suggest that the observed removal by Liu et al. could well have been due to bubble fractionation and scum formation.

The fact that a short term spike load was not metabolized, even though the biosolids were acclimated to resin acids, has important implications for full scale treatment systems. It would appear that, for short term loading fluctuations of resin acids, the only option to prevent a toxicity breakthrough, is a strategy of physical removal. Even though the bench scale reactors were operated at an unusually short HRT, the removal of influent bioavailable organic carbon appeared to be complete. It should therefore, be possible to treat pulp mill effluent at a relatively high rate if pulping process transients and treatment shock loads could be avoided or managed. From this experiment, it also seems unlikely that even secondary systems with HRTs as high as 12 hours can safely rely solely on biological mechanisms of resin acid removal.

To completely avoid toxicity breakthrough due to resin acids, mills may need to establish some form of tertiary treatment unit operation. The method of choice to manage resin acid shock loads depends on pH. Under acidic conditions, a strategy to rapidly exclude a colloidal contaminant should successfully eliminate resin acids from the water column. Under alkaline conditions, bubble fractionation to adsorb and separate surfactant-like contaminants would be appropriate. For neutral or variable aqueous pH conditions, a combination of exclusion and sorption

separation methods should be employed to reliably attenuate influent transient loads.

Due to the short HRT used for this investigation, if the resin acid shock load had disrupted the metabolic activity of the microbial community as a whole, then one would have expected to observe either a transient drop in biomass level, or a transient increase in effluent TOC. There was no evidence to suggest any associated change in biomass quantity, or the effluent TOC level. However, there was evidence to suggest a shift in community structure due to the sudden shock load. Therefore, although a shock load of resin acids at constant pH did not appear to adversely affect the overall microbial activity, it seems likely that some species suffered within the communities. The idea of plasticity of microbial communities was introduced to describe the ability of the community structure to rapidly change in response to environmental stimuli. The high growth rate, short SRT fraction of the community was shown to change more readily to the shock load.

4.5 Conclusions

With respect to objective C in Chapter 1, in this experiment there was no evidence to suggest that a shock load of resin acids at constant pH was detrimental to the overall health of the reactor biomass. However, a shift in microbial community structure did result from the sudden environmental change. Microbial fatty acids were used to quantify, characterize and compare biofilm and suspended communities during the transient experiment. Compositional analysis clearly distinguished between the biofilm and suspended microbial communities and demonstrated a pH influence on the communities. A new methodology for quantifying population dynamics was developed and provided meaningful insight to the experimental results.

With respect to objective D in Chapter 1, sorption onto biomass can increase resin acid residence time in a secondary wastewater treatment process. Resin acid sorption onto a biofilm was reversible and was influenced by pH. Sludge wasting is, therefore, a mechanism of resin acid removal during sudden periods of elevated resin acid loading. Biological acclimation to increased resin acid levels was found not to be significant in a twelve hour period during the wash-out of a shock load. Although the bioreactors were acclimated to remove a low, steady state influent concentration of resin acids, even at an unusually short HRT, the experimental data suggested that biological oxidation of transient loads is not an adequate removal mechanism. Selective withdrawal of resin acids by bubble fractionation and scum formation was found to be a major route of removal that was most pronounced under slightly alkaline bioreactor conditions. Scum management (removal and destruction) and tight pH control should, therefore, be a part of treatment plant operations at pulp mills.

The results of this experiment demonstrated that acidic or alkaline pH treatment conditions do not influence the extent of biological removal of TOC from primary bleached kraft mill effluent. In addition, a transient resin acid loading did not appear to impede the steady state bioreactor performance. However, over the duration of the experiment, there was no evidence to suggest that the added resin acids were metabolized. Therefore, an event of toxicity breakthrough was generated in the laboratory. This observation raises the issue of the requirement for microbial

acclimation to loading fluctuations. To consider the significance of microbial acclimation in resin acid removal, a second continuous flow experiment was necessary. The objective of this subsequent study was to determine the influence of pH on the metabolic response time necessary for microbial communities to adapt to a change in resin acid loading (Objective E - Chapter 1). The outcome of this final study is reported in Chapter 5, Transient Resin Acid Loading During Continuous Biological Treatment.

4.6 References

- Adamson, A. W. (1982). *Physical Chemistry of Surfaces*, John Wiley & Sons.
- Aitchison, J. (1986). *The Statistical Analysis of Compositional Data*, Chapman and Hall.
- Aldenderfer, M. S., and Blashfield, R. K. (1984). *Cluster Analysis*, Sage Publications.
- Amy, G. L., Bryant, C. W., Alleman, B. C., and Barkley, W. A. (1988). Biosorption of organic halide in a kraft mill generated lagoon. *Journal of the Water Pollution Control Federation*, 60(8), 1445-1453.
- Bailey, J. E., and Ollis, D. F. (1986). *Biochemical Engineering Fundamentals*, McGraw-Hill.
- Bell, J. P., and Tsezos, M. (1987). Removal of hazardous organic pollutants by biomass adsorption. *Journal of the Water Pollution Control Federation*, 59(4), 191-198.
- Bicho, P., and Sadler, J. (1994). Mechanisms to improve biomass yield and granulation in UASB reactors treating BCTMP pulp mill wastewater: Analysis for impact of resin acids. , Forest Products Biotechnology, University of British Columbia.
- Branion, R. (1992). Treatment of thermomechanical pulping wastewaters. #13(RC 18), #13(RC 20), STDF-AGAR 13(SA-2), Science Council of British Columbia Research Grants, Vancouver.
- Broch-Due, A., Anderson, R., and Kristofferson, O. (1994). Pilot plant experience with an aerobic moving bed biofilm reactor for treatment of NSSC wastewater. *Water Science and Technology*, 29(5-6), 283-294.
- Bruun, H. (1952a). An interpretation of the effect of ionization upon monolayer properties of rosin acids. *Acta Chemica Scandinavica*, 6, 955-957.
- Bruun, H. (1952b). Properties of monolayers of rosin acids. *Acta Chemica Scandinavica*, 6, 494-501.
- Carter, C. W., and Suffet, I. H. (1982). Binding of DDT to dissolved humic materials. *Environmental Science and Technology*, 16(11), 735-740.
- Christodoulatos, C., and Mohiuddin, M. (1996). Generalized models for prediction of pentachlorophenol adsorption by natural soils. *Water Environment Research*, 68(3), 370-378.
- Colodey, A. G., and Wells, P. G. (1992). Effects of pulp and paper mill effluents on estuarine and marine ecosystems in Canada: a review. *Journal of Aquatic Ecosystem Health*, 1, 201-226.
- Dobbs, R. A., Wang, L., and Govind, R. (1989). Sorption of toxic organic compounds on wastewater solids: correlation with fundamental properties. *Environmental Science and Technology*, 23(9), 1092-1097.
- Gilbert, R. O. (1987). *Statistical methods for environmental pollution monitoring*, Van Nostrand Reinhold Company.
- Hall, E. R., and Liver, S. F. (1996). Interactions of resin acids with aerobic and anaerobic biomass - II. Partitioning on biosolids. *Water Research*, 30(3), 672-678.
- Hansch, C., and Leo, A. (1995). *Exploring QSAR: Fundamentals and applications in chemistry and biology*, American Chemical Society.
- Harwood, J. L., and Russell, N. J. (1984). *Lipids in Plants and Microbes*, George Allen & Unwin, London.
- Hassett, J. P., and Anderson, M. A. (1979). Association of hydrophobic organic compounds with dissolved organic matter in aquatic systems. *Environmental Science and Technology*, 13(12), 1526-1529.
- Incropera, F. P., and de Witt, D. P. (1981). *Fundamentals of Heat Transfer*, John Wiley & Sons.
- Israelachvili, J. N. (1985). *Intermolecular and surface forces: With application to colloidal and biological systems*, Academic Press.
- Jacobsen, B. N., Arvin, E., and Reinders, M. (1996). Factors affecting sorption of pentachlorophenol to suspended microbial biomass. *Water Research*, 30(1), 13-20.
- Jafvert, C. T., Westall, J. C., Grieder, E., and Schwarzenbach, R. P. (1990). Distribution of hydrophobic ionogenic organic compounds between octanol and water: Organic Acids. *Environmental Science and Technology*, 24(12), 1795-1803.

- Karickhoff, S. W., Brown, D. S., and Scott, T. A. (1979). Sorption of hydrophobic pollutants on natural sediments. *Water Research*, 13, 241-248.
- Kukkonen, J. (1992). Effects of lignin and chlorolignin in pulp mill effluents on the binding and bioavailability of hydrophobic organic pollutants. *Water Research*, 26(11), 1523-1532.
- Kukkonen, J., and Oikari, A. (1992). Effects of kraft lignin and chlorolignin on the binding and bioavailability of benzo(a)pyrene to *Daphnia magna* Straus. *Bulletin for Environmental Contamination and Toxicology*, 48, 781-788.
- Kulovaara, M., Kronberg, L., and Pensar, G. (1987). Recoveries of some chlorophenolics and resin acids from humic water. *The Science of the Total Environment*, 62, 291-296.
- Leach, J. M., Mueller, J. C., and Walden, C. C. (1977). Biodegradability of toxic compounds in pulp mill effluents. *Transactions of the technical section CPPA*, 3(4), TR126-TR130.
- Levenspiel, O. (1972). *Chemical Reaction Engineering*, John Wiley & Sons.
- Levenspiel, O. (1984). *The Chemical Reactor Omnibook*, OSU Book Stores, Inc.
- Liu, H. W., Lo, S. N., and Lavallée, H. C. (1996). Mechanisms of removing resin and fatty acids in CTMP effluent during aerobic biological treatment. *Tappi Journal*, 79(5), 145-154.
- Liver, S. F., and Hall, E. R. (1996). Interactions of resin acids with aerobic and anaerobic biomass - I. Degradation by non-acclimated inocula. *Water Research*, 30(3), 663-671.
- Mackay, D., Bobra, A., Shiu, W. Y., and Yalkowsky, S. H. (1980). Relationships between aqueous solubility and octanol-water partition coefficients. *Chemosphere*, 9, 701-711.
- Marton, J. (1964). On the structure of Kraft lignin. *Tappi Journal*, 47(11), 713-719.
- Maze, C., and Burnet, G. (1969). A non-linear regression method for calculating surface tension and contact angle from the shape of a sessile drop. *Surface Science*, 13, 451-470.
- McLeay, D. (1987). Aquatic Toxicity of Pulp and Paper Mill Effluents: A Review. *EPS Report 4/PF/1*, Environment Canada.
- McLeay, D. J., Walden, C. C., and Munro, J. R. (1979a). Effect of pH on toxicity of kraft pulp and paper mill effluent to salmonid fish in fresh and seawater. *Water Research*, 13, 249-254.
- McLeay, D. J., Walden, C. C., and Munro, J. R. (1979b). Influence of dilution water on the toxicity of kraft pulp and paper mill effluent, including mechanisms of effect. *Water Research*, 13, 151-158.
- Metcalf & Eddy, I. (1991). *Wastewater Engineering: Treatment, Disposal, and Reuse*, McGraw-Hill, Inc.
- Muir, D. C. G., and Servos, M. R. (1996). Bioaccumulation of bleached kraft pulp mill related organic chemicals by fish. *Environmental Fate and Effects of Pulp and Paper Mill Effluents*, M. R. Servos, K. R. Munkittrick, J. H. Carey, and G. J. van der Kraak, eds., St. Lucie Press, 283-296.
- Nauman, E. B. (1987). *Chemical reactor design*, John Wiley & Sons.
- Neumann, A. W. (1974a). Contact angles and their temperature dependence: thermodynamic status, measurement, interpretation and application. *Advances in Colloid and Interface Science*, 4, 105-191.
- Neumann, A. W. (1974b). An equation-of-state approach to determine surface tensions of low-energy solids from contact angles. *Journal of Colloid and Interface Science*, 49(2), 291-304.
- Neumann, A. W., and Good, R. J. (1979). Techniques of measuring contact angles. *Surface and Colloid Science*, R. J. Good and R. R. Stromberg, eds., Plenum Press, 31-90.
- Ng, K. S. (1977). Detoxification of bleached kraft mill effluents by foam separation, PhD, University of British Columbia, Vancouver.
- Niimi, A. J., and Lee, H. B. (1992). Free and conjugated concentrations of nine resin acids in rainbow trout (*Oncorhynchus mykiss*) following waterborne exposure. *Environmental Toxicology and Chemistry*, 11, 1403-1407.
- Nyrén, V., and Back, E. (1958). The ionization constant, solubility product and solubility of abietic and dehydroabietic acid. *Acta Chemica Scandinavica*, 12(7), 1516-1520.
- Robinson, K. G., and Novak, J. T. (1994). Fate of 2,4,6-trichloro-(¹⁴C)-phenol bound to dissolved humic acid. *Water Research*, 28(2), 445-452.
- Rusten, B., Mattsson, E., Broch-Due, A., and Westrum, T. (1995). The Kaldnes moving bed process for

- wastewater treatment at pulp and paper mills. *Filtration & Separation*(5), 389-395.
- Sarkanen, K. V., and Ludwig, C. H. (1971). *Lignins: Occurrence, Formation, Structure and Reactions*, John Wiley & Sons.
- Savitzky, A., and Golay, M. J. E. (1964). Smoothing and Differentiation of Data by Simplified Least Squares Procedures. *Anal. Chem.*, 36(8), 1627-1639.
- Schellenberg, K., Leuenberger, C., and Schwarzenbach, R. P. (1984). Sorption of chlorinated phenols by natural sediments and aquifer materials. *Environmental Science and Technology*, 18(9), 652-657.
- Selvakumar, A., and Hsieh, H. (1988). Competitive adsorption of organic compounds by microbial biomass. *Journal of Environmental Science and Health*, A23(8), 729-744.
- Shimp, R., and Pfaender, F. K. (1985). Influence of naturally occurring humic acids on biodegradation of monosubstituted phenols by aquatic bacteria. *Applied and Environmental Microbiology*, 49(2), 402-407.
- Sikkema, J., de Bont, J. A. M., and Poolman, B. (1994). Interactions of cyclic hydrocarbons with biological membranes. *Journal of Biological Chemistry*, 269(11), 8022-8028.
- Sikkema, J., De Bont, J. A. M., and Poolman, B. (1995). Mechanisms of membrane toxicity of hydrocarbons. *Microbiological Reviews*, 59(2), 201-222.
- Soltes, E. J., and Zinkel, D. F. (1989). Chemistry of rosin. Navel Stores, D. F. Zinkel and J. Russel, eds., Pulp Chemicals Association, 261-345.
- Strehler, A., and Welander, T. (1994). A novel method for biological treatment of bleached kraft mill wastewaters. *Water Science and Technology*, 29(5-6), 295-301.
- Taylor, S., and Ross, P. (1993). Biosolids in Eurocan pulp mill effluent. , British Columbia Ministry of Environment.
- Weber, W. J. J. (1972). *Physicochemical processes for water quality control*, John Wiley & Sons.
- Westall, J. C. (1985). Influence of pH and ionic strength on the aqueous-nonaqueous distribution of chlorinated phenols. *Environmental Science and Technology*, 19, 193-198.
- White, D. C. (1983). Analysis of microorganisms in terms of quantity and activity in natural environments. *Microbes in their natural environments*, R. Whittenberg and J. W. T. Wimpenny, eds., Society for General Microbiology, 37-66.
- Yan, G., and Allen, D. G. (1994). Biosorption of high molecular weight organochlorines in pulp mill effluent. *Water Research*, 28(9), 1933-1941.
- Zanella, E. (1983). Effect of pH on acute toxicity of dehydrabiatic acid and chlorinated dehydroabiatic acid to fish and Daphnia. *Bulletin for Environmental Contamination and Toxicology*, 30, 133-140.

Chapter 5
Transient Resin Acid Loading During Continuous Biological Treatment

Summary

The objective of this investigation was to determine the time scale for microbial response to transient loads of resin acids during continuous biological treatment (Objective E - Chapter 1). Biological treatment systems have limitations, particularly under dynamic loading conditions. These limitations were explored by subjecting well acclimated bench scale moving bed bioreactors to step changes in resin acid loading. The results indicated that lag time and physiological state are important parameters of biological treatment. The capacity of a treatment system to degrade resin acids was found to be a function of the loading history. Time lag for a microbial response to a shift-up in resin acid loading was significant and was also affected by the treatment system pH. Hence, the prevailing bioreactor operating conditions, in conjunction with the period and amplitude of loading transients were shown to influence the extent of biological removal of resin acids. Consequently, transient loading conditions cannot be neglected in the design of biological unit processes used for the removal of specific contaminants from wastewater.

Table of Contents

5.1 Introduction	264
5.1.1 <i>Microbial Acclimation</i>	264
5.1.2 <i>Sorption to Biomass Revisited</i>	272
5.1.3 <i>Experimental Approach and Method Specific Issues</i>	272
5.2 Methods and Materials	275
5.2.1 <i>Bioreactor design and operation</i>	275
5.2.2 <i>Sampling and Chemical Analysis</i>	276
5.2.3 <i>Suspended solids control study</i>	277
5.2.4 <i>Suspended solids batch growth experiment</i>	279
5.3 Results	281
5.3.1 <i>Bioreactor Operating Conditions</i>	282
5.3.2 <i>The Effect of Resin Acids on Treatment Performance</i>	285
5.3.3 <i>Biomass Characterization</i>	290
5.3.4 <i>Population Dynamics</i>	299
5.3.5 <i>Induction and Kinetics of Resin Acid Metabolism</i>	303
5.3.6 <i>Assessment of the Interpretation of Fatty Acid Compositions</i>	307
5.3.7 <i>The Contribution of the Biofilm Biomass in Resin Acid Metabolism</i>	312
5.3.8 <i>Suspended Solids Batch Growth Experiment</i>	314
5.4 Discussion	324
5.5 Conclusions	332
5.6 References	334

5.1 Introduction

The previous investigation provided some insight into the fate of a spike load of resin acids added to a continuous flow biological treatment system. It was found that sorption to the biofilm prolonged the contaminant retention time. Further, scum formation resulted in significant partitioning of the contaminant to the liquid surface. Scum formation and the influence of sorption were the most extensive under alkaline conditions in which resin acids were dissolved and thereby, more mobile surfactants. Although the bioreactors were well acclimated to resin acids, the results indicated that little, if any, biological removal occurred for the added spike load. While the biological removal of the spike load was negligible, trend analysis of microbial fatty acid compositions did indicate a strong concentration-dependent community response by the faster growing suspended biomass. This microbial response was quantified by a new measure, which expressed the rate change in the microbial community structure. Although the shock load did not appear to impede overall biological activity in the bioreactors, the sudden environmental change did appear to alter the balance in the community structure.

The purpose of the present investigation was, in part, to reaffirm the above mentioned observations and data interpretation for the community structure based on microbial fatty acid spectra. However, since in the previous investigation (Chapter 4) biodegradation of the resin acid spike input was not evident, the main objective for the present study was to monitor the acclimation process required before the onset of significant biological removal of transient resin acid input as a function of pH (Objective E - Chapter 1). Therefore, acclimation of microbial communities was the main theme for the present study.

5.1.1 Microbial Acclimation

Microbial acclimation can be observed as a lag in metabolic activity. Such lag phases are usually measured by a delay in microbial growth and/or substrate depletion. A lag in a microbial system can be broadly defined as a period of "deficiency" existing within the organisms or in the extracellular medium (Barford et al. 1982). During the lag phase, adaptations are made and this

deficiency is, in some way, accommodated. Microbial lag can be the result of internal causes such as an inappropriate enzyme spectrum, metabolic deterioration, or minor metabolic imbalances. External causes of lag may involve the required build up of an extracellular pool of metabolic intermediates, the need to produce extracellular enzymes, the removal or sequestering of a toxic substance, or the need to accumulate dissolved CO₂ in the medium.

The occurrence of a lag phase for microbial systems is a well known phenomenon. Individual bacteria require time to acclimate to their nutritional environment (Metcalf & Eddy 1991). However, biological treatment systems comprise complex interacting mixed populations, with each individual species having its own characteristic responses to changing conditions of nutritional status. Therefore, in a study of the acclimation of microbial communities to changing environmental conditions, one must consider the relative importance of lag times both at the level of the individual organism and at the level of the community. The net result of accommodating any “deficiency” may be expressed in terms of well adjusted individuals, or in terms of a whole new ecology of microorganisms.

The distinctive phases exhibited during the growth of microorganisms have been recognized since the turn of the century (Panikov 1995). The lag phase was initially postulated as a resting phase that could be restored to active metabolism by external nutrient stimulation. Latent cells were assumed to germinate into active cells with germination times following a Pearson distribution.

The conundrum in understanding the lag phase for a cell in a simple mathematical context, is that a cell is comprised of a number of autonomously functioning subsystems (Panikov 1995). Cellular optimisation for growth involves many levels of control acting in concert to adjust the cellular interface and the internal composition of metabolic components (Barford et al. 1982). Interactions and relationships at the community level add an additional layer of complexity of adjustment and optimization. Adaptation by individuals to changing environmental or nutritional conditions may or may not be adequate to ensure the survival of that species within a community. Competition among different species for a common substrate will favour the most

adapted organisms at the time (Panikov 1995).

The response to a change in environmental conditions, such as a change in substrate concentration, will depend to a large extent on the past history of the community (Panikov 1995). Physiological state, introduced in the discussion of Chapter 3, figures significantly in the acclimation process. Physiological state can, for example, be observed during chemostat operation at different dilution rates. For steady state continuous cultures, regular dilution rate-dependent cellular variations in RNA content, cell size and stored polysaccharide concentrations can be observed (Panikov 1995). These variations are attributed to differences in growth rate, which is controlled by the selected dilution rate. A change in dilution rate forces a change to a new physiological state, but this change may involve a protracted transient process. The batch growth cycle is itself an example of such a transient process. From the outset during batch growth, cellular characteristics are continually changing (Bailey and Ollis 1986; Herbert 1974) in response to the continually changing medium conditions.

Batch growth may be thought of as a kind of "shift-up", where cells are suddenly exposed to a nutrient rich environment. For a typical "shift-up" experiment (Barford et al. 1982), the rate of RNA synthesis increases almost instantaneously and overshoots the rate ultimately assumed. The other rates of macromolecular synthesis initially remain constant. Eventually all activities accelerate to levels commensurate with the new environment. The order and timing of processes such as DNA synthesis, protein synthesis and cell division reflect a complex hierarchy of coordinated cell control functioning over a spectrum of time scales (Barford et al. 1982). Thus, the expression "balanced growth" during batch cultivation is a misnomer, since steady state conditions for cellular constituents are never really achieved. For the case of a mixed culture during batch growth, the likely progression of successive dominant species further negates any notion of steady state growth. The outcome of a batch growth experiment is very much a function of the starting conditions of both community and medium.

The nature of the substrate under "shift-up" conditions is also an important consideration. Generally, the enzymes required to catabolize an energy source can be constitutive or inducible.

The nature of a lag period is very much dependent on the type of enzyme required (Barford et al. 1982). Constitutive enzymes are synthesized independently of the cell's surroundings. Production of inducible enzymes requires environmental stimulation. For example (Barford et al. 1982), consider the growth of *E. coli* on a mixture of xylose and glucose in continuous culture. During batch growth, the consumption of these two substrates is diauxic, with glucose consumed preferentially. Enzymes involved in the consumption of glucose are constitutive and those necessary for xylose metabolism are inducible. Xylose enzymes can be repressed in the presence of glucose. As a result, switching from glucose to xylose metabolism in continuous culture requires a long transient, since the enzymes for xylose must be induced. Conversely, a change from xylose to glucose results in a relatively smooth transition, since the necessary enzymes for glucose are constitutive.

From well-controlled observations of the lag phase during batch growth, two distinct patterns have emerged (Panikov 1995). In one case, a group of microorganisms exhibited a simple inverse relationship between the duration of the lag phase and the inoculum growth rate. These inocula were obtained from a chemostat operating at steady state. The inoculum growth rates were manipulated by maintaining the chemostat at a number of dilution rates. While the length of the lag phase could be changed, the final maximum specific growth rate was found to be constant for each species tested.

Another group of microorganisms exhibited a biphasic growth pattern during the lag period. These other organisms displayed an initial high level of metabolic activity immediately after inoculation. This burst of activity was associated mainly with the production of reserve compounds such as polysaccharides or cell wall components. This first process slowed and was followed by a period of reduced metabolic activity. The length of this second phase of reduced metabolic activity was again inversely dependent on the growth rate of the inoculum. These observations of pure culture lag times have implications for full scale treatment systems.

Important control parameters for the design and operation of activated sludge treatment processes are the food to microorganism (F/M) ratio and the solids retention time (SRT) (Metcalf

& Eddy 1991). These parameters are controlled by manipulating the removal of waste activated sludge (WAS). Since *in situ* growth rate influences lag time, it is apparent that sludge age will affect the response time to an elevated loading of a specific contaminant. A longer SRT will likely result in a more protracted acclimation period to that specific contaminant. Typically, the objective of tuning F/M and SRT is to achieve the goals of establishing good biosolids settling characteristics and optimal BOD removal. Bioreactor operational conditions for optimal response dynamics to changing contaminant loading need to be established.

Typically, the modelling and design of the activated sludge process are based on Monod kinetics with endogenous metabolism. The biosolids are viewed as a single “pseudo-species” (Chapter 3) with the same overall metabolic activity of the underlying complex community (Bailey and Ollis 1986). Such a simplified approach has been successful for treatment plant design based on the removal of lumped parameter substrate measures such as biochemical oxygen demand (BOD). However, for treatment plant design for the removal of specific aquatic contaminants, the simplified Monod approach may be inadequate. Any inadequacy would stem from the fact that while the influent BOD levels may not vary significantly, the concentration of specific contaminants could fluctuate appreciably. An increase in a specific contaminant level imposes “step-up” conditions that will result in a lag period if enzyme induction is required. Contaminant breakthrough during the acclimation period could have a harmful environmental impact in the receiving environment.

Thirty years ago Powell (1967; 1969) recognized the deficiency of the Monod model which describes the growth rate as depending on the instantaneous value of the substrate concentration. However, this important recognition still does not seem to have infiltrated the engineering approach to biological wastewater treatment design. One method to mathematically express the contribution of the past to the present is by the application of a delay kernel or memory function (MacDonald 1982):

$$\bar{p}(t) = \int_{-\infty}^t G(t-\tau)p(s(\tau))d\tau \quad , \quad G(\infty) = 0 \quad \text{and} \quad \int_0^{\infty} G(u)du = 1 \quad (5-1)$$

where p may be a substrate (s) dependent property, such as the Monod growth rate, and G is a weighting distribution function. Thus the value \overline{p} assumed by the system at time t is weighted by the driving force of steady-state values that have been striven for in the past. Organisms growing under conditions of a changing environment will, therefore, spend considerable time and energy in adjusting their physiology and metabolism to their surroundings, in comparison to the situation under stable environmental conditions (Pickett 1982).

Continual change and cycling necessitates adaptation for survival. Most industrial and domestic wastewaters vary considerably, both in terms of hydraulic and organic loading. However, most research on wastewater treatment appears to be focused on steady state removal of aquatic contaminants. Efficacy of biological treatment at steady state does not guarantee a similar performance under transient conditions. Full scale systems may never truly reach a steady state. Thus some doubt should be cast on the reliability of a biological system to consistently remove toxic aquatic contaminants until a better understanding of the impact of process transients is established. The development and application of generalized theories or models of non-steady state microbial growth are currently lacking (Panikov 1995).

There are good reasons to consider non-steady state experimentation with biological treatment systems (Panikov 1995). Such experiments permit a wider range of hypotheses to be tested and yield data concerning the dynamic behaviour of the studied system. This kind of information is valuable since, in practice, disturbances to cultivation conditions are unavoidable. Bench scale experimental conditions of non-steady state growth can be induced by deliberate perturbations of operational parameters such as substrate loading, hydraulic retention time, solids retention time, pH and temperature.

Three classes of periodic reactor operation have been defined (Pickett 1982) and these are illustrated in Figure 5-1. Quasi-steady periodic operation occurs when the period of the input oscillation is large with respect to the system response time. For such operation, the system can closely follow any transient input function. Relaxed steady state operation is the other extreme.

In this case, the system is unable to follow the rapid cycling and eventually a “relaxed” steady state is established. Intermediate between these two extremes is a situation in which the response time is of the same order of magnitude as the forcing function. Biological reactor operation typically falls into this latter class of operation. In a biological system, the response is dependent on both the frequency and the amplitude of the applied transient input (Pickett 1982).

The effects of input cycle time and amplitude have been studied using *E. coli* growing in continuous culture on glucose (Pickett 1982). With moderate frequency and amplitude the cultures exhibited a regular cyclic behavioural pattern with a similar frequency to the changing feed input. The lag time between stimulus and response was dependent on cycle time and became independent of amplitude above some threshold value. Interestingly, the response to shift-down in glucose concentration was always more rapid than the response to shift-up. With increasing input frequency, no extensive change in the culture could be observed. Thus the system moved from intermediate periodic operation to a relaxed steady state. From these

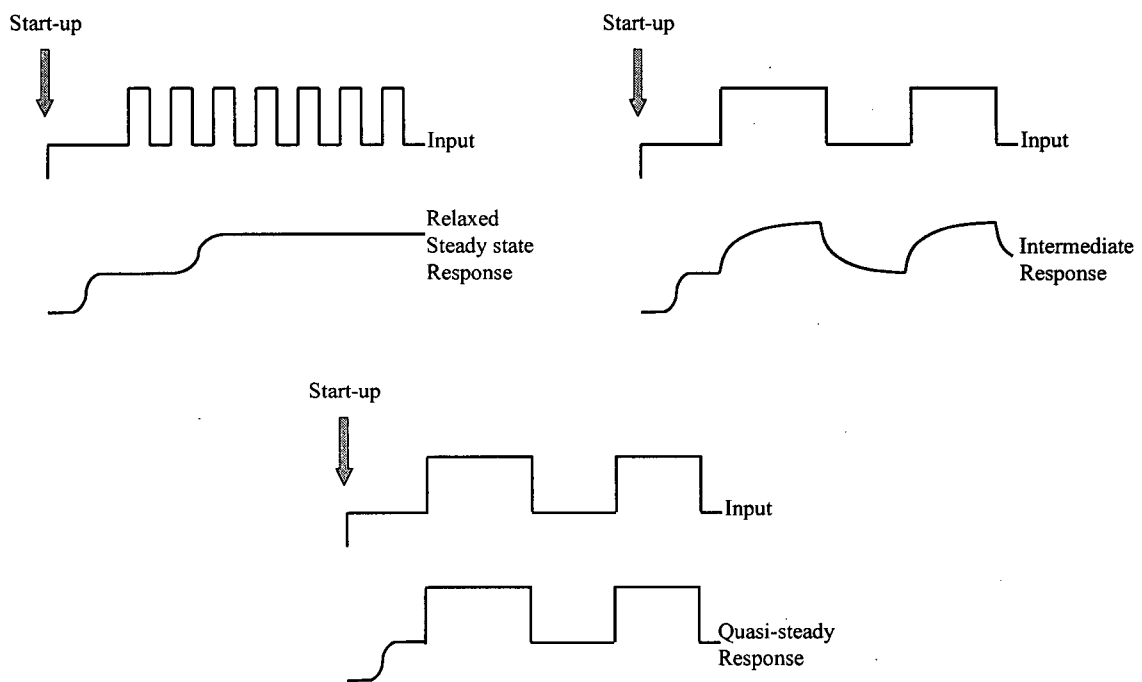


Figure 5-1. The three classes of periodic bioreactor operation (adapted from Pickett (1982)). The input would be the contaminant loading and the response would be the corresponding uptake rate. Depending on frequency of the applied stimulus and the time scale of system response, either relaxed, intermediate or quasi-steady periodic operation will ensue.

observations, it is not surprising that little biological removal of a resin acid shock load could be detected in the previous investigation (Chapter 4). Therefore, although tighter mill control can help to minimize the losses of resin acids in wastewater, acute toxicity removal in downstream biological treatment systems may be still be insufficient, particularly under dynamic loading conditions. The nature and the cause of these limitations are not fully understood. Time lags for microbial enzyme induction in response to a shift-up in resin acid loading have not been addressed in the literature. This omission is surprising considering the expected variability of resin acid loading in pulp mill effluents. Therefore, the present investigation was undertaken as an important step towards characterizing the dynamic response of microbial systems to resin acid loading transients.

For the present investigation, all the operational conditions were kept constant except for the resin acid loading. Of interest was the transient response under alkaline (pH 8) and acidic (pH 6) conditions. Small variations in pH can quench optimal enzyme activity (Pickett 1982). From the results of Chapter 3, resin acid metabolites from two different metabolic pathways were observed, depending on pH condition. Differences in pH appeared to select for two separate groups of resin acid degrading microorganisms that could also have quite different transient response characteristics. Thus one objective, of operating bioreactors under alkaline and acidic conditions in parallel, was to look for differences in the transient response of the distinct groups of resin acid-degrading microorganisms that would be cultured.

To simplify the interpretation of the experimental results for the present investigation, the system feed was monitored as total resin acids (TRA) and acid soluble total organic carbon (TOC). The resin acids were mainly abietic and dehydroabietic acids, accompanied by minor amounts of the pimaranes. The data from the previous investigation indicated that a sudden short-term transient input of resin acids affected the community structure without altering the metabolic activity of the community as a whole. While there was no direct evidence of inhibition, the data suggested that some members of the community were adversely affected by the shock. Therefore, it was of interest to observe the impact of a "shift-up" resin acid loading on the community structure over

a longer period of exposure. The purpose of this limited investigation was not to definitively solve the transient response model, but to merely assess the role of transient effects in resin acid removal and toxicity breakthrough.

5.1.2 Sorption to Biomass Revisited

In the previous investigation (Chapter 4), sorption of resin acids to the suspended carrier biofilm was found to follow the model of Langmuir sorption that was rate-limited by film diffusion. For the present investigation, resin acid sorption was anticipated to be an important aspect of the data analysis. However, due to the planned decreased sampling frequency over a longer period of bioreactor operation, there was some question about the extent to which sorption kinetics would be followed with the longer sampling interval.

In order to determine the extent to which the kinetics of resin acid sorption should be included in the data analysis for the present investigation, the time scale for sorption was assessed. Thus the model equation (4-17) was integrated using the estimated model parameters in Table 4-16 to solve the problem of a sudden exposure of resin acids to a "clean" biofilm. The results of this integration for the conditions of pH 6 and pH 8 are illustrated in Figure 5-2. Since more than 90 percent of the equilibrium loading was estimated to be reached after approximately 5 hours, sorption kinetics could be safely neglected for sampling intervals of this magnitude. In other words, for sampling intervals of approximately 5 hours and greater, resin acids sorbed to the carrier biofilm could be considered to be in equilibrium with the bulk liquid concentration.

5.1.3 Experimental Approach and Method Specific Issues

To satisfy the principal objective (Objective E - Chapter 1), two moving bed bioreactors were monitored in parallel as before (Chapter 4), but in this case, a more sustained transient resin acid input was applied. Again, pH 6 and pH 8 operating conditions were used to consider pH-dependence in the microbial response.

Two sequential step inputs of resin acids were fed to the well-acclimated bench scale, completely

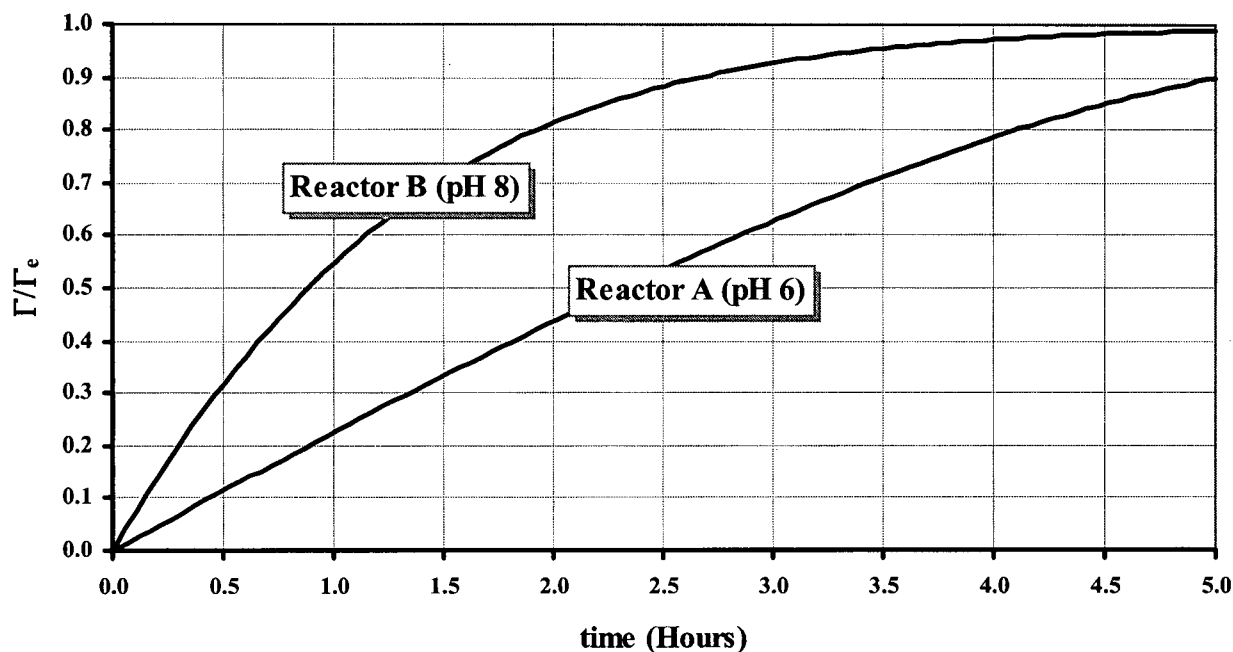


Figure 5-2. Kinetics of sorption of resin acids to a biofilm based on the results of Chapter 4. The model curves estimate the progression of surface loading (Γ) with respect to the equilibrium level (Γ_e) for pH 6 and pH 8. For both pH conditions, more than 90 percent of the approach to equilibrium is predicted to have occurred after 5 hours.

mixed, moving bed bioreactors. From the first step input, it was of interest to assess the rate of acclimation. The purpose of the second step was to determine the extent to which an improved capacity to remove resin acids would be retained by the bioreactors.

Finally, suspended biomass samples from the two reactors were used to inoculate sterile batch media containing pH-adjusted reactor influent enriched with resin acids. The kinetics of growth and substrate removal in the complex medium was monitored. The physiological state for the respective inocula were assessed in terms of lag time in substrate removal. In this manner, the condition of the two bioreactor communities that had experienced the same contaminant loading history at pH 6 and pH 8, respectively, could be compared.

Once again, microbial fatty acid compositions were used to monitor the community structure. The question of interference from non-viable (wood-derived) sources of fatty acids was considered explicitly in a control study involving the filtration of replicate samples. The method ambiguity regarding the potential combined contributions of species content and individual

adaption in any observed fatty acid compositional changes, was also re-addressed. The hypothesis of species level membrane adaptations dominating the fatty acid profile changes was tested by comparing the fatty acid compositions during periods of high, medium and low rates of resin acid metabolism.

5.2 Methods and Materials

5.2.1 Bioreactor design and operation

For these experiments, both microbiological inoculum and primary mill effluent were kindly supplied by Western Pulp Partnership in Squamish, British Columbia as described in Chapter 4.

The bioreactors were acclimated over a month of continuous operation and then closely monitored over a three week period (March-April 1997). During acclimation, primary-clarified bleached kraft mill effluent (BKME) was delivered weekly in about five 25 L Nalgene carboys. The BKME in each carboy was adjusted to pH 10 with 50 mL of 2 N NaOH, and was stored at 4°C. Just prior to the experiment, twenty carboys of primary effluent were collected from the mill, pH-adjusted and stored at 4°C (April 8, 1997). The bulk shipment of the BKME was made to ensure a consistent feed during the experiment.

The reactors were acclimated for 2 days to this BKME feed stock and the experimental phase commenced on April 10, 1997. Approximately on a daily basis, the contents of one carboy were screened to remove fibre fines and then decanted into the 50 litre feed holding tank, which was also refrigerated at 4°C. Sampling was undertaken over the course of each day. After drawing the last evening samples, any surface scum and growth were cleaned from the two reactors. Any influence on the data from this disturbance was assumed to have been attenuated by the next morning's sample.

Primary effluent was pumped (Cole Parmer MasterFlex) at a constant rate from the holding tank to the two parallel bench scale moving bed bioreactors. These bench scale bioreactors were the same design as described in Chapter 4, but had to be re-constructed anew due to embrittlement of the old reactor tanks. The logistics of effluent consumption and sampling over a three week time period required that a longer HRT (≈ 5 hours) be used than before. Since a greater number of the ANOX lab scale plastic carriers were going to be sacrificed, the initial number of carriers was increased to about 1050. This number was estimated from the total carrier dry weight and the average weight per carrier.

Table 5-1. Chemical amounts used to mix 1 L of concentrated tracer stock solutions. The stock without abietic acid (Na-BLK) was used as the control. The abietic acid (Sigma-Aldrich Canada Ltd.) was saponified by boiling in the lithium (Li-ABA) or sodium (Na-ABA) salt solutions. The tracer feed was made by diluting 130 mL of the saponified concentrated stock in 1 L of 0.0125 N NaOH.

Concentrated Tracer Stock	Chemical Weight (grams)				
	NaCl	NaOH	LiCl	LiOH·H ₂ O	Abietic Acid
Li-ABA			24.24	4.20	10.00
Na-ABA	33.73	3.95			10.00
Na-BLK	33.73	3.95			

A constant drip feed of concentrated ammonium chloride (6 g/L) supplied excess nitrogen and phosphoric acid dosing (Cole Parmer Series 7142 pH/pump system) maintained excess phosphorus at a constant pH of 6 and 8 in reactor A (“Acidic”) and B (“Basic”), respectively. The pH levels were continuously logged to a strip chart recorder. The pH was maintained to within ± 0.1 pH units.

In addition to the nitrogen and phosphorus feed supplements, a tracer solution was also continuously fed (Cole Parmer MasterFlex) into the two bioreactors (Figure 5-3 and Figure 5-4) and this feed provided the transient resin acid input. Three tracers were prepared from concentrated stock solutions (Table 5-1). Tracer feed consisted of 130 mL aliquots of the stock solution diluted with 1 L of 0.0125 N NaOH. Switching of the tracer feed enabled the determination of lithium and resin acid residence time distribution functions. The biosolids were monitored in parallel to test for a biological response to the controlled changes in input. Lithium was used as the control tracer for assessing the reactor mixing conditions. The tracer feed schedule and the sampling times are shown in Figure 5-5.

5.2.2 Sampling and Chemical Analysis

Sampling protocols and chemical analyses have been described in Chapter 4. Resin acids and microbial fatty acids were monitored from aqueous samples drawn from the bioreactors (“suspended”) and collected from the overflow (“effluent”). With sacrificed biofilm carriers sorbed resin acids and (“biofilm”) microbial fatty acids were monitored. During the periods when the Li-ABA tracer was either applied or removed (Figure 5-5), additional samples were drawn

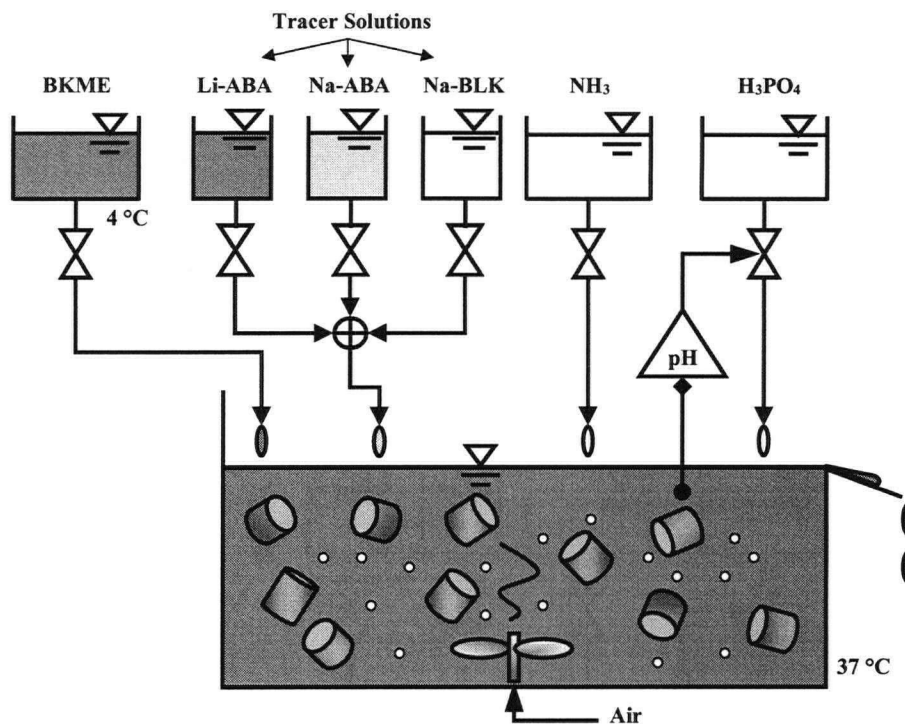


Figure 5-3. Idealized schematic of the experimental bench scale moving bed bioreactor (MBBR). Two parallel bioreactors (one at pH 6.0 and the other at pH 8.0) were continuously fed primary-clarified bleached kraft mill effluent. The effluent was kept at 4 °C and pH 10. Additional nutrients were supplied to maintain excess levels of nitrogen and phosphorus. The phosphorus was added at a rate to maintain constant pH in the bioreactors. The bioreactors were thermostated at 37 °C. During the experiment, the bioreactors were also continually fed from one of three possible tracer solutions (see also Figure 5-4, Figure 5-5, and Table 5-1).

from the reactors for lithium analysis by flame emission spectrophotometry. Reactor performance was measured in terms of total organic carbon (TOC) removal. Effluent flow was checked regularly by weighing a timed collection of sample from the overflow. Nitrogen and phosphorus levels were followed throughout the experiment.

5.2.3 Suspended solids control study

During the experiment, a set of additional samples was drawn from the two bioreactors and the BKME feed in order to explicitly consider the contribution of background free fatty acids to the assumed suspended biomass fatty acid composition. Triplicate whole, filtrate and filter samples were obtained. The whole samples were 5 mL aliquots drawn from the two reactors and the BKME feed as usual. The filtrate and filter samples were obtained by passing a 5 mL aliquot through a glass fibre filter (Whatman GF/F). The aqueous samples were processed as usual

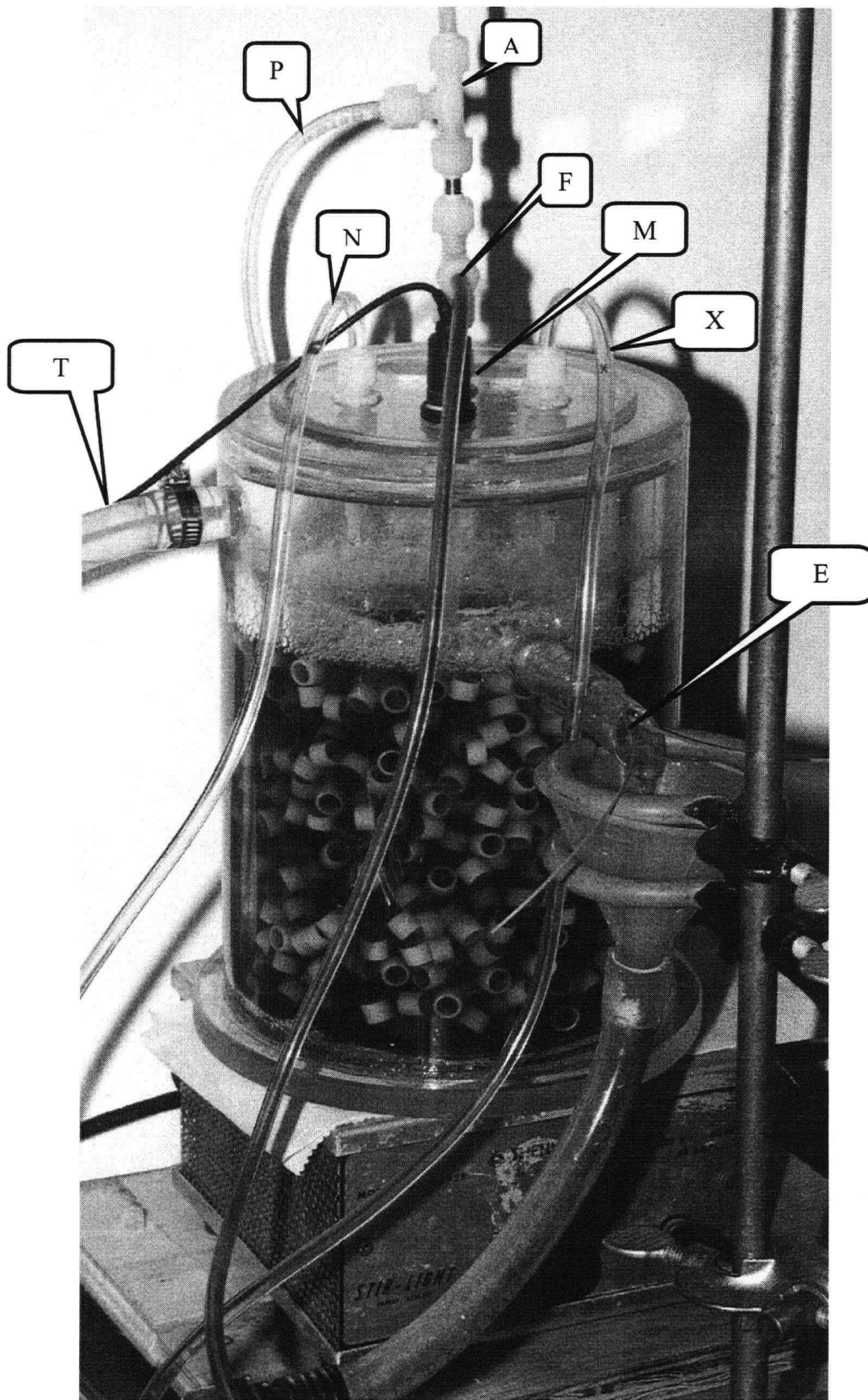


Figure 5-4. Photograph of the bench scale MBBR. Air (A), BKME feed (F), and phosphorus (P) were supplied through a common $\frac{1}{4}$ inch stainless steel tube down the axis of the Plexiglas tank in close proximity to the magnetic stir bar. The pH probe (M) can be seen supported by the top plate. The extra drip feed port (X) was used for the tracer input. Treated effluent exited the reactor by a constant level overflow (E). Thermostated water (T) was constantly supplied to the water jacket to maintain the bioreactor temperature.

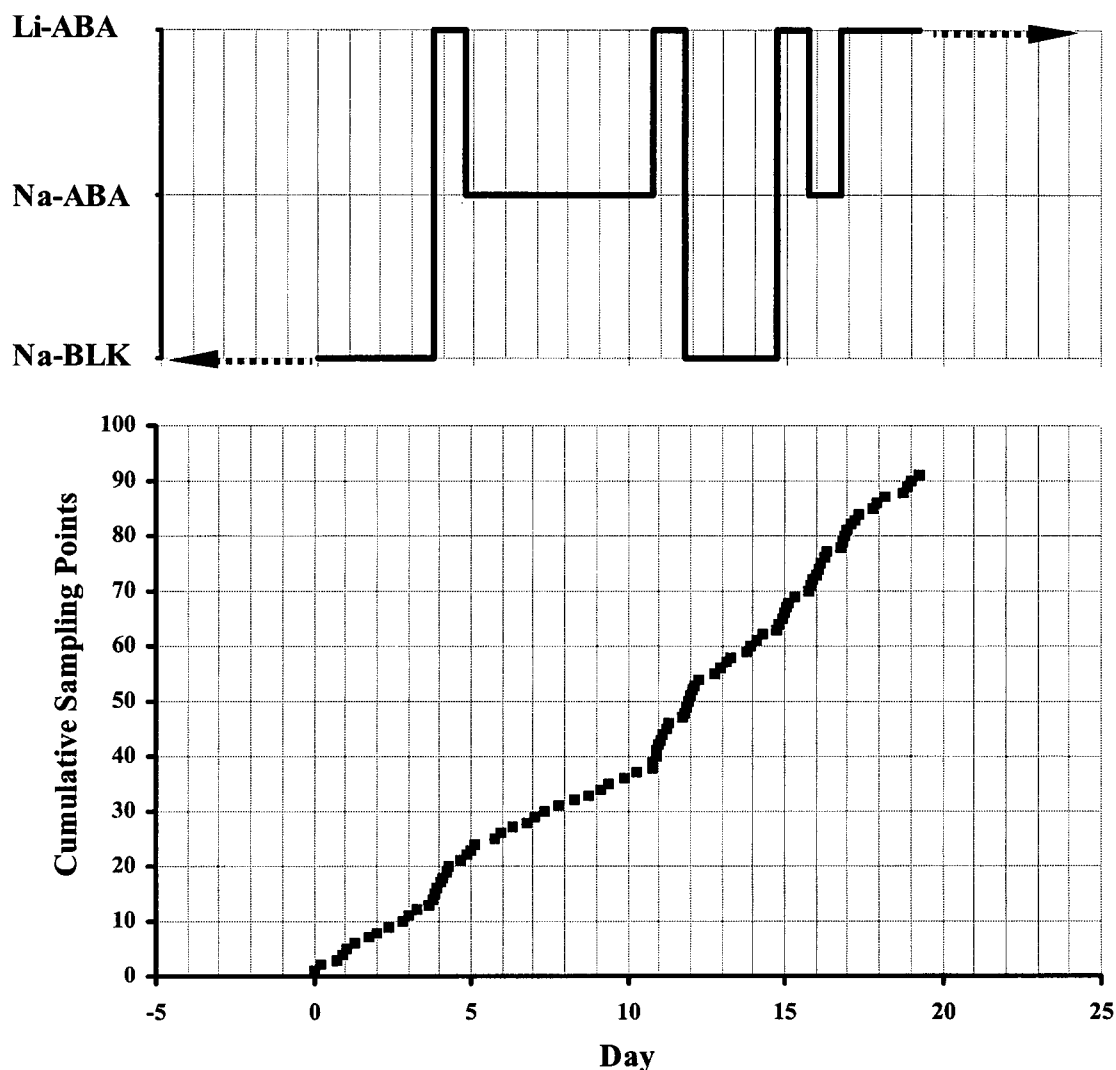


Figure 5-5. Tracer feed selection (Top) and sampling (Bottom) during the experiment. Three types of tracer solutions were fed to the bioreactors, namely, abietic acid saponified with lithium hydroxide (Li-ABA), abietic acid saponified with sodium hydroxide (Na-ABA) and the same sodium hydroxide solution without any resin acids (Na-BLK). Chemical content of the tracer solutions are given in Table 5-1.

(Chapter 4), and the filter samples were processed as described in Chapter 3.

5.2.4 Suspended solids batch growth experiment

A batch growth experiment was performed in order to estimate the readily biodegradable fraction of the TOC. In addition, it was of interest to consider, as a function of pH, microbial induction for resin acid metabolism, using batch cultivation conditions with the bioreactor suspended biomass as inoculum, in a medium of fresh BKME feed enriched with resin acids. The objective of this consideration of the batch growth kinetics was to compare the physiological state

of the microbial communities in the two parallel reactors with the same history, but differing in pH.

Batch medium was prepared by first heating two litres of BKME feed to 55°C and then, with constant agitation, adding 110 mL of the Na-ABA tracer solution (Table 5-1). As previously described (Chapter 3), the resin acid-enriched BKME feed was then decanted in 500 mL aliquots into shake flasks containing pre-weighed phosphorus salts to produce duplicate sets of 100 mM P-buffered media at pH 6 and 8. The media were autoclaved and, 12 hours prior to inoculation, adjusted to 37°C in an temperature-controlled room.

The batch growth experiment was performed approximately 12 hours after the last sampling event for the bench scale moving bed bioreactors. Bioreactor operating conditions were maintained after the last sampling event as shown in Figure 5-5. Aliquots of 5 mL from each of the two continuous systems were used to inoculate the respective shake flasks at pH 6 and 8. Just prior to inoculation, 5 mL of sterile 10% NH_4Cl was added to each shake flask. The pH was then checked and trimmed by dropwise addition of 50% H_2SO_4 . The inoculated shake flasks were agitated on a reciprocating table at 40 rpm to maintain aerobic growth conditions at 37°C. Activity in the flasks was monitored for approximately 30 hours after inoculation by periodic sampling to determine changes in TOC, resin acids and biomass levels. Sampling and analysis were as described in Chapter 3.

5.3 Results

The experimental results have been organized into eight subsections, each describing very specific aspects of the data reduction and interpretation. First (Section 5.3.1), the bioreactor operating conditions are presented. The moving bed bioreactors were found to be operating as completely stirred vessels over the duration of the experiment. The volumetric inflow and outflow rates were determined from measurements of the lithium tracer and, in addition, the average phosphorus and nitrogen concentrations. In section 5.3.2, the bioreactor performance was considered based on the removal of influent total organic carbon. The results indicated that a loss of TOC removal efficiency was associated with the applied load of resin acids. Next in Section 5.3.3, the suspended and biofilm reactor biomass were assessed in terms of the measured microbial fatty acid concentrations. From a comparison of the fatty acid compositions between the present and the previous (Chapter 4) investigations, it was found that, while pH exerted a stronger effect on the respective biofilm communities, HRT was the important factor influencing the suspended microbial communities. The results also suggested that community dominance in a bioreactor correlates with a relative degree of sensitivity to the bioreactor operating conditions.

Analysis of the population dynamics (Section 5.3.4), in terms of the time rate of change of the microbial fatty acid compositions (Chapter 4), indicated that resin acid loading fluctuations of less than about 10 hydraulic retention times would be too rapid to permit community level adjustment. Hence, community adjustment was indicated as the first step in the acclimation to a shift-up in resin acid input. The eventual metabolism of the elevated resin acid input was seen to progress in a manner dependent on the operating pH (Section 5.3.5). The ultimate extent of resin acid removal was better under alkaline conditions, corresponding to the previously observed (Chapter 2 and Chapter 3) increase in resin acid bioavailability under alkaline batch treatment conditions.

In section 5.3.6, the ambiguity of the interpretation of microbial fatty acid compositional change is considered more closely. The experimental results supported the notion that changes in fatty acid spectra for mixed cultures are overwhelmed by changes in the balance of species. In other words, an indication of fatty acid compositional change, relating to species level membrane

adaptations, was not detected. Following, the data of resin acid sorption to the biofilm biomass is presented in Section 5.3.7. Based on the sorption data, it was concluded that the contribution of the biofilm biomass towards resin acid metabolism must have been negligible for the present investigation. In contradiction to the results of Chapter 4, for longer contact times, resin acids under acidic aqueous conditions exhibited hysteresis effects in sorption. Thus, resin acids do not appear to adsorb reversibly in acidic aqueous conditions.

Finally, the results of the batch growth experiment to consider differences in physiological state are presented in Section 5.3.8. The data clearly demonstrated a difference in the physiological state for the communities of resin acid-degrading organisms obtained from the two parallel bioreactors. Furthermore, the results bring into question the commonly applied assumption of a constant growth yield coefficient for mixed culture batch growth experiments that are used to establish Monod kinetic parameters for microbial communities.

5.3.1 Bioreactor Operating Conditions

The goal of the first stage of data analysis was to characterize the bioreactor operating conditions. The average effluent flow rates for the two moving bed bioreactors are given in Table 5-2. Figure 5-6 shows the bioreactor lithium levels due to the tracer input feed that contained resin acids saponified by lithium salts. The average level of lithium in the Li-ABA (Table 5-1) tracer feed was 523 ± 36 mg Li/L. Based on the results of Chapter 4, the bioreactors were assumed to be ideally mixed. Therefore, the time rate change of the bioreactor lithium concentration could be modelled (Levenspiel 1984) by the equation:

$$\frac{\partial L_e}{\partial t} = \frac{Q_t}{V} L_t - \frac{Q_e}{V} L_e = \frac{1}{\theta_H} (D_f \cdot L_t - L_e), \quad D_f = \frac{Q_t}{Q_e}, \quad \theta_H = \frac{V}{Q_e} \quad (5-2)$$

where L is the lithium concentration in the effluent (e) and tracer feed (t), Q similarly represents the respective effluent and tracer feed volumetric flow rates, V is the reactor liquid volume, θ_H is the hydraulic retention time, and D_f is the tracer dilution factor.

The model of equation (5-2) was fitted to the experimental data by successive fourth order

Table 5-2. MBBR volume estimated from measurements of effluent flow. From the wash-in and out functions for step changes of lithium salt loading, the reactors were determined to be ideally mixed and an HRT was calculated.

Parameter	Reactor A pH = 6.0 ± 0.1	Reactor B pH = 8.0 ± 0.1	Units	Description
Q _e	426 ± 16	401 ± 16	mL/hr	Effluent flow rate
D _f	0.0562	0.0557	-	Lithium dilution factor
HRT	5.25	5.28	hr	Hydraulic retention time
V	2234	2117	mL	Liquid volume

Table 5-3. Average nutrient levels (phosphorus and nitrogen) for the two MBBR reactors and the BKME feed.

	Reactor A pH = 6.0 ± 0.1	Reactor B pH = 8.0 ± 0.1	Feed
Total-P (mg P/L)	378 ± 17	119 ± 14	4.1 ± 0.4
Kjeldahl-N (mg N/L)	38 ± 2	33 ± 2	14.3 ± 1.5

Runge-Kutta integration with non-linear regression parameter optimization (see Chapter 2.2.3, Non-linear Regression Analysis). Using the best fit model parameters that are listed in Table 5-2, the model for ideally mixed conditions can be seen to provide a good representation of the experimental data in Figure 5-6. From the lithium tracer model parameters, the liquid volume could be derived from the estimated effluent flow rate and HRT (Table 5-2).

The average measured nutrient levels in the two reactors as well as in the feed are given in Table 5-3. In a similar fashion to that of the previous investigation, the experimental feed and supplemental influent flows were calculated based on considerations of continuity and conservation of mass. In this case the additional inflow (Q) had to also be accounted for. By continuity:

$$Q_e = Q_f + Q_N + Q_P + Q_t \quad (5-3)$$

$$Q_e - Q_t = Q_e(1 - D_f) = Q_f + Q_N + Q_P$$

where the subscripts f, P, and N refer to BKME feed, phosphorus and nitrogen inflow rates respectively. Conservation of nitrogen (N) and phosphorus (P) were described by:

$$N_f Q_f + N_N Q_N = N_e Q_e \quad (5-4)$$

$$P_f Q_f + P_P Q_P = P_e Q_e$$

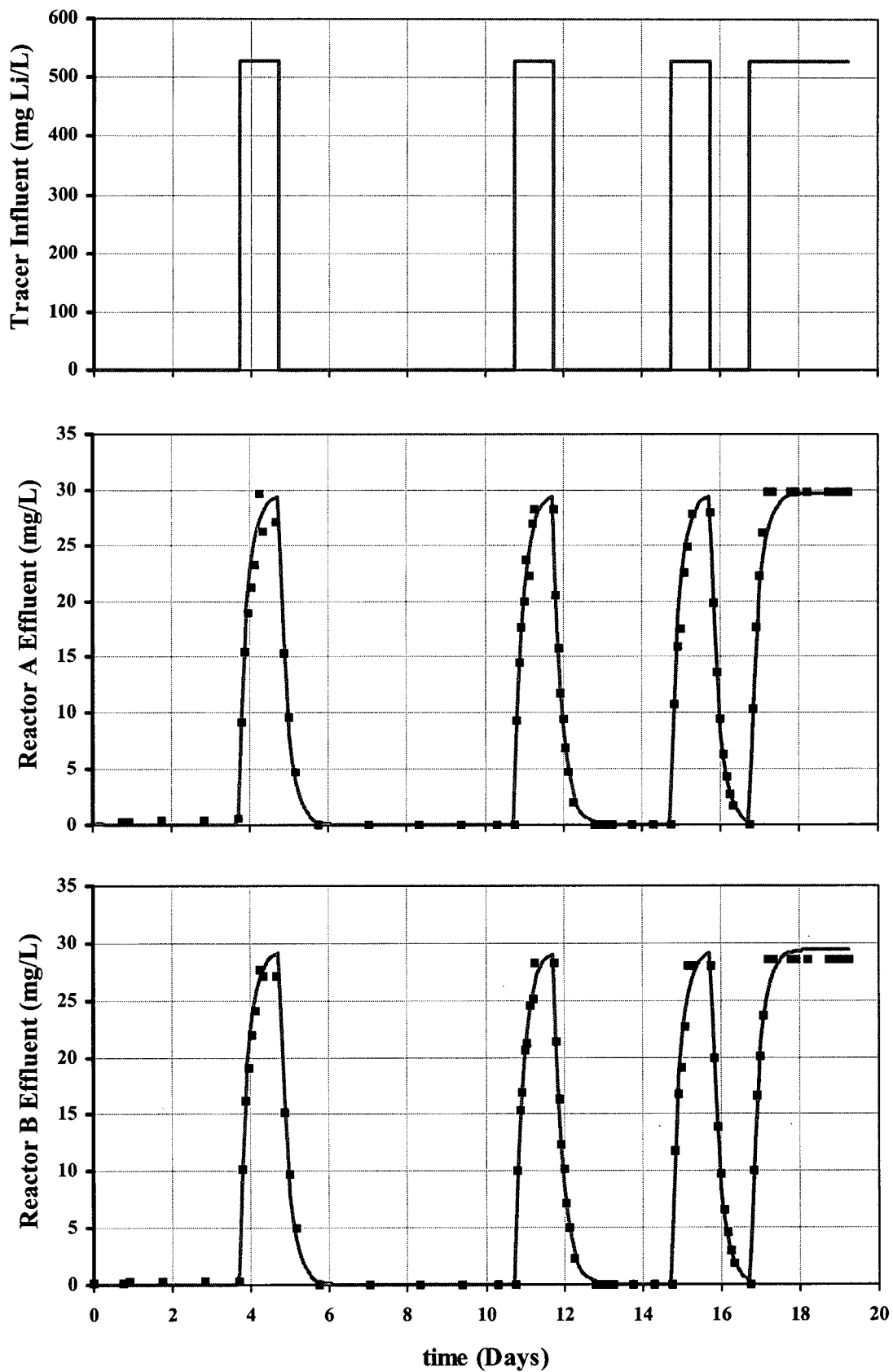


Figure 5-6. Lithium input (top) and the measured lithium effluent levels in reactor A (middle) and B (bottom) during the course of the experiment. The lithium data are described by the model given in equation (5-2). Least squares model parameters were determined by iterative numerical integration and non-linear optimisation.

Table 5-4. Estimated bioreactor volumetric inflow rates based on the conservation of mass balance for lithium, phosphorus and nitrogen and flow continuity. Volumetric flow rates are in mL/hr.

Flow Variable	Reactor A	Reactor B	Description
Q_e	426	401	MBBR effluent (total) flow
Q_f	335	364	BKME feed rate
Q_t	24	22	Tracer flow
Q_N	7	5	N-feed rate
Q_P	59	10	P-feed rate

where N and P are nitrogen and phosphorus concentrations with the same subscript notation defined by equation (5-3). The estimated volumetric inflow rates are listed in Table 5-4.

5.3.2 The Effect of Resin Acids on Treatment Performance

The performance of the bioreactors was expressed as the efficiency of removal of influent total organic carbon (TOC). The mean TOC concentrations in the BKME feed and in the effluents of reactors A and B are reported in Figure 5-7. TOC removal efficiency was calculated as follows:

$$\varepsilon^f = 100 \cdot \left(\frac{Q_f TOC^f - Q_e TOC^e}{Q_f TOC^f} \right) \% \quad (5-5)$$

where ε^f is the removal efficiency, TOC^f is the BKME feed TOC level and TOC^e is the effluent TOC level. On average, reactor A and B removed 37 and 44 percent of the BKME influent TOC respectively. The TOC level in the BKME feed was observed to decay slightly over time (Figure 5-8) following first order kinetics:

$$TOC^f = TOC_0^f \exp(-k^f t) \quad (5-6)$$

The initial BKME feed TOC (TOC_0^f) was about 486 mg C/L and the decay rate constant (k^f) was estimated to be 0.0082 day⁻¹. Thus, while the BKME feed TOC levels were similar to those of the previous experiment (Chapter 4), significantly less TOC removal was observed for the same bioreactors, now operating at a longer HRT. In the previous experiment, both reactors were

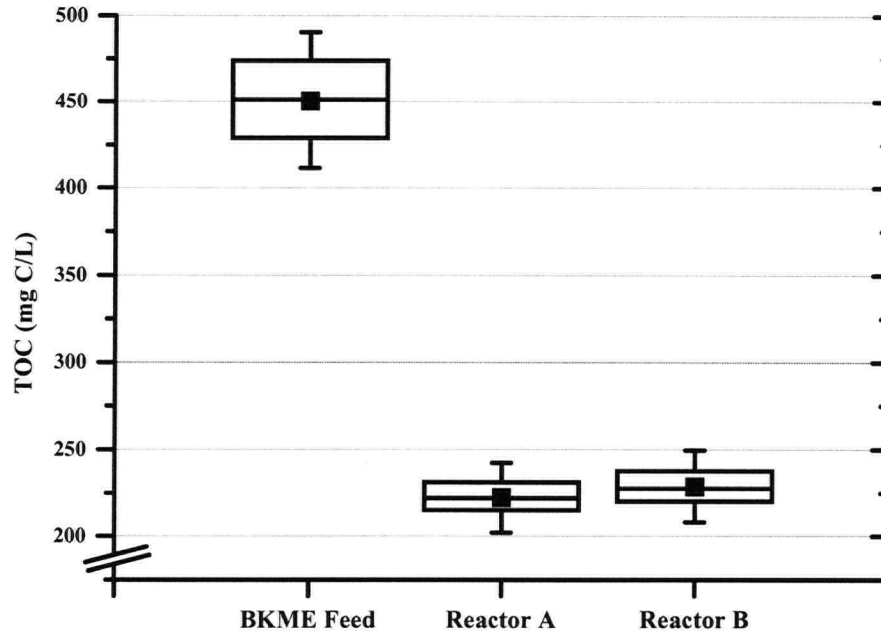


Figure 5-7. Average TOC levels in the BKME feed and the two bioreactors from 84 samples taken over the 21 day experiment. Correcting for the feed dilution due to the supplementary influent flows, the TOC removal efficiencies were 37 and 44 percent for reactors A and B respectively.

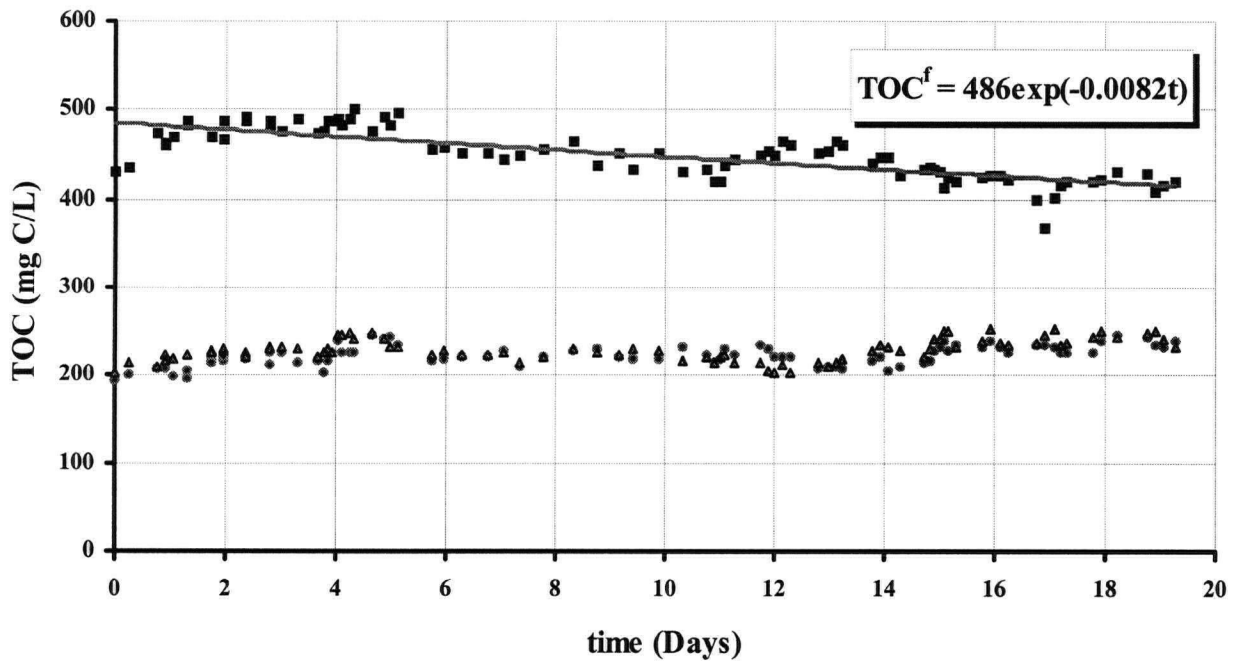


Figure 5-8. Measured TOC levels over time for the BKME feed (■), reactor A (●) and reactor B (▲). The BKME feed TOC (TOC^f) decayed over time following first order kinetics.

observed to remove about 57 percent of the influent BKME TOC.

There was no observed reduction in the effluent TOC levels corresponding to the TOC decay of the stored feed. Instead, the removal efficiency was observed to decrease over time. Considering the estimated first order decay in BKME feed TOC, the TOC removal efficiency should have followed an equation of form:

$$\varepsilon^r = 100 \cdot \left(1 - \frac{TOC^e}{TOC_0^f} \exp(k^f t) \right) \% \quad (5-7)$$

Therefore, the removal efficiency data were modelled with the following equation:

$$\varepsilon^r = 100 \cdot \left(1 - \varepsilon^0 \exp(k^\varepsilon t) \right) \% \quad (5-8)$$

where ε^0 is a constant and k^ε describes the rate of the decrease in removal efficiency. It was expected that if the decrease in removal efficiency was due only to the reduction in feed TOC levels, then the estimated rate constant k^ε would be approximately equal to k^f . The removal efficiency data and the model curves for equation (5-8) are shown in Figure 5-9. The initial removal efficiencies for reactor A and B were 44 and 50 percent respectively. The best fit rate constant k^ε was found to be equal to 0.014 day^{-1} , significantly larger than k^f . Thus the actual extent of TOC removal apparently decreased over the course of the experiment, beyond that accountable for by the slight reduction in influent TOC concentration. It was possible that this observed decrease in TOC removal performance could be associated with the applied load of resin acids to the system.

To address this possibility, the TOC removal efficiency data were further considered by calculating the residuals (Figure 5-10) with respect to the estimated model of equation (5-8). For each reactor, a cluster of outlying points of improved TOC removal efficiency was observed and these appeared to fall well outside the background scatter. This group of outlying points was determined to be significantly different from the rest of the residual errors. It was interesting to find that the occurrence of this group of outlier points corresponded roughly with the timing of

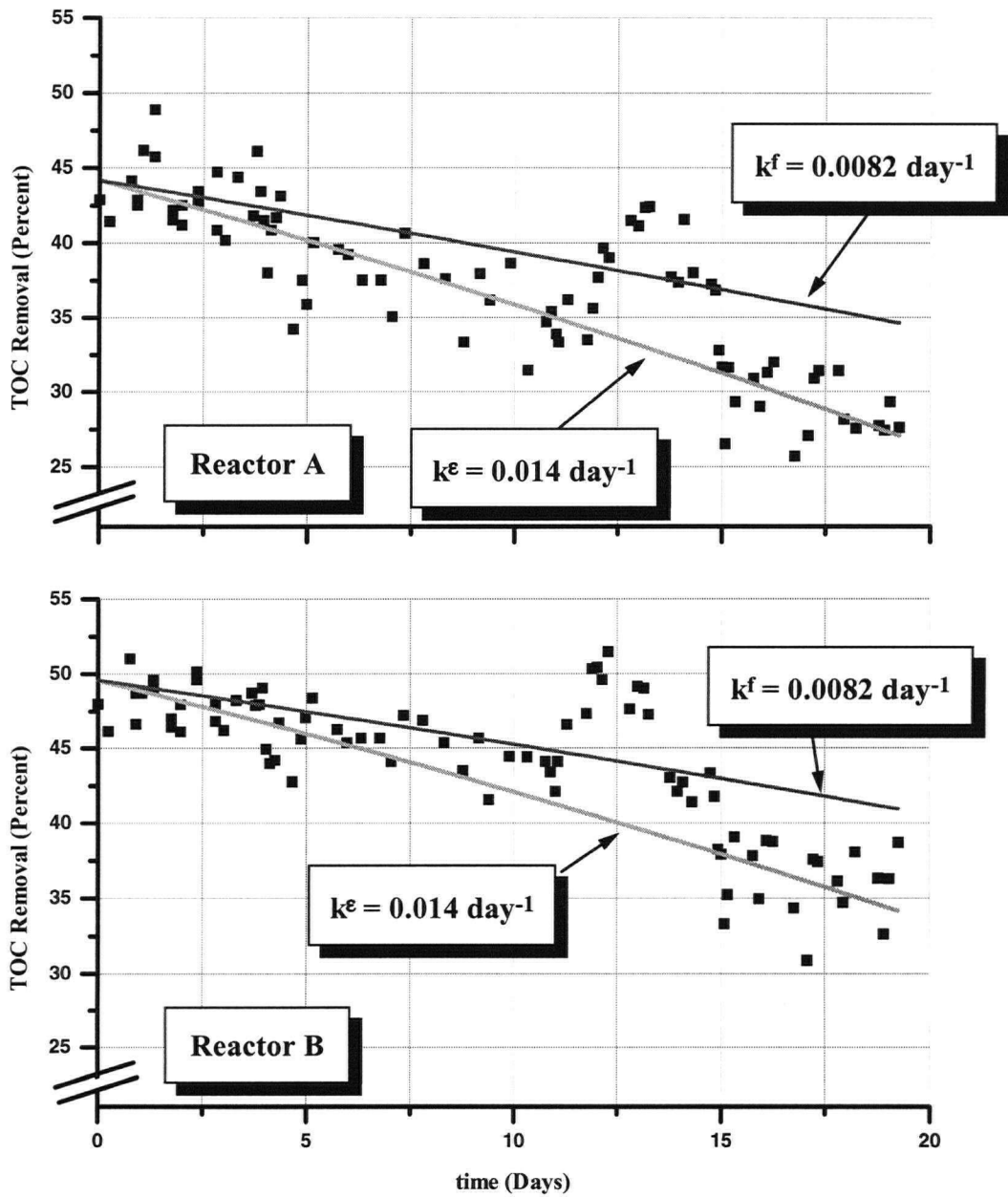


Figure 5-9. Progress of TOC removal for reactors A and B over time. Model curves (equation (5-8)) are shown along with the experimental data. The estimated decay rate coefficient (k^e) was 0.014 day^{-1} which indicated a reduction in the reactor performance that was greater than that expected from BKME feed decay ($k^f = 0.0082 \text{ day}^{-1}$) alone.

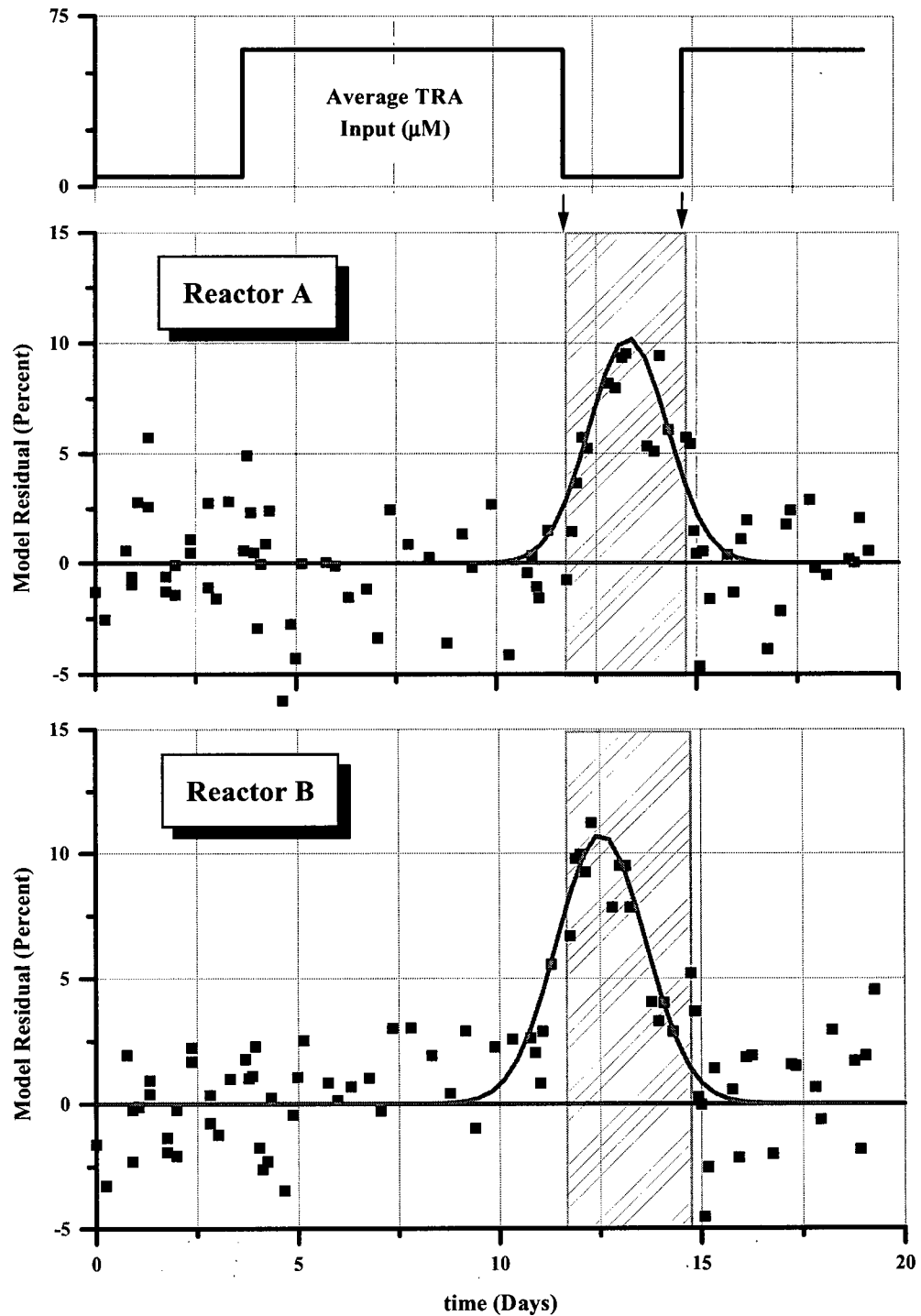


Figure 5-10. The residual errors between the models plotted in Figure 5-9 and the measured TOC removal efficiencies. A cluster of outlier residual values were found in the period corresponding to the removal of the augmented resin acid input. The outlying points were statistically significant and indicated an improvement in reactor performance corresponding to reduced resin acid loadings.

low resin acid loading (Figure 5-10). Therefore, the data suggested that with the additional resin acid loading there was an apparent suppression in TOC removal, since a temporary relief in resin acid loading was associated with a temporary improvement in TOC reduction.

5.3.3 Biomass Characterization

Biomass levels were once again assessed in terms of total fatty acids (TFA). The spectra of identified fatty acids are reported in Table 5-5. Box plots for the TFA levels are presented in Figure 5-11. For comparison, the TFA levels reported in Chapter 4 are shown as well. Increasing the hydraulic retention time had the effect of increasing the proportion of suspended growth. Also, the biomass levels in the reactor effluent were, on average, less than the levels measured within each of the reactors. Approximately 10 and 11 percent of the suspended biomass in reactor A and B were being retained, respectively. Some degree of settling of the suspended biosolids is believed to have prevented complete discharge at the overflow. This indicated that the residence time for the suspended growth extended slightly beyond the hydraulic retention time.

From the estimated total amount of biomass in the two reactors (Table 5-6) the biofilm and suspended biomass levels could be compared on a common basis. The total biofilm biomass was estimated based on the data presented in Table 5-7. The contribution of the biofilm to the overall biomass content was reduced as a consequence of the increased HRT used for this investigation. Similar to the results reported in Chapter 4, the acidic conditions of reactor A promoted a significantly higher overall total reactor biomass content without any associated improvement in TOC removal.

The marker dienoic fatty acid, octadecadienoic acid, gave a first impression of the significance of background interference from wood-derived fatty acids (Chapter 4) on estimated TFA biomass levels. On average, the level of 18:2(9c,12c) in the BKME feed was reduced by about 80 percent from the BKME feed by passage through the MBBRs (Table 5-5). The complete removal of 18:2(9c,12c) would have provided strong support for the assumption that the fatty acid spectra

Table 5-5. Average extracted fatty acid liquid concentrations and surface loadings for suspended and biofilm samples. Samples were obtained over 96 hours of operation. Fatty acids are identified by their shorthand designation (Chapter 3). Equivalent chain length (ECL) values are also reported.

Fatty Acid	ECL	BKME Influx (μmoles/L)	Reactor A			Reactor B		
			Suspended (μmoles/L)	Effluent (μmoles/L)	Biofilm (nmoles/cm ²)	Suspended (μmoles/L)	Effluent (μmoles/L)	Biofilm (nmoles/cm ²)
3OH-10:0	11.350	0.080 ±0.129	1.199 ±0.131	1.082 ±0.115	0.707 ±0.124	1.542 ±0.319	1.360 ±0.277	0.568 ±0.097
12:0	12.000	0.223 ±0.466	1.069 ±0.138	1.099 ±0.138	0.643 ±0.187	1.028 ±0.171	0.882 ±0.124	0.552 ±0.103
i14:0	13.628				0.310 ±0.050	0.354 ±0.083	0.336 ±0.058	0.371 ±0.090
14:0	14.000		0.381 ±0.080	0.346 ±0.088	0.607 ±0.075	0.412 ±0.112	0.377 ±0.107	0.303 ±0.065
i15:0	14.632		0.424 ±0.124	0.378 ±0.116	1.558 ±0.124	0.499 ±0.189	0.621 ±0.208	0.665 ±0.115
a15:0	14.709		0.532 ±0.184	0.473 ±0.214	1.519 ±0.147	1.596 ±0.166	1.512 ±0.176	1.018 ±0.215
15:0	15.000		0.390 ±0.079	0.284 ±0.089	0.418 ±0.045	0.806 ±0.207	0.770 ±0.178	0.307 ±0.041
3OH-14:0	15.431		0.330 ±0.050	0.272 ±0.037	0.478 ±0.057	0.434 ±0.059	0.377 ±0.058	0.293 ±0.028
i16:0	15.631				0.301 ±0.033	0.271 ±0.053	0.255 ±0.054	0.365 ±0.062
16:1w7c	15.772	5.789 ±1.214	14.684 ±1.211	13.458 ±1.181	2.747 ±0.667	15.161 ±2.923	13.140 ±2.609	1.600 ±0.280
16:0	16.000	2.142 ±0.190	12.701 ±1.258	11.123 ±1.112	7.924 ±1.023	13.303 ±2.722	11.560 ±2.405	3.633 ±0.536
i17:0	16.632				0.188 ±0.033			
a17:0	16.714				0.429 ±0.109	0.509 ±0.423	0.505 ±0.491	0.294 ±0.057
17:1w9c	16.763	1.849 ±0.449						
cy17:0w7	16.836		0.646 ±0.090	0.540 ±0.103	2.833 ±0.320	0.839 ±0.230	0.751 ±0.213	1.793 ±0.269
17:0	17.000	0.334 ±0.040	0.281 ±0.040	0.248 ±0.029	0.536 ±0.102	0.481 ±0.176	0.440 ±0.156	0.172 ±0.041
2OH-16:0	17.182		1.903 ±0.926	1.664 ±0.870	0.921 ±0.256			0.878 ±0.293
18:2(9c,12c)	17.648	1.418 ±0.707	0.305 ±0.137	0.334 ±0.133		0.333 ±0.076	0.378 ±0.076	
18:1w9c	17.720	1.598 ±0.684	0.297 ±0.037	0.262 ±0.043		0.425 ±0.077	0.413 ±0.078	
18:1w7c	17.781	1.399 ±0.574	6.489 ±0.563	5.895 ±0.453	6.549 ±0.962	8.301 ±1.438	7.485 ±1.264	3.801 ±0.578
18:1w7t	17.827				0.430 ±0.069			0.335 ±0.053
n18:0	18.000	0.621 ±0.089	0.716 ±0.082	0.644 ±0.082	2.097 ±0.463	0.958 ±0.091	0.861 ±0.088	0.754 ±0.218
cy19:0w9	18.846		0.566 ±0.126	0.513 ±0.100	9.862 ±2.169	0.806 ±0.266	0.665 ±0.138	1.960 ±0.366
Total		15.453 ±1.804	42.912 ±2.092	38.613 ±1.936	41.055 ±2.763	48.061 ±4.317	42.689 ±3.841	19.663 ±1.070

Table 5-6. Estimated TFA biomass levels (μmoles) for Reactors A and B. Biomass levels are also reported for the previous investigation for comparison. The increase in HRT can be seen to promote a greater level of suspended growth and of biomass overall. In the previous investigation reactor A maintained about 20 percent more biomass. For this investigation reactor A contained 44 percent more biomass.

	$\theta_H = 2.8 \text{ hr}$ (Chapter 4)		$\theta_H = 5.3 \text{ hr}$ (This Investigation)	
	Reactor A	Reactor B	Reactor A	Reactor B
Total Suspended	46	56	95	100
Total Biofilm	145	102	152	71
Total Biomass	191	158	247	171

Table 5-7. Values used to determine the total biofilm area.

Variable	Value	Units	Description
W_c	0.221 ± 0.018	g	Average weight
ρ_c	0.985	g/cm^3	Plastic density
A_c	$3.588 + 0.286$	cm^2	Average surface area
N	1057 ± 85		Number of units
A	3793	cm^2	Total biofilm area

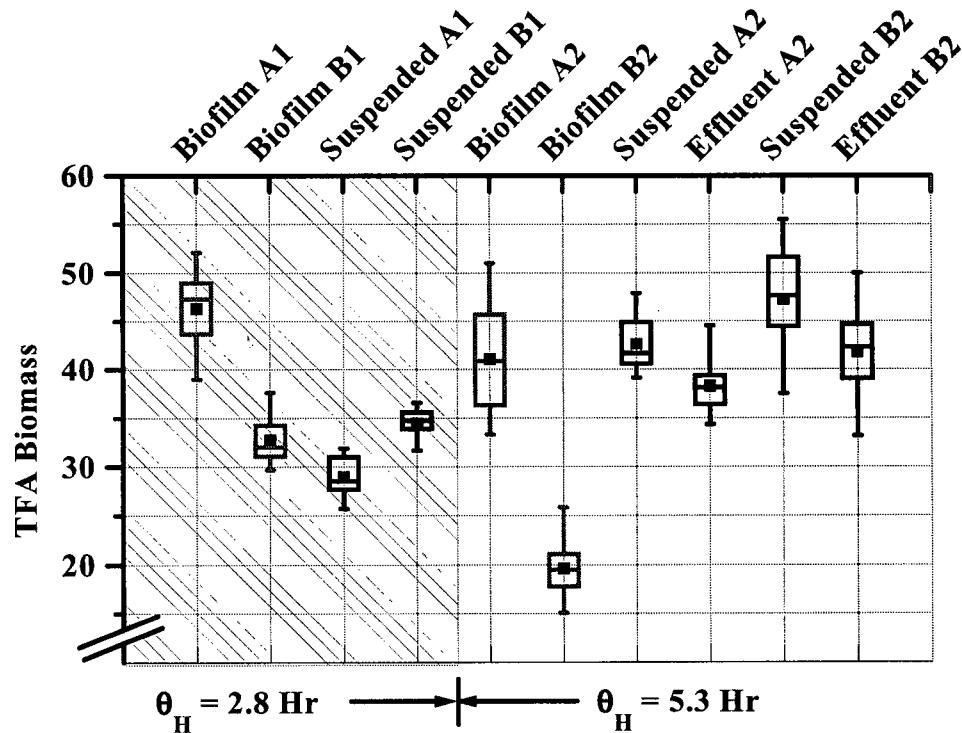


Figure 5-11. Biomass levels as total fatty acid (TFA). Levels in reactors A and B are given for both the previous experiment reported in Chapter 4 (1) and for the current investigation (2). The units are nmoles/cm^2 for biofilm surface loadings and $\mu\text{moles/L}$ for suspended and effluent concentrations. Effluent levels refer to samples taken of the effluent overflow. Increased HRT promoted higher suspended growth and less biofilm. On average, suspended biomass levels in the reactors were slightly greater than the effluent levels found in the overflows, indicating some suspended biomass retention.

obtained from the two reactors were exclusively derived from the viable biomass content (Chapter 4). The detection of this fatty acid in the suspended and effluent fatty acid spectra did not necessarily indicate that the spectra were "contaminated" by free fatty acids of wood origin. Dienoic fatty acids are also present in the membranes of fungi (Harwood and Russell 1984) and it is not unreasonable to speculate that the longer HRT used for this investigation promoted some level of fungal growth. Therefore, additional evidence was required to be able to conclude that the bioreactor fatty acid spectra were due primarily to the presence of viable microorganisms.

This necessary experimental evidence was obtained with the data collected from the suspended solids control experiment (Section 5.2.3). Figure 5-12 expresses the proportions of suspended and dissolved total resin acids (TRA) and total fatty acids (TFA) as percentages of the total concentrations. Measurements in triplicate were processed for samples from reactor A (pH 6), reactor B (pH 8) and the BKME feed (pH 10). Resin acids and fatty acids are both hydrophobic carboxylic acids. Increasing pH increases the solubility of resin acids (Chapter 3) and fatty acids alike. As expected, the TRA data indicated a higher dissolved fraction at higher pH. On the other hand, the relative amounts of suspended TFA in reactors A and B were approximately the same. The dissolved fraction of TFA in reactors A and B was only 2 percent. In contrast, TFA in the BKME feed was almost 80 percent dissolved. This result was interpreted to indicate that the high proportion of suspended TFA in the two reactors resulted predominantly from the contribution of the TFA from biosolids.

This interpretation of the TFA data was considered further by comparing the whole, filtrate and filter fatty acid compositions obtained for the suspended solids control study. Figure 5-13 presents the dendrogram produced from an analysis of compositional similarity (Chapter 3). The clusters illustrated that the whole sample spectra from reactors A and B were most similar to the filter spectra. Conversely, the filtrate spectra from A and B were grouped with the filtrate and whole sample spectra of the BKME feed. Thus, the cluster analysis demonstrated that the soluble fraction of the TFA spectra exhibited some degree of similarity to the BKME feed, but the whole samples were most similar to the suspended fraction. Since the soluble fraction of the TFA

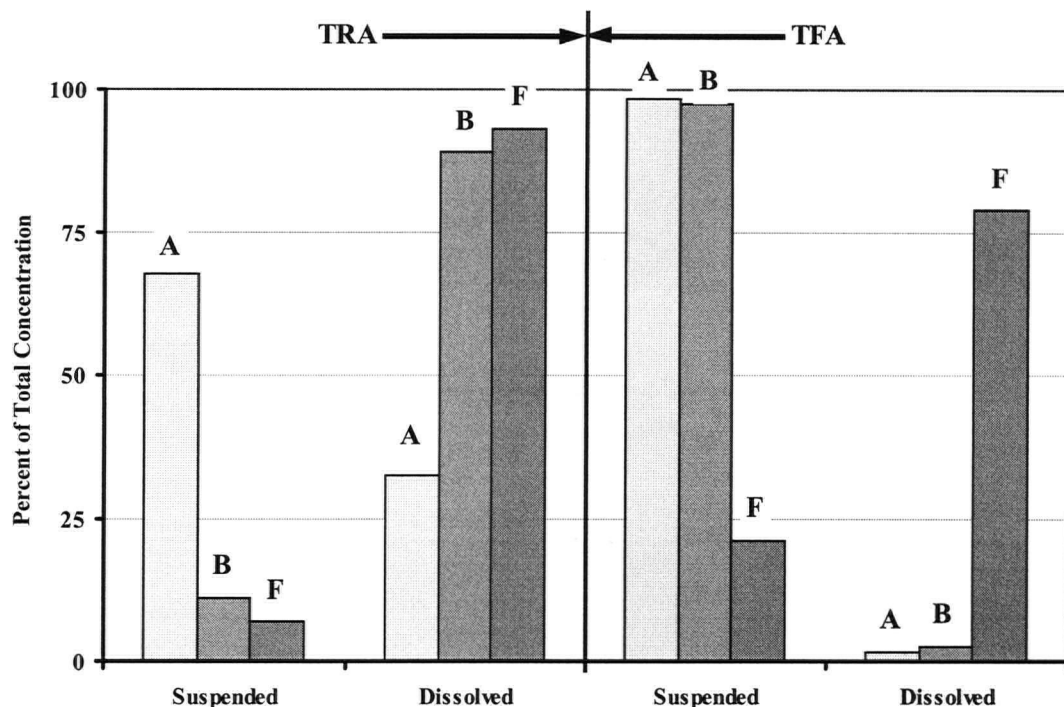


Figure 5-12. Amounts of suspended and dissolved total resin acids (TRA) and total fatty acids (TFA) expressed as a percent of the total concentration. Triplicate whole, filter and filtrate samples were taken for reactor A (A) at pH 6.0, reactor B (B) at pH 8.0 and the BKME feed (F) at pH 9.5. TRA data followed the expected trend with pH for the solubility of a hydrophobic carboxylic acid (Chapter 3). On the other hand, the suspended fraction of the TFA for reactors A and B was not sensitive to pH. Therefore, aqueous TFA samples were dominated by suspended solids considered to be viable biomass.

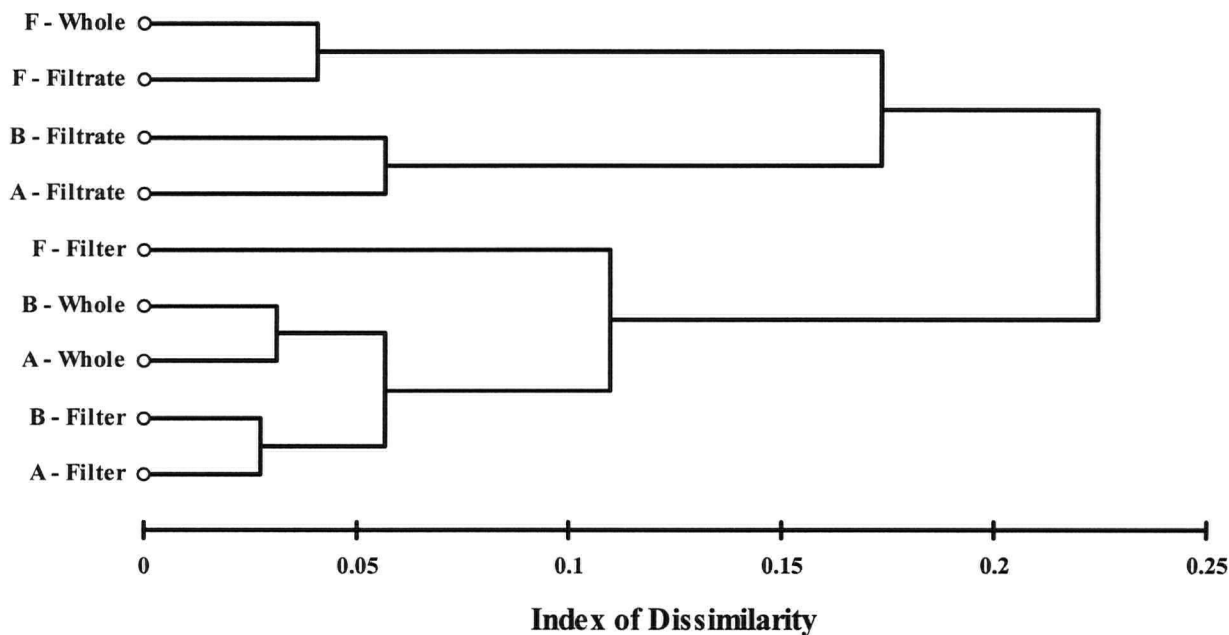


Figure 5-13. Dendrogram relating the similarities of fatty acid spectra from whole, filter and filtrate samples drawn from reactor A (A), reactor B (B) and the BKME feed (F). The matrix of similarities was calculated following the method described in Chapter 3. The dendrogram was formed by Ward's method (Aldenderfer and Blashfield 1984). These results indicate the distinction between the fatty acid composition of the feed and the bioreactors. Fatty acid spectra for the whole aqueous samples from the two bioreactors most closely resemble those of the suspended solids. The suspended solids contributions to the TFA of the two bioreactors was 98% of the total.

spectra from reactors A and B was only two percent of the total, it was felt that the degree of interference from free fatty acids was, therefore, negligible.

It was interesting to also note from Figure 5-13 that the BKME feed filter fatty acid spectra were clustered with the reactor A and B whole and filter samples. Therefore, a proportion of the fatty acids extracted from the feed were likely derived from viable microorganisms that may have been responsible for reducing the level of TOC in the BKME feed reservoir.

Averaged fatty acid spectra were used for a comparison of the suspended and biofilm communities in this and the previous experiment reported in Chapter 4. An analysis of similarity (Figure 5-14) yielded the interesting result that the biofilm communities were most similar between the two experiments and the suspended communities were most similar within each experiment. This result suggested that pH exerted a more pronounced effect on the biofilm community development and, in contrast, HRT was the important factor for the suspended biomass community.

Some degree of selection was also apparent from a comparison of the suspended and effluent communities sampled in this investigation (Figure 5-15). The respective suspended and effluent fatty acid spectra were related, although they were sufficiently different to be discriminated by logcontrast canonical component analysis (Figure 5-16). This result highlights the fact that the peculiarities of bioreactor design and operation impose some degree of selective pressure on the biomass. In this case, the method of effluent withdrawal retained some organisms preferentially to others. The relative impact of such selective pressures can be assessed by community analysis using microbial fatty acids.

The suspended and biofilm communities were discriminated by LCCA (Figure 5-17). The difference between suspended and biofilm communities accounted for most of the variance in a similar way to the results reported in Chapter 4. Once again the second two components appeared to be related to the influence of pH on the community development. In contrast to the previous investigation, here pH exerted a larger relative influence on the suspended biomass.

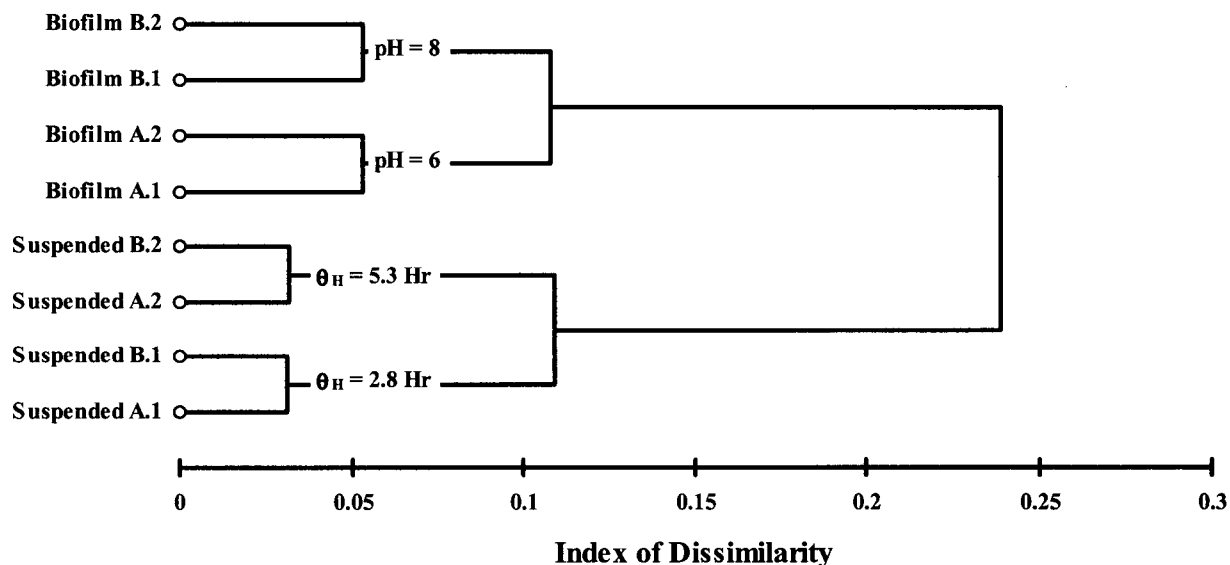


Figure 5-14. Dendrogram relating the similarities of fatty acid spectra from biofilm and suspended samples from reactor A (A) and reactor B (B) for the experiment reported in Chapter 4 (1) and the current investigation (2). The matrix of similarities was calculated following the method described in Chapter 3. The dendrogram was formed by Ward's method (Aldenderfer and Blashfield 1984) using XLSTAT Version 3.4. As indicated, fatty acid spectra for the biofilm biomass were grouped first corresponding to conditions of pH. In contrast, the spectra for the suspended biomass were grouped first according to the condition of HRT.

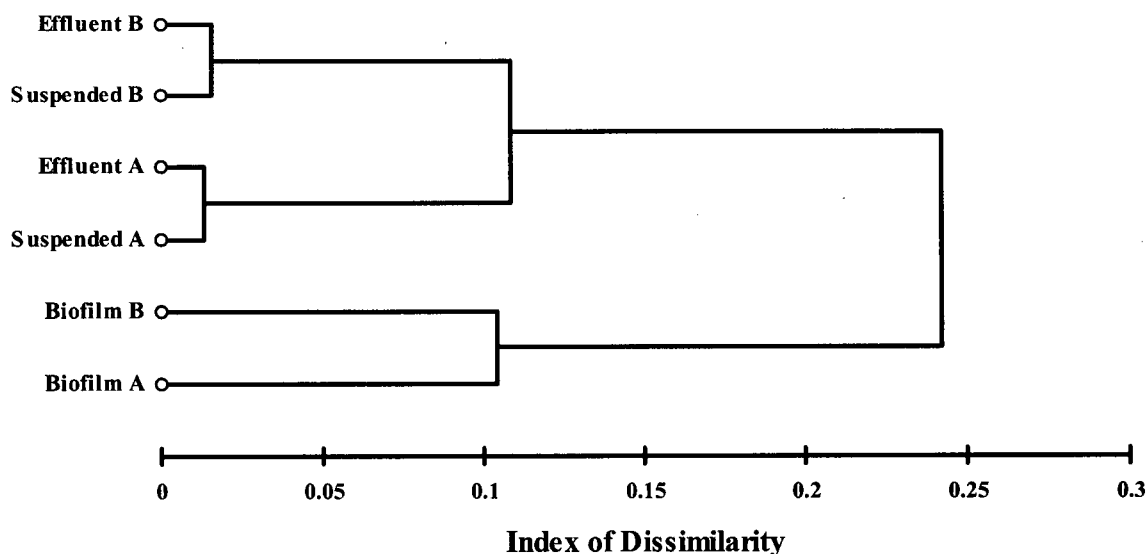


Figure 5-15. Dendrogram relating the similarities of fatty acid spectra from biofilm, suspended and effluent samples from reactor A (A) and reactor B (B) for the current investigation. The matrix of similarities was calculated following the method described in Chapter 3. The dendrogram was formed by Ward's method (Aldenderfer and Blashfield 1984) using XLSTAT Version 3.4. Fatty acid spectra from effluent samples were similar but distinctly different from those from suspended samples. It was also observed that the reactors retained about 10 percent of the suspended biomass (Figure 5-11). Therefore, there was some degree of selective biomass retention imposed by the bioreactor design.

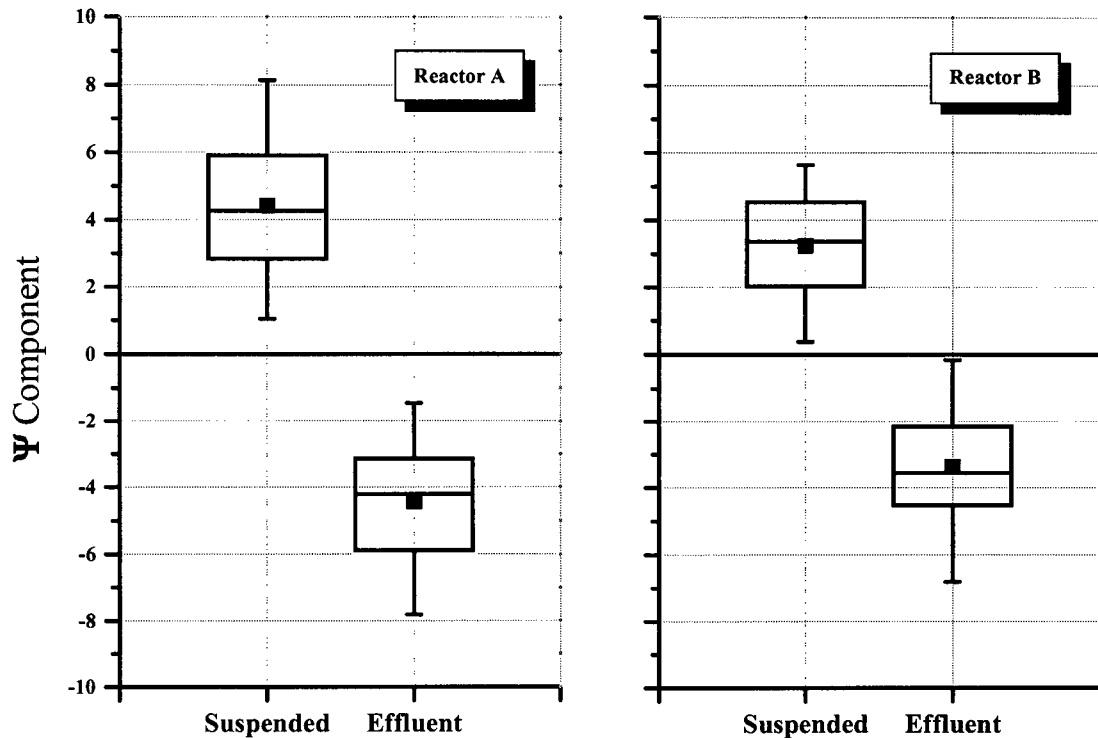


Figure 5-16 Discrimination between the suspended and effluent microbial communities based on their fatty acid spectra. The compositional data from the two sample groups were compared by logcontrast canonical component analysis. Only one logcontrast canonical component (LCC) results when there are just two categories. This component is the same as a discriminant score (Aitchison 1986). The LCC or logcontrast discriminant score was weighted by its eigen value (variance) to normalize the results between reactor A and B. Thus the data are plotted in terms of the weighted logcontrast canonical component (see Chapter 4). The compiled data represent spectra from 21 days of observation. The suspended (within reactor) and effluent (exiting) communities were concluded to be distinct.

Since, for this investigation, the suspended growth was the dominant fraction of the biomass, it is interesting to speculate that community dominance may correlate with environmental sensitivity.

In other words, the more predominant community of microorganisms in a bioreactor would appear to become more finely tuned to environmental operating conditions such as pH.

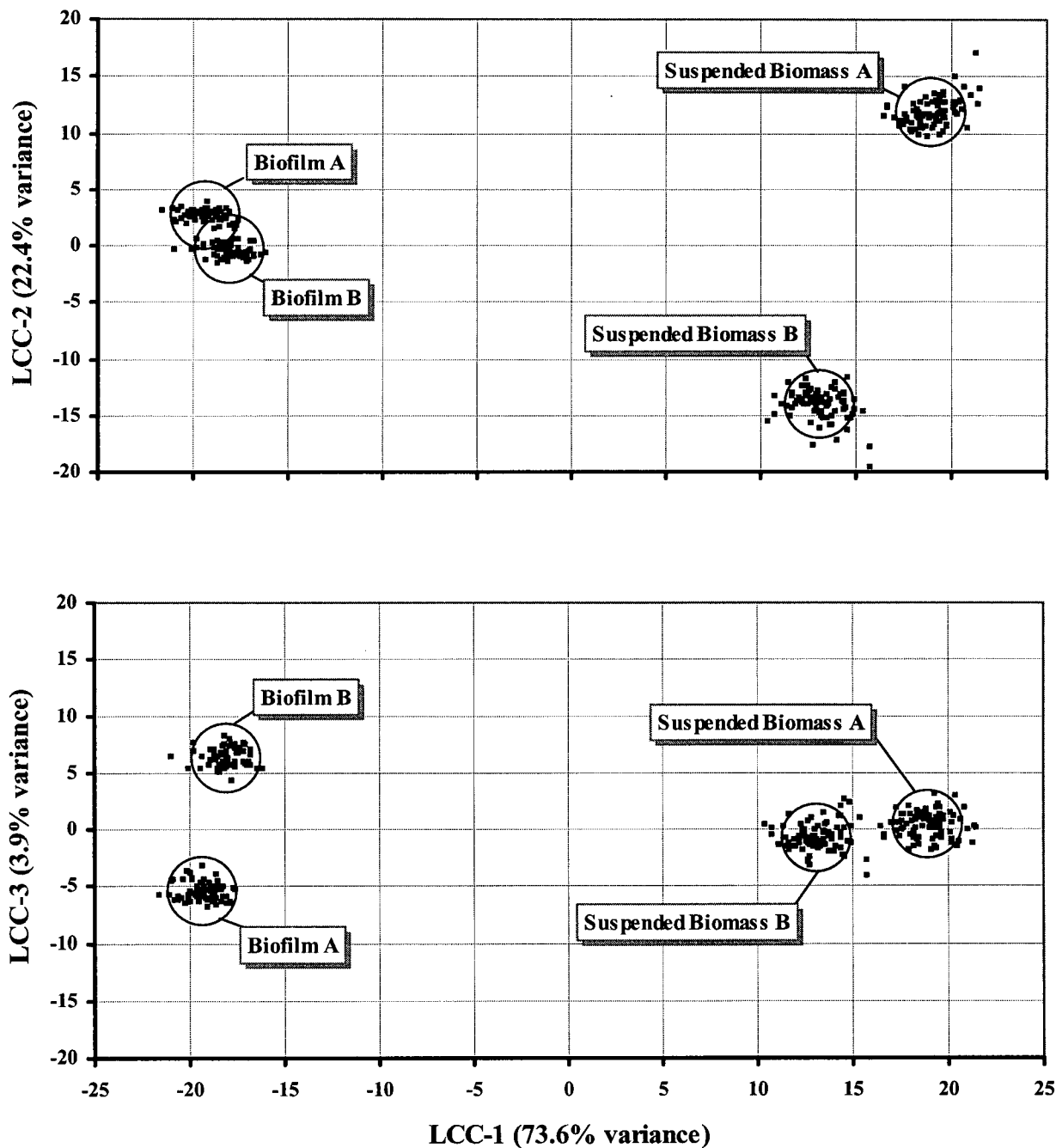


Figure 5-17. Logcontrast canonical components (LCC) of the fatty acid spectra for suspended and biofilm extracts. Individual observations are shown along with the mean values given by the centre of the circle around the respective data clusters. The canonical components were calculated using logratios with hexadecanoic acid (16:0) as the common divisor. The first component (LCC-1) distinguishes biofilm from suspended communities while the second and third components separate the influence of pH on the suspended and biofilm microbial ecology respectively.

5.3.4 Population Dynamics

Population dynamics were represented in terms of the state speed parameter, that was developed in Chapter 4 and defined by equation (4-42). State speed measures the time rate of change of microbial fatty acid compositions. If a change in the microbial fatty acid composition, for a complex community, is predominantly due to a change in the balance of species, then state speed provides an indication for the rate of transition in community structure. The results of the logcontrast canonical component analysis are reported in Tables 5-8 through to Table 5-11. As for the previous investigation, only the first three components were retained. Judging from the sum of the latent roots, the suspended and the biofilm biomass fatty acid spectra exhibited similar levels of variability, indicating a similar degree of compositional change over time. Hence, community structure was observed to be in a constant state of flux. As a result, a steady state

Table 5-8. Results of logcontrast canonical component analysis on the time series of suspended biomass samples taken from Reactor A. Sequential sub-groups of at least 5 observations were used.

Eigen Values				
Latent Root	λ_1	λ_2	λ_3	$\Sigma\lambda_i$
Eigen Value	55.80	25.24	13.80	94.83
Percent	52.33	23.67	12.94	88.93
Eigen Vectors				
Fatty Acid	ECL	b_1	b_2	b_3
3OH-10:0	11.350	-1.35	-10.33	-3.15
12:0	12.000	-2.86	3.11	-7.24
14:0	14.000	-4.79	-2.90	-8.49
i15:0	14.632	1.66	-4.23	3.97
a15:0	14.709	-1.72	8.09	3.80
15:0	15.000	-5.02	6.13	0.35
3OH-14:0	15.431	-2.08	0.48	0.17
16:1w7c	15.772	20.81	3.46	18.50
cy17:0w7	16.836	7.35	2.53	-3.45
17:0	17.000	-0.25	-2.41	0.60
2OH-16:0	17.182	-3.95	-2.05	-6.59
18:2(9c,12c)	17.648	-0.68	-7.98	4.73
18:1w9c	17.720	-2.00	9.26	-11.69
18:1w7c	17.781	27.89	4.41	-14.56
18:0	18.000	-0.55	6.89	11.25
cy19:0w9	18.846	-0.05	-4.70	-4.56

Table 5-9. Results of logcontrast canonical component analysis on the time series of suspended biomass samples taken from Reactor B. Sequential sub-groups of at least 5 observations were used.

Eigen Values				
Latent Root	λ_1	λ_2	λ_3	$\Sigma\lambda_i$
Eigen Value	101.08	24.81	9.96	135.85
Percent	67.07	16.46	6.61	90.14
Eigen Vectors				
Fatty Acid	ECL	b_1	b_2	b_3
3OH-10:0	11.350	11.50	-2.43	9.42
12:0	12.000	4.98	-11.81	-1.58
i14:0	13.628	-4.17	1.21	-0.68
14:0	14.000	-9.73	-11.39	4.80
i15:0	14.632	3.02	3.23	0.33
a15:0	14.709	-13.33	22.43	4.93
15:0	15.000	1.16	3.45	-1.27
3OH-14:0	15.431	2.99	-5.45	7.43
i16:0	15.631	-3.54	-5.75	-5.64
16:1w7c	15.772	-17.09	20.13	-11.53
a17:0	16.714	-0.03	-0.04	0.03
cy17:0w7	16.836	-4.59	1.59	-2.40
17:0	17.000	-0.22	-0.52	9.08
18:2(9c,12c)	17.648	0.14	3.80	7.39
18:1w9c	17.720	-4.67	-0.78	-0.62
18:1w7c	17.781	34.34	-8.90	-7.32
18:0	18.000	-13.49	3.66	-13.72
cy19:0w9	18.846	-0.25	-0.04	1.17

Table 5-10. Results of logcontrast canonical component analysis on the time series of biofilm biomass samples taken from Reactor A. Sequential sub-groups of at least 5 observations were used.

Eigen Values				
Latent Root	λ_1	λ_2	λ_3	$\Sigma\lambda_i$
Eigen Value	83.97	15.50	7.67	107.14
Percent	71.87	13.27	6.56	91.71
Eigen Vectors				
Fatty Acid	ECL	b_1	b_2	b_3
3OH-10:0	11.350	3.09	-1.17	3.44
12:0	12.000	3.46	1.47	0.46
i14:0	13.628	2.12	0.57	-0.14
14:0	14.000	-2.01	10.14	-9.66
i15:0	14.632	29.47	-26.80	17.87
a15:0	14.709	-24.86	7.03	0.30
15:0	15.000	1.68	-20.65	-11.58
3OH-14:0	15.431	-7.24	-5.90	10.30
i16:0	15.631	-6.41	19.26	1.35
16:1w7c	15.772	23.06	16.33	3.43
i17:0	16.632	-7.91	-3.05	2.63
a17:0	16.714	-1.13	-4.29	1.30
cy17:0w7	16.836	-12.02	7.41	-22.77
17:0	17.000	6.95	-3.97	-1.63
18:1w7c	17.781	-3.79	21.29	-21.40
18:1w7t	17.832	-1.85	0.36	5.23
18:0	18.000	-9.80	19.41	8.95
cy19:0w9	18.846	42.23	-20.94	-19.55

Table 5-11. Results of logcontrast canonical component analysis on the time series of biofilm biomass samples taken from Reactor B. Sequential sub-groups of at least 5 observations were used.

Eigen Values				
Latent Root	λ_1	λ_2	λ_3	$\Sigma\lambda_i$
Eigen Value	58.20	24.94	12.46	95.61
Percent	56.30	24.13	12.06	92.48
Eigen Vectors				
Fatty Acid	ECL	b_1	b_2	b_3
3OH-10:0	11.350	-6.27	1.85	3.93
12:0	12.000	-3.74	0.28	6.16
i14:0	13.628	0.01	-0.97	-0.06
14:0	14.000	31.90	12.17	-11.80
i15:0	14.632	-41.33	-31.46	20.10
a15:0	14.709	18.53	-7.15	-4.61
15:0	15.000	1.39	-3.72	-13.25
3OH-14:0	15.431	-4.95	0.76	13.05
i16:0	15.631	38.13	15.10	-32.09
16:1w7c	15.772	-6.04	23.42	-10.73
a17:0	16.714	9.66	-1.99	-0.14
cy17:0w7	16.836	-6.50	28.37	41.46
17:0	17.000	5.36	-2.58	-0.64
2OH-16:0	17.182	-3.16	-1.96	-3.66
18:1w7c	17.781	8.97	-12.89	8.36
18:1w7t	17.827	-6.40	1.96	-0.09
18:0	18.000	8.75	3.20	2.12
cy19:0w9	18.846	-8.70	5.57	-5.99

microbial community may not ever be achieved during biological treatment of complex wastewaters, even though steady state treatment performance is reached.

Figures 5-18 through to 5-21 show the variation of the first two weighted canonical components (Ψ_1 and Ψ_2) along with the derived state speed. The suspended biomass seemed to exhibit the strongest dynamic responses to the shift-up and shift-down in resin acid input. In Figures 5-18 and 5-19, a definite peak in the community state speed appears to be closely associated with the timing of the leading edge of the initial resin acid shift-up. The duration of this peak, or apparent suspended biomass community response, was approximately 10 HRT cycles. It can be seen, further in Figures 5-18 and 5-19, that the period of the shift-down in resin acids resulted in a second peak in community state speed, that carried over into the second shift-up. If population dynamics exhibit some level of inertia, this could explain the apparent lack of reaction to the

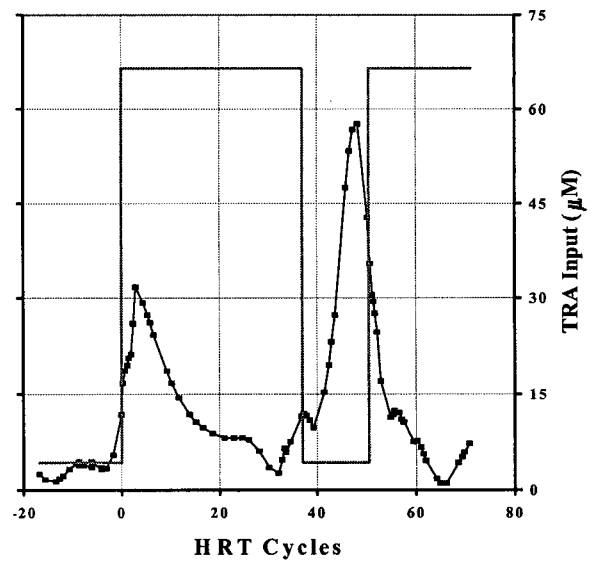
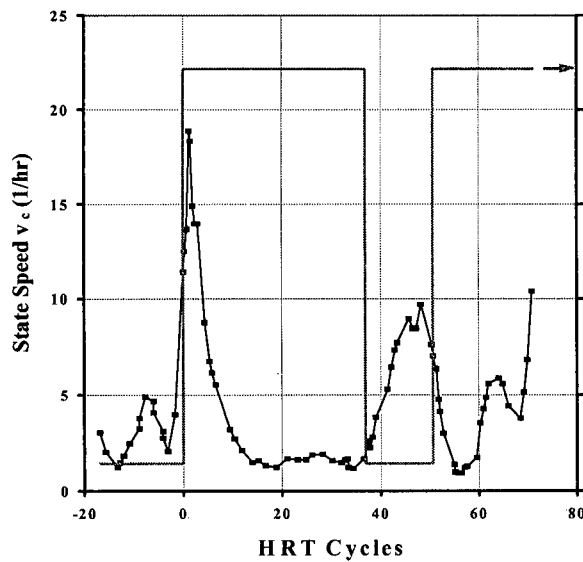
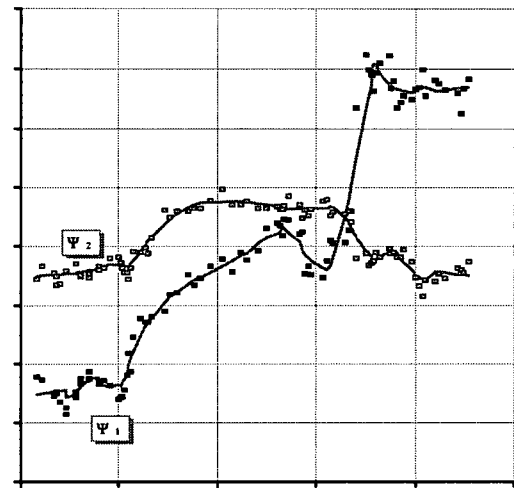
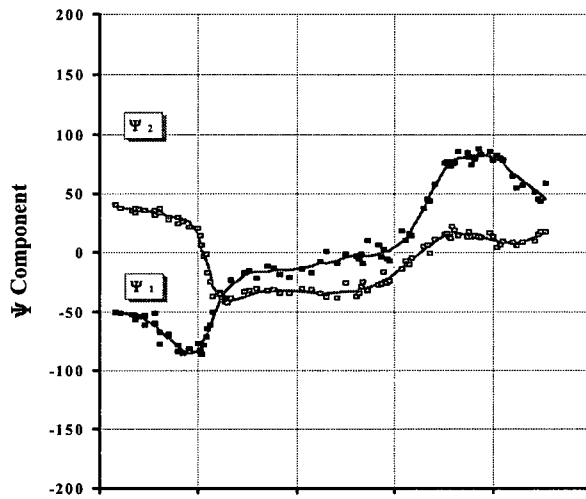


Figure 5-18. Reactor A suspended biomass community state and population dynamics. The community state (Top) is shown in terms of the first two weighted canonical components (Ψ_1 and Ψ_2). The logcontrast canonical component analysis was performed using 16:0 as the common divisor with the time series data sequentially sub-grouped in packets of 5 observations. State speed (Bottom) were calculated based on equation (4-42) as described in the results section of Chapter 4. For reference, the total resin acid (TRA) step input sequence is also plotted (Bottom).

Figure 5-19. Reactor B suspended biomass community state and population dynamics. The community state (Top) is shown in terms of the first two weighted canonical components (Ψ_1 and Ψ_2). The logcontrast canonical component analysis was performed using 16:0 as the common divisor with the time series data sequentially sub-grouped in packets of 5 observations. State speed (Bottom) were calculated based on equation (4-42) as described in the results section of Chapter 4. For reference, the total resin acid (TRA) step input sequence is also plotted (Bottom).

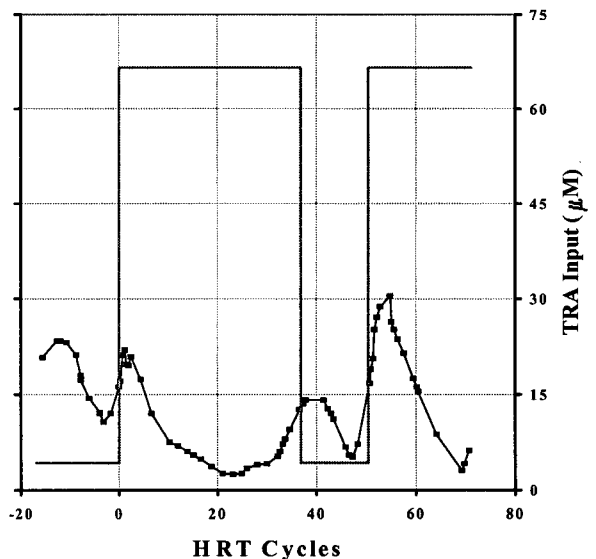
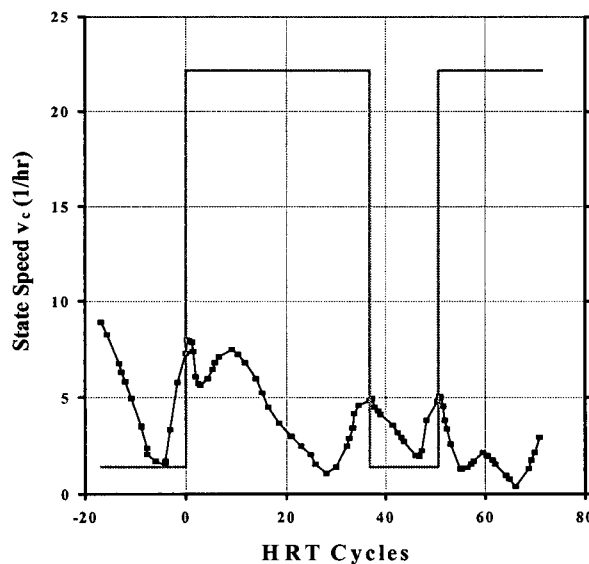
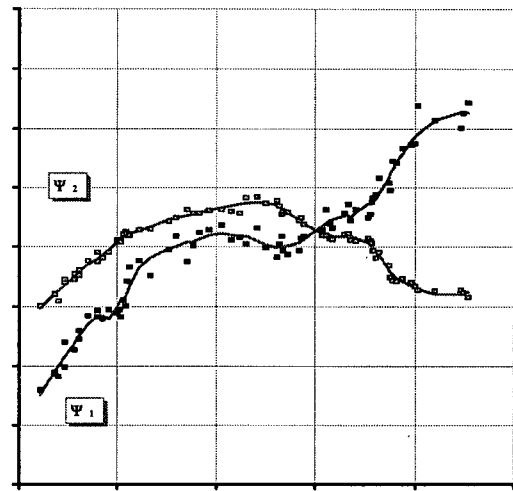
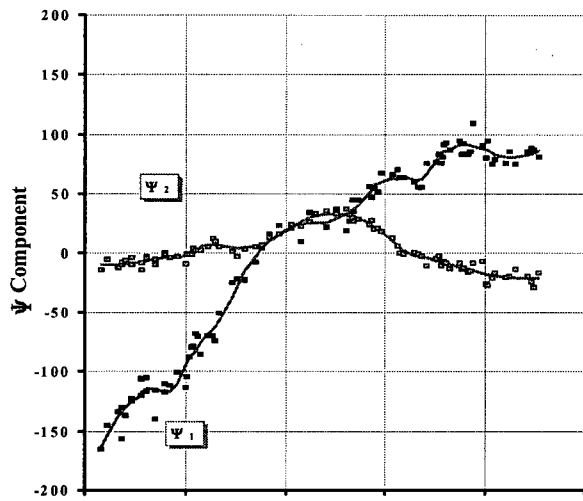


Figure 5-20. Reactor A biofilm biomass community state and population dynamics. The community state (Top) is shown in terms of the first two weighted canonical components (Ψ_1 and Ψ_2). The logcontrast canonical component analysis was performed using 16:0 as the common divisor with the time series data sequentially sub-grouped in packets of 5 observations. State speed (Bottom) were calculated based on equation (4-42) as described in the results section of Chapter 4. For reference, the total resin acid (TRA) step input sequence is also plotted (Bottom).

Figure 5-21. Reactor B biofilm biomass community state and population dynamics. The community state (Top) is shown in terms of the first two weighted canonical components (Ψ_1 and Ψ_2). The logcontrast canonical component analysis was performed using 16:0 as the common divisor with the time series data sequentially sub-grouped in packets of 5 observations. State speed (Bottom) were calculated based on equation (4-42) as described in the results section of Chapter 4. For reference, the total resin acid (TRA) step input sequence is also plotted (Bottom).

second step in Figures 5-18 and 5-19. Therefore, it is likely that, for this particular system, loading fluctuations of periods less than about 10 HRT cycles would not allow sufficient time for community level adjustment. Fluctuations on a time scale less than the natural response time will lead to some form of relaxed steady state operation (Figure 5-1). To strengthen this interpretation of the observed population dynamics, it was necessary to consider how the observations of state speed related to the kinetics of resin acid removal.

5.3.5 Induction and Kinetics of Resin Acid Metabolism

The estimation of the rate of total resin acid (TRA) removal was based on the following mass balance:

$$\frac{\partial m_a}{\partial t} = m'_i - m'_e - m'_b - m'_r \quad (5-9)$$

where m_a is the bioreactor aqueous mass, m'_i is the influent mass flow rate, m'_e is the effluent mass flow rate, m'_b is the biofilm mass loading rate, and m'_r is the biological removal rate. The terms in equation (5-9) are related to measurable experimental quantities in the following way:

$$m_a = Vc_a, \quad m'_i = Q_i c_i + Q_f c_f, \quad m'_e = \alpha Q_e c_a, \quad m'_b = A \frac{\partial \Gamma_b}{\partial t}, \quad m'_r = k_r X \quad (5-10)$$

where c is the resin acid molar concentration, α is a correction factor, Γ_b is the biofilm surface loading, k_r is the specific TRA uptake rate, and X is the biomass concentration. The other parameters and subscripts have already been defined in Table 5-2, Table 5-4 and Table 5-7. The factor (α) corrected for selective withdrawal of resin acids due to bubble fractionation. From the comparison of the suspended and effluent total resin acid concentrations, the correction factor was determined to be 0.96 and 1.09 for reactors A and B respectively (Figure 5-22). Thus acidic conditions (Reactor A) resulted in some level of clarification of the particulate resin acids not entrained in the overflow. If biological removal of the added resin acids had not been induced, a build up of resin acids in the acidic MBBR would be expected. Conversely for the alkaline conditions of reactor B, sorption and bubble fractionation augmented the TRA withdrawal rate at

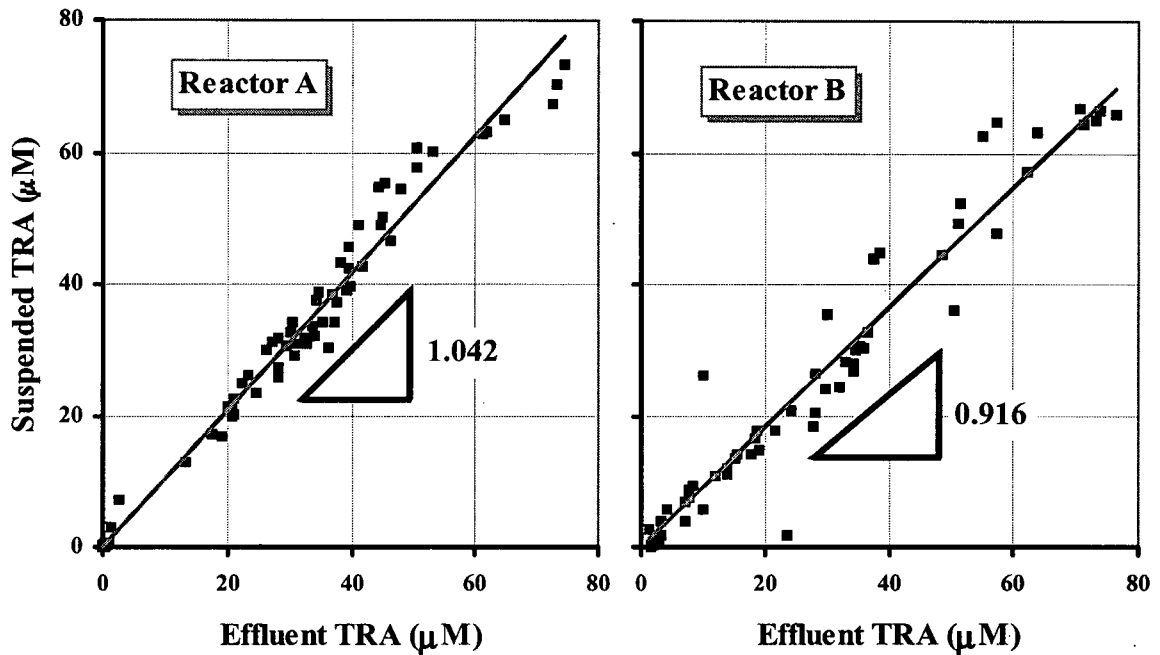


Figure 5-22. Retention (Reactor A) and selective withdrawal (Reactor B) of total resin acids (TRA). Suspended TRA refers to samples obtained from the bioreactor aqueous samples. Effluent TRA samples were drawn from collected effluent overflow. Reactor A effluent levels were approximately 4 percent lower than the suspended TRA. Reactor B effluent levels were approximately 8 percent higher than the suspended TRA. Retention of TRA at pH 6 was due to particulate settling and additional withdrawal of TRA at pH 8 was due to bubble fractionation.

the overflow.

Substituting the quantities in equation (5-10) into equation (5-9) and solving for the specific total resin acid biodegradation rate yields the following equation:

$$k_r = \frac{1}{X} \left(\frac{Q_t}{V} c_t + \frac{Q_f}{V} c_f - \alpha \frac{Q_e}{V} c_a - \frac{A}{V} \frac{\partial \Gamma_b}{\partial t} - \frac{\partial c_a}{\partial t} \right) \quad (5-11)$$

The TRA uptake rate (k_r) was calculated from the experimental data using the TRA data and the estimated reactor parameters reported in Table 5-2, Table 5-4 and Table 5-7. The time series of TRA concentrations and loadings were smoothed using a Savitzky-Golay (1964) sort of least squares sliding polynomial (see Chapter 4.3 Results). The first derivative of this sliding polynomial was used to estimate the rates of change of aqueous TRA concentration and surface loading. Since the suspended biomass was observed to exhibit the strongest coherent response to the resin acid step changes, it was assumed that metabolism of resin acids was most likely

determined by this community of microorganisms within each reactor. Hence, the suspended biomass as total fatty acid (TFA) was chosen as the most appropriate measure for biomass (X) in equation (5-11). This biomass assumption was also supported by the sorption data that are reported in Section 5.3.7.

The derived trends for the rate of TRA uptake are shown in Figure 5-23. On the common time scale, the community state speed for the suspended microorganisms are also plotted in Figure 5-23. With the initial step-up, it was of interest to observe that the peak in community state speed preceded the eventual increase in capacity to remove TRA. Therefore it appears that a community shift was required before a subsequent build-up of the necessary catabolic enzymes. The TRA shift-down also seemed to correspond with a community adjustment of the suspended biomass.

For the second TRA step, it is evident that the biomass did not fully retain the previously attained heightened capability to degrade resin acids. Between the two bioreactors, the retained level of TRA catabolic activity was greater for reactor B. The trend in the last set of sample points indicated that TRA catabolic activity was not going to be sustained. Further, the reduction in k_r at the tail end of the experiment again appeared to coincide with a trend of increasing community state speed. If this trend of the final data points in Figure 5-23 were to continue, it would suggest that although a pool of catabolic enzymes for resin acids still remained after the TRA shift-down period, community level adjustment may pre-empt TRA metabolism for reasons that are at this time unclear. The presence of an excess carbon source creates conditions for competition and competitive exclusion. It is not unreasonable to speculate that some level of community change is likely to be closely associated with any change in nutritional status.

Speculation regarding the driving forces that induce population dynamics and changes in metabolic activity is an interesting academic undertaking. Whatever the underlying community and metabolic processes that are stimulated, these results clearly demonstrate that a capacity to degrade resin acids is readily gained and lost. The time required to shift up or down is of sufficient duration to be considered a matter of serious contemplation in treatment process design,

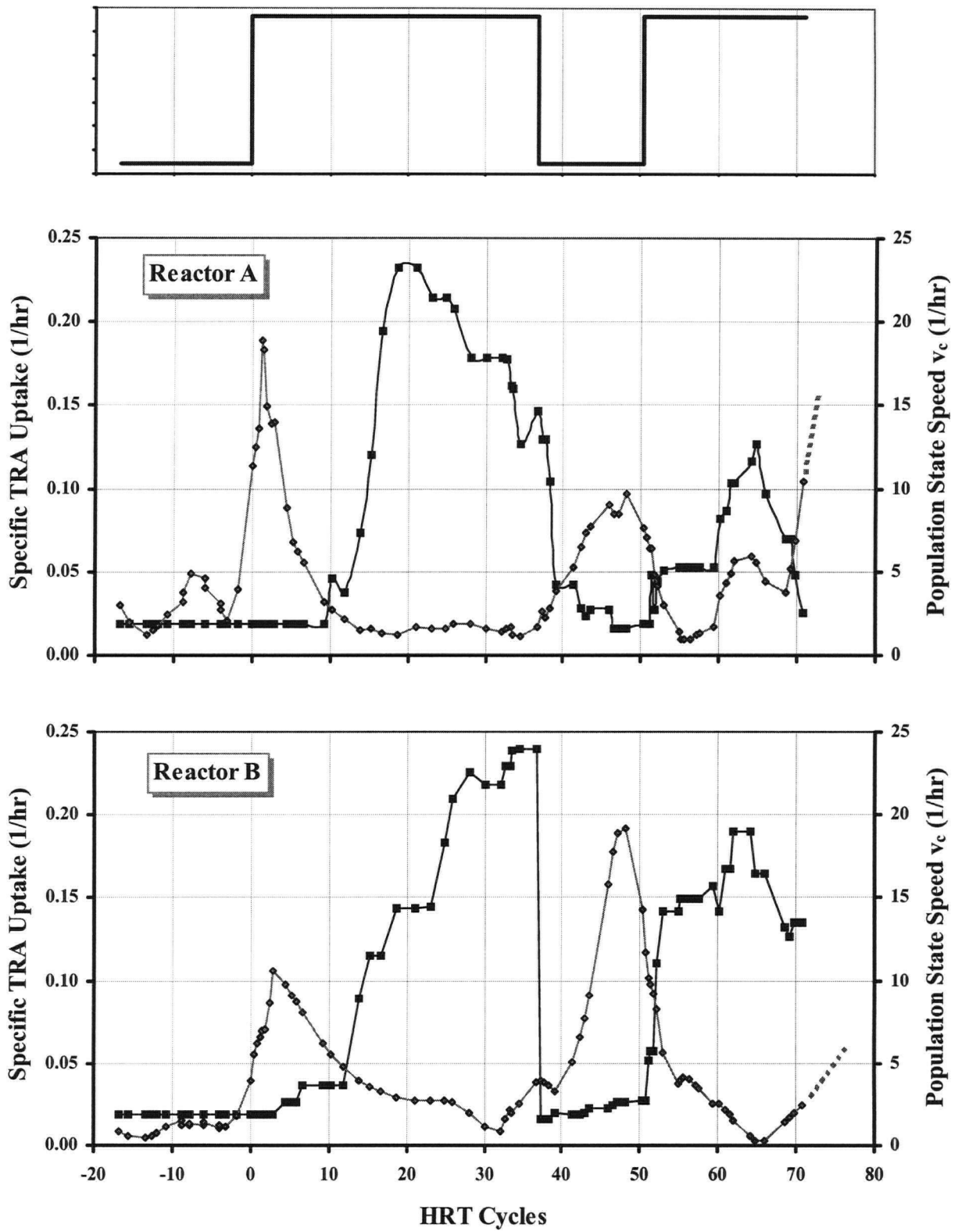


Figure 5-23. The time course of the estimated total resin acid (TRA) specific uptake rate (■) in response to the step changes of the influent loading. The respective suspended biomass population state speed (◆) are also shown. The population state speed appear to correlate well with the first shift-up and shift-down in TRA loading. Due to the time scale of the population response, it appears that the system was not able to adequately follow the second shift-up.

when assessing the risks and the potential impact of toxicity breakthrough.

The transient response to the initial shift-up practically spanned the entire duration of the step (Figure 5-24). The first 10 HRT cycles were dominated by a community level response and the next 25 HRT cycles probably involved the build-up of catabolic enzymes. Such a long transient had not been expected for a bioreactor already acclimated to resin acids. It therefore seems likely that TRA fluctuations with periods less than this observed two step lag phase will produce relaxed steady state operational conditions. The extent of contaminant removal for a relaxed steady state would be compromised and could result in chronic toxicity breakthrough. Therefore, the determination of characteristic response times is essential if a more realistic understanding of biological removal of specific contaminants is going to be achieved.

It was of further interest to note that the transient response towards an increased TRA uptake rate differed markedly between the two reactors. The approach to a new steady state was asymptotic for reactor B and asymptotic following an overshoot for reactor A. The net result was that the ultimate extent of resin acid removal for the shift-up was much better under alkaline conditions. Effluent concentrations towards the end of the first step were 29 μM for reactor A and 8 μM for reactor B. The extent of TRA removal under acidic conditions corresponds to the expected reduction in bioavailability determined from batch growth experiments (Chapters 2).

5.3.6 Assessment of the Interpretation of Fatty Acid Compositions

Community level changes, rather than adaptation of individuals, is the assumed interpretation of community state speed, based on fatty acid compositional analysis. This interpretation is based on the combination of results presented in Chapter 3. However, this view is open to challenge since it is well known that, for any individual organism, a change in substrate can induce a change in that particular organism's fatty acid composition. Studies of monocultures have shown that the composition of phospholipids is affected by environmental conditions (Lechevalier and Lechevalier 1988).

The purpose of this section is to consider the hypothesis that the observed fatty acid

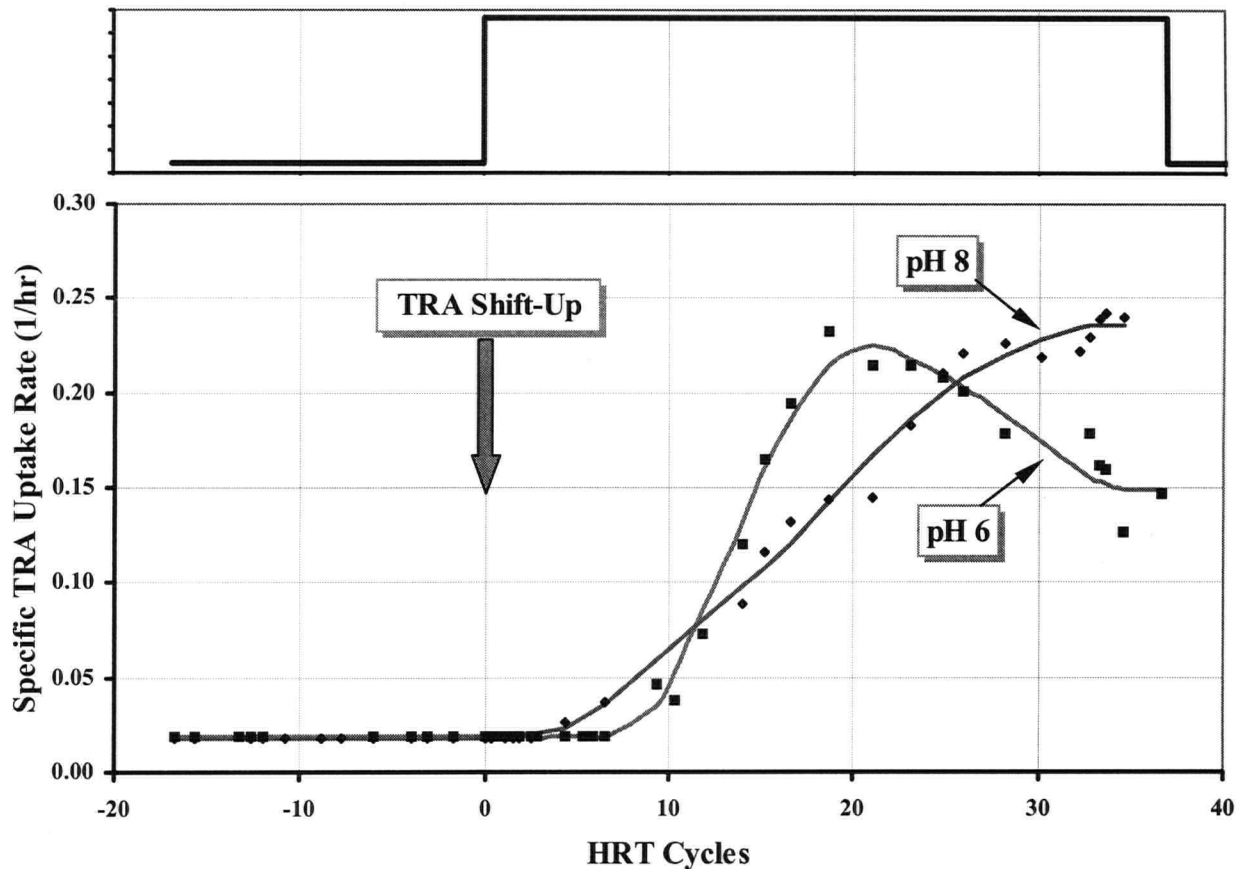


Figure 5-24. The transient response to a shift-up in total resin acids (TRA) was found to differ significantly with pH. Both bioreactors were initially removing resin acids (in the BKME feed) at a similar rate. Reactor A (pH 6) responded more quickly. However, after an initial overshoot, the new steady-state uptake rate was almost 40 percent lower than in Reactor B. Reactor B (pH 8) asymptotically approached the new steady-state level. The time scale for the transient response was greater than 30 HRT cycles.

compositional changes could be explained by membrane adaptations of individual species rather than a change in the balances of species. It is plausible that a species might adjust its membrane fatty acid composition to maintain fluidity (Chapter 3) and/or to optimize contaminant transport into the cell for metabolism. Resin acids are naturally occurring compounds and therefore the existence of a diversity of competent microorganisms in the environment should not be unreasonable to assume. The existence of microbial diversity is difficult to prove. However, the results of Chapter 3 do suggest diversity for resin acid-degrading bacteria. Therefore, consider the idea that populations of resin acid-degrading bacteria were widely distributed in the bioreactor microbial community. Suppose further that microbial membrane adaptation was necessary for the regulation of passive transport of resin acids into the cell. It then follows that membrane adjustment would need to precede metabolism. The observed peak in state-speed did precede increased metabolic activity on resin acids with the introduction of the first step load. If

membrane adjustment was indeed necessary for regulating resin acid transport into the cell, then the level of adjustment should correspond to the level of metabolic activity on resin acids.

Therefore, to test for the possibility that individual microbial adaptations dominated the observed fatty acid compositional changes, three time periods of the experiment were compared. On the time scale of HRT cycles (η) as shown in Figure 5-23, these time periods were (1) initial conditions of a low TRA uptake rate ($\eta < 0$), (2) a period of a high TRA uptake rate ($20 < \eta < 35$), and (3) a period of an intermediate TRA uptake rate ($55 < \eta < 75$). Fatty acid compositional data for each of these periods were grouped and then compared by logcontrast canonical component analysis. It was felt that if adaptation of individuals had been a key factor, then the uptake rate of resin acids would exhibit a strong correspondence to one of the canonical components.

The results of this compositional analysis are plotted in Figure 5-25 and Figure 5-26. The rate of resin acid uptake did not seem to correlate with either of the two logcontrast canonical components. The change in the fatty acid compositions indicated a transformation rather than a reversible adaptation. Transformation of the fatty acid spectra does not support the hypothesis of adaptation by individual populations. It therefore follows that changes in the fatty acid spectra for mixed cultures are likely to be overwhelmed by changes in the balance of species. This would suggest that the best way to interpret adaptation to environmental change by mixed cultures is with the principle of competitive exclusion. Since each microorganism exhibits distinct optima in environmental conditions for growth, changes to the growth conditions will hinder some organisms while favouring others. Those favoured organisms (or groups of organisms) would tend to dominate under new conditions at the expense of the others. Those species that rise in their dominance will depend not only on the new conditions, but on the culture history as well. Inhibition due to the presence of a hydrophobic substrate is believed to have been the cause of the interpreted shift in the community structure.

Therefore, the hypothesis of membrane adaptation as an explanation of the fatty acid change was rejected. This also means that the assumption of a wide distribution of participating populations of resin acid-degrading bacteria in the bioreactor community is not substantiated. While the

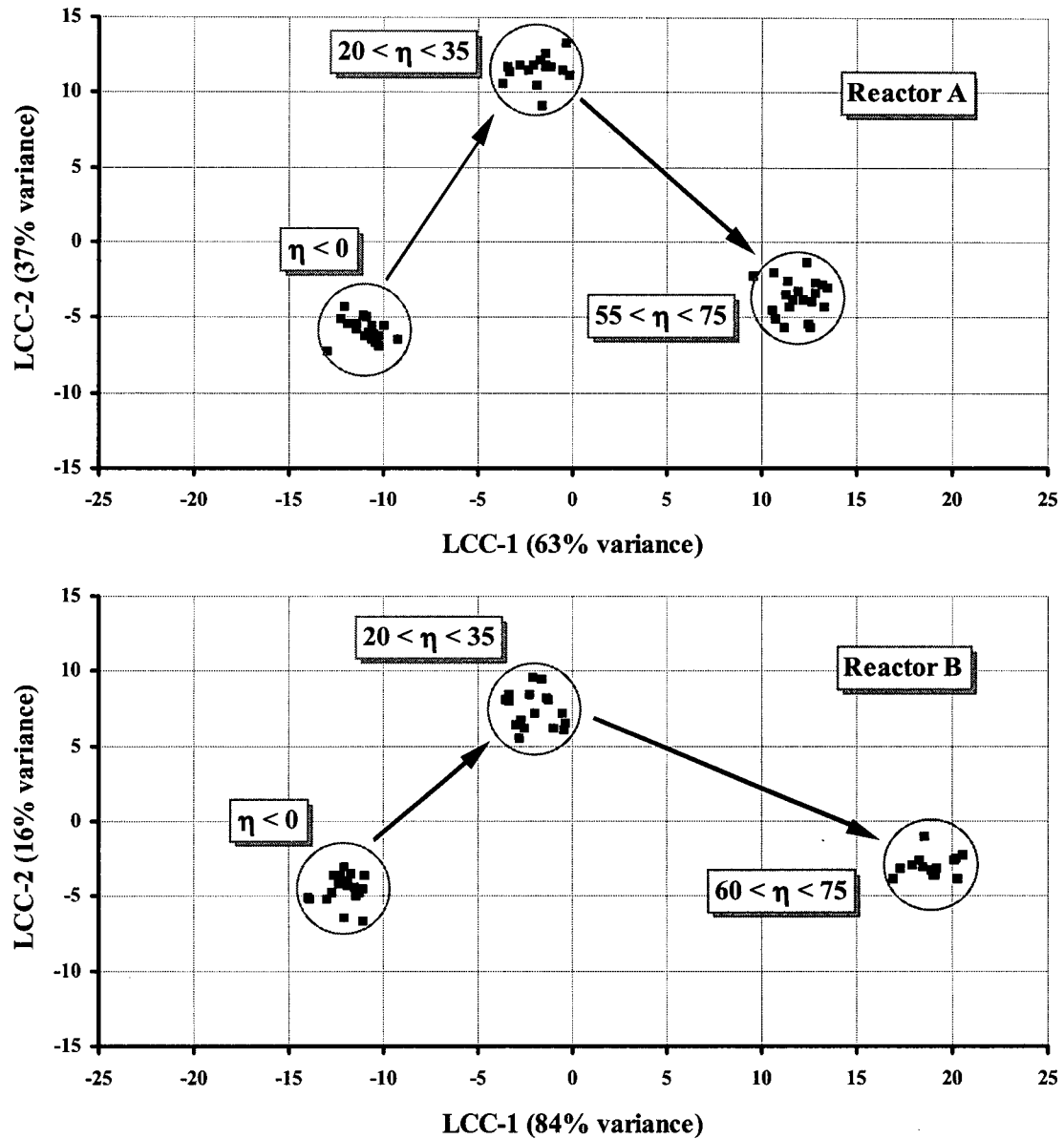


Figure 5-25. Logcontrast canonical component analysis of fatty acid compositions for the suspended biomass in reactor A (Top) and reactor B (Bottom) over selected time periods. The time periods on the scale of HRT cycles (η) as shown in Figure 5-23 reflect times of initial conditions ($\eta < 0$), of a high level of resin acid uptake ($20 < \eta < 35$), and of an intermediate resin acid uptake rate ($60 < \eta < 75$). Neither of the logcontrast canonical components (LCC) appear to correlate to the resin acid uptake rate. Hence it seems most likely that the fatty acid compositions reflect a change in the composition of microbial communities.

sudden addition of resin acids into the bioreactors appeared to have resulted in a community shift, that is not to say that the community shift was caused by populations of resin acid-degrading bacteria. The relative size of the sub-community degrading the resin acids is a question that needs to be addressed in future research.

The duration of lag periods is known to be influenced by growth rate (see Section 5.1.1). Within the moving bed bioreactors the suspended and biofilm communities represented communities with

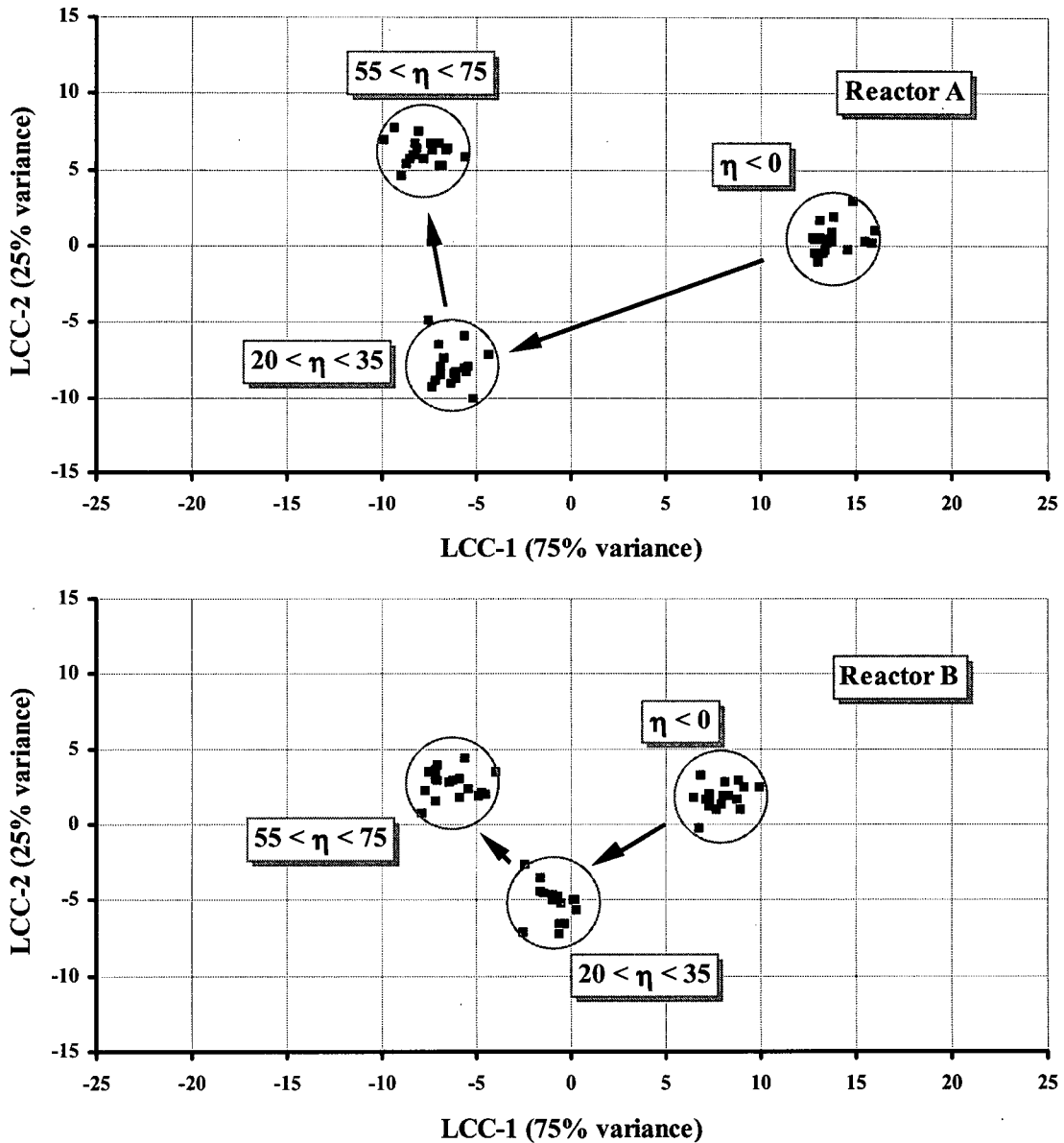


Figure 5-26. Logcontrast canonical component analysis of fatty acid compositions for the biofilm biomass in reactor A (Top) and reactor B (Bottom) over selected time periods. The time periods on the scale of HRT cycles (η) as shown in Figure 5-23 reflect times of initial conditions ($\eta < 0$), of a high level of resin acid uptake ($20 < \eta < 35$), and of an intermediate resin acid uptake rate ($60 < \eta < 75$). Neither of the logcontrast canonical components (LCC) appear to correlate to the resin acid uptake rate. Hence it seems most likely that the fatty acid compositions reflect a change in the composition of microbial communities.

distinctly different effective growth rates. The age distribution in a steadily growing culture is related to the distribution of the generation times and the youngest organisms are present in greatest numbers (Herbert 1974). Therefore, relatively young, fast growing cells dominated the suspended community. These cells exhibited the strongest response to the resin acid step input.

5.3.7 *The Contribution of the Biofilm Biomass in Resin Acid Metabolism*

For the previous calculation of the specific TRA uptake rate it was assumed that the biofilm biomass did not contribute to resin acid metabolism. This assumption was based on the observation that the population dynamics for the suspended biomass exhibited a strong relationship to the TRA shift-up and shift-down sequences. The validity of this assumption was considered by looking at the progression of sorption and desorption as function of the aqueous TRA concentration. Since the sampling interval was in the order of 5 hours, the TRA biofilm loading was considered in terms of equilibrium conditions, neglecting contaminant transport kinetics (Section 5.1.2).

Evidence of significant biodegradation of resin acids in the biofilm should have been observable as an apparent clockwise hysteresis in the sorption/desorption pattern (Chapter 4.1.3). The biofilm sorption data for the two bioreactors are presented in Figure 5-27 and Figure 5-28. Biofilm TRA loading under alkaline conditions (Figure 5-28) closely followed the model of equilibrium Langmuir sorption in agreement with the assumption of negligible biofilm activity towards resin acids. Biofilm TRA loading for reactor A (Figure 5-27) showed evidence of a counter clockwise hysteresis. A counter clockwise hysteresis gives an indication of irreversibility in the sorption process. Therefore the sorption data for reactor A also supported the assumption of negligible biofilm biodegradation of resin acids. Hence, loading transients are initially accommodated through biodegradation, by young, fast-growing organisms in the biological treatment process.

The nature of the sorption pattern at pH 6 contradicted the finding in Chapter 4 of reversible sorption during short-term exposure. Unfortunately, the present experiment was not designed to elucidate the more complex long-term sorption kinetics observed for resin acids under acidic conditions. However, the data do indicate that presence of resin acids on the biofilm augmented the extent of sorption. Apparently, resin acids on the biofilm behaved somewhat like an organic surface phase with a high affinity for extracting additional resin acids from aqueous solution.

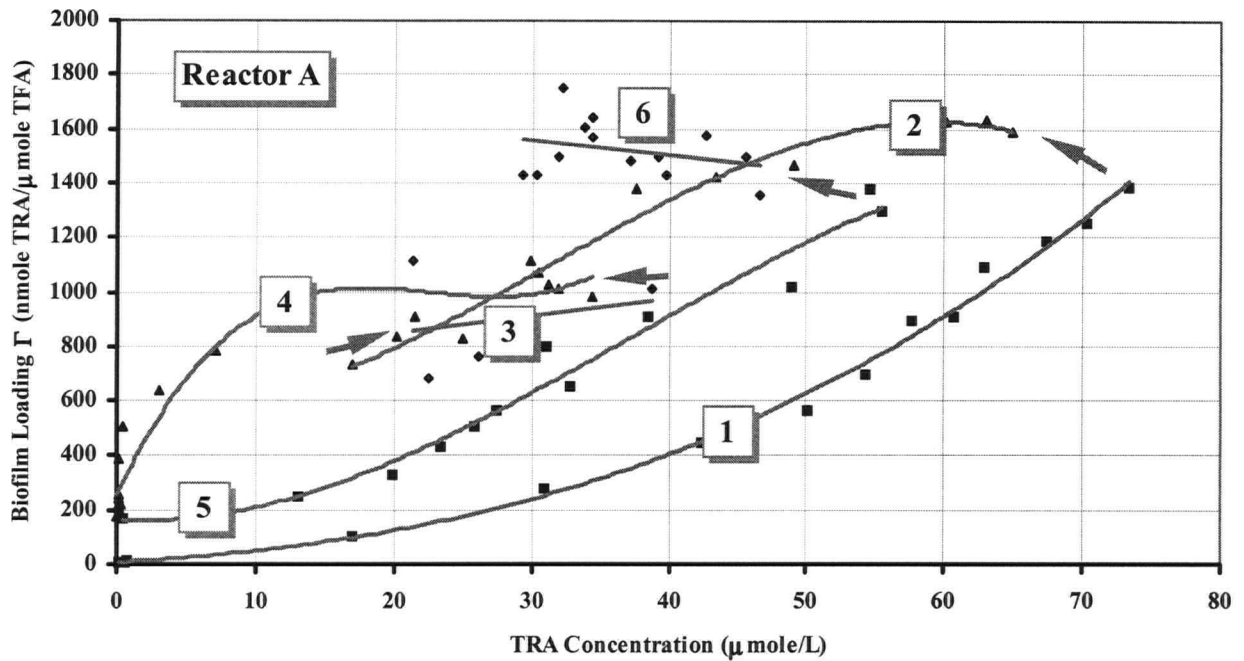


Figure 5-27. The history of total resin acid (TRA) sorption to the carrier biofilm for the acidic conditions (pH 6) of reactor A. A counter clockwise hysteresis was observed for periods of sorption (■ - 1 and 5) followed by desorption (\blacktriangle - 2 and 4). Two indeterminate regions of sorption or desorption are also noted (\blacklozenge - 3 and 6). Since the sampling interval was on the order of 5 hours, equilibrium Langmuir sorption conditions should have been observed according to the results reported in Chapter 4. However, these results indicated that reversible Langmuir sorption is not an appropriate model for resin acids under acidic conditions over a longer time frame. The counter clockwise hysteresis indicates some degree of irreversibility.

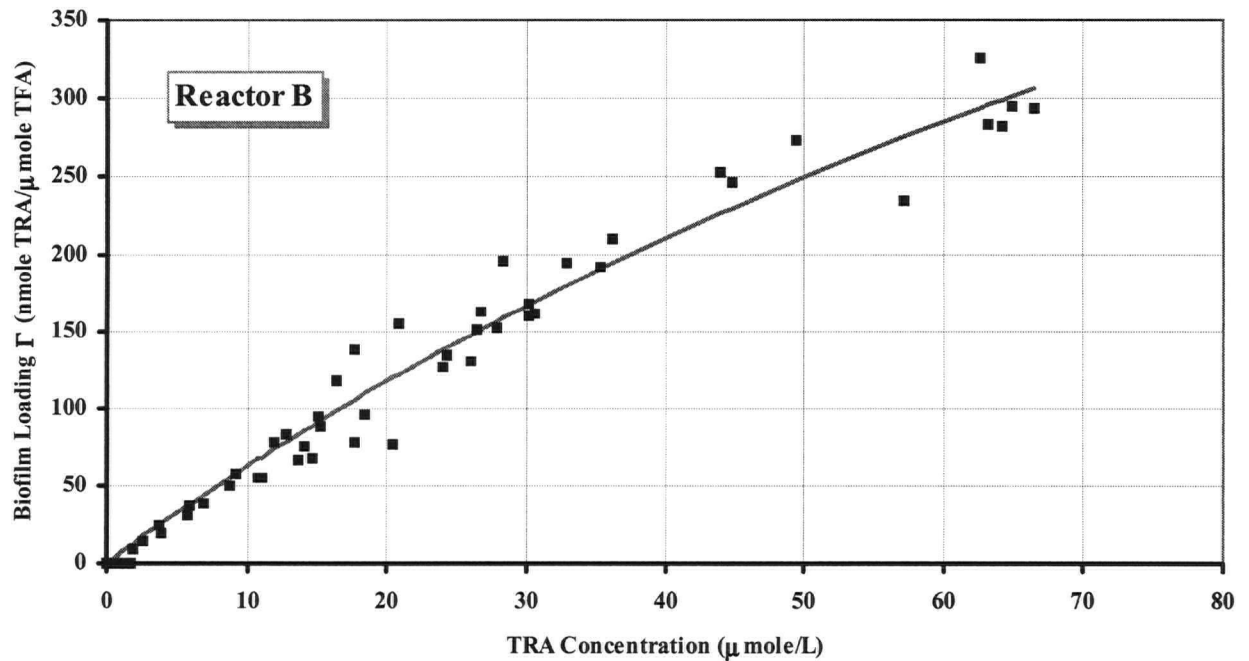


Figure 5-28. The history of total resin acid (TRA) sorption to the carrier biofilm for the alkaline conditions (pH 8) of reactor B. As predicted from the results of Chapter 4, equilibrium Langmuir sorption conditions were observed. The model curve, obtained by least squares nonlinear regression, estimated Langmuir constants $\{\Gamma_L, K_e\}$ of $\{984 \text{ nmole TRA}/\mu\text{mole TFA}, 147 \mu\text{M TRA}\}$.

5.3.8 Suspended Solids Batch Growth Experiment

The final part of this investigation involved batch growth in fresh media inoculated with suspended biomass from the two moving bed bioreactors at the respective pH conditions (Section 5.2.4). Duplicate shake flasks were inoculated at pH 6 (A1 and A2) and pH 8 (B1 and B2). The objective of this study was to compare the kinetics of mixed culture growth on a complex medium that included resin acids, at the two pH levels. Since both bioreactors were exposed to the same resin acid step load sequence, it was of interest to compare the physiological state of the suspended communities as a function of pH.

Physiological state can be qualitatively assessed from observations of the lag phase during batch growth (Panikov 1995). Referring to the r -parameter of physiological state (Chapter 3), a longer lag phase would indicate an initial r -state closer to zero. Using inocula from a chemostat, relative differences in the duration of the lag phase reflect relative differences in physiological state. The assumed working definition of the duration of the lag phase was the time required for the batch system to achieve maximum growth. When multiple substrates are being considered, the physiological state with respect to each substrate can be similarly compared by the time to reach the respective maximum specific removal rate.

To simplify the analysis, the carbon sources were grouped as total resin acids (TRA) and acid soluble total organic carbon (TOC). Kinetics of batch growth for the consumption of two substrates has been previously modelled for pure culture systems (Hegewald and Knorre 1978). This model was based on the following set of equations:

$$\begin{aligned}\frac{\partial X}{\partial t} &= \mu_T X \\ \frac{\partial S_1}{\partial t} &= -\frac{1}{Y_1} \mu_1 X, \quad \mu_1 = \mu_1(S_1, S_2, t) \\ \frac{\partial S_2}{\partial t} &= -\frac{1}{Y_2} \mu_2 X, \quad \mu_2 = \mu_2(S_1, S_2, t) \\ \mu_T &= \mu_1 + \mu_2\end{aligned}\tag{5-12}$$

where X is the biomass concentration, μ_T is the specific growth rate, S_i is the concentration of substrates 1 and 2, Y_i is the biomass yield coefficient on substrates 1 and 2, and μ_i is the growth rate on substrates 1 and 2. For this investigation, substrates 1 and 2 were TOC and TRA respectively. The biomass growth rate (μ_T) constant was expressed in terms of TFA.

In order to consider the experimental data against the framework of this two-substrate model, the TOC and TRA data were scaled to common units of micromolar carbon. The TFA growth and TOC depletion data (Figure 5-29) were empirically found to be well described by a Logistic sigmoidal function of the form:

$$y_L = \frac{A_i - A_f}{1 + \left(\frac{t}{t_{pk}} \right)^p} + A_f \quad (5-13)$$

The TRA depletion curves were also sigmoidal but were found to be better represented by the Boltzman equation:

$$y_B = \frac{A_i - A_f}{1 + \exp\left(\frac{t/t_{pk}}{\delta}\right)} + A_f \quad (5-14)$$

The best-fit parameters describing the experimental data were determined by least-squares nonlinear regression (Microcal Origin Version 4.00) and these values are listed in Table 5-12 through to Table 5-14. Function representations of the experimental data were used for the estimation of biomass growth and substrate depletion rates reported below. The extent of TRA removal (Table 5-14) was once again greater under alkaline conditions. The results for TOC removal could not be interpreted as definitively.

Figure 5-30 summarizes the TOC removal data for this and the previous investigation. Note that the bioreactor effluent levels were corrected for dilution by supplementary nutrient input. The final TOC concentration for the batch growth experiment was not consistently less than the effluent TOC for both of the continuous flow bioreactors. This variability in TOC reduction

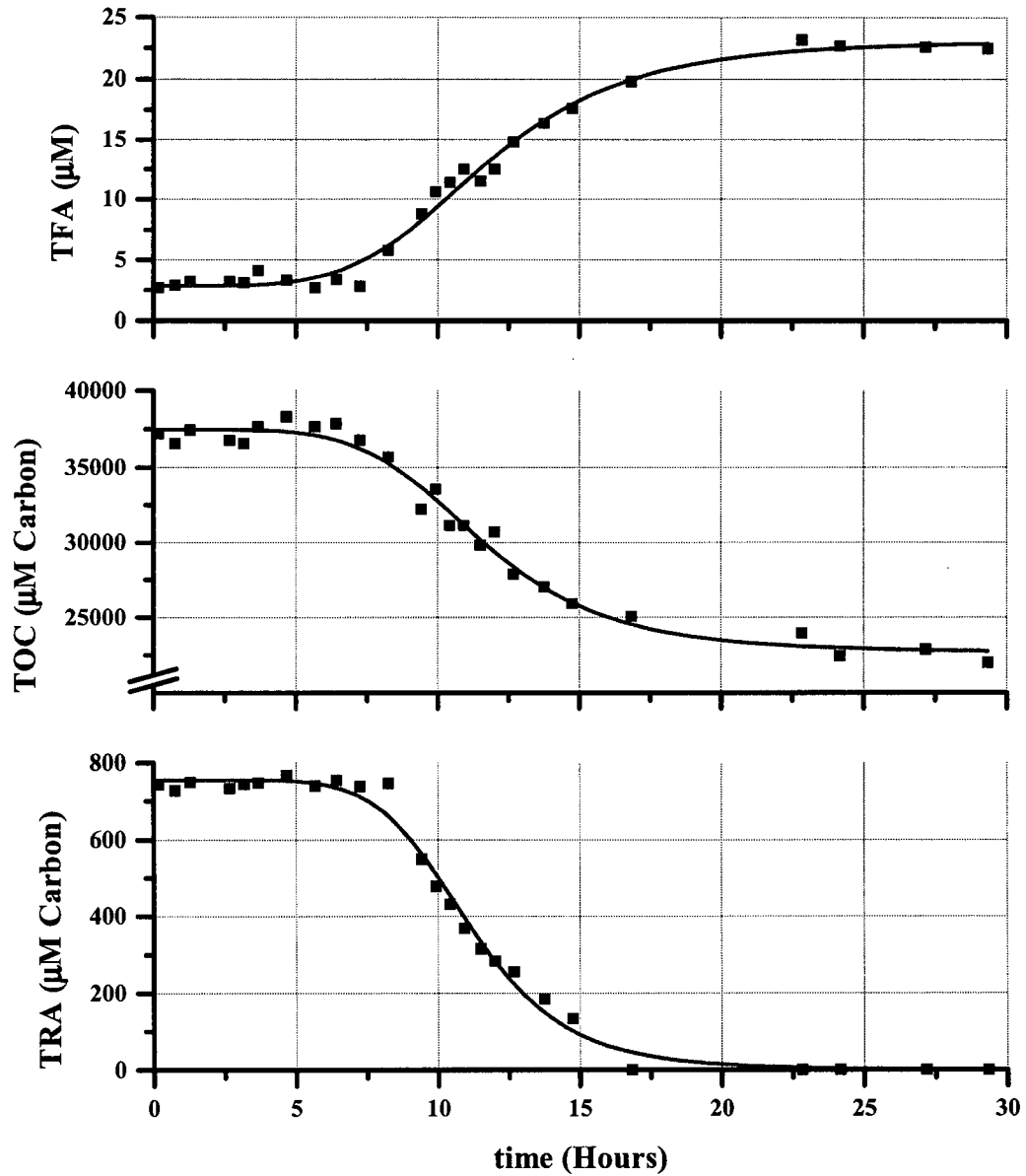


Figure 5-29. Shake flask B1 data illustrating the results of batch growth on BKME spiked with resin acids at pH 8. Biomass was measured as total fatty acid (TFA). The multiple carbon sources were approximately represented as acid soluble total organic carbon (TOC) and total resin acids (TRA). These carbon sources were equivalently scaled in concentrations units of micromolar carbon. The TFA and TOC time series were empirically fitted with a Logistic sigmoidal function (Table 5-12 and Table 5-13). TRA data were fitted by a Boltzmann sigmoidal function (Table 5-14).

Table 5-12. Best fit parameters for a logistic function (equation (5-13)) empirically describing biomass production as total fatty acids (TFA) during replicate (1 and 2) batch growth as a function of pH on BKME effluent spiked with resin acids. The inocula were 5 mL samples drawn from the respective moving bed bioreactors.

Parameter	A1 - pH 6	A2 - pH 6	B1 - pH 8	B2 - pH 8	Units
TFA _i	3.24 ± 0.27	3.53 ± 0.62	2.85 ± 0.31	3.46 ± 0.35	μmole/L
TFA _f	23.11 ± 0.47	26.14 ± 0.93	23.16 ± 0.55	29.37 ± 0.49	μmole/L
ΔTFA	19.87 ± 0.54	22.61 ± 1.11	20.31 ± 0.63	25.91 ± 0.60	μmole/L
t _{pk}	12.66 ± 0.20	11.68 ± 0.27	11.72 ± 0.23	10.87 ± 0.12	Hours
p	5.97 ± 0.53	8.43 ± 1.51	4.65 ± 0.44	8.02 ± 0.70	-

Table 5-13. Best fit parameters for a logistic function (equation (5-13)) empirically describing acid soluble total organic carbon (TOC) depletion during replicate (1 and 2) batch growth on BKME effluent as a function of pH.

Parameter	A1 - pH 6	A2 - pH 6	B1 - pH 8	B2 - pH 8	Units
TOC _i	36295.15 ± 248.69	35885.53 ± 223.09	37479.57 ± 275.75	35776.24 ± 190.57	μmole C/L
TOC _f	19434.59 ± 730.88	20076.71 ± 357.26	22623.63 ± 452.18	21298.26 ± 285.78	μmole C/L
ΔTOC	16860.56 ± 772.03	15808.82 ± 421.19	14855.94 ± 529.62	14477.98 ± 343.49	μmole C/L
t _{pk}	13.76 ± 0.48	11.13 ± 0.19	11.58 ± 0.25	11.15 ± 0.15	Hours
p	3.67 ± 0.39	4.73 ± 0.39	5.13 0.58	5.96 ± 0.48	-
TOC _i	435.54 ± 2.98	430.63 ± 2.68	449.75 ± 3.31	429.31 ± 2.29	mg C/L
TOC _f	233.22 ± 8.77	240.92 ± 4.29	271.48 ± 5.43	255.58 ± 3.43	mg C/L
Removal	46%	44%	40%	40%	Percent

Table 5-14. Best fit parameters for a Boltzman function (equation (5-14)) empirically describing total resin acid (TRA) depletion during replicate (1 and 2) batch growth on BKME effluent as a function of pH.

Parameter	A1 - pH 6	A2 - pH 6	B1 - pH 8	B2 - pH 8	Units
TRA _i	731.80 ± 3.65	717.25 ± 4.85	763.84 ± 14.02	766.69 ± 12.92	μmole C/L
TRA _f	29.15 ± 7.25	20.44 ± 9.79	8.40 ± 16.61	1.80 ± 15.52	μmole C/L
ΔTRA	702.65 ± 8.12	696.81 ± 10.93	755.44 ± 21.74	764.89 ± 20.20	μmole C/L
t _{pk}	15.71 ± 0.08	15.61 ± 0.10	11.11 ± 0.17	11.04 ± 0.15	Hours
δ	1.00 ± 0.06	0.90 ± 0.07	1.67 ± 0.17	1.55 ± 0.15	
TRA _i	36.59 ± 0.18	35.86 ± 0.24	38.19 ± 0.70	38.33 ± 0.65	μmole/L
TRA _f	1.46 ± 0.36	1.02 ± 0.49	0.42 ± 0.83	0.09 ± 0.78	μmole/L
Removal	96%	97%	99%	100%	Percent

suggests that the extent of TOC removal may be dependent on the community of microorganisms. For instance, the increased load of resin acids resulted in a community shift while at the same time a steady decrease in the capacity to remove TOC was also observed. The final TOC levels in Figure 5-30 from the present investigation should be directly comparable, since the media were prepared from the same primary BKME effluent. Although the greatest extent of TOC removal was achieved in the previous investigation (Chapter 4), the significance of this result cannot be interpreted since it has not been established that, other than the feed TOC level, the actual

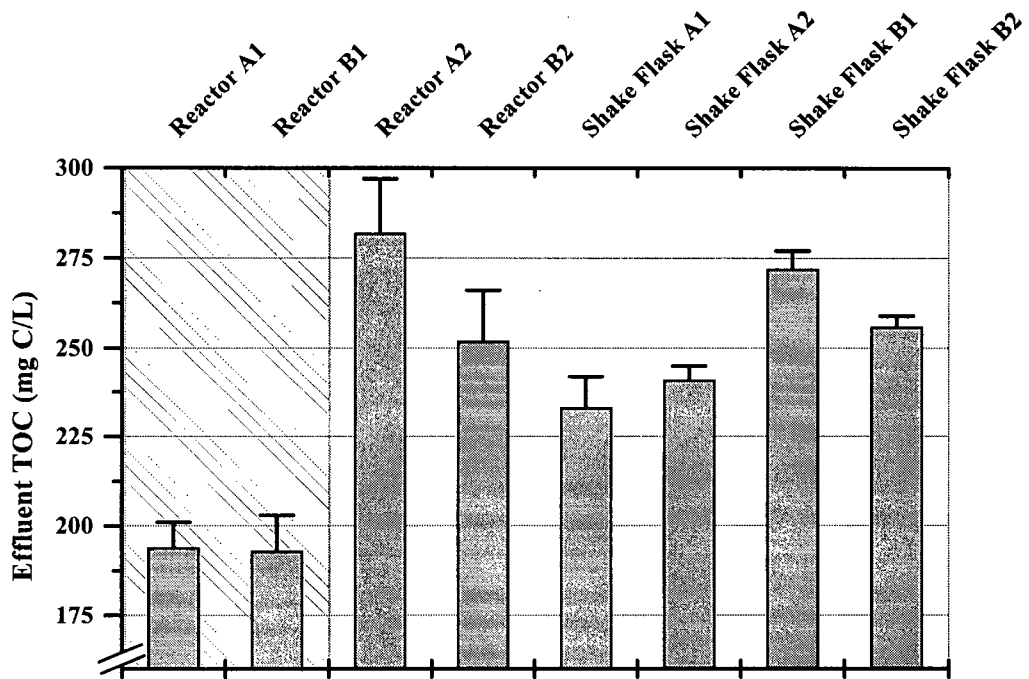


Figure 5-30. A comparison of effluent TOC levels from the moving bed bioreactors and after 30 hours of batch growth. Reactor effluent TOC levels have been corrected for the effect of feed dilution due to other input flows. Results are presented from the previous investigation (Reactor A1 and B1) as well as from the current study (Reactor A2 and B2). Replicate shake flasks were monitored at pH 6 (Flask A1 and A2) and at pH 8 (Flask B1 and B2). The greatest extent of TOC removal was achieved in the previous investigation with a reduced HRT but a more developed biofilm.

chemical make-up (biodegradable fraction) of the primary BKME effluent was similar in the two investigations.

From the functional representation of the experimental data it was possible to estimate the parameters from equation (5-12) as a function of time:

$$\begin{aligned} \mu_{TFA} = \mu_T &= \frac{1}{X} \frac{\partial X}{\partial t} \\ \frac{\mu_{TOC}}{Y_{TOC}} = \frac{\mu_1}{Y_1} &= -\frac{1}{X} \frac{\partial S_1}{\partial t} \\ \frac{\mu_{TRA}}{Y_{TRA}} = \frac{\mu_2}{Y_2} &= -\frac{1}{X} \frac{\partial S_2}{\partial t} \end{aligned} \quad (5-15)$$

The estimated specific growth rate (μ_{TFA}) values over time are shown in Figure 5-31. The

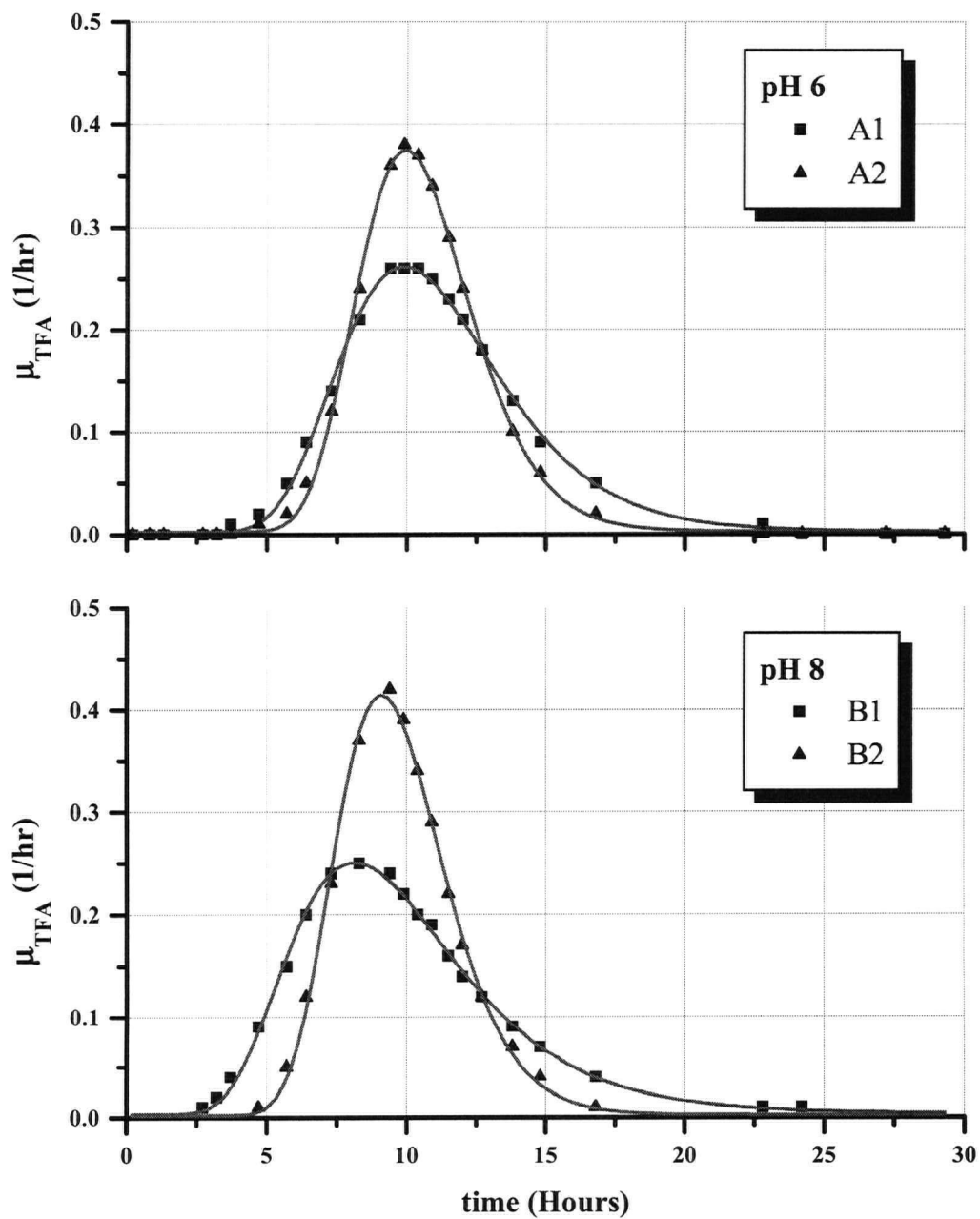


Figure 5-31. Mixed-culture batch growth rates estimated for replicate shake flasks at pH 6 (Top) and pH 8 (Bottom). The biomass growth rate (μ_T) for the model of equation (5-12) was determined from a Logistic sigmoidal representation of the TFA data (Table 5-12). The maximum growth rate was not sustained indicating that balanced growth was not achieved. The duration of the lag phase was taken as the time to reach the peak growth rate.

inoculum size used for this experiment was a bit too large, since logarithmic growth was not sustained in any of the batch cultures. Instead of a sustained exponential growth rate plateau, a peak growth rate was observed. In terms of the Monod equation, the half saturation constant must have been of comparable magnitude to the substrate concentration. However, for purposes of comparison, the duration of the lag phase could still be defined as the time required to reach peak growth kinetics.

The estimated growth rates on TOC and TRA are shown in Figure 5-32 and Figure 5-33. Once again, the peak rates were not well replicated, but consistent peak times were observed. Peak locations for TFA production and substrate (TOC and TRA) consumption were derived by fitting the data to either log-normal or Pearson VII peak functions (Microcal Origin Version 4.00).

These lag times are shown in Figure 5-34. While growth and substrate removal lags were relatively similar at pH 8, resin acid removal lag time was comparatively long at pH 6. This result demonstrates the importance of physiological state in the removal of specific contaminants. The time required for removal of a particular substrate depends on the extent to which members of a community have been induced to produce enzymes to grow and survive on that substrate.

Some further consideration was given to the batch experimental data to determine the extent to which traditional two substrate Monod kinetics (Hegewald and Knorre 1978) were representative. It is generally assumed that during batch growth the biomass yield coefficients are constant. Therefore it should have been possible to estimate the yield coefficients by multilinear regression analysis for the equation:

$$\mu_T = Y_1 \left(\frac{\mu_1}{Y_1} \right) + Y_2 \left(\frac{\mu_2}{Y_2} \right) \quad (5-16)$$

given sufficient experimental data of μ_T , μ_1/Y_1 , and μ_2/Y_2 . However the combined data presented in Figure 5-31 through to Figure 5-33 correlated poorly or inadmissibly with the model of equation (5-16). Therefore the assumption of a constant yield coefficient had to be rejected. This conclusion is also in agreement with the results reported in Chapter 3. For those batch

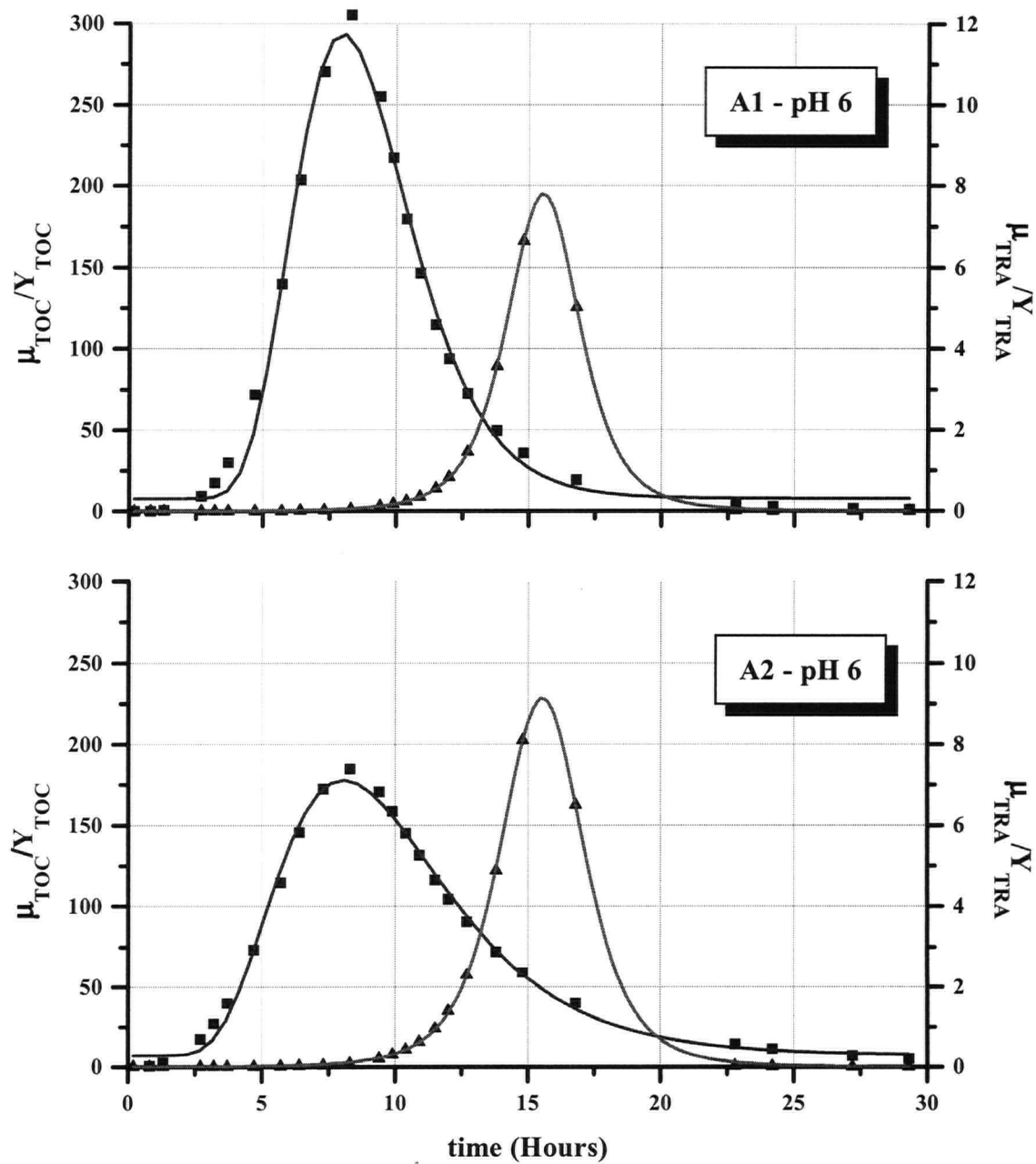


Figure 5-32. The estimated substrate-specific growth rates for replicate shake flasks at pH 6. Data are presented for the kinetics of TOC (■-Left axis) and TRA (▲-Right axis) removal for the model of equation (5-12). TOC and TRA were considered as substrate 1 and 2 respectively. The uptake kinetics were calculated from Logistic (Table 5-13) and Boltzman (Table 5-14) functional representation of the experimental data.

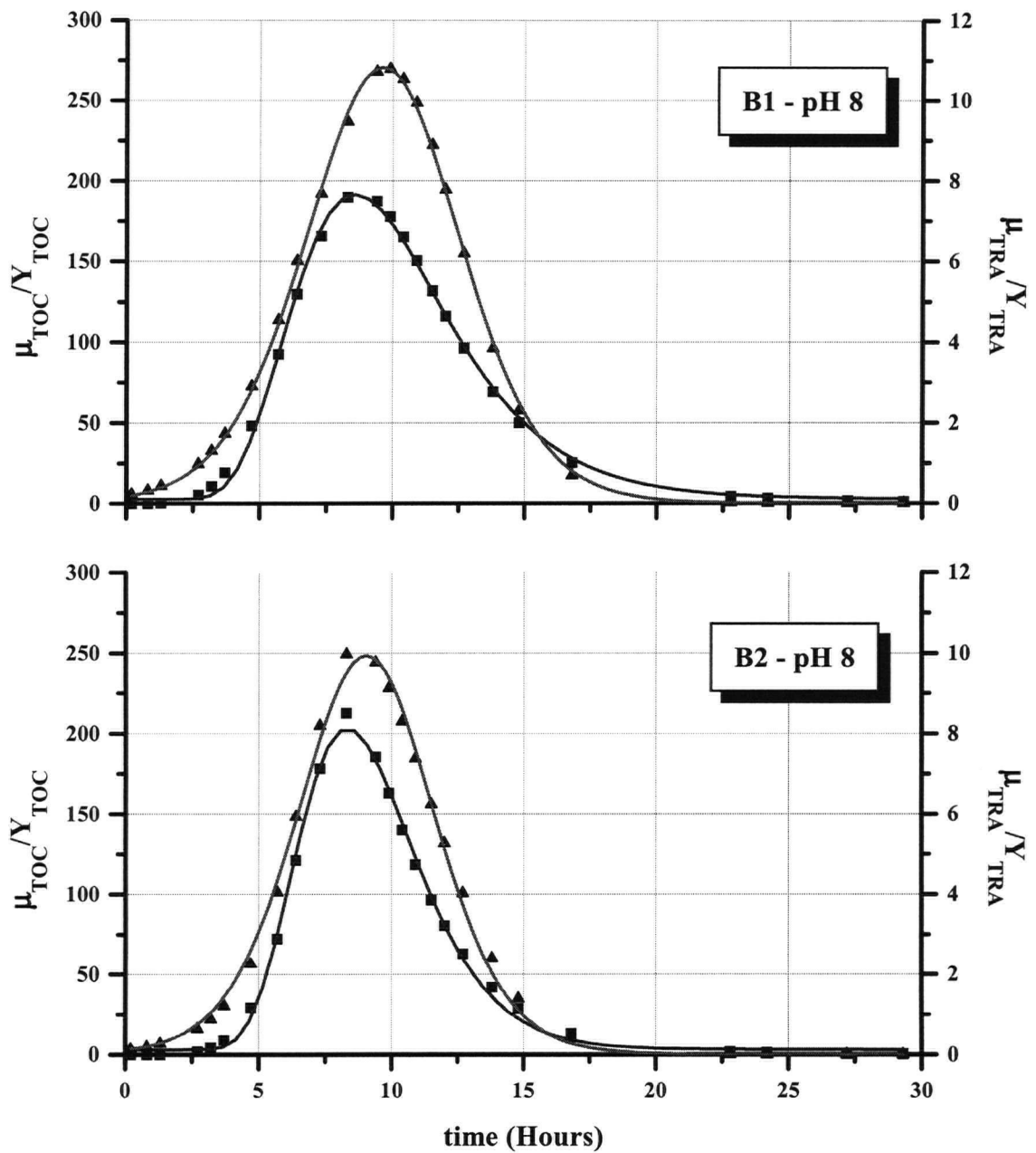


Figure 5-33. The estimated substrate-specific growth rates for replicate shake flasks at pH 8. Data are presented for the kinetics of TOC (■-Left axis) and TRA (▲-Right axis) removal for the model of equation (5-12). TOC and TRA were considered as substrate 1 and 2 respectively. The uptake kinetics were calculated from Logistic (Table 5-13) and Boltzman (Table 5-14) functional representation of the experimental data.

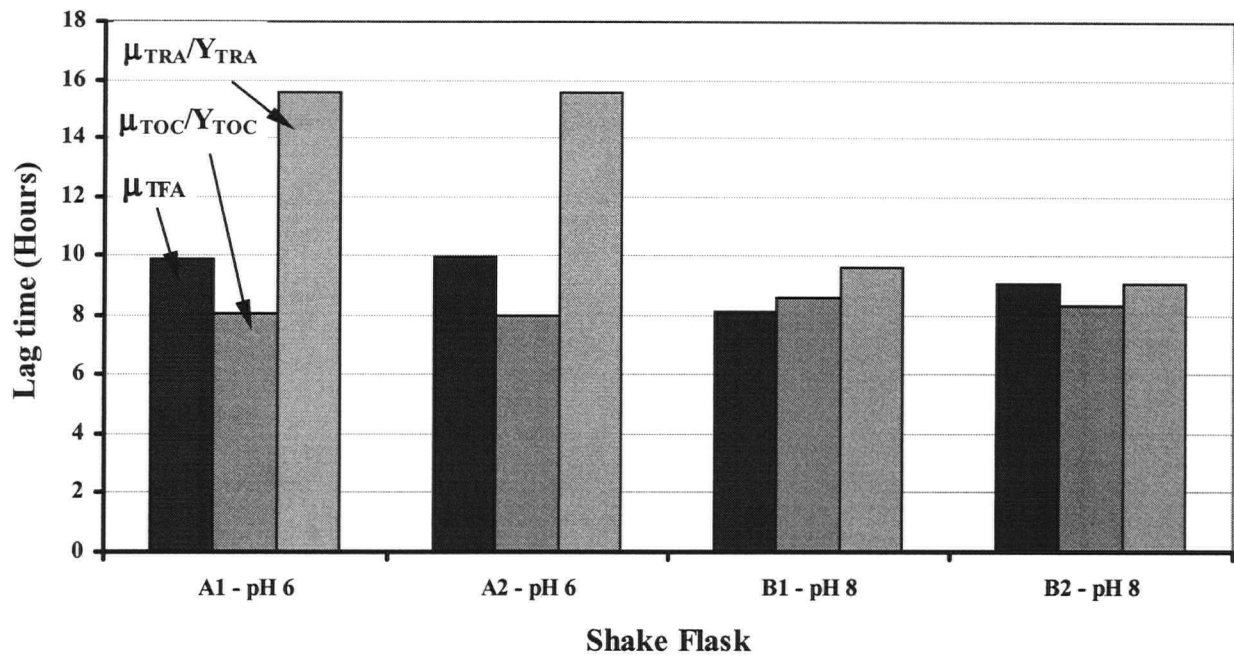


Figure 5-34. A comparison of lag times for growth (TFA) and for the specific removal of TOC and TRA. The lag times were estimated as the time to reach maximal values in Figures 5-31, 5-32 and 5-33. The peak locations were estimated from the growth rate data by empirical peak fitting. The growth rate and specific TOC removal rate data were modelled by a log-normal peak function. The specific TRA removal rate data fitted better to a Pearson VII function. Differences in the derived lag times were all significant with respect to the standard errors in peak estimation.

experiments it was found that the constancy of the yield coefficients deteriorated in the transition periods to and from exponential growth. These results indicate a potential for error in making the assumption of a constant yield coefficient. This assumption is almost universally made in the research literature for the analysis of experimental data obtained for determining Monod kinetic growth parameters.

5.4 Discussion

This investigation has served to demonstrate the important roles of population dynamics and physiological state in the removal of a specific class of aquatic contaminants during continuous biological treatment. The lag time necessary to accommodate shifts in the community and the supposed induction of catabolic enzymes represents an important limitation of a biological system in preventing toxicity breakthrough. Changes in microbial community structure due to a sudden increase in one contaminant can also impact on the extent of removal of other substrates. Observed variability in the extent of TOC reduction suggested that different communities of microorganisms differ in their capabilities for substrate utilization. Populations of microorganisms are in a continual state of flux. Sudden changes in the bioreactor environment will heighten the level of change in the community make-up above what may be an inherent background level.

It was apparent from this investigation that mixed cultures exhibit transient response patterns related to physiological state that have been previously observed for pure cultures (Panikov 1995). Continuous pure culture theory (Powell 1967) based on Monod kinetics and a delay kernel (equation(5-1)) predicts that the approach to a new equilibrium can be (1) monotonically asymptotic, (2) monotonically asymptotic after an initial overshoot, and (3) asymptotic with damped oscillation. The transient response for the rate of resin acid uptake after a shift-up in loading (Figure 5-24) was monotonically asymptotic at pH 8 and asymptotic with an overshoot at pH 6. The appearance of these two distinct patterns could be due to the fact that different communities of resin acid-degrading microorganisms are selected as a function of pH (Chapter 3). It is also possible that the threshold concentration for enzyme induction for acidic conditions is higher because of the reduction in resin acid bioavailability at low pH (Chapter 2).

Biological wastewater treatment design requires some accounting for lag phases, given the duration of the observed time delay for a system that was already acclimated to remove resin acids. The literature has clearly shown that pulp mill effluent is variable during normal mill operation (Beckett et al. 1992) and shutdown periods of several weeks are not uncommon. Mill shutdown can occur for reasons of scheduled maintenance, process upsets or an unexpected drop

in market prices. Operational changes or an operator error cannot always be avoided. Natural variations in wood extractive content can bring a sharp change in the distribution and concentration of resin acids in pulp mill sewers. With this in mind, transient state operation of pulp mill biological wastewater treatment processes is an unavoidable condition that requires a good engineering strategy, if toxicity breakthrough is to be wholly prevented.

This engineering strategy could be some form of preliminary, *in situ* or tertiary selective separation and storage system coupled with a physical oxidative unit process. The objective of an ancillary unit process that complements biological treatment should be to sustain removal during periods of acclimation and to filter out short-term load fluctuations. Due to the higher costs of physico-chemical wastewater treatment, a desirable feature of the backup system would be some form of proportional control. In other words, the application of the backup would only be required at times when the extent of biological removal is compromised.

Research on the dynamic response of a biological system to operational perturbations has provided a more realistic impression of system performance than an investigation of steady state resin acid removal, since true steady state conditions are probably never really achieved at full scale. Certainly when it comes to understanding treatment consistency for the removal of specific priority pollutants, response times for enzyme induction are important aspects of the process modelling and design. When considering the removal of a deleterious contaminant whose influent concentration is known to fluctuate, quasi-steady operation (Figure 5-1) should be the goal. Demonstration of a high removal efficiency under steady state conditions (Liu et al. 1993) is insufficient confirmation of the efficacy of a biological treatment process for the removal of specific aquatic contaminants.

In order to make appropriate design decisions, one must be appraised of the expected amplitude and period of influent fluctuation in relation to the biological response time scale. One must also consider the diversity of microorganisms capable of degrading a targeted contaminant in the complex wastewater (Chapter 3). It is important to know whether the treatment system must be carefully enriched to contain a very specialized community or if biological removal is made

possible by the induction of a relatively common set of enzymes. From the results in Chapter 3 and the present investigation, it would appear that resin acids fall into the latter category. A diversity of resin acid-degrading organisms was inferred from fatty acid profiles obtained during batch enrichment experiments. The need for enzyme induction was hypothesized to result in a significant delay in the growth of treatment capacity. Whether or not this conclusion is also valid for the more toxic chlorinated forms of resin acids needs to be determined. Knowing the specificity of populations that can dechlorinate contaminants in pulp mill effluent should provide additional fundamental insight that will help to furnish ideas and strategies for removal.

Novel ways to accommodate contradictory design constraints must also be considered. A complex wastewater contains many organic contaminants that need to be oxidized. For instance, a high SRT may favour the development of a community with organisms capable of removing the slowly degradable organic fraction. A short response time to changing influent conditions could necessitate the presence of a faster growing, low SRT community. At some intermediate SRT, an optimal combination between rapidly adapting generalists and well-established specialists may be reached. Perhaps the combination of biofilm and suspended growth used for this investigation is the most efficacious manner to provide a high degree of plasticity under the range of demands placed on a biological wastewater treatment system. Alternatively, a move away from combined sewers and large-scale treatment systems makes a lot of sense. Specialized industrial kidneys treating more specific process waters will permit a higher level of optimization in contaminant removal.

Fatty acid compositional analysis has been a useful tool to fingerprint and compare microbial communities in lab scale wastewater treatment systems. Quantitative assessment of community variability within and between experiments provided important insight about the relative sensitivity of microbial communities to the bioreactor operating conditions. Fatty acid compositions of individual organisms are known to be influenced by environmental parameters. However, the data from this investigation and the one in Chapter 3 indicated that changes in the balance of species most likely dominate compositional changes of fatty acids for mixed cultures.

Unfortunately, proof by inference is not rigorous. In future work it would be of considerable benefit to more definitively establish the deduced interpretation of competitive exclusion for fatty acid profiles from mixed cultures. This work should help to define the limitations of this approach to measuring population dynamics. Concurrent assessment of 16s rDNA patterns is one way to test the extent to which fatty acid spectral changes for mixed cultures reflect changes in microbial communities (Cloete and Muyima 1997).

Assuming that the interpretations drawn for this work would be confirmed by direct measurement of genetic material, fatty acid profile analysis remains a preferred method of community analysis. Compared to the current genetic methods, fatty acid sample processing is less laborious and is also amenable to some degree of automation. From one sample assay, information about biomass and community structure are concurrently obtained. Using dedicated equipment, sample turnaround time for fatty acids is about one and a half hours. The detailed sampling for this investigation would not have been possible, both in time and expense, had a 16s rDNA approach been used instead.

Wastewater engineers are currently trained to monitor changes in biomass without regard for microbial content. This investigation illustrates that a more comprehensive assessment of biomass kinetics involves a rate change in community structure as well as a rate change in biomass. In fact, the biomass can remain relatively constant in amount while still being quite dynamic in quality. Considering changes in biomass quantity alone may provide sufficient information when looking at the dynamic response of a pure culture system. However, fundamental gains in mixed culture wastewater treatment technology will likely be reached from a better understanding of the dynamics of mixed culture "quality". Measurement of population dynamics as the rate change of mixed culture fatty acid compositions is one approach for following mixed culture quality.

Identification of species-specific characteristics seems to have been a lost caveat in the application of the pioneering research of Jacques Lucien Monod (1949). The Monod equation describes the S-shaped growth dynamics of a batch culture with three parameters, namely (1) the growth yield Y , (2) the maximum growth rate μ_m , and (3) the growth rate saturation constant K_s . With values

in hand for these three parameters for a particular organism, it is possible to predict the growth dynamics. Predictive capability is the real power in much engineering activity. It should be noted however, that Monod's findings were specific to a limited range of medium conditions and neglected the lag and the cell death phases (Panikov 1995). Even with these restrictions, the parameters $\{Y, \mu_m, K_s\}$ can still be said to be characteristic properties of a particular organism. In the recognition that kinetics based on the Monod equation can be applied to fit the data obtained from mixed culture experiments (Chiu et al. 1972), there comes a realization of engineering potential. However, in surveying the scientific wastewater literature, one might be given the false impression that the kinetic parameters are thought to be a characteristic property of the wastewater. A model that provides a good fit to experimental data is a convincing result but is not a rigorous test of the relevance of the model when it comes to more general predictive capability.

Experimental data, using Monod kinetics, obtained for any given wastewater are notoriously variable (Grady et al. 1996). This lack of experimental reproducibility fuels a continued quest for representative parameter estimates, which are necessary for modelling and design (Magbanua Jr et al. 1998). Experimental variability may be due to experimental errors, changes in pseudo-species or differences in physiological state. It seems to be generally accepted that, to be the most useful, experimentally-determined kinetic parameters must accurately represent the ability of the bacterial community *in situ*. However even measurements of the extant or *in situ* kinetic parameters on individual substrates for biosolids in a well controlled continuous flow bioreactor vary considerably over time (Ellis et al. 1998). The pitfall is that it is not the wastewater that determines the kinetic parameters, but rather the biosolids. Evidence from this investigation indicates a continual change in the biosolids and that implies a continual change in the kinetic parameters. Physiological state further influences microbial kinetics. For this reason, the recommended method used to determine the kinetic constants is designed to maintain the physiological state of the bacteria sampled from the treatment system (Grady et al. 1996).

For batch assays, one approach to closely reproduce the *in situ* conditions is to maintain the

substrate to biomass ratio (S_0/X_0) of the sampled wastewater environment. A reported rule of thumb is to maintain a S_0/X_0 ratio of less than two (Chudoba et al. 1991; Chudoba et al. 1992). However, these precautions do not seem to help in removing or understanding the inherent experimental variability. Perhaps it makes more sense to attempt to define the variability in the maximum possible removal rate from batch replicate experiments with enrichment communities at a high S_0/X_0 ratio. Experimental variability can be related to pseudo-species diversity, and a factor of physiological state can be incorporated to help explain the behaviour of the real system. This approach will provide experimental data and model parameters that can be more meaningfully compared between studies.

Repeated batch experiments reported in Chapter 3 indicated that changes in pseudo-species influence the growth-linked resin acid removal kinetics. With this knowledge, one may ask what kinetic values are the best to use for treatment design? Using average values (Magbanua Jr et al. 1998) would mean that during steady state operation there is a reasonable probability that there will be times when the process is under-designed and that introduces a high risk of toxicity breakthrough. More conservative parameters may be obtained by applying a factor of safety to the mean values. How big should that factor of safety be? There is a severe penalty for over-design since the larger the factor of safety the more expensive the capital and operating costs will be. Thus, expense needs to be weighed against risks. What is a reasonable risk when it comes to potential environmental impact? Kinetic parameter variability in relation to pseudo-species variability is a useful quotient to consider. Smaller factors of safety would apply if it has been determined that large pseudo-species variability does not relate to large kinetic parameter variability.

Modelling and design solely on the basis of steady state Monod kinetic parameters (Liu et al. 1996b) can help to establish the ultimate potential of a given biological system. However, this investigation demonstrates that real performance depends on physiological state and the time scale of transients relative to that of metabolic response. Different pseudo-species have different metabolic response characteristics. A realistic assessment of the expected performance of a

biological wastewater treatment system requires the incorporation of a parameter of physiological state. Physiological state is not an independent layer of added complexity. It has implication for the current practice used for the determination of *in situ* Monod kinetic parameters that is not generally considered. Experiments with low S_0/X_0 ratios for the determination of extant kinetic parameters must overcome three technical hurdles. The first is the estimation of the capable fraction of the biomass. The second is the measurement of low substrate concentrations from restricted sample sizes. The third is the detection of a small biomass increase relative to a large mean.

The capable fraction of the biomass is thought to be proportional to the COD fraction of the target compound with respect to the untreated wastewater. This is not an unreasonable approximation assuming only growth-linked removal kinetics. Note however, that biomass yield for a resin acid-degrading community inoculated into either resin acid medium or sodium acetate medium differed by 20 percent (Chapter 3). Very sophisticated techniques in differential respirometry have been developed (Ellis et al. 1996; Ellis et al. 1998) to indirectly monitor substrate depletion in batch or fed-batch assays. To estimate heterotrophic growth it is assumed that substrate depletion is related to growth through a constant yield coefficient (Henze et al. 1986). However, this apparent yield coefficient is not a constant, but is a function of physiological state (Panikov 1995).

Biomass yield has been observed to vary in chemostat culture as a function of the dilution rate. Maximum yield occurs at subcritical dilution rates and declines with dilution rate (Panikov 1995). For a single microbial population, the change in yield relates to changing maintenance requirements, which are a function of physiological state. This dependency can be expressed as (Panikov 1995):

$$\left(\frac{\mu}{Y}\right) = \left(\frac{\mu}{Y^{MAX}}\right) + Q_m \quad (5-17)$$

where Y^{MAX} is the maximum possible substrate to biomass conversion and Q_m is the maintenance coefficient. Low dilution rates create conditions of low S_0/X_0 ratios. Changes in the balance of

species in batch or continuous cultivation of a microbial community can also result in a change in the overall community growth characteristics. Hence the assumed constancy of yield during batch growth is not necessarily true. A recent detailed study of *in situ* growth dynamics of activated sludge using batch assays indicates that the yield coefficient is not a constant for these kinds of measurements (Pollard et al. 1998). For these experiments, the rate change in biomass was estimated directly by the thymidine assay and the active biomass level was measured by acridine orange DNA staining and epifluorescence. The results of the batch growth tests for the present investigation also did not support the assumption of a constant yield coefficient. For batch conditions, a constant yield is achieved only during exponential growth when Y approaches Y^{MAX} and when the community composition is relatively stable. It must be concluded, therefore, that although *in situ* uptake kinetics can be empirically described by a Monod model, the experimental conditions may fall outside the range of validity. Such data must be treated with some reserve unless it can be explicitly shown that the model assumptions were valid. In any event, any estimated kinetic parameter values are not characteristic of the system but are a product of the physiological state of the "pseudo-species" at the time of measurement.

Finally, the long-term sorption behaviour of resin acids in slightly acidic conditions could not be modelled by a Langmuir isotherm. This result emphasizes the role of pH on the fate of these compounds. Previous studies (Hall and Liver 1996; Liu et al. 1996a) did not indicate the sensitivity of resin acids to the condition of pH. The present investigation along with other research (Christodoulatos and Mohiuddin 1996; Jacobsen et al. 1996; Westall 1985) on the fate of hydrophobic organic acids, indicates the importance of pH control. The way in which resin acids accumulated on the carriers at pH 6 corresponds to the old adage in chemistry that "likes attract like". This behaviour may be similar to the accumulation of extractives in the formation of stickies during paper making (Doshi and Dyer 1997). It would be interesting to explore the extent to which colloidal dispersions of resin acids may be sequestered by a suitable non-aqueous organic phase. A solvent sublation process using mineral oil as the collector (Matis 1995) could be quite effective for effluent pre-treatment to reduce extractive loading to the biobasin. The collected mineral oil could be cleaned and reused or else combusted and its heat content utilized.

5.5 Conclusions

In agreement with the results reported in Chapter 4, changes in the influent concentration of resin acids to a biological wastewater treatment system influenced the microbial community structure. Microbial population dynamics can be assessed from changes in microbial fatty compositions. This monitoring approach has been helpful in the consideration of community sensitivity to operational conditions such as pH, SRT and HRT. The combination of rapid sample processing and computer based data reduction makes fatty acid analysis an attractive research tool and a potential method for full scale system monitoring.

With respect to objective E in Chapter 1, the duration of the acclimation period after a shift-up in resin acids was similar for the pH 6 and pH 8 operating conditions. However, the nature of the microbial response was different and likely dependent on the microbial content which was itself pH-dependent. The measured extent of resin acid removal was greater at pH 8, in agreement with the observations from Chapter 3, of a greater residuum under acidic conditions.

Physiological state cannot be overlooked when considering the efficacy of a biological system for the removal of a specific aquatic contaminant. After experiencing identical contaminant loading histories, the conditions of the suspended biomass at pH 6 and pH 8 with respect to resin acid removal were distinct. Thus, the demonstration of biodegradability and high steady state removal efficiency are promising but insufficient criteria for a biological approach to wastewater treatment. Even if a treatment system is acclimated to remove background levels of a particular contaminant, there is a likelihood of toxicity breakthrough following loading transient. The capacity of microbial communities to degrade substrates requiring induction of metabolic pathways is readily gained and lost. The transient lag time depends on physiological state, which is related to SRT for activated sludge treatment systems. The requirements of SRT may be conflicting. A low SRT appears to be necessary to maintain younger dividing organisms that respond quickly to change. A high SRT would be necessary to enrich for a population of microorganisms that is more specialized in its ability to remove the more recalcitrant substrates.

In the present (Chapter 5) and the previous investigations (Chapters 2 to 4), pH has been repeatedly found to be important to the fate of resin acids in pulp mill effluent. Shifting from pH 6 to 8 dramatically changes the extent to which these compounds could be biologically removed. Not only does pH influence physico-chemical interactions of resin acids by altering their form in solution, but the microbial content and metabolic response have also been shown to be affected.

5.6 References

- Aldenderfer, M. S., and Blashfield, R. K. (1984). *Cluster Analysis*, Sage Publications.
- Bailey, J. E., and Ollis, D. F. (1986). *Biochemical Engineering Fundamentals*, McGraw-Hill.
- Barford, J. P., Pamment, N. B., and Hall, R. J. (1982). Lag Phases and Transients. Microbial Population Dynamics, M. J. Bazin, ed., CRC Press, 55-90.
- Beckett, R., Wood, J. W., and Dixon, D. R. (1992). Size and chemical characterization of pulp and paper mill effluents by flow field fractionation and resin adsorption. *Environmental Technology*, 13, 1129-1140.
- Chiu, S. Y., Fan, L. T., Kao, I. C., and Erickson, L. E. (1972). Kinetic behaviour of mixed populations of activated sludge. *Biotechnology and Bioengineering*, 14, 179-199.
- Christodoulatos, C., and Mohiuddin, M. (1996). Generalized models for prediction of pentachlorophenol adsorption by natural soils. *Water Environment Research*, 68(3), 370-378.
- Chudoba, P., Capdeville, B., and Chudoba, J. (1991). Synchronised division of activated sludge microorganisms. *Water Science and Technology*, 25, 817-822.
- Chudoba, P., Capdeville, B., and Chudoba, J. (1992). Explanation of biological meaning of S_0/X_0 ratio in batch cultivation. *Water Science and Technology*, 26, 743-751.
- Cloete, T. E., and Muyima, N. Y. O. (1997). *Microbial Community Analysis*, IAWPRC, London.
- Doshi, M. R., and Dyer, J. M. (1997). Paper Recycling Challenge, Volume I, Stickies. , Doshi & Associates.
- Ellis, T. G., Barbeau, D. S., Smets, B. F., and Grady, C. P. L., Jr. (1996). Respirometric technique for determination of extant kinetic parameters describing biodegradation. *Water Environment Research*, 68, 917.
- Ellis, T. G., Smets, B. F., and Leslie Grady Jr., C. P. (1998). Effect of simultaneous biodegradation of multiple substrates on the extant biodegradation kinetics of individual substrates. *Water Environment Research*, 70(1), 27-38.
- Grady, C. P. L. J., Smets, B. F., and Barbeau, D. S. (1996). Variability of kinetic parameter estimates: a review of possible causes and a proposed terminology. *Water Research*, 30(3), 742-748.
- Hall, E. R., and Liver, S. F. (1996). Interactions of resin acids with aerobic and anaerobic biomass - II. Partitioning on biosolids. *Water Research*, 30(3), 672-678.
- Harwood, J. L., and Russell, N. J. (1984). *Lipids in Plants and Microbes*, George Allen & Unwin, London.
- Hegewald, E., and Knorre, W. A. (1978). Kinetics of growth and substrate consumption of *Escherichia coli* ML 30 on two carbon sources. *Zeitschrift für Allgemeine Mikrobiologie*, 18(6), 415-426.
- Henze, M., Grady Jr, C. P. L., Gujer, W., Marais, G. v. R., and Matsuo, T. (1986). *Activated Sludge Model 1*, IAWPRC, London.
- Herbert, D. (1974). The chemical composition of micro-organisms as a function of their environment. Microbial Growth, P. S. S. Dawson, ed., Halsted Press, 204-229.
- Jacobsen, B. N., Arvin, E., and Reinders, M. (1996). Factors affecting sorption of pentachlorophenol to suspended microbial biomass. *Water Research*, 30(1), 13-20.
- Lechevalier, H., and Lechevalier, M. P. (1988). Chemotaxonomic use of lipids - an overview. Microbial Lipids, C. Ratledge and S. G. Wilkinson, eds., Academic Press, 869-902.
- Levenspiel, O. (1984). *The Chemical Reactor Omnibook*, OSU Book Stores, Inc.
- Liu, H. W., Lo, S. N., and Lavallée, H. C. (1993). Study of the performance and kinetics of aerobic biological treatment of a CTMP effluent. *Tappi Journal*, 94(12), 172-176.
- Liu, H. W., Lo, S. N., and Lavallée, H. C. (1996a). Mechanisms of removing resin and fatty acids in CTMP effluent during aerobic biological treatment. *Tappi Journal*, 79(5), 145-154.
- Liu, H. W., Lo, S. N., and Lavallée, H. C. (1996b). Theoretical study on two-stage anaerobic-aerobic biological treatment of a CTMP effluent. *Water Quality Research Journal of Canada*, 31(1), 1-35.

- Magbanua Jr, B. S., LU, Y., and Leslie Grady Jr, C. P. (1998). A technique for obtaining representative biokinetic values from replicate sets of parameter estimates. *Water Research*, 32(3), 849-855.
- Matis, K. A. (1995). Flotation science and engineering. , Marcel Dekker.
- Metcalf & Eddy, I. (1991). *Wastewater Engineering: Treatment, Disposal, and Reuse*, McGraw-Hill, Inc.
- Monod, J. (1949). The Growth of Bacterial Cultures. *Annual Review of Microbiology*, 3, 371-394.
- Panikov, N. S. (1995). *Microbial Growth Kinetics*, Chapman & Hall.
- Pickett, A. M. (1982). Growth in a Changing Environment. Microbial Population Dynamics, M. J. Bazin, ed., CRC Press, 91-124.
- Pollard, P. C., Steffens, M. A., Biggs, C. A., and Lant, P. A. (1998). Bacterial growth dynamics in activated sludge batch assays. *Water Research*, 32(3), 587-596.
- Powell, E. O. (1967). The growth rate of microorganisms as a function of substrate concentration. *Microbial Physiology and Continuous Culture*, E. O. Powell, C. G. T. Evans, R. E. Strange, and D. W. Tempest, eds., Her Majesty's Stationary Office.
- Savitzky, A., and Golay, M. J. E. (1964). Smoothing and Differentiation of Data by Simplified Least Squares Procedures. *Anal. Chem.*, 36(8), 1627-1639.
- Westall, J. C. (1985). Influence of pH and ionic strength on the aqueous-nonaqueous distribution of chlorinated phenols. *Environmental Science and Technology*, 19, 193-198.

Chapter 6

Recommendations and Future Applications

Summary

The limitations to the biological removal of resin acids can be influenced by the pH condition, within the narrow range typically used to biologically treat pulp mill effluent. Generally, alkaline pH conditions promote a greater extent and rate of removal. Harvesting and oxidation of scum from biobasins and clarifiers is recommended due to the tendency of acutely toxic hydrophobic contaminants to accumulate at the surface. In addition, future developments are required in online water quality measurement to prevent the discharge of toxic effluents through continuous influent and effluent monitoring.

The contributions made, with the present investigation, in the areas of surface tension and microbial fatty acid measurements are novel and have engineering application in future modelling and monitoring of the behaviour of microbial wastewater treatment processes.

Table of Contents

6.1 Introduction	337
6.2 Mechanisms of pH Influence in the Biological Removal of Resin Acids	337
6.2.1 <i>pH Versus Contaminant Retention Time (Objective D)</i>	339
6.2.2 <i>pH Versus Community Structure and Bioactivity (Objectives B, C and E)</i>	340
6.2.3 <i>pH Versus Resin Acid Bioavailability (Objective A)</i>	341
6.2.4 <i>Recommendations</i>	342
6.3 Research Contributions and Future Work	344
6.3.1 <i>Modelling of Biological Wastewater Treatment</i>	345
6.3.2 <i>Modelling Contaminant Transport</i>	347
6.3.3 <i>Control of Biological Wastewater Treatment</i>	348

6.1 Introduction

The purpose of this chapter is twofold. First, based on the experimental results, theoretical developments and discussions presented in the four preceding chapters, it is now of interest to return to the thesis question that motivated the research project. The objective is to consider the extent to which the original thesis question has been answered and how that information should influence current pulp mill practices. Second, through the course of the investigation, a number of ideas and concepts have been developed that have potential engineering application. The spin-off contributions of this research are in the areas of modelling and process control for biological wastewater treatment. The full development of these ideas are left for future work and, consequently, they lie beyond the scope of the present dissertation. However, due to their potential, they warrant some discussion which I hope will provide seeds for thought, and further research and development.

6.2 Mechanisms of pH Influence in the Biological Removal of Resin Acids

It has been repeatedly shown that the properties of resin acids in aqueous solution change significantly within the narrow pH range that is typical for biological treatment of pulp mill effluent. The probability of resin acid removal was postulated to be significantly pH-sensitive within this narrow pH range. It was stated in Chapter 1, that the probability of biological removal of a contaminant in a bioreactor depends on: (i) the contaminant bioavailability, (ii) the state of the selected microbial community, and (iii) the contaminant retention time.

The influence of a pH change on resin acid removal can be direct. For instance, microbial community structure and activity in a bioreactor are known to be influenced by the pH. The pH-dependency of resin acid removal can also be indirect. Resin acid solubility is a function of hydrophobicity, which is a function of pH. The kinetics and extent of contaminant adsorption are functions of contaminant hydrophobicity. Adsorption interactions can prolong the contaminant retention time during secondary treatment. Hydrophobic compounds are also known to inhibit microbial activity. Limitations of contaminant aqueous solubility are known to restrict the

contaminant bioavailability. Thus, the objective of the thesis was not to prove pH-dependency but rather to quantify the extent of pH-dependency for the biological removal of resin acids.

Over the course of the present investigation it has been shown that a change of pH, within the typical narrow range used for biological treatment of pulp mill effluent, significantly influences all three of the above factors, which in turn, affect the observed biological removal. Prior to the present investigation, there has been no clear quantification of this pH-dependency reported in the research literature. The contribution in this consideration of each of the three factors, has been a fundamental advancement in the understanding of resin acid fate during biological treatment.

This fundamental advancement has been achieved by working to unambiguously separate the direct dependency of microbial activity on pH, from the pH-dependent change of resin acid hydrophobicity on biological removal. The separation of contributing factors was accomplished by undertaking four separate experimental investigations that addressed the following five research objectives:

- A. To determine the influence of resin acid solubility on contaminant bioavailability (Chapter 2).
- B. To determine the influence of pH on the microbial community structure and the uptake rate of resin acids (Chapter 3).
- C. To determine the influence of resin acid hydrophobicity on microbial activity (Chapter 4).
- D. To determine the influence of resin acid hydrophobicity on contaminant sorption to biomass and, consequently, retention time (Chapter 4).
- E. To determine the influence of pH on the time lag in increased metabolic activity for resin acid biodegradation (Chapter 5).

The experience gained from the four investigations has engineering application in the future design of secondary biological processes treating pulp mill effluent.

6.2.1 pH Versus Contaminant Retention Time (Objective D)

To begin, consider how pH influences the contaminant retention time. Resin acid hydrophobicity decreases with pH. Under slightly acidic conditions, strong associations result between these contaminants and other particulate or dissolved organic matter in solution. So long as conditions remain acidic, the associations become less reversible with age (Chapter 5). Thus over longer periods of contact time under acidic conditions, the extent of resin acid adsorption departs from a standard isotherm model (Chapters 2 and 4) and grows in a manner that might be better modelled by equations of multilayer adsorption, organic phase extraction, or solid crystal growth.

While the extent of resin acid adsorption under acidic conditions will ultimately surpass levels predicted from studies that revealed short term reversible interactions, the rate of adsorption under acidic conditions appears to be a rate limiting step (Chapters 2 and 4). In other words, resin acid mobility, and consequently, the rate of adsorption, under alkaline conditions is much more rapid. Thus, a prolonged retention time due to resin acid adsorption was predicted to be greater for alkaline aqueous conditions (Chapter 4). Since film diffusion limits the adsorption process, high solute mobility under alkaline conditions makes the largest contribution to extension of the contaminant retention time due to adsorption interactions, at least in the short term.

It must be kept in mind that the prolonged retention of resin acids due to adsorption under alkaline conditions requires that the formation of surface foam does not facilitate a route for treatment process short-circuiting (Chapter 4). Scum is typically seen on the biobasins and clarifiers at pulp mills. Chances are that this scum will contain resin acids or other similar deleterious aquatic contaminants. Unfortunately, the benefit of a longer contaminant retention time due to adsorption will not likely contribute, as one would expect, to an improved probability for biodegradation in the biobasin, if one considers the results of community structure and bioactivity.

6.2.2 pH Versus Community Structure and Bioactivity (Objectives B, C and E)

Resin acids were readily biodegradable for all pH conditions tested (Chapter 3). Thus, a study that considers the influence of pH on just the removal of resin acids, might conclude that biological removal of resin acids is insensitive to pH. However, the observed change in community fatty acid chemotypes between experiments and as a function of pH, indicates that a diversity of resin acid-degrading bacteria exists in nature. Each community of resin acid-degrading bacteria achieved significantly different maximal rates of resin acid removal. Therefore, resin acid removal is quite pH-sensitive since community structure was shown to be pH-dependent and removal rates were in turn, community-dependent. However, the influence of pH-dependent changes in community structure were overshadowed by the observed response time to transient loading conditions.

Lag times for the acclimation of mixed culture populations to elevated resin acid loadings were unexpectedly long (Chapter 5). The time scale of prolonged contaminant retention in the biobasin due to adsorption was short with respect to the time scale required for microbial acclimation (Chapters 4 and 5). The duration of the lag time was independent of pH, although the community structure was sensitive to pH (Chapter 3), as was the nature of the transient response (Chapter 5). Acclimation was observed to be a two phase process (Chapter 5). A sudden input of resin acids stimulated a change in the community structure. As the community structure became established, biological removal became significant.

Physiological state is, therefore, a key factor governing the removal of resin acids. Under batch growth conditions (Chapter 3), the two resin acids were degraded in order of their relative concentrations. An identical cultivation history under acidic and alkaline continuous flow conditions, produced resin acid-degrading communities with distinctly different physiological states with respect to resin acid metabolism (Chapter 5). The trends of mixed culture acclimation to a resin acid shift-up, under continuous flow conditions (Chapter 5), were similar to those predicted for pure culture chemostat systems. Thus, the community response may be approximated by a model "pseudo-species". Such modelling neglects the change in the maximal

kinetic rates associated with a change in pseudo-species, but it promises to yield a more realistic representation of bioreactor dynamic behaviour. The pseudo-species physiological state for resin acid removal depends on the contaminant loading. Thus, the capacity to degrade resin acids is readily gained and lost in a bioreactor (Chapter 5).

The success of biological removal of resin acids appears to be limited by the extent to which steady state conditions in the bioreactor can be considered to be typical. A change in bioreactor pH selects for alternate communities of organisms that degrade resin acids. With a change in the community, there is a change in the maximum specific uptake rate. The long acclimation time observed for a resin acid shift-up, indicates that sudden increases in resin acid influent loadings will most likely result in an event of toxicity breakthrough.

If influent loading fluctuations are infrequent, the environmental impact of an occasional toxicity breakthrough event may be considered to be of sufficiently low significance to warrant strong remedial action to the current treatment practices. Such a complacent opinion will hopefully be swayed by ethics, engineering ambition, and, the risk of legal liability. The industry incentive of progressive systems closure, should also promote the necessity for robustness in contaminant removal. Inconsistent removal of resin acids from reused process waters will detract from the product quality due to the formation of "stickies" (Chapter 1).

6.2.3 pH Versus Resin Acid Bioavailability (Objective A)

Compounds like resin acids are believed to be degraded intercellularly, and to be transported into the cell by passive diffusion through a membrane having a molecular weight cut-off of about 1000 Daltons. It appeared that molecular associations between resin acids and other compounds in pulp mill effluent became significant under slightly acidic conditions (Chapters 2 and 3). As a consequence threshold concentrations for biological removal will increase below a neutral pH level. Such a threshold defines a concentration where the delivery rate of a contaminant to a microbial cell is insufficient to sustain growth. The decreased extent of removal under acidic conditions was observed for both batch and continuous treatment conditions

(Chapters 2, 3 and 5). However, note that threshold concentrations were also detected above neutral pH.

For alkaline batch growth conditions, a threshold concentration for resin acid biodegradation was consistently about 0.15 mg/L and, therefore, still significant (Chapter 3). Threshold concentrations can be reduced by the contributions of uncoupled and co-metabolic mechanisms of biological removal (Chapter 3). The importance of these other removal mechanisms during full scale biological treatment of pulp mill effluent has not been established. Until contributions of uncoupled growth and co-metabolism can be well defined and predicted, it does not seem prudent to rely on these secondary mechanisms of biological removal.

These secondary mechanisms of biological removal may depend on the presence of certain microorganisms and/or other substrates. The organic content of pulp mill effluent is known to be variable and the results of the present work indicate that the community of microorganisms during wastewater treatment is also continually changing (Chapter 5). Therefore, it is not unreasonable to speculate that the contributions of uncoupled and co-metabolic mechanisms of biological removal will not be consistent. Hence, threshold concentrations observed during batch, growth-linked biodegradation experiments represent an important, conservative limit to be expected for biological removal.

6.2.4 Recommendations

It must be concluded that there are pH-related limitations to biological removal of resin acids from pulp mill effluent and that the extent of these limitations depend, both directly and indirectly, on pH. How might the fundamental information acquired over the course of the present investigation be applied to improve upon the current practices of secondary treatment for bleached kraft mill effluent? There are three practical recommendations, that could be applied, namely:

- i) well controlled alkaline treatment conditions,

- ii) scum harvesting and parallel treatment, and
- iii) continuous monitoring in conjunction with mill shut-down protocols.

The bioavailability and the rate of removal were observed to be improved under alkaline conditions. Therefore, alkaline pH control near 7.5 is recommended in order to promote an optimal (more) stable microbial community in the biobasin.

However, alkaline treatment conditions also promote the greatest amount of scum formation. Thus, scum formed on biobasins and clarifiers should be considered for its potential to harbour acutely toxic contaminants. Due to the observed lag times for resin acid removal, a sudden re-entrainment of resin acids from the scum into the biobasin will likely not be attenuated.

Therefore, foam and scum formation require separate handling and treatment.

Harvesting and parallel treatment of surface scum is an innovative strategy for reducing the chances of toxicity breakthrough, by reducing the mass of resin acids and like compounds, that need to be biodegraded during continuous treatment. Due to the inconsistency of scum formation, the technology selected to process this waste stream should be able to operate intermittently. The most efficient methods to separate and convey surface scum in conjunction with its treatment need to be established. The effectiveness and economics of either biological or physical treatment need to be compared. For example, sequencing batch biological treatment or a physical unit process such as batch wet-oxidation are two approaches that could be investigated.

Finally, the best method to prevent toxicity breakthrough is to sense its onset and, consequently, divert the discharge of acutely toxic wastewater. Diversion of mill wastewater to holding tanks would be the first stage in an unscheduled emergency mill shut-down, and this is a practical issue of planning, space and economics. Detecting the onset of a breakthrough event is a technological problem in process monitoring. The onset of an event may be obvious due to a known process spill. However, the onset of an event may be less apparent. The cause could be due to an upstream change such as the wood-chip furnish, or it could be due to a downstream change such as an unexplained reduction in metabolic activity in the biobasin. Therefore, the process

monitoring equipment required for detecting early stages of an event of toxicity breakthrough, needs to be located both upstream and downstream of the biological treatment system. Upstream monitoring would raise the alarm of a change in the mill sewer that could compromise success in biological treatment. Downstream monitoring would signal a trend of reduced capacity in the biological treatment system. The problem is to determine what parameter would be best monitored.

Bioassays would be the most direct method of detecting the presence of toxic contaminants, but these require much manual intervention and time. Furthermore, an early warning for the onset of an event should ideally be before the final effluent is acutely toxic. The monitoring strategy can be one of assaying for specific contaminants on a semi-continuous basis. However, trace analysis can involve complicated and time consuming methodologies.

Alternatively, it may be possible to measure a more holistic water quality parameter that can be shown to infer (with high probability) the presence of deleterious chemicals. For example, surface tension monitoring (Chapter 2) is one method that can indicate an overall change in the content of resin acid-like contaminants in the effluent. Other examples for such holistic water quality parameters could be the change of the infra-red or UV absorbance spectra of the wastewater. The advantage of following a water quality parameter such as surface tension, lies in the simplicity of sample processing and the rapidity of the measurement. The disadvantage of such a non-specific assay is in the chance of raising a false alarm or of missing the event. Due to the economic expense of an unscheduled mill shut-down, decisions must be based on reliable information. Therefore, rapid, and ideally automated, methods of effluent monitoring need to be developed and tested. Non-specific signals of water quality change require the characterisation of the effluent such that reliable inferences can be made.

6.3 Research Contributions and Future Work

The application and developments made in the areas of surface tension and microbial fatty acid measurements have been novel contributions that have engineering application in modelling

and monitoring the behaviour of microbial wastewater treatment processes. The significance of these research tools has been discussed in the preceding chapters. The purpose here is to highlight these contributions in order to recommend how they might be applied for future work.

6.3.1 Modelling of Biological Wastewater Treatment

Representative modelling of biological wastewater treatment is required for research into, and the design of, robust biological unit processes used to reduce contaminant concentrations in wastewater. Modelling necessitates assumptions that serve tractable mathematical constructs. These constructs form the basis of much engineering decision-making. However, since modelling is, in itself, such a specialized discipline of applied mathematics and numerical processing, there can be some diversion between the “model world” and “experimental reality”. Due to the almost universal use of Monod kinetics for the design and simulation of biological wastewater treatment, it is important to continually be appraised of any experimental evidence that define limitations for the use of the Monod model.

The present investigation has brought into question the omission of a threshold concentration and the assumed consistency of the yield coefficient in classical Monod kinetics. Further, the model expectations for the performance of a biological unit process, fed fluctuating substrate concentrations, would be improved by the incorporation of a parameter of physiological state.

The monitoring of microbial fatty acid compositions were instrumental in arriving at these insights. Total fatty acid as a biomass measure was used in conjunction with measurements of substrate depletion to establish growth kinetics and to test explicitly the assumptions of the model. Under certain circumstances, the assumptions of complete substrate removal and of a constant growth yield coefficient may be valid. If they are valid, this considerably simplifies the experimental effort in measuring kinetic parameters. However, had the growth kinetics for Chapters 2 and 3 been estimated using respirometric measures applied to the classical Monod assumptions, then the threshold concentrations would have been incorrectly interpreted as a change in the growth yield coefficient. Interpretation of such respirometric data would have been

further compromised by neglecting the lag phase which was not consistent in duration. Had the kinetics been estimated by the substrate depletion curve alone, the unknown duration of the lag phase would also have lead to an erroneous estimation of the half saturation constant and the growth yield coefficient. Consider, for example, the parameters estimated in Chapter 2, in absence of adequate data for biomass production. A good fit to experimental data does not guarantee that the model is correct. Model assumptions need to be tested experimentally.

Therefore, research into the microbial kinetics of unfamiliar systems requires that both substrate depletion and biomass production be carefully monitored. Once the model assumptions have been explicitly tested, then in continued research it may be possible to reduce the experimental burden, with confidence in the validity of the estimates of the model parameters. For example, the growth kinetics on sodium acetate (Chapter 3) could have been well characterized with knowledge of the initial substrate concentration and data for biomass production.

Given the choice between monitoring substrate depletion or biomass production for mixed cultures, the most informative choice appears to be biomass production. Following biomass production in terms of microbial fatty acids furnishes data that helps to distinguish the mixed culture of one experiment from another. The results of mixed culture research have limited value unless the communities in experiments can be compared. For example, the observed variability in the removal rate of resin acids (Chapter 3) could not have been adequately interpreted, if it could not have been established that the communities involved were distinctly different. The quotient of community diversity with respect to removal rate variability is a parameter that has application in deciding on factors of safety in treatment plant design (Chapters 3 and 5). Growth kinetics of microbial communities involve both a rate change in biomass and a rate change in structure. The rate change in structure or population dynamics can be assessed by a parameter of state-speed that quantifies the kinetics of fatty acid compositional change (Chapters 4 and 5).

Advancement in modelling microbiological unit processes will be made with the incorporation of a parameter of physiological state. Response kinetics for the acquisition, and the dissipation, of capacity to remove specific aquatic contaminants were found to be very important facets in the

performance of a laboratory scale treatment system (Chapter 5). Modelling the community as a single pseudo-species, it was possible to reproduce the experimental observations of biphasic growth on resin acids during batch cultivation, by using the parameter of physiological state (Chapter 3). Similarly, the dynamic response of a continuous flow treatment system to a shift-up in resin acid loading, resembled classical model chemostat behaviour predicted for pure cultures (Chapter 5). Therefore, although community structure and, thus the pseudo-species, in continuous flow treatment systems are dynamic (Chapter 4 and 5), assuming a representative and constant pseudo-species can still be informative for modelling transient response under non-steady loading conditions. Both theoretical and experimental research on the parameter of physiological state will help to improve future engineering of wastewater treatment systems.

6.3.2 Modelling Contaminant Transport

The uptake of hydrophobic contaminants such as resin acids may be rate limited by diffusion. This limitation means that optimization of biological removal may be reached by somehow improving the contaminant mobility. For example, it is possible to use surfactants to solubilize hydrophobic contaminants in order to improve their bioavailability. The questions for a research investigation may be, what kind of surfactant and at what concentration.

A biological approach for an extensive screening program into enhanced treatability by using chemical additives may eventually lead to promising results. This kind of testing would likely be some form of factorial experimental design using a number of surfactants at different concentrations in batch culture. However, a more fundamental understanding of how the chemical additives influence bioavailability could reduce the required extent of trial and error during biological experimentation. If chemical additives were first screened for an ability to measurably enhance the contaminant transport, the biological trials would have a better chance of success.

Contaminant transport can be sensed and modelled from dynamic surface tension measurements (Chapter 2). Therefore, the maximum bubble pressure method combined with quasi-static

isotherm modelling is a useful research tool for studying contaminant fate. Such a research tool warrants further use and development.

6.3.3 Control of Biological Wastewater Treatment

If bacteria could only talk, what might engineers and plant operators ask the community in a biological wastewater treatment process? Perhaps the most pressing question when it comes to the control of biological treatment systems is: “are you happy?”. Such a question is currently considered by assessing the overall level of metabolic activity within the biobasin using respirometric techniques. However, a high level of metabolic activity does not guarantee treatment performance. Therefore, a complementary question that needs to be asked is: “who are you?”, followed by: “are you still there?”.

Optimal biological treatment requires the maintenance of desirable biosolids attributes, such as good settleability, while achieving maximal reduction in contaminant concentrations. Presumably, the community that achieves this optimal treatment performance may be susceptible to small perturbations in environmental factors. In other words, the many distinct communities of microorganisms that can potentially arise in a biobasin, can be thought of as metastable community structures. The community structure is metastable since it is forced to change given a sufficient external stimulus.

A number of different communities could achieve similar levels of treatment performance, while the characteristics of other communities that evolve could compromise the *modus operandi* of the treatment process. For instance, a high degree of contaminant reduction may still be achieved during sludge bulking, but the process will fail due to a lack of biosolids settleability. Therefore, monitoring community structure and population dynamics with respect to the unit process operating conditions would advance the application of control strategies.

From the present investigation, the monitoring of microbial community structure with microbial fatty acid compositions is one potential method of rapid community analysis. By correlating finger prints of the community structure (Chapters 3, 4 and 5) to biosolids characteristics, it might

be possible, over time, to see emerging patterns that can be linked to desirable or problematic operating conditions. By relating the sensitivity of the community to environmental perturbations, the best operational adjustments that need to be made in response to an undesirable community shift may be determined. Therefore, future investigations that provide a more fundamental understanding of community structure and its relationship to biological wastewater treatment control will be important contributions with exciting engineering application.

Appendix A Experimental Data

Summary

This appendix contains a list of the data tables that have been provided in electronic format on the accompanying computer disk. The data are organized by chapter as worksheets in Microsoft Excel 97 formatted files, namely, Chapter2.xls, Chapter3.xls, Chapter4.xls and Chapter5.xls. These files can be viewed and printed using the shareware Microsoft program Excel Viewer (Version 8.0). The minimum system requirements to install the viewer are as follows: (1) Personal computer with a 486 or higher processor, (2) Microsoft Windows 95 operating system or Windows NT, (3) 4 MB of memory for use on Windows 95 (8 MB recommended); 12 MB of memory for use on Windows NT Workstation, (4) 7 MB of hard disk space required (for installation only, 9 MB of hard disk space required), (5) VGA or higher-resolution video adapter, and (6) Microsoft Mouse or compatible pointing device. Of course, any spreadsheet software that supports the Excel 97 file format can be similarly used to view the data and if desired, the data can be further manipulated.

Table of Contents

A-2 Chapter 2 Data	351
A-3 Chapter 3 Data	351
A-4 Chapter 4 Data	353
A-3 Chapter 5 Data	354

A-2 Chapter 2 Data

The data in the following list of tables is contained in the Excel 97 file Chapter2.xls:

Table A-2.1. Raw data from Chapter 2 for mixed culture batch growth on abietane resin acids at pH 6. The results of the dynamic surface tension measurements are tabulated along side the history of resin acid depletion.

Table A-2.2. Raw data from Chapter 2 for mixed culture batch growth on abietane resin acids at pH 7. The results of the dynamic surface tension measurements are tabulated along side the history of resin acid depletion.

Table A-2.3. Raw data from Chapter 2 for mixed culture batch growth on abietane resin acids at pH 8. The results of the dynamic surface tension measurements are tabulated along side the history of resin acid depletion.

A-3 Chapter 3 Data

The data in the following list of tables is contained in the Excel 97 file Chapter3.xls:

Table A-3.1. Raw data from Chapter 3 (Figure 3-7) for mixed culture batch growth on Lauryl Tryptose Broth. The data show replicate samples of fatty acids obtained by PLFA and WCFA techniques. Concentrations are in micromolar units.

Table A-3.2. Replicate batch growth data from Chapter 3, for mixed culture batch growth on Lauryl Tryptose Broth. The data show the results of whole cell fatty acids extracted over the course of the growth cycle. With respect to Table A-3.3, the replicates are identified as A (Top) and B (Bottom).

Table A-3.3. Replicate batch growth data from Chapter 3, for mixed culture batch growth on Lauryl Tryptose Broth. The data show results of total fatty acid (mM TFA) biomass derived from Table A-3.2, along side data of protein biomass (mg/L Bovine Serum Albumin or BSA), and dry weight biomass (mg/L Dry Wt.).

Table A-3.4. Batch Growth Experiment A (March 1996) from Chapter 3. The table lists raw data as a function of time (Hour) for a medium pH of 6.04. The two dominant microbial fatty acid along with dehydrabietic (DHA), abietic (ABA), 6-dehydo-dehydroabietic (6-d-DHA), and 7-keto-dehydroabietic (7-k-DHA) acid micromolar concentrations are reported.

Table A-3.5. Batch Growth Experiment A (March 1996) from Chapter 3. The table lists raw data as a function of time (Hour) for a medium pH of 7.03. The two dominant microbial fatty acid along with dehydrabietic (DHA), abietic (ABA), 6-dehydo-dehydroabietic (6-d-DHA), and 7-keto-dehydroabietic (7-k-DHA) acid micromolar concentrations are reported.

Table A-3.6. Batch Growth Experiment A (March 1996) from Chapter 3. The table lists raw data as a function of time (Hour) for a medium pH of 7.55. The two dominant microbial fatty acid along with dehydrabietic (DHA), abietic (ABA), 6-dehydo-dehydroabietic (6-d-DHA), and 7-keto-dehydroabietic (7-k-DHA) acid micromolar concentrations are reported.

Table A-3.7. Batch Growth Experiment A (March 1996) from Chapter 3. The table lists raw data as a function of time (Hour) for a medium pH of 8.06. The two dominant microbial fatty acid along with dehydrabietic (DHA), abietic (ABA), 6-dehydo-dehydroabietic (6-d-DHA), and 7-keto-dehydroabietic (7-k-DHA) acid micromolar concentrations are reported.

Table A-3.8. Batch Growth Experiment A (March 1996) from Chapter 3. The table lists raw data as a function of time (Hour) for a medium pH of 8.44. The two dominant microbial fatty acid along with dehydrabiatic (DHA), abiatic (ABA), 6-dehydo-dehydroabiatic (6-d-DHA), and 7-keto-dehydroabiatic (7-k-DHA) acid micromolar concentrations are reported.

Table A-3.9. Batch Growth Experiment B (June 1996) from Chapter 3. The table lists raw data as a function of time (Hour) for a medium pH of 5.50. The microbial fatty acid along with dehydrabiatic (DHA), abiatic (ABA), 6-dehydo-dehydroabiatic (6-d-DHA), and 7-keto-dehydroabiatic (7-k-DHA) acid micromolar concentrations are reported.

Table A-3.10. Batch Growth Experiment B (June 1996) from Chapter 3. The table lists raw data as a function of time (Hour) for a medium pH of 6.01. The microbial fatty acid along with dehydrabiatic (DHA), abiatic (ABA), 6-dehydo-dehydroabiatic (6-d-DHA), and 7-keto-dehydroabiatic (7-k-DHA) acid micromolar concentrations are reported.

Table A-3.11. Batch Growth Experiment B (June 1996) from Chapter 3. The table lists raw data as a function of time (Hour) for a medium pH of 6.51. The microbial fatty acid along with dehydrabiatic (DHA), abiatic (ABA), 6-dehydo-dehydroabiatic (6-d-DHA), and 7-keto-dehydroabiatic (7-k-DHA) acid micromolar concentrations are reported.

Table A-3.12. Batch Growth Experiment B (June 1996) from Chapter 3. The table lists raw data as a function of time (Hour) for a medium pH of 7.03. The microbial fatty acid along with dehydrabiatic (DHA), abiatic (ABA), 6-dehydo-dehydroabiatic (6-d-DHA), and 7-keto-dehydroabiatic (7-k-DHA) acid micromolar concentrations are reported.

Table A-3.13. Batch Growth Experiment B (June 1996) from Chapter 3. The table lists raw data as a function of time (Hour) for a medium pH of 7.02. The microbial fatty acid along with dehydrabiatic (DHA), abiatic (ABA), 6-dehydo-dehydroabiatic (6-d-DHA), and 7-keto-dehydroabiatic (7-k-DHA) acid micromolar concentrations are reported.

Table A-3.14. Batch Growth Experiment B (June 1996) from Chapter 3. The table lists raw data as a function of time (Hour) for a medium pH of 7.55. The microbial fatty acid along with dehydrabiatic (DHA), abiatic (ABA), 6-dehydo-dehydroabiatic (6-d-DHA), and 7-keto-dehydroabiatic (7-k-DHA) acid micromolar concentrations are reported.

Table A-3.15. Batch Growth Experiment B (June 1996) from Chapter 3. The table lists raw data as a function of time (Hour) for a medium pH of 8.08. The microbial fatty acid along with dehydrabiatic (DHA), abiatic (ABA), 6-dehydo-dehydroabiatic (6-d-DHA), and 7-keto-dehydroabiatic (7-k-DHA) acid micromolar concentrations are reported.

Table A-3.16. Batch Growth Experiment B (June 1996) from Chapter 3. The table lists raw data as a function of time (Hour) for a medium pH of 8.53. The microbial fatty acid along with dehydrabiatic (DHA), abiatic (ABA), 6-dehydo-dehydroabiatic (6-d-DHA), and 7-keto-dehydroabiatic (7-k-DHA) acid micromolar concentrations are reported.

Table A-3.17. Batch Growth Experiment C (November 1996) from Chapter 3. The table lists raw data as a function of time (Hour) for a medium pH of 5.95. The microbial fatty acid along with dehydrabiatic (DHA) and abiatic (ABA) acid micromolar concentrations are reported.

Table A-3.18. Batch Growth Experiment C (November 1996) from Chapter 3. The table lists raw data as a function of time (Hour) for a medium pH of 6.45. The microbial fatty acid along with dehydrabiatic (DHA) and abiatic (ABA) acid micromolar concentrations are reported.

Table A-3.19. Batch Growth Experiment C (November 1996) from Chapter 3. The table lists raw data as a function of time (Hour) for a medium pH of 6.96. The microbial fatty acid along with dehydrabiatic (DHA) and abiatic (ABA) acid micromolar concentrations are reported.

Table A-3.20. Batch Growth Experiment C (November 1996) from Chapter 3. The table lists raw data as a function of time (Hour) for a medium pH of 7.47. The microbial fatty acid along with dehydrabiatic (DHA) and abiatic (ABA) acid micromolar concentrations are reported.

Table A-3.21. Batch Growth Experiment C (November 1996) from Chapter 3. The table lists raw data as a function of time (Hour) for a medium pH of 8.04. The microbial fatty acid along with dehydrabiatic (DHA) and abiatic (ABA) acid micromolar concentrations are reported.

Table A-3.22. Batch Growth Experiment C (November 1996) from Chapter 3. The table lists raw data as a function of time (Hour) for a medium pH of 5.99. The microbial fatty acid along with sodium acetate (NaAc) micromolar concentrations are reported. The community was enriched on resin acids.

Table A-3.23. Batch Growth Experiment C (November 1996) from Chapter 3. The table lists raw data as a function of time (Hour) for a medium pH of 6.46. The microbial fatty acid along with sodium acetate (NaAc) micromolar concentrations are reported. The community was enriched on resin acids.

Table A-3.24. Batch Growth Experiment C (November 1996) from Chapter 3. The table lists raw data as a function of time (Hour) for a medium pH of 6.98. The microbial fatty acid along with sodium acetate (NaAc) micromolar concentrations are reported. The community was enriched on resin acids.

Table A-3.25. Batch Growth Experiment C (November 1996) from Chapter 3. The table lists raw data as a function of time (Hour) for a medium pH of 7.51. The microbial fatty acid along with sodium acetate (NaAc) micromolar concentrations are reported. The community was enriched on resin acids.

Table A-3.26. Batch Growth Experiment C (November 1996) from Chapter 3. The table lists raw data as a function of time (Hour) for a medium pH of 8.09. The microbial fatty acid along with sodium acetate (NaAc) micromolar concentrations are reported. The community was enriched on resin acids.

A-4 Chapter 4 Data

The data in the following list of tables is contained in the Excel 97 file Chapter4.xls:

Table A-4.1. Raw data from Chapter 4 for the suspended biomass from reactor A (pH 6.0). The micromolar fatty and resin acid concentrations are given as a function of time. The resin acid concentrations are given in terms of pimaranes (PIM), abietanes (ABA), and chlorinated dehydroabietanes (CL-DHA).

Table A-4.2. Raw data from Chapter 4 for the suspended biomass from reactor B (pH 8.0). The micromolar fatty and resin acid concentrations are given as a function of time. The resin acid concentrations are given in terms of pimaranes (PIM), abietanes (ABA), and chlorinated dehydroabietanes (CL-DHA).

Table A-4.3. Raw data from Chapter 4 for the biofilm biomass from reactor A (pH 6.0). The fatty and resin acid surface loadings (nmole/cm²) are given as a function of time. The resin acid concentrations are given in terms of pimaranes (PIM), abietanes (ABA), and chlorinated dehydroabietanes (CL-DHA).

Table A-4.4. Raw data from Chapter 4 for the biofilm biomass from reactor B (pH 8.0). The fatty and resin acid surface loadings (nmole/cm²) are given as a function of time. The resin acid concentrations are given in terms of pimaranes (PIM), abietanes (ABA), and chlorinated dehydroabietanes (CL-DHA).

Table A-4.5. Raw data from Chapter 4 for the fatty acids present in the BKME feed. The micromolar fatty and resin acid concentrations are given as a function of time. The micromolar resin acid concentrations are given as a function of time in terms of pimaranes (PIM) and abietanes (ABA).

Table A-4.6. Raw data from Chapter 4 for the acid soluble total organic carbon levels (mg/L) as a function of time for reactor A, reactor B and the BKME feed.

Table A-4.7. Raw data from Chapter 4 for the lithium concentrations (mg/L) as a function of time in reactor A (Li.A) and reactor B (Li.B).

A-3 Chapter 5 Data

The data in the following list of tables is contained in the Excel 97 file Chapter5.xls:

Table A-5.1. Raw data from Chapter 5 for the suspended biomass and resin acids in reactor A (pH 6.0). The micromolar fatty and resin acid concentrations are given as a function of time. The resin acid concentration is given in terms of total resin acid (TRA).

Table A-5.2. Raw data from Chapter 5 for the effluent biomass and resin acids from reactor A (pH 6.0). The micromolar fatty and resin acid concentrations are given as a function of time. The resin acid concentration is given in terms of total resin acid (TRA).

Table A-5.3. Raw data from Chapter 5 for the suspended biomass and resin acids in reactor B (pH 8.0). The micromolar fatty and resin acid concentrations are given as a function of time. The resin acid concentration is given in terms of total resin acid (TRA).

Table A-5.4. Raw data from Chapter 5 for the effluent biomass and resin acids from reactor B (pH 8.0). The micromolar fatty and resin acid concentrations are given as a function of time. The resin acid concentration is given in terms of total resin acid (TRA).

Table A-5.5. Raw data from Chapter 5 for the biofilm biomass and adsorbed resin acids in reactor A (pH 6.0). The fatty and resin acid surface loadings (nmole/cm²) are given as a function of time. The resin acid concentrations are given in terms of total resin acids (TRA).

Table A-5.6. Raw data from Chapter 5 for the biofilm biomass and adsorbed resin acids in reactor B (pH 8.0). The fatty and resin acid surface loadings (nmole/cm²) are given as a function of time. The resin acid concentrations are given in terms of total resin acids (TRA).

Table A-5.7. Raw data from Chapter 5 for the fatty and resin acids in the BKME feed. The micromolar fatty and resin acid concentrations are given as a function of time. The resin acid concentration is given in terms of total resin acid (TRA).

Table A-5.8. Raw data from Chapter 5 for the acid soluble total organic carbon levels (mg/L) as a function of time for reactor A, reactor B and the BKME feed.

Table A-5.9. Raw data from Chapter 5 for the lithium concentrations (mg/L) as a function of time in reactor A, reactor B and in the tracer feed.

Table A-5.10. Raw data from Chapter 5 for the resin acid concentrations (μM) in the tracer feed.

Table A-5.11. Raw data from Chapter 5 for batch growth at pH 6.0 on BKME enriched with resin acids using the suspended biomass from reactor A for the inoculum.

Table A-5.12. Replicate data from Chapter 5 for batch growth at pH 6.0 on BKME enriched with resin acids using the suspended biomass from reactor A for the inoculum.

Table A-5.13. Raw data from Chapter 5 for batch growth at pH 8.0 on BKME enriched with resin acids using the suspended biomass from reactor B for the inoculum.

Table A-5.14. Replicate data from Chapter 5 for batch growth at pH 8.0 on BKME enriched with resin acids using the suspended biomass from reactor B for the inoculum.